

# Università degli Studi di Napoli *Federico II*

DOTTORATO DI RICERCA IN  
**FISICA FONDAMENTALE ED APPLICATA**

Ciclo: XXVII

Coordinatore: Prof. Raffaele Velotta

## Gamma-Ray Burst observations by the Square Kilometre Array. New perspectives

Settore Scientifico Disciplinare FIS/05

**Dottorando**

[Alan Cosimo Ruggeri](#)

**Tutore**

[Prof. Salvatore Capozziello](#)

Anni 2012/2015



*Non fidarti di coloro che in ogni momento ti riempiono di lodi e ti inondano di complimenti. I veri amici sono quelli che hanno il coraggio di dirti che sei un cretino, quando ritengono che tu stia sbagliando.*

Un cretino

*Don't trust people who compliment and praise you at anything. Good friends are brave enough to call you an idiot, when you are wrong.*

An idiot



# Papers related to the Ph.D.

1. Capozziello S., De Laurentis M., **Ruggeri A. C.** Dark energy observational tests and the SKA perspective. In Feretti L., Prandoni I., Brunetti G., Burigana C., Capetti A., Della Valle M., Ferrara A., Ghirlanda G., Govoni F., Molinari S., A. P., Scaramella R., Testi L., Tozzi P., Umana G., Wolter A., *editors*, *Italian SKA White Book*. INAF Press, 2014. ISBN ISBN 978-88-98985-00-5
2. Capozziello S., De Laurentis M., Luongo O., **Ruggeri A.C.** Cosmographic Constraints and Cosmic Fluids. *Galaxies*, 1:216260, December 2013. doi: 10.3390/galaxies1030216
3. Amati L., **Ruggeri A. C.**, Stratta G., Capozziello S., De Laurentis M., Della Valle M., Luongo O. The SKA contribution to GRB cosmology. *Science with the Square Kilometre Array*, Accepted.
4. **Ruggeri A. C.**, Dainotti M. G., Capozziello S. Possible detection of Gamma Ray Bursts in the radio band by the Square Kilometre Array. *Mon. Not. R. Astron. Soc.*, Submitted, 2015

Two internal reports for the *SKA-dish consortium* with the SAM/EIE Companies:

1. Parziale S., **Ruggeri A.C.**, Aurigemma R., Formentin F., De Lorenzi S., “Feed location maintenance concept analysis”
2. Parziale S., **Ruggeri A.C.**, Aurigemma R., De Lorenzi S., “Feed Indexer and PAF de-rotation”



# *Abstract*

Doctor of Philosophy

## **Gamma-Ray Burst observations by the Square Kilometre Array. New perspectives**

by Alan Cosimo Ruggeri

Gamma-Ray Bursts (GRBs) are the most powerful astrophysical source in the universe and have been studied since the '70s. Nevertheless, these objects are still not completely understood and many hypotheses have not been confirmed yet. Past and current observations have been made mostly at gamma, X and optical frequencies. This thesis aims to promote radio GRB observations, in order to thin out a menagerie of different opinions about these sources. In fact, GRBs have been prevalently studied as single cases, more often highlighting their peculiar features than elucidating their common characteristics, and thus leading to fragment the problem. Here the general properties are discussed, so that the attention is moved from the exception to the general case. In other words, this work suggests viewing GRBs in a broad ensemble instead of searching out single cases to explain every peculiarity and as a result increasing the number of possible groups to categorize them.

This work concerns astrophysics, Gamma-Ray Bursts (GRBs) sources, the *Square Kilometre Array* (SKA) radio telescope, radio observations and cosmology. For this reason, it has been divided into three parts, with six chapters in total. Each chapter is a step that leads to the next one following a precise scheme. In the end, all this work highlights both the importance of GRB radio observations and their real feasibility.

The first part concerns the high energies and consists of two chapters. The first chapter contains an overview about GRB state of the art, showing how from the gamma range the GRB afterglow emission reaches the lower frequency range up to the radio band. The second chapter passes from the theory to the practice, where different GRB satellite missions are listed with their gamma payloads, having thus an idea about GRB detection.

The second part is dedicated solely to the radio observations. Chapter 3 regards radio instrumentations and so the SKA is introduced here. This chapter may need some elucidation. My Ph.D. has been carried out between the University and the *Società Aerospaziale Mediterranea S.c.r.l.* company, hence on one hand I have been able to conduct a study about GRBs, on the other hand I have had the opportunity to collaborate with a company in charge of designing the feed indexer of the SKA. This mechanical

component will be assembled with the telescope antenna to select the receivers during the radio observations and details are contained in the chapter.

Since the SKA is a interferometer, chapter 4 regards the radio interferometry. This brief introduction to interferometry helps for the reading of the next chapter, where GRB radio observations are discussed. Chapter 5 concerns principally three works in radio astronomy. Firstly, the first radio observations ever for a very large GRB sample are presented. Secondly, the first considerations deduced from analyses of those first results. Finally, a work of mine currently submitted to the *Monthly Notices of the Royal Astronomical Society* where it is discussed the GRB detection rate for the SKA.

After discussions of observational techniques, detections and possible observational studies in the radio band about GRBs, the third part and its last chapter close the thesis by explaining what advantages a precise and complete study of GRBs can provide for cosmology. Indeed, these sources will be able to shine a light on the various cosmological models created to attempt to explain the expansion of the universe. This last point will be possible only when GRBs are studied proceeding with the precise method suggested here, considering GRBs as complex sources which must be observed and analyzed at all available wavelengths.

## *Acknowledgements*

I acknowledge my supervisor, Prof. Salvatore Capozziello, and the project “Dottorato in Azienda” by Regione Campania.

Thanks to the *Società Aerospaziale Mediterranea S.c.r.l.* (SAM) Company and its Pres. ing Luigi Iavarone. Thanks to my company supervisor, ing. Renato Aurigemma. Acknowledgements also to the *European Industrial Engineering S.r.l.* (EIE - Group) Company for their collaboration with the SAM.

An additional acknowledgement to Prof. Patrick Alan Woudt of the the University of Cape Town (UCT), who allowed me time abroad in South Africa, at the Department of Astronomy of the UCT. Many thanks for his help and our discussions concerning radio astronomy.

Also acknowledgements to the “SKA guys”, in particular Thomas Kusel, Jean Kotze and Niesa Burgher. Thanks to them I was able to go the MeerKAT situ, in the Karoo Desert.



# Contents

<b>Papers related to the PhD</b>	<b>v</b>
<b>Abstract</b>	<b>vii</b>
<b>Acknowledgements</b>	<b>ix</b>
<b>List of Figures</b>	<b>xv</b>
<b>List of Tables</b>	<b>xxi</b>
<b>Physical Constants</b>	<b>xxiii</b>
<b>Symbols</b>	<b>xxv</b>
<b>I Gamma Ray Bursts, the theoretical and observational state of the art</b>	<b>1</b>
<b>1 Theories about GRBs</b>	<b>3</b>
1.1 Introduction . . . . .	3
1.2 GRB parameter dictionary . . . . .	5
1.3 GRBs and their classification . . . . .	6
1.3.1 Short Gamma Ray Bursts . . . . .	7
1.3.2 Long Gamma Ray Bursts . . . . .	9
1.3.3 Intermediate class and other bursts . . . . .	10
1.4 The fireball model . . . . .	10
1.5 Frame and temporal conversions in relativistic ejecta . . . . .	12
1.5.1 Relativistic dynamics . . . . .	14
1.5.2 Photosphere and optical depth . . . . .	15
1.6 Light curve and spectrum . . . . .	17
1.6.1 Photosphere, shocks and thick and thin shells . . . . .	17
1.6.2 Prompt . . . . .	20
1.6.3 Afterglow . . . . .	24
1.7 Jets . . . . .	35
1.8 Gamma band vs Radio band . . . . .	37

---

<b>2 Satellite missions</b>	<b>39</b>
2.1 ULYSSES . . . . .	40
2.1.1 Hard X-ray detectors . . . . .	40
2.1.2 Soft X-ray detectors . . . . .	40
2.2 INTErnational Gamma-Ray Astrophysics Laboratory - INTEGRAL . . . . .	41
2.2.1 SPectrometer on INTEGRAL (SPI) . . . . .	41
2.2.2 Imager on Board the Integral Satellite (IBIS) . . . . .	41
2.2.3 Joint European X-Ray Monitor (JEM-X) . . . . .	41
2.2.4 Optical Monitoring Camera (OMC) . . . . .	42
2.3 Compton Gamma Ray Observatory . . . . .	43
2.3.1 Burst And Transient Source Experiment (BATSE) . . . . .	44
2.3.2 Imaging Compton Telescope (COMPTEL) . . . . .	44
2.3.3 Energetic Gamma Ray Experiment Telescope (EGRET) . . . . .	44
2.3.4 Oriented Scintillation Spectrometer Experiment (OSSE) . . . . .	45
2.4 BeppoSAX . . . . .	45
2.4.1 Low Energy Concentrator Spectrometer (LECS) . . . . .	46
2.4.2 Medium Energy Concentrator Spectrometers (MECS) . . . . .	46
2.4.3 High Pressure Gas Scintillation Proportional Counter (HPGSP) . . . . .	47
2.4.4 Phoswich Detector System (PDS) . . . . .	47
2.4.5 Wide Field Cameras (WFCs) . . . . .	48
2.5 High Energy Transient Explorer - HETE-2 . . . . .	49
2.5.1 Soft X-ray Camera (SXC) . . . . .	50
2.5.2 Wide-field X-ray Monitor (WXM) . . . . .	50
2.5.3 French Gamma Telescope (FREGATE) . . . . .	50
2.5.4 Results . . . . .	51
2.6 Swift . . . . .	52
2.6.1 Burst Alert Telescope (BAT) . . . . .	52
2.6.2 X-ray Telescope (XRT) . . . . .	53
2.6.3 Ultraviolet/Optical Telescope (UVOT) . . . . .	54
2.7 “Astrorivelatore Gamma a Immagini LEggero” - AGILE . . . . .	54
2.7.1 Gamma-Ray Imaging Detector (GRID) . . . . .	54
2.7.2 Hard X-ray Imaging Detector (Super-AGILE) . . . . .	55
2.8 Fermi . . . . .	55
2.8.1 Large Area Telescope (LAT) . . . . .	56
2.8.2 GLAST Burst Monitor (GBM) . . . . .	56
<b>II Gamma Ray Bursts by the Square Kilometre Array</b>	<b>59</b>
<b>3 The Square Kilometre Array</b>	<b>61</b>
3.1 The SKA - Overview . . . . .	61
3.2 The collaboration with the SAM company . . . . .	65
3.3 The feed indexer - Up and down configuration . . . . .	65
3.4 PAF and SPF feed indexer and PAF de-rotation . . . . .	68
3.5 Feed indexer deformation range . . . . .	71
3.6 SKA scientific books . . . . .	72

<b>4 Observational techniques for radio detections</b>	<b>73</b>
4.1 Radio interferometry . . . . .	73
4.1.1 Form of the observed electric field and synthesis imaging . . . . .	73
Measurements taken within a plane . . . . .	76
Sources in a small region of sky . . . . .	76
4.2 Signal acquisition in radio interferometry . . . . .	78
4.2.1 Frequency conversion . . . . .	81
4.2.2 The $u-v$ plane . . . . .	83
4.2.3 Antenna placing and synthesis arrays . . . . .	86
4.3 Sensitivity and angular resolution . . . . .	87
4.4 Convolution and deconvolution . . . . .	90
<b>5 GRB radio observations</b>	<b>93</b>
5.1 Studies of GRBs in radio band . . . . .	94
5.2 Two possible GRB populations by radio afterglows . . . . .	102
5.3 A statistics about possible observable GRBs by the SKA . . . . .	106
5.3.1 The sky above the SKA and its shadow cone . . . . .	106
5.3.2 Sample selection . . . . .	107
5.3.3 Serendipitous detections of radio GRBs by the SKA . . . . .	111
5.4 Measure unit conversions and Spectrum Energy Distribution . . . . .	117
5.5 Bolometric-equivalent energy and $k$ -correction . . . . .	118
5.6 Discussions . . . . .	121
5.7 Appendix of the chapter . . . . .	124
<b>III GRBs and Cosmology</b>	<b>131</b>
<b>6 Cosmology with GRBs</b>	<b>133</b>
6.1 A short discussion of cosmology	
Between theories and observations . . . . .	133
6.2 Cosmography . . . . .	136
6.3 GRBs for cosmological constraints . . . . .	139
<b>7 Conclusions</b>	<b>141</b>
<b>A Long table 5.4</b>	<b>143</b>
<b>Bibliography</b>	<b>301</b>
<b>Acknowledgements II</b>	<b>325</b>



# List of Figures

1.1	Histogram taken by [1] which shows GRB durations measured by BATSE.	7
1.2	The short bursts (squares) appears to be harder than the long ones (circles) [2].	8
1.3	Swift/XRT light curve of GRB 060428A, which shows all the phases seen in early GRB X-ray afterglows (but with an unusual dual-slope energy injection phase) [3].	8
1.4	Illustration of the emission from spherical relativistic shells in the source frame and the relativistic time delay leading to the relation between source frame and observer time. [4]	13
1.5	This spheroid is the locus of the points in which the radiation has the same time. Photons isotropically leave from the source $S$ and with $\Gamma = (1 - \beta^2)^{-1/2} \gg 1$ make the surface in the figure after an observer time $t$ . Most of radiation arrives from the observer direction (“OBS”) side and it is strongly Doppler-boosted inside the light cone $1/\Gamma$ . The line of sight parallel and perpendicular apparent axes of the ellipsoid are $r_{\perp} \sim \Gamma ct$ and $r_{\parallel} \sim 2\Gamma ct$ . [4]	14
1.6	A schematic behaviour of the Lorentz factor during the jet. Along the x-axes the radius where the saturation radius $r_s$ , the photospheric radius $r_{\text{ph}}$ , the internal shock (or magnetic dissipation) radius $r_{\text{is}}$ and the external shock $r_{\text{ext}}$ appear as the outflow runs. Thermal $\gamma$ -rays are produced by photosphere, the internal shock and dissipation region produce the non-thermal $\gamma$ -rays. The afterglow is finally produced by the external shock region [4].	19
1.7	Spectrum fit of 1B 911127. The low-energy spectral index is $-0.968 \pm 0.022$ , while it is $-2.427 \pm 0.07$ in the high-energy, after the energy break at $149.5 \pm 0.07$ keV [5].	21
1.8	Synchrotron spectrum of a relativistic shock with a power-law electron distribution. In the upper sketch, the fast cooling is shown, which is expected at early times ( $t < t_0$ ). The spectrum consists of four segments, identified as A, B, C, and D. Self-absorption is important below $\nu_a$ . The frequencies, $\nu_m$ , $\nu_c$ , and $\nu_a$ , decrease with time as indicated; the scalings above the arrows correspond to an adiabatic evolution, and the scalings below, in square brackets, correspond to a fully radiative evolution. Below, the slow cooling, which is expected at late times ( $t > t_0$ ). The evolution is always adiabatic. The four segments are identified as E, F, G, and H [6].	29

1.9	The synchrotron light curve plot is ignoring the self-absorption. In the upper panel the high-frequency case ( $\nu > \nu_0$ ) is represented. The four segments that are separated by the critical times, $t_c$ , $t_m$ , and $t_0$ , correspond to the spectral segments in 1.8 with the same labels (B, C, D, and H). The time dependence of the observed flux are reported on the slopes. The values within square brackets correspond to the radiative evolution (which is restricted to $t < t_0$ ), whereas the other values correspond to adiabatic evolution. In the lower panel the low-frequency case ( $\nu < \nu_0$ ). Credit by [6]. . . . .	33
2.1	Here two sketches of Hard X-ray (left) and Soft X-ray detectors (right) are showed [7]. . . . .	40
2.2	The figures show, on the left, the Imager IBIS in its whole scheme. On the right a detail on ISGRI. Figures taken from [8]. . . . .	42
2.3	The CGRO satellite with its instruments in highlight [9]. . . . .	43
2.4	The figures show, on the left, the BeppoSAX satellite for whole. On the right, a back-zoom of the payload [10, 11]. . . . .	46
2.5	Sketch of a WFC. In the right part of the picture the coded-mask can be seen, while after 70 cm the described detector is shown. Between the detector and the mask there is a stainless steel structure to detect only X-ray photons. . . . .	49
2.6	A single SXC unit consists of a pair of 2048x4096 CCDs (15 $\mu\text{m}$ pixel size) at 10 cm behind a finely-ruled mask. The CCDs are oriented so that their columns are parallel to the mask elements. The CCDs are read out in continuous-clocking, row-summing mode, so they operate essentially as one-dimensional images. . . . .	51
2.7	An image of the two XWM detectors [12]. . . . .	52
2.8	An image of the BAT [13]. . . . .	53
3.1	Parameters for comparable telescopes, from the table 1 of [14]. . . . .	64
3.2	An artist's impression of a MeerKAT antenna to show the FI placed on the frame between the reflector and the sub-reflector. On the FI are also placed some feeds. Credit by the SKA Africa. . . . .	66
3.3	Four sketches about the feed up and feed down configurations. Here it is easy to see the feed positions on the dishes and elevation motions. These sketches are taken from an internal company report of the SAM and the EIE-Group companies about dish-antenna maintenance. . . . .	67
3.4	This figure reports a sketch of an parabolic and elliptic sectors. These sectors are bi-dimensional cuts of the reflector and the sub-reflector of the SKATEL.DSH.MGTCSIROTS004 . . . . .	68
3.5	Here the feed up and feed down configurations with SPF installed. These figures are taken from an internal report of the SAM and the EIE-Group companies and sent to the SKA-dish consortium. . . . .	69
3.6	Here the feed up and feed down configurations with PAFs installed. These figures are taken from an internal report of the SAM and the EIE-Group companies and sent to the SKA-dish consortium. . . . .	70
3.7	In the left panel, a sketch of the SPSs and SKA Mid FI. In the right panel, PAFs and SKA Survey FI. A possible platform and an dish-antenna-interface structure are sketched below the FIs . . . . .	71

3.8	A draft exploded diagram of the Band 2 PAF, that shows gears of the de-rotating system too. . . . .	71
3.9	In the upper row, three sketches of the maximum displacement of the FI front at an elevation of $30^\circ$ . In lower row, the maximum global displacement. The color scale used indicates blue as the smaller displacement. . .	72
4.1	The source is located at $\vec{R}$ and causes the electromagnetic wave $\vec{E}(\vec{R}, t)$ . It is detected by an astronomer at $\vec{r}$ [15]. . . . .	74
4.2	This figure shows the phase center tracking (even called <i>phase reference position</i> ), to derive the interferometer response to a source, here represented by contours [16]. . . . .	77
4.3	A simplified block diagram of an interferometer with two elements [16]. . .	79
4.4	Sketch of an interferometer system, with frequency conversion instruments. Amplifiers and filters are not drawn in the diagram [16]. . . . .	82
4.5	The $(u, v, w)$ and $(l, m, n)$ coordinate systems used respectively to express the interferometer baselines and the source brightness distribution [16]. . .	84
4.6	During the Earth's rotation, any baseline vector $\vec{b}$ traces out a circular locus in a plane orthogonal to the rotation axis (coincident with the polar axis, $\delta = 90^\circ$ in celestial declination). As for a baseline vector totally in the East-West direction, $\vec{b}$ is perpendicular to the rotation axis [16]. . .	84
4.7	The North spherical cap where the source lies, with its tangent plane on the North pole and the source projection onto this last plane. The spacing-vector loci for an East-West baseline array are shown too, it has the origin of the $(u, v, w)$ system, where $w$ have the direction of the North pole [16]. . . . .	85
4.8	In the a sketch there is the VLA configuration, with 27 antennas. In the b sketch are shown transfer functions at four declinations. At $\delta = 0^\circ$ and $45^\circ$ for a time of $\pm 4\text{h}$ ; $\delta = -30^\circ$ for $\pm 3\text{h}$ ; finally, a snapshot of $\pm 5\text{m}$ pointing to the Zenith. Credit by [16]. . . . .	88
4.9	Visibility depending on the $u$ - $v$ distances. . . . .	89
4.10	A visual product of visibility and imaging. . . . .	90
4.11	A visual product of visibility and imaging [17]. . . . .	91
5.1	$k$ -corrected radio spectral luminosities at 8.5 GHz. The black circles are radio-detected afterglows, whereas the red triangles are the non-detected $3\sigma$ luminosity upper limits, with respect to the rest-frame time. The luminosity curve for the average cosmological burst varies over a small range, but there are also a number of low-luminosity events [18]. . . . .	95
5.2	The first panel shows the radio light curves at 8.5 GHz for the LGRBs in the rest-frame time. The red thick solid line represents the mean light curve. The pink shaded area represents the 75% confidence band. The second panel shows the same plot for time but in the observer-time frame [18]. . . . .	95
5.3	In the first panel, a histogram of the fluence distribution for sample of 304 used by Chandra and Frail. In the second panel they reported the fluence distribution of the radio-detected sample (hatched histogram) and the non-detected sample (filled histogram) [18]. . . . .	97

5.4	These sketches show the distributions of the GRBs detected by <i>Swift</i> , taken from the “Swift GRB Table and Lookup” website on the 13th February 2015. In the top, there are 911 detections of GRBs, in the middle panel 80 SGRBs (duration $\leq$ 2 seconds, as option required to the web site) and in the bottom 805 LGRBs (with duration $>$ 2 seconds). Here, detections where the fluences in the channel 15 - 150 keV are available.	98
5.5	Light curves of the radio density for a GRB at different frequencies. Apart from the redshift and the circumburst density with their values reported in the top of the plot, the other fixed parameters are: $E_{\text{KE,iso}} = 10^{53}$ erg; $\theta_j = 0.2$ rad; $\epsilon_e = 0.1$ ; $\epsilon_B = 1\%$ and $p = 2.2$ [18–20]. The light curves are generated with only a forward shock component. Credit by [18].	101
5.6	In the top left panel, the density varies and the parameters are fixed as follows: $z = 3$ ; $E_{\text{KE,iso}} = 10^{53}$ erg; $\theta_j = 0.2$ rad; $\epsilon_e = 0.1$ ; $\epsilon_B = 1\%$ and $p = 2.2$ . In the top right panel, the magnetic energy density varies and the parameters are fixed in this way: $z = 3$ ; $n = 10 \text{ cm}^{-3}$ $E_{\text{KE,iso}} = 10^{53}$ erg; $\theta_j = 0.2$ rad; $\epsilon_e = 0.1$ and $p = 2.2$ . In bottom left panel, the kinetic energy varies and the parameters are fixed as follows: $z = 3$ ; $n = 10 \text{ cm}^{-3}$ ; $\theta_j = 0.2$ rad; $\epsilon_e = 0.1$ ; $\epsilon_B = 1\%$ and $p = 2.2$ . In the bottom right panel, the redshift varies and the parameters are fixed as follows: $n = 10 \text{ cm}^{-3}$ ; $E_{\text{KE,iso}} = 10^{53}$ erg; $\theta_j = 0.2$ rad; $\epsilon_e = 0.1$ ; $\epsilon_B = 1\%$ and $p = 2.2$ . Credit by [18].	103
5.7	Light curves of some LGRBs and corresponding redshift, as reported in the inner panel. The three dashed lines indicate the EVLA $3\sigma$ sensitivity limits with an observational integration time of 1 hour [18].	104
5.8	In the first and second panels, the synthetic model of the 8.5 GHz flux density compared to the corresponding <i>R</i> -band optical and 1 keV X-ray flux densities. In the third panel, the comparison of the flux densities between the optical and X-ray frequencies. The model is the same as that used in figure 5.5 [18].	104
5.9	Distribution of redshifts for GRBs where the $z$ was known. Data taken from table 1 of [18], plotted by [21] distinguishing between radio-bright (in red) and radio-faint (in blue) GRBs. No difference is highlighted.	105
5.10	In the upper panel, the 2D a sketch of the Earth, with the polar axes, the South African (mean) antenna latitude $O$ , the horizon line (in blue) and the lowest angle-limit line (red) for the antenna. In the lower panel, the rotation simulates the Earth rotation and a shadow-cone is traced by the red line.	108
5.11	In this pie chart, the percentages are shown, out of 7516 distinct GRBs, occurring from the 18th January 1990 to the 12th May 2014, for GRANAT, Ulysses, CGRO, Konus/Wind, BeppoSAX, HETE-2, INTEGRAL, <i>Swift</i> , Agile and <i>Fermi</i> missions. As it is possible to see in the colour-key-box, I have considered single events for different missions/instruments, as well as same GRBs observed simultaneously by two or three satellite missions (or instruments) in yellow and pearl grey, respectively. To summarize: 58 GRBs observed by GRANAT (1% of 7516), 1885 by CGRO/BATSE (nt) (27%), 2063 by CGRO/BATSE (t) (25%), 153 by Konus/Wind (2%), 401 by BeppoSAX (5%), 70 by HETE-2 (< 1%), 78 by INTEGRAL (1%), 659 by <i>Swift</i> (9%), 26 by Agile (< 1%), 1091 by <i>Fermi</i> (15%), total GRBs observed in a pair and in a triple have been 979 (13%) and 52 (< 1%), respectively. See table 5.5 for the sake of clarity.	113

- 5.12 In this figure I have considered different missions, instruments and catalogues. I report GRBs observed by GRANAT, Ulysses, CGRO/BATSE, CGRO/COMPTON, Konus/Wind, BeppoSAX, HETE-2, INTEGRAL, *Swift*, Agile and *Fermi*. I also plot the non-triggered GRBs by CGRO/-BATSE. In the Y-axis the (progressive) number of GRBs detected by a mission/instrument is reported; in the X-axis the time of the detection expressed in years. Detections since 18th January 1990 done by GRANAT until 12th May 2014 done by *Fermi* and *Swift* are here plotted. . . . . 113
- 5.13 Polar plots show 6508 points out of 7516, i.e. GRBs with celestial declination  $< 50^\circ$  (dashed circle), observed by GRANAT (coral), CGRO/BATSE (triggered and non-triggered GRBs are dark grey and violet, respectively), Konus/Wind (yellow-green), BeppoSAX (blue), HETE-2 (cyan), INTEGRAL (purple), *Swift* (red), Agile (lime green) and *Fermi* (orange). The first plot shows the north celestial hemisphere that SKA can observe, i.e. the “central hole” delimited by the black dashed circle is due to the shadow cone, where it will not be able to observe; the second plot shows the south celestial hemisphere. RA and DEC are expressed in J2000 coordinates. For the sake of clarity, I have avoided plotting the same sources in different catalogues repeatedly, e.g. Ulysses sources do not appear among these points because they are already plotted with triggered CGRO/BATSE GRBs. . . . . 114
- 5.14 Plot of fluxes reported in table 5.7. The points are plotted only if the row shows four values at the various frequencies (19.6 EH $\zeta$ , 1.3 EH $\zeta$ ,  $4.56 \cdot 10^2$  TH $\zeta$ , 8.46 GHz). . . . . 123



# List of Tables

1.1	Temporal index $\alpha$ and spectral index $\beta$ in various afterglow models, the convention $F_\nu \propto t^\alpha \nu^\beta$ is adopted, from [6, 22–25]. The assumption $\nu_a < \min[\nu_m, \nu_c]$ is made. (Under certain conditions, e.g. for the wind fast cooling case in some limited regime, the higher $\nu_a$ case is relevant <sup>289</sup> , so that the values collected here are no longer valid). The jet model applies for the sideways expanding phase, which is valid for both ISM and wind cases and is usually in the slow cooling regime [26]. . . . .	32
1.2	Temporal exponents of the peak frequency, the maximum flux, the cooling frequency and the flux at a given bandwidth (respectively, $\nu_m$ , $F_{\nu_m}$ , $\nu_c$ , $F_\nu$ ) for the forward (f) and reverse (r) shocks. They are calculated in the adiabatic regime $\nu_m < \nu < \nu_c$ ( $F_\nu \propto F_{\nu_m}(\nu_m/\nu)^\beta \propto t^{-\alpha}\nu^{-\beta}$ , where $\beta = (p - 1)/2$ ), and in the cooling regime $\nu_c < \nu_m < \nu$ ( $F_\nu \propto (\nu_c/\nu_m)^{1/2}(\nu_m/\nu)^\beta \propto t^{-\alpha}\nu^{-\beta}$ where $\beta = p/2$ ). For $s = 1$ this gives the usual (i.e. without “refreshment”) forward and reverse shock behaviour [4, 27, 28]. . . . .	34
2.1	Some specifications of IBIS [29]. . . . .	42
2.2	Some specifications of the JEM-X [30]. . . . .	42
2.3	Some specifications of the OMC [31]. . . . .	43
2.4	Summary of the CGRO detector characteristics. Here it is also indicated the detection position precision. This table has been taken by the website of Astrophysics Science Division at NASA/GSFC [32]. . . . .	45
2.5	In the FoV, “37’ diameter circular” is equivalent to say 0.299 square degrees. The FWHM is the Full Width at Half Maximum of the total Gaussian signal. The energies are the central values of the two band windows of the range 0.1 - 10.0 keV. This table is part of the original table 1 in [33]. . . . .	47
2.6	The FoV value reported in the table is equivalent to 0.685 square degrees. The way to write $r_{50}$ and $r_{80}$ indicates the angular resolution values at radii encircling 50% and 80% of the total signal. The angular resolution energies are the central values of the three band windows of the energy range [34]. . . . .	47
2.7	Some PDS characteristics, extracted from table 1 of [35]. . . . .	48
2.8	Some WFC characteristics, extracted from table 1 of [36]. * $1mCrab \approx 2.410^{11}\text{ergs}^{-1}\text{cm}^2$ in the 210 keV X-ray band. . . . .	49
2.9	Some SXC characteristics [37]. . . . .	50
2.10	Some WXM characteristics [38]. . . . .	51
2.11	Some WXM characteristics [38]. . . . .	51
2.12	Some BAT characteristics [13]. . . . .	53

2.13 Some BAT characteristics [39]. . . . .	53
2.14 Some specifications of UVOT [40]. . . . .	54
2.15 Some specifications of GRID, taken from tables 2 and 3 in [41]. . . . .	55
2.16 Some specifications of the Super-Agile detector, taken from table 3 in [41]. Some value of them (specially if not written in the text) could be better then written only here. The reason is that the original table is early to the mission of 3 years, so the real instrumental specifications can be better. However reported information is good for this thesis and its aims. . . . .	55
2.17 Some specifications of the LAT. . . . .	56
2.18 Some specifications of the GBM. LED is Low-Energy Detector; HED is High-Energy Detector. Information taken from [42]. The symbol “-” indicates that the values have to be estimated yet. . . . .	57
 3.1 The planned FoVs at the SKA observational frequencies. See [14] for details.	65
3.2 Physical and electronic characteristics of the PAFs and SPF are summarized. The symbol * in the 3, 4, and 5 Bands simply indicates that 65 kg is the total weight of these three feeds. . . . .	68
 5.1 $P$ values for the K-S test for the radio detected vs non-detected GRB sample by [18]. . . . .	100
5.2 $R$ -index values between different GRB parameters [18]. . . . .	100
5.3 The median properties about radio-faint and -bright GRBs. $p$ is the value of the K-S test. $F_X^{11\text{hr}}$ and $F_R^{11\text{hr}}$ are respectively the flux at 0.3-10 keV and the flux density at the optical $R$ -band [21]. . . . .	105
5.4 This table is a collection and merging of all catalogues mentioned in this paper. In the columns, respectively: RA and DEC in degrees; detection year, month and day; name of the list related to a satellite; source name. For more details see the appendix. The full table is attached in appendix A. . . . .	111
5.5 Number of GRBs detected by different instruments of catalogues used and their combinations. GRA = GRANAT; BT = BATSE triggered; BNT = BATSE non-triggered; COMP = COMPTEL; Uly = Ulysses; KW = Knous/Wind; BeS = BeppoSAX; Agi = Agile; Fer = <i>Fermi</i> ; INT = INTEGRAL; HET = HETE-2; Swi = <i>Swift</i> . . . . .	112
5.6 Below, values of the angular coefficients of figure 5.12 are reported. . . . .	117
5.7 This table is a fusion between tables 1 and 4 from [18], but the orginal $S_{15-150}$ fluence, the R-band optical and the 4.86 GHz radio flux densities have been converted into $\text{erg cm}^{-2} \text{ s}^{-1}$ units, as indicated in section 5.4. The first three columns indicate the GRB name, right ascension and celestial declination. Forth, fifth and sixth columns with Y or N indicate wheter a GRB has a signal in the X, optical and radio band. The last five columns are the fluxes in the 15 - 150 keV and 0.3 - 10 keV energy ranges, at the optical R-band, at the 4.86 GHz radio band, redshift and equivalent isotropic bolometric energy. The apex “11h” indicates the value of the flux at 11 hour since the burst. The symbol “-” indicates not defined values. . . . .	127

# Physical Constants

Boltzmann constant	$k_B$	=	$1.380\ 648\ 8(13) \times 10^{-16}$ erg K <sup>-1</sup>
Electric charge	$e$	=	$-1.602\ 176\ 565(35) \times 10^{-19}$ C
Electron mass	$m_e$	=	$0.510\ 998\ 910(13)$ MeV/c <sup>2</sup>
Planck constant	$h$	=	$4.135\ 667\ 516(91) \times 10^{-15}$ eV s
Proton mass	$m_p$	=	$938.272\ 046(21)$ MeV/c <sup>2</sup>
Speed of Light	$c$	=	$2.997\ 924\ 58 \times 10^8$ m s <sup>-1</sup> (exact)



# Symbols

$S$	Fluence	$\text{erg cm}^{-2}$
$F$	Flux	$\text{erg cm}^{-2} \text{ s}^{-1}$
$F_\nu$	Flux Density	$\text{W m}^{-2} \text{ Hz}^{-1}$
$L$	Luminosity	$\text{erg s}^{-1} \text{ Hz}^{-1}$
$B$	Magnetic field	$1 \text{ G} = 10^{-4} \text{ kg C}^{-1} \text{ s}^{-1}$
$P$	Power	$\text{erg s}^{-1}$



*Dedicated to my parents. Thanks for all your support.*



**Part I**

**Gamma Ray Bursts,  
the theoretical and observational  
state of the art**



# Chapter 1

## Theories about GRBs

### 1.1 Introduction

Gamma Ray Bursts (GRBs) are the shortest and most powerful astrophysical events in the whole universe. They can emit an immense amount of electromagnetic energy within a few seconds, but gamma emission can last even for hours. This energy can reach magnitudes of  $10^{54}$  erg which roughly corresponds to the luminosity of the visible Universe in 1 second. In fact, the Sun has a luminosity of  $1L_{\odot} \sim 10^{33}$  erg/s and in a galaxy there are  $\sim 10^{12}$  stars. Because the number of galaxies in the universe has a magnitude of  $10^9$ , multiplying all these magnitude, the result is  $\sim 10^{54}$  erg/s which is the luminosity of the known universe. Another example is that the electromagnetic energy emitted in a few seconds from a GRB is comparable to the quantity of energy that the Sun emits in about ten billion years.

For these outstanding characteristics, GRBs were studied fervently since news of them began to circulate. Unfortunately, serious study did not coincide with their accidental discovery and astrophysical studies started several years later. Indeed, the *Vela* satellite detected the first GRB in 1963 during the Cold War, but it was a military mission to monitor nuclear tests on the Soviet Union, hence its data were classified. Data became available after the US military veto was dismissed and the official announcement occurred in 1974 with [43].

Since that moment, high-energy observations opened a new window and technology has started to improve in this sector. Today, despite the fact that GRBs are the brightest sources in the universe, there are many unclear aspects that must be understood. There are a multitude of theories and models that try to explain the physics of these phenomena, but none of these has been confirmed to be the definitive model. The principle issue is that GRB spectra are very different from each other and this makes them

difficult to study, because different spectra correspond to various physical combinations and complexities. They are cosmological objects and occur at any point in the universe, namely at any redshift, and for this reason a strong selection effect plays an important rule in discussions about GRB. Furthermore, GRB observations are not simple because their emission must be re-scaled considering relativistic effects, they are random, their progenitors have not been identified yet with certainty, and many other aspects.

In general, GRBs are extremely peculiar sources, thus some sporadic cases are sometimes considered as prototypes for a class, but GRBs are currently divided into two broad classes, long and short bursts, and the subdivision is based on a temporal edge. If the gamma peak lasts more than 2 seconds then the GRB belongs to long bursts, otherwise it belongs to short bursts. It is though that long and short bursts are associated to different progenitors.

Since the variety of light curves and of spectra is large, many efforts have been concentrating on a possible standardization which is focused on the phenomenology of the GRB emission rather than on explanations provided by theoretical models. These attempts of a standardization are principally centered on high energies (i.e.,  $\gamma$ -rays, X-rays), even though some recent studies are properly extending the frequency range. The general aim is to discover a common behaviour for a little group of GRBs which follows precise and sharp characteristics in a well-defined class.

The only way to categorize objects so different from each other is to analyze them in all respects, in order to find common characteristics. In other words, it is necessary to observe GRBs at many spectral bands to consider their complete envelopes in a large energy. To study in detail a big number of Spectral Energy Distributions (SEDs) could allow scientists to highlight emission processes that are only shown in very large spectral ranges.

The purpose of this work is to delineate a path towards radio GRB observations. In this sense, chapter 1 summarizes the state of art concerning GRBs, starting with a generic introduction about these sources, reporting then the more substantiated model that describes the emission mechanism, subsequently focusing attention on spectra and light curves highlighting how the GRB emission evolves across frequencies (from gamma to lower energies), and finally relays some brief considerations regarding radio and gamma band observations.

After this GRB overview, the topic moves to observational instruments. Chapter 2 reports almost all of the satellite missions dedicated to GRB detection. For each mission I have listed gamma instrumentations of the satellite payload and their features. From gamma instruments the discussion arrives at radio instruments. Chapter 3 speaks about the Square Kilometre Array, the radio telescope which will improve the radio GRB detections, thanks to its sensitivity and angular resolution. Here, the design of the *feed*

*indexer* for this radio telescope is also discussed. This is a rotating platform where the radio receivers will be placed and I am collaborating with the *Società Aerospaziale Mediterranea* to design it.

The focus moves from the radio instrument to observational techniques, and so chapter 4 introduces the radio interferometry. After some basics of radio interferometry, the topic proceeds towards radio observations for GRBs in chapter 5. This chapter provides basics for the approach to the GRB radio studies. It reports the first studies about a large sample of GRBs observed in radio band and the first important considerations deduced from those analyses. The chapter closes with the potentiality of the Square Kilometre Array to detect and observe GRBs and discussions about this.

In the end, chapter 6, after a brief excursus regarding cosmology, focuses on cosmography and on how GRBs can improve cosmological models, adding data in the acceleration transition epoch.

## 1.2 GRB parameter dictionary

Before of the specific discussions about GRBs, this brief section reports a short vade-mecum. It gathers some parameters/terms generally used for GRBs. It is inserted essentially for convenient and quick checks.

$L_{\text{bol}}$ : is the GRB luminosity. It is equal to:

$$L_{\text{bol}} = 4\pi d_L^2 F_{\text{bol}}; \quad (1.1)$$

$d_L$ : the luminosity distance is usually

$$d_L(z) = \frac{c}{H_0} (1+z) \int_0^z \frac{dz'}{\sqrt{\Omega_M(1+z')^3 + \Omega_k(1+z')^2 + \Omega_\Lambda}}, \quad (1.2)$$

where  $\Omega_M + \Omega_k + \Omega_\Lambda = 1$  and these addends are the cosmological parameters;

$F_{\text{bol}}$ : bolometric flux;

$P$ : radiation power;

$P_\nu$ : power spectral;

$E_{\text{peak}}$  or  $E_p$ : the peak energy;

$E_{\text{iso}}^{\text{bol}}$ : the equivalent isotropic (covering  $4\pi$  sterad) bolometric energy;

$E_\gamma$ : the GRB average energy integrated in the prompt emission;

$E_{\gamma, \text{iso}}$  is the GRB average energy integrated in the prompt emission, covering  $4\pi$  sterad;

$\tau_{\text{lag}}$ : the detecting time-frame between the arrival of the high energy photons and low energy ones [44];

$T_{90}$ : defined as the time interval over which a burst emits from 5% of its total measured counts to 95% [45];

$T_{50}$ : is the time interval in which the integrated counts from the burst increases from 25% to 75% of the total counts [1];

$\theta_j$ : the jet opening angle;

$t_j$ : jet break (time), the time when the relativistic collimation angle of the bulk-emission beam spreads sideways, out of the jet edge. This quantity and  $\theta_j$  are related to each other;

$\Gamma$ : it generally indicates the bulk Lorentz factor, but subscripts/apexes can characterize it;

$\gamma$ : it generally indicates the *non-bulk* Lorentz factor, e.g. for particles. Some subscript/apex can characterize it;

### 1.3 GRBs and their classification

GRBs have been separated in two broad classes after the acquisitions of the BATSE/C-GRO detector and the result of this distinction is shown in 1.1. The border between *short* GRBs (SGRBs) and *long* GRBs (LGRBs) is at  $T_{90} = 2\text{s}$  [46, 47]. As shown in figure 1.2, because initial data have showed SGRBs typically harder<sup>1</sup> than LGRBs this has leaded to think that these two group were activated by two different types of trigger. However, by additional analyses, it was seen that both LGRBs and SGRBs have similar behaviours, therefore they could have analogous origin, but with little differences. Indeed, the most discussed central engine envisages a central black hole (BH) with a surrounding torus produced by two different ways for each type of bursts, either a massive stellar core collapse for LGRBs, or a (observationally more uncertain) merger of NS-NS/BH-NS binaries for SGRBs. In both cases, the BH could be preceded by a temporary massive, highly magnetized NS [4].

There are three kinds of fuels from which energy can be drown: gravitational binding energy of the torus, the angular momentum of the BH and the magnetic energy stored

---

<sup>1</sup>The *hardness ratio* is defined as the ratio between the fluences (namely the flux integrated over time) of two channels of BATSE,  $\text{HR} = F_3/F_2$ . The channel 3 was 100-300 keV, the channel 2 was 50-100 keV [2].

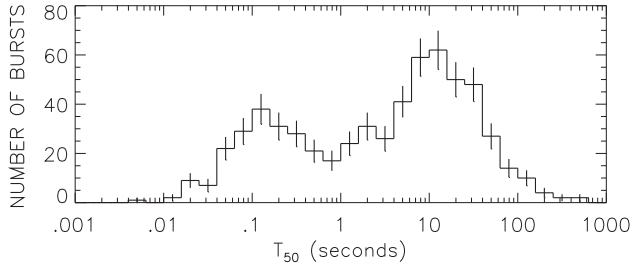


FIGURE 1.1: Histogram taken by [1] which shows GRB durations measured by BATSE.

during the collapse (basically, an energy exchange from the previous two). Apart from the third case, there are two main ways to extract energy from the accretion disk and the BH spin. There are the neutrino-drive wind [48–52] and the Blandford-Znajek mechanism [53]. These ways produce an optically thick  $e_{\pm}$  jet or fireball, but the Blandford-Znajek mechanism is dynamically Poynting-dominated, namely dominated by strong magnetic fields threading the BH [54–57].

A gamma,  $e^{\pm}$  fireball is expected in every model as a product of the transient core collapse or merging. These cataclysmic events could lead to important build-up of the magnetic stress [58]. When magnetohydrodynamic fields with  $B \lesssim 10^{15}$  Gauss are mixed with relativistic electrons and positrons, there are the conditions driving to a highly relativistic expansion with  $\Gamma \gg 1$ . Some fraction of baryons is very likely present in the fireball, but it is difficult to quantify without 3D magnetohydrodynamic simulations which can address baryon entrainment. However, if a GRB is arisen by a massive star, the expectation is that the fireball is collimated along the rotation axis, because of the transverse pressure of the stellar accretion fast-rotating disk.

The *Swift* satellite is increasing GRB data by the XRT and UVOT instruments. Independently from the short and long classes, most of GRB X-ray emissions show light curves like in figure 1.3. The X-ray afterglow begins with a steep time decay, just after the end of prompt  $\gamma$ -ray emission, then it continues with a much shallower time decay associated to X-ray flares lasting for  $\sim 1000$  s, followed by two different slope trends (pre-Swift era, they were roughly  $-1.2$  and  $-1.7$  [59, 60]). Sometimes, in the last part the slope changes again, ascribed to beaming due to a finite jet opening angle.

### 1.3.1 Short Gamma Ray Bursts

This class of bursts were re-considered after the detection of their optical counterpart by the *Swift* and the HETE-2 missions.

SGRBs are typically observed in host galaxies with a wide range of star formation properties, included those with a low formation rate. These hosts have properties substantially

different than galaxies hosting LGRBs [61, 62], and this lead to think that these classes have two different origins. Moreover, no evidence for simultaneous SNe has been found around SGRBs [63], on the contrary for long bursts. This reinforces the interpretation that SGRBs are generated from an old population of stars, probably due to mergers of compact binaries as mentioned above [63].

With respect to LGRBs, the short bursts generally have a lower isotropic-equivalent luminosity and total energy output ( $E_{\text{iso}} \sim 10^{50}$  erg). Their afterglows are faint and, in the few cases where a jet break has been measured, the jet opening angle seems to be wider than angle in LGRBs,  $\theta_j \sim 5^\circ - 25^\circ$  [64]. In about 25% of SGRBs, a longer ( $\sim 100$  s) light curve tail is discovered. It has a spectrum softer than the initial episode [65]. This is not in accordance with numerical simulations of NS-NS or NS-BH mergers, since they suggest that the disk of disrupted matter should increase in at most a few

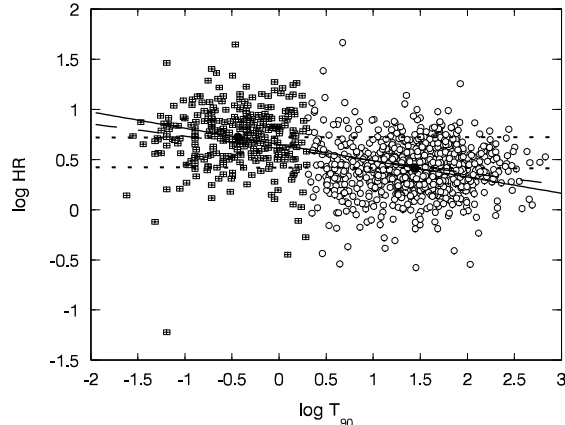


FIGURE 1.2: The short bursts (squares) appears to be harder than the long ones (circles) [2].

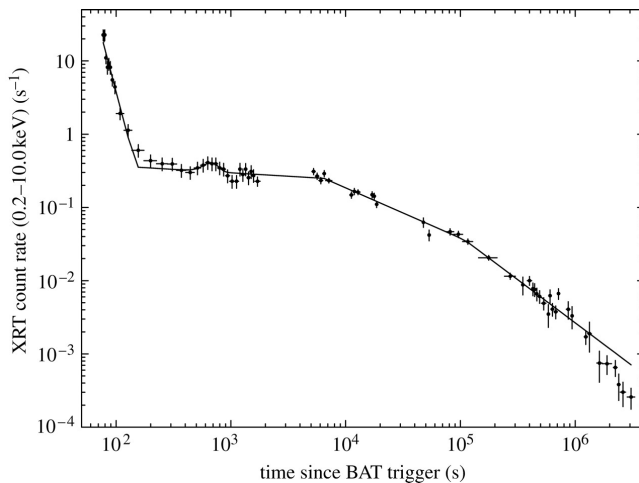


FIGURE 1.3: Swift/XRT light curve of GRB 060428A, which shows all the phases seen in early GRB X-ray afterglows (but with an unusual dual-slope energy injection phase) [3].

seconds [63]. However, if the disk is highly magnetized, a longer accretion timescale may be considered [66], as well as if the merger results in a temporary magnetar whose magnetic field holds back the accretions disk until the central object collapses into a BH [67, 68].

### 1.3.2 Long Gamma Ray Bursts

LGRBs are found in early-type galaxies [69–71], where blue massive stars are forming, and spread over a large redshift range from  $z = 0.0085$  up to  $z \sim 8$ . The metallicity of these host galaxies is generally lower with respect to the metallicity of the average of massive star forming galaxies [71–73] and this provides an expected redshift distribution ( $\sim 40\%$  has  $z \gtrsim 4$  [74]). In principle, this class of burst may be detected until  $z \lesssim 25 - 30$  [75–77].

Most of them that occur near enough for SN detection has an accompanying Type Ib or Ic SNe (e.g., GRB 980425/SN 1998bw [78], GRB 030329/SN 2003dh [79], GRB 031203/SN 2003lw [80], GRB 060218/SN 2006aj [81], XRF 060218/SN 2006aj [82], GRB 021211/SN 2002lt [83], XRF 020903/SN 1998bw [84], GRB 050525A/SN 2005nc [85]) in host young galaxies where short-lived massive formation is present. This has been supporting the advancing evidence that these bursts are caused by collapsing objects. That is where the central core of a massive star collapses to a compact object such as a (BH) or possibly a magnetar [67].

The gamma emission duration of these sources (from  $\sim 2$  s to  $\sim 10^3$  s) is normally ascribed to the time for the accretion of the matter falling into the central BH which must be formed as the core of the massive star collapses. This accretion process around a BH engenders a relativistic jet which breaks through the collapsing core and the stellar envelope along the direction of the rotation axis [4].

[86] and [87] have studied a mechanism of collapse related to a massive core, considering magnetohydrodynamic effects in the accretion disk and BH. The resulting accretion time is short enough to be associated with SGRBs, however a magnetic tension can extend the accretion time leading to a LGRBs. Basically, the energy for long bursts is provided by either a conversion of the BH rotational energy, mediated by the forming torus, or gravitational energy always generated by the torus falling onto the BH created by the massive core collapse. In both cases, the torus has a accretion lifetime depending on the duration of the prompt phase [4]. As for other mechanisms it is possible to see [88–92].

The most distant LGRBs are intrinsically the brightest, typically  $E_{\text{iso}} \gtrsim 10^{55}$  erg, but a selection effect is a reasonable doubt, because faint luminosity cannot be detected if too far. The current record holder being GRB 090423 at a spectroscopically confirmed redshift  $z = 8.2$  [93], and GRB 090429B, at a photometric redshift  $z \sim 9.4$  [94].

These bursts provide spectroscopic information about the chemical composition of the intervening intergalactic medium at epochs in which the universe was 20 times younger than today. LGRBs might contribute with information of star formation rate at high-redshift universe, since their explosions at the endpoint of the live of massive stars are approximately proportional to this rate. However, there might be evolutionary biases, such as a dependence of LGRBs on the metallicity of host galaxies, which must be taken into account [67, 95, 96].

### 1.3.3 Intermediate class and other bursts

Obviously, categorizing GRBs to only two class is not the best way to distinguish them, indeed in these two classes it is possible to find many peculiarity, perhaps too much. For this reason, one can try to increase the number of classes, identifying some peculiarity to establish a new group. For the sake of the completeness, some brief information is mentioned here.

Analyses carried out by [97] have suggested a possible re-interpretation of the current classes, leading an intermediate class studied by [98, 99]. The afterglows of this class are characterized by a soft long bump following the main event and by a late time evolution similar to the long GRBs ones, showing a “canonical” behaviour [100]. In several cases, X-ray flares are present [101] and they are harder than LGRBs [102].

An interesting type of object has been revealed by the *Swift* satellite. Sources of this type are located in the centre of the host galaxy and present bursts characterized by unusually persistent and prolonged emission. The prototype of this class is Sw J164449.3 [103]. They could be triggered the tidal disruption of a star by a massive BH. This effect has been predicted for long time, since the 1970s and more details can be seen in [67]. In the end, other objects produce bursts that cannot be classified into the two classes. These burst are extreme magnetar flares due to sudden readjustment in the magnetosphere of highly magnetized NS ( $B \gtrsim 10^{14}$  G) [67].

## 1.4 The fireball model

As said, GRBs are discovered in the end of sixties years and they were more understood only in the end of nineties years after the BeppoSAX mission. After the first studies, times and energies measured for those bursts have led to particular objects with stellar sizes, so an explanation to justify such a emission was suggested in [104] with their *relativistic fireball model*. They showed that under some conditions and relativistic

velocities ( $\Gamma \gg 1$ ) an expanding sphere of plasma with proper characteristics may appear more energetic than it is actually.

During the burst, a part of the total energy (a fraction of the order  $10^{50}$ - $10^{52}$  erg) remains trapped in a fireball made up  $e^\pm$  pairs,  $\gamma$ -rays and baryons, in addition a magnetic field having a comparable amount of energy (or also larger) can be contained. In this fireball, the amount of energy is mainly observed as non-thermal  $\gamma$ -ray emission. Although this electromagnetic energy is a little percentage respect to total, it is the most powerful if compared with else explosive event in the universe.

In this model the leading mechanism for the electromagnetic radiation observed from GRBs is based on a relativistic fireball generated by a core collapse or a merger. Because the fireball is expanding, the radiation pressure exceeds self-gravity, hence the luminosity is greater than Eddington luminosity, that is

$$L_E = 4\pi G \frac{M m_p c}{\sigma_T} = 1.25 \times 10^{38} (M/M_\odot) \text{ erg s}^{-1}, \quad (1.3)$$

where  $\sigma_T$  is the Thomson scattering cross-section for the electron.

Initially, fireball models were assumed to reach relativistic expansion velocities and their emission was thermal like [104–107]. However, ultimate expansion velocity depends on the baryon load of the fireball [108], in fact if the fireball energy involved all the baryons in the core (magnitude of solar masses) than the expansion would be sub-relativistic. But the region where the fireball originates is likely baryon-depleted, with a tendency to form high-entropy radiation bubbles, which are plasma clouds with high energy and low mass. Dynamically dominant magnetic fields would also tend to involve fewer baryons [4]. Indeed, a phenomenological argument shows that the expansion must be highly relativistic, because most of GRB spectral energy is observed above 0.5 MeV. In this case, the mean free path for the  $\gamma\gamma \rightarrow e^\pm$  process in an isotropic plasma (good assumption for a sub-relativistic expanding fireball) would be very short. Since a lot of bursts have a spectrum above 1 GeV, a reasonable process inside the flow must maintain energies above the threshold  $m_e c = 0.511$  MeV [109], avoiding the photon-photon interactions that degrade the energy. For this reason, it seems necessary that the flow has an expanding velocity associated to a high Lorentz factor  $\Gamma$ , so that the relative collision angle between photons is less than  $\Gamma^{-1}$  and the threshold for the pair creation is then diminished. Following [109, 110], when Lorentz factor is above to

$$\Gamma \gtrsim 10^2 \left( \frac{\epsilon_\gamma}{10 \text{ GeV}} \frac{\epsilon_t}{\text{MeV}} \right)^{1/2},$$

where  $\epsilon_\gamma$  are bullet photons and  $\epsilon_t$  are the targets photons with  $\sim 1$  MeV, then bullet photons avoid the annihilation against the target ones. We have a relativistic velocity with  $\Gamma \gtrsim 1$ .

Additional details about the discussed model can be seen in [4]. However, although the fireball model is the theory conventionally more accredited, there are others theories that rely their models on different assumptions. In this sense, [111] and its electromagnetic model can be cited.

## 1.5 Frame and temporal conversions in relativistic ejecta

For this discussion three frame will be considered:  $S_*$ ,  $\tilde{S}$  and  $S$ . The first symbol is referred to the frame of exploded star from which the fireball has been originated, the second refers to the rest frame, co-moving with the expanding fireball surface, and the last frame is the terrestrial frame. It is important to note that  $S_*$  and  $S$  measure the same velocities in  $\tilde{S}$ , apart from the cosmological redshift and negligible proper motions. The emitted gas moves relativistically with velocity  $\beta = v/c = (1 - \Gamma^{-2})^{1/2}$  relatively to  $S_*$ .

The lengths, times, thermodynamic and radiation quantities of the gas are best evaluated in  $\tilde{S}$  and Lorentz transformations will be used to change frame. Thus, a proper length  $d\tilde{r}$  in the co-moving frame has a length  $dr_* = dr = \tilde{r}/\Gamma$  in the stellar/Earth frame (as usual Fitz-Gerald contraction). The time follows standard dilatations when one measures two different instants in the same place ( $dr_* = dr = 0$ ), indeed a proper time interval  $d\tilde{t}$  changes into  $dt_* = dt = \tilde{t}\Gamma$  in the  $S_*$  frame. Even though  $S_*$  and  $S$  are substantially the same, a terrestrial observer must consider the classical light travel time delay (Doppler) effect, i.e. [112]. Hence, by supposing a static space with static sources, the only thing with different measure on  $\tilde{S}$  between  $S_*$  and  $S$  is the time of arrival of signals.

By fixing an expanding radial direction from the origin of the explosion, it is possible to characterize an angle between that direction and the observer line of sight, it will be read  $\theta$ . When a photon is in the point  $r_{*1} \equiv r_1$ , its time of arrival from the fireball origin to the Earth is  $t_1 = t_{*1} + d/c$ , where  $t_{*1}$  is the time to reach  $r_{*1}$  in the stellar frame while  $d$  is the distance between  $r_{*1}$  and the Earth. A second photon emitted from  $r_{*2} \equiv r_2$  at the time  $t_{*2}$  will be detected at the time  $t_2 = t_{*2} + (d/c - \beta dt_* \cos \theta)$ , where  $dt_* = t_{*2} - t_{*1}$ . It is possible to see an illustration in figure 1.4. For an observer in a terrestrial lab, the time difference between the instants  $t_1$  and  $t_2$  is read  $dt$  as follows [4]:

$$dt = dt_*(1 - \beta \cos \theta) \simeq dt_* \left( \frac{1}{2\Gamma^2} + \frac{\theta^2}{2} \right) \simeq dr \frac{1 + \Gamma^2 \theta^2}{(2\Gamma^2 c)} \simeq \frac{dr}{2\Gamma^2 c}, \quad (1.4)$$

where  $\Gamma \gg 1$  is assumed for an approaching gas ( $-\pi/2 < \theta < \pi/2$ ) along a radial direction and which is moving inside a light cone  $\theta \ll \Gamma^{-1}$ .

As said, the stellar and terrestrial frames are the same each others, but both are different with the rest frame of the relativistic moving fireball. The general relation between theirs

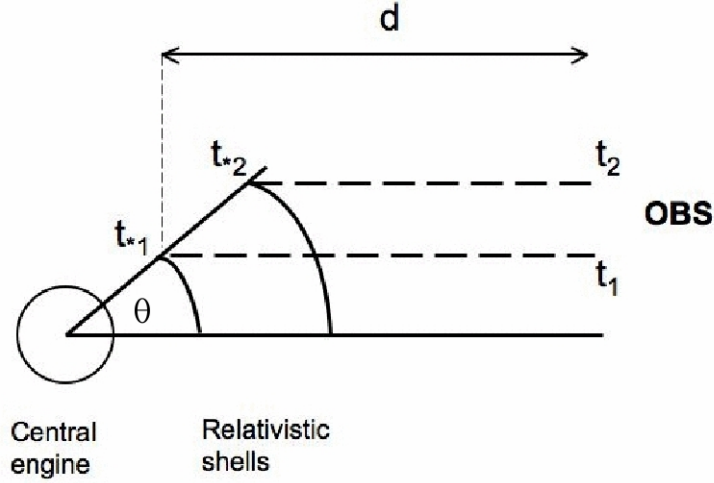


FIGURE 1.4: Illustration of the emission from spherical relativistic shells in the source frame and the relativistic time delay leading to the relation between source frame and observer time. [4]

and the co-moving frame are given through the Doppler factor  $\mathcal{D}$ ,

$$\mathcal{D} = \frac{1}{\Gamma(1 - \beta \cos \theta)}. \quad (1.5)$$

Usually, when gas is approaching (blueshift, namely  $\theta \rightarrow 0$ ),  $\Gamma \gg 1$  and  $\theta < 1/\Gamma$  then  $\mathcal{D} \sim 2\Gamma$ ; on the other hand, when gas is receding (redshift, namely  $\theta \rightarrow -\pi$ ) then  $\mathcal{D} \sim (2\Gamma)^{-1}$ . Now it is possible to write the time relation between  $S$  and  $\tilde{S}$  frames:

$$dt = \mathcal{D}^{-1} d\tilde{t} = \Gamma(1 - \beta \cos \theta) d\tilde{t} \simeq d\tilde{t}/(2\Gamma), \quad (1.6)$$

because  $dt = \Gamma d\tilde{t}$  and that in above relation it needs the cosmological correction, so all equation have to be multiplied by the factor  $(1+z)$ . In figure 1.5 is showed the spheroid of the relation expansion in function of the  $\theta$  angle.

The complete relations to change from a relativistic co-moving frame to a not-relativistic frame can be obtained using relativistic invariants (frequency, solid angle, temperature, volume, specific intensity, specific emissivity, radial width and specific absorption coefficient) and written in terms of the Doppler factor [112]:  $\nu = \mathcal{D}\tilde{\nu}$ ,  $d\Omega = \mathcal{D}^{-2} d\tilde{\Omega}$ ,  $T(\nu) = \mathcal{D}\tilde{T}(\tilde{\nu})$ ,  $dV = dV_f$ ,  $I_\nu(\nu) = \mathcal{D}^3 \tilde{I}_{\tilde{\nu}}$ ,  $j_\nu = \mathcal{D}^2 \tilde{j}_{\tilde{\nu}}$ ,  $\delta r = \mathcal{D}\delta\tilde{r}$ ,  $\mu_\nu(\nu) = \mathcal{D}^{-1} \tilde{\mu}_{\tilde{\nu}}(\tilde{\nu})$ . Where the absorption coefficient is  $\mu_\nu = n\sigma_\nu \text{ cm}^{-1}$ , where  $n$  is the density and  $\sigma_\nu$  the cross section, therefore  $\nu\mu_\nu$  and the optical depth  $d\tau = \mu_\nu d(\delta r)$  are invariants too.

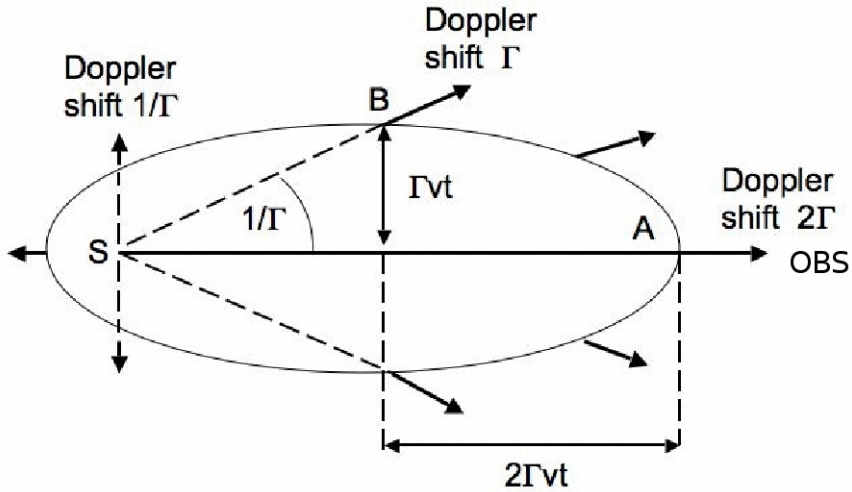


FIGURE 1.5: This spheroid is the locus of the points in which the radiation has the same time. Photons isotropically leave from the source  $S$  and with  $\Gamma = (1 - \beta^2)^{-1/2} \gg 1$  make the surface in the figure after an observer time  $t$ . Most of radiation arrives from the observer direction (“OBS”) side and it is strongly Doppler-boosted inside the light cone  $1/\Gamma$ . The line of sight parallel and perpendicular apparent axes of the ellipsoid are  $r_{\perp} \sim \Gamma c t$  and  $r_{\parallel} \sim 2\Gamma c t$ . [4]

### 1.5.1 Relativistic dynamics

Initially, when an outflow is ejected its high optical depth allows an expansion that can be considered adiabatic and within a radius  $r_0$ , there is an energy  $E_0$  imparted to a mass  $M_0 \ll E_0/c^2$ . The dominant pressure will be radiation one and the associated adiabatic index is  $\gamma_a = 4/3$ . Its co-moving temperature  $\tilde{T}$  (or the co-moving random Lorentz factor per particle  $\tilde{\gamma}$ ) evolves with its volume  $\tilde{V}$  as  $\tilde{T} \propto \tilde{V}^{1-\gamma_a}$ . It means  $\tilde{T} \propto \tilde{\gamma} \propto r^{-1}$  and so by conservation of the energy if the internal energy per particle decreases then the bulk energy per particle (namely the bulk Lorenz factor) must increase, so that  $\gamma\Gamma = \text{constant} \propto r$ . If the initial value of the random internal energy per particle was  $\gamma_0 = \eta = E_0/M_0c^2$ , the bulk Lorentz factor can increase up to  $\Gamma_{\max} \sim \eta$  when the expansion reaches a radius  $r/r_0 \sim \eta$ . Beyond this value the flow begins to coast, and  $\Gamma_{\max} \sim \text{const}$  [105–107, 113]

$$\Gamma(r) = \begin{cases} r/r_0 & \text{for } r/r_0 \lesssim \eta, \quad r \lesssim r_s, \\ \eta & \text{for } r/r_0 \gtrsim \eta, \quad r \gtrsim r_s, \end{cases} \quad (1.7)$$

where  $r_s$  is a saturation radius beyond which the Lorentz factor is saturated. The acceleration increases the radial velocity of particles, starting from a sphere with radius  $r_0$  up to the saturation radius  $r_s$ , these particles expand with their shell whose lab-frame width is initially small,  $\delta r \sim \delta r_0 \sim r_0$ . The radial velocity-spread is  $\Gamma^{-2}$  which causes a gradual enlargement of the lab-frame radial width  $\delta r/r \sim \delta v/v \sim \Gamma^{-2}$ . This spread becomes relevant only well beyond  $r_s$ .

The co-moving radial width  $\tilde{\delta r}$  is related with the lab width through the relativistic invariants in the end of the section 1.5. In this case  $\tilde{\delta r} \sim \delta r \Gamma$  and so

$$\tilde{\delta r} \sim \begin{cases} \delta r_0 \Gamma \sim r & \text{for } r \lesssim r_s, \\ \delta r_0 \eta & \text{for } r_s \lesssim r \lesssim r_\delta, \\ r/\eta & \text{for } r \gtrsim r_\delta. \end{cases} \quad (1.8)$$

Considering that the transverse dimensions (with respect to the motion) are invariant the co-moving volume is

$$\tilde{V} \sim 4\pi r^2 \tilde{\delta r}, \quad (1.9)$$

following the cases in Eq. 1.8. Hence the co-moving particle density  $\tilde{n}$  is proportional to  $\tilde{V}^{-1}$ .

In a relativistic gas with polytropic index equal to  $4/3$ , that is valid as long as the pressure is radiation-dominant, for an adiabatic expansion at high initial optical depths, the co-moving temperature, internal energy and volume are related as follows [4]

$$\frac{\tilde{T}}{T_0} = \frac{\tilde{E}}{E_0} = \left( \frac{\tilde{V}}{V_0} \right)^{-1/3} \simeq \begin{cases} \frac{\delta r_0}{r} & \text{for } r \lesssim r_s, \\ \frac{\delta r_0}{r_s} \left( \frac{r_s}{r} \right)^{2/3} = \eta^{-1/3} \left( \frac{\delta r_0}{r} \right)^{2/3} & \text{for } r_s \lesssim r \lesssim r_\delta, \\ \frac{\delta r_0}{r_s} \left( \frac{r_s}{r} \right)^{2/3} \frac{r_\delta}{r} = \eta^{1/3} \frac{\delta r_0}{r} & \text{for } r \gtrsim r_\delta, \end{cases} \quad (1.10)$$

where such equations are referred to the release of mass  $M_0$  and energy  $E_0$  corresponding to  $\eta = E_0/(M_0 C^2)$  and originating inside a region of dimensions  $\delta r_0 \sim r_0$ .  $M_0$  and  $E_0$  leave this region in a relativistic rest-frame time,  $\delta t_0 \sim \delta r_0/c$ .

For typical BHs, or compact stellar merging scenarios, the volume of the energy release is of several Schwarzschild radii ( $2G M_{\text{BH}}/c^2$ ).

### 1.5.2 Photosphere and optical depth

When the expanding relativistically fireball is in the early phase,  $e^\pm$  pairs are in equilibrium [105–107] and dominate the scattering optical depth. While it has been expanding its temperature decreases below  $\tilde{T} \sim 17$  keV, so the equilibrium of the pairs is broken and is supplanted by recombination, that occurs at radii below the saturation radius.

Thereafter, when there are low values of baryon loads (i.e. a dimensionless entropy  $\eta \lesssim 10^5$ ) the density of the baryonic electrons associated with the protons ( $n_e = n_p$ ) is very greater than the residual freeze-out density of remained pairs. The scattering optical depth is still large at the saturation radius quite because of baryonic electrons. For a minishell of initial width  $\delta r_0$  the optical Thomson scattering depth varies as [114]

$$\tau_T = \frac{M_0 \sigma_T}{4\pi r^2 m_p} = \tau_0 \frac{\delta r_0}{r}^2, \quad (1.11)$$

where  $\tau_0 = E_0 \sigma_T / (4\pi r_0^2 m_p c^2 \eta)$ , for  $r \lesssim r_\delta$ . In general, for bursts with relevant duration (e.g., 10 s), different parts of the flow have different densities at any instant, and are both above than below  $r_s$ . This case can be defined as *wind* regime and  $\eta \equiv L/(Mc^2)$  and the relativistic fluid differential equations are used, instead of integral conservation laws. Again, the Lorentz factor linearly increases and saturates at  $r_s = \eta r_0$  as in Eq. 1.7 ( $r_0 = \delta r_0$  is the minimum variability radius) and the adiabatic behaviour of Eqs. 1.10 is maintained for energy, etc.

The particle density is given by the mass conservation equation:

$$\tilde{n}_p = \frac{\dot{M}}{4\pi r^2 m_p c \Gamma} = \frac{L}{4\pi r^2 m_p c^3 \Gamma \eta}. \quad (1.12)$$

whereas the optical depth is

$$\tau_T = \int_r^\infty \tilde{n}_e \sigma_T \sqrt{\frac{1-\beta}{1+\beta}} d\tilde{r} \sim \frac{\tilde{n}_e \sigma_T r}{\Gamma \eta}, \quad (1.13)$$

within the global photosphere [108]

$$r_{\text{ph}} \simeq \frac{\dot{M} \sigma_T}{8\pi m_p c \Gamma^2} \simeq 6 \times 10^{11} L_{51} \eta_2^{-3} \text{ cm}. \quad (1.14)$$

The co-moving and observer-frame temperature of the flow behave as

$$\tilde{T} \propto \begin{cases} r^{-1} & \text{if } r < r_s, \\ r^{-2/3} & \text{if } r > r_s, \end{cases}; \quad T = \tilde{T} \Gamma \sim \begin{cases} T_0 & \text{if } r < r_s, \\ T_0 \left(\frac{r}{r_s}\right)^{-2/3} & \text{if } r > r_s. \end{cases} \quad (1.15)$$

The radiation escaping from a given radius  $r$  can reach only observers within a light cones of  $\theta = \Gamma^{-1}$ . The observer-frame time delay between the central line of sight and the edges of the cone is

$$t_{\text{ang}} \simeq t \simeq \frac{r}{c}(1-\beta) \sim \frac{r}{2c, \Gamma^2} \quad (1.16)$$

and it is named *angular time*. This time is the same as Eq. 1.6. Whether  $t_{\text{ang}}$  is longer than the total duration of GRB, then the observed duration of the photometric radiation

is equal to the angular time, otherwise the photometric radiation is expected the total duration of the burst.

## 1.6 Light curve and spectrum

An important distinction to underline is between light curve and spectrum. A light curve is the trend of the luminosity (or flux, or photon counter, or flux density) in time, at a precise frequency. On the other hand, a spectrum is still the behaviour of the light intensity, but in function of the frequency and not of time. In other words, the temporal range is (more or less) fixed and the flux varies with the frequency.

The light curves and spectra, both of the prompt and of the afterglow emission are described and shortly explained in this section. However, it is worthwhile to stress that GRB emissions do not follow a particular single curve and, for this reason, finding a common feature to set them is extremely difficult. In practice peculiar light curve and spectrum are found for any GRB, so the real goal is identify some common characteristics that explain their physics, modifying only those external parameters which rule the complete phenomenon. In spite of the thousands of observations and provided data, there are many ideas but none definitive.

### 1.6.1 Photosphere, shocks and thick and thin shells

The black body emission with the contribute of the comptonization in the higher energy part should consist the spectrum of the photosphere, but the observed spectrum is strongly non-thermal, following a broken power law. In addition, during the expansion, the energy is converted from internal into kinetic, hence the conversion becomes more inefficient when the fireball is optically thin, since most of energy transfers to protons rather to photons. For a high  $\eta$  photosphere forming before of the saturation radius, the radiative luminosity is constant, because  $\Gamma \propto r$  and  $\tilde{E}_{\text{rad}} \propto r^{-1}$ . But, if the photosphere with a more moderate  $\eta$  is emitting after the saturation radius,  $E_{\text{rad}} \propto (r/r_s)^{-2/3}$  and the baryonic kinetic energy is  $E_k \sim E_0 \sim \text{const}$  [4].

When the flow becomes optically thin, a re-conversion via shocks of the kinetic energy of the flow into random energy is an energetically efficient way to have a non-thermal spectrum. These collisionless shocks can be expected to accelerate particles to ultra-relativistic energies via the Fermi process, so that the relativistic electrons can emit through synchrotron and inverse Compton emissions. For a colliding outflow with  $\Gamma_0 = \eta$  and total energy  $E_0$ , the effects of the shock become relevant after having across the

external medium through a distance [115]

$$r_d \simeq \left( \frac{3 E_0}{4\pi n_{\text{ext}} m_p c^2 \eta^2} \right)^{1/3}, \quad (1.17)$$

where  $n_{\text{ext}}$  is the density of the external medium, while the timescale in which the deceleration occurs at the observe frame is

$$t_d \simeq \frac{r_d}{2c\Gamma}. \quad (1.18)$$

At this radius the bulk Lorentz factor is almost halved and the amount of external matter swept since the beginning of the impact is  $M_0/\eta$ , where  $M_0$  is the ejecta mass.

Apart from collision with the external medium, some collisions can occur inside the ejecta itself, if later portions of the jet is faster than the previous one, overcoming this last. In this case there will be *internal shocks* which lead to quick time-varying MeV  $\gamma$ -rays and to p-p collisions and, subsequently,  $\pi^0$  decay  $\gamma$ -rays [4, 116]. The former can be considered the core of the burst.

A variability in time should depend on a variability in the central engine which would depend on flares or intermittence of the accretion disc. For the observer, the radiation originated beyond the scattering photosphere. After the saturation radius  $r_s = r_0 \eta = r_0 \Gamma$ , the Thomson optical depth becomes  $\tau_T = \tilde{n}_e \sigma_T r / \Gamma = 1$  and the photosphere radius is

$$r_{\text{ph}} \simeq \begin{cases} 1.2 \cdot 10^{12} L_{51}^{1/3} r_{07}^{2/3} \eta_2^{-1/3} \text{ cm} & \text{if } r < r_s, \\ 1.2 \cdot 10^{12} L_{51} \eta_2^{-3} \text{ cm} & \text{if } r > r_s. \end{cases} \quad (1.19)$$

Whether the photosphere is formed above or below  $r_s$ , it depends on a critical value of the entropy,  $\eta_s = 562(L_{51}/r_{07}^{1/4})$ . If the entropy is grater then the photosphere occurs below, otherwise on the contrary. As long internal shocks are generated above  $r_s$  and the wind photosphere, the entropy must be

$$33 \left( \frac{L_{51} r_{0,7}}{t_v} \right)^{1/5} \lesssim \eta \lesssim 562 \left( \frac{L_{51}}{r_{0,7}} \right)^{1/4}, \quad (1.20)$$

where  $t_v$  is the time of the variability. In this case the energy does not emit through a quasi-thermal radiation from the photosphere. Figure 1.6 shows the radial variation of  $\Gamma$  and the location of the different characteristic radii and which region produce the various emissions.

The internal shocks have the advantage to be able to explain complicate light curves. Although the internal shocks explain the  $\gamma$ -ray radiation from GRBs via inverse Compton and/or synchrotron processes, the spectral slop at low energy (20 - 50 keV) is still unclear. There are serious issues when the efficiency is taken into account, because

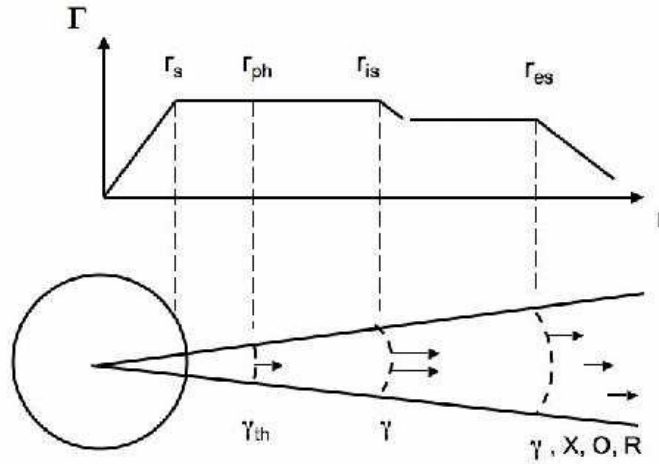


FIGURE 1.6: A schematic behaviour of the Lorentz factor during the jet. Along the x-axes the radius where the saturation radius  $r_s$ , the photospheric radius  $r_{ph}$ , the internal shock (or magnetic dissipation) radius  $r_{is}$  and the external shock  $r_{ext}$  appear as the outflow runs. Thermal  $\gamma$ -rays are produced by photosphere, the internal shock and dissipation region produce the non-thermal  $\gamma$ -rays. The afterglow is finally produced by the external shock region [4].

following estimations it results moderate in the bolometric sense (5 - 20%) and higher values ( $\lesssim 30$  - 50) considering a highly varying  $\Gamma$  factors in different shells of the jet [4], but adding the problem to expect large variations in  $E_p$  between spikes of the same GRB. However, the inverse Compton losses are predominant on the total efficiency, and it is  $\sim 1$  - 5% both if the MeV is due to the IC and by synchrotron in the 25 - 2000 keV (BATSE) range.

Independently of the burst duration, both forward and reversal shocks are expected, they are formed as soon as the jet starts its motion, with initially a radiation weak but which progressively becomes more powerful. Indeed, even if since the beginning the forward shock (FS) has got a highly relativist bulk Lorentz factor ( $\Gamma \sim \eta$ ), the reverse shock (RS) starts with sub-relativistic velocities that increases as the external matter is swept-out by the relativist outflow. The RS intensity increases with time only if the external-medium density follows a trend shallower than  $r^{-2}$ , while the intensity is constant when the density profile is  $r^{-2}$  below  $r_\delta$ .

For impulsive burst, namely when the deceleration time of the outflow is greater than the GRB time, the time needs to decelerate the jet corresponds to peak-emission duration. After the fist shock the expansion goes into a self-similar expansion as  $\Gamma \propto r^{-3/2}$  and  $t_d$  corresponds to time taken by the RS to across the ejecta. In this time the shell shocked has almost the same  $\Gamma$  of the FS but there is a relevant difference; in fact, while the

particles in the FS are highly randomly relativistic, those in the RF are only partially relativistic, and this produces a spectrum centered on optical band [4].

The external shock dynamics is different when the outflow time is greater than the deceleration time [87]. When the density of the external medium is considered as a constant and the same for the kinetic luminosity, in a intermediate time lesser than burst duration the bulk Lorenz factor is proportional to  $r^{-1/2}$ , then transitioning to a self-similar expansion where  $\Gamma \propto r^{-3/2}$  at the burst time (and not at  $t_d$  as previously).

There is substantial difference that depends on the observer-frame time of the transition to the self-similar expansion. Letting  $t_{\text{GRB}}$  as the time of the burst, the transition time can occur at either  $t_{\text{GRB}}$  or  $t_d$ . If  $\Gamma_0 \sim \eta$  is the initial Lorentz factor can be considered two cases:  $\eta < \Gamma(t_d)$  and  $\eta > \Gamma(t_{\text{GRB}})$ . The former case is said *thin shell*, where the deceleration and transition occur at  $r_d$  and  $t_d$  and the RS is partially relativistic. On the contrary, the latter case is said *thick shell*, where the transition and the deceleration occur at  $t_{\text{GRB}}$  and at a radius

$$r_{\text{TS}} \simeq 2ct_{\text{GRB}}\Gamma^2(t_{\text{GRB}}). \quad (1.21)$$

In this second case, at  $t_{\text{GRB}}$ , the RS reaches a relativistic velocity with a Lorentz factor of  $\sim \eta/(2\Gamma(t_{\text{GRB}})) \gg 1$  in the frame of the contact discontinuity, while the FS Lorentz factor is about  $\Gamma(t_{\text{GRB}})$  [4].

### 1.6.2 Prompt

The prompt emission is the first radiation that unveils a GRB and which alerts most of gamma satellite instruments, in order to start an observation on that particular area of the sky. The observed energy range at this stage is between  $\sim 0.05 - 2$  MeV. As shown in figure 1.7, the generic phenomenological photon spectrum consist of a broken power law in the mentioned range, then it extends as a power law again down into the X-ray, and up into energy range of some GeV. The photon energy flux is proportional to  $E^{-\beta}$  for classical GRBs, where the  $\beta$  index is  $\sim 1$  or  $\sim 2$ , if the energy is greater than an energy break typically  $E_b \sim 0.2$  MeV [5].

Initially, by missions pre-BATSE, the cutoff at the energy break suggested a bremsstrahlung emission, but with the discovery of the power law beyond  $E_b$ , the more natural emission to explain that spectral shape was the synchrotron process.

An easy way to start the explanation about the synchrotron shock model begins from the back shock, behind the FS. Because of the relativistic strong transition, after the

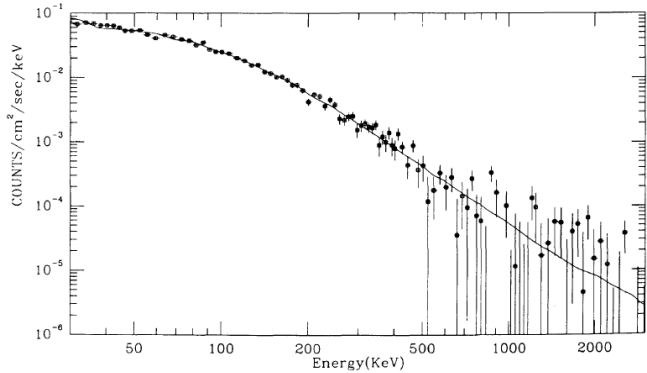


FIGURE 1.7: Spectrum fit of 1B 911127. The low-energy spectral index is  $-0.968 \pm 0.022$ , while it is  $-2.427 \pm 0.07$  in the high-energy, after the energy break at  $149.5 \pm 0.07$  keV [5].

shock the particle density  $n$  and the internal energy density  $\varepsilon$  are

$$\begin{aligned} n_2 &= (4\Gamma_{21} + 3)n_1 \simeq 4\Gamma_{21}n_1, \\ \varepsilon_2 &= (\Gamma_{21} - 1)n_2 m_p c^2 \simeq \Gamma_{21}n_2 m_p c^2 \simeq 4\Gamma_{21}n_1 m_p c^2, \end{aligned} \quad (1.22)$$

where the numbers 1 and 2 indicate respectively the zone post and pre shock, therefore  $\Gamma_{21}$  is the Lorentz factor between the two fluids, downstream and upstream (unshocked). The unshocked material is considered cold. Both relations are measured in the co-moving frames of 1 and 2 fluids. The Lorentz factor  $\Gamma_{21}$  can be approximated to the Lorenz factor  $\Gamma$  of the shock front since [4]

$$\Gamma_{21} = \frac{1}{\sqrt{2}}\Gamma, \quad \text{for } \Gamma_{21} \gg 1. \quad (1.23)$$

For internal shocks  $\Gamma_{21}$  can be replaced by a relative Lorentz factor  $\Gamma_r \sim 1$ .

In the co-moving frame, behind the shock, when a proton passes through a shock front with  $\Gamma_{21}$ , acquires a random internal energy  $\gamma_{p,m} \sim \Gamma$  [117]. These turbulent motions generate dynamo effects, building the magnetic field up [117, 118], as inferred for the SN remnant shocks. The efficiency of this process is not certain, but the resulting magnetic field after the shock can be parametrized by an energy density which is a fraction  $\epsilon_B$  of the equipartition value relative to the random proton energy density resulting [4]:

$$\tilde{B} \approx \Gamma \sqrt{32\pi \epsilon_B n_{\text{ext}}(\tilde{\gamma}_p - 1)m_p c^2}, \quad (1.24)$$

where the internal energy of the post-shock proton is [116, 117]

$$(\tilde{\gamma}_p - 1)m_p c^2 \sim 1 \quad \text{for internal shocks} \quad (1.25)$$

$$(\tilde{\gamma}_p - 1)m_p c^2 \sim \Gamma \quad \text{for external shocks} \quad (1.26)$$

One should also consider the Fermi acceleration, due to scattering of protons and electrons caused by irregularities in the magnetic field, which is present both back and in front of the FS. This acceleration leads to a relativistic power-law energy distribution as

$$N(\gamma) \propto \gamma^{-p}, \quad (1.27)$$

where  $p \geq 2$ . Even though knowing the particle energy distribution is necessary to understand the radiation produced by a plasma, details of Fermi acceleration are not completely understood, so it is not discussed here, but for more information see [119–124] and [125–127].

Reasonably, the thermal electrons and protons injected into the acceleration process have the same the minimum Lorentz factor,

$$\gamma_{e,m} \approx \Gamma, \quad (1.28)$$

therefore, both before and after the acceleration, electrons have an energy less than  $\sim m_e/m_p$  with respect to the proton energy. However, the energy can redistribute among particles, because of chaotic electric and magnetic fields that mediate collisionless shocks, up to some fraction  $\epsilon_e$  of the value equipartition of the thermal energy, and thus [118, 128]

$$\gamma_{e,m} \approx \epsilon_e \frac{m_p}{m_e} \Gamma. \quad (1.29)$$

Letting  $\zeta_e$  as the fraction of all shocked thermal electrons that achieve this initial equipartition value  $\epsilon_e$  and to be injected into the acceleration process, then the initial minimum random Lorentz factor of the electrons is [4, 129]

$$\gamma_{e,m} \approx \frac{\epsilon_e}{\zeta_e} \frac{m_p}{m_e} \Gamma. \quad (1.30)$$

Integrating over the power-law distribution, it gives

$$\gamma_{e,m} = g(p) \frac{\epsilon_e}{\zeta_e} \frac{m_p}{m_e} \Gamma, \quad (1.31)$$

where  $g(p) = (p - 2)/(p - 1)$ . Hereafter, the subscript “e” in  $\gamma_{e,m}$  will be omitted in this subsection.

Assuming that the radiative losses are a few, one can consider the adiabatic regime. In this case the optically thin synchrotron spectrum in the observer frame is [130]

$$F_\nu \propto \begin{cases} \nu^{1/3} & \text{if } \nu < \nu_m \\ \nu^{-(p-1)/2} & \text{if } \nu > \nu_m \end{cases} \quad (1.32)$$

where  $\nu_m$  is the synchrotron-peak frequency related to the magnetic field and to the energy of the plasma emitter. This frequency is equal to [4]

$$\nu_m \approx \frac{3}{8\pi} \frac{e\tilde{B}}{m_e c} \Gamma \gamma_m^2 \approx \tilde{B} \Gamma \gamma_m^2 \text{ MHz}. \quad (1.33)$$

For high energy, the slope of the synchrotron prompt emission is  $\beta_2 = (p - 1)/2$ , close to the mean of the Band fit [4, 5]; for low energy, the slope is almost flat ( $\beta_1 \sim 0$ ), relying on observations from a range of  $\tilde{B}$  values [4].

Another important point about the synchrotron emission is the self-absorption frequency  $\nu_a$ . At low energy, the spectrum is remarkably modified, indeed it is

$$F_\nu \propto \nu^2 \quad \text{if } \nu_a < \nu_m; \quad (1.34)$$

while, as for high energy, it is contaminated by the inverse Compton effect emission [116, 118, 128, 131–133] which extends the spectrum up to the GeV range.

Although the synchrotron emission is the most straightforward physical mechanism that explains GRB spectrum, many effects can modify it. One of these factors is the fast cooling. This triggers when the co-moving synchrotron cooling time, which is

$$\tilde{t}_{\text{sc}} = \frac{9 m_e^3 c^5}{4, e^4 \tilde{B}^2 \gamma_e} \sim \frac{7 \cdot 10^8}{\tilde{B}^2 \gamma_e} \text{ s}, \quad (1.35)$$

is less than the co-moving dynamic time

$$\tilde{t}_{\text{dyn}} \approx \frac{r}{2 c \Gamma}. \quad (1.36)$$

Under this condition, the electrons cool down and their energy decreases to a critical value

$$\gamma_c = \frac{6\pi m_e c}{\sigma_T \tilde{B} \tilde{t}_{\text{dyn}}} \quad (1.37)$$

and the spectrum becomes [134, 135]

$$F_\nu \propto \nu^{1/2} \quad \text{if } \nu > \nu_c \approx \frac{3}{8\pi} \frac{e\tilde{B}}{m_e c} \Gamma \gamma_c^2. \quad (1.38)$$

Even in low energy, the synchrotron as unique emission process is incompatible for some GRBs. Indeed, for this fraction of sources, the spectral index  $\beta_1$  at  $\nu > \nu_m$  results grater than 1/3. [4] gathers some explanations for this behaviour: synchrotron self-absorption in the X-ray band, or in the optical range up-scattered to X-rays [108]; jitter radiation or low-pitch angle scattering [50, 136]; time-dependent acceleration and radiation [137], where low-pitch angle diffusion can also explain high energy indices steeper than predicted by isotropic scattering; observational selection effects [54].

Another point to stress is regard to the break energy in the prompt GRB spectra. Indeed, it is mainly in the 50-500 keV range. Many efforts have been done to show whether this value is due to observational biases, or not. From the Eq. 1.33, the peak frequency depends on the bulk Lorentz factor, but this last should be random. Thus, the point is whether the peak emission is caused by the synchrotron process, or by another effects. An option is associated to the pair-recombination temperature to the black body emission of the fireball photosphere [138]. In this case, the slope at low energy should be steep because of the Rayleigh-Jeans part of the photosphere, whereas the spectrum would need another explanation at high energies. In an accelerating regime, such a photosphere radiation might occur only with a very poor-baryonic load.

In [118, 128, 139–142] a generic model has been proposed. It includes two emissions coming from separate zones, the non-thermal component due to internal shocks and a thermal component due to the photosphere. The non-thermal component is subject to the pair breakdown, which can produce both steep slopes at low energy, preferred break energies and power laws at high energy. A scattering depth, from thin to thick, can lead to a Compton equilibrium which gives spectral peaks in the appropriate energy range [143, 144]. Apart from this peak and fitting slope, it is important to highlight that the Compton equilibrium of internal shock electrons (or pairs) with photometric photons leads to a high radiative efficiency [145–147]. This model gives reasonable physical explanations for the Amati and Ghirlanda relations [148, 149], between the spectral peak energy and the isotropic equivalent energy.

For the sake of the completeness, besides the prompt emission model described there are several alternative models. One of these considers highly magnetized or Poynting dominated ejecta [71, 150–154], so that the main  $\gamma$ -ray emission might arise from a magnetic reconnection or dissipation process. The central engine should be either a magnetar, or a temporary highly magnetized NS [155].

Other models include particular stars [156–158] and electric discharges from a charged black hole [159], leaving unaltered fireball-shock scenarios.

A model of a speculative radiation scenario considers plasma balls ejected with relativistic velocities, which rely on blue-shifted bremsstrahlung emission during the prompt, wheres the afterglow is generated by inverse Compton of the progenitor or the ambient [160, 161].

For more details on these and other models consult [4].

### 1.6.3 Afterglow

After the burst the ejecta continues its motion, colliding with the interstellar medium, and so the external shock starts. As the jet sweeps as new matter heaps, the bolometric

luminosity of the shock increases as  $L_{\text{bol}} \propto t^2$ , since, in that frame, the kinetic flux  $L_{\text{bol}}/4\pi r^2 \Gamma^2$  is balanced by the external ram pressure  $\rho_{\text{ext}} \Gamma^2$ , while  $\Gamma \sim \Gamma_0 = \eta \sim \text{const.}$  and  $r \propto 2\Gamma^2 ct \propto t$  [115]. The luminosity peak is reached at a radius  $r_d$  when the value of  $\Gamma$  has dropped to the half, namely at an observer time  $t_d$  (Eqs. 1.17 and 1.18). The bulk Lorentz factor and the radius vary as the matter is swept up following this trend [115, 146]

$$\Gamma \propto r^{-g} \propto t^{-g/(1+2g)}, \quad \text{then} \quad r \propto t^{1/(1+2g)}, \quad (1.39)$$

where  $g$  depends on the regime, if adiabatic or radiative. It is equal to  $3/2$  in the first case, while is  $3$  in the second.

After the peak of luminosity at the external shock, the bolometric luminosity should decay as  $t^{-1}$  in the adiabatic regime, or steeper in the radiative case, with a gradual dimming. Indeed, in the former regime the radiative cooling time is longer than the observer-frame dynamical time ( $t \sim r/2c\Gamma^2$ ), hence the energy

$$E = \frac{4\pi}{3} r^3 n_0 m_p c^2 \Gamma^2 \quad (1.40)$$

is approximately constant. On the other hand, in the radiative case the cooling time is shorter than the dynamic time and in this case the momentum is conserved ( $n_0 r^3 \Gamma \sim \text{const.}$ ) as in the snowplough phase of the SN remnants.

The relation between observed time and observed radius is generally  $t \sim r/Kc\Gamma^2$  where [162, 163]

$$\begin{aligned} K &= 2 && \text{in the constant } \Gamma \text{ regime,} \\ K &= 4 && \text{in the self - constant } \Gamma \text{ regime.} \end{aligned}$$

As regarding the spectrum of radiation, its evolution is discussed as an overview from  $\gamma$ -band to the radio range, following different papers (in particular [4, 6, 164]). The most likely emission in the afterglow phase is due to the synchrotron radiation, by accelerated electrons of a relativistic sphere which collides with an external medium [165–169].

The relativistic shock collides with a cold interstellar medium whose  $n$  is the particle density, usually measured in  $\text{cm}^{-3}$ . Behind the shock this density and its energy density are respectively given by  $4\gamma n$  and  $4\gamma^2 n m_p c^2$ , where  $\gamma$  is the Lorentz factor of the fluid after the shock [6]. A power-law of Lorentz factor  $\gamma_e$  is assumed for electrons accelerated in the shock, with a minimum Lorentz factor lets [6]

$$\gamma_m \equiv N(\gamma_e) d\gamma_e \propto \gamma_e^{-p} d\gamma_e, \quad (1.41)$$

with

$$\gamma_e \geq \gamma_m. \quad (1.42)$$

In order to keep a finite energy for electrons, the electron index  $p$  must be greater than 2 ( $p > 2$ ). Remembering that  $\epsilon_e$  is the constant fraction of the energy shock which loads electrons and  $\epsilon_B$  is the constant fraction transferred by the shock energy to the magnetic energy density (in general, the synchrotron emission is dominant on the Compton scattering when  $\epsilon_e > \epsilon_B$ ) [6], the formula for the minimum electron Lorentz factor can be written

$$\gamma_m = \epsilon_e \frac{m_p p - 2}{m_e p - 1} \gamma \quad (1.43)$$

and the magnetic field in its frame is

$$B = \gamma c \sqrt{32\pi m_p \epsilon_B n}. \quad (1.44)$$

Taking into account a plasma cloud where electrons randomly move within a magnetic field  $B$ , with a Lorentz factor  $\gamma_e \gg 1$ , the radiation power and the characteristic synchrotron frequency are the following:

$$P(\gamma_e) = \frac{1}{3} \frac{\sigma_T c}{2\pi} \gamma^2 \gamma_e^2 B^2, \quad (1.45)$$

$$\nu(\gamma_e) = \frac{eB}{2\pi m_e c} \gamma \gamma_e^2. \quad (1.46)$$

The  $\gamma$  and  $\gamma^2$  factors transform the results from the rest frame to the observer frame and  $e$  is the electron charge. The spectral power  $P_\nu$  is the power per unit frequency ( $\text{erg s}^{-1} \text{Hz}^{-1}$ ) and depends on  $\nu^{1/3}$  if  $\nu < \nu(\gamma_e)$ , while cuts off as an exponential if  $\nu > \nu(\gamma_e)$ . The peak of the  $P_\nu$  function occurs at  $\nu(\gamma_e)$  [6]:

$$P_{\nu,\max} \approx \frac{P(\gamma_e)}{\nu(\gamma_e)} = \frac{m_e \sigma_T c^2}{3e} \gamma B, \quad (1.47)$$

which does not depend on  $\gamma_e$ . The equation 1.47 is suitable in an adiabatic regime when the electron does not lose a relevant fraction of its energy by radiation. In this case  $\gamma_e$  must be less than a critical  $\gamma_c$ , which is when

$$\gamma \gamma_c m_e c^2 = P(\gamma_c) t, \quad (1.48)$$

so that

$$\gamma_c = \frac{6\pi m_e c}{\sigma_T} \cdot \frac{1}{\gamma B^2 t} = \frac{3m_e}{16\epsilon_B \sigma_T m_p c} \cdot \frac{1}{\gamma n^3 t}, \quad (1.49)$$

where the  $t$  refers to the observer-frame time [6].

Electrons with  $\gamma_e > \gamma_c$  lose energy in a time  $t$ , cooling down to  $\gamma_c$ . Doing this, the electron emission frequency decreases as  $\nu \propto \gamma_e^2$  (while the electron energy depends on  $\gamma_e$ ). Hence, if  $\nu(\gamma_c) = \nu_c < \nu < \nu(\gamma_e)$  the spectral power varies as  $\nu^{-1/2}$ . The complete

spectrum  $P_\nu$  then consists in three parts: a low-energy tail ( $\nu < \nu_c$ ) where  $P_\nu \propto \nu^{1/3}$ ; a power-law segment within  $\nu_c$  and  $\nu(\gamma_e)$  where  $P \sim \nu^{-1/2}$ ; and an exponential cutoff with  $\nu > \nu(\gamma)$  [6]. Thus, it is necessary to integrate over  $\gamma_e$  to calculate the total spectrum emits by a power-law distribution of electrons.

In the observer frame the frequency is

$$\nu_m \propto \gamma \tilde{B} \gamma_e^2, \quad (1.50)$$

where both the co-moving magnetic field  $\tilde{B}$  and the electron Lorentz factor  $\gamma_e$  could be proportional to  $\gamma$  [117]. This consideration implies that as  $\nu_m$  decreases in according to  $\gamma$ , the peak will move towards lower frequencies, and the spectrum would emit through X-rays, optical, IR and, finally, radio emissions in some weeks. The observation of a little linear polarization in some optical and IR afterglows (e.g. [170]) supports the synchrotron mechanism as afterglow emission.

For a spherical fireball propagating into an external environment, the bulk Lorentz factor as asymptotically decreases in time as  $t^{3/2}$  (in the adiabatic limit). The accelerated electron minimum random Lorentz factor and the turbulent magnetic field also decrease as the inverse power laws of the time.

The peak energy of the synchrotron corresponding to the time-dependent minimum Lorentz factor and magnetic field then moves to softer energies as  $t^{-3/2}$ . These energies can be generalized in a straightforward manner when in the radiative regime or in the presence of density gradients, etc [4].

As regarding the radio spectrum, it is expected optically thick in the beginning, because of self-absorption, and optically thin after some hours. Later about 10 minutes, the dominant radiation is emitted by the FS, and the flux at a given frequency  $\nu$  decays as

$$F_\nu \propto t^{-(3/2)\beta}, \quad (1.51)$$

while the synchrotron peak frequencies decreases as

$$\nu_m \propto t^{-3/2}, \quad (1.52)$$

both equations are valid as long as the expansion is relativistic. Eqs. 1.51 and 1.52 are referred to the standard (adiabatic) model, where a RS is not considered, and  $\beta = d \log F_\nu / d \log \nu$  is the photon spectral energy flux slope. In general, the relativistic FS

and its frequency peak follow these trends [4]:

$$\begin{aligned} F_\nu &\propto t^{\frac{3-2g}{1+2g}(1-2\beta)}, \\ \nu_m &\propto t^{\frac{-4g}{1+2g}}, \end{aligned} \quad (1.53)$$

where the constant  $g$  was introduced after the equation 1.39. However, a RS is expected with an initial optical high brightness, which should have a shorter decay than the FS. As for the transition to a non relativistic expansion can be seen in different works (e.g. in [171–173]).

At a given instant, its spectrum depends on the electronic energy co-moving distribution. The co-moving energy of an electron is  $\gamma_e m_e c^2$ , with bulk Lorentz factor  $\Gamma$ . The spectrum peak has a frequency observed

$$\nu = \Gamma \gamma_e \frac{e \tilde{B}}{2\pi m_e c}. \quad (1.54)$$

There are three electron characteristic energies associated to three frequencies: the injection frequency  $\nu_m$ , the cooling frequency  $\nu_c$ , the maximum synchrotron frequency  $\nu_M$ . However, it is possible to report a forth frequency  $\nu_a$ , at lower frequencies where the synchrotron self-absorption is present. Fixing a  $\Gamma$  (hence an  $r$  or a  $t$  too), an isotropic equivalent kinetic energy of the explosion, an electron index (reminding that  $p > 2$ ) and the efficiency factors  $\epsilon_e$  (the electron-proton coupling parameter),  $\zeta_e$ ,  $\epsilon_B$  (the magnetic coupling parameter), [4] reports these observer-frame frequencies depending on time, including the cosmological redshift:

$$\nu_m = 6 \cdot 10^6 \sqrt{(1+z) \epsilon_B E_{52}} \left( \frac{p-2}{p+1} \right)^2 \left( \frac{\epsilon_e}{\zeta_e} \right)^2 \left( \frac{t}{\text{day}} \right)^{-3/2} \text{GHz}, \quad (1.55)$$

$$\nu_c = 9 \cdot 10^3 [(1+z) \epsilon_B^3 E_{52}]^{-1/2} n^{-1} \left( \frac{t}{\text{day}} \right)^{-1/2} \text{GHz}, \quad (1.56)$$

where  $E_{52} = E/10^{52}$  erg and  $n$  in  $\text{cm}^{-1}$ . The synchrotron self-absorption frequency does not depend on the time and is

$$\nu_a = 2 [(1+z) \epsilon_e / \zeta_e]^{-1} [n^3 \epsilon_B E_{52}]^{1/5} \text{GHz} \quad (1.57)$$

and the maximum flux at a given frequency is

$$F_{\nu,\max} = 20(1+z) (n \epsilon_B)^{1/2} E_{52} d_{L,28} \text{ mJy}, \quad (1.58)$$

where the notation  $d_{L,28} = d_L/10^{28}$  cm.

There are two types of spectra, depending on whether  $\gamma_m > \gamma_c$  or  $\gamma_m < \gamma_c$ , that

correspond to  $\nu_m(\gamma_m) > \nu_c$  or  $\nu_m(\gamma_m) < \nu_c$  respectively. In the *fast cooling case* ( $\nu_m > \nu_c$ ) the flux has the following equations [4, 6]:

$$F_\nu = F_{\nu,\max} \cdot \begin{cases} (\nu_a/\nu_c)^{1/3}(\nu/\nu_a)^2, & \nu < \nu_a \\ (\nu/\nu_c)^{1/3}, & \nu_a \leq \nu < \nu_c \\ (\nu/\nu_c)^{-1/2}, & \nu_c \leq \nu < \nu_m \\ (\nu_m/\nu_c)^{-1/2}(\nu/\nu_m)^{-p/2}, & \nu_m \leq \nu \leq \nu_M \end{cases} \quad (1.59)$$

where, if  $N_e = 4\pi R^3 n/3$  is the number of swept-up electrons in the post shock fluid,  $F_{\nu,\max} \equiv N_e P_{\nu,\max}/(4\pi d_L^2)$  is the observed peak flux at a distance  $d_L$  from the source

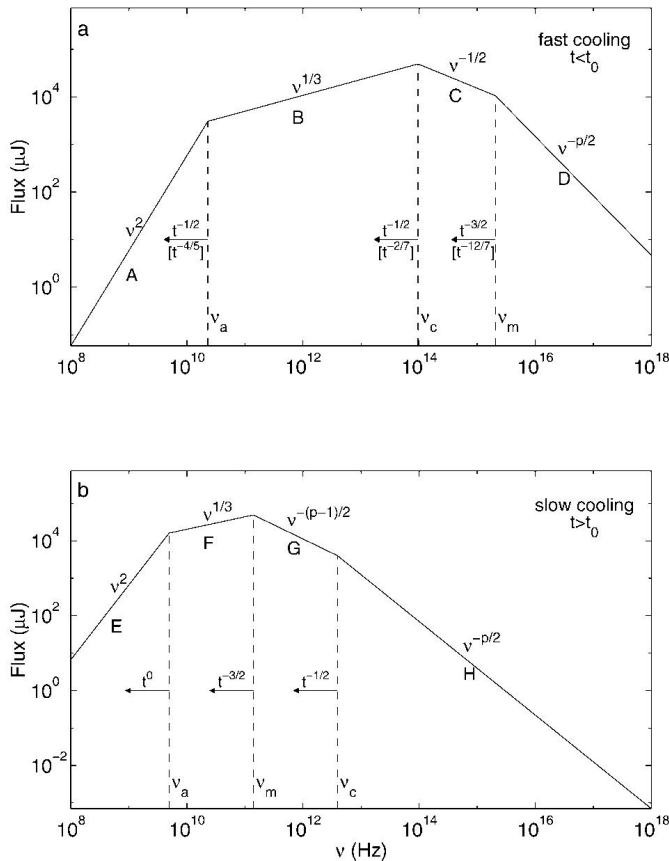


FIGURE 1.8: Synchrotron spectrum of a relativistic shock with a power-law electron distribution. In the upper sketch, the fast cooling is shown, which is expected at early times ( $t < t_0$ ). The spectrum consists of four segments, identified as A, B, C, and D. Self-absorption is important below  $\nu_a$ . The frequencies,  $\nu_m$ ,  $\nu_c$ , and  $\nu_a$ , decrease with time as indicated; the scalings above the arrows correspond to an adiabatic evolution, and the scalings below, in square brackets, correspond to a fully radiative evolution. Below, the slow cooling, which is expected at late times ( $t > t_0$ ). The evolution is always adiabatic. The four segments are identified as E, F, G, and H [6].

[6]. While, regarding to the *slow cooling case* ( $\nu_m < \nu_c$ ) the spectrum is [4, 6]:

$$F_\nu = F_{\nu,\max} \cdot \begin{cases} (\nu_a/\nu_m)^{1/3} (\nu/\nu_a)^2 & \nu < \nu_a \\ (\nu/\nu_m)^{1/3} & \nu_a \leq \nu < \nu_m \\ (\nu/\nu_m)^{-(p-1)/2} & \nu_m \leq \nu < \nu_c \\ (\nu_c/\nu_m)^{-(p-1)/2} (\nu/\nu_c)^{-p/2} & \nu_c \leq \nu \leq \nu_M \end{cases} \quad (1.60)$$

The trends of these cases are shown in figure 1.8. Table 1.1 is taken from [26], where the temporal indices  $\alpha$  and spectral indices  $\beta$  correspond to different FS spectral regimes of the previous equations 1.59 and 1.60, for a wind and a homogeneous external medium. A typical electron spectral index of shock acceleration is  $p \sim 2.2 - 2.5$  and it is compatible with the observations (e.g. [170]). As the expansion advances (and the density reduces) the emitted spectrum moves to longer wavelengths, and the flux starts to decay as a power law in time when it is observed in a given band. In this case the spectral index can change as the characteristic frequencies move through the spectrum. Some snapshots of afterglow spectra have been deduced by extrapolating measurements at different frequencies and time-frames, as in [169, 174]. In these works a time-depending model was used and a spherical symmetry was assumed. Changing physical parameters of the burst and environment, e.g. the total energy, the external medium density, the electron-proton and magnetic coupling parameters, various fits were obtained. Typical results are  $E \sim 10^{52} - 10^{54}$  erg,  $n_0 \sim 10^{-2} - 10$  cm $^{-3}$ ,  $\epsilon_e \sim 0.1 - 0.5$ ,  $\epsilon_B \sim 10^{-2}$ .

Before to close this section, some details about the RS. It is generally expected weakly relativistic as in the *thin shell case*, where the reverse electron Lorentz factor is

$$\gamma_e^r \sim \epsilon_e \frac{m_p}{m_e}, \quad (1.61)$$

while for the FS it is

$$\gamma_e^f \sim \epsilon_e \Gamma \frac{m_p}{m_e}. \quad (1.62)$$

The reverse electron emission is fainter than FS one. This because the RS has a total energy similar to the FS, but counts a number of electrons greater than  $\Gamma$  times, hence the energy per electron is  $\Gamma^{-1}$  times lower [164]. The pressure, and so the magnetic energy density, are the same both for the forward and the reverse shocked zone, therefore it is possible to write these relations [27]:

$F_{\nu,\max}^r = \Gamma F_{\nu,\max}^f$  The peak flux of the RS is larger than the FS, at any time, by a factor  $\Gamma$ .

$\nu_m^r = \nu_m^f / \Gamma^2$  The minimum electron frequency in the RS is lower than a  $\Gamma^2$  factor with respect to the FS.

$\nu_c^r = \nu_c^f = \nu_c$  The critical frequency is the same for both shocks when  $\epsilon_e$  is equal for both. In general, it is not true if a jet carries a strong magnetic field from the source

$\nu_a^{r,f} < \nu_m^{r,f}$  **and**  $\nu_a^{f,r} < \nu_c$  These relations are generally valid, as well as  $\nu_a^f < \nu_a^r$ . The flux temporal indices and characteristic frequencies for a standard afterglow are reported in table 1.2 for the r-case with  $s = 0$ .

Considerations and calculations regarding the afterglow light curves are present in [135], which is suggested to see. Figure 1.9 shows as the flux varies in time in the cases high frequency ( $\nu > \nu_0$ ) and low frequency ( $\nu < \nu_0$ ). The frequency  $\nu_0 = \nu_c(t_0) = \nu_m(t_0)$  follows from these equations:

$$\nu_c = \begin{cases} 1.3 \cdot 10^{13} \epsilon_B^{-3/2} E_{52}^{-4/7} \left(\frac{\gamma_0}{100}\right)^{4/7} n_1^{-13/14} \left(\frac{t}{\text{day}}\right)^{-2/7} \text{Hz} & \text{fully radiative evolution} \\ 2.7 \cdot 10^{12} \epsilon_B^{-3/2} E_{52}^{-1/2} n_1^{-1} \left(\frac{t}{\text{day}}\right)^{-1/2} \text{Hz} & \text{adiabatic evolution} \end{cases} \quad (1.63)$$

and  $t_0$  is the time when the transition between  $\nu_c$  and  $\nu_m$  occurs,

$$t_0 = \begin{cases} 210 \epsilon_B^2 \epsilon_e^2 E_{52} n_1 \text{ days} & \text{adiabatic,} \\ 4.6 \epsilon_B^{7/5} \epsilon_e^{7/5} E_{52}^{4/5} \left(\frac{\gamma_0}{100}\right)^{-4/5} n_1^{3/5} \text{ days} & \text{radiative.} \end{cases} \quad (1.64)$$

TABLE 1.1: Temporal index  $\alpha$  and spectral index  $\beta$  in various afterglow models, the convention  $F_\nu \propto t^\alpha \nu^\beta$  is adopted, from [6, 22–25]. The assumption  $\nu_a < \min[\nu_m, \nu_c]$  is made. (Under certain conditions, e.g. for the wind fast cooling case in some limited regime, the higher  $\nu_a$  case is relevant<sup>289</sup>, so that the values collected here are no longer valid). The jet model applies for the sideways expanding phase, which is valid for both ISM and wind cases and is usually in the slow cooling regime [26].

$\beta$	$\alpha (p > 2, p \sim 2.3)$	$\alpha(\beta)$	$\alpha (1 < p < 2, p \sim 1.5)$	$\alpha(\beta)$
<b>ISM, slow cooling</b>				
$\nu < \nu_a$	2	$\frac{1}{2}$		$\frac{17p-26}{16(p-1)} \sim -0.06$
$\nu_a < \nu < \nu_m$	$\frac{1}{3}$	$\frac{1}{2}$	$\alpha = \frac{3\beta}{2}$	$\frac{p+2}{8(p-1)} \sim 0.9$
$\nu_m < \nu < \nu_c$	$-\frac{p-1}{2}$	$\frac{3(1-p)}{4} \sim -1.0$	$\alpha = \frac{3\beta}{2}$	$-\frac{3(p+2)}{16} \sim -0.7$
$\nu > \nu_c$	$-\frac{p}{2}$	$\frac{2-3p}{4} \sim -1.2$	$\alpha = \frac{3\beta+1}{2}$	$-\frac{3p+10}{16} \sim -0.9$
<b>ISM, fast cooling</b>				
$\nu < \nu_a$	2	1		1
$\nu_a < \nu < \nu_c$	$\frac{1}{3}$	$\frac{1}{6}$	$\alpha = \frac{\beta}{2}$	$\frac{1}{6}$
$\nu_c < \nu < \nu_m$	$-\frac{1}{2}$	$-\frac{1}{4}$	$\alpha = \frac{\beta}{2}$	$-\frac{1}{4}$
$\nu > \nu_m$	$-\frac{p}{2}$	$\frac{2-3p}{4} \sim -1.2$	$\alpha = \frac{3\beta+1}{2}$	$-\frac{3p+10}{16} \sim -0.9$
<b>Wind, slow cooling</b>				
$\nu < \nu_a$	2	1		$\frac{13p-18}{8(p-1)} \sim 0.4$
$\nu_a < \nu < \nu_m$	$\frac{1}{3}$	0	$\alpha = \frac{3\beta-1}{2}$	$\frac{5(2-p)}{12(p-1)} \sim 0.4$
$\nu_m < \nu < \nu_c$	$-\frac{p-1}{2}$	$\frac{1-3p}{4} \sim -1.5$	$\alpha = \frac{3\beta-1}{2}$	$-\frac{p+8}{8} \sim -1.2$
$\nu > \nu_c$	$-\frac{p}{2}$	$\frac{2-3p}{4} \sim -1.2$	$\alpha = \frac{3\beta+1}{2}$	$-\frac{p+6}{8} \sim -0.9$
<b>Wind, fast cooling</b>				
$\nu < \nu_a$	2	2		2
$\nu_a < \nu < \nu_c$	$\frac{1}{3}$	$-\frac{2}{3}$	$\alpha = -\frac{\beta+1}{2}$	$-\frac{2}{3}$
$\nu_c < \nu < \nu_m$	$-\frac{1}{2}$	$-\frac{1}{4}$	$\alpha = -\frac{\beta+1}{2}$	$-\frac{1}{4}$
$\nu > \nu_m$	$-\frac{p}{2}$	$\frac{2-3p}{4} \sim -1.2$	$\alpha = \frac{3\beta+1}{2}$	$-\frac{p+6}{8} \sim -0.9$
<b>Jet, slow cooling</b>				
$\nu < \nu_a$	2	0		$\frac{3(p-2)}{4(p-1)} \sim -0.8$
$\nu_a < \nu < \nu_m$	$\frac{1}{3}$	$-\frac{1}{3}$	$\alpha = 2\beta - 1$	$\frac{8-5p}{6(p-1)} \sim 0.2$
$\nu_m < \nu < \nu_c$	$-\frac{p-1}{2}$	$-p \sim -2.3$	$\alpha = 2\beta - 1$	$-\frac{p+6}{4} \sim -1.9$
$\nu > \nu_c$	$-\frac{p}{2}$	$-p \sim -2.3$	$\alpha = 2\beta$	$-\frac{p+6}{4} \sim -1.9$

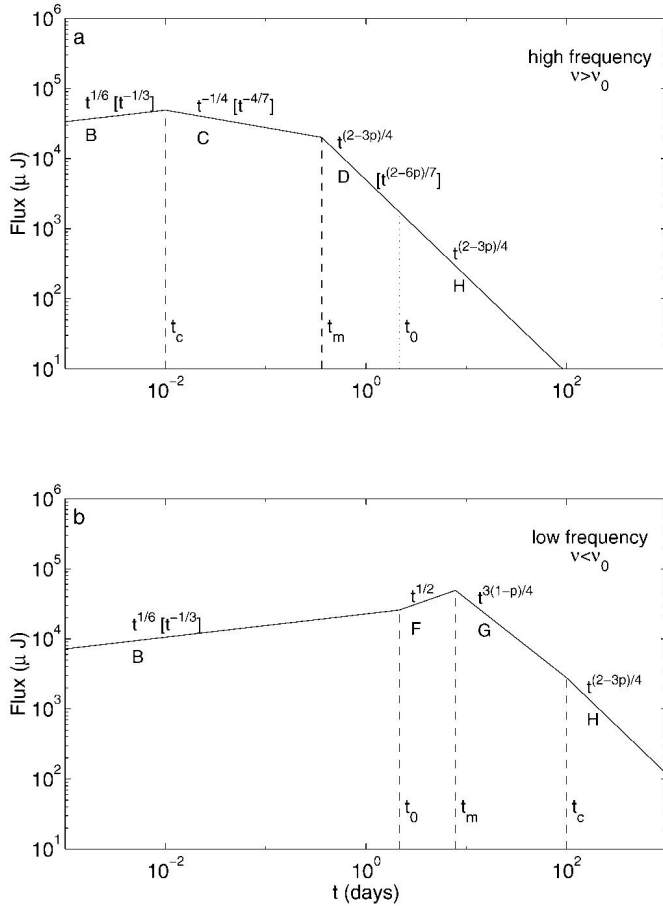


FIGURE 1.9: The synchrotron light curve plot is ignoring the self-absorption. In the upper panel the high-frequency case ( $\nu > \nu_0$ ) is represented. The four segments that are separated by the critical times,  $t_c$ ,  $t_m$ , and  $t_0$ , correspond to the spectral segments in 1.8 with the same labels (B, C, D, and H). The time dependence of the observed flux are reported on the slopes. The values within square brackets correspond to the radiative evolution (which is restricted to  $t < t_0$ ), whereas the other values correspond to adiabatic evolution. In the lower panel the low-frequency case ( $\nu < \nu_0$ ). Credit by [6].

TABLE 1.2: Temporal exponents of the peak frequency, the maximum flux, the cooling frequency and the flux at a given bandwidth (respectively,  $\nu_m$ ,  $F_{\nu_m}$ ,  $\nu_c$ ,  $F_\nu$ ) for the forward (f) and reverse (r) shocks. They are calculated in the adiabatic regime  $\nu_m < \nu < \nu_c$  ( $F_\nu \propto F_{\nu_m} (\nu_m/\nu)^\beta \propto t^{-\alpha} \nu^{-\beta}$ , where  $\beta = (p-1)/2$ ), and in the cooling regime  $\nu_c < \nu_m < \nu$  ( $F_\nu \propto (\nu_c/\nu_m)^{1/2} (\nu_m/\nu)^\beta \propto t^{-\alpha} \nu^{-\beta}$  where  $\beta = p/2$ ). For  $s = 1$  this gives the usual (i.e. without “refreshment”) forward and reverse shock behaviour [4, 27, 28].

Shock	$\nu_m$	$F_{\nu_m}$	$\nu_c$	$F_\nu$	
				$\nu_m < \nu < \nu_c$	$\nu > \max(\nu_c, \nu_m)$
f	$\frac{24-7k+sk}{2(7+s-2k)}$	$\frac{6s-6+k-3sk}{2(7+s-2k)}$	$-\frac{4+4s-3k-3sk}{2(7+s-2k)}$	$-\frac{6-6s-k+3sk+\beta(24-7k+sk)}{2(7+s-2k)}$	$-\frac{-4-4s+k+sk+\beta(24-7k+sk)}{2(7+s-2k)}$
r	$-\frac{12-3k+sk}{2(7+s-2k)}$	$\frac{6s-12+3k-3sk}{2(7+s-2k)}$	$-\frac{4+4s-3k-3sk}{2(7+s-2k)}$	$-\frac{12-6s-3k+3sk+\beta(12-3k+sk)}{2(7+s-2k)}$	$-\frac{8-4s-3k+sk+\beta(12-3k+sk)}{2(7+s-2k)}$

## 1.7 Jets

One of the most common assumptions regarding GRB is the isotropic emission of the burst, but it is not really so. All the energy with particles and photons are principally collimated in a relativistic jet, mentioned already in the previous sections. Nonetheless this assumption, the spherical-emission approximation is valid even for outflows collimating into jets of narrow solid angles, as well as the spherical snapshots spectral fits remain valid, because the assumption simply constrains the energy per solid angle only. Along the outflow direction is generated a light cone contained within a solid angle  $\Omega_j$  and the bulk Lorentz factor related to the ejecta is usually  $\Gamma \gtrsim \Omega_j^{-1/2}$  [114]. Outside this angle, nothing can be observed and the GRB cannot be detected. However, while the jet decelerates due to the interstellar medium,  $\Gamma$  decreases its value, the light-cone angle increases and variations are expected in the dynamics and light curve of the outflow. The jet opening angle is a formula depending on the observer time  $t_j$  at which the flux decay rate achromatically slips to a steeper value. At this time it is assumed that light-cone angle (or causal angle)  $\Gamma(t)^{-1}$  becomes comparable with the jet half-angle  $\theta_j$ , but later  $\Gamma(t)^{-1} > \theta_j$ . Assuming a standard adiabatic dynamics and a uniform distribution of the external medium, that jet opening half-angle is [4]

$$\theta_j \simeq 5^\circ \left( \frac{t_j}{\text{day}} \right)^{3/8} E_{\gamma,\text{iso},53}^{-1/8} n_{\text{ext}}^{1/8} \left( \frac{\eta_\gamma}{0.2} \right)^{1/8} \left( \frac{1+z}{2} \right)^{-3/8} \quad (1.65)$$

where  $E_{\gamma,53}$  is the isotropic equivalent  $\gamma$ -ray energy and  $\eta_\gamma$  is the radiative efficiency. When the causal angle is smaller than  $\theta_j$ , the radiation is emitted from an effective transverse surface

$$A \simeq r_\perp^2 \sim \left( \frac{r}{\Gamma} \right)^2 \propto \Gamma^2 t^2. \quad (1.66)$$

This area is different when the causal angle becomes larger than  $\theta_j$

$$A \simeq r^2 \theta_j^2. \quad (1.67)$$

After the break the flux becomes steeper, indeed the previous adiabatic behaviour with  $\Gamma \propto t^{-3/8}$  has a new factor  $\Gamma^2 \propto t^{-3/4}$ . If the collimation of the jet is not due to particular dynamical or magnetic effects, the ejecta is purely ballistic and can start expanding sideways. These sideways have co-moving speed of sound and lead to different decay  $\Gamma \propto t^{-1/2}$  and  $F \propto t^{-p} \propto t^{-2}$  [4].

Although Eq. 1.65 and its assumption of a uniform density of the external medium fit many afterglow, sometimes a wind-like distribution in the medium is preferred so that  $n_{\text{ext}} \propto r^{-2}$ . However, for a generic distribution  $n_{\text{ext}} \propto r^{-k}$  leads to a more general

expression of the collimation angle:

$$\theta_j \propto \left(\frac{E}{A}\right)^{-\frac{1}{8-2k}} \left(\frac{t_j}{1+z}\right)^{\frac{3-k}{8-2k}}. \quad (1.68)$$

Relativistic jets passing through an external medium with a wind-like density distribution may give rise to a shallow and very gradual break in the afterglow light curve [4].

Rescaling the isotropic energy of GRBs into the collimated ejecta, the original burst energy spread ( $E_{\gamma,\text{iso}} \sim 10^{51} - 10^{54}$  erg) is reduced by a magnitude and the mean value of a GRB becomes  $E_{\gamma,\text{iso}} \sim 1.3 \cdot 10^{51}$  erg. This energy is comparable with the core-collapse kinetic energy of SNe but, differently from this case, GRBs emit in gamma band and within a more collimated jet. Even considering the energy due to particles and magnetic fields to add to radiative inefficiencies, the resulting value maintains lower than  $10^{53.5} - 10^{54}$  erg. These upper limit are associated to either very-compacted object (NS-NS, NS-BH) mergers, or collapsar models by using magnetic hydrodynamics of the spin energetic of a central fast spinning BH and/or a torus disrupted. For more details see [4] and references therein.

An analytical discussion about the development of a jet and its  $\Gamma_j$  in a collapsar can be read in [175–178], but here some points are briefly summarized. In a massive-star burst, the jet blows as long as the central BH accretes, ejecting matter along the rotation axis with a relativistic speed. The dimensionless entropy of this jet must be comparable to or greater than the final bulk Lorentz factor once it has emerged from the star,  $\eta = L/Mc^2 \gtrsim \Gamma_j \gtrsim 100$  [4]. Although the jet has relativistic speeds when it is ejected, the jet head is quickly slowed down to sub-relativistic speeds of advance by the overburden of the stellar core and envelope. Its advance motion will gradually increase due to the density gradient of the star. Because of this speed difference the faster gas crashes into the slower one causing a spillover of energy and gas into a trans-relativistic cocoon which wastes heat around the jet and may be detected [145, 179]. Before to reach the He-core boundary layer ( $R_{\text{He}} \sim 10^{11}$  cm), the jet head will have a speed of  $v_i \sim c$  [4]. In the frame of the burst, this phase takes about 10 s, therefore this central engine must inject energy and momentum into the jet for at least this time. After the He-core border the density dramatically changes and an envelope with power-low extending hydrogen is expected. In this environment the  $\Gamma_j$  of jet head may reach a velocity similar to its final value ( $\Gamma \gtrsim 100$ , [177, 178]), after which it becomes ballistic and does not depend anymore on ejected matter from the BH. In accordance to [176], the mass overburden within the jet solid angle must be lesser than the total energy of the jet energy and divided by  $\Gamma_j c^2$ . Wolf-Rayet type stars may preserve this constrain, since their envelopes are swept by a stellar wind phase previous to the core collapse. They should lead to type Ib/c SNe,

which are the only SNe so far associated with some GRBs, as mentioned above. Regarding as relativistic jet ejected from a star it is possible to consult the literature, e.g. [180, 181].

## 1.8 Gamma band vs Radio band

In this first chapter a piece of the status of art about GRB studies has been reported, focusing the attention on the physical emission processes and the behaviour of the spectrum during the GRB emission, in particular about afterglow phase. The next chapter closes the part I and lists satellite missions dedicated to GRB observation used for last years. This is useful for giving an idea about observational energies, features and a general overview of the instrumentation to observe these sources outside the Earth's atmosphere.

Techniques used for gamma observations are very different from those used by any radio telescope. In front of all, a trivial but relevant point, observations are ground-based. In this sense, the chapters 2, 3 and 4 describe and highlight instruments and observational techniques for GRBs.

Even though GRBs are firstly detectable in gamma band, now it is clear how their remnants span and emit to a large range of frequencies. Therefore, it is true that satellite observations are the primary step for the GRB detection but they are not and cannot be the only observational channel. Moreover, satellite missions are even very expensive, with limited lifetimes and something could go amiss (e.g., malfunctioning, mission delays, wrong orbiting, etc). This does not mean to reduce the satellite GRB investigations but of supporting such missions with ground telescopes, promoting research towards lower frequencies. It is important to remember that radio band is not affected by radiation extinction, contrary to higher frequency. An accurate calorimetry for radio well-detectable GRBs would be possible. In addition, radio observations can obtain estimations of the effectiveness of the inverse Compton effect, since only radio frequencies can probe the density of the interstellar medium. In the end, redshift measures of the host galaxies can be obtained observing the hydrogen spin-flip at 1.4 GHz, to associate this fundamental information to GRBs.

In the following, radio data and observational considerations from recent works are reported. Furthermore, it is discussed what future technologies could contribute to an accurate radio study about GRBs.



## Chapter 2

# Satellite missions

In chapter 1 an overview has been written, reporting GRB studies carried out so far. Some satellite missions has been mentioned there and in this chapter most of gamma satellite missions are listed. The concept of satellite observation is extremely different from any other on-ground observation. Even though the space observations give the chance to detect radiations that will never reach to Earth, they are limited to the planned instrumentation. Nothing can be changed when a satellite is in orbit and no error is permitted. By describing various missions, it will be clear how each instrument was/is centered on a particular range of frequencies, in order to analyze a part of the  $\gamma$ -ray or X-ray spectrum.

This chapter describes a brief chronicle about gamma satellite missions that is useful as summary for a fast check of instrumentation on-board and its technical information. Here Field of View (FoV), angular resolution and material of detectors are reported. In general, a solid proportional counter is more precise than a gas detector, because the former can better estimate the colliding photon position. This and other details can be appreciated by comparing the tables of the different missions. Mission by mission the technology improves and detection precision increases.

Following information and figures have been mainly taken from the European Space Agency (ESA) and National Aeronautics and Space Administration (NASA) websites and a plenty of mission papers. Every satellite in this chapter has contributed to the publication of, at least, one GRB catalogue. These catalogues have been consulted for creating a unique catalogue described in chapter 5 and reported in the appendix of this thesis.

## 2.1 ULYSSES

The spacecraft was launched in the 6 October 1990 and Ulysses completed its mission in March 2008. This satellite had as principal aim the study of the Sun (magnetic field, cosmic rays, ions, etc.) and Jovian environment, but a part of its instrumentation was dedicated to cosmic GRBs. Only one instrument Gamma Ray Burst was sensitive at X-ray band (15 - 150 keV). This payload had to measure solar X-ray and cosmic gamma-ray bursts. It consisted of two detectors for soft ( $\sim$ 5 - 20 keV) and hard (15 - 150 keV) X-rays. A sketch of them is showed in figure 2.1.

None of those detectors had any angular resolution, indeed the GRB localization on Ulysses was done by triangulation and an accuracy of roughly an arcminute was reached in the best cases.

### 2.1.1 Hard X-ray detectors

The system consists of two hemispherical, 3 mm thick by 51 mm diameter CsI(Tl) scintillation crystals mounted via a plastic light guide to two photomultiplier tube detectors. It could see almost all the sky in the 15-150 keV energetic band ([7]).

### 2.1.2 Soft X-ray detectors

The soft X-ray sensors were designed as solar X-ray monitors. The energy band was  $\sim$  5 – 20 keV. A 100 mg/cm<sup>2</sup> beryllium foil front window rejects low energy X-rays and defines a conical field of view of 75° half-angle ([7]).

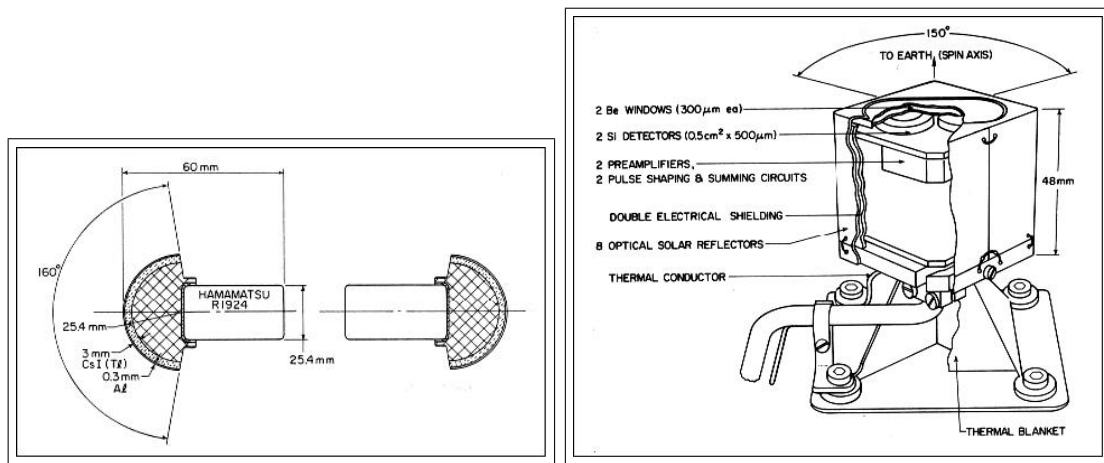


FIGURE 2.1: Here two sketches of Hard X-ray (left) and Soft X-ray detectors (right) are showed [7].

Unfortunately, these detectors never worked properly, because, during the storage period before launch, they became noisy and could not be replaced.

## 2.2 INTERNATIONAL GAMMA-RAY ASTROPHYSICS LABORATORY - INTEGRAL

Launched in October of 2002, still orbiting and operating, this ESA scientific mission is dedicated to celestial gamma-ray sources, using fine spectroscopy plus fine imaging thanks to its angular resolution of  $12'$  (FWHM). The energy range sensitivity is between 15 keV and 10 MeV, with concurrent source monitoring in the X-ray (3 - 35 keV) and optical (V-band at 550 nm) energy ranges. For an overview of the mission, information can be found in NASA-HEASARC website ([182]). INTEGRAL has get four instrument and for more specifications you can read [183].

### 2.2.1 SPectrometer on INTEGRAL (SPI)

This spectrometer is dedicated to spectral analyses of gamma-ray point-like sources and extended regions in the 20 keV - 8 MeV energy range. A hexagonal coded aperture mask is located 1.7 m above the detection plane in order to have a (fully coded) FoV of  $16^\circ$  with an angular resolution of  $\sim 2^\circ$ . For details see [184].

### 2.2.2 Imager on Board the Integral Satellite (IBIS)

The Imager IBIS provides a fine imaging in the energy range 15 keV - 10 MeV. A tungsten coded-aperture mask is at 3.2 meters above the detection plane and it is optimized for high angular resolution of  $12'$  (FWHM). The detector consists of two detects in tow planes: the upper is the Integral Soft Gamma-Ray Imager (ISGRI), with a  $2600 \text{ cm}^2$  layer of CdTe pixels, works in 15 keV - 1 MeV energy range; the bottom is the PIxellated Ceasium Iodide, with a  $3100 \text{ cm}^2$  layer of CsI pixels,covers 175 keV - 10 MeV energy range. The arrays are separated by 90 mm. A sketch of IBIS is shown in figure 2.2. In table 2.1 it is possible to read some characteristics of the IBIS.

### 2.2.3 Joint European X-Ray Monitor (JEM-X)

This instrument, combined with IBIS and SPI, improves the gamma-ray sources detection and identification, while the Integral gamma-ray improves data analysis and

TABLE 2.1: Some specifications of IBIS [29].

Parameter	Value
Energy range	15 keV - 10 MeV
Field of view:	8.33° × 8.00° (fully coded) 29.11° × 29.42° (zero response)
Angular resolution (FWHM)	12'
Point source location accuracy (90% error radius):	1' for SNR = 30 (ISGRI) 3' for SNR = 10 (ISGRI) 5' – 10' for SNR = 10 (PICsIT)

scientific interpretation. JEM-X provides images with an angular resolution of 3' in the 3-35 keV energy band. It consists of two identical instruments and uses the coded-mask technique for imaging, like the first ones. In table 2.2 a summary of its characteristics is listed.

TABLE 2.2: Some specifications of the JEM-X [30].

Parameter	Value
Energy range	3-35 keV
Field of view:	4.8° fully coded 7.5° half response 13.2° zero response
Angular resolution (FWHM)	3'
Point source location accuracy	1' (90% confidence, 15 $\sigma$ isolated source)
Typical Source Location (10 $\sigma$ source)	< 3'

#### 2.2.4 Optical Monitoring Camera (OMC)

The OMC catches photons in 500-850 nm wavelength range, allowing long observations of the visible light coming from gamma-ray and X-ray sources. In table 2.3 some characteristics are reported.

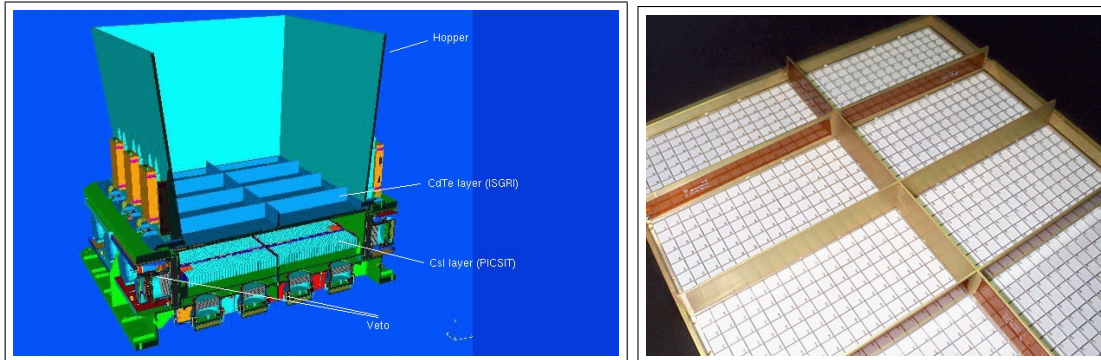


FIGURE 2.2: The figures show, on the left, the Imager IBIS in its whole scheme. On the right a detail on ISGRI. Figures taken from [8].

TABLE 2.3: Some specifications of the OMC [31].

Parameter	Value
Field of view	$4.979^\circ \times 4.979^\circ$
Angular resolution	$\sim 23''$ Gauss PSF (FWHM = $1.3 \pm 0.1$ pix)
Pixel size	$(13 \times 13)\mu\text{m}^2 = (17.5 \times 17.5) \text{ arcsec}^2$
Point source location accuracy	$\sim 2''$

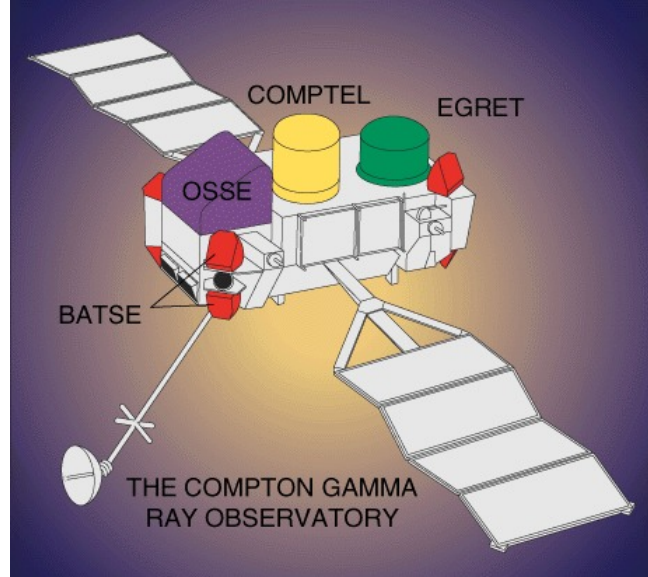


FIGURE 2.3: The CGRO satellite with its instruments in highlight [9].

## 2.3 Compton Gamma Ray Observatory

This mission is better known with its acronym CGRO and it was launched by NASA on the 5<sup>th</sup> April 1991. The satellite would have lasted for longer time, but one of its three stabilizing gyroscopes failed in December 1999<sup>1</sup>. It was safely de-orbited and re-entered the Earth's atmosphere on the 4<sup>th</sup> June 2000. CGRO was made up by four instruments: the Burst And Transient Source Experiment (BATSE); the Imaging Compton Telescope (COMPTEL); the Energetic Gamma Ray Experiment Telescope (EGRET); the Oriented Scintillation Spectrometer Experiment (OSSE). They covered a band of the electromagnetic spectrum from 30 KeV up to 30 GeV.

In figure 2.3 a draw of the satellite can be seen, whereas in table 2.4 it is possible to read some characteristics of each detector. Additional references about instrumentation and CGRO satellite can be found in [185].

The most important result of this satellite was the discover of the bi-modal distribution of GRB durations mentioned in chapter 1.

<sup>1</sup><http://spaceflightnow.com/cgroddeorbit/index.html>

### 2.3.1 Burst And Transient Source Experiment (BATSE)

BATSE was the principal detector dedicated to GRB observations. Since those objects came from any direction in the sky, it corroborated that they have cosmological origin. Moreover, it showed luminosity curves, leading off the first analyses about these mysterious phenomena. Its catalogue, containing 2702 detections, has been considered in chapter 5.

This detector served as the all-sky monitor for the CGRO, detecting and locating strong gamma transient sources (exactly the GRBs) as well as outbursts from other sources over the entire sky. There were eight BATSE detectors, one facing outward from each corner of the satellite, sensitive to gamma-ray energies  $\sim 25 - 2000$  keV. When gamma rays struck the NaI crystals inside the BATSE detectors, a flash of visible light was produced, caught and recorded by light-sensitive detectors. That signal was analyzed to determine the arrival time and energy of the original gamma ray [186].

### 2.3.2 Imaging Compton Telescope (COMPTEL)

The COMPTEL utilized the Compton effect and two layers of gamma-ray detectors to reconstruct an image of a gamma-ray source in the energy range from 1 to 30 MeV. Gamma rays from active galaxies, radioactive SN remnants, and diffuse gamma rays from giant molecular clouds could be studied. A part of the instrument was dedicated to a *burst mode* on two different energy ranges ( $\sim 0.1 - 1$  MeV and  $\sim 1 - 10$  MeV); these detectors are sensitive to incident radiation over 4 steradians.

The telescope had two layers of detectors. The upper detectors were filled with a liquid scintillator that scattered an incoming gamma-ray photon according to the Compton effect. Scattered photon was then absorbed by NaI crystals in the lower detectors. The instrument recorded in each layer of detectors all events data (time, location and energy), determining the direction and energy of the original gamma-ray photon and so reconstructing the source image and energy spectrum [187, 188].

### 2.3.3 Energetic Gamma Ray Experiment Telescope (EGRET)

The EGRET provides the highest energy gamma-ray window for the satellite. Its energy range is from 20 MeV to 30 GeV. It is from 10 to 20 times larger and more sensitive than previous detectors operating at these high energies. EGRET has made detailed observations of high-energy processes associated with diffuse gamma-ray emission, GRBs, cosmic rays, pulsars, and active galaxies, later known as blazars (this last objects, placed at cosmological distances, were discovered just by EGRET).

This instrument produces images using high-voltage gas-filled spark chambers. High-energy gamma-rays enter the chambers, producing an electron-positron pair which causes sparks. The particle path is recorded allowing the direction of the original gamma-ray to be determined. The particle energies are recorded by a NaI crystal below the spark chambers providing a measure of the original gamma-ray energy [189].

### 2.3.4 Oriented Scintillation Spectrometer Experiment (OSSE)

The OSSE consists of four NaI scintillation detectors, sensitive in the 0.05 - 10 MeV energy range. Each of these detectors can be individually pointed. This allows observations of a gamma-ray source to be alternated with observations of nearby background regions. An accurate subtraction of background contamination can then be made.

This instrument had to produce observations of the energy spectrum of nuclear lines in solar flares, the radioactive decay of nuclei in supernova remnants, and the signature of electron-positron annihilation in the Galactic center region [190].

TABLE 2.4: Summary of the CGRO detector characteristics. Here it is also indicated the detection position precision. This table has been taken by the website of Astrophysics Science Division at NASA/GSFC [32].

Instrument	Energy Range	FoV	Position Localization
OSSE	0.06 - 10.0 MeV	$3.8^\circ \times 11.4^\circ$	$10'$ square error box (Special mode: $0.1 \times$ Crab spectrum)
COMPTEL	0.8 - 30.0 MeV	$\sim 64^\circ$ (half angle)	$0.5^\circ - 1^\circ$ (90% confidence $0.2 \times$ Crab spectrum)
EGRET	20 MeV - 30 GeV	$\sim 0.6$ sr	$5'$ to $10'$ (1s radius; $0.2 \times$ Crab spectrum)
BATSE (Large area)	30 keV - 1.9 MeV	$4\pi$ sr	$3^\circ$ (strong burst)
BATSE (Spectroscopy)	15 keV - 110 MeV	$4\pi$ sr	—

## 2.4 BeppoSAX

SAX satellite, Italian acronym of “*Satellite per l’Astronomia X*”, was a program of the Italian Space Agency (ASI) with participation of the Netherlands Agency for Aerospace programs (NIVR). It was launched on the 30<sup>th</sup> April 1996 and renamed BeppoSAX in honor of Giuseppe Occhialini. The SAX finished its mission on the 30<sup>th</sup> April 2002, re-entering in atmosphere on the 29<sup>th</sup> April 2003.

The payload could observe at a range between 0.1 and 300 keV. It was made up by the Narrow Field Instruments (NFI) plus the Wide Field Camera (WFC) instruments. The NFI consists of four co-aligned detectors: one Low Energy Concentrator Spectrometer (LECS), three Medium Energy Concentrator Spectrometers (MECS), one High Pressure

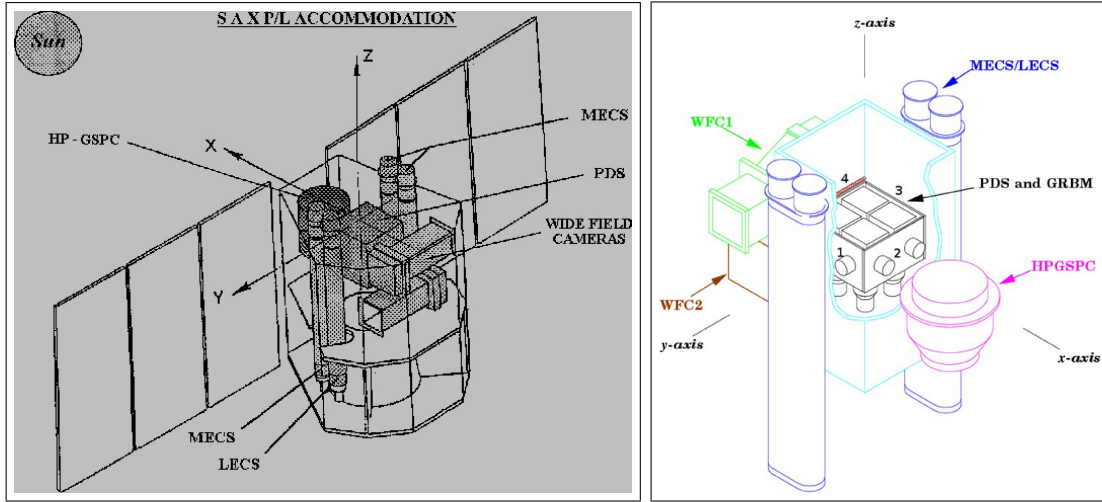


FIGURE 2.4: The figures show, on the left, the BeppoSAX satellite for whole. On the right, a back-zoom of the payload [10, 11].

Gas Scintillation Proportional Counter (HPGSP) and one Phoswich Detector System (PDS). The WFC instruments are tow units sensitive between 2-30 keV, with a field of view  $20^\circ \times 20^\circ$ . They are perpendicular to the NFI axis and point in opposite directions to each other. See figure 2.4 for a sketch of the satellite and its instrumentation. For a more details see [10, 33–36, 191].

#### 2.4.1 Low Energy Concentrator Spectrometer (LECS)

The LECS is a low energy (0.1 - 10.0 keV) telescope, identical to the other three MECS telescopes, but with a thin window position sensitive gas scintillation proportional counter in its focal plane. The detector unit consists of a gas cell, a photo-multiplier tube, front end electronics and two high-voltage supplies.

In table 2.5 some useful characteristics are reported: its field of view is  $\sim 0.3$  square degrees<sup>2</sup>; its angular resolution at 0.28 keV is  $9.7'$  at the Full Width at Half Maximum (FWHM), whereas at 6 keV is  $2.1'$  at the FWHM. Further and complete information can be read in [33].

#### 2.4.2 Medium Energy Concentrator Spectrometers (MECS)

A medium energy (1.3-10 keV) set of three identical grazing incidence telescopes with double cone geometry ([192, 193]), with position sensitive gas scintillation proportional counters in their focal planes ([194] and references therein). From table 1 in [34], table 2.6 is extracted.

<sup>2</sup>If  $\Omega$  is a solid angle and  $\alpha$  is the whole (plane) angle subtended by a cone, then  $\Omega = 2\pi \cdot (1 - \cos \alpha/2)$ . Remembering also that  $1\text{deg}^2 = (\pi/180)^2 \text{ sr}$ .

TABLE 2.5: In the FoV, “ $37'$  diameter circular” is equivalent to say 0.299 square degrees. The FWHM is the Full Width at Half Maximum of the total Gaussian signal. The energies are the central values of the two band windows of the range 0.1 - 10.0 keV. This table is part of the original table 1 in [33].

Parameter	Value
Field of View	$37'$ diameter circular
Angular resolution:	
arcmin at 0.28 keV	$9.7'$ FWHM
arcmin at 6 keV	$2.1'$ FWHM
Image pixel dimension	$17.4''$ by $17.4''$ square
Entrance window size	20 mm diameter

TABLE 2.6: The FoV value reported in the table is equivalent to 0.685 square degrees. The way to write  $r_{50}$  and  $r_{80}$  indicates the angular resolution values at radii encircling 50% and 80% of the total signal. The angular resolution energies are the central values of the three band windows of the energy range [34].

Parameter	Value
Energy Range	1.3 - 10 keV
Field of View	$28'$ radius
Angular resolution:	
arcsec at 1.5 keV	$r_{50} = 105''$ ; $r_{80} = 165''$
arcsec at 6.4 keV	$r_{50} = 7''$ ; $r_{80} = 150''$
arcsec at 8.1 keV	$r_{50} = 7''$ ; $r_{80} = 15''$
Image pixel dimension	$20''$ by $20''$ square

### 2.4.3 High Pressure Gas Scintillation Proportional Counter (HPGSP)

The basic mechanism of this instrument is quite well known and has been extensively described by different authors [195, 196].

After penetrating the beryllium window, the X-ray photon is absorbed by Xenon atoms via the photoelectric effect, since the photons enter a cell filled with Xenon (90%) and Helium (10%) gases at 5 atm. The photoelectron emitted gives rise to a localized cloud of secondary electrons at the position of X-ray absorption. After drifting through the so called drift region, the electron cloud, driven by a electric field, enters a scintillation region with higher electric field and in which the electrons acquire enough energy to excite the Xenon atoms. As a result of collisions, the excited atoms form excited diatomic Xenon molecules which then de-excite by the emission of vacuum ultra violet photons in the 1500-1950 Å range.

### 2.4.4 Phoswich Detector System (PDS)

The PDS consists of a square array of four independent NaI(Tl)/CsI(Na) scintillation detectors. A system be independently rocked back and forth to allow the simultaneous

monitoring of source and background. Its energy range was between 15-300 keV and with its high sensitivity, especially in the 20-100 keV band, this instrument offered the opportunity to perform observations of key importance in the hard X-ray band. The alternating current lateral shields are also used as *Gamma-Ray Burst Monitor* (GRBM). Finally a particle monitor provides information on high fluxes of environmental particles and triggers actions to prevent the damage of the detectors photo-multipliers.

For this work is important to highlight the GRBM capability. The lateral shields of the PDS were in fact used as detectors of GRBs of cosmic origin. The signals from each of the slabs in a programmable energy band, from  $\sim 20$  up to 600 keV, were sent to both a GRBM logic unit and a Pulse Height Analyzer, where the trigger condition was checked. A GRB event was triggered when at least two of the four lateral shields met the trigger condition. In this way it was expected to reduce the rate of false triggers caused by interactions of high energy particles in the shields. When a GRB condition was verified, the burst time profiles in the entire energy band from each of the four detectors were stored, together with the absolute time of the trigger occurrence [35]. A summary table of PDS features in 2.7.

TABLE 2.7: Some PDS characteristics, extracted from table 1 of [35].

Parameter	Value
Energy range	15-300 KeV
Effective area	640 cm <sup>2</sup>
Field of view (FWHM)	1.3° hexagonal
Minimum channel width of energy spectra	0.3 keV

#### 2.4.5 Wide Field Cameras (WFCs)

The WFCs were two 2-dimensional detectors consisted of energy sensitive proportional counters, filled with a Xenon gas at 2 atm, for position and energy. Both detectors were placed behind a metal coded-mask, useful to determine the sky position of a source. They could carry out spatially-resolved simultaneous monitoring of compact X-ray sources in crowded fields with high sensitivity, allowing for systematic spectral variability studies of different compact X-ray sources types over a large range of timescales. It could observe various classes of astrophysical objects with X-ray emission, ranging from nearby stars to active galactic nuclei, and X-ray spectrum of GRBs too. In addition, the WFCs monitored large sky regions for previously unknown X-ray sources, such as black hole candidates and neutron stars, for follow-up studies with the NFIIs on-board BeppoSAX. The field of view is 20° square (FWHM), though sources can be detected with less sensitivity in a field of 40°  $\times$  40° in total. The angular resolving power is 5 arcmin (FWHM), determined by the mask-detector distance, the size of the single mask elements

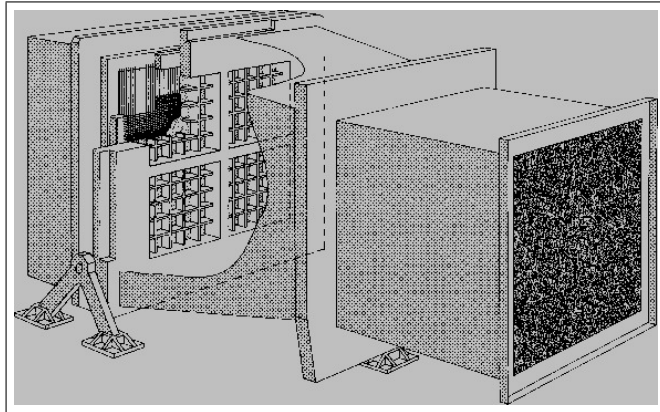


FIGURE 2.5: Sketch of a WFC. In the right part of the picture the coded-mask can be seen, while after 70 cm the described detector is shown. Between the detector and the mask there is a stainless steel structure to detect only X-ray photons.

( $256 \times 256$  in total) of about  $1 \times 1 \text{ mm}^2$  and, finally, the position detector resolution. A draw of it is shown in figure 2.5 and a summary of its characteristics are listed in table 2.8.

TABLE 2.8: Some WFC characteristics, extracted from table 1 of [36].  
 \*  $1mCrab \approx 2.410^{11} \text{ ergs}^{-1} \text{ cm}^2$  in the 210 keV X-ray band.

Parameter	Value
Energy range	1.8-28 keV
Effective area	$140 \text{ cm}^2$
Field of view	$20^\circ \times 20^\circ$ (FWHM)
Angular resolving power	5 arcmin
Source location accuracy	< 1 arcmin
Sensitivity in $10^5$ s	few mCrab*

## 2.5 High Energy Transient Explorer - HETE-2

This project was an international collaboration between USA, Japan, France, and Italy. The first HETE was lost during the launch on the 4<sup>th</sup> November 1996. A second launch was performed on the 9<sup>th</sup> October 2000. HETE-2 was fully operational on February 2001 and disused on October 2006. The satellite was designed to detect and localize GRBs. Indeed, its primary goal was to determine their origin and nature by simultaneous observation of soft and medium X-rays and gamma-rays. It is important to underline that the most of missions could detect from gamma band up to X-ray band, because gamma scintillators was not so precise to locate source coordinates, contrary to the X-ray detectors. In order to avoid imprecisions and to provide a precise localization, HETE-2 (and other satellites) used an observational large spectrum for an identification of counterparts to these explosions. Its energy range was between 0.5 and 400 keV.

The payload of this satellite was made up by two X-ray (0.5-25 keV) detectors and a gamma-ray telescope (6-400 keV): Soft X-ray Camera + Wide-field X-ray Monitor and French Gamma-ray Telescope, respectively. All instruments pointed in the anti-solar direction, sharing a common field of view of  $\sim 1.5$  sterad.

Initially, a processing software allowed the location to be calculated in real time on-board. Subsequently, ground post-burst analyses provided refined localizations.

### 2.5.1 Soft X-ray Camera (SXC)

This detector consisted in a pair of two CCD-based one-dimensional and a coded-aperture for X-ray images, a CCD localized X-rays parallel to the spacecraft X-axis, while the other was parallel to the Y-axis. Its energy range is 0.5 - 2 keV (a range in which a significant fraction of a GRB's energy might be radiated). Because of the small CCD pixel size ( $7.2 \text{ cm}^2$ ), the angular size of a SXC pixel is only 33 arcsec, in a field of view of 0.9 sterad. Table 2.9 reports some characteristics, while figure 2.6 shows an image of the SXC detector. [37].

TABLE 2.9: Some SXC characteristics [37].

Parameter	Value
Energy range	0.5-2 keV
Effective area	$7.2 \text{ cm}^2$
Field of view	0.91 sr
Focal Plane scale	33'' per CCD pixel
Localization Precision:	
Faint Burst	5 sigma - 15''
Bright Burst	22 sigma - 3'' (1 Crab; 10s)

### 2.5.2 Wide-field X-ray Monitor (WXM)

This detector consists of two identical units of one-dimensional position sensitive X-ray detectors. As the SXC, they are oriented orthogonally to each other. One WXM unit consisted of a one-dimensional coded mask and two 1-D position-sensitive proportional counters placed around 20 cm below the mask. The detection area of  $120 \times 83.5 \text{ mm}^2$  at the top side is sealed by  $100\mu\text{m}$ -thick Be windows [38]. Table 2.10 lists some specifications and figure 2.7 shows the complete detector. For details see [12].

### 2.5.3 French Gamma Telescope (FREGATE)

FREGATE was used as a burst trigger and to have moderate resolution spectra. Its principal objectives are the detection and spectroscopy of gamma-ray bursts and the

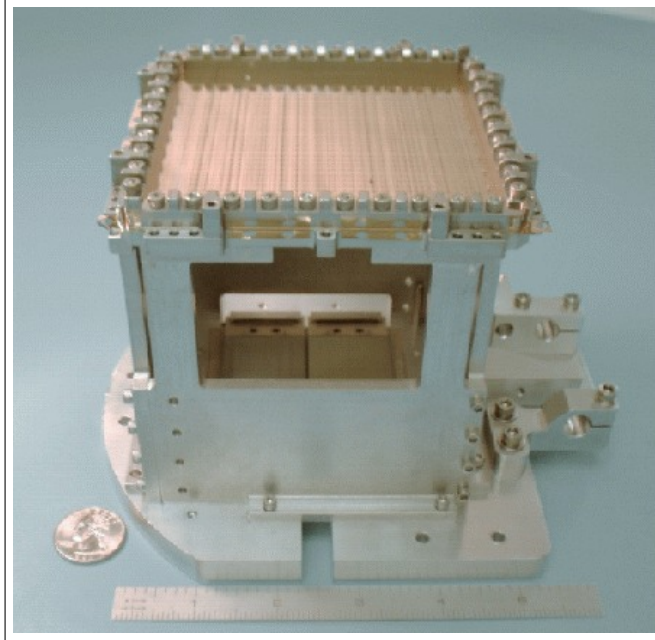


FIGURE 2.6: A single SXC unit consists of a pair of 2048x4096 CCDs (15  $\mu\text{m}$  pixel size) at 10 cm behind a finely-ruled mask. The CCDs are oriented so that their columns are parallel to the mask elements. The CCDs are read out in continuous-clocking, row-summing mode, so they operate essentially as one-dimensional images.

TABLE 2.10: Some WXM characteristics [38].

Parameter	Value
Energy Range	2-25 keV
Effective Area	175 $\text{cm}^2$ for each unit
Field of View	1.6 sr (FWZM)
Angular resolution	$\sim 11'$ (normal incidence, 8 keV)

monitoring of variable X-ray sources. It consisted in tow NaI crystal scintillators, read by a photomultiplier.

TABLE 2.11: Some WXM characteristics [38].

Parameter	Value
Energy Range	6-400 keV
Effective Area	120 $\text{cm}^2$
Field of View	3 SR

#### 2.5.4 Results

183 GRBs well localized, detected afterglows: 54 X-rays, 51 optical, 27 radio. HETE-2 localized burst GRB 030329/SN2003dh and this confirmed the GRB-SN connection.

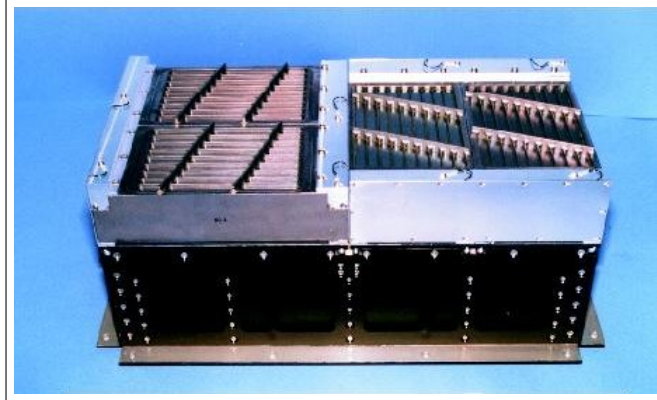


FIGURE 2.7: An image of the two XWM detectors [12].

## 2.6 Swift

Swift was launched on the 20<sup>th</sup> November 2004, with a consortium USA-UK-Italy and its mission is currently working. This mission wants to determine the origin of GRBs which are though as probes of the early universe. For this reason it observes at wavelength very different from other satellites. The energy range 0.2 - 150 keV is dedicated to gamma detections, while the UV/Optical telescope is between 170 - 650 nm for the afterglow observations.

It has three instruments on-board: the Burst Alert Telescope for gamma-ray band; the X-ray Telescope (XRT) and the Ultraviolet/Optical Telescope (UVOT). After that the BAT detects GRBs and accurately determines their sky positions, Swift relays a 3 arcmin position estimate to the ground within 20 s of the initial detection. The spacecraft, in less than  $\sim 90$  s, autonomously re-points itself to bring the burst location within the field of view of the sensitive narrow-field X-ray and UV/optical telescopes to observe the afterglow. In addition to an accurate position, Swift provides multi-wavelength light curves for the duration of the afterglow, a gamma-ray spectrum of the burst, X-ray spectra of the afterglow, and in some cases it can constrain the redshift of the burst. Swift is able to discover 100 GRBs per year, with a position precision of 0.5 - 5 arcsec for almost every source [197].

### 2.6.1 Burst Alert Telescope (BAT)

The BAT is a highly sensitive CdZnTe detector, with a coded-mask aperture at large FoV of 1.4 sterad (half coded). It provides triggers and 4-arcmin positions. The energy range is 15-150 keV for imaging with a non-coded response up to 500 keV. The BAT calculates an initial position and within a few minutes it decides whether the burst merits a spacecraft slew and, if so, moves itself. Further information on the BAT is

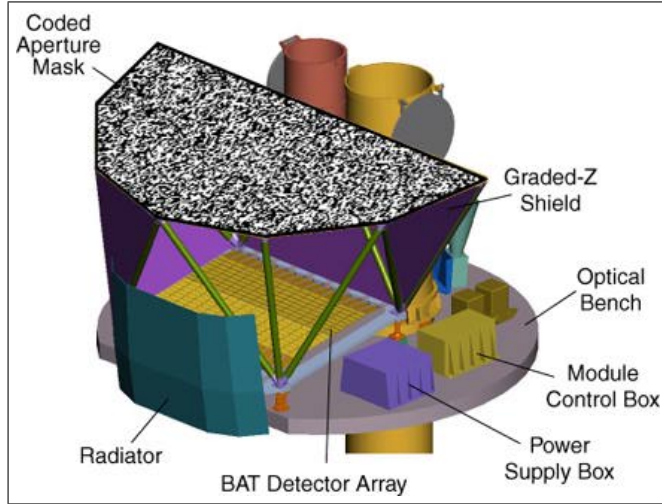


FIGURE 2.8: An image of the BAT [13].

given by [198, 199]. Some specifications are reported in table 2.12 and an image of it is shown in figure 2.8.

TABLE 2.12: Some BAT characteristics [13].

Parameter	Value
Energy Range	15-150 keV
Aperture	Coded-mask
Detecting Area	5200 cm <sup>2</sup>
Field of View	1.4 sr (partially-coded)
Telescope PSF	17'

## 2.6.2 X-ray Telescope (XRT)

The XRT is designed to measure the fluxes, spectra, and light curves of GRBs and afterglows over a wide dynamic range covering more than seven orders of magnitude in flux. This telescope can pinpoint GRBs to 5'' accuracy within 10 s of target acquisition for a typical GRB. It can study the X-ray counterparts of GRBs beginning 20-70 s from burst discovery and continuing for days to weeks. Table 2.13 summarizes some instrument's parameters. Further information can be found in [200, 201].

TABLE 2.13: Some BAT characteristics [39].

Parameter	Value
Energy Range	0.2-10 keV
Telescope PSF	18'' HPD at 1.5 keV
Detector Operation	Imaging, Timing, and Photon-counting
Pixel Scale	2.36 arcsec/pixel
Sensitivity	$2 \times 10^{-14}$ erg cm <sup>-2</sup> s <sup>-1</sup> in 104 s

### 2.6.3 Ultraviolet/Optical Telescope (UVOT)

This telescope is uniquely devoted for afterglow studies in UV and optical spectra. A characteristic of the UVOT is its rapid response to observe these gamma-ray counterparts and to determine their redshift while they are still bright, because optical afterglows decline in luminosity as  $t^{-1.1}$  to  $t^{-2.1}$ . Stars in the FoV of the UVOT provide an astrometric grid for the GRB field [40].

TABLE 2.14: Some specifications of UVOT [40].

Parameter	Value
Wavelength Range	170-650 nm
Field of View	$17' \times 17'$
Telescope PSF	$2.5''$ at 350 nm
Filters	7
Sensitivity	B = 22.3 in white light in 1000 s
Pixel Scale	0.502''
Brightness Limit	v = 7.4 mag
Camera Speed	11 ms

## 2.7 “Astrorivelatore Gamma a Immagini LEggero” - AGILE

AGILE is a totally Italian mission and dedicated to the gamma-ray observations. The satellite was launched on the 23rd April 2007, from the Indian base of Sriharikota and currently operating.

It combines two co-axial instruments: the AGILE Gamma-Ray Imaging Detector (30 MeV - 50 GeV) and a hard X-ray detector (18-60 keV). Their technology is based on solid-state silicon. The last component of the payload is a calorimeter which energy range is between 250 keV and 100 MeV, and an anti-coincidence system. These last instruments will not be described in the following. AGILE is used to study persistent and transient gamma-ray sources.

All these information has been taken by Agenzia Spaziale Italiana (ASI - Italian Space Agency) website. See [41, 202–204] for more details.

### 2.7.1 Gamma-Ray Imaging Detector (GRID)

It is sensitive in the energy range 30 MeV50 GeV. GRID consists of a Silicon-Tungsten tracker, a Cesium Iodide Mini-Calorimeter, an anti-coincidence system made of segmented plastic scintillators. Its trigger is based exclusively on Silicon plane detectors.

The use of solid components entails a good angular resolution of around 5-20 arcmin for bright sources in a FoV of  $\sim 3$  steradians. A summary of its capabilities is listed in table 2.15.

TABLE 2.15: Some specifications of GRID, taken from tables 2 and 3 in [41].

Parameter	Value
Energy Range	30 MeV - 50 GeV
Field of View	$\sim 3$ sr
PSF (68% containment radius):	$4.7^\circ$ at 0.1 GeV $0.6^\circ$ at 1 GeV $0.2^\circ$ at 10 GeV
Source Location Accuracy	5-20 arcmin with $S/N \sim 10$

## 2.7.2 Hard X-ray Imaging Detector (Super-AGILE)

This detector is positioned on top of the GRID Tracker and consists of an additional plane of four Silicon square units plus a coded mask. One of main goals of Super-AGILE is the simultaneous gamma-ray and hard X-ray detection of astrophysical sources (unprecedented for gamma-ray instruments). It has a precision in source positioning of 1-3 arcmins, depending on the source intensities.

TABLE 2.16: Some specifications of the Super-Agile detector, taken from table 3 in [41]. Some value of them (specially if not written in the text) could be better than written only here. The reason is that the original table is early to the mission of 3 years, so the real instrumental specifications can be better. However reported information is good for this thesis and its aims.

Parameter	Value
Energy Range	18-60 keV
Field of View	$107^\circ \times 68^\circ$ FW at Zero Sens.
Angular Resolution (pixel size)	$\sim 6'$
Required pointing reconstruction	$\sim 1'$
Source Location Accuracy	1-3 arcmin with $S/N \sim 10$

## 2.8 Fermi

Launched on the 11<sup>th</sup> June 2008 and currently in its circular orbit at 560 km above the Earth, the Fermi Gamma-ray Space Telescope (FGST, but formerly Fermi) is an international and multi-agency space observatory that studies the cosmos in the energy range between 8 keV and 300 GeV. Payload of Fermi consists of two instruments: the Large Area Telescope and the GLAST Burst Monitor. The former is Fermi's primary instrument, and the second one is the complementary instrument [205].

### 2.8.1 Large Area Telescope (LAT)

The LAT is made up by a tracker, a calorimeter, an anti-coincidence detector and a data acquisition system. It detects  $\gamma$ -rays through pair creations and the direction of the photon is obtained by the tracker sensitive from 30 MeV to greater than 300 GeV (its sensitivity is greater than 10 GeV because almost nothing is known about cosmic objects at these energies). Its FoV is 2 steradians and its angular resolution can measure the locations of bright sources to within 1 arcminute. The point spread function for on-axis gammas has a 68% containment radius of about  $3^\circ$  at 100 MeV and  $0.04^\circ$  at 100 GeV [206]. A summary of its specifications is in table 2.17.

TABLE 2.17: Some specifications of the LAT.

Parameter	Value
Energy Range	20 MeV - $\gtrsim 300$ GeV
Field of View	2 sr
Angular Resolution (SPF):	$3^\circ$ at 100 MeV $0.04^\circ$ at 100 GeV
Source Location Accuracy	$\sim 1'$

### 2.8.2 GLAST Burst Monitor (GBM)

The GBM is sensitive in the range 8 keV - 30 MeV. There are 12 sodium iodate detectors for X-rays and low-energy gamma-rays, and 2 bismuth germanate detectors for high-energy gamma-rays. By viewing the entire sky ( $4\pi$  steradians, apart from a piece occulted by Earth), GBM can detect  $\sim 250$  GRBs per year.

The low-energy (8 keV - 1 MeV) detectors provide rough locations of GRBs to within several degrees (they are mounted in four banks consisting of three detectors each, oriented to see different parts of the sky) but an accurate determination of the spectral continuum shape of their prompt emissions. The high-energy (150 keV - 30 MeV) ones are placed on opposite sides of the spacecraft, providing nearly full sky coverage. Table 2.18 summarizes characteristics of the GBM.

TABLE 2.18: Some specifications of the GBM. LED is Low-Energy Detector; HED is High-Energy Detector. Information taken from [42]. The symbol “-” indicates that the values have to be estimated yet.

Parameter	Value
Energy Range	8 keV to 1 MeV for LEDs 150 keV to 30 MeV for HEDs
On-board GRB Locations	< 15° in 1.8 sec (< 8° for $S/C < 60^\circ$ zenith)
Field of View	9.5 sr
Angular Resolution (SPF):	- for LEDs - for HEDs
Final Source Location Accuracy	~ 3°



## **Part II**

# **Gamma Ray Bursts by the Square Kilometre Array**



## Chapter 3

# The Square Kilometre Array

In chapter 1, GRBs and an overview of them have been presented, while chapter 2 is dedicated to most of the satellite missions whose purpose is/was to observe these objects at very high frequencies ( $\gamma$  and X rays), principally during their emitting initial phases (for some hours). Before to present GRB radio studies, part II of this work is initially dedicated to radio instruments and radio observational techniques. In this chapter, some brief information is reported about the Square Kilometre Array (SKA), namely the instrument proposed for radio investigation of GRBs, and, in particular, this chapter is focused on the so called *feed indexer*. The feed indexer is an electromechanical rotating platform which will be used by the SKA dish antennas to allow a switch among the feeds.

A part of my PhD has been conducted in collaboration with an aerospace company, thus most of the information here has been taken from company reports and preliminary studies carried out on the SKA. Unfortunately, most of the info coming cannot be reported either because they are still preliminary or confidential. Where possible, some figures and analysis carried out during the collaboration have been reported.

### 3.1 The SKA - Overview

The first idea about the SKA was born in the September 1993. A concept of a new generation radio observatory in order to satisfy a lot of scientific goals, by using precise and avantgarde technical specifications.

On August 2000, in Manchester, the International Square Kilometre Array Steering Committee (ISSC) was signed by representatives of eleven Countries (Australia, Canada, China, Germany, India, Italy, the Netherlands, Poland, Sweden, the United Kingdom

and the United States). Other chronological dates and information are possible to find in the SKA web site (see [207]), but it is important to report the collaboration agreement upgraded in 2007, where it was establish the adding of the South Africa with its National Research Foundation.

Since December 2011, the project has been leading by the SKA organization that has the task to formalise relationships between the international partners and centralize the leadership of this scientific project. The SKA project involves so much institutions, to do truly it a global enterprise. In fact, 11 member countries are the core of the SKA (today: Australia, Canada, China, Germany, Italy, New Zealand, South Africa, Sweden, the Netherlands and the United Kingdom) and around 100 organizations across about 20 countries (adding: Brazil, France, Japan, South Korea, Poland, Portugal, Russia, Spain, the USA) have been participating in the design and development of the SKA.

This common effort aims to develop an instrument that will try to find answers for the five key science purposes: galaxy evolution, cosmology and dark energy; strong-field tests of gravity using pulsars and black holes; the origin and evolution of cosmic magnetism; probing the Cosmic Dawn; the cradle of life. Obviously, a flexible design has been considered to enable exploration of the unknown. To know further details about the key science projects, the unanswered questions in fundamental physics, astrophysics and astrobiology at which the SKA could answer, see [208]. In general, about this project there is the [SKA web site<sup>1</sup>](#).

The SKA will be the largest and most sensitive radio telescope ever built in the world, composed of three unique antenna designs which will be able to observe over a large frequency range, from 50 MHz to 20 GHz. The ranges of these three types of antennas will be for low, middle and high frequency. Respectively, the Low-Frequency Aperture Array (LFAA, or SKA-Low) will cover the lowest frequency band, from 50 MHz up to 350 MHz; the SKA Mid Frequency Aperture Array (MFAA) is scheduled in a later phase of the construction and will cover from 400 MHz upwards; finally, 3000 single dish antennas are planned to observe from around 350 MHz to 20 GHz, (for details see [14]). This huge international project will consist of two construction phases; phase 1 will take place from 2018 to 2023 providing an operational array of telescopes capable of carrying out the first scientific studies in low and mid frequencies; phase 2 and the high frequency dishes will then follow providing full sensitivity for frequencies up to 20 GHz. Most of the dish antennas will be located in South Africa's Karoo desert, whereas a smaller portion of them will be placed in the Australia's Murchison region, together with millions of dipole antennas for low-frequency array. The MFAA will consist of tens stations to deploy in South Africa. Dish receivers are planned to be of two types, i.e., Single Pixel Feeds (SPFs) and Phased Array Feeds (PAFs), with different reception

---

<sup>1</sup><https://www.skatelescope.org>

characteristics and will be assembled in South Africa and Australia, respectively. For this reason, two different names have been chosen to distinguish between these dishes, i.e., the SKA-Mid for the SPF types and the SKA-Survey for the PAFs. Current news and additional information can be read in the SKA organization's web site.

By using interferometry, the SKA will have a combined collecting area of about one square kilometre, with its 15 m diameter dishes, and LFAA and MFAA antennas. This radio telescope will reach a sensitivity of  $400 \mu\text{Jy}$  in 1 minute, in the range between 70 and 300 MHz. The sensitivity formula, where the lowest measurable flux density  $S$ , for a single dish, is reported below:

$$S = \frac{T_{\text{sys}}}{\sqrt{2\Delta\nu \cdot \tau}} \cdot \frac{a_{\text{ric}}}{g}, \quad (3.1)$$

where  $T_{\text{sys}}$ ,  $\Delta\nu$  and  $\tau$  are the system temperature, the pass-band and the acquisition integration time;  $g$  is the antenna gain and  $a_{\text{ric}}$  is a factor which depends on the kind of receiver. The SKA telescope will have sensitivities of  $3.72$ ,  $2.06$  and  $0.72 \mu\text{Jy}\cdot\text{hr}^{-1/2}$ , respectively for the SKA-Survey, SKA-Low and SKA-Mid [14]. Their planned field of views (FoVs) are reported in the table 3.1.

For a more precise idea, see figure 3.1 in which a comparison with current radio telescopes is shown.

Thanks to the interferometric technique with a baseline of about 3000 km and a planned angular resolution of 0.1 arcsec at 1 GHz, the SKA will be able to take surveys of the sky at a rate faster than any survey telescope ever existed. It will perform continuum surveys looking at vast swathes of the radio-wavelength sky from the southern hemisphere and part of the northern one, making a detailed map as the thousands of telescopes work in unison. The continuity of the surveys will allow the observations of transients, such as GRBs. It will make it possible to obtain their light curves in radio frequencies, which are currently detectable only with significant difficulty, and only in cases where they are bright in this band. Instrumental synergies between gamma satellite missions and radio telescopes, e.g., *Swift* and AMI (Arcminute Microkelvin Imager) [209, 210], will give an excellent chance to improve studies about GRBs (or transients, in general). In fact, high frequency dishes could be on-target for a few minutes since the burst, thus obtaining early-time light curves of GRBs. Furthermore, thanks to the FoV and range of the LFAA, one will have the opportunity to observe transients whose GRBs either elude gamma-ray satellites, or are impossible to detect at high energies such as orphan afterglows [211]. In these cases no gamma-alert is needed, just because only the afterglow could be observed and the initial gamma emission cannot reach the Earth.

For additional info about scientific purposes and applications of this telescope, consult the SKA science books too (e.g. [212] and the international white book, currently in

Table xxx: Parameters for Comparable Telescopes															
	eMERLIN	JVLA	GBT	GMRT	Parkes MB	LOFAR	FAST	MeerKAT	WSRT	Arecibo	ASKAP	SKA1-survey	SKA1-low	SKA-mid	
$A_{eff}/T_{sys}$	$m^2/K$	60	265	275	250	100	61	1250	321	124	1150	65	391	1000	1530
FoV	$deg^2$	0.25	0.25	0.015	0.13	0.05	0.13	0.0017	0.05	0.25	0.003	30	18	27	0.49
Receptor Size	m	25	25	101	45	39	300	13.5	25	225	12	15	35	15	
Fiducial Frequency	GHz	1.4	1.4	1.4	1.4	1.4	0.12	1.4	1.4	1.4	1.4	1.67	0.11	1.67	
Survey Speed FoM	$deg^2 m^4 K^{-2}$	$9.00 \times 10^3$	$1.76 \times 10^3$	$1.14 \times 10^3$	$8.13 \times 10^3$	$6.50 \times 10^3$	$5.21 \times 10^3$	$2.66 \times 10^3$	$8.86 \times 10^3$	$3.80 \times 10^3$	$3.97 \times 10^3$	$1.27 \times 10^5$	$2.75 \times 10^5$	$2.70 \times 10^7$	$1.30 \times 10^9$
Resolution	arcsec	$10\text{--}150 \times 10^3$	1.4–44	420	2	650	5	88	11	16	192	7	0.9	11	0.22
Baseline or Size	km	217	1–35	0.1	27	0.064	100	0.5	4	2.7	225	6	50	50	200
Frequency Range	GHz	1.3–1.8, 4–8, 22–24	1–50	0.2–50+	0.15, 0.23, 0.33, 0.51, 1.14	0.441 ± 0.24	0.03–0.22	0.1–3	0.7–2.5, 0.7–10	0.3–8.6	0.3–10	0.7–1.8	0.65–1.67	0.050–0.350	0.35–14
Bandwidth	MHz	400	1000	400	450	400	4	800	1000	160	1000	300	500	250	770
Cont. Sensitivity	$\mu Jy \cdot hr^{-1/2}$	27.11	3.88	5.89	6.13	16.26	266.61	0.92	3.20	20.74	0.89	28.89	3.72	2.06	0.72
Sensitivity, 100 kHz	$\mu Jy \cdot hr^{-1/2}$	17.14	3.88	3.73	411	1029	1696	82	310	830	89	1532	263	103	63
SEFD	Jy	46.0	10.4	10.0	11.0	27.5	45.2	2.2	8.5	22.3	2.4	42.5	7.1	2.8	1.7

Notes to Table													
eMERLIN	Frequencies non-contiguous												
JVLA	Multiple antenna configurations												
GBT	Single dish												
GMRT	Frequencies non-contiguous												
Parke's MB	Multi-beam (13)												
LOFAR	Parameters for all NL stations												
FAST	Single dish												
MeerKAT	SKA Precursor												
WSRT	Frequencies non-contiguous												
Aracibo	Single dish												
ASKAP	SKA Precursor												
SKA1-survey	Muli-beam (36)												
SKA1-low	Mixed 13.5-m & 15-m dishes												
SKA-mid	$\Omega_{fov} = (\pi/4)(66\lambda/Ddish)^2$												
Notes: All (cont'd)	Fiducial frequency: Most Parameters												
	SEFD derived from $A_{eff}/T_{sys}$												
	Sensitivity derived from SEFD & BW												
	System efficiency assumed 100%.												

FIGURE 3.1: Parameters for comparable telescopes, from the table 1 of [14].

TABLE 3.1: The planned FoVs at the SKA observational frequencies. See [14] for details.

Frequency Range GHz	FoV ( $^{\circ}$ ) <sup>2</sup>
0.07-0.3	200
0.3 - 1	1-200
1 -20	$\lesssim 1$

press<sup>2</sup>).

## 3.2 The collaboration with the SAM company

During my PhD, I have collaborated with a company in charge of designing the rotating platform, dedicated to the SKA, which will be used to switch among the different feeds planned for the SKA. The company mentioned is the *Società Aerospaziale Mediterranea S.c.r.l.* (SAM) and the platform is called the feed indexer (FI). For this reason I will write about the studies and considerations done during the concept design of the FI. The collaboration with the SAM has consisted in a scientific support about antennas, studies of deformations, company meetings and a abroad mission. Regarding the last, a profitable partnership has been established with the South African SKA Office (in Cape Town) and the EMSS company (Cape Town). The latter is a company in charge of manufacturing the feeds for the SKA (and currently for the MeerKAT precursor).

## 3.3 The feed indexer - Up and down configuration

The figure 3.2 shows a picture of the MeerKAT, where the FI placed on the telescope frame between the reflector and the sub-reflector. The FI design covers studies of the placing, encumbrance, deformations and translational and rotational degrees of freedom of the FI on the dish. The SAM is in charge of its design, so part of the company task is also focused on the choice of material to be used, considering the SKA constraints and costs. A study of maintenance has been carried out too.

A preliminary study was performed on the the position and shape of the platform. The SKA organization asked for analysis concerning the up and down configurations. Roughly, the difference between these two configurations concerned the position of the receivers and two different elevation rotations of the dish. In figure 3.3 some sketches of the “feed up” and “feed down” configurations are shown. These sketches are taken

---

<sup>2</sup>[http://arxiv.org/find/all/1/all:+EXACT+Science\\_with\\_the\\_Square\\_Kilometer\\_Array/0/1/0/all/0/1](http://arxiv.org/find/all/1/all:+EXACT+Science_with_the_Square_Kilometer_Array/0/1/0/all/0/1)



FIGURE 3.2: An artist’s impression of a MeerKAT antenna to show the FI placed on the frame between the reflector and the sub-reflector. On the FI are also placed some feeds. Credit by [the SKA Africa](#).

from an internal official report about antenna maintenance, sent first to the SKA-dish consortium, then used for a final report forwarded to the SKA organization. They are covered by company confidentiality, so references cannot be reported.

These preliminary considerations led to a maintenance-concept analysis, as well as testing possible positions for all the various combinations (i.e., PAF-feed down, SPF-feed down, PAF-feed up, SPF-feed up). These tests were necessary to verify whether the whole ensemble, i.e. receiver components plus feed indexer, would have interfered with the ray tracing of the electromagnetic waves collected and focused by reflectors.

By starting from simple bi-dimensional mathematical formula and some indications, such as shown in figure 3.4, a 3D-simulation has been created. The strongest constraint for these test-sketches is that the secondary focus must lay on all feed surfaces. Figures 3.5 and 3.6 show the four options, mentioned above, among feed-up and feed-down configurations for the SPFs and for PAFs. Although the sketches show simulations in a preliminary phase, they contributed heavily to the choice for the definitive configuration. However, it should be noted that the ray tracing simulations were not decisive in this choice. The placement of FIs and feeds was fine for both configurations, and for all practical purposes there was not an encumbrance in the light paths. The minimum verified clearances were:

**Feed-up configurations:** 28.7 cm with the SPFs; 43.5 cm with the PAFs.

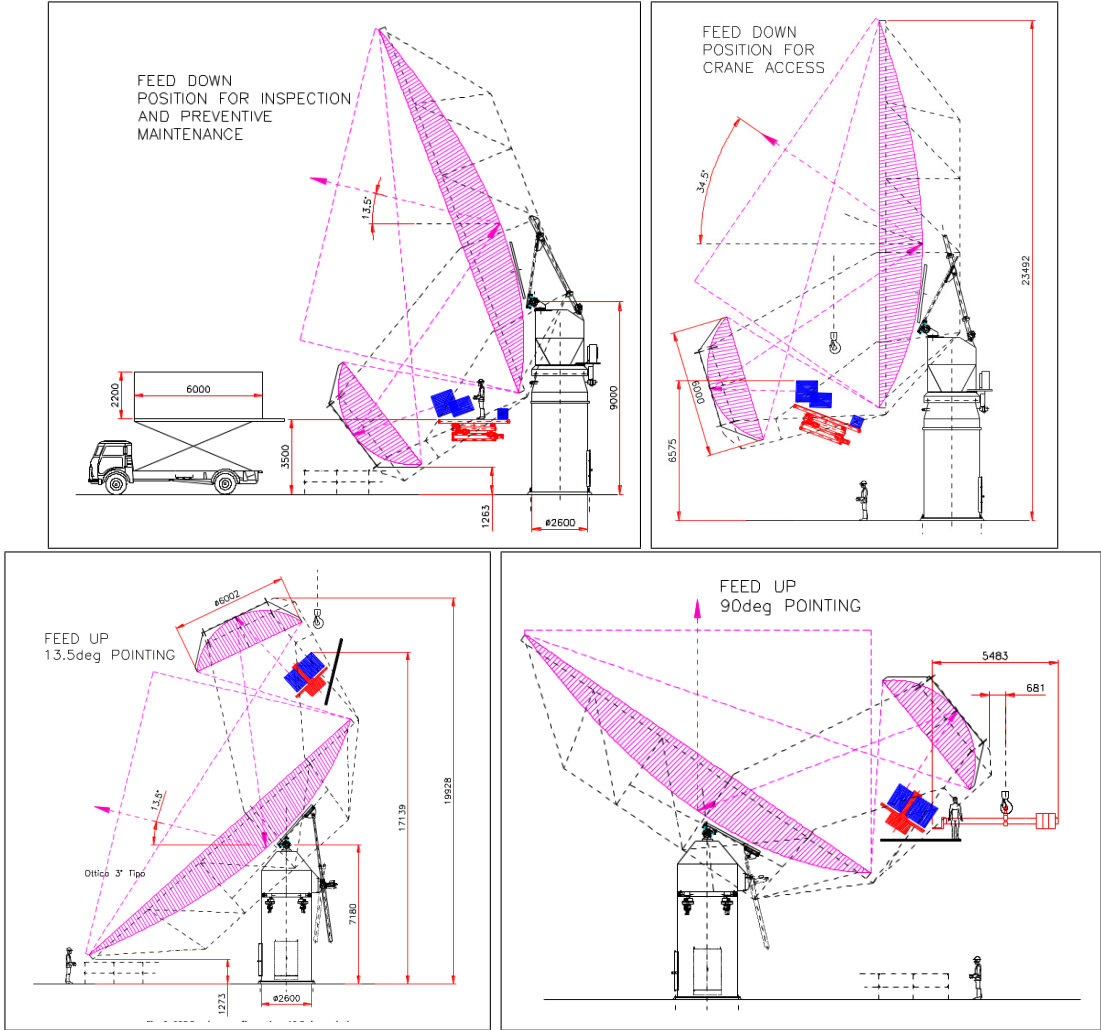


FIGURE 3.3: Four sketches about the feed up and feed down configurations. Here it is easy to see the feed positions on the dishes and elevation motions. These sketches are taken from an internal company report of the SAM and the EIE-Group companies about dish-antenna maintenance.

**Feed-down configurations:** 76.5 cm with the SPF; 66.5 cm with the PAFs.

Even observational advantages have not been crucial to decide between these configurations (there were small differences in the illuminated sub-reflector surfaces). In the end, the feed-down configuration was preferable for technical constructive reasons and maintenance costs. In other words, the feed-down configuration is easier to produce and maintain, and is overall more economical. In fact, the cost per single dish must be multiplied by the final number of antennas that will be built (about 3000, when the SKA will be fully operational), and this factor is definitely important.

As for the maintenance, the study performed with the SAM has shown that working in the feed-down configuration is more accessible and convenient. On the contrary, the feed-up configuration makes any procedure more complex, both for duration and position. Furthermore, extra support vehicles would have been necessary to go on the

TABLE 3.2: Physical and electronic characteristics of the PAFs and SPFs are summarized. The symbol \* in the 3, 4, and 5 Bands simply indicates that 65 kg is the total weight of these three feeds.

Feed	Frequency range GHz	Expected Diameter m	Weight kg
PAFs			
Band 1	0.35 - 0.90	2.34	300
Band 2	0.65 - 1.67	1.27	200
Band 3	1.5 - 4.0	0.53	100
SPFs			
Band 1	0.35 - 1.05	-	80
Band 2	0.95 - 1.76	-	64
Band 3	1.65 - 3.05	-	65*
Band 4	2.80 - 5.18	-	65*
Band 5	4.6 - 13.8	-	65*

feed-indexer and work on components placed there (e.g., feeds, helium pumps, vacuum systems, etc).

### 3.4 PAF and SPF feed indexer and PAF de-rotation

As mentioned above, the FI will have to support two kinds of feeds (i.e. PAFs and SPFs) and they are very different from each other. Initially, SKA-organization constraints imposed that the FI was the same for both components, but this was unreasonable and, after some meetings in South Africa, this constrain has been canceled. Now, two different designs will be produced for the Survey and Mid configurations.

Table 3.2 reports the sizes and the weights of the feeds. The values reported here

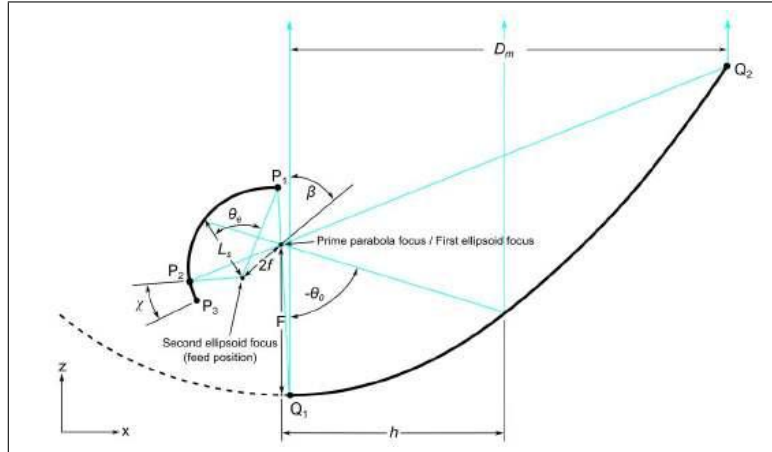


FIGURE 3.4: This figure reports a sketch of an parabolic and elliptic sectors. These sectors are bi-dimensional cuts of the reflector and the sub-reflector of the SKA-TEL.DSH.MGTCSIROTS004

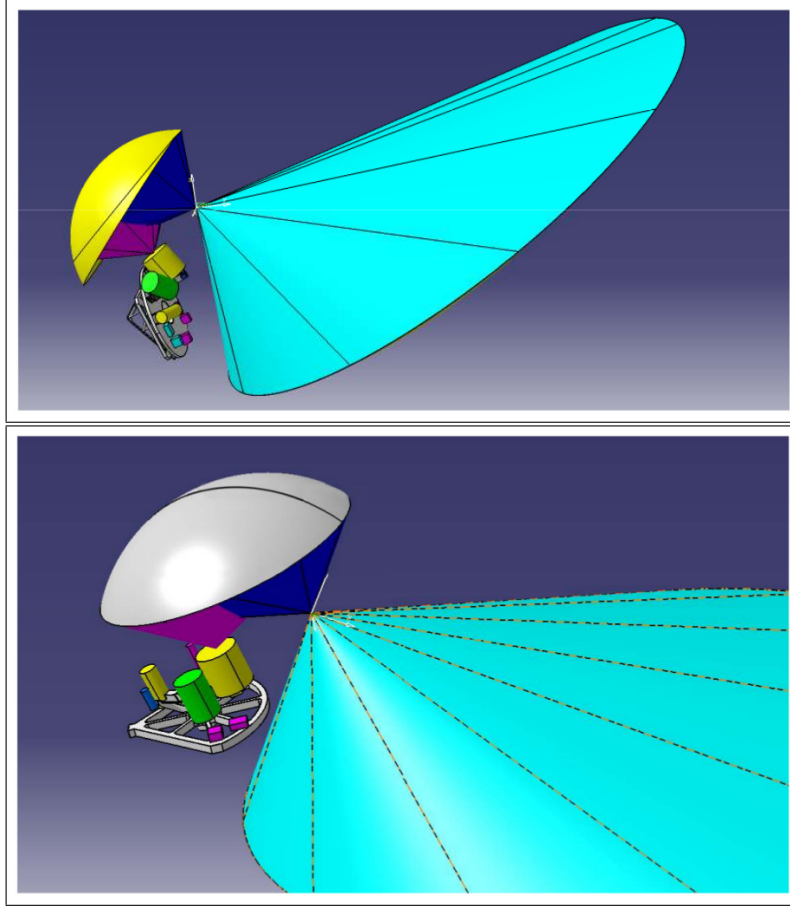


FIGURE 3.5: Here the feed up and feed down configurations with SPFs installed. These figures are taken from an internal report of the SAM and the EIE-Group companies and sent to the SKA-dish consortium.

might be changed before actual production. By reading weights in the table, it is clear that the two kinds of feeds are really different. As their names suggest, the SPF are single feeds, hence they consist of single horns that collect a specific radio frequency. Only Bands 1 and 2 will be populated during the first phase of construction. The feed packages are mounted on the FI, and only one band will be available for observation at any given time. For Bands 1 to 4, the entire bandwidth is digitised. For Band 5, two individually tuneable sub-bands of 2.5GHz bandwidth each are required. On the other hand, the PAF is an array of feeds, more or less similar to a CCD (charge-coupled device) detector. For this reason, a de-rotating system is planned for the PAF detectors, to maintain the same (fixed) piece of sky above the PAF during any observation. Currently, both the FIs and the feeds are in the design phases, but some sketches of them, as well as some preliminary exploded diagrams to connect feeds with the FI structure, can be shown. Figure 3.7 shows the FI-PAF and FI-SPF configurations, whereas figure 3.8 shows an exploded-diagram example of the band-2 PAF. It is important to state that shapes and gears are drafts at this stage and a lot of sketches are only estimates which will lead to further considerations.

In figure 3.8 it is possible to see a system of gears and rolls that allows the PAF rotation. Since the PAF is an array of feeds, the sky imaging observed by this receiver must stay unmoving during any source tracking. In fact, while the tracking is in progress the antenna continually changes elevation and azimuth. Since the PAF has two dimensions, it must be spun to maintain the same orientation between it and the sky.

At the beginning, three different types of de-rotating systems were suggested: mechanical, electronic and via-software reducing. In the end, the mechanical solution was chosen. This option is probably the best one, since signal-deconvolution works will be particularly stressing for computers of the SKA, which will produce several terabytes per a single observation. On the other hand, an electronic de-rotation, by modifying the feed-array beam, might have introduced some noise into detections. Obviously, many studies must be done also on the de-rotating system, considering possible electromagnetic interferences too.

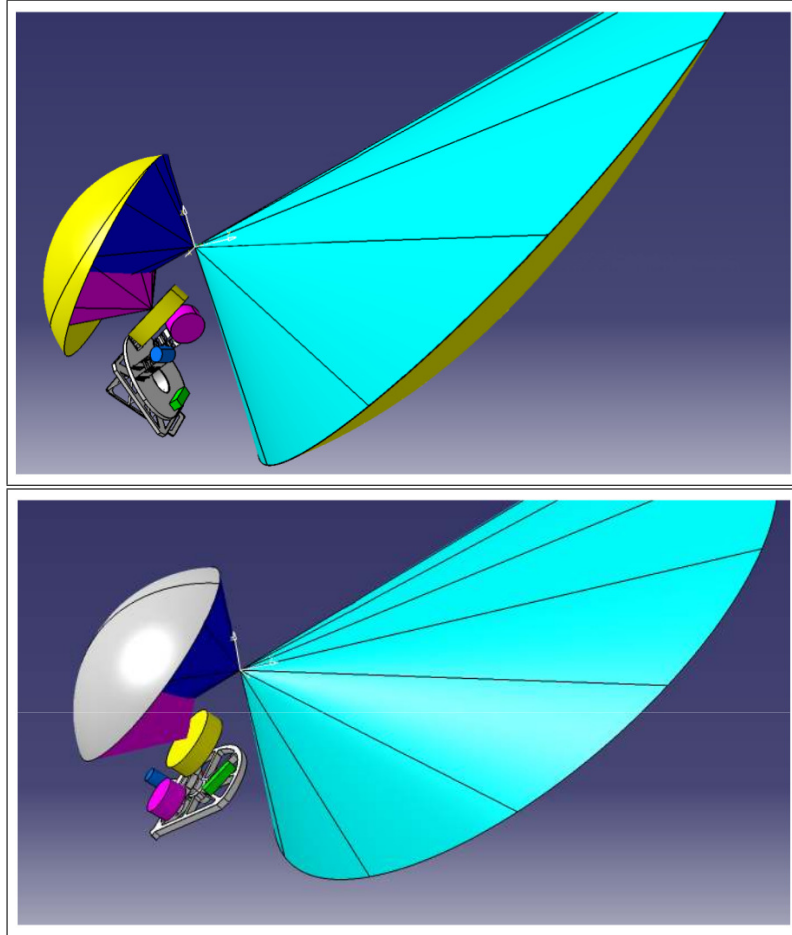


FIGURE 3.6: Here the feed up and feed down configurations with PAFs installed. These figures are taken from an internal report of the SAM and the EIE-Group companies and sent to the SKA-dish consortium.

### 3.5 Feed indexer deformation range

More detailed specifications (size, weights, components, component placements on the FI) are being available, and thus improved analyses have been performed since the last year. The stiffness required to the FI is extremely high and this is due to the high precision on the focus position. In the SKA, deformations are tolerated up to a magnitude of a few centimeters for the entire antenna. Obviously, most of deformations are expected to be due to the frame and dish, therefore the FI must have a displacement range of about 1-2  $\mu\text{m}$ .

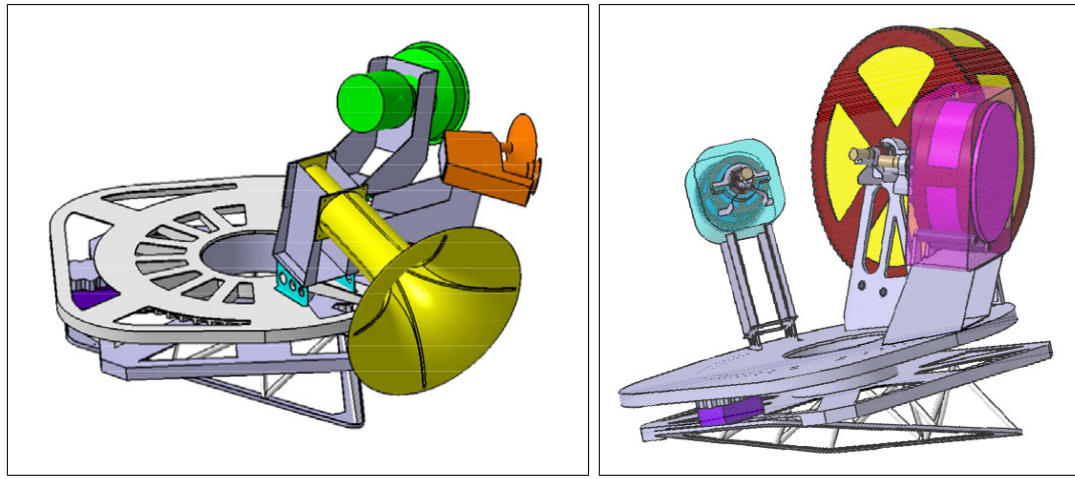


FIGURE 3.7: In the left panel, a sketch of the SPSs and SKA Mid FI. In the right panel, PAFs and SKA Survey FI. A possible platform and an dish-antenna-interface structure are sketched below the FIs .

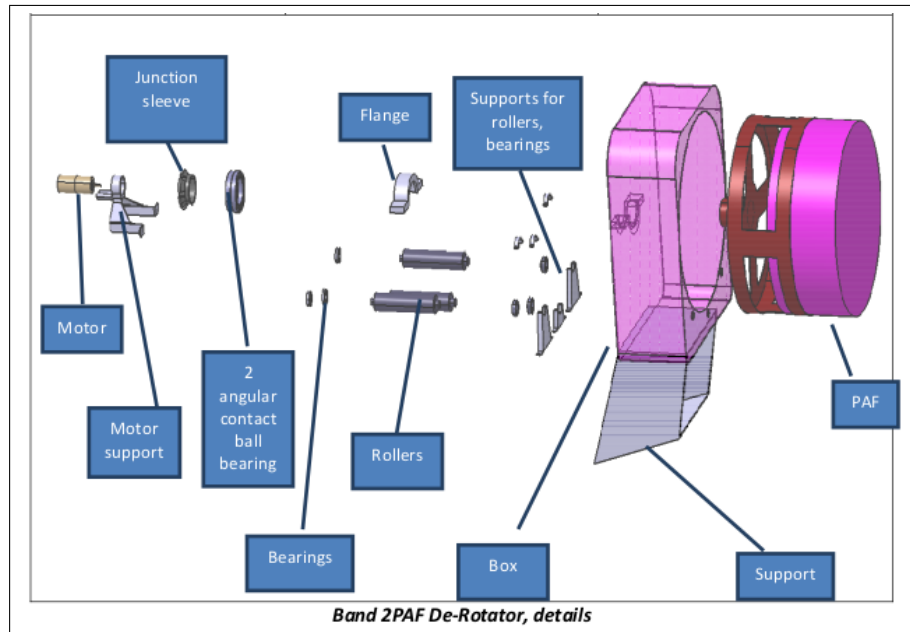


FIGURE 3.8: A draft exploded diagram of the Band 2 PAF, that shows gears of the de-rotating system too.

With the SAM, some preliminary Finite Element Model (FEM) analyses have been performed. The platform has been loaded with all the planned components, (i.e., vacuum pump station, helium system, power supply and electrical panels, radio frequency over fiber transmitter) using weights and (approximate) sizes to consider the real barycenter of each object. The analysis has envisaged different tilts to predict the load on the FI as the antenna elevation changes. Currently, the analysis done by the SAM simulate deformations, the SPF FI displacements are within the constraints, and no definitive FEM analysis has been done on the PAF FI. Additional studies will need to improve the platform in order to reach a good combination among the total weight, the stiffness and costs. All the obtained results cannot be reported but figure 3.9 shows an output of a FEM analysis at 30° of elevation for the SPF FI, using data provided by SKA Dish consortium and the EMSS. In this analysis, gravitational displacements and environmental factors (e.g., wind, thermal expansion) have been considered.

### 3.6 SKA scientific books

Apart from this technical experience, I want to highlight that there are also two my contributions for the *Italian SKA White Book* [213] and for the *Science with the Square Kilometer Array* (Amati et al., accepted<sup>3</sup> [214]).

---

<sup>3</sup>[http://arxiv.org/find/all/1/all:+EXACT+Science\\_with\\_the\\_Square\\_Kilometer\\_Array/0/1/0/all/0/1](http://arxiv.org/find/all/1/all:+EXACT+Science_with_the_Square_Kilometer_Array/0/1/0/all/0/1)

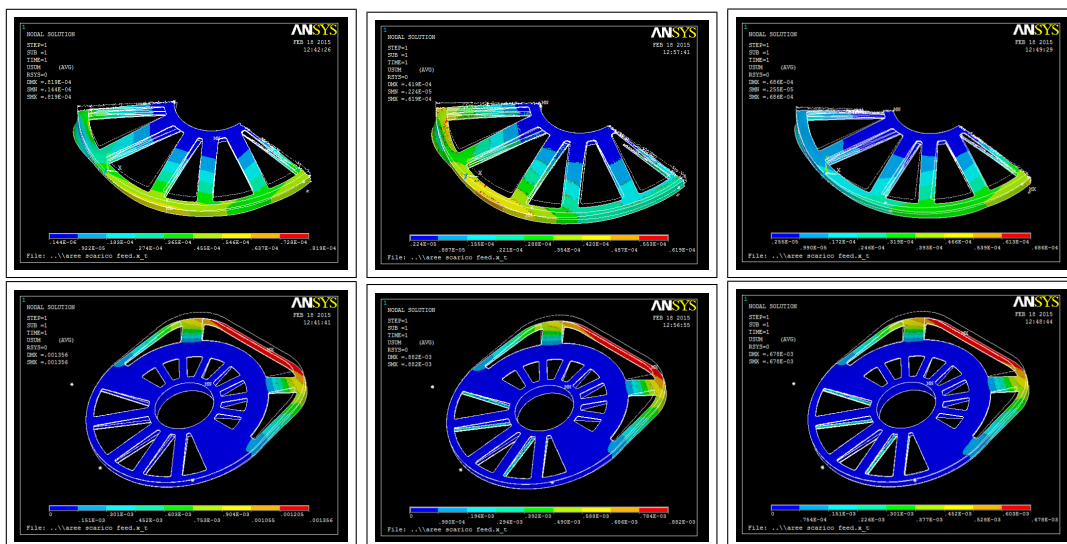


FIGURE 3.9: In the upper row, three sketches of the maximum displacement of the FI front at an elevation of 30°. In lower row, the maximum global displacement. The color scale used indicates blue as the smaller displacement.

# Chapter 4

## Observational techniques for radio detections

After a brief introduction of the SKA in the chapter 3, this chapter is dedicated to the interferometric technique that this radio telescope will use. The SKA will have about 3000 dish antennas and will be placed on two continents. The following discussion will explain the necessity of these large numbers and the distant locations of the antennas, and how these features improves the data acquisition.

### 4.1 Radio interferometry

The SKA is commonly called a telescope but it is really a *radio interferometer*. A radio interferometer is an array of radio antennae that observe in synergy and, obviously, is based on electromagnetic wave interferometry. In order have a very complete view of this aspect, it is suggested to see [17].

#### 4.1.1 Form of the observed electric field and synthesis imaging

When a source emits, its electromagnetic radiation follows Maxwell's equations and will propagate away from the source to eventually reach an astronomer. In figure 4.1, an astrophysical source is located at  $\vec{R}$ , causing a time-variable electric field indicated by  $\vec{E}(\vec{R}, t)$ , which an astronomer may detect at  $\vec{r}$ .

If we have a varying field observed in finite time intervals, then it is possible to express the magnitude of the field as the real part of the sum of a Fourier series where the only time-varying functions are exponentials. Because the Maxwell's equations are linear, one

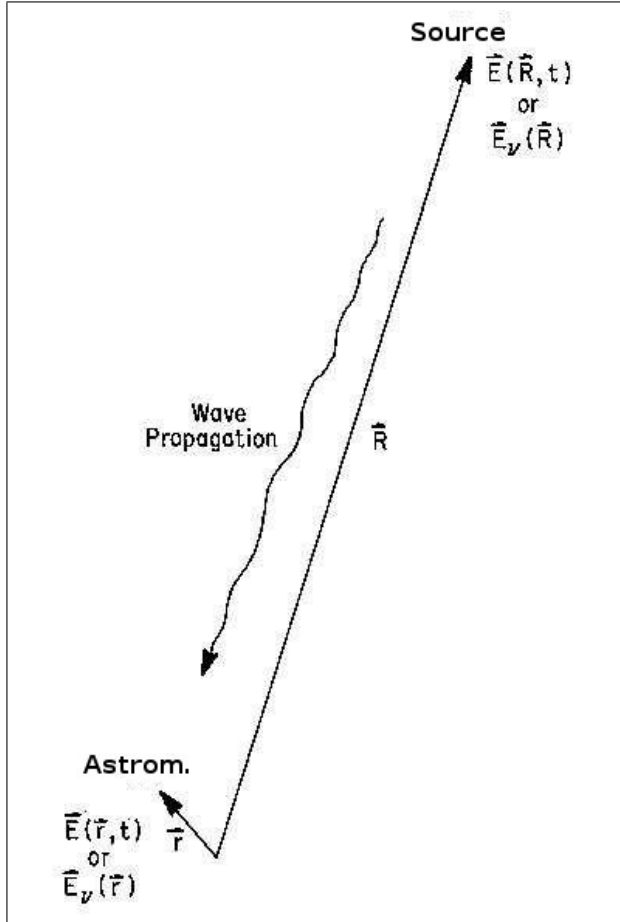


FIGURE 4.1: The source is located at  $\vec{R}$  and causes the electromagnetic wave  $\vec{E}(\vec{R}, t)$ . It is detected by an astronomer at  $\vec{r}$  [15].

may deal with the coefficients of this series, rather than with the general time-varying field. Following the explanation of B.G. Clark in [15],  $\vec{E}_\nu(\vec{R})$  will indicate the *quasi-monochromatic components* of the electric field in this Fourier series and the field will be represented as complex quantities (i.e.,  $A e^{i\alpha}$ ). Only a single quasi-monochromatic component will be considered in the following account.

The electric field measured at any point is a superposition of the various electromagnetic sources, mathematically it is an integral of all these contributes and over all the space:

$$\vec{E}_\nu(\vec{r}) = \int \int \int P_\nu(\vec{R}, \vec{r}) \vec{E}_\nu(\vec{R}) \, dx \, dy \, dz, \quad (4.1)$$

where the function  $P_\nu(\vec{R}, \vec{r})$  is called the propagator, and describes how the electric field at  $\vec{R}$  influences the electric field at  $\vec{r}$ .

In order to simplify the equation 4.1, some assumptions are introduced. Firstly, the vectorial field  $\vec{E}_\nu(\vec{r})$  will be treated as a scalar, hence polarization phenomena are not now considered, the multiplication in Eq. 4.1 is regarded as scalar, and the propagator will also be a scalar instead of a tensor function (as a complete derivation would have it).

The second assumption is that the observed sources are a long way away, so that it is impossible to describe the emitting region in its third dimension, i.e., the depth. In other words, every source is placed on the celestial sphere, therefore its emission will derive from a spherical surface with distance  $|\vec{R}|$ . For this reason,  $E_\nu(\vec{R})$  will be substituted with  $\mathcal{E}_\nu u(\vec{R})$ , which indicates a distribution of the electric field on a surface. The third assumption is that the radiation passes through empty space to reach the astronomer. In this way, Huygens' Principle states that  $P_\nu(\vec{R}, \vec{r})$  takes a very simple form:

$$E_\nu(\vec{r}) = \int \mathcal{E}_\nu(\vec{R}) \frac{e^{2\pi i \nu |\vec{R} - \vec{r}|/c}}{|\vec{R} - \vec{r}|} dS, \quad (4.2)$$

where  $dS$  is the surface area element of the celestial sphere. This equation is the general form of the quasi-monochromatic component of the field at a particular frequency due to all sources of cosmic electromagnetic emission.

One of the properties of  $E_\nu(\vec{r})$  is the correlation of the field at two different points. The correlation of the locations  $\vec{r}_1$  and  $\vec{r}_2$  is defined as the expectation value of a product:

$$V_\nu(\vec{r}_1, \vec{r}_2) = \langle \vec{E}_\nu(\vec{r}_1) \vec{E}_\nu^*(\vec{r}_2) \rangle, \quad (4.3)$$

where the raised asterisk indicates the complex conjugate. Inserting Eq. 4.2 into Eq. 4.3 and exchanging the right variables, resulting:

$$V_\nu(\vec{r}_1, \vec{r}_2) = \left\langle \int \int \mathcal{E}_\nu(\vec{R}_1) \mathcal{E}_\nu^*(\vec{R}_2) \frac{e^{2\pi i \nu |\vec{R}_1 - \vec{r}_1|/c}}{|\vec{R}_1 - \vec{r}_1|} \frac{e^{-2\pi i \nu |\vec{R}_2 - \vec{r}_2|/c}}{|\vec{R}_2 - \vec{r}_2|} dS_1 dS_2 \right\rangle. \quad (4.4)$$

At this point, the fourth assumption is useful, because it says that the radiation from astronomical sources is spatially incoherent, namely  $\langle \mathcal{E}_\nu(\vec{R}_1) \mathcal{E}_\nu^*(\vec{R}_2) \rangle$  is zero if  $\vec{R}_1 \neq \vec{R}_2$ . Therefore, the signals coming from two different points of the astrophysical object and measured by the same antenna has a null expectation. Exchanging the integrals with the expectation in Eq. 4.4 the the resulting equation is:

$$V_\nu(\vec{r}_1, \vec{r}_2) = \int \langle |\mathcal{E}_\nu(\vec{R})|^2 \rangle \frac{e^{2\pi i \nu |\vec{R} - \vec{r}_1|/c}}{|\vec{R} - \vec{r}_1|} \frac{e^{-2\pi i \nu |\vec{R} - \vec{r}_2|/c}}{|\vec{R} - \vec{r}_2|} |\vec{R}|^2 dS. \quad (4.5)$$

Using the unit vector, the observed intensity and the solid angle:

$$\vec{s} = \vec{R}/|\vec{R}|, \quad I_\nu = |\mathcal{E}_\nu(\vec{s})|^2 |\vec{R}|^2, \quad d\Omega = \frac{dS}{|\vec{R}|^2}$$

and using the previous assumption  $|\vec{R}| \gg |\vec{r}|$ , so that

$$|\vec{R} - \vec{r}_1| - |\vec{R} - \vec{r}_2| \simeq -(\vec{r}_1 - \vec{r}_2) \cdot \vec{s} \text{ and } |\tilde{\vec{R}} - \tilde{\vec{r}}_2| \simeq |\tilde{\vec{R}}|,$$

then Eq. 4.5 can be rewritten as

$$V_\nu(\vec{r}_1, \vec{r}_2) \approx \int I_\nu(\vec{s}) e^{-2\pi\nu\vec{s}\cdot(\vec{r}_1 - \vec{r}_2)/c} d\Omega. \quad (4.6)$$

The function  $V_\nu$  is called the *spacial coherent function*, or the *spacial autocorrelation function*, of the field  $E_\nu(\vec{r})$ . It is important to underline that this function depends only on the separation vector  $\vec{r}_1 - \vec{r}_2$  of the two points and not on their modulus. This means that correlation properties of the radiation field can be ascertained by holding one observation point fixed and adjusting the second one. Practically speaking, an interferometer is practically a device that measures the spacial autocorrelation function.

Eq. 4.6 is invertible, within reasonable and well-defined limits. This aspect is extremely important because through the function  $V_\nu$  one can measure the intensity distribution of any emitting source. To obtain the invertibility condition another assumption is needed, but, in this case, there are two options:

**Measurements taken within a plane** One option is to confine measurements in a single plane, choosing a convenient coordinate system and measuring distances in terms of the wavelength, so that the vector spacing of the separation variable in  $V_\nu$  will be  $\vec{r}_1 - \vec{r}_2 = (x, y, 0) = \lambda(x/\lambda, y/\lambda, 0) = \lambda(u, v, 0)$  (remembering that  $z = 0$  for the new reference frame). In this coordinate system the components of  $\vec{s}$  are  $(l, m, \sqrt{1 - l^2 - m^2})$ .

With such considerations, the spacial coherent function becomes:

$$V_\nu(u, v, w \equiv 0) = \int \int I_\nu(l, m) \frac{e^{-2\pi\nu(ul+vm)}}{\sqrt{1 - l^2 - m^2}} dl dm \quad (4.7)$$

This last equation is a Fourier transform relation between  $V_\nu(u, v, 0)$  and  $I_\nu(l, m) \cdot (1 - l^2 - m^2)^{-1/2}$  (called modified intensity). It is worthwhile to stress that in this reference frame the vector  $\vec{R}$  has only the last component not equal to zero and angles are expressed in direction cosines.

**Sources in a small region of sky** The second option for the fifth simplifying assumption is that the all of radiation comes from only a little piece of the sky. In this case, if  $\vec{s}_0$  points the centre of the source and  $\vec{s}$  points in a direction very close to the centre, then  $\vec{s} = \vec{s}_0 + \vec{\sigma}$  and all terms of  $\vec{\sigma}$  greater than the fist order will be considered negligible. The statement that  $|\vec{s}| = |\vec{s}_0| = 1$  leads to

$$(\vec{s}_0 + \vec{\sigma}) \cdot (\vec{s}_0 + \vec{\sigma}) \approx 1 + 2\vec{s}_0 \cdot \vec{\sigma}. \quad (4.8)$$

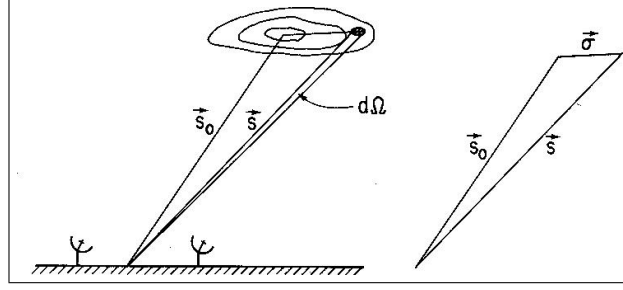


FIGURE 4.2: This figure shows the phase center tracking (even called *phase reference position*), to derive the interferometer response to a source, here represented by contours [16].

Therefore  $\vec{s}_0$  and  $\vec{\sigma}$  are perpendicular.  $\vec{s}_0$  is the *phase tracking center* and is sketched in figure 4.2. By choosing a convenient coordinate system measured in terms of wavelength, where  $\vec{s}_0 \equiv (0, 0, 1)$ ,  $\vec{s} \equiv (l, m, \sqrt{1 - l^2 - m^2}) \cong (l, m, 1)$ ,  $\vec{\sigma} \cong (l, m, 0)$  and  $\vec{r}_1 - \vec{r}_2 \equiv (u, v, w)$  (as previously), Eq. 4.6 is modified in this way:

$$V'_\nu(u, v, w) = e^{-2\pi i w} \int \int I_\nu e^{-2\pi i (ul + um)} dl dm. \quad (4.9)$$

Now it is possible to define the coherence function relative to  $\vec{s}_0$  as

$$V_\nu(u, v) = V'_\nu(u, v, w) e^{2\pi i w} = \int \int I_\nu e^{-2\pi i (ul + um)} dl dm. \quad (4.10)$$

In this case,  $I_\nu(l, m)$  and  $V_\nu(u, v)$  are linked by a Fourier transform,

$$I_\nu(l, m) = \int \int V_\nu(u, v) e^{2\pi i (ul + vm)} du dv. \quad (4.11)$$

For the sake of the clarity, the spacial autocorrelation function is not known everywhere in the  $u - v$  plane, but only where an antenna can sample the signal. A *sampling function*  $S(u, v)$ , which is null everywhere but where data have been taken, *i.e.* where antennas had been working. Doing thus, one could calculate the *dirty image* function

$$I_\nu^D(l, m) = \int \int V_\nu(u, v) S(u, v) e^{2\pi i (ul + vm)} du dv. \quad (4.12)$$

The functions  $I_\nu^D(l, m)$  and  $I_\nu(l, m)$  are related by a convolution,

$$I_\nu^D = I_\nu \otimes B, \quad (4.13)$$

where  $\otimes$  denotes the convolution and

$$B(l, m) = \int \int S(u, v) e^{2\pi i (ul + vm)} du dv, \quad (4.14)$$

which is known as *synthesized beam* or *point spread function* corresponds to the sampling function  $S(u, v)$ . Hence, following Eq. 4.13,  $I_\nu^D$  is the real intensity distribution  $I_\nu$  convolved with the synthesized beam  $B$ .

For the sake of the clarity, Eq. 4.2 is not complete; in fact there is the normalized reception pattern factor to consider,  $\mathcal{A}_\nu(s)$ . This value has not been reported from the beginning to facilitate the writing of previous equations. Considering just Eq. 4.10, its complete form is termed the complex visibility:

$$V(u, v) = \int \int \mathcal{A}_\nu(l, m) I_\nu e^{-2\pi i(ul+um)} dl dm, \quad (4.15)$$

it is referred to the phase tracking center that one chooses. The  $\mathcal{A}_\nu$  factor does not consider receivers as point-like, so its sensitivity depends on the arrival direction of the signal. This factor can be taken into account in the last step to derive the sky intensity and then to divide the derived intensities. But, even though this division improves the estimate of the final intensities, it introduces a lot of errors in directions far from the center of the element primary beam, where one is dividing by small numbers [15]. However, apart from the real complexity of  $\mathcal{A}_\nu(s)$ , it rapidly decreases to zero but within some  $s_0$  (namely the pointing center for the array elements), therefore the assumption to neglect the terms of  $\sigma$  greater than the first order (Eq. 4.8) is generally accepted.

## 4.2 Signal acquisition in radio interferometry

After having seen that the measure of the radio mutual coherence can give images, this section is dedicated to the analysis of the electric field after it is received by antennas. In particular, the discussion is limited to two only antennas, but concepts here are sufficient to understand fundamentals of radio interferometry. To write this section, I follow [16].

Synthesis arrays produce images by Fourier transform from measurements of the complex visibility. As mentioned this method can be explained through arrays with two elements, as in figure 4.3. In figure,  $\vec{s}$  is the unit vector which points the source (the same for both the antennas),  $\vec{b}$  is the baseline, that is the distance between the antennas, and  $\theta$  the angle between the vector  $\vec{s}$  and the zenith. The same wavefront reaches the first antenna a time  $\tau_g$  later than the second one, and this time is the *geometrical delay*, given by

$$\tau_g = \frac{\vec{b} \cdot \vec{s}}{c} = \frac{|\vec{b}\vec{s}|}{c} \cos \theta. \quad (4.16)$$

After the reception, the signals pass through amplifiers with some filters centered on the frequency of the observation  $\nu$  and with a bandpass  $\Delta\nu$ . Then signals are combined

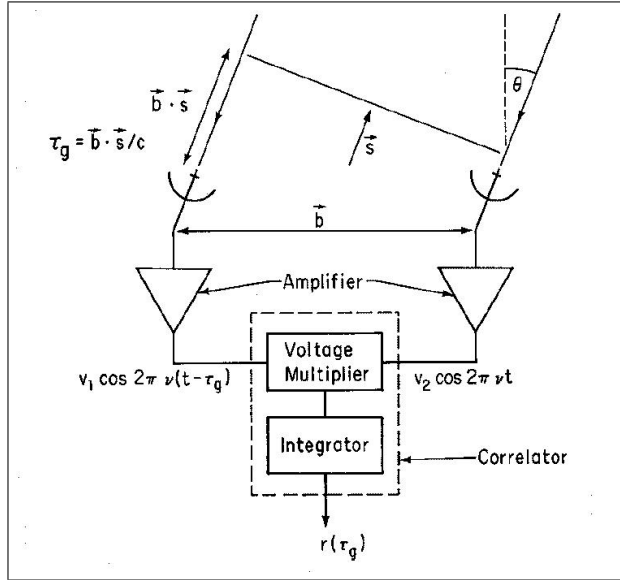


FIGURE 4.3: A simplified block diagram of an interferometer with two elements [16].

by a correlator, that is a voltage multiplier followed by a time averaging (integrating) circuit [16]. Assuming that  $V_1(t) = v_1 \cos \omega(t - \tau_g)$  and  $V_2(t) = v_2 \cos \omega t$  are the input quasi-monochromatic waveforms, the correlator multiplies these inputs, then averages them and a filter cuts the higher frequencies (i.e.,  $2\omega$ ). In other words:

$$\begin{aligned}
 r(\tau_g) &= v_1 v_2 \cos \omega t, \cos[(t - \tau_g)\omega] = \\
 &= \frac{1}{2} v_1 v_2 [\cos \omega t + \cos(2\omega t - \omega \tau_g)] \propto \\
 &\propto v_1 v_2 \cos \omega \tau_g.
 \end{aligned} \tag{4.17}$$

The oscillations in the cosine function represent the motion of the source through the interferometer fringe pattern, and the temporal variation of the geometrical delay is very slow with respect to the Earth's rotation which does not attenuate the fringes by the averaging.

The interferometer output is expressed in terms of radio brightness, then integrated over a solid angle (all the sky is  $4\pi$  sterad). The symbol used here to indicate the brightness (or even the intensity), in the direction  $\vec{s}$ , at the frequency  $\nu$ , is  $I_\nu(\vec{s})$ , using units given in  $\text{W m}^{-2} \text{Hz}^{-1} \text{sr}^{-1}$ . Thus, a signal power received from a solid angle of  $d\Omega$ , in a bandpass  $\Delta\nu$  is  $A(\vec{s})I(\vec{s})\Delta\nu d\Omega$ , where  $A(\vec{s})$  is the effective area that collects the radiation in the direction  $\vec{s}$  (in the following this area will be considered the same for all antennas). By

omitting constant factors, the resulting output from  $d\Omega$  is

$$dr = A(\vec{s}) I(\vec{s}) \Delta\nu \cos(\omega\tau_g) d\Omega. \quad (4.18)$$

This last equation in terms of  $\vec{b}$  and  $\vec{s}$  and integrated over the source solid angle gives

$$r = \Delta\nu \int_S A(\vec{s}) I(\vec{s}) \cos \frac{\vec{b} \cdot \vec{s}}{c} d\Omega. \quad (4.19)$$

To justify this last result, some assumptions have been considered:  $\Delta\nu$  is small enough to ignore variations in  $\nu$  for  $A$  and  $I$ , the emitted source wavefront is plane when received and signal components emitting from the different points of the source are uncorrelated, namely that the source is spatially incoherent.

Once the phase reference position  $\vec{s}_0$  is fixed (remind figure 4.2), the synthesized FoV can be centered, and Eq. 4.19 becomes

$$\begin{aligned} r &= \Delta\nu \cos \left( \omega \frac{\vec{b} \cdot \vec{s}_0}{c} \right) \int_S A(\vec{\sigma}) I(\vec{\sigma}) \cos \left( \omega \frac{\vec{b} \cdot \vec{s}}{c} \right) d\Omega + \\ &\quad - \Delta\nu \sin \left( \omega \frac{\vec{b} \cdot \vec{s}_0}{c} \right) \int_S A(\vec{\sigma}) I(\vec{\sigma}) \sin \left( \omega \frac{\vec{b} \cdot \vec{s}}{c} \right) d\Omega. \end{aligned} \quad (4.20)$$

The complex visibility, already mentioned in the section 4.1.1, can be re-written as [16]

$$V \equiv |V| e^{i\phi_V} = \int_S \mathcal{A}(\vec{\sigma}) I(\vec{\sigma}) \exp \left[ -i\omega \frac{\vec{b} \cdot \vec{\sigma}}{c} \right] d\Omega, \quad (4.21)$$

with  $\mathcal{A} \equiv A(\vec{\sigma})/A_0$ , namely the normalized antenna reception pattern and  $A_0$  the maximum response at the centre of the beam. This last equation represents the response of the system to the brightness distribution  $\mathcal{A}(\vec{\sigma})I(\vec{\sigma})$ . By splitting the real and imaginary parts in Eq. 4.21, results in

$$A_0 |V| \cos \phi_V = \int_S A(\vec{\sigma}) I(\vec{\sigma}) \cos \left( \omega \frac{\vec{b} \cdot \vec{\sigma}}{c} \right) d\Omega \quad (4.22)$$

and

$$A_0 |V| \sin \phi_V = - \int_S A(\vec{\sigma}) I(\vec{\sigma}) \sin \left( \omega \frac{\vec{b} \cdot \vec{\sigma}}{c} \right) d\Omega, \quad (4.23)$$

which are substituted into Eq. 4.21 to give the following equation

$$r = A_0 \Delta\nu |V| \cos \left( \omega \frac{\vec{b} \cdot \vec{s}_0}{c} - \phi_V \right). \quad (4.24)$$

Taking interferometric measurements means to measure the amplitude and phase of the

fringe pattern from Eq. 4.24, subsequently deriving the amplitude and the phase of  $V$  by the appropriate calibration [16]. As mentioned in the previous section, the Fourier transform of the visibility (Eq. 4.21) gives the intensity distribution of a source. Thus  $V$  must be measured over a sufficiently wide range of  $\nu \vec{b} \cdot \vec{\sigma}/c$ , that can be envisaged as the baseline viewed from the direction of the source, measured in wavelengths [16].

Now, It is useful to stress how  $\Delta\nu$  influences  $r(\tau_g)$ . If Eq. 4.18 is integrated over the source with an infinitesimal bandwidth  $d\nu$ , then it can written

$$dr = A_0|V| \cos(2\pi\nu\tau_g - \phi_V) d\nu, \quad (4.25)$$

and hence

$$\begin{aligned} r &= A_0|V| \int_{\nu_0-\Delta/2}^{\nu_0+\Delta/2} \cos(2\pi\nu\tau_g - \phi_V) d\nu = \\ &= A_0|V|\Delta\nu \frac{\sin(\pi\Delta\nu\tau_g)}{\pi\Delta\nu\tau_g} \cos(2\pi\nu_0\tau_g - \phi_V), \end{aligned} \quad (4.26)$$

where  $\nu_0$  is the observational central frequency in the passband. Therefore the fringes follow a sinc-function expansion, also referred to as the *bandwidth pattern*. The complete fringe amplitude appears only at a direction normal to the baseline, that is at  $\tau_g = 0$ . The range within which the fringe amplitude is greater than the 99% corresponds to

$$\frac{\sin \pi \Delta\nu\tau_g}{\pi \Delta\nu\tau_g} \approx 1 - \frac{(\pi \Delta\nu\tau_g)^2}{6} > 0.99. \quad (4.27)$$

This condition is respected for  $|\Delta\nu\tau_g| < 0.078$ , if  $\pi \Delta\nu\tau_g \ll 1$ . In practice, if one wanted to observe with large hour-angle, a computer-controlled delay should be included within the system to compensate for  $\tau_g$  [16].

### 4.2.1 Frequency conversion

In order to work in a simple way with the source signal ( $\nu_{\text{RF}}$ ), this is mixed with a fixed frequency of an local oscillator ( $\nu_{\text{LO}}$ ), to obtain as output two intermediate frequencies ( $\nu_{\text{IF}}$ ):

$$\nu_{\text{RF}} + \nu_{\text{LO}} \quad (4.28a)$$

$$\nu_{\text{RF}} - \nu_{\text{LO}}. \quad (4.28b)$$

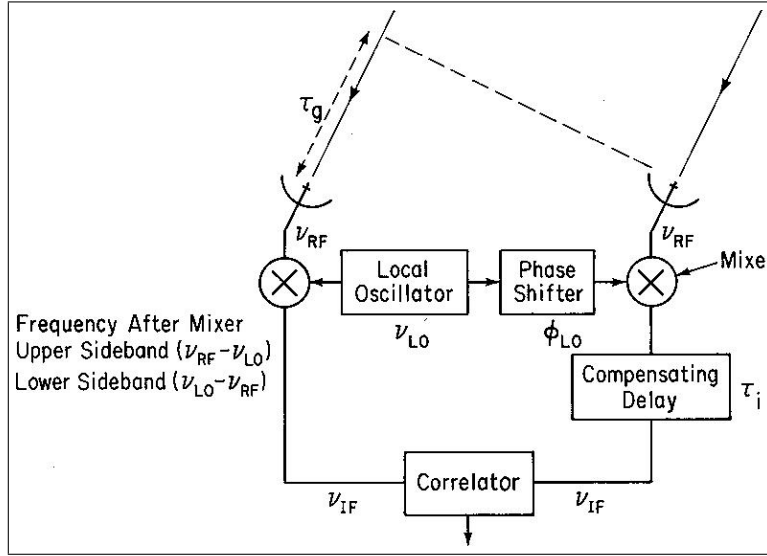


FIGURE 4.4: Sketch of an interferometer system, with frequency conversion instruments. Amplifiers and filters are not drawn in the diagram [16].

Since these outputs are usually filtered, only the lower  $\nu_{\text{IF}}$  (the upper sideband in applied for  $\nu_{\text{RF}}$ ) is considered and the following relation for next calculations

$$\nu_{\text{RF}} = \nu_{\text{IF}} + \nu_{\text{LO}} . \quad (4.29)$$

As a final addition, there is an instrumental delay  $\tau_i$  to compensate for  $\tau_g$ . Figure 4.4 can help to see the all processes. The final response can be written by considering the phase differences  $\phi_1$  and  $\phi_2$  imposed on the  $\nu_{\text{RF}}$  of the antennas 1 and 2, before reaching the correlator. As for the upper sideband, the phase differences are

$$\begin{aligned} \phi_1 &= 2\pi\nu_{\text{RF}}\tau_g = 2\pi(\nu_{\text{IF}} + \nu_{\text{LO}})\tau_g \\ \phi_2 &= 2\pi\nu_{\text{IF}} + \phi_{\text{LO}} , \end{aligned} \quad (4.30)$$

where  $\phi_{\text{LO}}$  is the phase difference of the local oscillator signal at the two mixers.

From Eq. 4.25 and suitable modifications, the upper-sideband response is [16]

$$\begin{aligned} r &= A_0|V| \int_{\nu_{\text{IF}_0}-\Delta/2}^{\nu_{\text{IF}_0}+\Delta/2} \cos(\phi_1 - \phi_2 - \phi_V) d\nu = \\ &= A_0|V|\Delta\nu \frac{\sin(\pi\Delta\nu\Delta\tau)}{\pi\Delta\nu\Delta\tau} \cos[2\pi(\nu_{\text{LO}}\tau_g + \nu_{\text{IF}_0}\Delta\tau_i) - \phi_{\text{LO}} - \phi_V] , \end{aligned} \quad (4.31)$$

where  $\Delta\tau = \tau_g - \tau_i$  is the tracking error of the compensating delay  $\tau_i$ . Here the output fringe oscillations depend on the  $\nu_{\text{LO}}$ , rather than the observational frequency  $\nu_0$  as in Eq. 4.27. For the sake of the clarity, if the lower sideband with Eq. 4.28a is chosen the

phase difference equations are [16]:

$$\begin{aligned}\phi_1 &= -2\pi(\nu_{\text{IF}} - \nu_{\text{LO}})\tau_g \\ \phi_2 &= 2\pi\nu_{\text{IF}} - \phi_{\text{LO}}, \\ r_l &= A_0|V|\Delta\nu \frac{\sin(\pi\Delta\nu\Delta\tau)}{\pi\Delta\nu\Delta\tau} \cos[2\pi(\nu_{\text{LO}}\tau_g - \nu_{\text{IF}_0}\Delta\tau_i) - \phi_{\text{LO}} - \phi_V].\end{aligned}\quad (4.32)$$

### 4.2.2 The $u$ - $v$ plane

In previous sections basic concepts of radio interferometry have been reported, concerning signal emission, pointing and frequency conversion. Also a brief introduction about  $(u, v, w)$  coordinates has been given, but in this section the coordinate system for imaging is explained in detail, drawing from [17] and, in particular, [16].

The baseline vector of the system of reference consist of the  $u$ ,  $v$  e  $w$  components, which are measured in wavelengths (the same as the observational frequency). The axes of the tern have directions respectively towards East, North and the phase tracking center; while the sky positions are defined as  $l$  and  $m$ , which are the direction cosines of  $u$  and  $v$  axes. Figure 4.5 can help to envisage this scheme.

The centre of the synthesized image has the direction of the unit vector  $\vec{s}_0$  and the projection of the celestial sphere, centered at and normal to the previous point, is the  $(l, m)$  plane. Distances in  $l$  and  $m$  are proportional to the sines of the angles that open from the direction  $\vec{s}_0$ . In this frame, I can write

$$\begin{aligned}\frac{\nu}{c}\vec{b} \cdot \vec{s} &= ul + vm + nw, \\ \frac{\nu}{c}\vec{b} \cdot \vec{s}_0 &= w, \\ d\Omega = \frac{dl \ dm}{n} &= \frac{dl \ dm}{\sqrt{1 - l^2 - m^2}}.\end{aligned}\quad (4.33)$$

By using this coordinate system, Eq. 4.21 becomes [16]

$$V(u, v, w) = \int_{-\infty}^{+\infty} \int_{-\infty}^{+\infty} \mathcal{A}(l, m) I(l, m) \frac{e^{-2\pi i [ul + vm + w(\sqrt{1-l^2-m^2} - 1)]}}{\sqrt{1 - l^2 - m^2}} dl \ dm, \quad (4.34)$$

noting that the integrand is made equal to zero if  $l^2 + m^2 \geq 1$ . It is obvious from the equation that the visibility is a function of  $I$  and  $\mathcal{A}$ . In order to obtain  $I(l, m)$  by a two-dimensional Fourier transform, the third component should be nullified. This is possible under two conditions: either the baselines are coplanar, namely when the tip

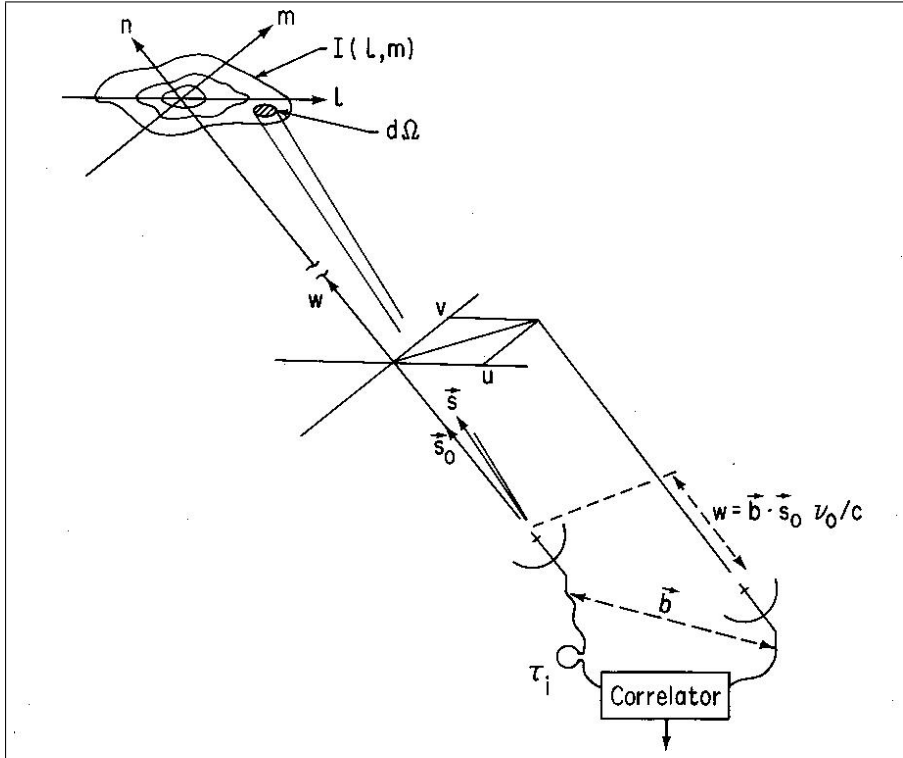


FIGURE 4.5: The  $(u, v, w)$  and  $(l, m, n)$  coordinate systems used respectively to express the interferometer baselines and the source brightness distribution [16].

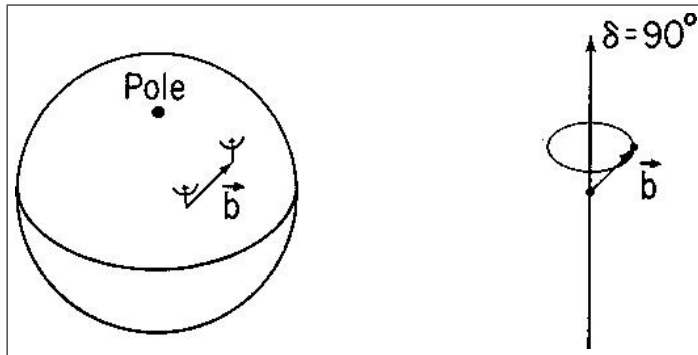


FIGURE 4.6: During the Earth's rotation, any baseline vector  $\vec{b}$  traces out a circular locus in a plane orthogonal to the rotation axis (coincident with the polar axis,  $\delta = 90^\circ$  in celestial declination). As for a baseline vector totally in the East-West direction,  $\vec{b}$  is perpendicular to the rotation axis [16].

of the baseline vector traces out a circle concentric with the Earth's rotation axis, as in figure 4.6, or when the baseline vectors are entirely in the East-West direction, in which case all traces are concentric, with different radii and in the same plane. In general, this latter condition is always respected for a two-antenna array, choosing the  $w$ -axis in the celestial-pole direction, so that  $w = 0$ . Now, Eq. 4.34 has lost the  $w$ -component and its Fourier transform is

$$\frac{\mathcal{A}(l, m) I(l, m)}{\sqrt{1 - l^2 - m^2}} = \int_{-\infty}^{+\infty} \int_{-\infty}^{+\infty} V(u, v) e^{2\pi i (ul + vm)} du dv. \quad (4.35)$$

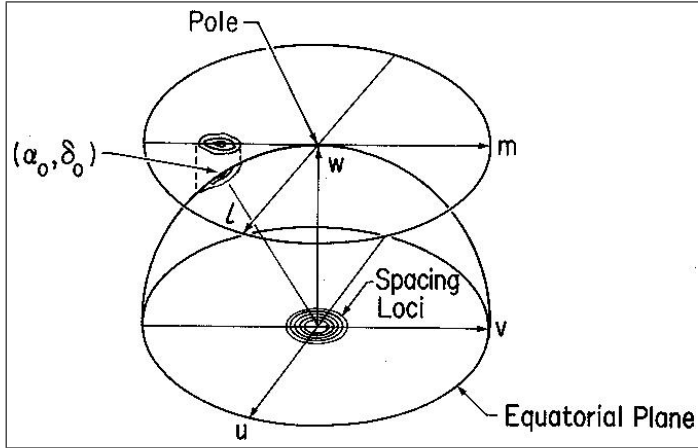


FIGURE 4.7: The North spherical cap where the source lies, with its tangent plane on the North pole and the source projection onto this last plane. The spacing-vector loci for an East-West baseline array are shown too, it has the origin of the  $(u, v, w)$  system, where  $w$  have the direction of the North pole [16].

The last equation can be used throughout the North hemisphere. As an example, figure 4.7 shows how the spacings of antenna pairs for an East-West array are projected from the  $u$ - $v$  plane on the  $l$ - $m$  plane.

When radio observations are done, small areas of the sky are usually selected to be imaged by the antenna beams. Pointing on the celestial coordinates  $(\alpha_0, \delta_0)$ , it is possible to choose the direction of the  $u$ -axis as in figure 4.7, so that  $l$  is small within the region to observe and it is about equal to the angular distance on the sky. A problem with  $m$  remains, since it is the angular distance measured from the pole and therefore  $m = \sin(90^\circ - \delta_0) = \cos \delta_0$ . Furthermore, the scale of the image is compressed in the  $m$ -direction by a factor  $\sin \delta$ . The best solution is to center the system of reference on  $(\alpha_0, \delta_0)$  of the image. To do this it is sufficient to rotate the axes around the  $u$ -direction as long as the  $w$ -axis points the center of the image and substituting  $w = -v \cos \delta_0$  in Eq. 4.34, which derives from the location of the baselines in the equatorial plane. Now, there are only two variables in the integral and the Fourier transform is applicable.

When the source is close to the celestial equator, baselines parallel to the Earth's rotation axis are preferred, though they are not coplanar in the  $(u, v, w)$  space. In this case, a new system of three coordinates is required to accommodate the spacing vectors and to reduce Eq. 4.34 to a two-dimensional Fourier transform. One has this system if  $|l|$  and  $|m|$  are small enough to write

$$\left( \sqrt{1 - l^2 - m^2} - 1 \right) w \approx -\frac{1}{2}(l^2 + m^2)w \approx 0. \quad (4.36)$$

Thus Eq. 4.34 becomes

$$V(u, v, w) = \int_{-\infty}^{+\infty} \int_{-\infty}^{+\infty} \mathcal{A}(l, m) I(l, m) e^{-2\pi i(ul+vm)} dl dm. \quad (4.37)$$

In practice, when  $|l|$  and  $|m|$  are small, the field imaging will also be small, and the visibility upon  $w$  is negligible. In the end, the image of Eq. 4.37 is

$$\mathcal{A}(l, m) I(l, m) = \int_{-\infty}^{+\infty} \int_{-\infty}^{+\infty} V(u, v) e^{2\pi i(ul+vm)} du dv. \quad (4.38)$$

This last equation is valid only if the condition

$$\pi(l^2 + m^2)w \ll 1 \quad (4.39)$$

is respected. Arrays which do not have coplanar baselines as the Earth rotates have a phase error  $\pi(l^2 + m^2)w$ , with Eq. 4.37 and radiation emanating from  $(l, m)$ . This limits the dimensions of the source to image, unless special procedures are used.

### 4.2.3 Antenna placing and synthesis arrays

As mentioned previously, when a pair of antennas tracks a point with celestial coordinates  $(h, \delta)$ , the tip of their baseline trace out a curve due to the Earth's rotation. In the commonly used reference system, multiple-element antenna arrays trace out ellipses in the  $u-v$  plane and these ellipses have equations which depend on the celestial declination of the observed point. Thus a general antenna-spacing ellipse is

$$u^2 + \left( \frac{v - (L_z/\lambda) \cos \delta}{\sin \delta} \right)^2 = \frac{L_X^2 + L_Y^2}{\lambda^2}, \quad (4.40)$$

where  $L_X$ ,  $L_Y$  and  $L_Z$  are Cartesian-coordinate distances between two antennas. The center and the semi-axes of this ellipse are respectively:

$$C_e \equiv \left( 0; \frac{L_z \cos \delta}{\lambda} \right), \quad (4.41a)$$

$$r_{\text{eli}} = \frac{\sqrt{L_X^2 + L_Y^2}}{\lambda}. \quad (4.41b)$$

For an array with many antennas the ensemble of elliptical loci is called a *transfer function*, or *sampling function* [16].

The number of pairs of baselines in an array with  $n_{\text{ant}}$  antennas is

$$N_b = \frac{1}{2} n_{\text{ant}} (n_{\text{ant}} - 1), \quad (4.42)$$

and, in general, the rate at which visibility measurements can be done is proportional to the square of the total antenna number. The arrangement of antennas in the plane ( $u, v$ ) is the *sampling of visibility function*. This configuration usually depends on the angular-resolution range that is required, since resolution and FoV are related to the available baselines of the array.

The antenna configuration and an example of the transfer function for the Very Large Array (VLA) are shown in figure 4.8. In the upper panel (4.8a) there is a configuration in which the radial distance from the array center to the  $n_i$  antenna on each branch is proportional to  $n^{1.716}$ . With this power-law design, no two spacings on any branch are equal. The array is rotated of  $5^\circ$  from the North-South line, to avoid exact East-West baselines. This example can be seen with more detail in [16].

### 4.3 Sensitivity and angular resolution

In this quick introduction to the radio interferometry and antennas, I introduce, without describing in detail, two important parameters. Sensitivity and angular resolution are certainly two of the primary features to know about any telescope.

The sensitivity is the lowest measure that a receiver can measure. If I term the sensitivity of an antenna as  $S_{\text{ant}}$ , its equation is:

$$S_{\text{ant}} = \frac{T_{\text{sys}}}{\sqrt{2\Delta\nu\Delta T}}. \quad (4.43)$$

where  $\Delta\nu$  is already mentioned,  $\Delta T$  is the integration time for an acquisition, and  $T_{\text{sys}}$  is the *system temperature*. In general, for radio telescope, a temperature is related to the received flux density, as

$$\text{SEFD} = \frac{T_{\text{sys}}}{g}, \quad (4.44)$$

where SEFD is the *system equivalent flux density* and  $g$  is named gain, which depends on the antenna and receiver features.

The system temperature collects many temperatures measured by the receiver, and is a sum of

$$T_{\text{sys}} = T_{\text{rx}} + T_{\text{sp}} + T_{\text{atm}} + T_{\text{Gal}} + T_{\text{CMB}} \quad (4.45)$$

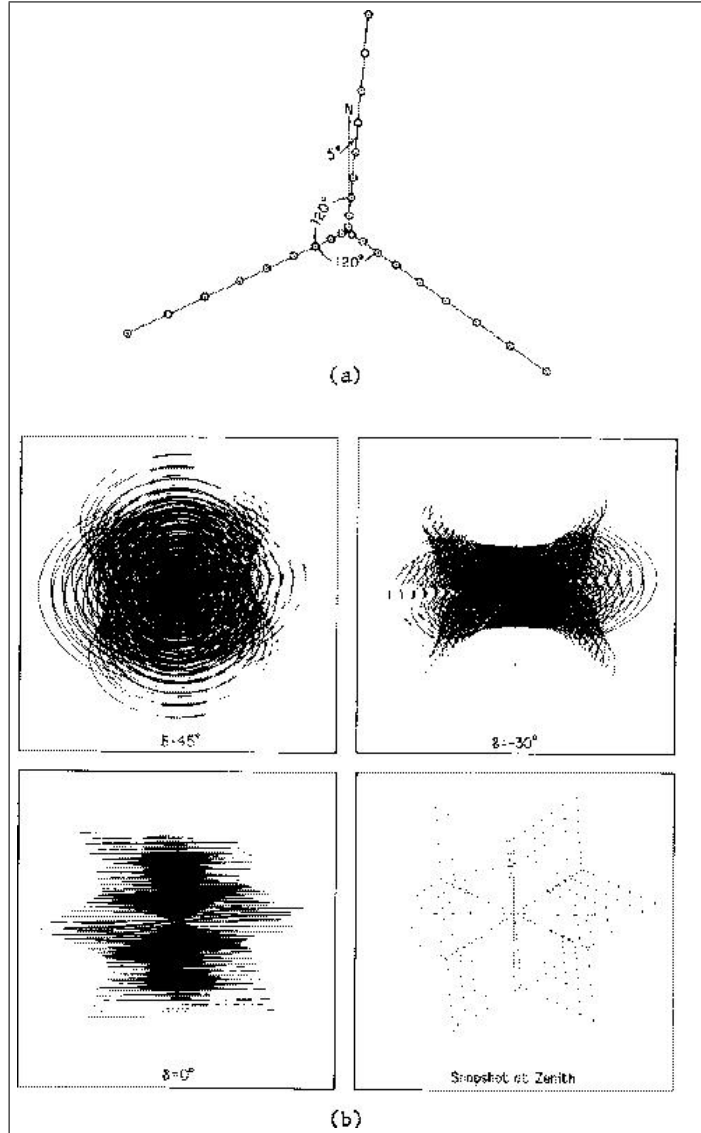


FIGURE 4.8: In the a sketch there is the VLA configuration, with 27 antennas. In the b sketch are shown transfer functions at four declinations. At  $\delta = 0^\circ$  and  $45^\circ$  for a time of  $\pm 4\text{h}$ ;  $\delta = -30^\circ$  for  $\pm 3\text{h}$ ; finally, a snapshot of  $\pm 5\text{m}$  pointing to the Zenith. Credit by [16].

where, respectively they are: the temperature inserted by the receiver, i.e., electrical noise; the spillover temperature, namely radio signal emitted by the Earth and intercepted by the beam of the antenna; the temperature of the Earth atmosphere, that is the radio signal emitted by it; the temperature of the radio Galactic background; finally, the the temperature of the Cosmic Background Radiation. The radio-source signal is often termed as *antenna temperature*,  $T_{\text{ant}}$ , and must be added to the system temperature. As regarding a two-element radio interferometer, assuming (obviously) the same integrator time and bandpass, the lowest flux density measured is

$$S_{\text{2RI}} = \sqrt{\frac{\text{SEFD}_1 \cdot \text{SEFD}_2}{2 \Delta\nu \Delta T}}. \quad (4.46)$$

For a  $n_{\text{ant}}$ -antenna array the sensitivity of a synthesis image is

$$I_{\text{arr}} \propto \frac{\langle \text{SEFD} \rangle}{\sqrt{2 \Delta\nu \Delta T}} \frac{1}{\sqrt{n_{\text{ant}} (n_{\text{ant}} - 1)}}, \quad (4.47)$$

where  $\langle \text{SEFD} \rangle$  is the geometric mean of all the antenna SEFD of the array, and the unit is Jansky per synthesized beam area.

As for the angular resolution, its formula is

$$\vartheta_{\text{HPBW}} = 2063 \frac{\lambda}{B_{\max}} \text{ mas}. \quad (4.48)$$

However, there is another important parameter to take into account. It is the largest *angular scale* (also named *spatial frequency*),

$$\vartheta_{\text{LAS}} = 2063 \frac{\lambda}{2 B_{\min}} \text{ mas}. \quad (4.49)$$

Both results are in mas, if the wavelengths are measured in cm while the maximum and minimum baselines, respectively  $B_{\max}$  and  $B_{\min}$ , are expressed in km. When  $B_{\min}$  is too large, one losses information on the total flux; while, if  $B_{\max}$  is too short, then information of the size on the source can be lacking as well as information on its whole structure. In other words, a very compact array has a  $u$ - $v$  sample with short baselines, the flux is measured very well but one loses details on the internal structure of the source and on its high spatial frequency. On the other hand, an widespread array without short baselines can measure a source structure well, with high spatial frequency, but the flux is reduced. See also figure 4.9. In general, the choice of the radio interferometer for studies about astrophysical sources has to base on precise purposes.

It is worthwhile to stress that the FoV is different from the angular scale (in general the latter is less than the former).

GRBs are extremely faint sources, so a preliminary study should be done with a compact array, in order to collect their fluxes rather than structures. Furthermore, to investigate

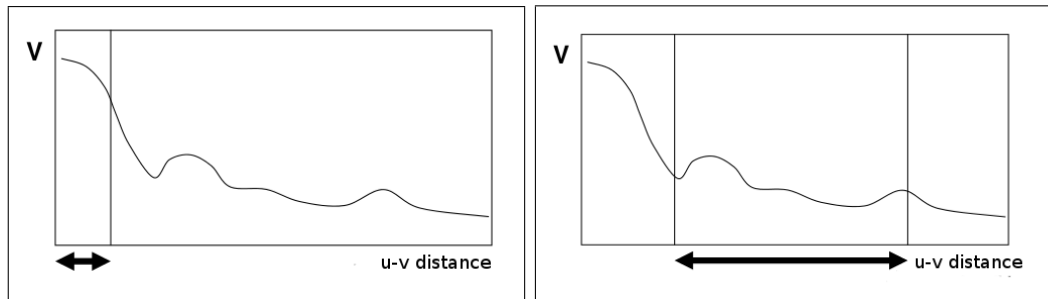


FIGURE 4.9: Visibility depending on the  $u$ - $v$  distances.

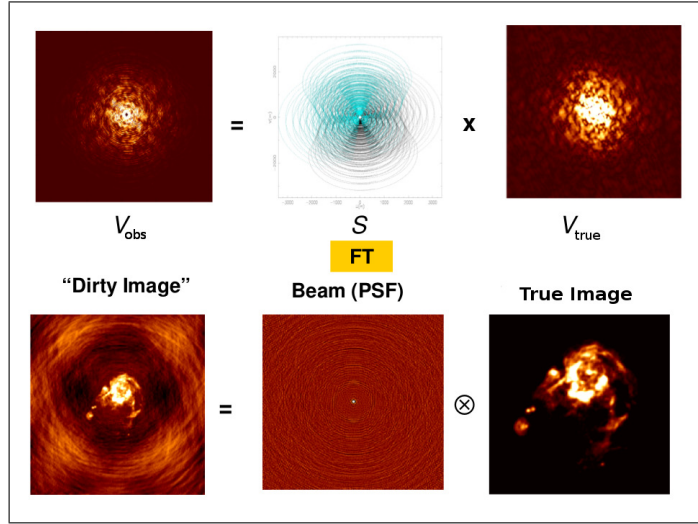


FIGURE 4.10: A visual product of visibility and imaging.

common characteristics it is more important to analyse all the flux, e.g. unresolved sources.

## 4.4 Convolution and deconvolution

When one observes using arrays, the actual coverage of the  $u$ - $v$  plane is incomplete. In fact, it is sampled only where antennas are placed. However, after integrating for long time, the transfer function traced out by the baseline tips increase points in that plane. Therefore, the final resulting visibility is not ideal, but it is generated by a smaller ensemble of the ideal coverage. In other words, the visibility is

$$V_{\text{obs}}(u, v) = V_{\text{true}}(u, v) \times S(u, v), \quad (4.50)$$

where

$$S(u, v) = \sum_k \delta(u_k, v_k) \quad (4.51)$$

and  $k$  runs over the antennas of the array. Factors in Eq. 4.50 inserted into the Fourier transform give a convolution product:

$$I_{\text{obs}}(l, m) = \iint_S [V_{\text{true}}(u, v) \times S(u, v)] e^{2\pi i(lu + mv)} du dv \rightarrow I_d(u, v) = I_{\text{true}}(u, v) \otimes B(l, m), \quad (4.52)$$

where the subscript “d” is for “dirty” and  $B(l, m)$  is the point spread function (PSF). Through the convolution, the resulting image is a sum of many beams, each centered on the source. Figure 4.10 shows an explanatory sketch of the last equations.

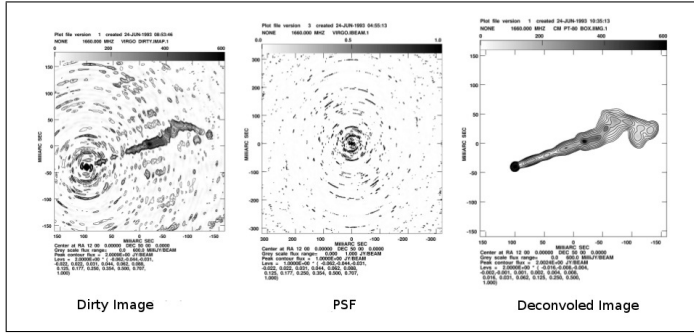


FIGURE 4.11: A visual product of visibility and imaging [17].

After an image has been acquired by the PSF, the deconvolution process starts. The CLEAN algorithm is one of methods used to deconvolve a dirty image. It consists in an iterative process that sequentially subtracts beam detection from the dirty image. To state more clearly, it is a cycle with four steps:

1. Identify the brightest point,  $I_{\max}$ , in the image
2. Subtract 1 beam detection from  $I_{\max}$
3. Write a table (called *clean components*) specifying positions in the imaging map and intensity at that point:  $(x_i, y_i, I_i)$ , , where  $i$  is the iteration number
4. if the peak in the residual map is greater then the RMS, then go to step 1.

From the residual image, one adds the (convoluted) clean components of a “clean” beam, that is a bi-dimensional Gaussian. Figure 4.11 can help to clarify the iteration.

For more detail see also [17] and, in particular, [215].

In the chapter 5, some GRB-radio works are discussed and the GRB radio fluxes are also reported. In general, because of their faint emissions, data reductions of GRBs are very difficult to obtain. In fact, it is very complex to separate the background dirty image from the GRB signal. Furthermore, identifying the source with good precision in the image is another not a trivial difficulty to solve.



## Chapter 5

# GRB radio observations

Part I speaks generically about GRBs, debating basically about  $\gamma$ -Ray and X-Ray detections, which classify these sources. There, it has been also introduced the importance of lower band observations and detailed how optical and infrared, can be used to discover and to study non-manifest features for higher energies. For this reason, observations in radio band will provide additional information that might not be evident for all higher bands.

Previous chapters of part II have introduced the SKA telescope and radio interferometry, to provide essential knowledge to read this chapter which closes the part II and is focused on radio GRB observations, to point out their chances to provide fundamental data, practical applications and issues. It will also report my current submitted paper and the aim proposed in this work.

GRB afterglow luminosities cross frequencies from X-rays to radio during decay. The radio decay takes many days, or even weeks after the burst, while the highest frequencies last for some minutes or hours. Considering the burst of each event as the zero time, every frequency has an own luminosity peak, which generally appears later as the wavelength increases, i.e. this peak is moved in time since the gamma burst, as well the decay becomes longer. As an example, the peak of a GRB afterglow emission crosses the millimeter and submillimeter range during the first hours to days.

In general, even though radio observations have been limited until now because of the current low sensitivity, the SKA will change this situation and studies of these crossings will be crucial for the constraining models.

## 5.1 Studies of GRBs in radio band

In this section a precise study of GRBs by Chandra & Frail [18] is reported. They were the first to start a systematic study in radio bands on GRBs. For the first time, a large sample of radio GRB was presented in a work, instead of deep studies about single events. Their work is important not only for its results but also for analyses and procedures adopted. They attempt to understand and find relations between the radio band and higher frequencies comparing each others.

A number of 304 (pre-*Swift* and *Swift* eras) GRBs have been observed between 0.6 - 600 GHz bands, by the the Very large Array (VLA), the EVLA (the Expanded VLA), the Australia Telescope Compact Array (ATCA), the Westerbork Synthesis Radio Telescope (WSRT), the Giant Metrewave Radio Telescope (GMRT) and, finally, the Very Long Baseline Array (VLBA) with its millisecond angular resolution to observe five GRBs. Observations, data reductions and analyses of this sample lasted for 15 years (GRB observed since January 1997 to January 2011). Observations were done with the interferometric mode, with a typical integration time of 30 minutes and a bandwidth of 100 MHz. Out of 304 GRBs, 95 are detections while the 206 are non-detections, where they considered as “detection” when the signal was greater than  $3\sigma$  of the instrumental sensitivity and as “non-detections” when the GRB radio acquisition was less then  $3\sigma$  (as regarding sensitivity, see chapter 4).

Before continuing to their results and considerations, a quick presentation of relevant formulae is useful. Here the formula to convert the radio flux density  $F$  into spectral luminosity  $L$  is

$$L = 4\pi F \frac{d_L^2}{1+z}, \quad (5.1)$$

where  $d_L$  is the luminosity distance at redshift  $z$  (more details in the part III). Chandra and Frail multiplied Eq. 5.1 by a  $k$ -correction factor equal to

$$k = (1+z)^{\alpha-\beta}, \quad (5.2)$$

in order to incorporate the  $k$ -correction so as to rescale values into the rest frame follows:

$$L_k = k L = 4\pi F d_L^2 (1+z)^{\alpha-\beta-1} \quad (5.3)$$

In Eqs. 5.2 and 5.3,  $\alpha$  and  $\beta$  are respectively the time and the frequency indices in  $F \propto t^\alpha \nu^\beta$ . To have an optically thin, post-jet-break, flat light curve [216], they got values of  $\alpha = 0$  and  $\beta = 1/3$ . Doing so, they obtained the average luminosity of  $1.1 \times 10^{31}$  erg s $^{-1}$  Hz $^{-1}$  for detections, and the average of  $6.4 \times 10^{30}$  erg s $^{-1}$  Hz $^{-1}$  for non-detection. In their work, through figure 5.1, a difference between low-luminosity

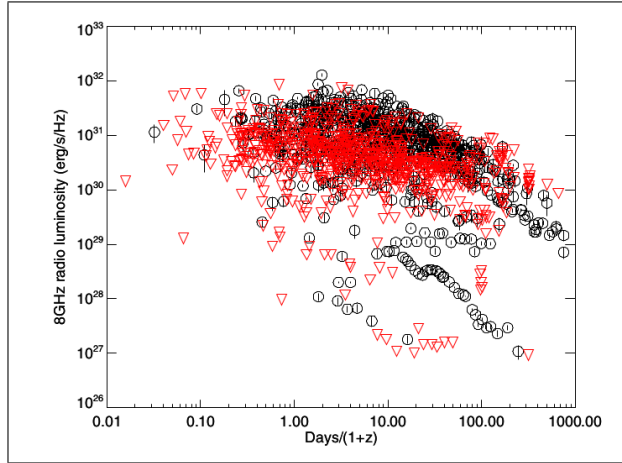


FIGURE 5.1:  $k$ -corrected radio spectral luminosities at 8.5 GHz. The black circles are radio-detected afterglows, whereas the red triangles are the non-detected  $3\sigma$  luminosity upper limits, with respect to the rest-frame time. The luminosity curve for the average cosmological burst varies over a small range, but there are also a number of low-luminosity events [18].

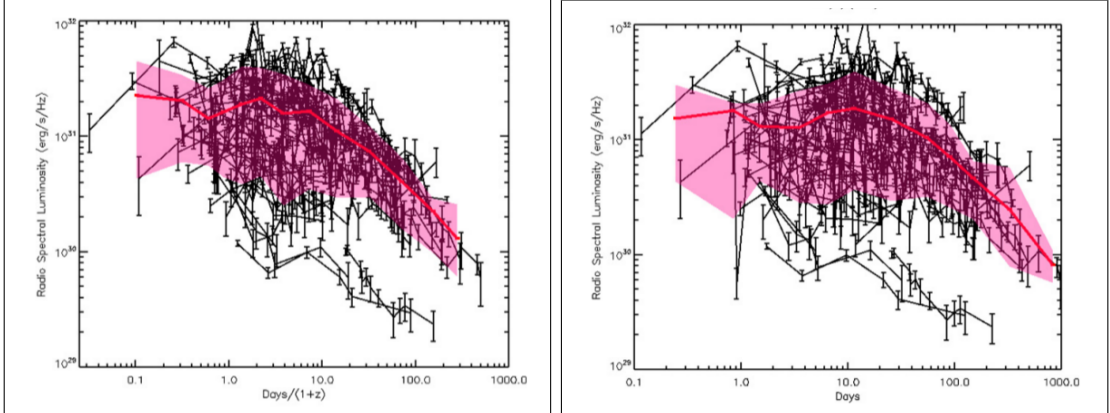


FIGURE 5.2: The first panel shows the radio light curves at 8.5 GHz for the LGRBs in the rest-frame time. The red thick solid line represents the mean light curve. The pink shaded area represents the 75% confidence band. The second panel shows the same plot for time but in the observer-time frame [18].

and standard events is distinguished. Figure 5.2 shows the mean 8.46 GHz light curves of the cosmological LGRBs of  $\sim 2 \times 10^{31}$   $\text{erg s}^{-1} \text{ Hz}^{-1}$  that have peaks until 10-20 days in the observer frame, while these days become 3-6 in the rest frame. After these days, the curves decay as a power law with an index of  $-1$ . In the rest-frame plot there are two different peaks at two instants. The first peak appears between 0.1 and 0.2 days, while the second around the day 2, in the middle there is a dip that has its bottom in about 24 hours. The dip most likely indicates the transition between two different emission processes (reverse and forward shocks). In their study, they collected 65 detections with more than three observations in a single band. By fitting observational data with the

forward shock formula [217],

$$f(t) = \begin{cases} F_{\max} t_{\max}^{-1/2} t^{1/2} & \text{for } t < t_{\max} \\ F_{\max} t_{\max} t^{-1} & \text{for } t > t_{\max}, \end{cases} \quad (5.4)$$

the peak flux densities at the peak times have been determined.

Even though this last formula does not perfectly represent the exact light curve evolution in the radio band, it is good enough to have approximate values of the peak flux density  $F_{\max}$  at the time  $t_{\max}$ . When curves show two peaks, the authors ignored the first peak because it might be a reverse shock and they searched to isolate the forward component emission only.

The curves show that the peak times happen between 3 and 9 days after the burst, at the rest frame and at 8.5 GHz. However, I want to highlight that, even though the peak is in the 8.5 GHz range, the rest-frame peak frequency is different, since it depends on the  $z$ . In other words, when one observes at a given frequency, this is the observer-frame frequency, therefore any peak has got its own frequency emission in its rest frame different from the detected frequency. In this case, different peaks for each frequency should be classified to try to discover a trend. For this reason the SED is quite important. Citing Chandra & Frail, the peak could be due either to the  $\nu_{\max}$  passing the radio frequencies, or to the jet brake and thus the radio emission stops rising, both suppositions could occur around that temporal range. The luminosity distribution peaks in the range of  $10^{31} - 10^{32}$  erg s $^{-1}$  Hz $^{-1}$ . The upper limit detections are clustered between 60 and 3000  $\mu$ Jy. Although observations at 1.4 GHz were done only when the flux density at 8.46 GHz was very high, it is important to note that on a sample of 55 GRB, only 12 of them were detections at the lower frequency.

In regards to the redshift distribution, they took 147 out of 304 redshifts known and made a histogram, dividing them into radio detection and non-detection groups. They found no correlation between radio detections and measured redshifts, and this result was confirmed by the Kolmogorov - Smirnov test (K-S test). This means that GRBs (at least in radio band) do not have a preferred distribution in  $z$ -range considered.

Analysing the fluence (erg cm $^{-2}$ ) between 15 - 150 keV, at the observer frame, they think to have found two different classes overlapping with their radio detected and non-detected sources. They underline that the non-detections mostly (176 out of 206) place below  $10^{-6}$  erg cm $^{-2}$ , but the detections are mostly (82 out of 95) greater than  $10^{-6}$  erg cm $^{-2}$ . Basically, the non-detected radio afterglows tend to have lower values of fluence, and those detected vice-versa. This consideration is supported by the K-S test which gives a value  $P = 2.61 \times 10^{-7}$ . On the other hand, this could depend on an instrumental threshold, due to the dim radio afterglow. Indeed, if the fluence radio threshold was

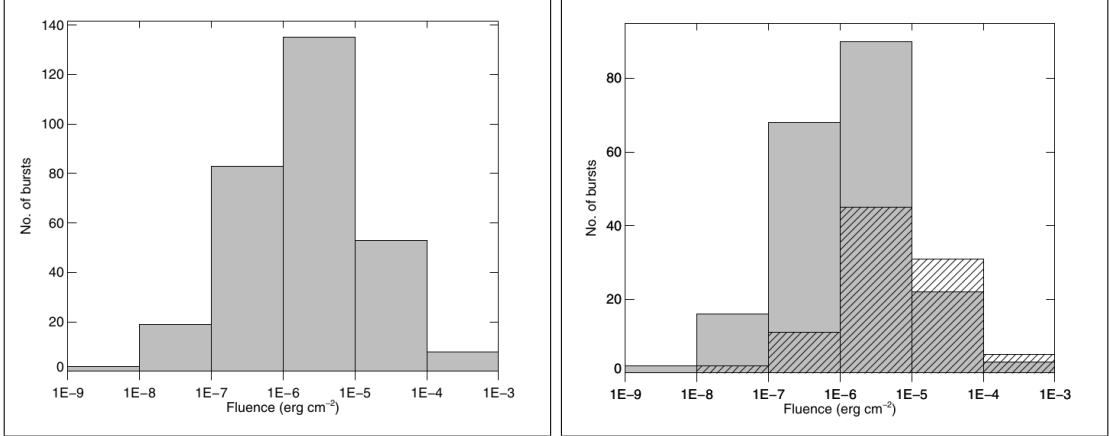


FIGURE 5.3: In the first panel, a histogram of the fluence distribution for sample of 304 used by Chandra and Frail. In the second panel they reported the fluence distribution of the radio-detected sample (hatched histogram) and the non-detected sample (filled histogram) [18].

between  $10^{-6}$  and  $10^{-5}$   $\text{erg cm}^{-2}$ , then most of non-detections would stay under this limit, unlike the detections. However, the first panel of figure 5.3 could indicate that the fluences between  $10^{-6}$  and  $10^{-5}$   $\text{erg cm}^{-2}$  is a fluence mean of their sample and this is supported by figure 5.4. Therefore there is a possibility that the GRB mean emission is related to the radio emission.

If the redshift was known, they calculated the isotropic-equivalent  $\gamma$ -ray energies  $E_{\text{iso}}^{\text{bol}}$  of the GRB prompt emission, adopting the rest-frame passband in the range 1- $10^4$  keV. W the energy of the burst was not known, they used the prompt best-fit models with either a band function [5], a cutoff power-law function, or a simple power law ([218] for details), starting from “GCN circulars archive”. Then, they adopted a  $k$ -correction method of [219]. Since the isotropic energy is related to the collimated jet, the jet break  $t_j$  is fundamental to calculate it. A formula to estimate the collimation angle  $\theta_j$  is in [220]:

$$\theta_j = 0.057 \left( \frac{t_j}{\text{day}} \right)^{3/8} \left( \frac{2}{1+z} \right)^{3/8} E_{\text{iso},53}(\gamma) \left( \frac{\eta_\gamma}{0.2} \right)^{1/8} \left( \frac{n}{0.1 \text{ cm}^{-3}} \right)^{1/8}, \quad (5.5)$$

where  $E_{\text{iso},53}$  is the isotropic  $\gamma$ -ray energy in  $10^{53}$  erg unit,  $\eta_\gamma$  is the efficiency of the fireball in converting the energy in the ejecta into gamma rays and  $n$  is the mean circum-burst density. From Eq. 5.5, the beaming fraction [18]

$$f_b = (1 - \cos \theta_j) \approx \theta_j^2 / 2 \quad (5.6)$$

is needed to calculate the beaming-corrected bolometric energy:

$$E_{\text{true}}^{\text{bol}} = f_b E_{\text{iso}}^{\text{bol}}. \quad (5.7)$$

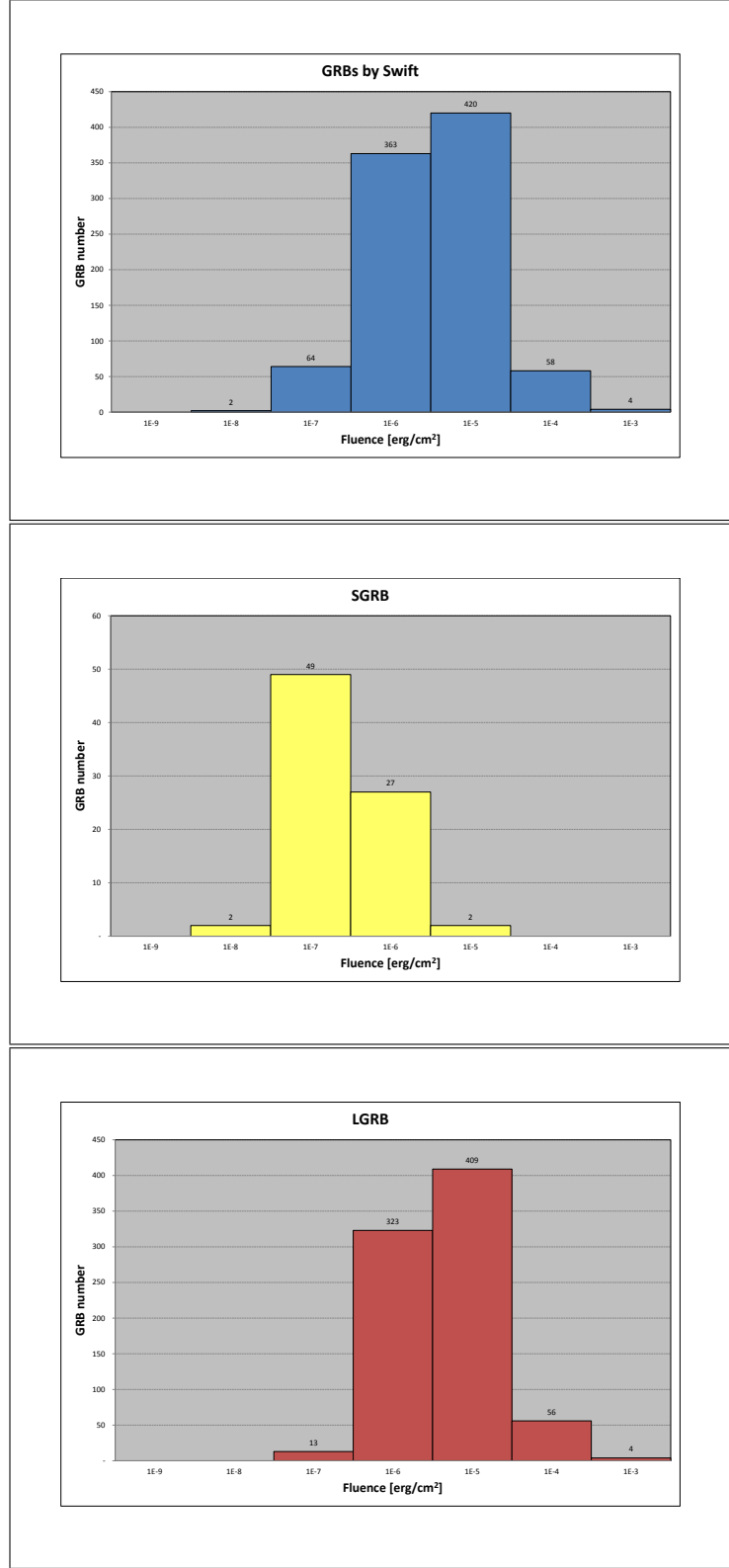


FIGURE 5.4: These sketches show the distributions of the GRBs detected by *Swift*, taken from the “[Swift GRB Table and Lookup](#)” website on the 13th February 2015. In the top, there are 911 detections of GRBs, in the middle panel 80 SGRBs (duration  $\leq 2$  seconds, as option required to the web site) and in the bottom 805 LGRBs (with duration  $> 2$  seconds). Here, detections where the fluences in the channel 15 - 150 keV are available.

Most of radio detections (60 out 95) have an isometric-equivalent energy  $\geq 13^{53}$  erg, whereas radio non-detections they are only 9 out of 206 above this value. The sources show the same behaviour with the beaming-corrected energies, but at lower energies, since the beaming correction reduces them. Thus, both beaming-corrected and isometric bolometric energies can be an efficient indicator of the radio detectability. Doing the K-S test for the bolometric and the beaming-corrected energies results respectively in  $P = 9.97 \times 10^{-7}$  and  $P = 3.47 \times 10^{-3}$ . Thus the isotropic-equivalent energy is a stronger indicator than the beaming-corrected energy for detectable radio GRBs [18].

Chandra and Frail also examined the X-ray and R-band optical fluxes. The higher band considered has an energy range between 0.3 and 10 keV (for fluxes measured by BeppoSAX the range is 1.6 - 10 keV, but it is usually corrected), starting at 11 hours after the burst, and then flux-corrected for the Galactic extinction. The cooling frequency is expected to occur at 11 hours, when the frequencies transition from X-ray to optical bands [221]. A flux with a frequency above the cooling frequency is independent of the circumburst density [18]. They obtained the X-ray fluxes from different works (i.e., [222–225]), or from the *Swift* /XRT repository [226] if the X-ray 11 hours fluxes were not available in literature, searching X-Ray flux value at  $11 \pm 0.5$  hours. When the datum at  $\sim 11$  hour was totally absent, they extrapolated the flux by a power law with a temporal index  $\alpha_X$  ( $F_X \propto t^{\alpha_X}$ ) equal to  $-1.17$  for LGRBs and equal to  $-1.22$  for SHBs [221]. For the R-band, they used the density flux ( $\mu\text{Jy}$ ) at 11 hours. If data were not available in published references, flux density values were taken from the GCN circulars, then those values were extrapolated at 11 hours through the best-fit temporal decay index as reported in those tables. If this index could not be obtained, they used a function

$$F_R \propto t^{\alpha_R}, \quad (5.8)$$

with  $\alpha_R = -0.85$  for long bursts and  $\alpha_R = -0.68$  for short bursts. For GRBs where an R-band magnitudes were not present, they adopted the spectral index  $\beta_R = -1$  (in  $f \propto v^{\beta_R}$ ) to convert the magnitudes in that band. They also corrected the flux density using the Galaxy extinction by [227] and used the **NICMOS unit conversion tool**<sup>1</sup> to convert into  $\mu\text{Jy}$  all fluxes obtained.

As for the X-ray flux, the radio detections peak between  $10^{-12} - 10^{-11}$  erg  $\text{cm}^{-2} \text{s}^{-1}$ , while the radio non-detections peak between  $10^{-13} - 10^{-12}$  erg  $\text{cm}^{-2} \text{s}^{-1}$ . As for R-band optical flux densities, the detected sample peaks between  $10 - 100 \mu\text{Jy}$ ; while the flux for non-detected sample is between  $1 - 10 \mu\text{Jy}$  (as usual, these are fainter than the detections). Likewise for the isotropic-equivalent energy, they suggest that the X-ray fluxes and the dust-extinction-corrected optical magnitudes could be useful for the radio

---

<sup>1</sup>[http://www.stsci.edu/hst/nicmos/tools/conversion\\_form.html](http://www.stsci.edu/hst/nicmos/tools/conversion_form.html)

TABLE 5.1:  $P$  values for the K-S test for the radio detected vs non-detected GRB sample by [18].

Parameter	P Value
Redshift	0.61
Beamed $\gamma$ -ray energy	$3.47 \times 10^{-3}$
X-ray flux (0.3-10 keV)	$3.61 \times 10^{-6}$
Isotropic-equivalent $\gamma$ -ray energy	$9.97 \times 10^{-7}$
Fluence	$2.61 \times 10^{-7}$
Optical R-band flux density	$1.30 \times 10^{-9}$

detectability of bursts. The K-S test favoured the optical fluxes. This is not surprising since the optical band is closer to the radio one with respect to the X-Ray band. For the sake of clarity, table 5.1 from [18] shows the K-S test.

Their work continues investigating correlations between the peak radio flux density (or luminosity) at 8.46 GHz and various LGRB properties in  $\gamma$ -band (e.g., fluence, isotropic and beaming-corrected energies), and also measurements in optical and X-Ray bands. The estimate of the correlations is given in terms of the Pearson's correlation coefficient, or  $R$ -index. To verify the  $R$ -index, they plotted three graphs, where the peak flux density at 8.46 GHz of their radio detections was versus the corresponding 15 - 150 keV fluences, the X-ray 11-hours fluxes and the R-band optical flux densities. A final graph relates the energies  $E_{\text{iso}}^{\text{bol}}$  to the corresponding peak luminosities at 8.46 GHz of their radio-detected sources. There is only a positive correlation and it is for optical flux density to the peak intensity of the radio afterglows. In table 5.2 all the  $R$ -index values obtained by [18] are reported.

Another interesting point to report from [18] concerns synthetic radio curves. In order to have a comparison between radio data curves and afterglow curves by theoretical models, they plotted the curves, changing some parameters, i.e., the circumburst density, the kinetic energy, the redshift, the beaming angle and the microscopic shock parameters (the electron energy density  $\epsilon_e$ , the magnetic energy density  $\epsilon_B$  and the electron spectral index  $p$ ). By varying those parameters, it has also been possible to determine their dependence in the light curves.

Figure 5.5 shows the temporal evolution of the flux densities, where they fix parameters

TABLE 5.2:  $R$ -index values between different GRB parameters [18].

Parameter 1	Parameter 2	$R$ -index value
Peak radio flux density	Fluence	0.02
Peak radio flux density	Optical flux	0.62
Peak radio flux density	X-ray flux	-0.05
Peak radio luminosity	Isotropic-bolometric energy	0.12

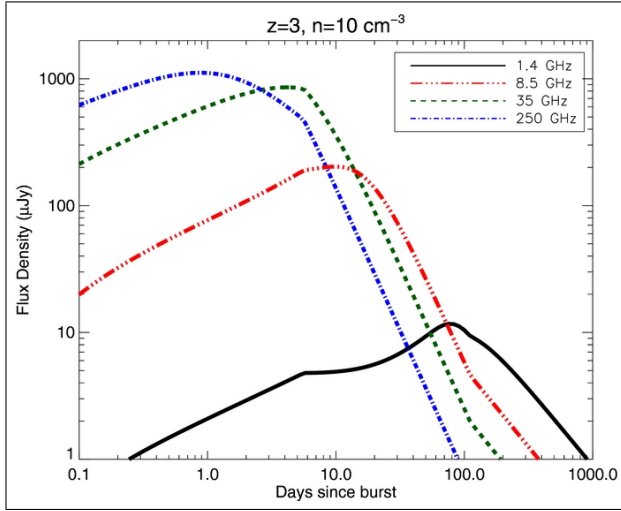


FIGURE 5.5: Light curves of the radio density for a GRB at different frequencies. Apart from the redshift and the circumburst density with their values reported in the top of the plot, the other fixed parameters are:  $E_{\text{KE,iso}} = 10^{53}$  erg;  $\theta_j = 0.2$  rad;  $\epsilon_e = 0.1$ ;  $\epsilon_B = 1\%$  and  $p = 2.2$  [18–20]. The light curves are generated with only a forward shock component. Credit by [18].

(i.e.,  $E_{\text{KE,iso}} = 10^{53}$  erg;  $\theta_j = 0.2$  rad;  $\epsilon_e = 0.1$ ;  $\epsilon_B = 1\%$  and  $p = 2.2$ ) and change the observational frequencies. While the frequency increases, the peak flux density increases too but the time-to-peak reduces, as expected. Other light curves are calculated and plotted, all at 8.46 GHz but varying the density, kinetic energy and microscopic parameters. The dependences on the  $\epsilon_e$  and  $p$  are not so relevant [18]. From figure 5.6 (in the top-left panel) it is easy to see the strong dependence on the  $n$ , but it is explainable for two reasons. Initially, the radio synchrotron emission enhances its flux because of the increasing number of emitting particles, however, when the density continues to increase, there is a reduction of the emission due to the emergence of the synchrotron self-absorption effect. The brightest curves are with  $n = 1$  and  $n = 10$   $\text{cm}^{-3}$ ; this means that radio afterglows are biased to a narrow range of densities [18]. With a low  $n$  there is an intrinsic weakness of the emission, but when  $n$  is too high the synchrotron self-absorption suppresses the radio afterglow emission for a long time. This may justify why some of the bright GRBs are faint in radio band [18] but it might be used to fix constraints for radio emission (and detection). In the top-right panel of figure 5.6 the peak of the light curve increases in time and flux as  $\epsilon_B$  increases. This is because the synchrotron emission becomes more efficient, but if the density is too high, the flux does not increase anymore as the magnetic energy density increases and there is only a shift of the peak time to a later time, due to the effects of the large synchrotron absorption frequency which inhibit the emission [18]. In the bottom left panel of figure 5.6, the dependence of the light curve on the kinetic energy is trivial. The curve at  $10^{53}$  erg is equal to the results of their 8.46 GHz data analyses; furthermore, its beaming-corrected energy is  $2 \times 10^{51}$  erg, which is at least consistent with the kinetic energy

derived from radio calorimetry [228, 229].

In the last panel of figure 5.6, the redshift dependence is shown. The flux density reduces as the  $z$  increases, but, for  $z \gtrsim 3$ , the negative- $k$  correction effects start and the peak radio flux density falls only slightly despite the increase of  $z$  [18]. This means all GRBs with  $E_{\text{EK,iso}} \geq 10^{53}$  erg could be detectable by the EVLA with an observational integration time of 20-30 minutes, independently of their redshift [18]. In figure 5.7 some LGRB light curves are shown at different redshifts, observed at 8.5 GHz, with the sensitivity limits of the EVLA set at  $z = 1, 3$ , and 8.

In the last figure 5.8, again reported by [18], there are the relationships for their standard afterglow model at radio, optical and X-ray bands. It is important to recall that these radio observations were sensitivity limited as well as limited in time range over which the correlations can be observed. In other words there have not been simultaneous observations at different bands. Finally, another complication is the radio-flux-density temporal evolution, which it is more complex than the almost monotonic evolutions of the X-ray and optical frequencies.

## 5.2 Two possible GRB populations by radio afterglows

One year after the paper of [18], the radio non-detections and detections of the Chandra & Frail's sample were thought as belonging to two distinct populations [21]. Hancock et al. named the first group as *radio-faint* (RF) and the second as *radio-bright* (RB). They do this to note that the detection rates at radio wavelengths are significantly lower than those at X-rays and optical frequency, and that this difference could not depend on an instrumental sensitivity. In fact, the difference between radio afterglow detections and non-detections can depend on either distance (and hence redshift), instrumental sensitivity, or intrinsic peculiarities in GRBs. The first case is unlikely, since the distributions of detections and non-detections in  $z$  are basically the same (as said in [18] too). In other words, if radio afterglows were not all comparable, then the RBs should be observed at low redshifts, while the RFs should stay further, but this is not the case, as shown in figure 5.9, where RF and RB are equally distributed.

In the second case, it should be possible to extract the mean afterglow flux from detections by visibility stacking, to understand the extent to which instrumental sensitivity is relevant for detection of RB and RF GRBs [230]. Image-based stacking has been used in astronomy, when sources are individually too faint to detect. This technique investigates the mean properties of similar objects.

Stacking involves creating a calibrated image of each object under consideration and

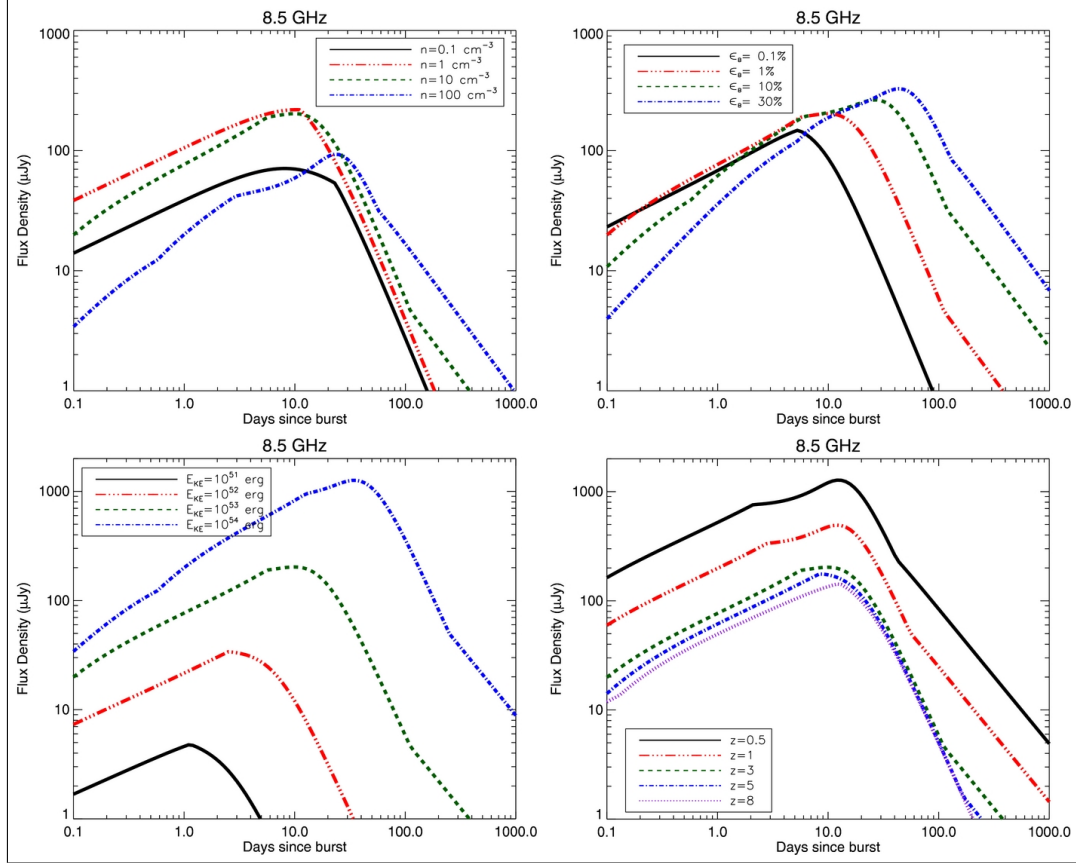


FIGURE 5.6: In the top left panel, the density varies and the parameters are fixed as follows:  $z = 3$ ;  $E_{\text{KE,iso}} = 10^{53}$  erg;  $\theta_j = 0.2$  rad;  $\epsilon_e = 0.1$ ;  $\epsilon_B = 1\%$  and  $p = 2.2$ . In the top right panel, the magnetic energy density varies and the parameters are fixed in this way:  $z = 3$ ;  $n = 10 \text{ cm}^{-3}$ ;  $E_{\text{KE,iso}} = 10^{53}$  erg;  $\theta_j = 0.2$  rad;  $\epsilon_e = 0.1$  and  $p = 2.2$ . In bottom left panel, the kinetic energy varies and the parameters are fixed as follows:  $z = 3$ ;  $n = 10 \text{ cm}^{-3}$ ;  $\theta_j = 0.2$  rad;  $\epsilon_e = 0.1$ ;  $\epsilon_B = 1\%$  and  $p = 2.2$ . In the bottom right panel, the redshift varies and the parameters are fixed as follows:  $n = 10 \text{ cm}^{-3}$ ;  $E_{\text{KE,iso}} = 10^{53}$  erg;  $\theta_j = 0.2$  rad;  $\epsilon_e = 0.1$ ;  $\epsilon_B = 1\%$  and  $p = 2.2$ . Credit by [18].

then forming a weighted sum of these images [21]. If images and pixels have uncorrelated Gaussian noise, then the stacking of  $N$  images will improve the sensitivity of a factor  $\propto \sqrt{N}$ . As for radio interferometry, [231] note that there is an objective difficulty to reach the ideal sensitivity with stacked images, due to a spatially correlated noise produced by the nature of interferometric images and their deconvolution. The true mean does not coincide with the mean of noisy data, and the relation between the population mean and the stacked value depends on the structure of the underlying noise in a nonlinear way. However, this problem is avoided in [230], where the visibility stacking stacks radio observations with different  $u - v$  coverages and the calibrated visibility data is combined before imaging takes place [21].

In short, observations are calibrated, imaged and manually cleaned, removing radio background sources, as long as only the GRB flux is in the visibility data for the final stacked observation. At the end of the procedure, the stacked sensitivity obtained was

worse than the ideal sensitivity expected from a single observation of equivalent integration time. The reason for this unexpected result probably depends on radio faint remains of background sources, which are impossible to separate out from RF GRBs. However, stacked images were more sensitive than any of the individual observations [21].

Because the means between RB and RF GRBs differ by up to three orders of magnitude, these could be two different populations, due to intrinsic differences.

In their analysis, they compared fluxes predicted by models with three different radio luminosity GRB distributions (i.e., Gaussian, flat and decreasing power law) with the stacked observations. The result is that RB GRB models are consistent with stacked observations, but RF GRBs are not. In fact, the flux of the RF model is five times greater than flux of stacked observations. Since they considered models where RB and

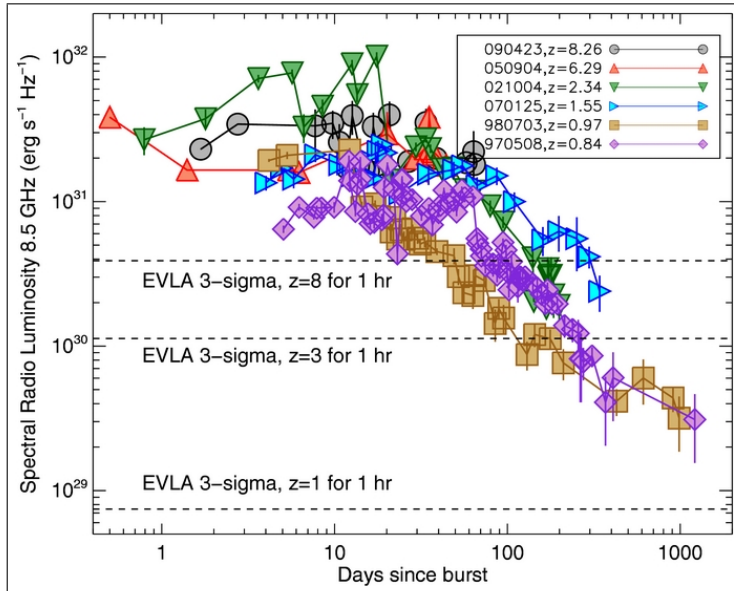


FIGURE 5.7: Light curves of some LGRBs and corresponding redshift, as reported in the inner panel. The three dashed lines indicate the EVLA  $3\sigma$  sensitivity limits with an observational integration time of 1 hour [18].

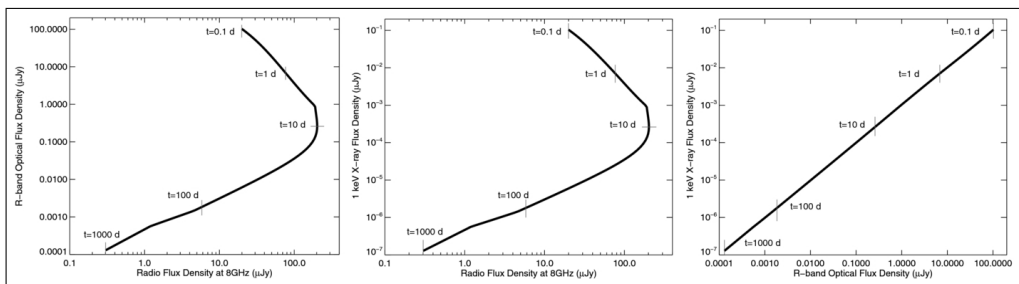


FIGURE 5.8: In the first and second panels, the synthetic model of the 8.5 GHz flux density compared to the corresponding  $R$ -band optical and 1 keV X-ray flux densities. In the third panel, the comparison of the flux densities between the optical and X-ray frequencies. The model is the same as that used in figure 5.5 [18].

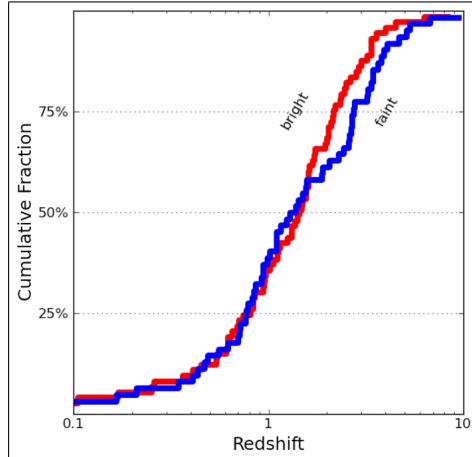


FIGURE 5.9: Distribution of redshifts for GRBs where the  $z$  was known. Data taken from table 1 of [18], plotted by [21] distinguishing between radio-bright (in red) and radio-faint (in blue) GRBs. No difference is highlighted.

TABLE 5.3: The median properties about radio-faint and -bright GRBs.  $p$  is the value of the K-S test.  $F_X^{11\text{hr}}$  and  $F_R^{11\text{hr}}$  are respectively the flux at 0.3-10 keV and the flux density at the optical  $R$ -band [21].

Parameter	Population		$p$
	Faint	Bright	
Redshift	1.3	1.4	0.32
$T_{90}(\text{s})$	34	62	$8.3 \cdot 10^{-3}$
$S_\gamma/(10^{-6} \text{ erg cm}^{-2})$	1.6	5.7	$1.5 \cdot 10^{-5}$
$F_X^{11\text{hr}}/10^{-13} \text{ erg cm}^{-2} \text{ s}^{-1}$	6.4	23	$8.9 \cdot 10^{-5}$
$F_R^{11\text{hr}}/\mu\text{Jy}$	5.8	41	$6.0 \cdot 10^{-11}$
$E_{\text{bol}}/(10^{52} \text{ erg})$	2.1	10	$4.8 \cdot 10^{-5}$

RF GRBs were in the same class but with different luminosity, this hypothesis must be false, therefore bright and faint radio afterglows should arise by two distinct populations.

Nevertheless, these two populations are not completely sharp, especially for first two weeks since the burst. In later time, fainter radio afterglows will tend to dim. The correct fraction between RF and RB is  $\sim 30 - 40\%$  and  $\sim 60 - 70\%$ , respectively.

With an additional investigation, they show that the two populations follow particular distributions at different wavelengths. Even though the 20 - 40% of RF GRBs could be bright, the difference between the group seems to be real. This difference between these two populations seems to be confirmed also for other frequencies, as shown in table 5.3, but the difference is less prevalent as wavelength becomes shorter than the radio band.

The two different radio emissions could depend on different radiation processes, environments, or also on diverse explosion mechanisms. However, if two different prompt emission processes existed, then one would find a bimodal distribution of the gamma-ray

efficiency  $\epsilon_\gamma$

$$\epsilon_\gamma = \frac{E_{\text{iso}^{\text{bol}}}}{E_{\text{iso}^{\text{bol}}} + E_{K,\text{iso}}} . \quad (5.9)$$

For example one could be based on an electromagnetic model [111], another on the fireball model [232]. In the former case, the baryon emission is very low, the  $\epsilon_\gamma$  is high, and therefore the afterglow is faint or non existent; in the latter case, an intermediate baryon loading will involve a radio bright afterglow, with an higher  $\epsilon_\gamma$  than previously. However, even if only the fireball model was used, an explanation for the two radio populations through the  $\epsilon_\gamma$  would be still possible. Very strong magnetic fields produce a less efficient prompt emission, because [233]

$$\epsilon_\gamma \propto B^{-1} . \quad (5.10)$$

Although the best candidate for GRB progenitors are black holes, millisecond magnetars would also be a good option [234]. In this case the magnetic field can reach value of  $10^{14} - 10^{15}$  G, which is much greater than the expected magnetic field within the innermost orbit of a black hole ( $\lesssim 10^8$  G). Thus, GRBs generated by magnetars have a low  $\epsilon_\gamma$  and a faint radio emission, whereas black hole driven GRBs would have higher  $\epsilon_\gamma$  and a brighter radio emission.

### 5.3 A statistics about possible observable GRBs by the SKA

After the review of the first and very precise study of a large GRB sample discussed in section 5.1 and recent hypotheses about their radio populations in section 5.2, in this section a work of mine is reported [235], currently submitted to MNRAS review. Therein, the GRB detection rate has been calculated for the SKA. To do this, many catalogues of GRB satellite missions have been consulted. The created final list can be used as a starting point for quick searches, recalling the original catalogue and all information concerning a GRB contained there.

#### 5.3.1 The sky above the SKA and its shadow cone

Firstly, it is necessary to select which part of the sky will be observable to the SKA, from its position on the Earth. Starting from a circle, pole axis and equator can be traced, and now it is possible to take into account the (roughly averaged) latitudes where antennas will be placed, i.e.,  $\sim -30.7^\circ$  in South Africa and  $\sim -26.7^\circ$  in Australia, on its edge. The point on the latitude closest to the equator is chosen to draw a tangent (the *horizon*

(line). Now if the circle is rotated around the pole axis, a sphere and a double cone whose vertex is on the pole axes (below the south pole) is traced out. For our case, only the cone which contain the sphere can be shaded. As a last step, the minimum elevation of the SKA dish antenna, i.e.  $\sim 13.5^\circ$ <sup>2</sup>, is taken into account. This angle must be added from the horizon line, because of a structural mechanical limit of the dish antennas. For the sake of the clarity, a radio telescope is generally used to observe at higher elevation (e.g.,  $\gtrsim 20$ ) to have a cleaner signal without emission effects due to the atmosphere which decrease the intensity of the observed radiations. These steps are drawn in figure 5.10 to show the final shadow-cone for the SKA. The final angle to consider, between the red line and the polar axes, in figure 5.10, is

$$\vartheta_s = \vartheta_l + 13.5^\circ = 40.2^\circ \simeq 0.702 \text{ rad}, \quad (5.11)$$

where the shadow cone has a solid angle  $\Omega_s$  calculated as:

$$\Omega_s = \int_0^{2\pi} d\phi \int_0^{\vartheta_s} d\vartheta \sin \vartheta, \quad (5.12)$$

resulting in

$$\Omega_s = 2\pi \cdot [-\cos \vartheta]_0^{\vartheta_s} = 1.484 \text{ sr}. \quad (5.13)$$

Even if it is only an approximation, this integral gives a satisfying idea of the observable sky above the SKA.

### 5.3.2 Sample selection

GRBs are sources detected by gamma satellites, hence these cosmological objects must be collected in literature and gamma catalogues. The following satellite missions and the associated catalogues have been taken into account: Agile with [236–239], BeppoSAX with [240], CGRO with [241–243] and the *batsegrb* catalogue [244, 245] in HEASARC web site<sup>3</sup>, *Fermi* with [246, 247] and the *fermigbrst* catalogue in HEASARC archive<sup>4</sup> [246–249], GRANAT, HETE-2, INTEGRAL with [250–252], Konus/Wind with [237], *Swift* with [253] and the “*Swift* GRB Table and Lookup”<sup>5</sup>; ULYSSES with [254]. By cross-correlating of different catalogues, I have created a list with 7516 distinct GRBs shown in table 5.4. Considering only GRBs that have coordinates in various catalogues, coincidences have been found in order to identify equal sources and discard duplicates.

<sup>2</sup>the minimum elevation must be  $< 15^\circ$ , as imposed by constraint [14]

<sup>3</sup><http://heasarc.gsfc.nasa.gov/W3Browse/cgro/batsegrb.html>.

However, <http://gammaray.msfc.nasa.gov/batse/grb/catalog/current/> is another useful web site.

<sup>4</sup><http://heasarc.gsfc.nasa.gov/W3Browse/fermi/fermigbrst.html>

<sup>5</sup>[http://swift.gsfc.nasa.gov/archive/grb\\_table](http://swift.gsfc.nasa.gov/archive/grb_table)

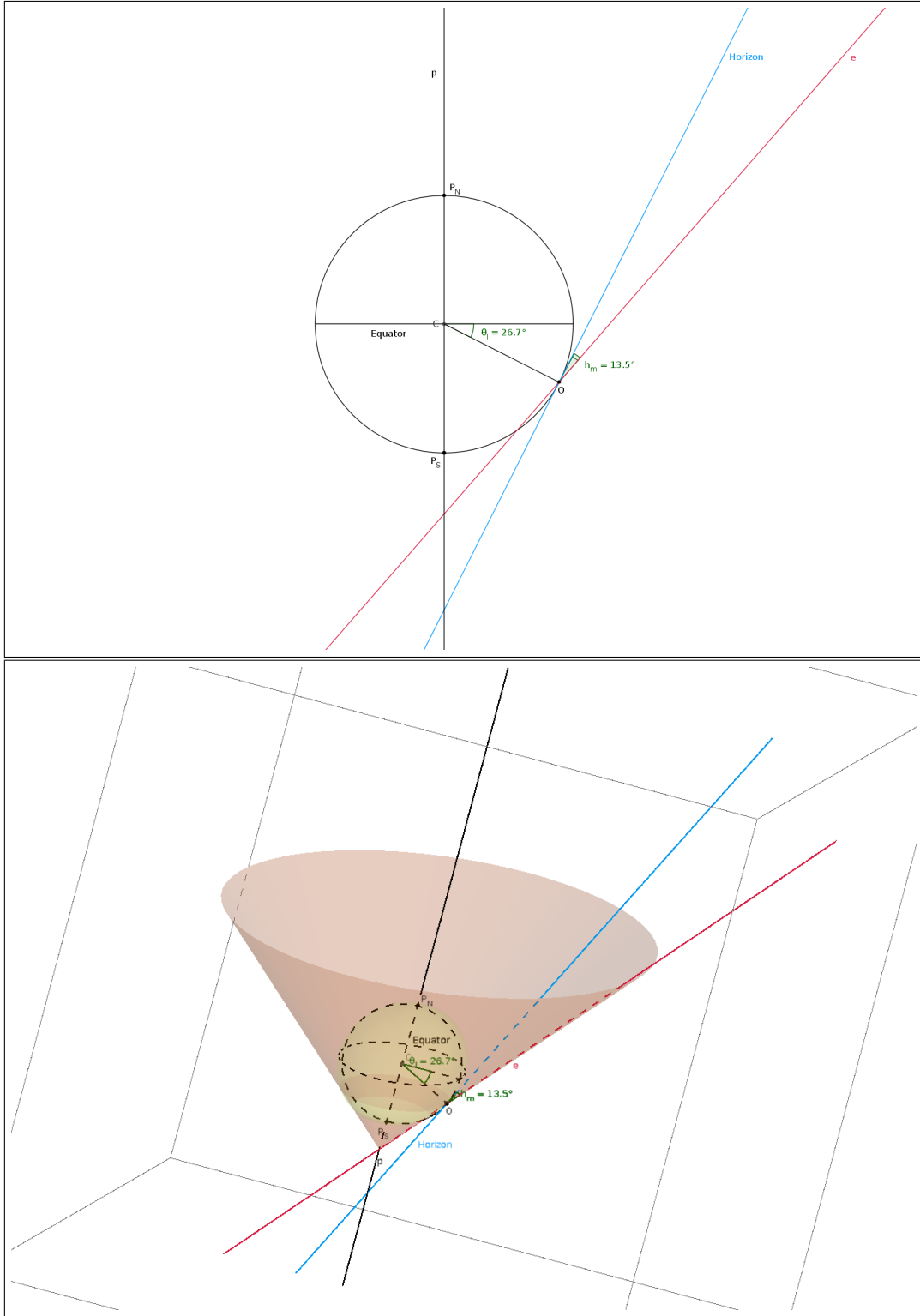


FIGURE 5.10: In the upper panel, the 2D a sketch of the Earth, with the polar axes, the South African (mean) antenna latitude  $O$ , the horizon line (in blue) and the lowest angle-limit line (red) for the antenna. In the lower panel, the rotation simulates the Earth rotation and a shadow-cone is traced by the red line.

Table 2 in [254] has 218 GRBs, but, as mentioned in the associated paper, they are all coincident with 218 GRBs triggered by CGRO/BATSE.

The catalogues in [241] and in [242] (both focused on BATSE receiver on-board CGRO) have been considered. The former counts 3906 GRBs (2068 triggered and 1838 non-triggered), whereas the second one contains 873 (only non-triggered). Precisely, 725 non-triggered plus 15 triggered elements out of (Kommers') 873 objects were considered by Stern like coincident GRBs in his catalogue. 133 GRBs by Kommers plus 1838 by Stern have been taken to make up a “BATSE non-triggered catalogue” (BNT) with 1971 GRBs in total. Subsequently, using the *batsegrb* catalogue, and merging this with the previous 2068 GRBs in the Stern catalogue, the “BATSE triggered catalogue” (BT) with 2703 elements has been obtained. Finally, 4674 GRBs detected by BATSE/CGRO instrument have been selected. Apart from BATSE catalogues, also table 8 in [243] has been consulted, for the COMPTEL instrument. In that table, the precise detection time lacks, but thanks to reported days and coordinates it has been possible to establish that 29 out of 31 sources were present in BT catalogue, 1 out of 31 source was in BNT catalogue, and the last one had a coincidence with BT and GRANAT detections.

By considering table 2 in [240], the catalogue counts 873 GRBs with their own coordinates. In order not to repeat the same source between the BeppoSAX and CGRO catalogues, I consider two GRBs equal if their detection intervals are  $\leq 0.005$  days (that is  $\sim 7$  minutes) and if they are within an angle of  $146^\circ$  (both RA and DEC)<sup>6</sup>. This solution is ad hoc for our tasks, but a similar method was used by Stern matching between non-triggered sources in his table and sources in Kommers' table. Finally, 421 (340 of which are in BT, while the remaining 81 are in BNT) are common sources between BeppoSAX and CGRO. A similar comparison has been done with other missions working in the same time-frame of BeppoSAX.

For HETE-2 mission, the following catalogues have been consulted: “*hete2grb*: HETE-2 Gamma-Ray Bursts”<sup>7</sup> by MIT<sup>8</sup> (Massachusetts Institute of Technology) and “*hete2gcn*: HETE-2 GCN Triggers Catalog”<sup>9</sup>. In these catalogues, because not every GRB has coordinates, I have cross-correlated the 84 GRBs of the first catalogue with the 1235 rows of the second one, thus obtaining 71 GRBs in common, associating them to their respective coordinates. No GRBs in common between HETE-2 and BeppoSAX, Konus/Wind, *Swift*, only 1 with INTEGRAL is in common.

---

<sup>6</sup>The estimate for maximum location error is  $63.7^\circ$  in [241] for BATSE; the maximum location error is  $83^\circ$  in [240] for BeppoSAX. However, the most discriminating factor is generally the time, indeed changing angular range modifies their overlapping of just a few elements.

<sup>7</sup><http://heasarc.gsfc.nasa.gov/W3Browse/hete-2/hete2grb.html>

<sup>8</sup><http://space.mit.edu/HETE/Bursts/>

<sup>9</sup><http://heasarc.gsfc.nasa.gov/W3Browse/hete-2/hete2gcn.html>

Then, I have considered the current missions, *Swift* and *Fermi*, using tables in [246, 247, 253] and the HEASARC archive. Until 12th of May 2014, *Fermi* satellite has reported 1359 GRBs and *Swift* has reported 869<sup>10</sup>. As previously, two detections are considered equal if they lie in a time range of 0.005 days and an angular range<sup>11</sup> of 45°. I find 193 common sources between *Fermi* and *Swift*, but all coincidences with other missions are reported in table 5.5.

Unfortunately for the Agile mission, contrary to *Fermi*, *Swift* or CGRO, a large unique catalogue dedicated to gamma-ray bursts does not exist, thus I have consulted the above-mentioned catalogues, and the *Swift* web site. I have always taken into account GRBs with their respective coordinates, thus obtaining the “Agile list” which collects 89 sources. Sources collected in literature are the results of triangulations with various instruments (e.g., Konus/Wind, INTEGRAL, HETE-2, Suzaku, etc) where the Agile contribution was used. The GRBs of table 2 presented in [239] are InterPlanetary Network (IPN) identifications and the *Fermi*/GMB was used for some of these triangulations. In those cases, they have already been included in *Fermi* catalogues, cited here, and hence excluded from this final Agile list.

Konus/Wind, GRANAT and INTEGRAL, they have the same issue as Agile. In fact, I have matched various catalogues (i.e., [250], [251], [252], [237]), in order to identify single different objects with respective coordinates, and to have a reasonable list for each of these missions. For this purpose, the **SIMBAD Astronomical Database** and HEASARC database have also been used. From the latter, the *grbcat*<sup>12</sup> catalogue and the *phebus*<sup>13</sup> catalogue [255–258] (this last in particular way for GRANAT) have been consulted. In this case, if the sources were without coordinates, I searched in SIMBAD or in *grbcat* catalog. Obviously, great care was taken not reporting duplicates among catalogues of the same satellite. I have matched these last catalogues with previous ones by GRB names and detection time, in a similar way as previously mentioned.

Distributions of GRBs are presented in figure 5.11, where the pie chart shows 12 different pieces divided into three groups: the first one whose objects have been detected by only one mission or one instrument (10 difference pieces); a piece where same objects have been detected by two instruments (the “couples” piece); finally, the last one where GRBs have been detected by three instruments simultaneously (the “triples” piece). For clarity, table 5.5 shows all the combinations, also distinguishing the triggered and non-triggered GRBs detected by BATSE.

<sup>10</sup>I report that in [253] there are 3 elements more with respect to the web table in “*Swift* GRB Table and Lookup”, but they have not been counted.

<sup>11</sup>The most position error (90% error radius) in [253] is of 6.4'; the maximum positional uncertainty in *Fermi* catalogue is 45.7°.

<sup>12</sup><http://heasarc.gsfc.nasa.gov/W3Browse/gamma-ray-bursts/grbcat.html>

<sup>13</sup><http://heasarc.gsfc.nasa.gov/W3Browse/gamma-ray-bursts/phebus.html>

TABLE 5.4: This table is a collection and merging of all catalogues mentioned in this paper. In the columns, respectively: RA and DEC in degrees; detection year, month and day; name of the list related to a satellite; source name. For more details see the appendix. The full table is attached in appendix A.

RA deg	DEC deg	Year	Month	Day	Cat.	GRB Name
174.680	-44.320	1990	01	18.73618	GRA	GRB900118
91.160	-82.010	1990	01	20.85941	GRA	GRB900120
113.280	27.890	1990	01	23.07098	GRA	GRB900123A
357.190	-38.560	1990	01	23.78091	GRA	GRB900123B
131.630	-38.180	1990	01	26.75309	GRA	GRB900126
338.040	35.360	1990	02	22.49763	GRA	GRB900222
124.580	38.840	1990	03	8.39725	GRA	GRB900308A
323.250	-31.780	1990	03	27.43366	GRA	GRB900327
206.920	-12.250	1990	04	4.74625	GRA	GRB900404
85.110	82.030	1990	04	13.42455	GRA	GRB900413B
...	...	...	...	...	...	...

Overlapping missions can more easily be seen in figure 5.12, where detections are plotted in function of the time. The trigger time has been used to do this plot, which is conventionally written as “year, month, day, universal time” (YYYY MM DD hh:mm:ss). I wrote a routine that works as a counter, translating dates and hours in progressive numbers starting at the first gamma detection (18th January 1990) until the last considered for my estimation (12th May 2014). Table 5.6 lists an approximate detection-rate for each fitted line. As for this last point, it is worthwhile to stress that many missions were not exclusively dedicated for GRB exploration, so those rates are only indicative; in fact some tables found in literature are not complete for each mission and they report only partial GRB detections. However, the most plausible detection-rates are CGRO, BeppoSAX, *Swift* and *Fermi*.

To conclude, figure 5.13 shows 6508 GRBs which occurred from 18th January 1990 to 12th May 2014 in two polar plots, corresponding to the north and south celestial hemispheres that the SKA will be able to observe, as mentioned in the beginning of this section. More details about the routine developed by me though IDL software are in section 5.7.

### 5.3.3 Serendipitous detections of radio GRBs by the SKA

From my final list, I compute a rough estimate of how many GRBs could be observed by the SKA, for a potential GRB survey. I take into account the first GRB detection for each instrument and not the life time of the instrument itself so that the potential initial problems of the detection are already taken into account. However I’m aware that for a

TABLE 5.5: Number of GRBs detected by different instruments of catalogues used and their combinations.

GRA = GRANAT; BT = BATSE triggered; BNT = BATSE non-triggered; COMP = COMPTEL; Uly = Ulysses; KW = Knous/Wind; BeS = BeppoSAX; Agi = Agile; Fer = *Fermi*; INT = INTEGRAL; HET = HETE-2; Swi = *Swift*.

Mission	GRB Number
GRA	58
GRA-BT	26
GRA-BT-COMP	1
GRA-BT-Uly	14
GRA-BNT	1
KW	153
KW-BT	26
KW-BT-BeS	18
KW-Agi	4
KW-Agi-Fer	7
KW-BNT	3
KW-BeS	15
KW-BNT-BeS	2
KW-INT	1
KW-Fer	22
HET	70
INT	78
INT-HET	1
INT-Swi	6
INT-Fer	14
INT-Fer-Agi	1
Agi	26
Agi-Fer	31
Agi-Swi	11
Agi-Fer-Swi	9
BT	2063
BT-Uly	204
BT-COMP	29
BT-BeS	322
BNT	1885
BNT-COMP	1
BNT-BeS	79
BeS	401
Swi	659
Swi-Fer	184
Fer	1091
Total	7516

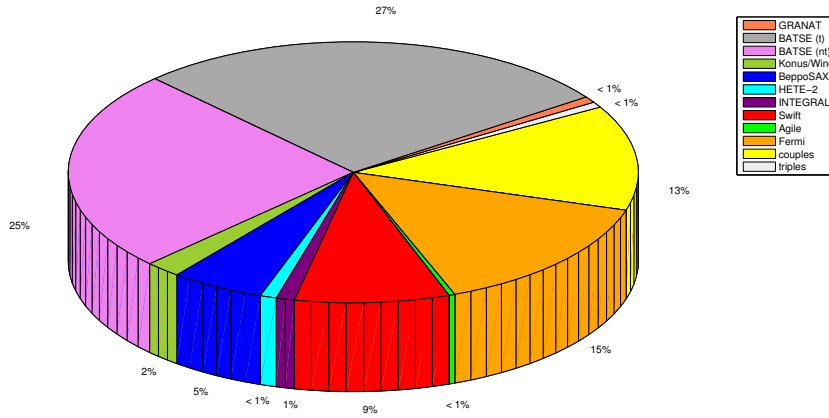


FIGURE 5.11: In this pie chart, the percentages are shown, out of 7516 distinct GRBs, occurring from the 18th January 1990 to the 12th May 2014, for GRANAT, Ulysses, CGRO, Konus/Wind, BeppoSAX, HETE-2, INTEGRAL, *Swift*, Agile and *Fermi* missions. As it is possible to see in the colour-key-box, I have considered single events for different missions/instruments, as well as same GRBs observed simultaneously by two or three satellite missions (or instruments) in yellow and pearl grey, respectively. To summarize: 58 GRBs observed by GRANAT (1% of 7516), 1885 by CGRO/BATSE (nt) (27%), 2063 by CGRO/BATSE (t) (25%), 153 by Konus/Wind (2%), 401 by BeppoSAX (5%), 70 by HETE-2 (< 1%), 78 by INTEGRAL (1%), 659 by *Swift* (9%), 26 by Agile (< 1%), 1091 by *Fermi* (15%), total GRBs observed in a pair and in a triple have been 979 (13%) and 52 (< 1%), respectively. See table 5.5 for the sake of clarity.

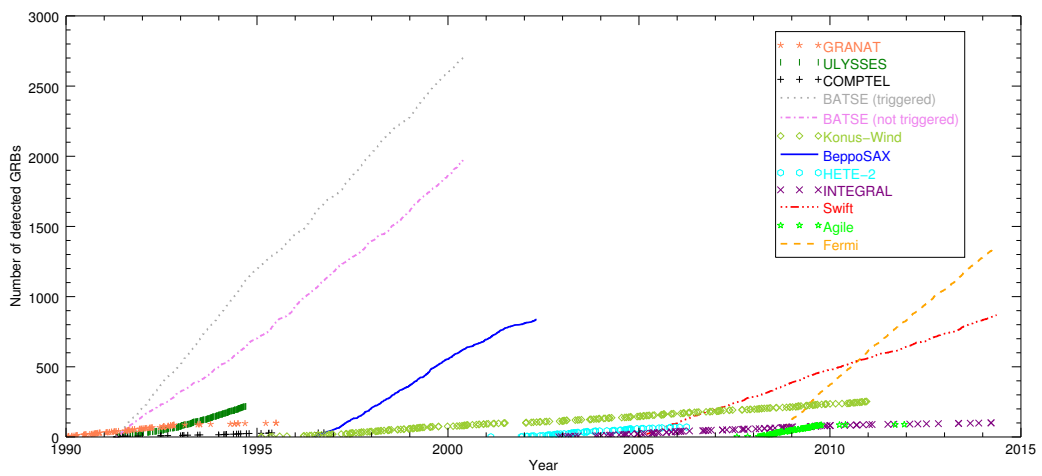


FIGURE 5.12: In this figure I have considered different missions, instruments and catalogues. I report GRBs observed by GRANAT, Ulysses, CGRO/BATSE, CGRO/-COMPTON, Konus/Wind, BeppoSAX, HETE-2, INTEGRAL, *Swift*, Agile and *Fermi*. I also plot the non-triggered GRBs by CGRO/BATSE. In the Y-axis the (progressive) number of GRBs detected by a mission/instrument is reported; in the X-axis the time of the detection expressed in years. Detections since 18th January 1990 done by GRANAT until 12th May 2014 done by *Fermi* and *Swift* are here plotted.

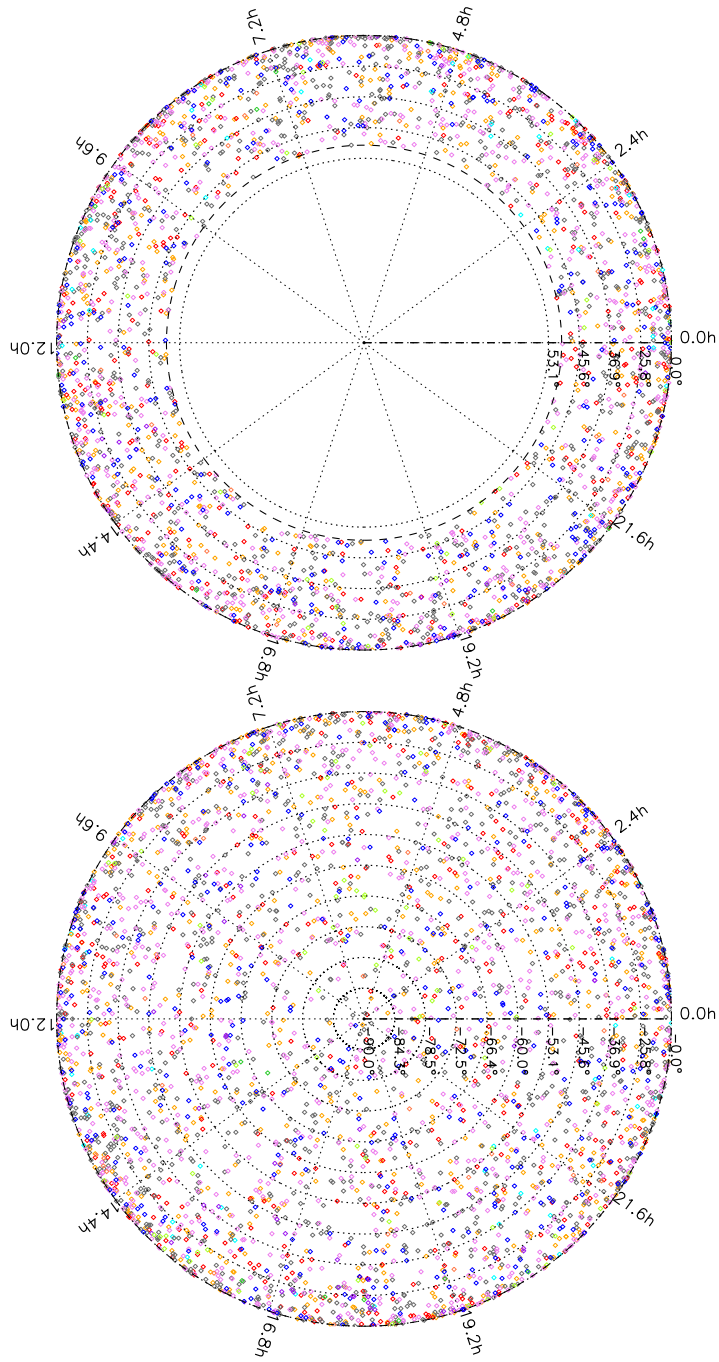


FIGURE 5.13: Polar plots show 6508 points out of 7516, i.e. GRBs with celestial declination  $< 50^\circ$  (dashed circle), observed by GRANAT (coral), CGRO/BATSE (triggered and non-triggered GRBs are dark grey and violet, respectively), Konus/Wind (yellow-green), BeppoSAX (blue), HETE-2 (cyan), INTEGRAL (purple), *Swift* (red), Agile (lime green) and *Fermi* (orange). The first plot shows the north celestial hemisphere that SKA can observe, i.e. the “central hole” delimited by the black dashed circle is due to the shadow cone, where it will not able to observe; the second plot shows the south celestial hemisphere. RA and DEC are expressed in J2000 coordinates. For the sake of clarity, I have avoided plotting the same sources in different catalogues repeatedly, e.g. Ulysses sources do not appear among these points because they are already plotted with triggered CGRO/BATSE GRBs.

more refined calculation I should also have taken into account the fraction of time in which the instruments are operational. Moreover, another issue arises in this calculation because of the limited knowledge of the GRB radio brightness distribution. Indeed, [18] have shown that the current sample is sensitivity limited, therefore the brightness of GRBs at radio wavelengths and the sensitivity of the SKA at various frequencies cannot not be taken into account.

In sec. 5.3.2, I have explained how the GRB list has been acquired. I now consider sources with declination lesser than  $50^\circ$ ; these are 6508, hence let  $N_{\text{GRB}} = 6508$ , because the number of GRBs within a spherical cap is equal to  $(4\pi - \Omega_s)$  sterad. As already mentioned, the SKA FoV is  $\sim 1$  square degree ( $\Omega_{\text{HF}} \simeq 3.05 \cdot 10^{-4}$  sr) at the high-frequency (1 - 20 GHz). Then, assuming a uniform distribution for GRBs detected within the telescope beam and with a time-frame of 24.33 years I can obtain the probability of observing a GRB by the SKA:

$$P_{\text{HF}} = \frac{N_{\text{GRB}}}{4\pi - \Omega_s} \cdot \frac{\Omega_{\text{HF}}}{24.33 \text{ y}} = 7.36 \cdot 10^{-3} \frac{\text{GRB}}{\text{y}}. \quad (5.14)$$

This number shows that the SKA in its high-frequency range has an extremely low probability to serendipitously detect radio transients associated to GRBs. In fact, this value was estimated using all data here considered in our table and, in a time-frame of almost 25 years.

I have repeated the same calculation, but focusing on the *Fermi* and *Swift* missions. In our final catalogue, the first *Swift* detection was on 2004/12/17 and the last one is on 2014/05/12, counting 869 GRBs; on the other hand, *Fermi* observed its first GRB on the 2008/07/14 and the last one on the 2014/05/12, having 1359 sources in total. Excluding the sources with a declination  $\geq 50^\circ$ , they become 1194 by *Fermi* ( $N_{\text{Fer}}$ ) for 2129 days, and 736 by *Swift* ( $N_{\text{Swi}}$ ) for 3433 days. For these two missions, in their own time-frames, the probabilities to detect in a serendipitous way a GRB per year within the high-frequency SKA are:

$$\begin{aligned} P_{\text{HF,Fer}} &= \frac{N_{\text{Fer}}}{4\pi - \Omega_s} \cdot \frac{\Omega_{\text{HF}}}{2129/365.25 \text{ y}} = \\ &= \frac{1194}{11.082 \text{ sr}} \cdot 5.22 \cdot 10^{-5} \frac{\text{sr}}{\text{y}} = \\ &= 5.63 \cdot 10^{-3} \frac{\text{GRB}}{\text{y}}; \end{aligned} \quad (5.15)$$

$$\begin{aligned}
P_{\text{HF,Swi}} &= \frac{N_{\text{Swi}}}{4\pi - \Omega_s} \cdot \frac{\Omega_{\text{HF}}}{3433/365.25 \text{ y}} = \\
&= \frac{736}{11.082 \text{ sr}} \cdot 3.24 \cdot 10^{-5} \frac{\text{sr}}{\text{y}} = \\
&= 2.15 \cdot 10^{-3} \frac{\text{GRB}}{\text{y}}.
\end{aligned} \tag{5.16}$$

These numbers are still very low. However, looking at table 5.6, even if I use the CGRO, that is the mission with the most efficient rate-detection, considering both triggered and non-triggered data (4036 GRBs within 3324 days), the result will be  $1.22 \cdot 10^{-2}$  GRB/y. If I take into account the Earth rotation during an observation in order to increase these numbers, the previous results will be multiplied by about 2.5 times. Therefore, in the best case, the SKA could detect  $\sim 2.5 \cdot 1.22 \cdot 10^{-2}$  GRB per year, at its high-frequency.

The situation changes for low-frequency antennae and their FoV. In fact, the SKA-Low has a FoV equal to 200 square degrees, that corresponds to a solid angle  $\Omega_{\text{LF}} \simeq 6.1 \cdot 10^{-2}$  sterad. At the low frequency, a slightly smaller spherical cap than before must be consider, because dipole antenna can observe with a scan angle of  $\pm 45^\circ$  with respect to the zenith (as constraint reported by [259]). Following Eqs. 5.11 and 5.13, I have to add  $45^\circ$  to  $\vartheta_l$  instead of  $13.5^\circ$ , in order to obtain the new  $\Omega_{s,\text{LF}} \simeq 4.310$  sterad. Thus, with a DEC less than to  $18^\circ$  ( $\simeq 90^\circ - \vartheta_l - 45^\circ$ ), the number of GRBs detected by *Fermi* is 880. In this case:

$$\begin{aligned}
P_{\text{LF,Fer}} &= \frac{880}{4\pi - \Omega_{s,\text{LF}}} \cdot \frac{\Omega_{\text{LF}}}{2129/365.25 \text{ y}} = \\
&= \frac{880}{8.256 \text{ sr}} \cdot 1.05 \cdot 10^{-2} \frac{\text{sr}}{\text{d}} = 1.12 \frac{\text{GRB}}{\text{y}}.
\end{aligned} \tag{5.17}$$

As previously done for the dishes, I can consider the Earth rotation, thus doubling the SKA-Low FoV. In doing so, I obtain a probability of 2.23 GRB per year.

Contrary to the SKA dishes, the LFAA might be a GRB-radio monitoring, but, more study about GRB low radio band observations and in particular about its sensitivity should be investigated. Indeed, currently, the expected GRB afterglow signal at 50-350 MHz range will be lower than high-frequency one, hence the LFAA could have serious difficulty detecting it.

However, SKA dishes will be used principally to go on-source with specific (and precise) coordinates, namely after the GRB alert. Indeed, GRBs will not be detected randomly, but moving antennae on-source after a satellite detection (e.g., Robo-AMI above-mentioned). Only with a real synergy among the radio band and the other wavelengths ( $\gamma$ -ray, X-ray, optical, infrared), the SKA will considerably be to contribute to

TABLE 5.6: Below, values of the angular coefficients of figure 5.12 are reported.

Instrument	Angular Coefficient
GRANAT	21.17
Ulysses	66.36
COMPTEL	5.78
BATSE (t)	295.78
BATSE (nt)	216.93
Konus/Wind	16.01
BeppoSAX	159.28
HETE-2	16.99
INTEGRAL	9.80
<i>Swift</i>	90.85
Agile	33.82
<i>Fermi</i>	230.97

a data increment, and hence the statistics, and finally to enhance the understanding of the GRB physics. On the other hand, a serendipitous SKA detection could be give an important contribution to the GRB world. It is true that prompt radio emissions are not probably exist, but also it true they have never been directly observed by a radio telescope. This situation might be purely random. Even by Robo AMI, go on source after  $\sim 4$  minutes is too late for a *prompt* radio observation.

## 5.4 Measure unit conversions and Spectrum Energy Distribution

GRBs are observed in different bands and there is a preferred measure of unit for each band. A measure can usually be given either in luminosity  $L$  ( $\text{erg s}^{-1} \text{ Hz}^{-1}$ ), fluence  $S$  ( $\text{erg cm}^{-2}$ ), flux  $F$  ( $\text{erg cm}^{-2} \text{ s}^{-1}$ ) or flux density  $F_\nu$  ( $\text{W m}^{-2} \text{ Hz}^{-1}$ ). Since I want to compare different wavelengths to each other, I must have the same measure unit. For convenience, the relations among there units is written here:

$$L = \frac{4\pi F_\nu d_L^2}{1+z}$$

$$F = F_\nu \Delta\nu$$

$$S = F \Delta t,$$

where  $\Delta\nu$  and  $\Delta t$  are respectively the bandwidth and the integration time during the acquisition.

In order to plot an SED of the 95 GRBs detected by [18], I choose to convert everything into fluxes. Taking into account tables 1 and 4 in that work, from the fluence at 15-150 keV I can obtain the flux by multiplying by the  $T_{90}$ . Furthermore, from data in flux density, I can calculate the flux of the source knowing the bandwidth (100 MHz at radio band and R-band<sup>14</sup> at optical wavelengths). Also, the conversion from energies into frequencies, or wavelengths, is given by using the Planck constant

$$E = h\nu = hc\lambda. \quad (5.18)$$

Finally, the flux density is expressed in  $\mu\text{Jy}$ , so in cgs system it is

$$1 \mu\text{Jy} = 10^{-6} \text{ Jy} = 10^{-32} \frac{\text{W}}{\text{m}^2 \text{ Hz}} = 10^{-29} \frac{\text{erg}}{\text{s cm}^2 \text{ Hz}}. \quad (5.19)$$

In practice, if I have an R-band flux density  $F_\nu = 6.5 \mu\text{Jy}$ , it must be multiplied by the bandwidth 138 nm (converted into cgs system and frequency, it is  $138 \cdot 10^{-7} \text{ cm} \cdot 3 \cdot 10^{10} \text{ cm/s}$ ) and the conversion factor is  $10^{-29} \text{ erg s}^{-1} \text{ cm}^{-2} \text{ Hz}^{-1}$ . Thus the result in flux is  $F = 2.691 \cdot 10^{-23} \text{ erg cm}^{-2} \text{ s}^{-1}$ .

As mentioned in section 5.1, where I explain in detail the paper of [18], they have not listed every value at each frequency, so I want to report in section 5.5 some commonly used methods to extrapolate and “*k*-correct” data.

## 5.5 Bolometric-equivalent energy and *k*-correction

In section 5.1, I introduce how Chandra and Frail made their data extrapolation. Here I want to explain in detail how to make an calculation and then the *K*-correction of the equivalent-bolometric energy. To do this, I follow papers already cited in the text, i.e. [5, 219].

When a GRB is detected by a satellite, the satellite detectors usually measures a part of its real bolometric fluence  $S_{\text{bol}}$ . This last is typically measured in energy per unit area and, obviously, is the fluence at the observer frame. In general, the formula to obtain the equivalent-bolometric energy is

$$E_{\text{iso}}^{\text{bol}} = \frac{4\pi d_L}{1+z} S_{\text{bol}}, \quad (5.20)$$

---

<sup>14</sup>Its Full Width Half Maximum (bandwidth  $\Delta\lambda$ ) is 138 nm, its Effective Wavelength Midpoint  $\lambda_{\text{eff}}$  for standard filter is at 658 nm [260].

which considers the energy on a spherical surface with radius  $d_L$ .

In particular, the (real) bolometric energy is difficult to measure, due to the limited-energy bandpass of detectors, therefore a satellite detector really measures the fluence per energy units, often labeled as  $S_{[e_1, e_2]}$ . The fluence per unit energy is defined as [219]

$$S_{[e_1, e_2]} = \int_{E_1}^{E_2} E S_0 \Phi(E) dE, \quad (5.21)$$

where  $\Phi(E)$  is the time integrated spectral shape of a the observed GRB and  $S_0$  is a normalization factor (photons per unit area per unit energy), both of which are acquired by measures. Although the spectrum could be measured point by point, it is not done in practice. Acquisitions are at different sparse intervals, and for this reason analytic fits are used. Non-thermal spectra are well described by the background-subtracted continuum Band function:

$$\Phi(E) = \begin{cases} A \left( \frac{E}{100 \text{ keV}} \right)^\alpha e^{-E/E_0} & \text{if } E \leq E_{\text{break}} \\ A \left( \frac{E_{\text{break}}}{100 \text{ keV}} \right)^{(\alpha-\beta)} \left( \frac{E}{100 \text{ keV}} \right)^\beta e^{\beta-\alpha} & \text{if } E > E_{\text{break}} \end{cases} \quad (5.22)$$

where  $A$  is a normalization constant and

$$E_{\text{break}} \equiv (\alpha - \beta) E_0 \quad (5.23)$$

and

$$E_0 = \frac{E_p}{2 + \alpha}. \quad (5.24)$$

In the last equation,  $E_p$  is the energy peak of the prompt, which typically occurs between 50 and 500 keV. Commonly the two spectral indexes are  $\alpha \sim -1$  and  $\beta \sim -2$ ; however, many standard energy spectra can follow Eq. 5.22, as a single power law ( $E_0 = \infty$ ), energy exponential ( $\alpha = -1$  and  $\beta = -\infty$ , for optically thin thermal bremmstrahlung without the Gaunt factor) and photon exponential ( $\alpha = 0$ ,  $\beta = -\infty$ ) [5]. Eqs. 5.22 seems to adequately fit the spectral energy shape in the range of BATSE (20-2000 keV [5, 261]), also extending it out to tens of MeV [262].

Once the bandpass fluence is obtained in Eq. 5.21, there is a point to note. Even though this value is measured between a range  $e_1$  and  $e_2$ , it has to be converted to the source co-moving frame, to know the energy interval at the rest frame. Basically,  $S_{[e_1, e_2]}$  should be seen like  $S_{[E_1/1+z, E_2/1+z]}$ , and so Eq. 5.21 can be rewritten as [219]

$$E_{[E_1, E_2]} = S_{[e_1, e_2]} k[e_1, e_2, E_1, E_2, z, \Phi(E)], \quad (5.25)$$

where,  $\Phi(E)$  is given by Eq. 5.22 and the  $k$ -correction is

$$k[e_1, e_2, E_1, E_2, z, \Phi(E)] \equiv \frac{I[E_1/(1+z), E_2/(1+z)]}{I[e_1, e_2]}, \quad (5.26)$$

with  $I[i_1, i_2] \equiv S_{[i_1, i_2]} / S_0$ . It is trivial to note that if the fixed co-moving bandpass is equal to the redshift detector bandpass, then  $e_1 = E_1/(1+z)$ ,  $e_2 = E_2/(1+z)$  and  $k = 1$ .

Often information about the GRB spectrum and fluence measures are available and thus mathematical extrapolations are necessary. Although spectra of GRBs are very different and only one model cannot fit all of them, the  $\phi(E)$  can be used with an empirical numerical correction of 1.06 times the median energy implied over the template spectra used by [219] (to consult for more details).

From [219], I report the error estimation on the  $k$ -correction method. The fluence of a GRB is essentially determined by a spectrum which is the response of a detector, given by its predicted total count. The spectral shape and normalization are found by iteration as long as the predicted counts best match the raw counts, hence there is a likely covariance among  $S_0$  and the parameters of  $\Phi(E)$ . This covariance is rarely reported, perhaps because of the complex dependence on the detector responses. For this reason, in the next error estimate done by [219],  $\Phi(E)$  and  $S_0$  are considered as uncorrelated. Furthermore, since the redshift error is negligible with respect to the uncertainty in the measure of the fluence, it can therefore be ignored in the next calculations.

From Eq. 5.25 uncertainty in the energy is given by

$$\sigma_{E_{[E_1, E_2]}}^2 = \left( \frac{E_{[E_1, E_2]}}{S_{[e_1, e_2]}} \right)^2 \sigma_{S_{[e_1, e_2]}}^2 + \left( \frac{E_{[E_1, E_2]}}{k} \right)^2 \sigma_k^2. \quad (5.27)$$

By adopting the Band function 5.22 and assuming that  $E_0$ ,  $\alpha$  and  $\beta$  are uncorrelated, the uncertainty in  $k$  is

$$\begin{aligned} \sigma_k^2 &= \\ &= \left\{ \frac{k}{I[E_1/(1+z), E_2/(1+z)]} \frac{\partial}{\partial \alpha} [I[E_1/(1+z), E_2/(1+z)]] - \frac{k}{I[e_1, e_2]} \frac{\partial}{\partial \alpha} [I[e_1, e_2]] \right\}^2 \sigma_\alpha^2 + \\ &+ \left\{ \frac{k}{I[E_1/(1+z), E_2/(1+z)]} \frac{\partial}{\partial \beta} [I[E_1/(1+z), E_2/(1+z)]] - \frac{k}{I[e_1, e_2]} \frac{\partial}{\partial \beta} [I[e_1, e_2]] \right\}^2 \sigma_\beta^2 + \\ &+ \left\{ \frac{k}{I[E_1/(1+z), E_2/(1+z)]} \frac{\partial}{\partial E_0} [I[E_1/(1+z), E_2/(1+z)]] - \frac{k}{I[e_1, e_2]} \frac{\partial}{\partial E_0} [I[e_1, e_2]] \right\}^2 \sigma_{E_0}^2. \end{aligned} \quad (5.28)$$

In the previous equation, the different  $\partial I[x_1, x_2]/\partial y$  are:

$$\frac{\partial}{\partial E_0} [I[x_1, x_2]] = \begin{cases} \int_{x_1}^{x_2} \Phi(E) \left(\frac{E}{E_0}\right)^2 dE, & \text{if } E \leq E_{\text{break}} \\ \int_{x_1}^{x_2} \Phi(E) \frac{E_{\text{break}}}{E_0}, & \text{if } E > E_{\text{break}}; \end{cases} \quad (5.29)$$

$$\frac{\partial}{\partial \alpha} [I[x_1, x_2]] = \begin{cases} \int_{x_1}^{x_2} E \Phi(E) \ln\left(\frac{E}{100 \text{ keV}}\right) dE, & \text{if } E \leq E_{\text{break}} \\ \int_{x_1}^{x_2} E \Phi(E) \ln\left(\frac{E_{\text{break}}}{100 \text{ keV}}\right) dE, & \text{if } E > E_{\text{break}}; \end{cases} \quad (5.30)$$

$$\frac{\partial}{\partial \beta} [I[x_1, x_2]] = \begin{cases} 0, & \text{if } E \leq E_{\text{break}} \\ \int_{x_1}^{x_2} E \Phi(E) \ln\left(\frac{E}{E_{\text{break}}}\right) dE, & \text{if } E > E_{\text{break}}. \end{cases} \quad (5.31)$$

In practice, it is extremely difficult (if not impossible) to observe a complete spectrum, and thus extrapolations are the only methods to obtain its shape. This leads to systematic uncertainties when the Band function does not fit a spectrum well, outside the observed bandpass. However, most of energy of a GRB is emitted around  $E_0$  (more or less 100-400 keV in the [5] sample), therefore the extrapolation of a spectrum will not grossly affect the derived energy [219].

## 5.6 Discussions

In the previous sections I have spoken about radio GRB observations, data extrapolations, radio GRB populations, GRBs with the observable sky above the SKA and  $k$ -correction, all these topics are used for this section.

In general, extrapolations among different bands should be avoided, so radio afterglow simulations should be made but this is beyond this work. In chapter 1 it has been mentioned that different emission processes come into play from gamma to radio bands, and extrapolations could therefore lead to shortcomings, but an attempt for this will be done at a next work. However, taking into account the simple consideration made by Chandra & Frail, expanded later by Hancock et al., I can apply their first studies to my sample. Thus, considering the  $S_\gamma$  value for FR population in table 5.3, it is possible to draw GRBs with  $S_\gamma \geq 1.6 \cdot 10^{-6}$  erg cm $^{-2}$  from *Swift* table considered in this work.

With a very generic calculation one can take into account only the radio detections in [18] and considering their sample as a projection of a real partition for the radio

detectability. In this case the detection rate for GRBs in radio band would be

$$\frac{304}{95} = 31.3\%. \quad (5.32)$$

Considering my calculation on all GRBs collected, the probability to have GRBs in the sky above the SKA is

$$\frac{6508}{7516} = 86.6\%. \quad (5.33)$$

Therefore, the probability to have a radio detectable GRB above the SKA is 27.1%.

Limiting the calculation on the *Swift* observations taken from the “[Swift GRB Table and Lookup](#)” (time-frame 17<sup>th</sup> December 2004 - 18<sup>th</sup> March 2015) some estimation can be carried out. There are 951 GRBs in total but 200 are without coordinates, 121 are with a declination grater than 50° (out of the SKA view), 16 GRBs does not have a determinate fluence between 15-150 keV.

Considering the fluence threshold and the percentage found by Chandra & Frail for radio detections over this threshold, i.e.  $S_{15-150} = 10^{-6}$  erg cm<sup>-2</sup> and 86.3%, it is simple to see that 345 GRBs have  $\delta < 50^\circ$  and  $S_{15-150} \geq 10^{-6}$  erg cm<sup>-2</sup>. Therefore, for the SKA the percentage of detecting GRBs in radio band and in the “*Swift* world” is at least

$$\frac{345 \cdot 86.3\%}{951} = 31.3\%. \quad (5.34)$$

Limited to GRBs observed by *Swift* within the observable sky of the radio telescope (excluding also GRBs without determinate coordinates), the percentage increases to

$$\frac{345 \cdot 86.3\%}{951 - 200 - 121} = 47.3\%. \quad (5.35)$$

On the other hand, it is possible to take into account the values calculated by Hancock et al., using again the same *Swift* data. In this case, the median value of fluence at 15-150 keV associated to RF GRBs is  $16 \cdot 10^{-7}$  erg cm<sup>-2</sup>, so the detection rate for the SKA becomes

$$\frac{266}{951} = 28.0\%, \quad (5.36)$$

which increases if the GRBs out of the SKA shadow cone are excluded

$$\frac{266}{951 - 200 - 121} = 42.2\%. \quad (5.37)$$

Even considering only *Swift* data, the estimations of radio detectability of GRB afterglows are more or less the same, namely around the 30%.

It is important to note that the RF upper limit calculated in [21] is 40 μJy. The planned sensitivity of the SKA will reach the nJy, so RF GRBs will not be a unsurmountable for this telescope.

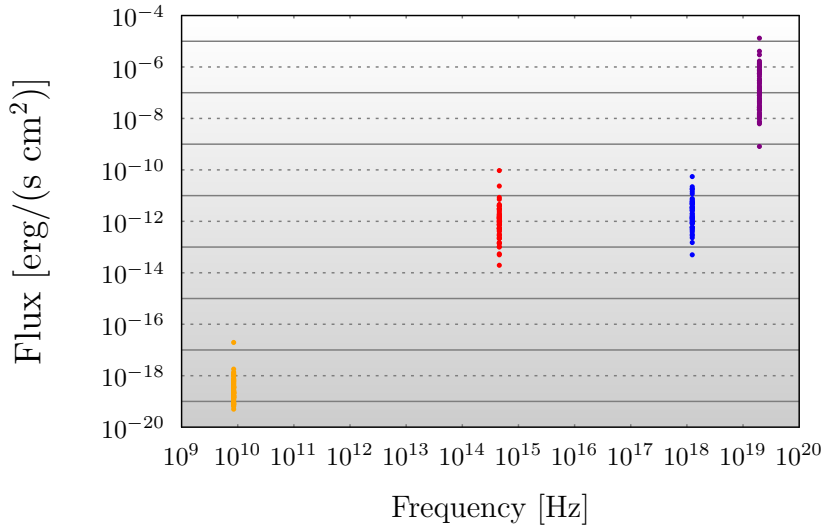


FIGURE 5.14: Plot of fluxes reported in table 5.7. The point are plotted only if the row shows four values at the variuos frequencies (19.6 EH $\zeta$ , 1.3 EH $\zeta$ ,  $4.56 \cdot 10^2$  TH $\zeta$ , 8.46 GHz).

By available data in [18], table 5.7 and figure 5.14 have been created. The table shows 64 GRBs and corresponding celestial coordinates observed at different frequencies. It is basically a merging of tables 1 and 4 in [18], but filtered by a conversion of units. The used procedure to have values in fluxes is the same described in section 5.4, where the time considered for conversion from fluence has been the  $T_{90}$ . To convert flux densities for radio and optical bands, their acquisition bandwidths have been considered. The symbols “Y” and “N” in columns 3<sup>th</sup>, 4<sup>th</sup> and 5<sup>th</sup> indicate if the signal was detected at X-ray, optical and radio frequencies.

As regarding figure 5.14, it shows a plot with four frequencies, i.e. 19.6 EH $\zeta$ , 1.3 EH $\zeta$ ,  $4.56 \cdot 10^2$  TH $\zeta$ , 8.46 GHz vs measured or extrapolated fluxes. Data are taken from the table 5.7, but only where fluxes have all four values. It is clear as the flux decreases with the wavelength. This is only a first step for more accurate analyses in next works.

Without others radio observations, it is impossible to be more precise, but these results about the detection rate are relevant enough to encourage a study in this direction. Additional radio data will give the possibility to find correlations with higher frequencies, although very different physical processes drive the GRB emission for each band.

As will be seen in detail in part III, the final goal concerning GRBs will be to use them as *distance indicators*. In order to find a relation between GRBs and their distances, it is worthwhile to note that only observational quantities should be used. However, to obtain a common light curve for GRBs, as Phillips did for SNeIa [263], will be more difficult.

As often mentioned, GRBs spread in a very large range of variables and such variables are largely changeable. Another point is their redshifts and their luminosity time decays. When one considers a luminosity curve, the time decay should be referred to the rest frame, but if this time is considered then one should consider the real frequencies, namely the emitted frequency in the rest frame. If the redshift is known, both these corrections are possible, therefore it is possible to obtain a distance only for GRBs where the  $z$  is known and the SKA can help in this analysis by indirect observations (e.g., the spin-flip emission of the hydrogen at 1.4 GHz from the host galaxy).

## 5.7 Appendix of the chapter

Table 5.4 is the merging of catalogues mentioned and explained in part in section 5.3.2. For each row there are seven columns. The first two columns are GRB coordinates (RA J2000 and DEC J2000) in decimal degrees; the third, fourth and fifth are the acquisition time with year, month, day (days are decimal and contain information about hours, minutes and seconds); the sixth column is the referring mission and, finally, the source name.

In the sixth column only one of the missions which detected that GRB is reported, but, as previously mentioned, some GRBs have been detected by more than one mission, hence they could be reported in more than one catalogue.

As for source name, I have reported the same name of the catalogue considered in the sixth column. No official names were found for the BNT GRBs, therefore only “GRB” has been written in the last column. Furthermore, BT source names are the same used in the HEASARC web table, with a final dash instead of the common progressive letters. However, sources have been sorted by detection time, so it is possible to read all GRBs with a temporal logic.

The references used for every mission are reported in the table 5.4:

### - GRANAT satellite (cat. GRA)

References in the *phebus* catalogue [255–258].

### - BATSE/CGRO (t) (cat. BT)

references in the *batseggrb* catalogue [244, 245] and [241].

### - BATSE/CGRO (nt) (cat. BNT)

references in the [241] and [242].

### - Konus/Wind (cat. K/W)

references in the [237].

- **BeppoSAX (cat. BeS)**

references in the [240].

- **HETE-2 (cat. HET)**

references in the “*hete2grb*: HETE-2 Gamma-Ray Bursts” by **MIT** (Massachusetts Institute of Technology) and “*hete2gen*: HETE-2 GCN Triggers Catalog”.

- **INTEGRAL (cat. INT)**

references in the [250], [251] and [252]. We matched with the the “*Swift GRB Table and Lookup*” (selecting INTEGRAL mission).

- ***Swift* (cat. Swi)**

references in [253] and “*Swift GRB Table and Lookup*”.

- **Agile (cat. Agi)**

references in [236], [237], [238] and [239] and I matched them with “*Swift GRB Table and Lookup*” (selecting Agile mission).

- ***Fermi* (cat. Fer)**

references in [246], [247] and the *fermigbrst catalogue* in HEASARC archive.

The following list clearly explains how all matchings have been done. As mentioned in section 5.3.2, different GRB catalogues, gathering in each list only a single mission (the only exception was CGRO with two different catalogues). Equal events from various tables have been make as one. For doing this, the lists have been matched each other, using the following criteria:

- The Agile list was matched with all other lists. A GRB was the same if it exploded within 0.005 days with respect to another one, and if they had a difference  $\leq 90^\circ$  in RA and in DEC each other. Even if the Agile angular resolution was within a few arcmin, many GRBs were localized by satellite triangulations and other satellite were not so fine in localization accuracy. To be sure, a much larger angular range has been used. More details about this mission can be read at the [ASI web site](#).
- The BeppoSAX list was matched with all CGRO lists, as explained previously (time delay of 0.005 and angular range  $\leq 146^\circ$ ).
- Among BATSE/CGRO lists I did not change the criterion used by [241].
- *Swift* list was matched with *Fermi* one, with a delay of 0.005 days and angular range of  $45^\circ$ .
- The GRANAT list was matched with all other lists, using only a time delay of 0.005 days.

- The HETE-2 list was matched with BeppoSAX and *Swift* lists: angular range of  $83^\circ$  and time delay of 0.005 days.
- The INTEGRAL list was matched with Hete-2, *Fermi* and *Swift* lists. Time delay 0.005 and angular range  $90^\circ$ .
- The Konus/Wind list was matched with all other lists, with a delay 0.005 and angular range  $90^\circ$ .

The time delay of 0.005 days (that is  $\sim 7$  minutes between an explosion and the next) is in common. We changed angular ranges instrument by instrument, depending on their error positions, or FoV, or angular resolution. These angular values are probably large, but a conservative case has been preferred. However, the most relevant matching filter was the time delay and, that other criteria could be used.

This research has made also use of the Jochen Grainer's table on

<http://www.mpe.mpg.de/~jcg/grbgen.html> [264].

TABLE 5.7: This table is a fusion between tables 1 and 4 from [18], but the original  $S_{15-150}$  fluence, the R-band optical and the 4.86 GHz radio flux densities have been converted into  $\text{erg cm}^{-2} \text{s}^{-1}$ -units, as indicated in section 5.4. The first three columns indicate the GRB name, right ascension and celestial declination. Forth, fifth and sixth columns with Y or N indicate whether a GRB has a signal in the X, optical and radio band. The last five columns are the fluxes in the 15 - 150 keV and 0.3 - 10 keV energy ranges, at the optical R-band, at the 4.86 GHz radio band, redshift and equivalent isotropic bolometric energy. The apex “11h” indicates the value of the flux at 11 hour since the burst. The symbol “-” indicates not defined values.

Name	RA	DEC	X	O	R	$F_{15-150}$	$F_{0.3-10}^{11\text{h}}$	$F_{\text{R-band}}^{11\text{h}}$	$F_{\text{radio}}$	$z$	$E_{\text{iso}}^{\text{bol}}$
970508	06:53:49.2	+79:16:19	Y	Y	Y	7.92857e-08	5.70000e-13	1.41304e-13	9.58000e-19	0.835	7.10E+51
970828	18:08:31.7	+59:18:50	Y	N	Y	7.89116e-07	1.99000e-12	-	1.44000e-19	0.958	2.96E+53
980329	07:02:38.0	+38:50:44	Y	Y	Y	7.51724e-07	6.00000e-13	5.00000e-14	3.32000e-19	2.95	2.10E+54
980519	23:22:21.5	+77:15:43	Y	Y	Y	1.81000e-07	3.90000e-13	1.35652e-12	2.05000e-19	-	-
980703	23:59:06.7	+08:35:07	Y	Y	Y	2.23333e-07	1.40000e-12	7.71739e-13	1.37000e-18	0.966	6.90E+52
981226	23:29:37.2	-23:55:54	Y	N	Y	1.34000e-08	2.80000e-13	-	1.37000e-19	1.11	5.9E+51
990510	13:38:07.1	-80:29:48	Y	Y	Y	1.61333e-07	3.47000e-12	3.95435e-12	2.55000e-19	1.619	1.78E+53
991208	16:33:53.5	+46:27:21	X	Y	Y	1.34833e-06	-	8.53261e-12	1.80400e-18	0.706	1.10E+53
000210	01:59:15.6	-40:39:33	Y	N	Y	4.09000e-06	3.10000e-13	-	9.30000e-20	0.850	2.00E+53
000301C	16:20:18.6	+29:26:36	X	Y	Y	3.47000e-07	-	1.44130e-12	5.20000e-19	2.034	4.37E+52
000418	12:25:19.3	+20:06:11	X	Y	Y	7.16667e-07	-	6.97826e-13	1.08500e-18	1.119	7.51E+52
000911	02:18:34.4	+07:44:29	X	Y	Y	1.65000e-08	-	1.24565e-12	2.63000e-19	1.059	8.80E+53
000926	17:04:09.7	+51:47:10	X	Y	Y	1.45200e-06	-	2.29130e-12	6.29000e-19	2.039	2.70E+53
001007	04:05:54.3	-21:53:46	X	Y	Y	1.45333e-07	-	3.03261e-12	2.22000e-19	-	-
001018	13:14:10.3	+11:48:32	X	X	Y	6.38710e-07	-	-	5.90000e-19	-	-
010222	14:52:12.5	+43:01:06	Y	Y	Y	2.97059e-07	7.05000e-12	1.67174e-12	9.30000e-20	1.477	1.33E+54
010921	22:55:59.9	+40:55:53	X	Y	Y	2.96667e-07	-	3.12391e-12	2.29000e-19	0.450	9.00E+51
011030	20:43:35.4	+77:17:20	Y	N	Y	-NaN	1.80000e-11	-	1.39000e-19	3	-

Table 5.7: continue into the next page...

Table 5.7: ... continues from the previous page

Name	RA	DEC	X	O	R	$F_{15-150}$	$F_{0.3-10}^{1\text{lh}}$	$F_{\text{R-band}}^{1\text{lh}}$	$F_{\text{radio}}$	$z$	$E_{\text{iso}}^{\text{bol}}$
011211	11:15:18.0	-21:56:56	Y	Y	Y	6.20000e-09	1.80000e-11	5.17391e-13	1.62000e-19	2.140	6.30E+52
020305	12:42:27.94	-14:18:11.8	X	Y	Y	2.65182e-08	-	1.46957e-12	7.60000e-20	2.8	-
020405	13:58:03.12	-31:22:21.9	X	Y	Y	1.23750e-06	-	1.26739e-12	1.13000e-19	0.690	1.10E+53
020819B	23:27:19.47	+06:15:56.0	X	N	Y	7.94000e-08	-	-	2.91000e-19	0.410	7.90E+51
021004	00:26:54.68	+18:55:41.6	Y	Y	Y	2.26000e-08	8.40000e-13	3.02826e-12	7.80000e-19	2.330	3.80E+52
021206	16:00:46.85	-09:42:33.5	X	N	Y	1.32000e-05	-	-	1.37000e-19	-	-
030115A	11:18:32.60	+15:02:59.0	X	Y	Y	2.62500e-08	-	1.04348e-13	8.30000e-20	2.500	3.91E+52
030226	11:33:04.93	+25:53:55.3	Y	Y	Y	3.92754e-08	1.35000e-12	1.03913e-12	1.71000e-19	1.986	1.20E+53
030227	04:57:33.00	+20:29:09.0	Y	Y	Y	2.16061e-08	9.00000e-13	1.39130e-13	6.40000e-20	-	-
030329	10:44:49.96	+21:31:17.4	Y	Y	Y	1.07619e-06	5.48600e-11	9.40870e-11	1.95670e-17	0.169	1.80E+52
030418	10:54:33.69	-07:01:40.8	X	Y	Y	9.72727e-09	-	5.10870e-13	6.90000e-20	-	-
030723	21:49:24.40	-27:42:47.4	Y	Y	Y	8.12903e-10	1.50000e-13	5.19565e-13	2.04000e-19	-	-
031203	08:02:30.36	-39:51:00.1	Y	Y	Y	4.43333e-08	4.50000e-13	4.16304e-12	7.24000e-19	0.105	1.15E+50
050401	16:31:28.82	+02:11:14.8	Y	Y	Y	2.49091e-07	3.51000e-12	5.43478e-14	1.22000e-19	2.898	3.20E+53
050416A	12:33:54.60	+21:03:24.0	Y	Y	Y	1.22333e-07	2.53000e-12	2.15217e-13	3.73000e-19	0.650	1.00E+51
050509C	12:52:53.94	-44:50:04.1	Y	Y	Y	7.56000e-09	-	4.08696e-13	3.44000e-19	-	-
050525A	18:32:32.57	+26:20:22.5	Y	Y	Y	1.70000e-06	5.15000e-12	9.43478e-13	1.64000e-19	0.606	2.04E+52
050603	02:39:56.89	-25:10:54.6	Y	Y	Y	5.30000e-07	3.30000e-12	1.90435e-12	3.77000e-19	2.821	5.00E+53
050713B	20:31:15.50	+60:56:38.4	Y	N	Y	2.54400e-08	1.18000e-11	-	3.43000e-19	-	-
050730	14:08:17.13	-03:46:16.7	Y	Y	Y	1.51592e-08	7.67000e-12	5.60870e-13	2.12000e-19	3.968	9.00E+52
050820A	22:29:38.11	+19:33:37.1	Y	Y	Y	1.43333e-08	2.21200e-11	1.89565e-12	1.50000e-19	2.615	2.00E+53
050824	00:48:56.05	+22:36:28.5	Y	Y	Y	1.15652e-08	1.37000e-12	2.15217e-13	1.52000e-19	0.830	1.50E+51
050904	00:54:50.79	+14:05:09.4	Y	Y	Y	2.77586e-08	5.00000e-14	4.34783e-13	7.60000e-20	6.290	1.30E+54

Table 5.7: continue into the next page...

Table 5.7: ...continues from the previous page

Name	RA	DEC	X	O	R	$F_{15-150}$	$F_{0.3-10}^{11h}$	$F_{R\text{-band}}^{11h}$	$F_{\text{radio}}$	$z$	$E_{\text{iso}}^{\text{bol}}$
060116	05:38:46.28	-05:26:13.1	Y	Y	Y	2.27358e-08	5.80000e-13	1.50000e-13	3.63000e-19	-	-
060218	03:21:39.68	+16:52:01.8	Y	Y	Y	1.22656e-08	4.88000e-12	2.35261e-11	4.71000e-19	0.033	2.90E+48
060418	15:45:42.40	-03:38:22.8	Y	Y	Y	8.08738e-08	9.40000e-13	5.43478e-13	2.16000e-19	1.490	1.00E+53
070125	07:51:17.77	+31:09:04.1	Y	Y	Y	1.07333e-06	3.78000e-12	4.51522e-12	1.02800e-18	1.548	9.55E+53
070612A	08:05:29.61	+37:16:15.1	X	Y	Y	2.87263e-08	-	7.16957e-12	1.02800e-18	0.617	9.12E+51
071003	20:07:24.22	+10:56:50.0	Y	Y	Y	5.60811e-08	5.57000e-12	3.91522e-12	6.16000e-19	1.604	3.24E+53
071010B	10:02:09.26	+45:43:50.3	Y	Y	Y	1.22222e-07	4.56000e-12	1.05000e-12	3.41000e-19	0.947	2.60E+52
071020	07:58:39.78	+32:51:40.4	Y	Y	Y	5.75000e-07	1.61000e-12	2.84783e-13	1.41000e-19	2.146	8.91E+52
080603A	18:37:37.97	+62:44:38.9	Y	Y	Y	7.00000e-09	1.58000e-12	2.89130e-13	2.07000e-19	1.687	-
081203B	15:15:11.67	+44:25:42.9	Y	Y	Y	9.13044e-08	5.87000e-12	7.32609e-13	1.62000e-19	-	-
081221	01:03:10.20	-24:32:53.2	Y	Y	Y	5.55882e-07	1.14000e-12	1.95652e-14	1.74000e-19	-	-
090313	13:13:36.21	+08:05:49.8	Y	Y	Y	2.12676e-08	3.19000e-12	1.67174e-12	4.35000e-19	3.375	4.57E+52
090323	12:42:50.29	+17:03:11.6	Y	Y	Y	5.50376e-07	2.81000e-12	8.95652e-13	2.43000e-19	3.57	4.10E+54
090328	06:02:39.6	-41:53:03.2	Y	Y	Y	9.47368e-07	6.14000e-12	1.46522e-12	6.86000e-19	0.736	1.00E+53
090423	09:55:33.29	+18:08:57.8	Y	Y	Y	6.25000e-08	5.00000e-13	-	5.00000e-20	8.260	1.10E+53
090424	12:38:05.11	+16:50:15.1	Y	Y	Y	4.36000e-07	2.30000e-13	7.65217e-13	2.36000e-19	0.544	4.47E+52
090715B	16:45:21.53	+44:50:20.0	Y	Y	Y	2.13962e-08	8.20000e-13	2.34783e-13	1.91000e-19	3.000	2.36E+53
090902B	17:39:45.6	+27:19:26.6	Y	Y	Y	0.00000	4.70000e-12	3.19565e-13	8.40000e-20	1.883	3.09E+54
091020	11:42:55.21	+50:58:42.2	Y	Y	Y	9.74359e-08	1.95000e-12	1.00000e-13	3.99000e-19	1.710	4.56E+52
100413A	17:44:53.22	+15:50:02.4	Y?	Y	Y	3.24607e-08	1.26000e-12	-	8.00000e-20	3.5	-
100414A	12:48:29.96	+08:41:34.9	Y	Y	Y	2.97692e-06	1.43700e-11	1.27174e-12	5.24000e-19	1.368	7.79E+53
100418A	17:05:27.18	+11:27:40.1	Y	Y	Y	4.85714e-08	1.07000e-12	2.65435e-12	1.21800e-18	0.620	5.20E+50
100906A	01:54:44.15	+55:37:50.5	Y	Y	Y	1.05263e-07	2.71000e-12	1.01304e-12	2.15000e-19	1.727	1.34E+53

Table 5.7: End table



## **Part III**

### **GRBs and Cosmology**



# **Chapter 6**

## **Cosmology with GRBs**

This thesis passes through three parts. The first part speaks about GRBs, their theories and gamma satellite instrumentation, while the second part is about radio observation, instruments, interferometric observational techniques and GRB study approaches in radio band. In this last part, I speak about GRBs for cosmology and what contributions they could give due to their intrinsic characteristics.

The first part of this chapter introduces some cosmological models that try to explain the evolution of the universe; basically, current state of the art of cosmology but without entering into details of each theory. Secondly, a discussion of cosmography and the procedures for testing any cosmological model. Finally, after the previous excursus, there is a section focused on improvement of models through the use of GRB probes and increased levels of GRB observations.

### **6.1 A short discussion of cosmology Between theories and observations**

The principle aim of cosmology is the understanding of the whole universe and the causes of its behaviour. In other words, cosmology studies the expansion of the universe at every point (or epoch), and attempts to understand its origin and its future. To explain (or better to justify) its expansion, there is a plethora of theories, models, discussions, with some cited more than others. [265] discusses several models and compares them to each other by cosmological observables.

Although general relativity and Einstein's equations are perfect to describe the Solar system and are in excellent agreement with local gravitational scales, several observations have shown that the universe is currently undergoing an accelerated phase. If

a homogeneous, isotropic, universe dominated by pressureless matter is assumed, then general relativity predictions indicate a decelerated expansion. Even taking into account contributions of spatial scalar curvature, radiation, baryons and dark matter, the measured cosmic acceleration is not explained. An additional component must exist, such as a fluid possibly of non-standard origin, to justify a similar speed up. In today's era of *precision cosmology*, tighter bounds of the observable universe have been measured, and definitively show that a possible new ingredient termed *dark energy*, is required in order to accelerate the universe in the present time.

The dark energy can be considered as a very special fluid with a negative pressure, which by expanding itself opposes the gravity. However, no known fluid behaves in this way and no standard fluid is able to generate a negative pressure, so alternatives have been postulated. They include exotic fluids, anti-gravitational effects due to curvature corrections, and quantum gravity effects.

The simplest explanation of the above problems is probably provided in the branch of quantum field theories. Indeed, by including the quantum vacuum energy term within the standard energy-momentum tensor, the corresponding energy density has an upper limit due to the Planck mass. The obtained vacuum energy contribution is different from zero, and it is usually interpreted as the *cosmological constant*,  $\Lambda$ . This constant is responsible for the acceleration, since the  $\Lambda$  fluid behaves as a non-interacting perfect fluid, which does not cluster, as confirmed by several observations. Furthermore, the equation of state related to the dark energy, that is the ratio between pressure and energy density ( $\omega = -P/\rho$ ), is equal to -1 at any epoch of the universe. Since a constant density is considered also the pressure must be a constant. Such a vacuum energy cosmological constant could be compatible with early time epoch, and have the corresponding  $\Lambda$ CDM ( $\Lambda$  Cold Dark Matter) model dominating at the present time, fitting the cosmological data. This model would seem to be perfect and in agreement with any epoch, but there are several theoretical issues that plague it. Two shortcomings are particularly significant. Firstly, the fine-tuning problem, a discordance of 123 magnitudes between theory and data; secondly, the *coincidence problem* highlights the fact that matter and dark energy densities are comparable only in our epoch. Because of these weak points, many other phenomenological models have been proposed.

A natural extension of  $\Lambda$ CDM is  $\omega$ CDM model, where a scalar field has been introduced within general relativity, providing a constant equation of state ( $\omega \equiv P/\rho = \text{const}$ ). Although the  $\omega$ CDM is a general case which converges on  $\Lambda$ CDM if  $z \ll 1$ , the origin of this *quintessence* dark energy term and its physical meaning in terms of thermodynamical fluid is not completely clear [265]. Thus, the  $\omega$ CDM model cannot be considered as a paradigm which can describe the dark energy dynamics.

A simple and immediate alternative is offered by the *varying quintessence* fluid that accounts for an evolving equation of state for the DE fluid, which leads to a time-dependent barotropic factor ( $\omega = \omega(z)$ ). By this class of models, the trend of the expansion of the universe can be fitted through observational data, since the  $\omega(z)$  is not defined *a priori*. Thus both  $\omega$  and its derivatives can be reconstructed by observations. In practice, it is demanded that the barotropic factor evolves as the universe expands, therefore this factor must be matched with cosmological data at different eras of the evolution of the universe.

Recently, several reconstruction methods have been implemented. One of the most relevant is provided by the Chevallier-Polarsky-Linder parametrization [266, 267] of the equation of state, where a Taylor expansion around the value of the cosmological scale factor  $a(t) = a_0 = 1$  of the barotropic factor is involved,

$$\omega(a) = \omega_0 + \omega_1(1 - a). \quad (6.1)$$

An advantage of this parametrization is to predict an early universe dominated by matter, in agreement with current early time bounds. However, the parametrization is affected by the degeneracy between  $\omega_0$  and  $\omega_1$  and the corresponding experimental difficulties of reconstructing the evolution of the dark energy at every epoch.

Another option regarding a particular hypothesis is offered by extending the standard Einstein-Hilbert action. Following this idea, dark energy effects can be reconstructed thanks to introductions of curvature corrections or quantum gravity modifications, where these effects are a consequence of an extended gravitational theory. In such a way, possibilities of extending general relativity span from the  $\mathcal{F}(R)$  gravity to Horava-Lifshiz corrections, and so on [268, 269]. However, the correct modification is not known *a priori*, and this gives a significant disadvantage.

It is easy to see that there are a lot of models but, more or less, each of them fits data in excellent agreement in the early and late times. The necessity of model-independent techniques and experimental tests, able to rule out cosmological models, is probably one of the most important prerogatives of modern cosmology. A first test to check models is cosmography which is discussed in this section 6.2. However there is another point important to highlight. As just mentioned, models fit well to early and late times, but there is a dearth of precise data for cosmological purposes in the intermediate  $z$ , between  $2 \lesssim z \lesssim 1000$ , where the redshift transition from a decelerated and accelerated expansion seems to occur. This means that models should be set exactly in this transition phase. Most of the available probes in this range are GRBs, reaching  $z \lesssim 10$ , but they cannot give “precise” information, since their luminosity has not been standardized yet and efforts in this sense are needed.

## 6.2 Cosmography

Cosmography was presented by Weinberg [270] and is an instrument able to directly compare cosmological observables in terms of data models, rather than cosmological models with data. In practice, cosmography relies only upon the cosmological principle and is totally model-independent, fixing cosmological constraints on late-time cosmology. This procedure can eventually discard those models that do not match the corresponding experimental limits, by making the simple assumption that the universe is homogeneous and isotropic. The prescription of this method consists in expanding the cosmological observables of interest around present time, obtaining Taylor series that can be matched directly with data. The degeneracy problem among cosmological models, which leads to the issue that different models fit data with high precision, is hence naturally alleviated.

Assuming a Friedmann-Robertson-Walker metric,

$$ds^2 = dt^2 - a(t)^2 \left( \frac{dr^2}{1 - k r^2} + r^2 \sin^2 \vartheta \, d\phi^2 + r^2 \, d\vartheta^2 \right), \quad (6.2)$$

with  $a(t)$  the scale factor and  $k$  the standard spatial curvature, cosmography can then be used to infer how much dark energy or other components are required to guarantee current observations, without postulating any cosmological model at the beginning of an analysis. The idea is to relate the cosmographic expansions to the free parameters of a given model [265].

Cosmography is a part of cosmology that tries to infer kinematical quantities and its framework is represented by assuming Taylor series of the scale parameter as the basic postulate. In doing so, the standard Hubble law can become an expansion at low  $z$ . From the Hubble law  $v = H_0 D$ , it is easy to obtain the following expression:

$$\frac{a_0}{a(t)} = 1 + \frac{H_0 D}{c}, \quad (6.3)$$

where, the subscript 0 commonly refers to the present time, hence  $a_0 = a(t = 0)$ ;  $H_0$  the Hubble's constant and  $D$  the causal distance crossed by photons from an emitter to an observer. Because

$$1 + z = 1 + \frac{v}{c}, \quad (6.4)$$

then

$$1 + z = \frac{a_0}{a(t)}, \quad (6.5)$$

which is the redshift definition in terms of the scale factor (hereafter  $c$  is considered equal to 1). Therefore, it is possible to expand this equation as  $z(D)$ . These steps represent

the base of the the scale factor expansion, yielding [265]:

$$a(t) \approx a_0 \left[ 1 + \frac{da}{dt} \Big|_{t_0} \Delta t + \frac{1}{2!} \frac{d^2 a}{dt^2} \Big|_{t_0} \Delta t^2 + \frac{1}{3!} \frac{d^3 a}{dt^3} \Big|_{t_0} \Delta t^3 + \frac{1}{4!} \frac{d^4 a}{dt^4} \Big|_{t_0} \Delta t^4 + \dots \right], \quad (6.6)$$

where  $\Delta t \equiv (t - t_0)$ . It is usually assumed that  $\Delta t > 0$ , in order to get the causality of cosmological observations. If  $a_0 = 1$ , the Eq. 6.6 becomes:

$$a(t) \approx 1 + H_0 \Delta t - \frac{q_0}{2} H_0^2 \Delta t^2 + \frac{j_0}{6} H_0^3 \Delta t^3 + \frac{s_0}{24} H_0^4 \Delta t^4 + \dots, \quad (6.7)$$

with the definition of the cosmographic series factors as:

$$H \equiv \frac{1}{a} \frac{da}{dt}, \quad q \equiv -\frac{1}{aH^2} \frac{d^2 a}{dt^2}, \quad j \equiv \frac{1}{aH^3} \frac{d^3 a}{dt^3}, \quad s \equiv \frac{1}{aH^4} \frac{d^4 a}{dt^4}. \quad (6.8)$$

The Hubble rate represents the first derivative with respect to cosmic time of  $\ln a(t)$ . The acceleration parameter  $q$  indicates if the universe is either accelerated or decelerated. The currently accelerating universe appears to have a  $q_0$  between  $-1$  and  $0$ . The  $j$  term is the *jerk* parameter and indicates the variation of acceleration. If it were positive, it would indicate that  $q$  changed sign in the past, at the transition redshift, corresponding to  $q = 0$ . Finally, the *snap* term  $s$  indicates if  $j$  changed sign as the universe expands. If it were negative, the jerk parameter would maintain the same sign of its present measurable value [265].

An expression for the luminosity distance  $d_L$  could be obtained by straightforward calculations, through an Taylor expansion around  $z \simeq 0$ . In particular, from the expression for the causal distance

$$D = \int_0^z \frac{d\psi}{H(\psi)}, \quad (6.9)$$

it is possible to write the luminosity distance, so defined:

$$d_L = (1+z) \int_0^z \frac{d\psi}{H(\psi)}. \quad (6.10)$$

By a Taylor expansion, the last equation gives as final result:

$$\begin{aligned} d_L(z) = d_H z & \left\{ 1 + \frac{1}{2} [1 - q_0] z - \frac{1}{6} (\Omega_0 - q_0 - 3q_0^2 + j_0) z^2 + \right. \\ & \left. + \frac{1}{24} [2 - 2q_0 - 15q_0^2 - 15q_0^3 + 5j_0(1+2q_0) + s_0 + 2\Omega_k(1+3q_0)] z^3 + o(z^4) \right\}, \end{aligned} \quad (6.11)$$

where  $d_H = 1/H_0$  is the Hubble's radius;  $\Omega_0$  the total energy density of the universe, which can be related to the spatial scalar curvature;  $\Omega_k \equiv kd_H^2/a^2$ , in terms of  $\Omega_k = \Omega_0 - 1$ . For this equation, the closure relation, i.e.  $\Omega_k = 0$ , can be assumed and hence a total density fixed to  $\Omega_0 = 1$  (this assumption is explained in the following

of this section).

It is interesting to note that cosmography could be extended into an inhomogeneous-universe framework (e.g., LemaitreTolmanBondi metric [271]) and a new set of cosmographic parameters should be defined.

Although cosmography is a powerful test, it is worthwhile to stress that assuming a precise model-independent procedure depends on  $\Omega_0$ , since the  $j_0$  parameter is linked to the total energy density of the universe. In fact, the Taylor's series cannot separate the sum  $\Omega_0 + j_0$ , and thus the jerk parameter cannot be performed alone. To reduce this issue, the scalar curvature must be set and this would be in contrast with the initial declaration of a model-independent test. Fortunately, it is possible to use this geometrical stratagem because the instrumental measures at the present time confirm that the universe can be fairly well approximated through a vanishing scalar curvature, and so, no generality is lost if  $\Omega_k = 0$ .

Another aspect to stress regards the approximation of the series. Even though the low order of the series propagates numerical departures within the error bars of the cosmographic parameter, a high order might increase the phase space, enlarging so the allowed-statistical regions of cosmic parameters. To alleviate these problems, different datasets can be considered, matching cosmological data with more than one survey compilation. Afterwards, all the observable quantities of interest may be truncated at an intermediate order of the Taylor series, in order to reduce systematics on measurements.

A last shortcoming concerns the divergence of Eq. 6.7 when  $z \rightarrow +\infty$ . Beyond the approximation of low redshift ( $z \gtrsim 1$ ), finite truncations could give systematics on the measurements of cosmological quantities, providing possibly misleading results. A method to alleviate this drawback consists in re-parameterizing the redshift variable, through the use of auxiliary variables, circumscribed within a low redshift domain, in which any possible parameterization of the redshift, for example parameterized by  $x$ , may be limited to  $x < 1$ . Some cases of this parametrization are discussed in [265].

In general, when the dark energy is considered as some mysterious fluid, this is naturally inserted into the Einstein's field equations to drive an accelerated universe expansion. Cosmography could discover the real nature of this strange substance by carrying out accurate analyses, refining the current theoretical knowledge on the observable universe, as well. An improvement of cosmographic analyses will be given by observational data but a crucial contribution will be provided by GRB observations.

### 6.3 GRBs for cosmological constraints

The problem of the divergence among models is real and too many theories seem to answer with a reasonable explanation about the universe expansion, but only observations can give an actual contribution to filter those theories which better match data. In section 6.2, it has been seen how cosmography can set cosmological parameters, however, it is important to remember that cosmography is only a tool. In fact, data can ignore models and theories, but constraints for these last are dictated by observations.

If one had sources whose luminosities were determinate, then their distances would be known, since the intensity is inversely proportional to the square of the distance. In other words, when an observer measures the radiation intensity of an astrophysical object which has a specific (and known) luminosity, he can obtain the distance of that object too. These specific objects are called *standard candles* or, more in general, *distance indicators*. The best examples are Cepheids and SNeIa [263, 272], but another recent example could be cited about SNeIc [273].

Although redshift and distance are linked to each other by Hubble's law [274], and redshift measurements can be carried out for many sources, it is still challenging to determine what their real distances are. The velocity of a source is given by the cosmological redshift, but this does not naturally give information of its position in the space. The point is that only if both velocity and position are known, it is possible to understand the real expansion of the universe. Currently, we have information of true velocity and position only for relatively few astrophysical objects and only in two "narrow" redshift ranges. Out of these ranges, distances and velocities are calculated from the model using assumed cosmological parameters. Unfortunately, inserting these parameters back into the model creates a *circular problem* because the parameters should be given by the data. An additional shortcoming is that this last redshift gap of imprecision is unfortunately huge.

As mentioned, the luminosity decreases as the square of the distance, therefore there is a selection problem which cannot be overcome if a source does not emit an extremely high intrinsic luminosity. For this reason, SNeIa have a natural limit for distance and other sources must be chosen as probes. As mentioned above, these more powerful probes could be GRBs, which span a broader redshift range than SNeIa  $z$  range.

A lot of efforts have been done trying to discover correlations that relate GRB luminosity to other burst parameters, in order to standardize these sources. In an upcoming paper (Del Vecchio et al.), various correlations will be compared, but in this work I want to report only the philosophy of a correlation.

Basically, a correlation tries to connect "visible" parameters as  $E_{\text{iso}}$  or  $E_{\gamma}$  with  $\theta_{\text{jet}}$ ,  $t_b$ ,

$E_{\text{peak}}$ , and so forth (e.g., [102, 275–277]). The purpose of such a correlation is a standardization for GRBs (or a smaller group which respect particular conditions) where they follow a luminosity law. In this way, one may use the correlation to potentially calculate the distance. Once the redshift is measured and the distance calculated, these data can be insert into Eqs. 6.8 and 6.11 to obtain cosmological parameters. Subsequently, the values of these parameters can test different models, in which the adopted Hubble’s parameter  $H(z)$  depends on the model (see [265] for details).

In any case, discovering a GRB relation between distance and redshift, would extend the Hubble diagram to redshifts where the universe velocity transition occurs. This would revolutionize in a decisive way any models, and for this reason such a relation is desired.

Most of current studies about correlations are focused on the X-ray band, but correlation between  $\gamma$ -ray and X-ray are also studied. This work promotes the enlargement of the GRB observation up to the radio wavelengths for many reasons. Firstly, a radio correlation might exist in radio band only; then, radio data would be able to confirm, or contest, correlations in higher bands, since no current correlation is certain. Secondly, even if physical emission processes are different, correlation between more than one band cannot be totally excluded from considerations. GRB studies in radio band could become crucial for discoveries in this sense, therefore observations by appropriate telescopes are necessary. All this work demonstrates that studies done in this way can give excellent results, and that radio observations are practicable.

## Chapter 7

# Conclusions

This thesis wanted to be a proposal in order to promote radio observations for sources that are conventionally known as gamma emitters and this aim has been reached through a precise scheme.

Starting from an excursus about GRB classifications, emission models, emission processes and spectral emission, it has been possible to see how GRBs are sources emitting at very different bands. On the second and third steps acquisition instruments are considered, both for gamma and radio frequencies. After a look at the SKA telescope, a more detailed discussion has been offered about my work in the *Società Aerospaziale Mediterranea* company, and so the feed indexer device for the SKA has been described. With basics of radio interferometry provided on the forth step, the SKA capacities have been highlighted, showing that a radio interferometer can contribute in a relevant way to accurate GRB analyses. In this sense, it is worthwhile to remember again that studies about GRBs must cover many frequencies of the electromagnetic spectrum. Only in this way it will be possible to recognise and understand common characteristics in GRB nature. Indeed, since each spectrum is peculiar enough for different GRBs, one will be able to standardize objects like these only when the complete behaviour of many multi-band GRB observations will have been understood.

Chapter 5 shows the effectiveness of radio observations, which, though these can observe aspects detectable only at radio wavelengths, must be combined with other higher-frequency telescopes. Synergies in this sense are crucial. In this chapter where recent and current works have been reported, it is shown how a methodical radio study provides important results for GRBs.

After all these steps, the last part explains how the astrophysical studies about GRBs can be extended to cosmology, contributing to fix important constraints which could to shine a light on the expansion of the universe.



## Appendix A

### Long table 5.4

This is the complete table 5.4. It is the collection and merging of all catalogues mentioned in this work. In the columns, respectively: RA and DEC in degrees; detection year, month and day; name of the list related to a satellite; source name.

The abbreviations in the sixth column correspond to: GRA = GRANAT; BT = BATSE triggered; BNT = BATSE non-triggered; COMP = COMPTEL; Uly = Ulysses; KW = Knous/Wind; BeS = BeppoSAX; Agi = Agile; Fer = Fermi; INT = INTEGRAL; HET = HETE-2; Swi = Swift.

More details are indicated in section 5.7.

RA deg	DEC deg	Year	Month	Day	Cat.	GRB Name
174.680	-44.320	1990	01	18.73618	GRA	GRB900118
91.160	-82.010	1990	01	20.85941	GRA	GRB900120
113.280	27.890	1990	01	23.07098	GRA	GRB900123A
357.190	-38.560	1990	01	23.78091	GRA	GRB900123B
131.630	-38.180	1990	01	26.75309	GRA	GRB900126
338.040	35.360	1990	02	22.49763	GRA	GRB900222
124.580	38.840	1990	03	8.39725	GRA	GRB900308A
323.250	-31.780	1990	03	27.43366	GRA	GRB900327
206.920	-12.250	1990	04	4.74625	GRA	GRB900404
85.110	82.030	1990	04	13.42455	GRA	GRB900413B
16.950	37.270	1990	04	14.60223	GRA	GRB900414
31.940	18.240	1990	04	15.26456	GRA	GRB900415
135.710	18.800	1990	06	16.16655	GRA	GRB900616B
35.910	59.230	1990	06	18.96692	GRA	GRB900618B
45.900	52.200	1990	06	25.91963	GRA	GRB900625
80.900	43.050	1990	06	28.47075	GRA	GRB900628

Continued on next column

Continued from previous column

RA deg	DEC deg	Year	Month	Day	Cat.	GRB Name
185.910	30.620	1990	07	8.47789	GRA	GRB900708A
252.790	16.200	1990	07	8.78118	GRA	GRB900708B
274.630	-40.980	1990	08	15.48278	GRA	GRB900815
276.310	-45.180	1990	09	1.06505	GRA	GRB900901
326.180	-14.770	1990	09	14.19907	GRA	GRB900914
133.140	-36.720	1990	09	25.85095	GRA	GRB900925B
169.680	-6.480	1990	09	29.07599	GRA	GRB900929
348.610	30.400	1990	10	9.01097	GRA	GRB901009
210.670	-13.240	1990	10	15.11269	GRA	GRB901015A
90.500	-26.000	1990	10	15.36444	GRA	GRB901015B
198.230	-46.270	1990	10	27.18133	GRA	GRB901027
104.750	52.930	1990	11	12.62334	GRA	GRB901112
39.900	25.310	1990	11	16.07095	GRA	GRB901116
30.390	72.400	1990	11	21.75499	GRA	GRB901121B
227.900	49.810	1991	01	17.04017	GRA	GRB910117
296.790	-70.880	1991	01	22.63449	GRA	GRB910122
303.440	-51.850	1991	02	2.87332	GRA	GRB910202B
212.940	58.540	1991	02	19.48986	GRA	GRB910219
184.100	6.380	1991	03	10.54309	GRA	GRB910310
96.960	14.970	1991	03	12.52997	GRA	GRB910312
77.629	13.690	1991	04	2.60295	GRA	GRB910402
209.420	-13.240	1991	04	8.93354	GRA	GRB910408A
280.460	34.050	1991	04	14.31142	GRA	GRB910414A
270.680	24.760	1991	04	21.38477	BT	4B910421
193.470	-8.380	1991	04	23.82969	BT	4B910423
68.400	-6.400	1991	04	24.07108	BNT	GRB
201.310	-45.410	1991	04	24.82184	BT	4B910424
91.290	-22.770	1991	04	25.02623	BT	4B910425-
335.940	25.770	1991	04	25.23441	BT	4B910425-
246.200	65.400	1991	04	26.06234	BNT	GRB
75.820	-19.510	1991	04	26.92647	BT	4B910426
32.400	-46.100	1991	04	27.17242	BNT	GRB
78.860	-15.590	1991	04	27.37872	BT	4B910427
174.750	14.330	1991	04	29.13322	BT	4B910429
315.300	-48.900	1991	04	29.24927	BNT	GRB
135.800	2.730	1991	04	30.71434	BT	4B910430
126.540	-0.230	1991	05	1.34738	BT	4B910501
114.480	-25.310	1991	05	2.47068	BT	4B910502-
46.220	-52.710	1991	05	2.94263	BT	4B910502-
87.450	38.740	1991	05	3.29460	BT	4B910503
214.700	-19.600	1991	05	3.30197	BNT	GRB
243.500	-36.000	1991	05	4.94859	BNT	GRB
177.680	44.440	1991	05	5.84394	BT	4B910505
48.200	14.800	1991	05	7.30245	BNT	GRB
299.550	-44.880	1991	05	7.60505	BT	4B910507
116.500	62.000	1991	05	8.79403	BNT	GRB
339.250	38.260	1991	05	9.12744	BT	4B910509
355.600	3.900	1991	05	10.75684	BNT	GRB

Continued on next column

Continued from previous column

RA deg	DEC deg	Year	Month	Day	Cat.	GRB Name
331.300	-27.900	1991	05	10.81694	BNT	GRB
266.480	58.300	1991	05	11.09153	BT	4B910511
90.860	71.580	1991	05	12.63552	BT	4B910512
192.700	-15.100	1991	05	16.53999	BNT	GRB
75.240	-55.930	1991	05	17.20995	GRA	GRB910517A
113.580	49.170	1991	05	17.45054	BT	4B910517-
356.910	25.280	1991	05	17.99693	BT	4B910517-
285.850	80.820	1991	05	18.14272	BT	4B910518-
218.400	33.000	1991	05	18.25985	BNT	GRB
249.020	-11.770	1991	05	18.62183	BT	4B910518-
292.000	-2.400	1991	05	19.11546	BNT	GRB
108.930	-33.750	1991	05	21.21848	BT	4B910521-
216.660	-34.520	1991	05	21.88487	BT	4B910521-
137.720	-50.890	1991	05	22.50845	BT	4B910522
106.990	0.360	1991	05	23.79404	BT	4B910523-
352.960	24.890	1991	05	23.98529	BT	4B910523-
234.300	26.800	1991	05	24.28564	BNT	GRB
216.030	-62.820	1991	05	25.81005	BT	4B910525
111.560	1.050	1991	05	26.14750	BT	4B910526-
30.540	-50.710	1991	05	26.19386	BT	4B910526-
344.100	-13.200	1991	05	28.83444	BNT	GRB
240.590	43.970	1991	05	28.89369	BT	4B910528
205.430	-27.400	1991	05	29.73335	BT	4B910529
22.200	-41.800	1991	05	30.19755	BNT	GRB
297.900	8.300	1991	06	1.72014	BNT	GRB
310.120	32.340	1991	06	1.80712	BT	4B910601
288.640	48.620	1991	06	2.50450	BT	4B910602-
142.760	53.990	1991	06	2.95487	BT	4B910602-
39.000	12.600	1991	06	3.81109	BNT	GRB
29.470	-35.250	1991	06	4.87564	BT	4B910604
143.900	34.200	1991	06	5.98109	BNT	GRB
172.300	-43.600	1991	06	6.83559	BNT	GRB
78.760	-9.360	1991	06	7.00843	BT	4B910607-
146.760	52.270	1991	06	7.18821	BT	4B910607-
255.200	25.000	1991	06	8.53868	BNT	GRB
0.500	31.900	1991	06	8.73743	BNT	GRB
239.120	-62.250	1991	06	8.96807	BT	4B910608
103.080	-12.070	1991	06	9.03365	BT	4B910609
243.700	37.300	1991	06	9.69788	BNT	GRB
310.300	4.400	1991	06	11.70819	BNT	GRB
52.100	49.500	1991	06	12.07303	BNT	GRB
72.800	16.400	1991	06	12.33343	BNT	GRB
337.070	15.420	1991	06	12.36755	BT	4B910612
174.750	-12.950	1991	06	14.07944	BT	4B910614-
65.900	36.100	1991	06	14.23756	BNT	GRB
20.060	-13.440	1991	06	14.40795	BT	4B910614-
139.400	25.400	1991	06	15.32985	BNT	GRB
61.700	66.100	1991	06	16.09808	BNT	GRB

Continued on next column

Continued from previous column

RA deg	DEC deg	Year	Month	Day	Cat.	GRB Name
172.600	42.800	1991	06	16.15881	BNT	GRB
356.720	-1.210	1991	06	16.44404	BT	4B910616
347.000	35.200	1991	06	17.08281	BNT	GRB
4.600	33.700	1991	06	18.12138	BNT	GRB
21.170	-36.570	1991	06	19.59344	BT	4B910619
67.920	22.500	1991	06	20.23438	BT	4B910620-
89.400	40.000	1991	06	20.24851	BNT	GRB
65.810	65.970	1991	06	20.76583	BT	4B910620-
177.900	53.700	1991	06	20.98852	BNT	GRB
326.870	-8.440	1991	06	21.08146	BT	4B910621-
226.920	-12.440	1991	06	21.67830	BT	4B910621-
8.460	-32.800	1991	06	22.69031	BT	4B910622
18.400	34.300	1991	06	23.36867	BNT	GRB
329.300	18.600	1991	06	24.51241	BNT	GRB
317.610	52.910	1991	06	25.22817	BT	4B910625
22.700	35.100	1991	06	25.62936	BNT	GRB
133.380	7.720	1991	06	26.30223	BT	4B910626
57.300	-17.600	1991	06	26.40899	BNT	GRB
256.400	48.700	1991	06	26.88009	BNT	GRB
197.990	-2.480	1991	06	27.18701	BT	4B910627
69.240	-58.420	1991	06	29.21928	BT	4B910629-
63.520	8.400	1991	06	29.83042	BT	4B910629-
304.700	35.130	1991	06	30.31738	BT	4B910630
61.350	-53.420	1991	07	1.16087	BT	4B910701
117.000	43.800	1991	07	2.18644	BNT	GRB
255.070	29.050	1991	07	2.19903	BT	4B910702-
87.560	24.820	1991	07	2.29159	BT	4B910702-
40.370	29.480	1991	07	3.21093	BT	4B910703
24.030	-65.980	1991	07	5.00628	BT	4B910705-
149.500	3.100	1991	07	5.41902	BNT	GRB
219.790	-43.590	1991	07	5.81551	BT	4B910705-
256.630	-43.690	1991	07	6.21168	BT	4B910706
211.100	-27.300	1991	07	7.26164	BNT	GRB
72.400	-48.500	1991	07	7.73328	BNT	GRB
12.090	15.120	1991	07	8.40395	BT	4B910708
172.770	81.670	1991	07	9.48150	BT	4B910709
248.140	-25.290	1991	07	10.19003	BT	4B910710
17.000	-26.300	1991	07	10.54918	BNT	GRB
76.900	-37.900	1991	07	10.63210	BNT	GRB
76.100	-75.800	1991	07	11.07201	BNT	GRB
209.870	-16.390	1991	07	11.39713	BT	4B910711
303.630	-57.090	1991	07	12.34428	BT	4B910712
17.200	-39.400	1991	07	12.57190	BNT	GRB
187.770	30.690	1991	07	13.85456	BT	4B910713
37.400	-47.100	1991	07	14.38352	BNT	GRB
348.800	-42.800	1991	07	14.44608	BNT	GRB
242.520	22.190	1991	07	14.86547	BT	4B910714
263.400	-66.700	1991	07	15.05624	BNT	GRB

Continued on next column

Continued from previous column

RA deg	DEC deg	Year	Month	Day	Cat.	GRB Name
231.000	3.700	1991	07	15.08656	BNT	GRB
321.430	53.830	1991	07	15.49586	BT	4B910715
110.700	-74.800	1991	07	16.38105	BNT	GRB
165.900	47.800	1991	07	16.44528	BNT	GRB
249.840	-58.210	1991	07	17.18963	BT	4B910717-
294.150	-7.210	1991	07	17.43267	BT	4B910717-
239.460	-16.140	1991	07	17.54682	GRA	GRB910717C
350.540	59.740	1991	07	18.10066	BT	4B910718-
82.800	22.780	1991	07	18.25125	BT	4B910718-
307.970	-46.030	1991	07	18.46479	BT	4B910718-
276.070	-18.580	1991	07	18.88020	BT	4B910718-
245.850	28.460	1991	07	19.45350	BT	4B910719
208.000	42.900	1991	07	19.83991	BNT	GRB
313.960	-32.810	1991	07	21.14006	BT	4B910721-
315.520	-14.290	1991	07	21.81264	BT	4B910721-
125.800	3.320	1991	07	22.48525	BT	4B910722
323.900	16.100	1991	07	23.10524	BNT	GRB
191.900	71.500	1991	07	23.33858	BNT	GRB
264.390	-0.030	1991	07	23.58773	GRA	GRB910723B
135.450	-13.580	1991	07	25.08829	BT	4B910725-
273.180	14.130	1991	07	25.55008	BT	4B910725-
70.600	41.200	1991	07	26.74186	BNT	GRB
222.300	6.100	1991	07	27.04633	BNT	GRB
355.200	25.400	1991	07	28.22105	BNT	GRB
243.600	82.300	1991	07	29.48367	BNT	GRB
249.540	-75.220	1991	07	30.17939	BT	4B910730-
84.000	49.000	1991	07	30.49044	BNT	GRB
132.530	56.130	1991	07	30.59154	BT	4B910730-
313.880	16.930	1991	07	30.93558	BT	4B910730-
187.500	19.900	1991	07	31.09475	BNT	GRB
81.440	-35.840	1991	08	2.03144	BT	4B910802-
199.570	-53.420	1991	08	2.63978	BT	4B910802-
266.900	-28.500	1991	08	3.09449	BNT	GRB
309.710	23.510	1991	08	3.35654	BT	4B910803
15.200	-10.600	1991	08	3.37285	BNT	GRB
313.270	-51.300	1991	08	5.44544	BT	4B910805
61.200	9.100	1991	08	5.71061	BNT	GRB
266.500	72.400	1991	08	5.77021	BNT	GRB
201.400	-55.400	1991	08	6.21873	BNT	GRB
155.660	27.120	1991	08	6.64204	BT	4B910806
257.800	-33.600	1991	08	7.11867	BNT	GRB
153.850	6.490	1991	08	7.30594	BT	4B910807
237.390	38.820	1991	08	9.04058	BT	4B910809-
195.430	19.370	1991	08	9.26042	BT	4B910809-
281.960	64.740	1991	08	9.81650	BT	4B910809-
175.300	-39.000	1991	08	11.60553	BNT	GRB
79.700	-72.160	1991	08	11.60685	BT	4B910811
39.410	-64.490	1991	08	13.56696	BT	4B910813

Continued on next column

Continued from previous column

RA deg	DEC deg	Year	Month	Day	Cat.	GRB Name
58.010	45.220	1991	08	14.46505	BT	4B910814-
60.000	35.300	1991	08	14.48543	BNT	GRB
163.810	-64.630	1991	08	14.58262	BT	4B910814-
346.350	30.430	1991	08	14.80177	BT	4B910814-
142.770	-36.050	1991	08	15.39638	BT	4B910815
313.410	-52.810	1991	08	15.60037	GRA	GRB910815C
183.500	-17.900	1991	08	15.90672	BNT	GRB
50.500	-14.700	1991	08	16.29940	BNT	GRB
221.030	-59.090	1991	08	16.50836	BT	4B910816-
172.600	1.480	1991	08	16.61855	BT	4B910816-
90.110	27.080	1991	08	17.70863	BT	4B910817
289.770	-30.010	1991	08	17.71488	GRA	GRB910817B
268.340	-27.090	1991	08	18.57275	BT	4B910818
173.800	-27.700	1991	08	19.54145	BNT	GRB
184.600	-53.500	1991	08	20.26672	BNT	GRB
311.600	40.000	1991	08	20.40318	BNT	GRB
230.300	-54.100	1991	08	20.90447	BNT	GRB
292.460	-63.520	1991	08	21.07129	BT	4B910821
353.690	-72.320	1991	08	21.44000	GRA	GRB910821B
269.870	43.740	1991	08	22.57707	BT	4B910822
105.650	8.060	1991	08	23.87597	BT	4B910823
69.120	48.510	1991	08	26.84512	BT	4B910826
121.610	-24.340	1991	08	27.31354	BT	4B910827
53.200	7.000	1991	08	27.69213	BNT	GRB
43.370	-32.070	1991	08	28.34514	BT	4B910828
304.000	57.600	1991	08	29.01759	BNT	GRB
59.030	22.960	1991	08	29.94425	BT	4B910829
202.100	14.700	1991	08	30.05958	BNT	GRB
208.180	-16.250	1991	09	1.22516	GRA	GRB910901
220.000	-47.800	1991	09	1.75873	BNT	GRB
117.600	62.900	1991	09	2.18235	BNT	GRB
54.000	7.400	1991	09	2.43345	BNT	GRB
299.080	-7.700	1991	09	2.95527	BT	4B910902
238.340	13.100	1991	09	3.40625	BT	4B910903
354.150	-17.090	1991	09	4.64919	BT	4B910904
0.000	-81.050	1991	09	5.99230	BT	4B910905
136.550	-28.230	1991	09	7.04540	BT	4B910907
147.500	4.300	1991	09	7.07082	BNT	GRB
230.800	-32.000	1991	09	8.39264	BNT	GRB
226.100	-15.530	1991	09	8.45874	BT	4B910908
146.400	-44.900	1991	09	10.15337	BNT	GRB
150.700	30.300	1991	09	10.17068	BNT	GRB
109.610	-10.310	1991	09	12.24736	BT	4B910912
170.800	-37.100	1991	09	12.51164	BNT	GRB
170.310	-33.400	1991	09	14.40275	BT	4B910914
194.200	63.500	1991	09	14.79778	BNT	GRB
181.500	24.500	1991	09	15.93654	BNT	GRB
32.560	-35.650	1991	09	16.68879	BT	4B910916

Continued on next column

Continued from previous column

RA deg	DEC deg	Year	Month	Day	Cat.	GRB Name
298.280	-30.240	1991	09	18.01993	BT	4B910918
170.300	-46.300	1991	09	18.73564	BNT	GRB
148.590	33.210	1991	09	19.95412	BT	4B910919
223.800	33.000	1991	09	20.23037	BNT	GRB
52.530	-22.570	1991	09	23.76627	BT	4B910923
148.300	61.600	1991	09	25.08287	BNT	GRB
265.670	-29.260	1991	09	25.14938	BT	4B910925
157.200	-1.360	1991	09	26.16713	BT	4B910926-
346.070	21.360	1991	09	26.76802	BT	4B910926-
182.050	17.130	1991	09	27.14290	BT	4B910927-
50.160	-39.650	1991	09	27.97700	BT	4B910927-
200.430	54.570	1991	09	28.36825	BT	4B910928-
35.300	-63.200	1991	09	28.66704	BNT	GRB
130.460	33.350	1991	09	28.94985	BT	4B910928-
170.000	75.400	1991	09	29.09532	BNT	GRB
356.560	39.950	1991	09	29.71663	BT	4B910929
93.430	44.510	1991	09	30.30860	BT	4B910930-
131.800	-20.620	1991	09	30.49688	BT	4B910930-
250.750	73.200	1991	10	1.37241	BT	4B911001
358.200	8.600	1991	10	1.45749	BNT	GRB
115.670	-73.690	1991	10	2.37005	BT	4B911002
54.700	-32.300	1991	10	3.97918	BNT	GRB
349.740	62.950	1991	10	4.06053	BT	4B911004
235.800	14.730	1991	10	5.31788	BT	4B911005
82.800	51.800	1991	10	6.24726	BNT	GRB
33.300	-45.440	1991	10	6.37632	BT	4B911006
308.910	40.590	1991	10	7.64733	BT	4B911007
49.700	66.100	1991	10	9.34882	BNT	GRB
192.900	-40.400	1991	10	10.22965	BNT	GRB
113.500	34.600	1991	10	10.46205	BNT	GRB
110.600	-2.400	1991	10	11.88701	BNT	GRB
331.900	30.000	1991	10	12.42764	BNT	GRB
144.500	17.100	1991	10	12.45201	BNT	GRB
117.200	-7.800	1991	10	12.54043	BNT	GRB
317.420	11.990	1991	10	16.24502	BT	4B911016-
300.060	-4.160	1991	10	16.45942	BT	4B911016-
224.500	25.800	1991	10	16.61304	BNT	GRB
325.700	-20.770	1991	10	18.13831	GRA	GRB911018A
285.200	69.200	1991	10	18.60666	BNT	GRB
33.600	21.100	1991	10	18.72041	BNT	GRB
54.000	-46.800	1991	10	19.03203	BNT	GRB
239.190	26.280	1991	10	19.29111	BT	4B911019
96.900	37.600	1991	10	20.34505	BNT	GRB
123.910	70.340	1991	10	22.17636	BT	4B911022
208.650	38.360	1991	10	24.84035	BT	4B911024
209.660	20.160	1991	10	25.07920	BT	4B911025-
316.350	36.660	1991	10	25.89253	BT	4B911025-
74.680	-22.270	1991	10	26.54654	BT	4B911026

Continued on next column

Continued from previous column

RA deg	DEC deg	Year	Month	Day	Cat.	GRB Name
358.180	69.620	1991	10	27.07306	BT	4B911027-
127.220	74.120	1991	10	27.43877	BT	4B911027-
11.300	-18.700	1991	10	29.20200	BNT	GRB
11.400	-70.100	1991	10	29.90839	BNT	GRB
19.900	13.400	1991	10	30.35057	BNT	GRB
284.540	21.340	1991	10	31.40024	BT	4B911031-
298.890	-28.890	1991	10	31.51339	BT	4B911031-
90.000	-56.100	1991	10	31.97986	BNT	GRB
74.530	-48.800	1991	11	1.11729	BT	4B911101
257.600	10.100	1991	11	2.24443	BNT	GRB
212.450	35.030	1991	11	4.62826	BT	4B911104
343.030	-35.160	1991	11	6.15418	BT	4B911106-
62.240	-66.250	1991	11	6.53675	BT	4B911106-
63.100	-34.800	1991	11	7.04809	BNT	GRB
310.500	22.300	1991	11	9.09442	BNT	GRB
112.010	-26.520	1991	11	9.14419	BT	4B911109
349.600	4.000	1991	11	9.17104	BNT	GRB
328.600	-5.900	1991	11	10.22672	BNT	GRB
306.400	14.560	1991	11	10.78916	BT	4B911110
218.090	10.870	1991	11	11.16648	BT	4B911111-
153.300	-10.300	1991	11	11.21818	BNT	GRB
97.500	-35.400	1991	11	11.58110	BNT	GRB
63.970	-51.370	1991	11	11.60925	BT	4B911111-
121.110	-21.280	1991	11	11.93040	BT	4B911111-
5.600	-37.800	1991	11	12.36248	BNT	GRB
340.320	-49.460	1991	11	13.57065	BT	4B911113
255.370	34.230	1991	11	17.05971	BT	4B911117-
225.720	11.200	1991	11	17.19145	BT	4B911117-
280.550	17.600	1991	11	17.61724	BT	4B911117-
167.030	-20.850	1991	11	18.79002	BT	4B911118-
21.900	19.000	1991	11	18.89404	BNT	GRB
253.490	-5.920	1991	11	18.98565	BT	4B911118-
152.500	33.000	1991	11	19.16037	BNT	GRB
261.620	-9.370	1991	11	19.23574	BT	4B911119-
42.430	67.770	1991	11	19.27016	BT	4B911119-
182.500	-44.100	1991	11	19.73972	BNT	GRB
6.690	66.040	1991	11	20.32846	BT	4B911120-
235.110	37.430	1991	11	20.47390	BT	4B911120-
74.300	35.100	1991	11	20.50876	BNT	GRB
280.970	31.080	1991	11	20.93580	BT	4B911120-
153.800	-63.400	1991	11	21.16434	BNT	GRB
82.100	15.700	1991	11	21.80926	BNT	GRB
106.150	-28.370	1991	11	22.63814	BT	4B911122
51.780	75.520	1991	11	23.18366	BT	4B911123-
22.810	30.340	1991	11	23.34413	BT	4B911123-
132.700	14.800	1991	11	23.89683	BNT	GRB
320.920	36.970	1991	11	24.44574	BT	4B911124
183.920	8.240	1991	11	25.95086	BT	4B911125

Continued on next column

Continued from previous column

RA deg	DEC deg	Year	Month	Day	Cat.	GRB Name
159.790	6.930	1991	11	26.53389	BT	4B911126
269.140	49.730	1991	11	27.18204	BT	4B911127-
310.130	24.550	1991	11	27.29259	BT	4B911127-
160.970	-74.590	1991	11	27.96428	BT	4B911127-
338.640	-10.360	1991	11	28.36301	BT	4B911128
326.680	2.490	1991	11	29.41448	BT	4B911129-
40.560	-21.010	1991	11	29.74990	BT	4B911129-
105.700	32.200	1991	11	30.79353	BNT	GRB
182.100	-5.700	1991	12	2.36961	BNT	GRB
172.500	-22.840	1991	12	2.85336	BT	4B911202-
235.880	-0.400	1991	12	2.99411	BT	4B911202-
68.690	-21.600	1991	12	4.72341	BT	4B911204
318.200	-65.100	1991	12	5.00907	BNT	GRB
103.970	-25.850	1991	12	5.96159	BT	4B911205
307.790	29.300	1991	12	7.41024	BT	4B911207
112.680	-21.140	1991	12	8.00400	BT	4B911208-
38.150	-53.110	1991	12	8.87850	BT	4B911208-
61.300	-71.500	1991	12	8.91821	BNT	GRB
74.610	24.160	1991	12	9.03944	BT	4B911209-
144.000	-4.400	1991	12	9.06816	BNT	GRB
46.110	-31.300	1991	12	9.68244	BT	4B911209-
259.980	-45.080	1991	12	9.77498	BT	4B911209-
294.870	-19.400	1991	12	10.87902	BT	4B911210
209.400	-45.740	1991	12	13.85807	BT	4B911213
82.400	-37.800	1991	12	14.75000	BNT	GRB
98.000	6.300	1991	12	16.19000	BNT	GRB
300.200	-16.900	1991	12	16.75160	BNT	GRB
6.960	22.670	1991	12	17.34868	BT	4B911217-
176.700	57.500	1991	12	17.38000	BNT	GRB
10.500	5.000	1991	12	17.87010	BNT	GRB
28.890	0.030	1991	12	17.94442	BT	4B911217-
354.250	-0.160	1991	12	19.37655	BT	4B911219-
218.650	-4.830	1991	12	19.91479	BT	4B911219-
17.000	84.900	1991	12	20.56000	BNT	GRB
146.600	70.500	1991	12	21.59885	BNT	GRB
215.820	-42.720	1991	12	21.91905	BT	4B911221
87.084	14.062	1991	12	22.62512	GRA	GRB911222
61.300	6.200	1991	12	22.66153	BNT	GRB
349.600	63.900	1991	12	22.88000	BNT	GRB
336.990	-50.420	1991	12	23.23400	BT	4B911223
255.940	10.620	1991	12	24.25398	BT	4B911224-
45.430	-10.790	1991	12	24.46039	BT	4B911224-
342.040	-17.710	1991	12	24.64969	BT	4B911224-
146.400	18.400	1991	12	24.69000	BNT	GRB
334.610	26.170	1991	12	25.37888	BT	4B911225-
143.500	32.400	1991	12	25.62000	BNT	GRB
253.310	-34.100	1991	12	25.71432	BT	4B911225-
111.290	-29.460	1991	12	26.15047	BT	4B911226

Continued on next column

Continued from previous column

RA deg	DEC deg	Year	Month	Day	Cat.	GRB Name
350.440	-68.250	1991	12	27.04575	BT	4B911227
280.190	43.690	1991	12	28.72368	BT	4B911228
139.200	10.200	1991	12	28.81000	BNT	GRB
147.800	-25.200	1992	01	5.35482	BNT	GRB
335.400	-53.800	1992	01	5.73700	BT	4B920105
93.600	50.400	1992	01	6.70567	BNT	GRB
213.200	-17.900	1992	01	7.88000	BNT	GRB
345.500	33.800	1992	01	9.26975	BNT	GRB
58.080	-20.800	1992	01	10.38748	BT	4B920110-
159.880	3.240	1992	01	10.46124	BT	4B920110-
357.710	10.550	1992	01	10.93170	BT	4B920110-
131.100	12.300	1992	01	11.41549	BNT	GRB
227.500	12.500	1992	01	12.36242	BNT	GRB
91.750	74.160	1992	01	13.86966	BT	4B920113
244.130	63.890	1992	01	14.72484	BT	4B920114
243.000	-6.200	1992	01	14.85455	BNT	GRB
140.240	11.780	1992	01	16.12104	BT	4B920116-
152.790	-81.320	1992	01	16.77124	BT	4B920116-
351.300	-1.600	1992	01	16.99475	BNT	GRB
52.200	-45.800	1992	01	17.44000	BNT	GRB
51.400	69.400	1992	01	19.30668	BNT	GRB
175.600	-10.800	1992	01	20.00000	BNT	GRB
300.310	-82.750	1992	01	20.93796	BT	4B920120
262.840	-57.730	1992	01	21.18958	BT	4B920121-
144.900	-0.100	1992	01	21.56000	BNT	GRB
30.430	28.560	1992	01	21.91446	BT	4B920121-
69.500	13.500	1992	01	22.10582	BNT	GRB
61.330	47.360	1992	01	22.39101	BT	4B920122
16.800	15.500	1992	01	23.25000	BNT	GRB
84.750	14.250	1992	01	23.48258	BT	4B920123
44.300	-47.200	1992	01	26.25000	BNT	GRB
322.370	-29.260	1992	01	27.89371	BT	4B920127
160.300	-28.900	1992	01	28.12000	BNT	GRB
96.730	15.710	1992	01	28.13296	BT	4B920128
7.300	-3.700	1992	01	28.94000	BNT	GRB
7.750	-51.060	1992	01	30.02057	BT	4B920130-
222.800	-25.500	1992	01	30.56000	BNT	GRB
54.590	-3.220	1992	01	30.95141	BT	4B920130-
43.600	17.800	1992	01	31.92899	BNT	GRB
344.300	51.300	1992	01	31.96097	BNT	GRB
308.400	85.600	1992	02	2.81000	BNT	GRB
269.740	-15.260	1992	02	3.65056	BT	4B920203
27.300	39.800	1992	02	3.95875	BNT	GRB
39.390	-15.830	1992	02	5.62814	BT	4B920205
295.540	30.380	1992	02	7.07247	BT	4B920207
329.660	-11.830	1992	02	9.68160	BT	4B920209-
288.230	60.750	1992	02	9.90330	BT	4B920209-
318.780	-40.430	1992	02	10.09439	BT	4B920210-

Continued on next column

Continued from previous column

RA deg	DEC deg	Year	Month	Day	Cat.	GRB Name
150.970	48.360	1992	02	10.41231	BT	4B920210-
326.880	21.350	1992	02	10.95297	BT	4B920210-
38.190	14.100	1992	02	12.17623	BT	4B920212
39.670	7.130	1992	02	14.71948	BT	4B920214
122.900	-17.100	1992	02	15.00000	BNT	GRB
264.100	-39.300	1992	02	15.81000	BNT	GRB
250.500	22.700	1992	02	15.88000	BNT	GRB
233.500	23.400	1992	02	16.50000	BNT	GRB
340.710	48.650	1992	02	16.57144	BT	4B920216-
322.900	18.200	1992	02	16.69000	BNT	GRB
156.920	1.170	1992	02	16.92940	BT	4B920216-
122.900	6.100	1992	02	17.16579	BNT	GRB
132.550	-29.580	1992	02	18.27875	BT	4B920218-
140.420	52.960	1992	02	18.46056	BT	4B920218-
39.470	27.470	1992	02	18.77943	BT	4B920218-
275.100	27.100	1992	02	19.12000	BNT	GRB
343.660	4.380	1992	02	20.54204	BT	4B920220
184.140	48.480	1992	02	21.26009	BT	4B920221
257.720	-51.590	1992	02	22.37869	BT	4B920222
169.650	-66.780	1992	02	24.11365	BT	4B920224-
161.790	27.470	1992	02	24.90140	BT	4B920224-
6.500	-48.000	1992	02	25.12000	BNT	GRB
100.060	50.630	1992	02	26.32927	BT	4B920226-
271.250	17.460	1992	02	26.34407	BT	4B920226-
68.360	66.840	1992	02	27.25059	BT	4B920227-
129.600	-32.500	1992	02	27.39012	BNT	GRB
201.300	-5.800	1992	02	27.56000	BNT	GRB
241.010	10.650	1992	02	27.74046	BT	4B920227-
202.280	50.560	1992	02	27.86806	BT	4B920227-
147.940	25.060	1992	02	28.62439	BT	4B920228
333.670	-5.250	1992	02	29.62787	BT	4B920229-
191.360	-51.060	1992	02	29.80645	BT	4B920229-
185.400	-51.300	1992	02	29.81000	BNT	GRB
344.180	16.830	1992	03	1.48220	BT	4B920301
115.280	-58.920	1992	03	2.01023	BT	4B920302-
341.930	20.670	1992	03	2.26140	BT	4B920302-
318.400	-10.900	1992	03	3.31000	BNT	GRB
161.030	46.960	1992	03	3.32743	BT	4B920303-
269.660	-18.710	1992	03	3.98124	BT	4B920303-
264.600	59.650	1992	03	5.04215	BT	4B920305-
247.670	-62.140	1992	03	5.40828	BT	4B920305-
134.380	80.520	1992	03	5.41868	BT	4B920305-
284.600	5.800	1992	03	6.19000	BNT	GRB
355.570	-45.150	1992	03	7.01255	BT	4B920307
143.500	-59.800	1992	03	7.69000	BNT	GRB
84.440	65.250	1992	03	8.20538	BT	4B920308-
251.470	43.500	1992	03	8.73176	BT	4B920308-
105.850	-5.910	1992	03	10.58558	BT	4B920310

Continued on next column

Continued from previous column

RA deg	DEC deg	Year	Month	Day	Cat.	GRB Name
129.760	-36.570	1992	03	11.09750	BT	4B920311
102.600	-66.750	1992	03	14.22266	BT	4B920314-
240.750	-4.560	1992	03	14.25171	BT	4B920314-
0.000	-60.480	1992	03	14.40407	BT	4B920314-
124.800	-41.800	1992	03	14.62547	BNT	GRB
264.620	29.160	1992	03	14.72325	BT	4B920314-
349.400	-58.800	1992	03	14.75000	BNT	GRB
320.580	-20.890	1992	03	15.18017	BT	4B920315-
202.010	-29.980	1992	03	15.47123	BT	4B920315-
131.440	28.730	1992	03	17.70515	BT	4B920317
254.500	-26.310	1992	03	18.45641	BT	4B920318-
194.970	27.730	1992	03	18.62984	BT	4B920318-
35.700	-26.500	1992	03	19.06000	BNT	GRB
39.350	-45.880	1992	03	20.42310	BT	4B920320-
323.870	57.810	1992	03	20.51318	BT	4B920320-
218.200	-4.700	1992	03	21.19000	BNT	GRB
181.610	-1.970	1992	03	21.51968	BT	4B920321-
233.000	31.830	1992	03	21.54223	GRA	GRB920321C
226.400	45.800	1992	03	21.56000	BNT	GRB
198.840	-34.350	1992	03	21.98264	BT	4B920321-
337.890	-34.660	1992	03	23.73537	BT	4B920323
158.950	-39.660	1992	03	24.87115	BT	4B920324
351.400	24.100	1992	03	25.46995	BNT	GRB
293.700	-48.680	1992	03	25.54037	BT	4B920325-
351.570	12.940	1992	03	25.72056	BT	4B920325-
341.600	-14.100	1992	03	25.84375	BNT	GRB
315.140	-4.300	1992	03	28.88875	BT	4B920328
18.210	-54.770	1992	03	29.69336	BT	4B920329
347.120	-33.490	1992	03	30.43964	BT	4B920330
7.900	30.300	1992	03	30.47319	BNT	GRB
73.800	17.400	1992	03	30.81000	BNT	GRB
27.520	57.680	1992	03	31.60569	BT	4B920331-
264.300	30.550	1992	03	31.76097	BT	4B920331-
94.500	58.300	1992	04	1.38000	BNT	GRB
306.100	12.100	1992	04	2.06000	BNT	GRB
323.780	23.880	1992	04	4.54981	BT	4B920404
357.000	34.130	1992	04	5.90383	BT	4B920405
289.910	-57.690	1992	04	6.11405	BT	4B920406
341.440	-10.680	1992	04	7.50255	BT	4B920407
235.600	71.300	1992	04	7.51448	BNT	GRB
154.480	-55.460	1992	04	8.45631	BT	4B920408-
138.960	40.830	1992	04	8.50412	BT	4B920408-
306.690	33.880	1992	04	8.73177	BT	4B920408-
244.970	71.000	1992	04	9.18192	BT	4B920409
278.970	68.980	1992	04	11.41428	BT	4B920411-
339.720	-28.420	1992	04	11.52425	BT	4B920411-
272.500	-57.200	1992	04	11.81000	BNT	GRB
231.320	-6.140	1992	04	12.83478	BT	4B920412

Continued on next column

Continued from previous column

RA deg	DEC deg	Year	Month	Day	Cat.	GRB Name
109.730	-48.890	1992	04	13.95523	BT	4B920413
300.000	-65.150	1992	04	14.77635	BT	4B920414-
112.500	-73.720	1992	04	14.97410	BT	4B920414-
238.900	-37.000	1992	04	17.81000	BNT	GRB
88.800	-27.000	1992	04	18.22356	BNT	GRB
156.970	66.880	1992	04	18.92147	BT	4B920418
149.720	-18.250	1992	04	19.45463	BT	4B920419-
231.200	-26.900	1992	04	19.69204	BNT	GRB
85.520	63.290	1992	04	19.83804	BT	4B920419-
320.510	13.450	1992	04	20.28638	BT	4B920420
5.960	53.160	1992	04	23.73638	BT	4B920423-
305.100	53.400	1992	04	23.88000	BNT	GRB
153.900	22.160	1992	04	23.92131	BT	4B920423-
346.350	32.100	1992	04	24.59733	BT	4B920424
269.600	7.600	1992	04	24.69000	BNT	GRB
335.300	-13.300	1992	04	25.56000	BNT	GRB
303.390	-35.980	1992	04	28.47071	BT	4B920428
190.800	51.700	1992	04	28.62000	BNT	GRB
179.080	-14.330	1992	04	29.79134	BT	4B920429
227.960	-73.510	1992	04	30.36418	BT	4B920430-
356.000	-10.600	1992	04	30.38000	BNT	GRB
37.610	-8.220	1992	04	30.66865	BT	4B920430-
123.430	-35.000	1992	05	1.88767	BT	4B920501
33.050	-17.730	1992	05	2.25207	BT	4B920502-
154.820	45.420	1992	05	2.72685	BT	4B920502-
131.990	-84.960	1992	05	2.79519	BT	4B920502-
146.760	41.980	1992	05	3.11839	BT	4B920503-
11.100	64.400	1992	05	3.19000	BNT	GRB
206.000	75.900	1992	05	3.36561	BT	4B920503-
45.370	69.940	1992	05	5.91308	BT	4B920505
271.570	-11.580	1992	05	7.05902	BT	4B920507
6.190	0.970	1992	05	8.16557	BT	4B920508
107.800	-26.200	1992	05	9.06000	BNT	GRB
212.700	74.600	1992	05	9.31000	BNT	GRB
341.220	-82.430	1992	05	9.47170	BT	4B920509
188.300	-16.000	1992	05	10.19000	BNT	GRB
125.040	-48.960	1992	05	11.26904	BT	4B920511-
63.100	-47.600	1992	05	11.81000	BNT	GRB
65.030	-45.600	1992	05	11.85944	BT	4B920511-
24.330	-37.010	1992	05	11.93648	BT	4B920511-
127.300	-18.800	1992	05	13.44000	BNT	GRB
211.160	-44.770	1992	05	13.70346	BT	4B920513
45.700	34.100	1992	05	14.81000	BNT	GRB
254.700	49.100	1992	05	14.81000	BNT	GRB
36.940	-82.840	1992	05	17.02405	BT	4B920517-
204.100	-16.470	1992	05	17.13744	BT	4B920517-
196.930	57.920	1992	05	17.60010	BT	4B920517-
247.300	33.900	1992	05	18.21946	BT	4B920518

Continued on next column

Continued from previous column

RA deg	DEC deg	Year	Month	Day	Cat.	GRB Name
163.700	30.900	1992	05	18.25000	BNT	GRB
34.000	17.800	1992	05	18.31000	BNT	GRB
292.100	13.300	1992	05	18.69000	BNT	GRB
355.240	-36.080	1992	05	19.02455	BT	4B920519-
319.940	44.170	1992	05	19.68882	BT	4B920519-
190.030	-51.940	1992	05	20.32012	BT	4B920520-
308.130	-8.600	1992	05	20.39667	BT	4B920520-
131.950	40.810	1992	05	21.13307	BT	4B920521
245.300	20.100	1992	05	21.25000	BNT	GRB
157.520	29.220	1992	05	24.16090	BT	4B920524
229.210	37.330	1992	05	25.02898	BT	4B920525-
299.630	-42.050	1992	05	25.14377	BT	4B920525-
14.650	-67.130	1992	05	25.30268	BT	4B920525-
104.490	39.310	1992	05	26.09880	BT	4B920526
162.680	18.130	1992	05	30.95827	BT	4B920530
86.840	-23.680	1992	05	31.67387	BT	4B920531
315.800	-38.200	1992	06	1.30855	BNT	GRB
4.700	-33.900	1992	06	2.25000	BNT	GRB
244.700	-4.900	1992	06	4.69000	BNT	GRB
289.640	-41.700	1992	06	5.71238	BT	4B920605
85.900	61.900	1992	06	5.81000	BNT	GRB
119.000	-34.000	1992	06	6.69000	BNT	GRB
335.720	-73.720	1992	06	6.86968	BT	4B920606
284.730	5.940	1992	06	7.82957	BT	4B920607
21.790	5.720	1992	06	8.60149	BT	4B920608
196.580	-5.580	1992	06	9.35150	BT	4B920609-
260.130	-72.080	1992	06	9.75824	BT	4B920609-
147.830	-17.810	1992	06	10.04993	BT	4B920610
312.910	-55.640	1992	06	13.60536	BT	4B920613-
352.550	-62.600	1992	06	13.85230	BT	4B920613-
258.360	-16.500	1992	06	15.25870	BT	4B920615-
309.400	62.800	1992	06	15.38000	BNT	GRB
353.290	-32.840	1992	06	15.41190	BT	4B920615-
16.650	24.230	1992	06	15.60066	BT	4B920615-
100.690	-64.520	1992	06	17.15588	BT	4B920617-
70.600	39.600	1992	06	17.19000	BNT	GRB
37.660	77.510	1992	06	17.22698	BT	4B920617-
19.040	21.470	1992	06	17.78047	BT	4B920617-
26.600	79.000	1992	06	17.88000	BNT	GRB
316.000	-46.070	1992	06	18.90981	BT	4B920618
96.000	2.000	1992	06	19.25000	BNT	GRB
140.170	-64.710	1992	06	19.35627	BT	4B920619-
185.200	-3.300	1992	06	19.38000	BNT	GRB
155.280	22.470	1992	06	19.54441	BT	4B920619-
133.500	-59.900	1992	06	19.56000	BNT	GRB
282.800	18.300	1992	06	19.74845	BNT	GRB
252.600	24.300	1992	06	19.75000	BNT	GRB
88.990	-43.420	1992	06	20.75918	BT	4B920620-

Continued on next column

Continued from previous column

RA deg	DEC deg	Year	Month	Day	Cat.	GRB Name
4.850	-0.360	1992	06	20.78961	BT	4B920620-
162.130	10.030	1992	06	20.95375	BT	4B920620-
41.400	-2.500	1992	06	21.81000	BNT	GRB
147.100	-39.400	1992	06	22.25000	BNT	GRB
54.160	-61.820	1992	06	22.26948	BT	4B920622-
162.100	47.170	1992	06	22.29519	BT	4B920622-
138.200	53.300	1992	06	22.31000	BNT	GRB
346.810	10.010	1992	06	22.53774	BT	4B920622-
159.530	-56.320	1992	06	22.67177	BT	4B920622-
67.550	3.050	1992	06	24.18862	BT	4B920624
173.000	33.200	1992	06	25.12000	BNT	GRB
1.000	50.900	1992	06	26.75000	BNT	GRB
136.900	6.000	1992	06	26.94000	BNT	GRB
212.600	-26.280	1992	06	27.42968	BT	4B920627-
166.020	-2.580	1992	06	27.54347	BT	4B920627-
296.300	66.850	1992	06	28.37617	BT	4B920628-
317.790	-27.320	1992	06	28.87341	BT	4B920628-
249.630	-26.140	1992	06	29.37979	BT	4B920629
357.780	13.200	1992	06	30.22497	BT	4B920630
314.640	33.440	1992	07	1.81829	BT	4B920701
276.640	-22.060	1992	07	7.04745	BT	4B920707
308.340	-49.910	1992	07	8.55787	BT	4B920708
337.600	-8.230	1992	07	10.00912	BT	4B920710-
53.850	17.340	1992	07	10.92598	BT	4B920710-
93.720	-7.550	1992	07	11.43626	BT	4B920711-
240.100	-53.300	1992	07	11.50000	BNT	GRB
276.540	73.380	1992	07	11.67293	BT	4B920711-
189.070	1.010	1992	07	14.21284	BT	4B920714-
215.480	-36.440	1992	07	14.54478	BT	4B920714-
140.360	-44.640	1992	07	14.84962	BT	4B920714-
285.770	53.740	1992	07	15.53573	BT	4B920715
221.800	49.800	1992	07	16.42671	BNT	GRB
326.840	-23.330	1992	07	17.28012	BT	4B920717-
20.750	-2.320	1992	07	17.65775	BT	4B920717-
159.300	-71.600	1992	07	17.69000	BNT	GRB
22.440	-3.980	1992	07	18.61154	BT	4B920718-
296.390	-55.980	1992	07	18.89772	BT	4B920718-
255.900	-52.400	1992	07	19.69000	BNT	GRB
203.020	36.870	1992	07	20.13338	BT	4B920720-
144.740	-10.300	1992	07	20.24506	BT	4B920720-
258.400	-65.770	1992	07	20.31464	BT	4B920720-
153.090	25.190	1992	07	21.06393	BT	4B920721-
19.920	-13.400	1992	07	21.12051	BT	4B920721-
331.700	51.200	1992	07	21.25000	BNT	GRB
0.640	-28.180	1992	07	21.26413	BT	4B920721-
37.550	33.490	1992	07	21.76236	BT	4B920721-
309.300	58.300	1992	07	22.75000	BNT	GRB
321.190	36.750	1992	07	22.88990	BT	4B920722

Continued on next column

Continued from previous column

RA deg	DEC deg	Year	Month	Day	Cat.	GRB Name
85.790	7.780	1992	07	23.04207	BT	4B920723-
268.290	-1.730	1992	07	23.54460	BT	4B920723-
287.080	27.330	1992	07	23.83552	GRA	GRB920723C
117.530	14.360	1992	07	24.71471	BT	4B920724
345.000	-49.300	1992	07	25.99999	BNT	GRB
180.100	-7.700	1992	07	27.00000	BNT	GRB
324.530	16.430	1992	07	27.49937	BT	4B920727
113.400	9.500	1992	07	27.69000	BNT	GRB
320.650	28.130	1992	07	28.48281	BT	4B920728
22.100	33.900	1992	07	30.54264	BT	4B920730-
241.670	-10.700	1992	07	30.89692	BT	4B920730-
202.410	79.080	1992	07	31.78559	BT	4B920731
157.860	68.900	1992	08	1.05324	BT	4B920801
101.350	-48.260	1992	08	2.19125	BT	4B920802
179.200	-52.400	1992	08	2.75000	BNT	GRB
222.850	30.970	1992	08	3.09032	BT	4B920803-
134.710	-36.120	1992	08	3.70399	BT	4B920803-
15.800	68.400	1992	08	3.94000	BNT	GRB
68.240	5.880	1992	08	4.69367	BT	4B920804-
286.400	50.690	1992	08	4.82873	BT	4B920804-
170.440	49.830	1992	08	4.95781	BT	4B920804-
187.300	30.100	1992	08	5.25000	BNT	GRB
105.580	22.930	1992	08	5.46799	BT	4B920805
125.000	1.700	1992	08	5.72609	BNT	GRB
284.740	-10.680	1992	08	6.75646	BT	4B920806
262.140	-5.780	1992	08	8.16353	BT	4B920808
128.800	-35.400	1992	08	8.75000	BNT	GRB
280.070	59.480	1992	08	11.11803	BT	4B920811-
101.330	16.830	1992	08	11.22076	BT	4B920811-
118.960	-3.970	1992	08	12.23156	BT	4B920812-
115.220	-37.910	1992	08	12.87463	BT	4B920812-
206.220	-28.340	1992	08	13.14848	BT	4B920813
258.680	-44.630	1992	08	14.25688	BT	4B920814-
226.620	-11.650	1992	08	14.55906	BT	4B920814-
241.710	66.160	1992	08	16.30251	BT	4B920816
324.500	-6.400	1992	08	18.38000	BNT	GRB
43.860	-24.980	1992	08	18.59007	BT	4B920818
356.800	28.400	1992	08	21.38000	BNT	GRB
354.500	-69.900	1992	08	24.00000	BNT	GRB
228.590	-51.790	1992	08	24.45351	BT	4B920824
165.600	23.200	1992	08	26.69000	BNT	GRB
354.500	-35.500	1992	08	29.34137	BNT	GRB
182.270	14.030	1992	08	29.50810	BT	4B920829
258.530	-73.990	1992	08	30.07313	BT	4B920830
261.650	16.060	1992	09	1.25435	BT	4B920901
239.700	0.300	1992	09	1.62000	BNT	GRB
279.150	-20.700	1992	09	2.02009	BT	4B920902-
52.580	-76.650	1992	09	2.76560	BT	4B920902-

Continued on next column

Continued from previous column

RA deg	DEC deg	Year	Month	Day	Cat.	GRB Name
61.970	-68.370	1992	09	3.03422	BT	4B920903
299.100	28.800	1992	09	3.06630	BNT	GRB
301.540	22.590	1992	09	3.97848	GRA	GRB920903C
215.800	34.700	1992	09	4.12000	BNT	GRB
126.600	-12.200	1992	09	6.09201	BNT	GRB
79.400	18.900	1992	09	7.31000	BNT	GRB
145.600	57.700	1992	09	7.69000	BNT	GRB
101.460	-20.720	1992	09	8.34844	BT	4B920908
140.000	-36.300	1992	09	8.79705	BNT	GRB
239.800	-51.700	1992	09	9.69000	BNT	GRB
33.500	41.600	1992	09	10.30564	BNT	GRB
256.110	-13.720	1992	09	12.19522	BT	4B920912
61.200	38.300	1992	09	12.56000	BNT	GRB
351.580	53.610	1992	09	13.16321	BT	4B920913
122.900	37.200	1992	09	13.87469	BNT	GRB
260.400	-34.600	1992	09	14.38000	BNT	GRB
205.000	25.300	1992	09	16.19000	BNT	GRB
14.390	47.540	1992	09	17.48296	BT	4B920917
188.600	-44.700	1992	09	20.05110	BNT	GRB
150.570	20.010	1992	09	20.05115	BT	4B920920
121.800	30.800	1992	09	20.88000	BNT	GRB
161.700	-0.800	1992	09	23.28560	BNT	GRB
338.100	-20.700	1992	09	24.38000	BNT	GRB
126.680	-68.740	1992	09	24.75763	BT	4B920924
129.720	-58.690	1992	09	25.36851	BT	4B920925-
201.110	42.200	1992	09	25.85465	GRA	GRB920925B
129.510	28.820	1992	09	25.86475	GRA	GRB920925C
160.260	67.380	1992	09	25.90644	BT	4B920925-
330.700	24.440	1992	09	25.94877	GRA	GRB920925E
322.770	9.380	1992	09	28.74397	BT	4B920928
297.100	-50.900	1992	09	30.19000	BNT	GRB
324.430	32.280	1992	10	1.16937	BT	4B921001-
238.730	-7.430	1992	10	1.29839	BT	4B921001-
1.000	-46.600	1992	10	2.19000	BNT	GRB
133.650	0.980	1992	10	2.47874	BT	4B921002-
231.950	11.980	1992	10	2.99376	BT	4B921002-
150.320	-14.710	1992	10	3.27477	BT	4B921003-
85.420	14.620	1992	10	3.94580	BT	4B921003-
52.100	-3.200	1992	10	4.50000	BNT	GRB
209.110	6.870	1992	10	4.78382	BT	4B921004
321.300	21.600	1992	10	7.06000	BNT	GRB
59.400	29.500	1992	10	8.12000	BNT	GRB
9.100	64.300	1992	10	8.81000	BNT	GRB
257.610	87.180	1992	10	8.88029	BT	4B921008
120.410	-29.100	1992	10	9.27860	BT	4B921009
323.550	55.550	1992	10	11.39823	BT	4B921011
115.800	8.800	1992	10	12.05726	BNT	GRB
312.800	26.600	1992	10	13.38000	BNT	GRB

Continued on next column

Continued from previous column

RA deg	DEC deg	Year	Month	Day	Cat.	GRB Name
87.260	1.530	1992	10	13.85593	BT	4B921013
117.710	33.410	1992	10	13.95882	GRA	GRB921013C
123.040	41.690	1992	10	15.06704	BT	4B921015
122.500	-18.300	1992	10	16.81596	BNT	GRB
198.490	-17.230	1992	10	17.99668	BT	4B921017
186.350	52.410	1992	10	18.38153	BT	4B921018
249.200	-63.700	1992	10	18.88000	BNT	GRB
241.050	36.240	1992	10	21.76440	BT	4B921021
200.150	-55.300	1992	10	22.20542	BT	4B921022-
253.780	-12.420	1992	10	22.63957	BT	4B921022-
108.170	45.030	1992	10	22.93639	BT	4B921022-
122.900	-81.100	1992	10	23.10612	BNT	GRB
256.500	26.000	1992	10	23.12000	BNT	GRB
224.440	19.270	1992	10	23.43517	BT	4B921023-
136.620	-33.950	1992	10	23.80191	BT	4B921023-
181.780	-70.900	1992	10	24.98594	BT	4B921024
98.900	-24.300	1992	10	25.56000	BNT	GRB
345.153	5.208	1992	10	25.58032	GRA	GRB921025A
250.000	-27.400	1992	10	25.69000	BNT	GRB
294.900	46.500	1992	10	25.99103	BNT	GRB
189.300	24.400	1992	10	26.00000	BNT	GRB
193.400	19.000	1992	10	26.00000	BNT	GRB
44.300	-55.200	1992	10	26.31000	BNT	GRB
56.000	41.600	1992	10	27.44246	BNT	GRB
212.200	-7.700	1992	10	27.94000	BNT	GRB
92.400	39.200	1992	10	28.75000	BNT	GRB
72.600	64.300	1992	10	29.50000	BNT	GRB
34.140	-1.570	1992	10	29.52634	BT	4B921029-
128.610	63.810	1992	10	29.76172	BT	4B921029-
86.160	6.860	1992	10	30.05314	BT	4B921030-
141.780	64.510	1992	10	30.98517	BT	4B921030-
204.970	17.330	1992	10	31.17308	BT	4B921031-
294.540	12.710	1992	10	31.75007	BT	4B921031-
324.620	47.360	1992	11	1.75273	BT	4B921101
218.300	-9.070	1992	11	2.39117	BT	4B921102-
218.080	-25.670	1992	11	2.65773	BT	4B921102-
134.420	-30.760	1992	11	2.95843	BT	4B921102-
86.300	73.400	1992	11	4.00000	BNT	GRB
96.600	4.300	1992	11	4.50000	BNT	GRB
158.300	-8.900	1992	11	5.25000	BNT	GRB
57.000	43.100	1992	11	7.55948	BNT	GRB
111.250	39.430	1992	11	8.38168	BT	4B921108
230.000	48.400	1992	11	9.25000	BNT	GRB
98.900	16.000	1992	11	9.79039	BNT	GRB
213.460	-33.070	1992	11	9.81955	BT	4B921109
33.570	-27.860	1992	11	10.11561	BT	4B921110-
155.340	17.190	1992	11	10.39436	BT	4B921110-
165.200	-74.500	1992	11	10.56000	BNT	GRB

Continued on next column

Continued from previous column

RA deg	DEC deg	Year	Month	Day	Cat.	GRB Name
59.890	33.810	1992	11	10.56874	BT	4B921110-
223.600	42.400	1992	11	11.19000	BNT	GRB
303.800	58.920	1992	11	11.27157	BT	4B921111-
51.920	-39.540	1992	11	11.39108	BT	4B921111-
292.900	8.400	1992	11	11.56000	BNT	GRB
170.530	-66.230	1992	11	12.23146	BT	4B921112-
288.690	-45.720	1992	11	12.39315	BT	4B921112-
76.940	-88.950	1992	11	12.53205	BT	4B921112-
124.400	26.800	1992	11	12.62000	BNT	GRB
77.980	30.210	1992	11	12.68627	BT	4B921112-
151.560	81.290	1992	11	13.01767	BT	4B921113
82.600	-30.100	1992	11	14.46609	BNT	GRB
306.440	-48.310	1992	11	15.82602	BT	4B921115
222.000	-5.100	1992	11	15.88000	BNT	GRB
20.500	-10.500	1992	11	16.50000	BNT	GRB
48.770	29.130	1992	11	17.14187	BT	4B921117
350.450	50.320	1992	11	18.92481	BT	4B921118
124.200	-18.500	1992	11	20.38000	BNT	GRB
307.000	-27.800	1992	11	22.31000	BNT	GRB
334.240	-53.250	1992	11	23.26287	BT	4B921123-
163.690	-33.580	1992	11	23.53917	BT	4B921123-
218.000	13.400	1992	11	23.62000	BNT	GRB
140.600	2.500	1992	11	24.06000	BNT	GRB
178.100	62.400	1992	11	25.38000	BNT	GRB
129.030	-63.150	1992	11	27.00564	BT	4B921127
22.100	-31.800	1992	11	27.56000	BNT	GRB
241.500	40.500	1992	11	28.12000	BNT	GRB
294.510	-38.960	1992	11	28.43394	BT	4B921128
353.300	-36.200	1992	11	28.81000	BNT	GRB
189.850	67.930	1992	12	2.25863	BT	4B921202
28.300	38.100	1992	12	2.56000	BNT	GRB
233.620	21.030	1992	12	3.90582	BT	4B921203
339.120	5.800	1992	12	5.02255	BT	4B921205
213.700	-21.400	1992	12	5.05512	BNT	GRB
114.700	-8.700	1992	12	6.50000	BNT	GRB
314.220	62.020	1992	12	6.73252	BT	4B921206-
176.480	45.720	1992	12	6.76689	BT	4B921206-
357.700	26.910	1992	12	7.04540	BT	4B921207-
306.330	-42.930	1992	12	7.66722	BT	4B921207-
7.440	55.750	1992	12	8.47192	BT	4B921208
143.700	-39.600	1992	12	8.62000	BNT	GRB
172.980	61.450	1992	12	9.11177	BT	4B921209-
69.600	-53.700	1992	12	9.31000	BNT	GRB
332.970	-52.020	1992	12	9.48309	BT	4B921209-
38.700	-42.000	1992	12	11.31000	BNT	GRB
18.390	47.470	1992	12	11.60455	BT	4B921211
302.400	25.700	1992	12	12.19000	BNT	GRB
20.500	-17.500	1992	12	13.62000	BNT	GRB

Continued on next column

Continued from previous column

RA deg	DEC deg	Year	Month	Day	Cat.	GRB Name
306.220	44.120	1992	12	14.58756	BT	4B921214
161.480	22.440	1992	12	16.35498	BT	4B921216
88.890	21.240	1992	12	17.81568	BT	4B921217
355.620	-55.310	1992	12	18.10420	BT	4B921218
231.800	24.600	1992	12	18.19000	BNT	GRB
335.980	-31.460	1992	12	19.56971	BT	4B921219
223.880	31.990	1992	12	20.05521	BT	4B921220
85.680	-15.640	1992	12	22.85617	BT	4B921222
195.300	61.000	1992	12	23.12949	BNT	GRB
206.330	-25.650	1992	12	27.53065	BT	4B921227
263.190	-55.670	1992	12	28.03288	BT	4B921228-
67.670	-57.710	1992	12	28.59710	BT	4B921228-
97.900	10.300	1992	12	28.62000	BNT	GRB
19.520	17.210	1992	12	30.37351	BT	4B921230-
150.540	28.630	1992	12	30.58734	BT	4B921230-
221.860	34.160	1992	12	30.65350	BT	4B921230-
303.600	-48.500	1993	01	2.31000	BNT	GRB
220.540	10.460	1993	01	2.46943	BT	4B930102
199.900	0.260	1993	01	3.05243	BT	4B930103-
198.660	25.220	1993	01	3.15987	BT	4B930103-
345.200	41.600	1993	01	3.38000	BNT	GRB
85.840	37.260	1993	01	4.04169	BT	4B930104-
312.270	29.110	1993	01	4.46096	BT	4B930104-
13.600	-68.300	1993	01	6.30795	BNT	GRB
199.460	-15.430	1993	01	6.40677	BT	4B930106-
252.710	70.520	1993	01	6.58084	BT	4B930106-
172.200	5.100	1993	01	6.62000	BNT	GRB
6.080	2.000	1993	01	6.65115	BT	4B930106-
124.790	-32.620	1993	01	6.83142	BT	4B930106-
94.620	-30.440	1993	01	8.10341	BT	4B930108
173.000	8.100	1993	01	8.31000	BNT	GRB
77.120	26.020	1993	01	9.43729	BT	4B930109
99.840	1.710	1993	01	10.07753	BT	4B930110-
239.920	28.800	1993	01	10.26567	BT	4B930110-
294.700	47.100	1993	01	10.81000	BNT	GRB
15.100	16.300	1993	01	11.36787	BNT	GRB
226.320	27.740	1993	01	12.15800	BT	4B930112-
210.100	51.920	1993	01	12.63752	BT	4B930112-
328.320	9.540	1993	01	13.00627	BT	4B930113-
341.750	-40.620	1993	01	13.25399	BT	4B930113-
42.110	84.410	1993	01	13.64652	BT	4B930113-
283.660	60.030	1993	01	14.03115	BT	4B930114-
90.990	-21.230	1993	01	14.18536	BT	4B930114-
246.990	15.910	1993	01	16.11600	BT	4B930116
219.200	-32.600	1993	01	18.75000	BNT	GRB
261.310	14.740	1993	01	20.98032	BT	4B930120
8.480	-20.810	1993	01	21.38692	BT	4B930121-
23.630	11.560	1993	01	21.50847	BT	4B930121-

Continued on next column

Continued from previous column

RA deg	DEC deg	Year	Month	Day	Cat.	GRB Name
290.100	44.600	1993	01	21.81346	BNT	GRB
59.500	-11.930	1993	01	22.51480	BT	4B930122
60.390	38.340	1993	01	23.78149	BT	4B930123
63.100	5.500	1993	01	23.98714	BNT	GRB
287.290	-79.450	1993	01	24.76178	BT	4B930124
139.380	-57.800	1993	01	25.86506	BT	4B930125
359.250	50.260	1993	01	26.47410	BT	4B930126
245.300	-19.960	1993	01	27.01994	BT	4B930127-
310.950	-39.630	1993	01	27.67669	BT	4B930127-
10.830	-9.990	1993	01	28.45977	BT	4B930128
182.040	-8.240	1993	01	31.78972	BT	4B930131-
79.830	-2.600	1993	01	31.88277	BT	4B930131-
95.500	-13.790	1993	02	1.36622	BT	4B930201-
188.790	84.740	1993	02	1.57745	BT	4B930201-
333.530	41.150	1993	02	1.69579	BT	4B930201-
356.100	-2.600	1993	02	2.72308	BNT	GRB
318.990	71.460	1993	02	3.04366	BT	4B930203-
150.840	68.810	1993	02	3.42748	BT	4B930203-
227.430	2.500	1993	02	3.47395	BT	4B930203-
121.640	64.830	1993	02	4.52536	BT	4B930204-
148.420	-48.750	1993	02	4.93947	BT	4B930204-
278.000	-45.740	1993	02	5.42397	BT	4B930205
248.400	27.600	1993	02	5.88000	BNT	GRB
10.350	-21.720	1993	02	6.05333	BT	4B930206-
233.510	-66.150	1993	02	6.62721	BT	4B930206-
321.500	-41.900	1993	02	6.80130	BNT	GRB
240.000	-57.000	1993	02	9.18208	GRA	GRB930209
239.300	-58.200	1993	02	9.19000	BNT	GRB
248.880	22.250	1993	02	10.09042	BT	4B930210
285.300	31.500	1993	02	11.88000	BNT	GRB
38.350	8.890	1993	02	12.47913	BT	4B930212
13.930	49.410	1993	02	13.36953	BT	4B930213-
199.970	-67.460	1993	02	13.53176	BT	4B930213-
255.350	17.990	1993	02	14.17243	BT	4B930214-
251.100	-35.200	1993	02	14.27357	BNT	GRB
282.830	-44.510	1993	02	14.31730	BT	4B930214-
194.800	26.770	1993	02	14.75902	BT	4B930214-
38.900	-7.700	1993	02	16.62000	BNT	GRB
117.780	0.980	1993	02	17.61433	BT	4B930217
118.270	51.620	1993	02	18.00421	BT	4B930218
318.100	2.200	1993	02	18.32859	BNT	GRB
21.500	65.000	1993	02	19.13936	BT	4B930219-
330.630	35.080	1993	02	19.16604	BT	4B930219-
242.820	57.510	1993	02	19.21404	BT	4B930219-
58.290	-30.050	1993	02	19.35414	BT	4B930219-
302.410	20.020	1993	02	19.87090	BT	4B930219-
209.120	-61.750	1993	02	20.06596	BT	4B930220
145.130	-25.850	1993	02	21.76607	BT	4B930221

Continued on next column

Continued from previous column

RA deg	DEC deg	Year	Month	Day	Cat.	GRB Name
337.300	-38.800	1993	02	22.11112	BNT	GRB
298.700	78.100	1993	02	27.81000	BNT	GRB
79.440	-9.770	1993	02	28.34164	BT	4B930228
28.600	16.800	1993	02	28.88000	BNT	GRB
296.210	-40.440	1993	03	1.65062	BT	4B930301
204.800	43.900	1993	03	2.19000	BNT	GRB
90.330	5.430	1993	03	2.89812	BT	4B930302
0.200	-55.500	1993	03	3.69000	BNT	GRB
79.330	16.440	1993	03	4.36021	BT	4B930304
40.920	-36.690	1993	03	5.29973	BT	4B930305-
96.460	11.750	1993	03	5.45089	BT	4B930305-
282.300	59.300	1993	03	5.69000	BNT	GRB
32.800	3.600	1993	03	5.90262	BNT	GRB
102.300	-27.300	1993	03	7.56000	BNT	GRB
85.500	-33.400	1993	03	8.31000	BNT	GRB
325.410	51.730	1993	03	9.13044	BT	4B930309-
151.900	-32.900	1993	03	9.27796	BNT	GRB
32.570	-28.160	1993	03	9.51940	BT	4B930309-
331.000	-59.300	1993	03	10.06000	BNT	GRB
284.350	-52.390	1993	03	10.30509	BT	4B930310
126.890	-32.380	1993	03	11.24766	BT	4B930311
88.700	-3.000	1993	03	13.29181	BNT	GRB
35.800	86.060	1993	03	13.45596	BT	4B930313
83.300	67.400	1993	03	14.81773	BNT	GRB
0.350	-10.890	1993	03	15.03456	BT	4B930315
226.400	-33.700	1993	03	15.44000	BNT	GRB
335.100	-85.000	1993	03	16.75000	BNT	GRB
12.820	-62.670	1993	03	16.94766	BT	4B930316
2.740	7.990	1993	03	17.66521	BT	4B930317
21.000	38.600	1993	03	18.19000	BNT	GRB
106.180	-19.140	1993	03	18.29816	BT	4B930318-
150.480	-18.850	1993	03	18.52075	BT	4B930318-
202.000	67.100	1993	03	20.94000	BNT	GRB
180.200	59.570	1993	03	24.19545	BT	4B930324
19.500	14.700	1993	03	25.02296	BNT	GRB
47.300	43.800	1993	03	25.62000	BNT	GRB
138.830	21.340	1993	03	26.21230	BT	4B930326-
273.520	-45.100	1993	03	26.26831	BT	4B930326-
172.200	-8.200	1993	03	27.44000	BNT	GRB
294.880	-34.060	1993	03	28.26384	BT	4B930328
179.250	-8.650	1993	03	29.13155	BT	4B930329
208.900	53.100	1993	03	30.35836	BNT	GRB
100.300	-56.500	1993	03	30.94000	BNT	GRB
43.000	47.270	1993	03	31.13284	BT	4B930331-
50.130	-36.830	1993	03	31.34410	BT	4B930331-
97.180	-33.580	1993	03	31.67142	BT	4B930331-
238.890	-33.030	1993	04	1.05146	BT	4B930401-
203.100	-48.610	1993	04	1.26497	BT	4B930401-

Continued on next column

Continued from previous column

RA deg	DEC deg	Year	Month	Day	Cat.	GRB Name
339.930	19.450	1993	04	1.41538	BT	4B930401-
42.920	-41.620	1993	04	3.52044	BT	4B930403
234.700	-60.100	1993	04	3.88000	BNT	GRB
30.510	16.100	1993	04	4.22620	BT	4B930404
198.180	-8.800	1993	04	5.37141	BT	4B930405-
200.060	13.020	1993	04	5.58323	BT	4B930405-
216.350	48.730	1993	04	5.88222	BT	4B930405-
299.810	29.010	1993	04	6.30307	BT	4B930406-
191.500	-76.600	1993	04	6.53873	BNT	GRB
139.630	-46.860	1993	04	6.71389	BT	4B930406-
12.140	-71.620	1993	04	6.91896	BT	4B930406-
269.600	-61.300	1993	04	8.06000	BNT	GRB
245.590	-46.800	1993	04	8.19325	BT	4B930408
314.100	58.700	1993	04	9.12000	BNT	GRB
295.830	43.180	1993	04	9.20152	BT	4B930409-
176.910	-39.750	1993	04	9.89282	BT	4B930409-
277.200	-23.000	1993	04	9.94000	BNT	GRB
25.040	-20.560	1993	04	10.12400	BT	4B930410
183.000	-56.400	1993	04	10.75000	BNT	GRB
60.000	-26.700	1993	04	13.91405	BNT	GRB
311.420	9.920	1993	04	14.10227	BT	4B930414
29.030	17.530	1993	04	15.38876	BT	4B930415
134.300	22.300	1993	04	15.64978	BNT	GRB
109.600	-20.000	1993	04	16.56000	BNT	GRB
144.550	-24.180	1993	04	16.93557	BT	4B930416
193.400	-2.500	1993	04	17.81000	BNT	GRB
311.650	21.370	1993	04	18.60993	BT	4B930418-
147.500	49.800	1993	04	18.79132	BNT	GRB
333.140	17.080	1993	04	18.94732	BT	4B930418-
36.130	-29.040	1993	04	20.22213	BT	4B930420-
241.710	-7.090	1993	04	20.76108	BT	4B930420-
324.000	-34.200	1993	04	20.96662	BNT	GRB
15.000	-22.400	1993	04	21.12000	BNT	GRB
69.000	-17.820	1993	04	21.18544	BT	4B930421-
234.190	-13.250	1993	04	21.90744	BT	4B930421-
53.100	-8.000	1993	04	22.56000	BNT	GRB
158.230	-37.050	1993	04	23.55300	BT	4B930423
230.100	-57.600	1993	04	24.44000	BNT	GRB
54.220	41.600	1993	04	24.80486	BT	4B930424
220.600	61.600	1993	04	25.00000	BNT	GRB
18.000	-35.190	1993	04	25.42882	BT	4B930425-
257.830	63.820	1993	04	25.62139	BT	4B930425-
45.450	-21.720	1993	04	26.38859	BT	4B930426-
37.800	-87.000	1993	04	26.50000	BNT	GRB
67.820	10.130	1993	04	26.52815	BT	4B930426-
67.900	29.100	1993	04	27.56000	BNT	GRB
129.850	-55.450	1993	04	28.04668	BT	4B930428
33.800	-26.900	1993	04	29.75000	BNT	GRB

Continued on next column

Continued from previous column

RA deg	DEC deg	Year	Month	Day	Cat.	GRB Name
106.330	20.970	1993	04	30.62591	BT	4B930430-
345.120	-7.070	1993	04	30.98719	BT	4B930430-
178.900	-32.200	1993	05	1.31000	BNT	GRB
254.720	-46.530	1993	05	2.57839	BT	4B930502
46.000	0.000	1993	05	2.65128	BNT	GRB
198.330	-63.520	1993	05	3.27258	BT	4B930503-
19.620	-22.260	1993	05	3.59554	BT	4B930503-
50.280	72.720	1993	05	3.70670	BT	4B930503-
5.370	-40.220	1993	05	3.86532	BT	4B930503-
101.830	-16.660	1993	05	6.23456	BT	4B930506-
64.450	-5.970	1993	05	6.62003	BT	4B930506-
259.300	34.400	1993	05	6.62000	BNT	GRB
255.350	-24.340	1993	05	6.75963	BT	4B930506-
76.000	43.700	1993	05	8.94000	BNT	GRB
150.670	55.000	1993	05	10.09942	BT	4B930510
270.160	41.220	1993	05	11.15809	BT	4B930511
281.920	78.030	1993	05	14.01825	BT	4B930514-
344.200	16.410	1993	05	14.70656	BT	4B930514-
317.600	57.600	1993	05	15.46819	BNT	GRB
332.990	40.250	1993	05	16.91773	BT	4B930516
209.800	0.000	1993	05	17.30471	BNT	GRB
5.850	22.850	1993	05	17.38474	BT	4B930517-
29.340	-5.960	1993	05	17.83298	BT	4B930517-
349.170	-37.510	1993	05	18.13919	BT	4B930518
288.900	-9.200	1993	05	19.38000	BNT	GRB
26.840	-41.460	1993	05	19.67631	BT	4B930519
203.150	-31.880	1993	05	21.11292	BT	4B930521
334.100	23.400	1993	05	21.76892	BNT	GRB
14.800	4.210	1993	05	23.82007	BT	4B930523
125.070	61.760	1993	05	24.66607	BT	4B930524-
351.160	-6.020	1993	05	24.73950	BT	4B930524-
85.850	-44.350	1993	05	26.85595	BT	4B930526
89.810	8.330	1993	05	28.51336	BT	4B930528
43.910	51.910	1993	05	29.15622	BT	4B930529
15.830	34.380	1993	05	30.39444	BT	4B930530-
188.090	35.160	1993	05	30.43391	BT	4B930530-
340.040	13.250	1993	05	31.66224	BT	4B930531
95.560	3.200	1993	06	1.25759	BT	4B930601-
127.120	39.350	1993	06	1.59709	BT	4B930601-
185.290	72.700	1993	06	1.84007	BT	4B930601-
263.220	37.660	1993	06	2.57157	BT	4B930602-
217.980	-32.340	1993	06	2.80895	BT	4B930602-
121.160	0.420	1993	06	3.57221	BT	4B930603
161.100	-36.010	1993	06	5.09362	BT	4B930605-
294.370	34.110	1993	06	5.28565	BT	4B930605-
252.640	-79.260	1993	06	6.30473	BT	4B930606-
144.500	10.700	1993	06	6.65354	BNT	GRB
151.650	31.200	1993	06	6.86814	BT	4B930606-

Continued on next column

Continued from previous column

RA deg	DEC deg	Year	Month	Day	Cat.	GRB Name
163.440	35.640	1993	06	7.88067	BT	4B930607
323.250	-10.220	1993	06	8.47860	BT	4B930608-
105.050	40.790	1993	06	8.82053	BT	4B930608-
240.300	-21.000	1993	06	8.94000	BNT	GRB
208.730	-16.380	1993	06	9.42181	BT	4B930609-
203.800	-18.210	1993	06	9.81006	BT	4B930609-
211.880	-1.910	1993	06	10.74458	BT	4B930610
103.070	-69.760	1993	06	12.03076	BT	4B930612-
88.190	36.010	1993	06	12.16524	BT	4B930612-
347.100	-1.080	1993	06	12.37081	BT	4B930612-
253.800	33.500	1993	06	12.62000	BNT	GRB
37.100	30.740	1993	06	12.69815	BT	4B930612-
316.230	-31.410	1993	06	13.92781	BT	4B930613
168.140	23.950	1993	06	14.15314	BT	4B930614-
33.300	-41.040	1993	06	14.69071	BT	4B930614-
33.650	-80.540	1993	06	14.91035	BT	4B930614-
177.400	-4.900	1993	06	16.25000	BNT	GRB
236.400	-4.600	1993	06	17.25000	BNT	GRB
217.400	-21.200	1993	06	17.56000	BNT	GRB
244.960	-68.140	1993	06	19.79927	BT	4B930619
59.010	-37.280	1993	06	20.37091	BT	4B930620
201.200	-44.610	1993	06	21.07428	BT	4B930621-
303.300	56.420	1993	06	21.70295	BT	4B930621-
132.370	7.440	1993	06	22.14462	BT	4B930622-
249.000	80.850	1993	06	22.20311	BT	4B930622-
261.550	46.230	1993	06	23.13164	BT	4B930623
21.800	-40.200	1993	06	26.08129	BNT	GRB
344.600	-37.700	1993	06	26.94000	BNT	GRB
152.000	-55.940	1993	06	27.06233	BT	4B930627
43.500	10.800	1993	06	27.17391	BNT	GRB
33.900	40.900	1993	06	27.80370	BNT	GRB
67.100	39.500	1993	06	30.69000	BNT	GRB
351.900	-60.100	1993	06	30.95883	BNT	GRB
298.720	6.330	1993	07	1.02212	BT	4B930701-
226.100	39.900	1993	07	1.62000	BNT	GRB
314.870	78.940	1993	07	1.92539	BT	4B930701-
299.400	23.100	1993	07	2.79089	BNT	GRB
311.060	8.040	1993	07	3.47674	GRA	GRB930703A
352.890	38.270	1993	07	4.62572	BT	4B930704-
100.900	60.800	1993	07	4.70076	BT	4B930704-
283.080	-39.240	1993	07	5.52718	BT	4B930705-
202.500	-63.500	1993	07	5.62000	BNT	GRB
78.270	-56.170	1993	07	5.99446	BT	4B930705-
278.550	-18.960	1993	07	6.21772	BT	4B930706-
174.900	-35.400	1993	07	6.25645	BNT	GRB
210.090	-1.360	1993	07	6.33971	BT	4B930706-
158.100	11.400	1993	07	8.16063	BNT	GRB
86.550	-69.020	1993	07	8.21711	BT	4B930708-

Continued on next column

Continued from previous column

RA deg	DEC deg	Year	Month	Day	Cat.	GRB Name
239.500	-43.340	1993	07	8.51255	BT	4B930708-
80.790	26.940	1993	07	8.81245	BT	4B930708-
194.410	-46.730	1993	07	9.25998	BT	4B930709-
351.810	-8.390	1993	07	9.72699	BT	4B930709-
26.350	40.190	1993	07	10.13507	BT	4B930710
316.500	-69.200	1993	07	10.15984	BNT	GRB
265.500	-10.990	1993	07	11.03574	BT	4B930711-
13.750	-9.090	1993	07	11.14725	BT	4B930711-
211.620	-37.390	1993	07	11.63235	BT	4B930711-
251.050	-50.560	1993	07	11.99578	BT	4B930711-
257.700	23.700	1993	07	14.67562	BT	4B930714
223.030	3.390	1993	07	15.62591	BT	4B930715
194.900	51.700	1993	07	17.19000	BNT	GRB
207.000	-73.700	1993	07	18.00000	BNT	GRB
287.650	-55.320	1993	07	19.37239	BT	4B930719-
212.180	1.360	1993	07	19.47068	BT	4B930719-
20.820	25.340	1993	07	20.60775	BT	4B930720-
95.510	47.170	1993	07	20.84894	BT	4B930720-
78.660	-33.150	1993	07	21.05373	BT	4B930721-
298.580	-40.790	1993	07	21.53165	BT	4B930721-
109.840	-16.000	1993	07	21.62144	BT	4B930721-
302.800	-56.300	1993	07	22.88000	BNT	GRB
198.100	40.300	1993	07	23.60524	BNT	GRB
289.600	58.310	1993	07	24.09850	BT	4B930724-
75.920	0.230	1993	07	24.65450	BT	4B930724-
50.050	-49.040	1993	07	24.69892	BT	4B930724-
267.150	13.110	1993	07	25.64433	BT	4B930725
57.800	43.900	1993	07	25.98098	BT	GRB
159.990	-23.890	1993	07	27.33924	BT	4B930727-
309.400	27.970	1993	07	27.56634	BT	4B930727-
86.100	16.800	1993	07	28.56000	BNT	GRB
304.550	27.950	1993	07	30.21786	BT	4B930730
116.530	45.490	1993	07	31.13647	BT	4B930731-
102.310	37.380	1993	07	31.26663	BT	4B930731-
292.780	46.020	1993	08	1.09183	BT	4B930801
161.200	-4.300	1993	08	1.98545	BNT	GRB
277.300	31.300	1993	08	2.50509	BNT	GRB
27.800	67.500	1993	08	4.69000	BNT	GRB
284.280	58.700	1993	08	5.08279	BT	4B930805-
334.550	-15.600	1993	08	5.52742	BT	4B930805-
351.930	-1.360	1993	08	7.66178	BT	4B930807-
275.100	-56.840	1993	08	7.91862	BT	4B930807-
163.390	-65.830	1993	08	9.10089	BT	4B930809-
37.970	-74.630	1993	08	9.21602	BT	4B930809-
273.460	42.630	1993	08	11.58451	BT	4B930811
346.600	78.700	1993	08	11.62000	BNT	GRB
198.300	-28.100	1993	08	12.25000	BNT	GRB
251.800	57.000	1993	08	12.49569	BNT	GRB

Continued on next column

Continued from previous column

RA deg	DEC deg	Year	Month	Day	Cat.	GRB Name
166.510	26.390	1993	08	12.53168	BT	4B930812
164.600	-44.700	1993	08	12.63583	BNT	GRB
36.600	80.600	1993	08	13.75000	BNT	GRB
283.600	-10.980	1993	08	15.22688	BT	4B930815
129.300	22.600	1993	08	15.75285	BNT	GRB
69.030	62.690	1993	08	16.03640	BT	4B930816
145.700	57.200	1993	08	16.69000	BNT	GRB
88.970	-48.250	1993	08	17.20047	BT	4B930817
105.770	-49.280	1993	08	19.67293	BT	4B930819
153.050	-51.880	1993	08	20.01289	BT	4B930820
166.300	-15.500	1993	08	20.25570	BNT	GRB
52.200	57.400	1993	08	20.75000	BNT	GRB
235.320	-7.940	1993	08	21.41086	BT	4B930821
162.400	-46.800	1993	08	21.62000	BNT	GRB
266.610	-6.870	1993	08	22.26565	BT	4B930822-
213.090	-0.680	1993	08	22.61449	BT	4B930822-
255.250	6.030	1993	08	24.26100	BT	4B930824
40.700	77.800	1993	08	25.50000	BNT	GRB
240.000	16.700	1993	08	26.41806	BNT	GRB
3.700	19.400	1993	08	26.50000	BNT	GRB
175.070	29.590	1993	08	26.79038	BT	4B930826
14.300	67.700	1993	08	27.62000	BNT	GRB
299.100	8.500	1993	08	27.68988	BNT	GRB
177.110	37.240	1993	08	28.06069	BT	4B930828
317.250	-38.210	1993	08	29.98520	BT	4B930829
223.290	-3.630	1993	08	31.38618	BT	4B930831
158.280	-38.360	1993	09	1.06126	BT	4B930901
233.420	49.000	1993	09	2.28987	BT	4B930902-
209.500	22.800	1993	09	2.44000	BNT	GRB
103.120	16.150	1993	09	2.89443	BT	4B930902-
88.670	-10.420	1993	09	3.01353	BT	4B930903-
242.840	-69.470	1993	09	3.10876	BT	4B930903-
201.330	10.630	1993	09	3.53654	BT	4B930903-
317.300	49.400	1993	09	4.64666	BNT	GRB
186.100	9.200	1993	09	4.98258	BNT	GRB
11.100	-46.700	1993	09	5.00932	BNT	GRB
310.950	-1.220	1993	09	5.14340	BT	4B930905-
330.050	-67.900	1993	09	5.91264	BT	4B930905-
244.000	9.400	1993	09	9.52199	BNT	GRB
15.830	36.840	1993	09	9.67654	BT	4B930909
143.500	-71.300	1993	09	10.14317	BNT	GRB
160.200	3.330	1993	09	10.31920	BT	4B930910-
157.720	-0.590	1993	09	10.33615	BT	4B930910-
167.590	-66.690	1993	09	10.50843	BT	4B930910-
178.310	52.870	1993	09	11.96946	BT	4B930911
294.270	44.270	1993	09	13.71194	BT	4B930913-
154.330	15.920	1993	09	13.73281	BT	4B930913-
34.260	34.290	1993	09	14.11750	BT	4B930914

Continued on next column

Continued from previous column

RA deg	DEC deg	Year	Month	Day	Cat.	GRB Name
23.960	-25.580	1993	09	16.14113	BT	4B930916-
280.710	65.390	1993	09	16.84679	BT	4B930916-
117.800	-61.500	1993	09	17.12000	BNT	GRB
326.400	-77.400	1993	09	18.44000	BNT	GRB
50.300	40.100	1993	09	21.88000	BNT	GRB
164.640	-32.080	1993	09	22.22010	BT	4B930922-
271.200	55.890	1993	09	22.26721	BT	4B930922-
12.800	-56.500	1993	09	22.69000	BNT	GRB
313.700	10.310	1993	09	24.04369	BT	4B930924
100.300	-7.100	1993	09	24.38000	BNT	GRB
96.980	-54.660	1993	09	25.57014	BT	4B930925
66.440	30.510	1993	09	26.70405	BT	4B930926
108.610	-9.520	1993	09	27.17926	BT	4B930927
241.800	-71.900	1993	09	27.25000	BNT	GRB
240.100	-72.100	1993	09	28.93980	BNT	GRB
264.800	-62.400	1993	09	28.94000	BNT	GRB
91.600	39.400	1993	09	28.94000	BNT	GRB
256.260	45.260	1993	10	1.05777	BT	4B931001
205.600	11.200	1993	10	1.06000	BNT	GRB
14.400	14.400	1993	10	1.75000	BNT	GRB
100.460	-45.960	1993	10	3.88922	BT	4B931003
124.120	-25.660	1993	10	5.66002	BT	4B931005
211.800	-47.100	1993	10	5.68385	BNT	GRB
66.310	65.280	1993	10	6.89711	BT	4B931006
226.100	-38.900	1993	10	6.94348	BNT	GRB
237.090	-12.540	1993	10	7.18355	BT	4B931007
315.900	-5.100	1993	10	7.19000	BNT	GRB
288.300	-15.200	1993	10	7.25000	BNT	GRB
4.300	37.900	1993	10	7.31000	BNT	GRB
280.110	-41.550	1993	10	8.03125	BT	4B931008-
311.500	-67.300	1993	10	8.06000	BNT	GRB
42.980	21.370	1993	10	8.30434	BT	4B931008-
165.400	33.930	1993	10	8.46471	BT	4B931008-
39.900	45.800	1993	10	8.62000	BNT	GRB
126.500	-14.800	1993	10	8.66172	BNT	GRB
260.300	55.500	1993	10	11.94000	BNT	GRB
315.300	-25.600	1993	10	11.97712	BNT	GRB
169.230	19.110	1993	10	13.62360	BT	4B931013-
211.550	14.390	1993	10	13.70415	BT	4B931013-
44.420	64.280	1993	10	13.71924	BT	4B931013-
3.600	36.300	1993	10	14.06000	BNT	GRB
57.860	-38.890	1993	10	14.49728	BT	4B931014-
272.500	9.340	1993	10	14.70905	BT	4B931014-
338.080	61.980	1993	10	15.41675	BT	4B931015
66.390	-46.920	1993	10	16.39184	BT	4B931016-
76.220	41.340	1993	10	16.52277	BT	4B931016-
181.440	-83.110	1993	10	17.05404	BT	4B931017
195.700	-61.600	1993	10	17.25000	BNT	GRB

Continued on next column

Continued from previous column

RA deg	DEC deg	Year	Month	Day	Cat.	GRB Name
241.240	-62.020	1993	10	18.24624	BT	4B931018
58.220	16.440	1993	10	19.40657	BT	4B931019-
242.920	-18.700	1993	10	19.76568	BT	4B931019-
289.000	9.000	1993	10	20.12000	BNT	GRB
211.510	-27.070	1993	10	21.37263	BT	4B931021-
85.890	30.820	1993	10	21.54192	BT	4B931021-
345.940	-12.110	1993	10	21.92575	BT	4B931021-
249.060	8.360	1993	10	22.41678	BT	4B931022
4.190	74.170	1993	10	23.17627	BT	4B931023
137.630	-8.490	1993	10	24.56191	BT	4B931024
166.300	19.800	1993	10	25.94000	BNT	GRB
51.360	-10.560	1993	10	26.48330	BT	4B931026
356.800	45.300	1993	10	26.94394	BNT	GRB
34.140	9.270	1993	10	30.30931	BT	4B931030-
326.410	58.240	1993	10	30.33937	BT	4B931030-
258.580	33.470	1993	10	30.79104	BT	4B931030-
62.000	-15.900	1993	10	30.90950	BNT	GRB
325.100	62.730	1993	10	31.17124	BT	4B931031
180.100	53.600	1993	10	31.25000	BNT	GRB
238.320	0.780	1993	11	1.13219	BT	4B931101-
200.300	-56.900	1993	11	1.25850	BNT	GRB
132.580	-2.050	1993	11	1.96780	BT	4B931101-
328.500	34.400	1993	11	2.62000	BNT	GRB
319.100	4.160	1993	11	3.26461	BT	4B931103-
87.880	65.050	1993	11	3.68453	BT	4B931103-
348.800	9.500	1993	11	3.75487	BNT	GRB
96.500	-27.300	1993	11	5.37831	BNT	GRB
44.600	73.300	1993	11	6.50000	BNT	GRB
196.750	-3.130	1993	11	6.85560	BT	4B931106
162.700	-45.200	1993	11	6.94000	BNT	GRB
99.400	-40.700	1993	11	7.31000	BNT	GRB
172.300	50.600	1993	11	8.42620	BNT	GRB
59.640	-6.350	1993	11	8.95251	BT	4B931108
110.680	39.510	1993	11	9.65067	BT	4B931109
217.590	-21.810	1993	11	10.71810	BT	4B931110
64.100	-49.000	1993	11	10.72845	BNT	GRB
235.800	37.100	1993	11	11.69000	BNT	GRB
311.510	55.950	1993	11	12.78186	BT	4B931112
49.100	-41.900	1993	11	13.06000	BNT	GRB
97.130	29.780	1993	11	13.73781	BT	4B931113-
107.820	-46.800	1993	11	13.96344	BT	4B931113-
29.040	-39.970	1993	11	14.21754	BT	4B931114
157.300	15.300	1993	11	14.26470	BNT	GRB
46.400	-24.500	1993	11	15.09300	BNT	GRB
64.290	25.320	1993	11	15.68990	BT	4B931115
272.600	-1.000	1993	11	15.75000	BNT	GRB
168.900	-9.400	1993	11	17.03875	BNT	GRB
348.990	-44.140	1993	11	17.91376	BT	4B931117

Continued on next column

Continued from previous column

RA deg	DEC deg	Year	Month	Day	Cat.	GRB Name
20.050	-6.160	1993	11	18.48041	BT	4B931118
149.300	37.300	1993	11	18.64485	BNT	GRB
319.670	23.030	1993	11	20.78429	BT	4B931120
159.700	-79.400	1993	11	25.88000	BNT	GRB
157.280	70.080	1993	11	26.19916	BT	4B931126-
3.290	-17.400	1993	11	26.81366	BT	4B931126-
250.810	-23.070	1993	11	27.03484	BT	4B931127
110.140	-50.660	1993	11	28.21380	BT	4B931128-
293.330	80.880	1993	11	28.32824	BT	4B931128-
142.640	18.210	1993	11	28.71126	BT	4B931128-
197.100	36.800	1993	12	2.91779	BNT	GRB
6.520	24.530	1993	12	3.04310	BT	4B931203
250.150	38.230	1993	12	4.40845	BT	4B931204-
221.180	-72.720	1993	12	4.60781	BT	4B931204-
247.120	-43.950	1993	12	5.44648	BT	4B931205-
15.560	66.490	1993	12	5.62491	BT	4B931205-
104.590	3.560	1993	12	6.36215	BT	4B931206-
175.200	-0.200	1993	12	6.44000	BNT	GRB
266.600	-5.620	1993	12	6.73368	BT	4B931206-
198.730	-29.930	1993	12	8.19259	BT	4B931208-
234.110	-40.290	1993	12	8.39909	BT	4B931208-
14.060	48.690	1993	12	9.54412	BT	4B931209-
19.400	-28.500	1993	12	9.88000	BNT	GRB
259.560	20.830	1993	12	9.96656	BT	4B931209-
359.180	44.750	1993	12	10.68887	BT	4B931210
72.120	30.570	1993	12	11.67292	BT	4B931211
247.610	28.440	1993	12	12.22855	BT	4B931212
182.200	71.200	1993	12	14.38000	BNT	GRB
329.800	-4.900	1993	12	15.12000	BNT	GRB
7.710	-49.870	1993	12	15.25854	BT	4B931215-
15.920	-18.250	1993	12	15.52639	BT	4B931215-
0.760	75.300	1993	12	17.50740	BT	4B931217
244.980	41.530	1993	12	18.80837	BT	4B931218
20.490	-74.720	1993	12	19.03201	BT	4B931219-
51.200	70.700	1993	12	19.04863	BNT	GRB
12.360	-3.600	1993	12	19.69061	BT	4B931219-
51.000	47.000	1993	12	20.15648	BNT	GRB
113.500	45.400	1993	12	20.19000	BNT	GRB
298.520	40.370	1993	12	20.65973	BT	4B931220
32.200	33.500	1993	12	20.75000	BNT	GRB
91.020	-43.170	1993	12	21.09016	BT	4B931221-
244.810	-17.420	1993	12	21.97992	BT	4B931221-
276.400	32.100	1993	12	22.12000	BNT	GRB
229.900	-41.700	1993	12	22.81000	BNT	GRB
192.520	28.650	1993	12	22.88998	BT	4B931222
221.600	37.600	1993	12	23.06000	BNT	GRB
256.790	41.240	1993	12	23.98219	BT	4B931223
13.490	-48.400	1993	12	25.21037	BT	4B931225-

Continued on next column

Continued from previous column

RA deg	DEC deg	Year	Month	Day	Cat.	GRB Name
264.800	40.700	1993	12	25.44000	BNT	GRB
4.850	9.870	1993	12	25.97236	BT	4B931225-
205.950	21.630	1993	12	26.84108	BT	4B931226
227.400	-20.800	1993	12	26.88000	BNT	GRB
93.800	-28.700	1993	12	26.88000	BNT	GRB
224.020	52.590	1993	12	28.01265	BT	4B931228
240.060	19.700	1993	12	29.30285	BT	4B931229-
83.400	70.200	1993	12	29.38000	BNT	GRB
55.610	38.080	1993	12	29.69741	BT	4B931229-
239.800	63.590	1993	12	30.85197	BT	4B931230
94.030	-6.520	1994	01	1.34847	BT	4B940101-
307.390	-14.540	1994	01	1.65955	BT	4B940101-
111.390	40.010	1994	01	1.91192	BT	4B940101-
189.270	62.840	1994	01	1.94584	BT	4B940101-
10.900	45.110	1994	01	2.11520	BT	4B940102
306.600	10.800	1994	01	2.50000	BNT	GRB
31.300	-52.100	1994	01	2.56000	BNT	GRB
8.800	-28.200	1994	01	3.25000	BNT	GRB
267.900	7.140	1994	01	3.92565	BT	4B940103
56.700	62.200	1994	01	4.81000	BNT	GRB
112.100	-69.400	1994	01	7.00000	BNT	GRB
234.300	16.200	1994	01	7.94000	BNT	GRB
76.230	-25.140	1994	01	8.27427	BT	4B940108
337.600	-10.800	1994	01	10.07806	BT	4B940110-
171.350	60.670	1994	01	10.39279	BT	4B940110-
268.900	-11.100	1994	01	11.12000	BNT	GRB
153.170	-56.330	1994	01	11.37057	BT	4B940111
115.400	-53.600	1994	01	11.88000	BNT	GRB
226.380	25.310	1994	01	12.53221	BT	4B940112-
44.950	59.920	1994	01	12.82885	BT	4B940112-
90.000	47.200	1994	01	13.54912	BNT	GRB
238.300	50.800	1994	01	13.62000	BNT	GRB
209.390	-23.160	1994	01	13.69993	BT	4B940113
340.570	-39.280	1994	01	14.23465	BT	4B940114-
97.400	-14.800	1994	01	14.89469	BT	4B940114-
216.000	54.010	1994	01	15.15521	BT	4B940115
353.400	24.400	1994	01	16.50000	BNT	GRB
59.500	16.700	1994	01	16.81000	BNT	GRB
287.700	-63.940	1994	01	18.45603	BT	4B940118
326.560	-71.630	1994	01	19.11263	BT	4B940119-
51.600	25.000	1994	01	19.38000	BNT	GRB
131.410	39.290	1994	01	19.65602	BT	4B940119-
133.900	76.000	1994	01	20.00668	BNT	GRB
101.500	-35.500	1994	01	20.44690	BT	4B940120-
146.750	85.060	1994	01	20.52219	BT	4B940120-
26.200	-42.600	1994	01	21.06000	BNT	GRB
234.400	-60.500	1994	01	24.18455	BNT	GRB
209.100	-54.400	1994	01	24.38257	BNT	GRB

Continued on next column

Continued from previous column

RA deg	DEC deg	Year	Month	Day	Cat.	GRB Name
98.500	-35.800	1994	01	24.52438	BNT	GRB
89.610	0.540	1994	01	24.58196	BT	4B940124
193.500	33.800	1994	01	25.56000	BNT	GRB
130.980	9.040	1994	01	26.32662	BT	4B940126-
22.070	52.590	1994	01	26.78918	BT	4B940126-
337.910	68.750	1994	01	27.39774	BT	4B940127
166.380	-0.050	1994	01	28.23997	BT	4B940128-
224.020	-15.220	1994	01	28.70214	BT	4B940128-
127.460	28.590	1994	01	29.44674	BT	4B940129
345.600	-14.800	1994	01	31.69000	BNT	GRB
188.300	-51.200	1994	01	31.81000	BNT	GRB
268.610	22.370	1994	02	1.31992	BT	4B940201-
353.460	28.320	1994	02	1.34350	BT	4B940201-
184.160	-40.950	1994	02	3.65759	BT	4B940203
246.300	-23.200	1994	02	3.69000	BNT	GRB
144.200	-59.960	1994	02	6.00600	BT	4B940206-
260.410	-46.470	1994	02	6.76792	BT	4B940206-
203.590	-40.350	1994	02	7.41728	BT	4B940207-
250.630	-9.060	1994	02	7.48029	BT	4B940207-
1.500	14.350	1994	02	9.83336	BT	4B940209
152.290	82.130	1994	02	10.80089	BT	4B940210
245.200	27.300	1994	02	11.43807	BNT	GRB
273.350	62.200	1994	02	11.56382	BT	4B940211-
25.620	-1.430	1994	02	11.67808	BT	4B940211-
191.900	-28.100	1994	02	13.08403	BNT	GRB
349.540	63.710	1994	02	13.51304	BT	4B940213
151.080	53.150	1994	02	14.02648	BT	4B940214-
357.960	-9.630	1994	02	14.38494	BT	4B940214-
96.430	-9.610	1994	02	14.48237	BT	4B940214-
190.350	21.290	1994	02	14.69861	BT	4B940214-
40.670	-29.940	1994	02	16.14778	BT	4B940216
353.100	53.350	1994	02	17.24784	BT	4B940217-
29.070	4.550	1994	02	17.96021	BT	4B940217-
114.100	-17.500	1994	02	18.81000	BNT	GRB
349.710	-19.690	1994	02	18.81422	BT	4B940218
63.500	0.110	1994	02	19.18526	BT	4B940219
200.200	22.500	1994	02	22.06000	BNT	GRB
66.000	39.170	1994	02	22.49367	BT	4B940222
18.150	15.740	1994	02	23.33350	BT	4B940223
136.950	-8.070	1994	02	24.67701	BT	4B940224
303.120	-21.950	1994	02	26.00826	BT	4B940226-
32.750	13.180	1994	02	26.19428	BT	4B940226-
349.270	6.280	1994	02	26.83008	BT	4B940226-
189.400	28.500	1994	02	27.52674	BNT	GRB
343.960	36.110	1994	02	27.87794	BT	4B940227
127.980	-12.360	1994	02	28.47847	BT	4B940228-
126.190	-11.290	1994	02	28.82309	BT	4B940228-
258.000	16.800	1994	03	1.09856	BNT	GRB

Continued on next column

Continued from previous column

RA deg	DEC deg	Year	Month	Day	Cat.	GRB Name
103.510	64.350	1994	03	1.84071	BT	4B940301
12.490	-23.970	1994	03	2.21426	BT	4B940302
192.230	58.680	1994	03	3.05687	BT	4B940303
288.610	11.790	1994	03	4.53541	BT	4B940304
31.700	-64.600	1994	03	4.56000	BNT	GRB
227.890	21.090	1994	03	5.37602	BT	4B940305-
191.280	40.830	1994	03	5.48869	BT	4B940305-
259.690	0.460	1994	03	5.65939	BT	4B940305-
300.820	15.100	1994	03	6.15085	BT	4B940306
192.370	-28.200	1994	03	7.33073	BT	4B940307
74.600	50.590	1994	03	10.91733	BT	4B940310
105.200	26.400	1994	03	11.52045	BNT	GRB
221.500	-56.170	1994	03	12.47804	BT	4B940312-
356.000	15.800	1994	03	12.56000	BNT	GRB
118.780	13.720	1994	03	12.76697	BT	4B940312-
109.450	-14.460	1994	03	13.54332	BT	4B940313
354.860	-2.140	1994	03	14.41654	BT	4B940314
29.200	29.800	1994	03	16.81000	BNT	GRB
165.680	81.290	1994	03	18.33536	BT	4B940318
261.100	35.900	1994	03	19.38000	BNT	GRB
68.740	-12.600	1994	03	19.99816	BT	4B940319
149.100	-12.300	1994	03	21.56000	BNT	GRB
160.330	3.100	1994	03	21.92022	BT	4B940321
213.890	8.370	1994	03	23.91988	BT	4B940323
197.000	14.400	1994	03	24.12000	BNT	GRB
50.100	-54.900	1994	03	24.26926	BNT	GRB
129.800	12.300	1994	03	25.19000	BNT	GRB
151.670	24.740	1994	03	26.30939	BT	4B940326
54.000	-2.500	1994	03	27.38000	BNT	GRB
38.850	53.230	1994	03	27.85043	BT	4B940327
97.180	-32.350	1994	03	28.50387	BT	4B940328
237.510	-68.890	1994	03	29.24266	BT	4B940329-
180.000	8.920	1994	03	29.49347	BT	4B940329-
204.910	-10.330	1994	03	29.76086	BT	4B940329-
139.100	-54.000	1994	03	30.06000	BNT	GRB
57.800	19.200	1994	03	30.31000	BNT	GRB
351.300	4.500	1994	03	30.56000	BNT	GRB
352.230	58.890	1994	03	30.71009	BT	4B940330-
193.800	-33.630	1994	03	30.86435	BT	4B940330-
199.600	-61.100	1994	03	30.94000	BNT	GRB
218.200	-73.200	1994	03	31.56000	BNT	GRB
157.810	57.530	1994	03	31.57838	BT	4B940331-
65.130	17.640	1994	03	31.87472	BT	4B940331-
240.100	-29.200	1994	04	2.38000	BNT	GRB
155.900	25.300	1994	04	2.44000	BNT	GRB
164.400	62.100	1994	04	3.86956	BNT	GRB
47.020	56.270	1994	04	4.64021	BT	4B940404
225.440	-39.100	1994	04	6.04924	BT	4B940406

Continued on next column

Continued from previous column

RA deg	DEC deg	Year	Month	Day	Cat.	GRB Name
24.700	48.000	1994	04	7.25000	BNT	GRB
59.030	-21.150	1994	04	7.49464	BT	4B940407-
22.540	40.000	1994	04	7.76391	BT	4B940407-
88.900	7.000	1994	04	7.81000	BNT	GRB
33.800	-60.500	1994	04	7.88000	BNT	GRB
265.600	4.600	1994	04	9.00682	BT	4B940409
194.300	-34.700	1994	04	9.06000	BNT	GRB
231.440	51.450	1994	04	10.61235	BT	4B940410-
254.890	30.800	1994	04	10.65628	BT	4B940410-
80.300	41.800	1994	04	11.31000	BNT	GRB
217.170	-38.350	1994	04	12.06980	BT	4B940412
292.200	-25.700	1994	04	12.25000	BNT	GRB
28.800	2.900	1994	04	13.25000	BNT	GRB
206.260	-23.230	1994	04	13.42536	BT	4B940413-
216.980	63.780	1994	04	13.59126	BT	4B940413-
135.940	-8.260	1994	04	13.98815	BT	4B940413-
216.360	71.570	1994	04	14.38692	BT	4B940414-
214.300	7.500	1994	04	14.50000	BNT	GRB
181.260	-26.150	1994	04	14.69891	BT	4B940414-
214.300	-8.800	1994	04	14.94000	BNT	GRB
294.630	10.950	1994	04	14.99823	BT	4B940414-
255.160	-28.190	1994	04	15.36921	BT	4B940415-
249.150	-14.470	1994	04	15.70918	BT	4B940415-
137.200	-1.800	1994	04	17.44000	BNT	GRB
40.400	-47.600	1994	04	17.69723	BNT	GRB
313.400	-36.600	1994	04	17.76145	BNT	GRB
138.200	-22.700	1994	04	18.25000	BNT	GRB
243.100	-18.500	1994	04	18.56000	BNT	GRB
192.200	-0.300	1994	04	19.25000	BNT	GRB
105.340	51.430	1994	04	19.61075	BT	4B940419-
359.860	-47.950	1994	04	19.79928	BT	4B940419-
183.600	-20.800	1994	04	21.92353	BT	4B940421
249.850	-2.900	1994	04	22.25496	BT	4B940422
7.520	-4.080	1994	04	23.97245	BT	4B940423
29.800	-45.210	1994	04	24.36014	BT	4B940424
172.100	-58.000	1994	04	24.94000	BNT	GRB
119.110	-22.170	1994	04	25.28745	BT	4B940425-
322.950	14.890	1994	04	25.50999	BT	4B940425-
280.840	82.990	1994	04	25.69799	BT	4B940425-
22.810	0.900	1994	04	26.22912	BT	4B940426
56.290	24.110	1994	04	27.19183	BT	4B940427
347.760	-1.560	1994	04	28.44204	BT	4B940428
35.100	-57.520	1994	04	29.03047	BT	4B940429-
34.500	-8.350	1994	04	29.21720	BT	4B940429-
122.700	-71.700	1994	05	3.12000	BNT	GRB
161.000	10.060	1994	05	3.21372	BT	4B940503
163.060	41.430	1994	05	4.36441	BT	4B940504
349.610	67.500	1994	05	6.85130	BT	4B940506

Continued on next column

Continued from previous column

RA deg	DEC deg	Year	Month	Day	Cat.	GRB Name
29.300	-25.800	1994	05	6.94000	BNT	GRB
278.800	51.500	1994	05	7.00000	BNT	GRB
207.360	-21.930	1994	05	7.81384	BT	4B940507
85.400	43.100	1994	05	8.44000	BNT	GRB
166.100	80.600	1994	05	11.12000	BNT	GRB
122.300	-9.400	1994	05	12.56000	BNT	GRB
92.200	-74.010	1994	05	12.70122	BT	4B940512-
232.970	55.880	1994	05	12.73461	BT	4B940512-
330.560	-58.190	1994	05	12.91124	BT	4B940512-
83.700	-11.900	1994	05	13.22334	BNT	GRB
313.900	-2.400	1994	05	13.74132	BNT	GRB
327.360	-9.510	1994	05	14.17206	BT	4B940514
84.600	-16.300	1994	05	14.69000	BNT	GRB
341.640	-41.360	1994	05	15.08485	BT	4B940515-
111.320	83.930	1994	05	15.72411	BT	4B940515-
175.520	12.960	1994	05	16.34183	BT	4B940516
167.400	-34.600	1994	05	16.74779	BNT	GRB
205.300	15.500	1994	05	17.19000	BNT	GRB
273.200	8.400	1994	05	17.31000	BNT	GRB
56.500	-52.500	1994	05	17.75000	BNT	GRB
323.500	6.930	1994	05	20.01504	BT	4B940520
129.190	-63.010	1994	05	21.48979	BT	4B940521-
69.200	40.700	1994	05	21.62000	BNT	GRB
295.760	50.610	1994	05	21.65677	BT	4B940521-
325.440	-76.440	1994	05	21.91833	BT	4B940521-
72.700	-44.100	1994	05	22.00000	BNT	GRB
243.200	18.400	1994	05	24.00000	BNT	GRB
135.460	-3.930	1994	05	24.26630	BT	4B940524-
120.800	7.900	1994	05	24.31000	BNT	GRB
157.680	11.560	1994	05	24.39582	BT	4B940524-
313.540	53.470	1994	05	26.14318	BT	4B940526-
73.400	-9.000	1994	05	26.31000	BNT	GRB
80.410	-30.390	1994	05	26.45517	BT	4B940526-
131.850	34.200	1994	05	26.84729	BT	4B940526-
29.540	-43.830	1994	05	27.54264	BT	4B940527-
268.780	-54.000	1994	05	27.67933	BT	4B940527-
163.640	-25.330	1994	05	29.13684	BT	4B940529-
100.930	-47.550	1994	05	29.50506	BT	4B940529-
66.190	-23.750	1994	05	29.68098	BT	4B940529-
214.840	58.930	1994	05	29.88815	BT	4B940529-
259.900	-82.300	1994	05	30.25000	BNT	GRB
111.420	-1.570	1994	05	30.37337	BT	4B940530
40.100	-1.700	1994	05	31.00773	BNT	GRB
18.230	58.420	1994	06	2.00993	BT	4B940602-
61.530	-8.890	1994	06	2.31775	BT	4B940602-
312.700	65.500	1994	06	4.25000	BNT	GRB
130.290	-45.670	1994	06	4.27738	BT	4B940604-
126.350	-13.420	1994	06	4.60911	BT	4B940604-

Continued on next column

Continued from previous column

RA deg	DEC deg	Year	Month	Day	Cat.	GRB Name
111.750	43.520	1994	06	5.62471	BT	4B940605
311.720	47.190	1994	06	6.51844	BT	4B940606
55.200	-54.800	1994	06	8.40509	BNT	GRB
284.140	23.340	1994	06	9.68689	BT	4B940609
114.200	-73.700	1994	06	10.94000	BNT	GRB
333.000	42.600	1994	06	11.69000	BNT	GRB
157.700	-31.600	1994	06	11.88000	BNT	GRB
69.050	0.160	1994	06	11.99389	BT	4B940611
167.100	-31.800	1994	06	12.19000	BNT	GRB
143.600	-49.300	1994	06	13.30808	BNT	GRB
287.300	-52.600	1994	06	13.38000	BNT	GRB
316.050	-16.140	1994	06	13.86021	BT	4B940613
158.910	9.880	1994	06	14.51912	BT	4B940614
49.300	76.400	1994	06	16.12000	BNT	GRB
165.040	-58.180	1994	06	16.20979	BT	4B940616-
51.000	76.400	1994	06	16.44000	BNT	GRB
336.220	-15.560	1994	06	16.45919	BT	4B940616-
346.680	11.220	1994	06	16.83148	BT	4B940616-
216.770	-9.270	1994	06	16.99648	BT	4B940616-
27.600	-60.500	1994	06	17.00000	BNT	GRB
299.050	-29.890	1994	06	19.89677	BT	4B940619
302.200	-45.200	1994	06	21.00000	BNT	GRB
214.080	5.990	1994	06	21.09340	BT	4B940621-
52.300	26.790	1994	06	21.50782	BT	4B940621-
277.650	-69.170	1994	06	21.62752	BT	4B940621-
46.300	-47.600	1994	06	21.88000	BNT	GRB
299.580	-31.240	1994	06	22.55436	BT	4B940622
71.200	3.200	1994	06	22.62000	BNT	GRB
183.000	4.600	1994	06	23.12000	BNT	GRB
276.200	-32.900	1994	06	23.21508	BNT	GRB
246.870	12.250	1994	06	23.22624	BT	4B940623-
210.510	43.780	1994	06	23.37215	BT	4B940623-
108.370	75.780	1994	06	23.78222	BT	4B940623-
33.880	-46.880	1994	06	23.99174	BT	4B940623-
282.450	-62.390	1994	06	24.60642	BT	4B940624-
24.000	10.990	1994	06	24.80686	BT	4B940624-
192.530	-15.370	1994	06	26.03191	BT	4B940626
256.000	-30.190	1994	06	28.21227	BT	4B940628
250.300	77.100	1994	06	28.25000	BNT	GRB
145.180	-6.430	1994	07	1.90740	BT	4B940701
83.900	54.900	1994	07	2.38000	BNT	GRB
29.730	-23.530	1994	07	2.39458	BT	4B940702
131.500	27.390	1994	07	3.19499	BT	4B940703-
210.280	-39.190	1994	07	3.55977	BT	4B940703-
27.700	15.110	1994	07	4.14453	BT	4B940704-
175.900	-29.600	1994	07	4.25000	BNT	GRB
326.800	30.900	1994	07	4.88000	BNT	GRB
212.490	47.250	1994	07	4.98064	BT	4B940704-

Continued on next column

Continued from previous column

RA deg	DEC deg	Year	Month	Day	Cat.	GRB Name
296.000	56.000	1994	07	5.31000	BNT	GRB
336.700	49.400	1994	07	6.12000	BNT	GRB
54.910	5.860	1994	07	6.24928	BT	4B940706-
265.110	26.400	1994	07	6.80872	BT	4B940706-
114.900	-23.000	1994	07	8.00000	BNT	GRB
176.600	-39.300	1994	07	8.44000	BNT	GRB
214.060	64.270	1994	07	8.60475	BT	4B940708-
53.400	35.810	1994	07	8.84002	BT	4B940708-
301.580	24.660	1994	07	8.86257	BT	4B940708-
72.020	-34.160	1994	07	9.47454	BT	4B940709
260.130	-8.620	1994	07	10.37571	BT	4B940710-
96.420	-36.590	1994	07	10.41353	BT	4B940710-
110.580	-25.250	1994	07	11.75980	BT	4B940711
66.700	-73.100	1994	07	12.00000	BNT	GRB
219.200	16.990	1994	07	12.03866	BT	4B940712
148.930	10.900	1994	07	13.45117	BT	4B940713
317.900	54.400	1994	07	13.50000	BNT	GRB
333.580	-42.100	1994	07	14.53776	BT	4B940714-
251.350	-32.090	1994	07	14.70002	BT	4B940714-
135.530	-19.200	1994	07	14.88773	BT	4B940714-
138.090	8.400	1994	07	15.67586	BT	4B940715-
214.870	-48.670	1994	07	15.95515	BT	4B940715-
238.490	-64.840	1994	07	16.40227	BT	4B940716-
127.190	88.100	1994	07	16.54297	BT	4B940716-
353.500	49.900	1994	07	16.56000	BNT	GRB
109.800	12.930	1994	07	17.14201	BT	4B940717-
102.210	-59.360	1994	07	17.36646	BT	4B940717-
110.130	48.870	1994	07	17.84927	BT	4B940717-
345.200	-32.600	1994	07	19.19000	BNT	GRB
252.300	31.100	1994	07	20.06000	BNT	GRB
337.300	-64.100	1994	07	20.38000	BNT	GRB
145.940	-62.530	1994	07	20.38432	BT	4B940720
339.900	47.900	1994	07	22.31000	BNT	GRB
280.340	-40.910	1994	07	22.34612	BT	4B940722
24.340	4.730	1994	07	24.96979	BT	4B940724
55.100	50.700	1994	07	25.75807	BT	4B940725
6.560	-49.890	1994	07	26.61098	BT	4B940726
342.100	25.400	1994	07	26.62000	BNT	GRB
154.560	0.280	1994	07	27.46271	BT	4B940727
312.500	-1.900	1994	07	27.50000	BNT	GRB
234.900	-76.200	1994	07	27.81000	BNT	GRB
42.570	-49.080	1994	07	28.12190	BT	4B940728-
291.220	4.450	1994	07	28.58796	BT	4B940728-
85.490	-39.870	1994	07	28.99924	BT	4B940728-
349.400	5.000	1994	07	29.06000	BNT	GRB
151.200	-52.900	1994	07	29.44000	BNT	GRB
79.700	-61.400	1994	07	30.44000	BNT	GRB
348.140	-62.860	1994	07	30.76208	BT	4B940730

Continued on next column

Continued from previous column

RA deg	DEC deg	Year	Month	Day	Cat.	GRB Name
121.340	-56.410	1994	07	31.02860	BT	4B940731
111.870	-60.890	1994	08	3.05781	BT	4B940803-
275.850	-6.930	1994	08	3.16669	BT	4B940803-
88.500	-37.300	1994	08	3.44000	BNT	GRB
160.100	40.000	1994	08	5.25853	BNT	GRB
138.000	42.000	1994	08	5.31581	BNT	GRB
199.060	53.280	1994	08	6.09010	BT	4B940806-
276.210	-31.330	1994	08	6.19362	BT	4B940806-
242.380	13.650	1994	08	6.39788	BT	4B940806-
26.750	-49.850	1994	08	6.82176	BT	4B940806-
81.670	50.650	1994	08	7.77160	BT	4B940807
289.830	45.440	1994	08	8.61763	BT	4B940808
150.300	40.900	1994	08	8.97728	BNT	GRB
155.880	-0.050	1994	08	9.31205	BT	4B940809
212.010	-17.470	1994	08	10.09910	BT	4B940810
145.300	42.000	1994	08	11.31000	BNT	GRB
75.800	78.230	1994	08	11.39514	BT	4B940811
340.490	-46.120	1994	08	12.01925	BT	4B940812-
241.200	-34.900	1994	08	12.31000	BNT	GRB
89.180	45.590	1994	08	12.50383	BT	4B940812-
231.220	-24.960	1994	08	12.63220	BT	4B940812-
272.100	17.300	1994	08	13.12000	BNT	GRB
103.800	-24.200	1994	08	14.50000	BNT	GRB
135.460	57.950	1994	08	14.84047	BT	4B940814
73.100	18.200	1994	08	15.75000	BNT	GRB
148.800	-18.700	1994	08	15.88000	BNT	GRB
167.300	43.700	1994	08	16.16566	BNT	GRB
198.300	-29.610	1994	08	16.44775	BT	4B940816
129.200	-35.600	1994	08	16.81831	BNT	GRB
280.840	3.470	1994	08	17.36130	BT	4B940817
160.500	-5.510	1994	08	19.98928	BT	4B940819
334.240	-45.200	1994	08	21.18354	BT	4B940821-
294.690	43.480	1994	08	21.91074	BT	4B940821-
134.400	-8.400	1994	08	22.39311	BT	4B940822
41.660	9.150	1994	08	23.13676	BT	4B940823-
101.080	12.230	1994	08	23.43887	BT	4B940823-
59.590	36.580	1994	08	23.68320	BT	4B940823-
96.610	-29.260	1994	08	25.04917	BT	4B940825
35.000	-17.900	1994	08	26.72405	BNT	GRB
93.590	-34.630	1994	08	26.87176	BT	4B940826
151.800	14.000	1994	08	26.93460	BNT	GRB
281.060	-4.520	1994	08	27.22091	BT	4B940827-
231.000	18.300	1994	08	27.28926	BNT	GRB
133.820	-16.970	1994	08	27.95015	BT	4B940827-
338.680	51.740	1994	08	28.28286	BT	4B940828
129.390	-15.480	1994	08	29.39395	BT	4B940829
193.660	25.660	1994	08	30.37497	BT	4B940830-
1.760	-6.290	1994	08	30.48425	BT	4B940830-

Continued on next column

Continued from previous column

RA deg	DEC deg	Year	Month	Day	Cat.	GRB Name
337.410	22.380	1994	08	30.54437	BT	4B940830-
270.220	8.320	1994	08	31.54532	BT	4B940831
54.830	-48.320	1994	09	1.89065	BT	4B940901
177.500	51.400	1994	09	2.25000	BNT	GRB
45.650	-11.390	1994	09	2.54743	BT	4B940902-
56.320	-7.430	1994	09	2.60407	BT	4B940902-
215.420	-65.970	1994	09	2.70840	BT	4B940902-
243.380	44.090	1994	09	4.16657	BT	4B940904
20.100	-38.600	1994	09	4.28605	BNT	GRB
281.290	-0.460	1994	09	5.92763	BT	4B940905
104.700	29.300	1994	09	6.75000	BNT	GRB
94.870	73.470	1994	09	7.35111	BT	4B940907
161.420	-31.810	1994	09	7.85856	GRA	GRB940907B
310.600	36.700	1994	09	8.88000	BNT	GRB
47.200	81.000	1994	09	9.00000	BNT	GRB
55.670	4.170	1994	09	9.20995	BT	4B940909
194.100	19.500	1994	09	9.50000	BNT	GRB
59.900	-30.900	1994	09	10.48709	BNT	GRB
332.010	-34.110	1994	09	10.81347	BT	4B940910-
224.280	8.620	1994	09	10.90645	BT	4B940910-
296.700	-74.200	1994	09	11.07987	BNT	GRB
35.530	-63.030	1994	09	11.68588	BT	4B940911
166.590	33.490	1994	09	13.61344	BT	4B940913
159.400	31.000	1994	09	13.94000	BNT	GRB
219.420	47.700	1994	09	15.28634	BT	4B940915
100.400	-49.300	1994	09	16.31000	BNT	GRB
113.740	26.820	1994	09	16.73668	BT	4B940916
303.300	-2.500	1994	09	17.31000	BNT	GRB
91.390	1.650	1994	09	17.71949	BT	4B940917
65.530	3.220	1994	09	18.61892	BT	4B940918
206.540	41.430	1994	09	19.02942	BT	4B940919
263.200	75.800	1994	09	20.08895	BNT	GRB
140.400	-9.100	1994	09	20.45383	BNT	GRB
112.050	24.570	1994	09	21.13111	BT	4B940921-
204.900	-17.770	1994	09	21.21404	BT	4B940921-
264.400	72.100	1994	09	23.31000	BNT	GRB
271.500	-54.200	1994	09	23.81000	BNT	GRB
82.300	12.800	1994	09	23.94000	BNT	GRB
227.100	11.800	1994	09	24.31000	BNT	GRB
154.500	-9.900	1994	09	25.00000	BNT	GRB
107.070	-20.390	1994	09	25.67502	BT	4B940925
98.200	19.000	1994	09	26.00147	BNT	GRB
48.700	-34.800	1994	09	26.06000	BNT	GRB
185.400	-11.000	1994	09	26.50000	BNT	GRB
153.870	19.130	1994	09	28.35972	BT	4B940928
78.100	58.600	1994	09	30.06000	BNT	GRB
78.700	32.000	1994	09	30.25000	BNT	GRB
170.800	69.000	1994	09	30.56000	BNT	GRB

Continued on next column

Continued from previous column

RA deg	DEC deg	Year	Month	Day	Cat.	GRB Name
129.900	10.500	1994	09	30.88000	BNT	GRB
301.800	30.600	1994	10	1.88000	BNT	GRB
186.900	35.040	1994	10	3.22035	BT	4B941003-
105.600	16.600	1994	10	3.70941	BT	4B941003-
155.900	2.000	1994	10	5.00000	BNT	GRB
251.490	7.010	1994	10	5.16990	BT	4B941005-
104.000	-30.100	1994	10	5.31000	BNT	GRB
329.900	44.950	1994	10	5.46449	BT	4B941005-
84.000	55.700	1994	10	5.94473	BNT	GRB
174.400	80.800	1994	10	6.40492	BNT	GRB
208.540	-36.370	1994	10	6.54507	BT	4B941006
0.700	78.000	1994	10	8.06000	BNT	GRB
305.620	-52.180	1994	10	8.56450	BT	4B941008
277.400	-8.800	1994	10	8.75000	BNT	GRB
352.230	-57.250	1994	10	9.14999	BT	4B941009
356.600	-61.800	1994	10	10.19000	BNT	GRB
211.100	-34.000	1994	10	10.81640	BNT	GRB
290.000	-58.400	1994	10	11.12000	BNT	GRB
324.700	-47.300	1994	10	11.38000	BNT	GRB
123.550	32.430	1994	10	11.69457	BT	4B941011
47.310	48.510	1994	10	12.12538	BT	4B941012
152.370	-24.320	1994	10	13.96287	BT	4B941013
31.660	7.430	1994	10	14.38898	BT	4B941014-
164.780	19.740	1994	10	14.96895	BT	4B941014-
24.600	31.500	1994	10	16.00000	BNT	GRB
27.800	-31.030	1994	10	16.34716	BT	4B941016
301.550	9.810	1994	10	17.43025	BT	4B941017-
207.370	-0.130	1994	10	17.68353	BT	4B941017-
55.740	-16.280	1994	10	18.25152	BT	4B941018-
329.020	-1.730	1994	10	18.35883	BT	4B941018-
54.600	-3.830	1994	10	18.49487	BT	4B941018-
6.090	-48.150	1994	10	18.54735	BT	4B941018-
55.000	-0.200	1994	10	18.56000	BNT	GRB
308.900	35.700	1994	10	18.88000	BNT	GRB
330.200	15.800	1994	10	19.39202	BNT	GRB
31.200	67.900	1994	10	20.25000	BNT	GRB
158.990	-2.720	1994	10	20.76390	BT	4B941020-
49.990	-24.740	1994	10	20.83713	BT	4B941020-
230.000	8.500	1994	10	22.39791	BNT	GRB
38.800	23.400	1994	10	22.44000	BNT	GRB
108.700	19.200	1994	10	23.06000	BNT	GRB
338.900	65.400	1994	10	23.19000	BNT	GRB
212.280	-82.350	1994	10	23.19065	BT	4B941023-
354.020	56.520	1994	10	23.51071	BT	4B941023-
205.960	-6.530	1994	10	26.11986	BT	4B941026-
278.100	-44.600	1994	10	26.25000	BNT	GRB
109.060	33.560	1994	10	26.92419	BT	4B941026-
66.190	81.150	1994	10	31.03266	BT	4B941031-

Continued on next column

Continued from previous column

RA deg	DEC deg	Year	Month	Day	Cat.	GRB Name
39.660	-57.290	1994	10	31.19617	BT	4B941031-
44.200	24.700	1994	10	31.38000	BNT	GRB
217.270	-24.160	1994	10	31.47360	BT	4B941031-
251.600	48.500	1994	10	31.56000	BNT	GRB
250.900	0.900	1994	11	1.44000	BNT	GRB
236.640	59.280	1994	11	1.85796	BT	4B941101
113.900	-39.200	1994	11	2.69000	BNT	GRB
345.300	18.500	1994	11	4.44000	BNT	GRB
52.100	63.300	1994	11	8.56000	BNT	GRB
36.620	66.590	1994	11	9.00043	BT	4B941109
329.800	-14.800	1994	11	9.25000	BNT	GRB
123.790	-38.140	1994	11	10.19751	BT	4B941110-
303.080	13.510	1994	11	10.61656	BT	4B941110-
97.540	32.650	1994	11	11.09723	BT	4B941111
197.820	86.190	1994	11	13.13429	BT	4B941113
98.040	35.410	1994	11	14.08516	BT	4B941114
159.960	-27.890	1994	11	15.26586	BT	4B941115
241.200	-14.500	1994	11	16.18000	BNT	GRB
284.600	30.500	1994	11	16.38000	BNT	GRB
125.940	-59.460	1994	11	16.80590	BT	4B941116
1.200	30.100	1994	11	19.06000	BNT	GRB
182.500	21.980	1994	11	19.81308	BT	4B941119
5.080	-46.600	1994	11	21.39286	BT	4B941121-
35.450	-66.370	1994	11	21.72567	BT	4B941121-
253.780	-6.140	1994	11	22.55111	BT	4B941122-
158.580	32.330	1994	11	22.85619	BT	4B941122-
38.400	52.300	1994	11	23.69000	BNT	GRB
74.550	22.050	1994	11	23.78098	BT	4B941123-
197.900	-6.200	1994	11	23.82677	BT	4B941123-
240.900	21.200	1994	11	25.44000	BNT	GRB
240.920	-18.480	1994	11	25.91980	BT	4B941125
13.810	-63.050	1994	11	26.01441	BT	4B941126-
306.490	21.650	1994	11	26.16335	BT	4B941126-
264.740	-61.300	1994	11	26.51529	BT	4B941126-
82.150	-32.980	1994	11	26.70442	BT	4B941126-
114.170	-32.580	1994	11	26.83100	BT	4B941126-
69.170	44.970	1994	11	27.60438	BT	4B941127
32.720	-72.830	1994	11	28.65066	BT	4B941128-
19.570	-33.950	1994	11	28.77879	BT	4B941128-
83.900	-11.200	1994	12	1.25000	BNT	GRB
282.980	24.370	1994	12	2.14742	BT	4B941202
309.200	30.200	1994	12	2.72598	BNT	GRB
3.050	-53.850	1994	12	3.71976	BT	4B941203
273.200	-46.500	1994	12	5.12000	BNT	GRB
126.250	3.540	1994	12	5.34418	BT	4B941205
188.500	-36.500	1994	12	10.38000	BNT	GRB
131.000	-32.000	1994	12	11.19000	BNT	GRB
222.000	15.100	1994	12	11.98646	BNT	GRB

Continued on next column

Continued from previous column

RA deg	DEC deg	Year	Month	Day	Cat.	GRB Name
331.100	-7.800	1994	12	13.55141	BNT	GRB
220.000	-54.770	1994	12	14.58936	BT	4B941214
134.580	23.400	1994	12	15.01817	BT	4B941215-
157.750	-18.080	1994	12	15.33948	BT	4B941215-
250.600	33.000	1994	12	16.44000	BNT	GRB
130.170	-80.370	1994	12	17.16772	BT	4B941217
253.300	1.600	1994	12	18.21171	BNT	GRB
185.700	48.300	1994	12	18.48642	BT	4B941218
69.700	-6.400	1994	12	22.19000	BNT	GRB
46.300	68.000	1994	12	22.25000	BNT	GRB
28.230	-39.160	1994	12	22.31420	BT	4B941222
224.920	46.620	1994	12	24.15432	BT	4B941224
138.240	3.910	1994	12	26.99478	BT	4B941226
353.780	-49.230	1994	12	28.31923	BT	4B941228
72.940	-64.960	1994	12	29.59655	BT	4B941229-
255.180	39.990	1994	12	29.95207	BT	4B941229-
210.670	-2.780	1994	12	30.77761	BT	4B941230-
149.000	14.000	1994	12	30.81000	BNT	GRB
172.720	-36.110	1994	12	30.87030	BT	4B941230-
173.250	39.760	1994	12	30.98876	BT	4B941230-
185.690	27.740	1995	01	1.06459	BT	4B950101
39.070	-34.940	1995	01	2.11490	BT	4B950102-
98.160	-3.160	1995	01	2.31699	BT	4B950102-
282.310	14.100	1995	01	3.67383	BT	4B950103
339.700	75.600	1995	01	3.81000	BNT	GRB
9.800	7.400	1995	01	4.25000	BNT	GRB
303.260	-15.630	1995	01	4.30462	BT	4B950104
273.200	-24.400	1995	01	4.31000	BNT	GRB
227.300	51.200	1995	01	4.38000	BNT	GRB
14.000	-58.300	1995	01	4.88000	BNT	GRB
23.310	-62.860	1995	01	5.22839	BT	4B950105
196.300	-1.700	1995	01	5.71074	BNT	GRB
17.710	-12.940	1995	01	8.08635	BT	4B950108
294.100	7.100	1995	01	9.24649	BNT	GRB
238.660	-34.730	1995	01	10.78345	BT	4B950110
336.240	-64.780	1995	01	11.19980	BT	4B950111-
19.570	-10.220	1995	01	11.51285	BT	4B950111-
24.300	-5.800	1995	01	11.56000	BNT	GRB
159.400	26.300	1995	01	12.71909	BNT	GRB
313.910	-24.150	1995	01	14.04215	BT	4B950114-
284.590	25.880	1995	01	14.95068	BT	4B950114-
38.940	14.620	1995	01	15.28693	BT	4B950115-
317.440	19.460	1995	01	15.98586	BT	4B950115-
125.700	-2.400	1995	01	16.33364	BNT	GRB
285.210	29.080	1995	01	17.06669	BT	4B950117-
323.700	-79.600	1995	01	17.56812	BNT	GRB
294.070	-48.600	1995	01	17.64591	BT	4B950117-
102.970	58.300	1995	01	18.51609	BT	4B950118-

Continued on next column

Continued from previous column

RA deg	DEC deg	Year	Month	Day	Cat.	GRB Name
38.200	-55.510	1995	01	18.71881	BT	4B950118-
340.310	-0.700	1995	01	19.92971	BT	4B950119
197.380	36.460	1995	01	20.45128	BT	4B950120
235.410	-76.800	1995	01	23.32088	BT	4B950123
345.600	60.000	1995	01	23.61236	BNT	GRB
195.800	-67.100	1995	01	23.62000	BNT	GRB
322.700	-37.500	1995	01	26.98757	BNT	GRB
254.620	5.340	1995	01	29.76110	BT	4B950129-
166.100	19.900	1995	01	29.81000	BNT	GRB
246.000	-48.900	1995	01	29.81000	BNT	GRB
346.650	-50.900	1995	01	29.91980	BT	4B950129-
56.640	-32.750	1995	01	30.88380	BT	4B950130
17.890	19.540	1995	01	31.48306	BT	4B950131
319.400	-58.800	1995	01	31.94000	BNT	GRB
274.600	42.700	1995	02	3.12000	BNT	GRB
69.590	-14.450	1995	02	6.44708	BT	4B950206-
241.650	-49.690	1995	02	6.82340	BT	4B950206-
169.330	84.300	1995	02	7.03219	BT	4B950207-
37.480	26.140	1995	02	7.30817	BT	4B950207-
170.600	-21.100	1995	02	7.81000	BNT	GRB
336.960	54.190	1995	02	8.09056	BT	4B950208
289.800	37.500	1995	02	8.18475	BNT	GRB
154.550	-27.480	1995	02	10.09748	BT	4B950210
242.800	-3.700	1995	02	10.81000	BNT	GRB
9.510	52.650	1995	02	11.10067	BT	4B950211-
325.600	3.300	1995	02	11.19000	BNT	GRB
64.350	-55.020	1995	02	11.83876	BT	4B950211-
256.820	47.280	1995	02	11.97668	BT	4B950211-
119.300	-17.900	1995	02	13.81000	BNT	GRB
123.800	49.590	1995	02	16.88828	BT	4B950216
26.800	-69.900	1995	02	20.38000	BNT	GRB
294.310	-32.150	1995	02	21.86465	BT	4B950221-
204.220	86.800	1995	02	21.98843	BT	4B950221-
325.560	-21.990	1995	02	23.09941	BT	4B950223
324.600	61.500	1995	02	24.38000	BNT	GRB
67.130	43.900	1995	02	25.63173	BT	4B950225-
75.970	-70.440	1995	02	25.71502	BT	4B950225-
158.990	-13.900	1995	02	26.61732	BT	4B950226
93.180	51.910	1995	02	27.58626	BT	4B950227
101.000	-42.700	1995	02	28.56000	BNT	GRB
307.960	12.920	1995	03	1.87686	BT	4B950301
206.650	60.220	1995	03	2.99507	BT	4B950302
113.580	-63.960	1995	03	3.26897	BT	4B950303
49.300	-27.100	1995	03	4.12000	BNT	GRB
242.070	-69.100	1995	03	4.43586	BT	4B950304
49.600	-5.600	1995	03	5.52938	BNT	GRB
197.200	-11.120	1995	03	5.62853	BT	4B950305
335.400	33.600	1995	03	5.69000	BNT	GRB

Continued on next column

Continued from previous column

RA deg	DEC deg	Year	Month	Day	Cat.	GRB Name
138.300	72.300	1995	03	8.08569	BNT	GRB
127.500	7.300	1995	03	8.25626	BNT	GRB
344.190	33.640	1995	03	10.90735	BT	4B950310
349.310	22.690	1995	03	11.46679	BT	4B950311
338.330	22.170	1995	03	12.78219	BT	4B950312
95.980	-3.040	1995	03	13.31775	BT	4B950313
30.800	-38.100	1995	03	13.81000	BNT	GRB
85.000	-12.960	1995	03	17.21942	BT	4B950317-
47.290	27.530	1995	03	17.82218	BT	4B950317-
74.670	9.530	1995	03	17.83469	BT	4B950317-
274.740	-2.220	1995	03	20.00307	BT	4B950320
214.000	-19.900	1995	03	20.25000	BNT	GRB
190.300	-2.900	1995	03	20.56000	BNT	GRB
136.900	25.600	1995	03	20.75000	BNT	GRB
245.620	-74.430	1995	03	21.14309	BT	4B950321
208.900	-57.600	1995	03	23.56174	BNT	GRB
18.800	-70.400	1995	03	25.25000	BNT	GRB
52.810	50.500	1995	03	25.29912	BT	4B950325-
66.220	-11.560	1995	03	25.73370	BT	4B950325-
54.120	38.010	1995	03	27.30494	BT	4B950327-
274.400	20.460	1995	03	27.99157	BT	4B950327-
29.650	-14.400	1995	03	28.90271	BT	4B950328
7.100	32.600	1995	03	30.81000	BNT	GRB
185.800	-20.000	1995	03	31.01510	BNT	GRB
197.930	56.950	1995	04	1.49354	BT	4B950401-
86.060	43.750	1995	04	1.86382	BT	4B950401-
10.400	30.000	1995	04	3.19000	BNT	GRB
36.390	10.710	1995	04	3.55541	BT	4B950403-
184.640	56.550	1995	04	3.98179	BT	4B950403-
13.740	57.500	1995	04	5.17660	BT	4B950405-
326.160	47.790	1995	04	5.43078	BT	4B950405-
47.400	45.900	1995	04	6.81000	BNT	GRB
118.800	-1.000	1995	04	7.14291	BNT	GRB
316.600	38.700	1995	04	7.25000	BNT	GRB
47.140	-58.720	1995	04	9.27269	BT	4B950409
322.300	-23.280	1995	04	10.79185	BT	4B950410
1.700	-32.700	1995	04	10.94000	BNT	GRB
119.600	-66.700	1995	04	11.50000	BNT	GRB
314.400	-79.200	1995	04	11.62000	BNT	GRB
317.360	2.650	1995	04	12.03338	BT	4B950412
347.900	83.700	1995	04	13.12000	BNT	GRB
261.260	64.370	1995	04	13.62729	BT	4B950413
322.500	79.200	1995	04	14.81000	BNT	GRB
349.600	13.400	1995	04	16.12000	BNT	GRB
186.320	30.200	1995	04	16.56042	BT	4B950416-
240.840	-10.930	1995	04	16.95322	BT	4B950416-
159.900	-34.000	1995	04	17.31000	BNT	GRB
136.170	-73.290	1995	04	17.50464	BT	4B950417

Continued on next column

Continued from previous column

RA deg	DEC deg	Year	Month	Day	Cat.	GRB Name
92.400	3.260	1995	04	18.96986	BT	4B950418
50.240	54.460	1995	04	19.47485	BT	4B950419
281.030	-46.470	1995	04	20.63471	BT	4B950420
317.900	-67.300	1995	04	21.25000	BNT	GRB
72.010	-63.060	1995	04	21.52072	BT	4B950421
13.900	47.900	1995	04	21.61234	BNT	GRB
189.600	68.700	1995	04	22.19000	BNT	GRB
84.800	-15.900	1995	04	24.25000	BNT	GRB
163.160	-35.250	1995	04	25.01064	BT	4B950425
226.100	2.500	1995	04	28.69000	BNT	GRB
47.600	-82.700	1995	04	30.12000	BNT	GRB
11.200	-80.500	1995	04	30.31000	BNT	GRB
57.340	29.020	1995	04	30.62765	BT	4B950430-
125.410	61.410	1995	04	30.69001	BT	4B950430-
330.000	-46.600	1995	05	1.06000	BNT	GRB
296.920	27.780	1995	05	1.14241	BT	4B950501
164.650	-27.860	1995	05	2.07413	BT	4B950502
157.400	14.200	1995	05	2.85916	BNT	GRB
159.160	-7.190	1995	05	3.77512	BT	4B950503
359.000	38.500	1995	05	3.94000	BNT	GRB
143.870	-70.210	1995	05	5.52308	BT	4B950505
11.300	-83.100	1995	05	6.56000	BNT	GRB
335.800	84.340	1995	05	6.97584	BT	4B950506
302.740	78.820	1995	05	9.53455	BT	4B950509-
44.440	22.930	1995	05	9.96951	BT	4B950509-
332.200	25.500	1995	05	10.00000	BNT	GRB
188.570	-65.480	1995	05	10.32500	BT	4B950510
66.200	68.800	1995	05	10.38000	BNT	GRB
246.700	13.000	1995	05	10.75000	BNT	GRB
125.300	32.400	1995	05	10.76848	BNT	GRB
231.700	-37.100	1995	05	10.94000	BNT	GRB
343.300	-32.400	1995	05	10.94000	BNT	GRB
255.200	-72.400	1995	05	11.94000	BNT	GRB
271.600	-72.910	1995	05	13.94565	BT	4B950513
266.100	-28.800	1995	05	14.75000	BNT	GRB
76.400	17.400	1995	05	14.88000	BNT	GRB
294.800	10.200	1995	05	15.62000	BNT	GRB
313.600	-26.000	1995	05	17.00000	BNT	GRB
290.100	-20.000	1995	05	17.12934	BNT	GRB
20.820	-47.150	1995	05	17.45574	BT	4B950517
162.700	-38.800	1995	05	18.12000	BNT	GRB
32.600	-62.400	1995	05	18.81000	BNT	GRB
155.100	-17.800	1995	05	19.44000	BNT	GRB
175.260	42.370	1995	05	19.75059	BT	4B950519
318.800	-51.800	1995	05	19.94000	BNT	GRB
142.000	-7.500	1995	05	20.77909	BNT	GRB
29.600	9.900	1995	05	21.10644	BNT	GRB
22.210	-26.860	1995	05	21.29117	BT	4B950521

Continued on next column

Continued from previous column

RA deg	DEC deg	Year	Month	Day	Cat.	GRB Name
65.900	25.800	1995	05	21.44000	BNT	GRB
88.520	-81.910	1995	05	22.27659	BT	4B950522-
155.100	71.300	1995	05	22.81000	BNT	GRB
109.560	19.280	1995	05	22.98707	BT	4B950522-
85.630	43.080	1995	05	23.23575	BT	4B950523-
38.400	12.700	1995	05	23.50020	BNT	GRB
15.000	18.900	1995	05	23.69000	BNT	GRB
72.160	38.910	1995	05	23.76927	BT	4B950523-
186.410	0.450	1995	05	24.17244	BT	4B950524
291.600	-1.600	1995	05	24.88000	BNT	GRB
322.736	68.062	1995	05	26.19229	K/W	950526_T16613
270.800	5.700	1995	05	26.92648	BNT	GRB
239.060	-20.820	1995	05	29.42701	BT	4B950529
46.400	-5.600	1995	05	30.19000	BNT	GRB
115.390	-21.600	1995	05	30.63675	BT	4B950530
55.400	11.800	1995	05	31.25000	BNT	GRB
274.710	17.790	1995	05	31.44427	BT	4B950531
48.400	-16.700	1995	06	1.50000	BNT	GRB
41.450	-58.500	1995	06	2.29622	BT	4B950602
43.500	-31.300	1995	06	2.56000	BNT	GRB
51.400	-33.700	1995	06	3.25000	BNT	GRB
256.200	83.200	1995	06	4.06000	BNT	GRB
114.200	40.800	1995	06	5.12000	BNT	GRB
316.600	-26.700	1995	06	7.42693	BNT	GRB
57.560	-53.600	1995	06	8.94065	BT	4B950608
100.100	-17.650	1995	06	10.07927	BT	4B950610
220.340	-79.560	1995	06	11.23738	BT	4B950611-
269.800	-69.500	1995	06	11.24447	BNT	GRB
147.200	11.890	1995	06	11.54595	BT	4B950611-
205.200	35.200	1995	06	11.94000	BNT	GRB
254.090	-0.480	1995	06	12.68729	BT	4B950612
137.400	-68.200	1995	06	14.00000	BNT	GRB
125.500	27.400	1995	06	14.26198	BNT	GRB
310.200	-48.500	1995	06	15.12000	BNT	GRB
69.200	65.900	1995	06	16.38727	BNT	GRB
297.700	-50.700	1995	06	16.44000	BNT	GRB
143.700	-60.700	1995	06	17.12031	BNT	GRB
290.940	-13.390	1995	06	19.22824	BT	4B950619
131.800	56.600	1995	06	19.56000	BNT	GRB
45.720	6.130	1995	06	20.03095	BT	4B950620
231.000	37.500	1995	06	20.62000	BNT	GRB
339.600	-46.900	1995	06	21.81000	BNT	GRB
257.600	-47.100	1995	06	21.94000	BNT	GRB
213.400	-1.500	1995	06	22.81000	BNT	GRB
136.900	20.800	1995	06	23.28098	BNT	GRB
295.960	36.460	1995	06	24.14586	BT	4B950624-
121.600	-27.000	1995	06	24.31200	BNT	GRB
133.800	-54.800	1995	06	24.75000	BNT	GRB

Continued on next column

Continued from previous column

RA deg	DEC deg	Year	Month	Day	Cat.	GRB Name
165.370	14.990	1995	06	24.97319	BT	4B950624-
133.400	7.800	1995	06	25.12000	BNT	GRB
137.200	42.300	1995	06	25.12000	BNT	GRB
271.640	-21.150	1995	06	25.16899	BT	4B950625
355.400	-55.800	1995	06	26.29273	BNT	GRB
147.100	-39.700	1995	06	26.75000	BNT	GRB
242.270	-49.370	1995	06	27.65715	BT	4B950627
180.000	-55.880	1995	06	28.02484	BT	4B950628
279.600	55.000	1995	06	28.88000	BNT	GRB
288.100	-5.000	1995	06	29.06000	BNT	GRB
83.130	9.470	1995	06	29.42867	BT	4B950629
174.280	21.480	1995	06	30.88237	BT	4B950630
320.140	-20.820	1995	07	1.14766	BT	4B950701-
214.800	-33.500	1995	07	1.25000	BNT	GRB
346.270	37.740	1995	07	1.27473	BT	4B950701-
160.400	36.500	1995	07	3.31405	BNT	GRB
49.500	10.000	1995	07	3.35347	BNT	GRB
192.400	24.600	1995	07	4.44000	BNT	GRB
248.800	68.000	1995	07	5.12000	BNT	GRB
210.500	-9.300	1995	07	5.94735	BNT	GRB
28.610	31.520	1995	07	6.49463	BT	4B950706
9.000	-10.600	1995	07	9.88000	BNT	GRB
55.900	-67.100	1995	07	10.10869	BNT	GRB
85.810	-24.010	1995	07	11.15959	BT	4B950711
286.670	30.040	1995	07	13.37242	BT	4B950713
258.600	-82.700	1995	07	13.69000	BNT	GRB
342.800	-27.100	1995	07	13.75000	BNT	GRB
29.000	64.030	1995	07	14.07161	BT	4B950714
62.700	-54.100	1995	07	15.19000	BNT	GRB
150.300	-45.700	1995	07	16.26963	BNT	GRB
95.940	5.090	1995	07	16.96008	BT	4B950716
214.000	-3.000	1995	07	17.12000	BNT	GRB
129.600	4.100	1995	07	17.81000	BNT	GRB
200.430	31.650	1995	07	18.74693	BT	4B950718
187.300	24.500	1995	07	19.38000	BNT	GRB
75.800	17.200	1995	07	21.56000	BNT	GRB
74.200	25.800	1995	07	22.75000	BNT	GRB
294.800	44.700	1995	07	23.75786	BNT	GRB
243.700	-78.000	1995	07	23.85194	BNT	GRB
12.540	-40.720	1995	07	26.59697	BT	4B950726
295.300	-4.600	1995	07	27.38000	BNT	GRB
183.840	-45.560	1995	07	28.37748	BT	4B950728
277.400	26.200	1995	07	28.50000	BNT	GRB
301.100	-78.400	1995	07	28.50000	BNT	GRB
324.500	-50.500	1995	07	29.25000	BNT	GRB
251.810	25.340	1995	07	30.41771	BT	4B950730
218.300	-13.400	1995	07	30.88000	BNT	GRB
138.120	7.520	1995	08	1.33078	BT	4B950801

Continued on next column

Continued from previous column

RA deg	DEC deg	Year	Month	Day	Cat.	GRB Name
29.170	-6.790	1995	08	2.23840	BT	4B950802
134.700	57.630	1995	08	3.75894	BT	4B950803
287.450	56.260	1995	08	4.08258	BT	4B950804-
186.670	24.940	1995	08	4.52520	BT	4B950804-
35.500	41.400	1995	08	4.56000	BNT	GRB
79.860	-39.380	1995	08	5.15573	BT	4B950805-
318.660	57.760	1995	08	5.43369	BT	4B950805-
12.000	25.000	1995	08	5.88000	BNT	GRB
272.750	-31.350	1995	08	6.00983	BT	4B950806-
164.480	35.730	1995	08	6.83969	BT	4B950806-
149.700	80.360	1995	08	8.15017	BT	4B950808
51.090	14.060	1995	08	9.99473	BT	4B950809
30.380	5.760	1995	08	10.12509	BT	4B950810
58.020	3.790	1995	08	12.65427	BT	4B950812
271.500	-35.900	1995	08	15.25000	BNT	GRB
262.810	3.210	1995	08	15.88523	BT	4B950815
196.000	32.400	1995	08	16.75000	BNT	GRB
182.250	39.810	1995	08	17.84659	BT	4B950817
278.650	33.870	1995	08	18.05791	BT	4B950818
279.500	-7.800	1995	08	19.05253	BNT	GRB
339.480	-61.250	1995	08	19.98303	BT	4B950819
245.240	-66.400	1995	08	22.15914	BT	4B950822-
125.670	-17.240	1995	08	22.38852	BT	4B950822-
240.900	86.100	1995	08	26.12000	BNT	GRB
118.600	5.100	1995	08	27.06000	BNT	GRB
323.100	-52.340	1995	08	30.17645	BT	4B950830-
330.070	-64.670	1995	08	30.43507	BT	4B950830-
131.380	46.220	1995	09	1.01789	BT	4B950901-
316.390	13.380	1995	09	1.46690	BT	4B950901-
264.200	69.350	1995	09	1.98571	BT	4B950901-
119.500	43.700	1995	09	3.22439	BNT	GRB
344.100	0.700	1995	09	3.38924	BNT	GRB
181.300	-18.200	1995	09	4.31000	BNT	GRB
169.520	64.420	1995	09	4.32154	BT	4B950904-
258.860	47.480	1995	09	4.60983	BT	4B950904-
99.000	44.600	1995	09	5.62000	BNT	GRB
302.120	49.460	1995	09	7.19036	BT	4B950907
85.460	4.310	1995	09	8.08667	BT	4B950908-
178.700	6.950	1995	09	8.35164	BT	4B950908-
216.360	-0.110	1995	09	9.98903	BT	4B950909
226.940	-10.730	1995	09	11.27258	BT	4B950911-
20.930	45.900	1995	09	11.36487	BT	4B950911-
162.400	-14.520	1995	09	11.61406	BT	4B950911-
69.700	54.030	1995	09	11.97281	BT	4B950911-
333.000	-34.300	1995	09	12.38000	BNT	GRB
45.540	-51.270	1995	09	14.08884	BT	4B950914-
313.600	72.390	1995	09	14.16736	BT	4B950914-
57.860	-34.950	1995	09	14.81969	BT	4B950914-

Continued on next column

Continued from previous column

RA deg	DEC deg	Year	Month	Day	Cat.	GRB Name
278.000	9.000	1995	09	16.03404	BNT	GRB
13.180	-0.060	1995	09	16.41050	BT	4B950916-
192.720	24.170	1995	09	16.89116	BT	4B950916-
292.870	-53.350	1995	09	17.81441	BT	4B950917-
339.870	-1.470	1995	09	17.99142	BT	4B950917-
39.270	53.620	1995	09	18.49208	BT	4B950918
74.680	32.450	1995	09	19.59545	BT	4B950919-
347.300	37.970	1995	09	19.98536	BT	4B950919-
164.800	42.000	1995	09	20.25000	BNT	GRB
350.710	-41.410	1995	09	20.75331	BT	4B950920
158.070	47.010	1995	09	21.24244	BT	4B950921-
87.740	6.000	1995	09	21.47708	BT	4B950921-
99.600	-25.500	1995	09	21.90150	BNT	GRB
244.650	39.770	1995	09	22.17933	BT	4B950922-
160.790	37.210	1995	09	22.30013	BT	4B950922-
167.650	46.690	1995	09	26.73980	BT	4B950926
184.300	-48.400	1995	09	30.75000	BNT	GRB
147.300	29.400	1995	10	1.44000	BNT	GRB
127.100	-0.300	1995	10	1.50000	BNT	GRB
214.040	50.730	1995	10	1.92645	BT	4B951001
46.050	-1.880	1995	10	2.89799	BT	4B951002
9.400	34.400	1995	10	3.23897	BNT	GRB
39.820	87.250	1995	10	3.38796	BT	4B951003
22.120	-4.480	1995	10	4.43321	BT	4B951004
214.000	-82.600	1995	10	5.19000	BNT	GRB
204.220	8.660	1995	10	7.05288	BT	4B951007
265.700	-30.500	1995	10	9.19000	BNT	GRB
163.100	-18.000	1995	10	10.06000	BNT	GRB
1.900	-14.400	1995	10	10.12000	BNT	GRB
159.500	-0.100	1995	10	10.88000	BNT	GRB
126.550	39.350	1995	10	10.88361	BT	4B951010
181.200	-64.300	1995	10	11.61553	BNT	GRB
40.860	-57.580	1995	10	11.89906	BT	4B951011
299.483	-5.263	1995	10	13.66084	K/W	951013_T57097
294.100	-6.500	1995	10	13.69000	BNT	GRB
252.680	48.610	1995	10	13.97094	BT	4B951013
184.200	8.100	1995	10	14.25000	BNT	GRB
167.850	-20.640	1995	10	14.50421	BT	4B951014-
318.920	38.080	1995	10	14.95024	BT	4B951014-
155.240	10.580	1995	10	15.53684	BT	4B951015-
2.990	-12.300	1995	10	15.68587	BT	4B951015-
35.820	-24.360	1995	10	16.02872	BT	4B951016-
118.990	-49.090	1995	10	16.82881	BT	4B951016-
199.800	-40.200	1995	10	17.75000	BNT	GRB
197.600	-38.900	1995	10	18.50000	BNT	GRB
39.100	39.800	1995	10	18.88000	BNT	GRB
161.510	-87.810	1995	10	19.55839	BT	4B951019
199.300	-48.300	1995	10	20.37851	BNT	GRB

Continued on next column

Continued from previous column

RA deg	DEC deg	Year	Month	Day	Cat.	GRB Name
356.430	6.640	1995	10	20.49854	BT	4B951020
340.000	4.400	1995	10	20.74177	BNT	GRB
61.700	81.500	1995	10	20.94000	BNT	GRB
109.600	-20.600	1995	10	22.65088	BNT	GRB
289.900	-37.300	1995	10	23.00000	BNT	GRB
164.000	15.300	1995	10	25.30725	BNT	GRB
223.200	-68.800	1995	10	25.69000	BNT	GRB
265.550	29.070	1995	10	28.06245	BT	4B951028
115.390	28.660	1995	10	30.22683	BT	4B951030-
105.830	18.710	1995	10	30.36086	BT	4B951030-
85.500	21.550	1995	10	30.47478	BT	4B951030-
217.440	45.950	1995	11	1.41947	BT	4B951101
337.480	-57.220	1995	11	2.02211	BT	4B951102-
138.570	46.990	1995	11	2.24509	BT	4B951102-
189.640	-35.230	1995	11	2.33213	BT	4B951102-
40.390	27.260	1995	11	4.06786	BT	4B951104-
264.530	-21.810	1995	11	4.23133	BT	4B951104-
189.390	-47.720	1995	11	4.73269	BT	4B951104-
17.900	43.110	1995	11	5.16385	BT	4B951105
180.000	-12.820	1995	11	7.30405	BT	4B951107-
11.990	29.340	1995	11	7.73100	BT	4B951107-
148.870	39.850	1995	11	7.94329	BT	4B951107-
17.680	-16.380	1995	11	10.96513	BT	4B951110
31.410	69.550	1995	11	11.89778	BT	4B951111
308.700	33.700	1995	11	11.94000	BNT	GRB
98.830	65.420	1995	11	12.58488	BT	4B951112-
324.600	-47.600	1995	11	12.65435	BNT	GRB
132.520	49.080	1995	11	12.76944	BT	4B951112-
225.700	16.900	1995	11	12.81000	BNT	GRB
355.110	-44.760	1995	11	13.97634	BT	4B951113
296.000	-45.400	1995	11	14.94000	BNT	GRB
193.800	-37.500	1995	11	15.11197	BNT	GRB
11.560	-27.250	1995	11	16.35403	BT	4B951116
285.790	37.050	1995	11	17.11711	BT	4B951117-
114.400	44.400	1995	11	17.38000	BNT	GRB
74.530	52.180	1995	11	17.70694	BT	4B951117-
133.100	10.000	1995	11	18.56000	BNT	GRB
11.150	74.960	1995	11	19.06459	BT	4B951119-
306.460	-40.710	1995	11	19.34528	BT	4B951119-
78.950	24.860	1995	11	19.85435	BT	4B951119-
136.910	-33.190	1995	11	20.14179	BT	4B951120-
89.870	64.320	1995	11	20.35799	BT	4B951120-
199.300	16.700	1995	11	20.38000	BNT	GRB
206.540	-21.700	1995	11	21.25788	BT	4B951121
4.700	16.300	1995	11	21.78691	BNT	GRB
235.500	-32.100	1995	11	23.39171	BNT	GRB
53.750	24.500	1995	11	23.75701	BT	4B951123
73.320	51.680	1995	11	24.24605	BT	4B951124-

Continued on next column

Continued from previous column

RA deg	DEC deg	Year	Month	Day	Cat.	GRB Name
157.300	47.600	1995	11	24.31000	BNT	GRB
117.180	-43.370	1995	11	24.45061	BT	4B951124-
277.280	-3.220	1995	11	25.02196	BT	4B951125
56.900	56.000	1995	11	26.44000	BNT	GRB
189.920	44.590	1995	11	27.51019	BT	4B951127
239.800	-18.100	1995	11	27.62000	BNT	GRB
141.900	56.300	1995	11	28.36610	BNT	GRB
250.640	50.310	1995	11	28.43520	BT	4B951128-
43.210	84.220	1995	11	28.90965	BT	4B951128-
177.400	34.200	1995	11	29.31000	BNT	GRB
328.060	-35.760	1995	12	2.45255	BT	4B951202
235.400	-78.400	1995	12	2.65707	BNT	GRB
279.840	-19.250	1995	12	3.04616	BT	4B951203
275.600	-13.800	1995	12	3.06000	BNT	GRB
137.200	-49.600	1995	12	3.57848	BNT	GRB
257.790	-24.010	1995	12	5.25207	BT	4B951205
73.500	-12.900	1995	12	7.38000	BNT	GRB
189.670	1.150	1995	12	7.56123	BT	4B951207
353.000	70.150	1995	12	8.22704	BT	4B951208-
248.400	37.800	1995	12	8.41385	BNT	GRB
57.660	-28.150	1995	12	8.49124	BT	4B951208-
72.650	-68.480	1995	12	8.97515	BT	4B951208-
316.500	50.500	1995	12	9.35950	BNT	GRB
41.700	-35.300	1995	12	9.38000	BNT	GRB
138.930	2.150	1995	12	9.81812	BT	4B951209
333.700	33.400	1995	12	10.18164	BNT	GRB
99.200	54.900	1995	12	10.85021	BNT	GRB
229.700	-29.900	1995	12	11.00000	BNT	GRB
81.160	-18.930	1995	12	11.24721	BT	4B951211-
58.660	13.730	1995	12	11.56828	BT	4B951211-
49.700	-36.300	1995	12	12.00000	BNT	GRB
238.900	-48.800	1995	12	12.81000	BNT	GRB
225.300	-19.900	1995	12	13.00000	BNT	GRB
283.980	-6.820	1995	12	13.20662	BT	4B951213
314.200	46.600	1995	12	13.37818	BNT	GRB
325.400	38.300	1995	12	13.38000	BNT	GRB
98.600	8.800	1995	12	13.38000	BNT	GRB
13.400	65.800	1995	12	14.50000	BNT	GRB
194.700	-17.400	1995	12	15.65189	BNT	GRB
49.900	88.200	1995	12	15.88000	BNT	GRB
63.400	20.800	1995	12	16.00000	BNT	GRB
290.400	-56.600	1995	12	17.19000	BNT	GRB
344.600	25.300	1995	12	17.81000	BNT	GRB
20.700	-20.700	1995	12	18.31000	BNT	GRB
192.700	20.300	1995	12	18.75000	BNT	GRB
13.200	6.700	1995	12	19.69000	BNT	GRB
240.790	60.510	1995	12	19.70231	BT	4B951219
297.900	28.900	1995	12	20.18907	BNT	GRB

Continued on next column

Continued from previous column

RA deg	DEC deg	Year	Month	Day	Cat.	GRB Name
104.530	23.200	1995	12	20.36901	BT	4B951220
226.350	-35.870	1995	12	24.07918	BT	4B951224
237.900	14.800	1995	12	24.31000	BNT	GRB
176.100	-15.800	1995	12	24.56000	BNT	GRB
49.200	-34.000	1995	12	26.25000	BNT	GRB
334.300	10.900	1995	12	27.81000	BNT	GRB
68.610	1.590	1995	12	27.91668	BT	4B951227
93.130	28.220	1995	12	28.65794	BT	4B951228
106.600	49.600	1995	12	29.01963	BNT	GRB
104.000	-55.900	1995	12	31.38000	BNT	GRB
174.100	66.000	1995	12	31.88000	BNT	GRB
135.600	21.700	1996	01	1.44000	BNT	GRB
147.300	62.200	1996	01	2.81000	BNT	GRB
64.320	-60.970	1996	01	2.84786	BT	4B960102
350.000	6.400	1996	01	3.17956	BNT	GRB
351.900	61.700	1996	01	3.50388	BNT	GRB
309.800	-34.600	1996	01	4.00000	BNT	GRB
322.700	-18.600	1996	01	5.81000	BNT	GRB
6.190	33.580	1996	01	6.71192	BT	4B960106
140.890	59.700	1996	01	7.09120	BT	4B960107
212.200	-30.800	1996	01	7.50000	BNT	GRB
226.800	71.000	1996	01	7.81000	BNT	GRB
98.200	-39.900	1996	01	8.44000	BNT	GRB
136.400	16.500	1996	01	9.56000	BNT	GRB
261.600	-20.100	1996	01	10.69000	BNT	GRB
138.070	48.170	1996	01	11.53847	BT	4B960111
36.820	57.230	1996	01	12.31388	BT	4B960112
175.100	22.500	1996	01	13.25000	BNT	GRB
97.400	23.000	1996	01	13.62000	BNT	GRB
230.270	6.200	1996	01	13.64843	BT	4B960113
144.400	14.200	1996	01	13.69000	BNT	GRB
57.400	52.300	1996	01	14.44000	BNT	GRB
216.190	-29.730	1996	01	14.51047	BT	4B960114
132.300	-50.200	1996	01	15.38000	BNT	GRB
228.580	17.120	1996	01	15.72329	BT	4B960115
296.700	-29.000	1996	01	16.88000	BNT	GRB
59.200	69.700	1996	01	17.25000	BNT	GRB
282.100	6.100	1996	01	19.38000	BNT	GRB
86.330	54.650	1996	01	19.40134	BT	4B960119-
274.900	-64.100	1996	01	19.44000	BNT	GRB
209.550	-8.700	1996	01	19.72641	BT	4B960119-
359.700	49.800	1996	01	20.44000	BNT	GRB
121.100	9.000	1996	01	20.94000	BNT	GRB
296.500	-36.000	1996	01	23.50000	BNT	GRB
51.040	54.050	1996	01	24.03919	BT	4B960124-
253.900	2.500	1996	01	24.25000	BNT	GRB
231.920	-4.230	1996	01	24.88072	BT	4B960124-
294.100	-22.400	1996	01	25.38000	BNT	GRB

Continued on next column

Continued from previous column

RA deg	DEC deg	Year	Month	Day	Cat.	GRB Name
171.770	58.890	1996	01	28.60884	BT	4B960128
90.730	-38.600	1996	01	29.31651	BT	4B960129-
192.740	-21.170	1996	01	29.64191	BT	4B960129-
305.830	-40.270	1996	01	30.10138	BT	4B960130
358.050	14.460	1996	02	1.90883	BT	4B960201
157.100	-51.400	1996	02	1.94000	BNT	GRB
170.700	-15.600	1996	02	1.94000	BNT	GRB
104.400	54.600	1996	02	2.06000	BNT	GRB
97.900	65.200	1996	02	2.50000	BNT	GRB
215.040	-64.630	1996	02	2.58740	BT	4B960202
145.500	26.000	1996	02	2.88000	BNT	GRB
249.900	-21.200	1996	02	3.00000	BNT	GRB
171.400	13.000	1996	02	4.38000	BNT	GRB
71.680	-75.670	1996	02	5.29865	BT	4B960205-
110.110	-41.990	1996	02	5.39918	BT	4B960205-
76.900	-1.000	1996	02	5.48642	BNT	GRB
232.700	-14.100	1996	02	6.00000	BNT	GRB
195.530	-9.070	1996	02	6.20714	BT	4B960206-
231.200	20.830	1996	02	6.53428	BT	4B960206-
29.110	-60.260	1996	02	7.67480	BT	4B960207
9.800	35.800	1996	02	7.75000	BNT	GRB
130.000	-20.300	1996	02	7.94000	BNT	GRB
118.500	62.200	1996	02	8.25696	BNT	GRB
351.000	-15.800	1996	02	9.61826	BNT	GRB
358.220	66.380	1996	02	9.86374	BT	4B960209
232.300	77.010	1996	02	10.40738	BT	4B960210
144.000	-15.400	1996	02	10.44000	BNT	GRB
346.900	-50.700	1996	02	11.01218	BNT	GRB
254.700	36.800	1996	02	11.81000	BNT	GRB
112.800	7.400	1996	02	12.54166	BNT	GRB
356.800	40.100	1996	02	13.11063	BNT	GRB
350.570	-4.400	1996	02	14.77631	BT	4B960214
158.800	25.600	1996	02	15.19000	BNT	GRB
300.200	-21.400	1996	02	15.69000	BNT	GRB
355.450	16.750	1996	02	16.66894	BT	4B960216
47.900	-17.600	1996	02	17.38000	BNT	GRB
256.120	19.610	1996	02	19.82801	BT	4B960219
175.650	79.540	1996	02	20.88488	BT	4B960220
47.770	-31.240	1996	02	21.22346	BT	4B960221
64.200	-40.300	1996	02	23.50440	BNT	GRB
245.500	-65.000	1996	02	24.02376	BNT	GRB
200.400	-54.400	1996	02	25.81000	BNT	GRB
60.610	-15.260	1996	02	29.94240	BT	4B960229-
358.220	12.400	1996	02	29.99728	BT	4B960229-
118.000	-23.900	1996	03	1.06000	BNT	GRB
211.700	-59.900	1996	03	2.88000	BNT	GRB
205.000	14.400	1996	03	3.31000	BNT	GRB
2.480	-22.950	1996	03	4.36809	BT	4B960304

Continued on next column

Continued from previous column

RA deg	DEC deg	Year	Month	Day	Cat.	GRB Name
72.800	23.400	1996	03	4.56000	BNT	GRB
3.900	45.100	1996	03	5.44000	BNT	GRB
63.800	-49.000	1996	03	5.88000	BNT	GRB
177.900	-8.300	1996	03	7.38000	BNT	GRB
253.100	-7.100	1996	03	9.06000	BNT	GRB
205.140	-74.610	1996	03	11.78124	BT	4B960311
237.700	1.800	1996	03	12.49763	BNT	GRB
237.370	-61.970	1996	03	12.53281	BT	4B960312
170.200	4.000	1996	03	15.12000	BNT	GRB
208.000	-34.800	1996	03	15.62000	BNT	GRB
353.000	44.000	1996	03	15.88000	BNT	GRB
223.000	-70.170	1996	03	16.77412	BT	4B960316
114.200	2.300	1996	03	18.94000	BNT	GRB
314.600	68.400	1996	03	19.25140	BNT	GRB
94.840	-47.720	1996	03	19.60177	BT	4B960319
231.800	3.800	1996	03	20.75000	BNT	GRB
22.500	49.400	1996	03	21.25000	BNT	GRB
7.560	67.050	1996	03	21.88288	BT	4B960321
96.980	-54.610	1996	03	22.22733	BT	4B960322-
177.520	-29.570	1996	03	22.52042	BT	4B960322-
215.900	-42.700	1996	03	22.69000	BNT	GRB
328.510	-7.610	1996	03	23.57289	BT	4B960323
131.640	-64.370	1996	03	25.69943	BT	4B960325-
48.430	-32.570	1996	03	25.80895	BT	4B960325-
208.300	-66.100	1996	03	26.88000	BNT	GRB
74.200	-44.800	1996	03	27.30032	BNT	GRB
92.600	11.300	1996	03	28.00000	BNT	GRB
104.500	-2.800	1996	03	29.25000	BNT	GRB
279.850	-67.990	1996	03	29.72900	BT	4B960329
26.110	-21.910	1996	03	30.01440	BT	4B960330
274.810	15.190	1996	03	31.03275	BT	4B960331-
111.860	-20.390	1996	03	31.24545	BT	4B960331-
110.710	23.520	1996	03	31.70968	BT	4B960331-
133.000	12.300	1996	04	2.44000	BNT	GRB
267.400	14.400	1996	04	3.06000	BNT	GRB
211.580	18.900	1996	04	3.35906	BT	4B960403-
106.980	19.810	1996	04	3.73501	BT	4B960403-
287.960	-19.240	1996	04	4.10296	BT	4B960404
278.300	75.400	1996	04	4.31000	BNT	GRB
69.680	26.790	1996	04	5.68866	BT	4B960405-
332.050	-14.220	1996	04	5.77921	BT	4B960405-
150.000	8.100	1996	04	7.23212	BNT	GRB
284.500	59.100	1996	04	8.12000	BNT	GRB
85.040	1.880	1996	04	8.92531	BT	4B960408
224.620	67.280	1996	04	9.51118	BT	4B960409-
15.520	42.420	1996	04	9.83076	BT	4B960409-
42.540	41.920	1996	04	9.89288	BT	4B960409-
38.700	-60.900	1996	04	10.50000	BNT	GRB

Continued on next column

Continued from previous column

RA deg	DEC deg	Year	Month	Day	Cat.	GRB Name
31.030	-3.870	1996	04	11.09465	BT	4B960411-
147.860	-5.740	1996	04	11.24501	BT	4B960411-
265.810	-1.190	1996	04	12.91322	BT	4B960412
351.040	-45.140	1996	04	14.15123	BT	4B960414
258.300	-7.600	1996	04	15.10330	BNT	GRB
159.100	-56.810	1996	04	15.20259	BT	4B960415-
73.400	7.000	1996	04	15.50000	BNT	GRB
215.590	9.090	1996	04	15.66172	BT	4B960415-
103.000	27.600	1996	04	15.81000	BNT	GRB
2.640	15.120	1996	04	15.90381	BT	4B960415-
66.850	73.600	1996	04	16.17292	BT	4B960416
249.700	-8.200	1996	04	16.33874	BNT	GRB
50.180	-4.270	1996	04	17.12736	BT	4B960417-
227.800	3.270	1996	04	17.87563	BT	4B960417-
170.500	0.420	1996	04	18.07066	BT	4B960418-
302.000	38.800	1996	04	18.12000	BNT	GRB
91.120	7.910	1996	04	18.17628	BT	4B960418-
69.300	5.700	1996	04	18.51304	BNT	GRB
110.320	-16.150	1996	04	18.77309	BT	4B960418-
234.250	-27.230	1996	04	20.19495	BT	4B960420
357.800	58.700	1996	04	20.79414	BNT	GRB
289.500	45.100	1996	04	21.19000	BNT	GRB
284.700	-65.900	1996	04	22.56000	BNT	GRB
134.800	27.200	1996	04	22.69415	BT	4B960422
199.440	-31.510	1996	04	23.50885	BT	4B960423
59.930	40.820	1996	04	25.01288	BT	4B960425-
9.800	56.510	1996	04	25.99990	BT	4B960425-
248.390	-45.950	1996	04	26.27637	BT	4B960426
329.700	17.000	1996	04	26.50000	BNT	GRB
198.800	1.000	1996	04	27.75000	BNT	GRB
304.240	35.130	1996	04	28.55037	BT	4B960428
65.800	34.200	1996	04	29.88000	BNT	GRB
11.800	-51.490	1996	04	30.57740	BT	4B960430
21.200	-26.700	1996	05	2.07757	BNT	GRB
299.900	-44.300	1996	05	4.19000	BNT	GRB
98.230	36.040	1996	05	5.66240	BT	4B960505
79.230	17.890	1996	05	7.98333	BT	4B960507
113.200	-47.700	1996	05	8.30042	BNT	GRB
141.970	-45.440	1996	05	8.56260	BT	4B960508-
258.320	-77.620	1996	05	8.79172	BT	4B960508-
306.440	-76.780	1996	05	9.50956	BT	4B960509
240.400	-16.000	1996	05	10.62000	BNT	GRB
205.000	-40.800	1996	05	11.17782	BNT	GRB
252.700	-45.200	1996	05	11.95755	BNT	GRB
251.010	-20.480	1996	05	12.88001	BT	4B960512
77.120	3.530	1996	05	13.92894	BT	4B960513
135.910	-25.520	1996	05	15.02357	BT	4B960515
278.250	-24.920	1996	05	16.03563	BT	4B960516-

Continued on next column

Continued from previous column

RA deg	DEC deg	Year	Month	Day	Cat.	GRB Name
75.700	4.400	1996	05	16.75000	BNT	GRB
208.760	61.880	1996	05	16.77592	BT	4B960516-
62.280	-18.070	1996	05	16.97509	BT	4B960516-
332.900	5.400	1996	05	18.50000	BNT	GRB
130.620	1.140	1996	05	18.52992	BT	4B960518
306.590	-4.532	1996	05	19.18479	K/W	960519_T15966
303.250	55.770	1996	05	21.33735	BT	4B960521-
251.550	41.070	1996	05	21.39128	BT	4B960521-
347.450	57.820	1996	05	22.27647	BT	4B960522
203.730	42.150	1996	05	23.46542	BT	4B960523-
46.750	-63.320	1996	05	23.68891	BT	4B960523-
27.620	39.270	1996	05	24.09946	BT	4B960524-
160.820	2.600	1996	05	24.37878	BT	4B960524-
358.520	-24.770	1996	05	24.83969	BT	4B960524-
139.070	53.770	1996	05	25.98090	BT	4B960525
106.300	26.900	1996	05	26.75000	BNT	GRB
186.070	1.080	1996	05	27.65882	BT	4B960527
291.860	22.030	1996	05	28.09332	BT	4B960528
143.900	15.000	1996	05	28.38000	BNT	GRB
232.700	-19.800	1996	05	29.30213	BNT	GRB
14.400	48.890	1996	05	29.50538	BT	4B960529
242.300	-64.400	1996	05	30.59354	BNT	GRB
143.410	-53.790	1996	05	30.72105	BT	4B960530
154.000	11.700	1996	05	31.06000	BNT	GRB
16.600	-27.900	1996	05	31.06000	BNT	GRB
34.210	-28.500	1996	05	31.07958	BT	4B960531-
180.000	80.770	1996	05	31.37270	BT	4B960531-
208.810	-56.480	1996	06	1.19850	BT	4B960601-
5.570	64.800	1996	06	1.75898	BT	4B960601-
10.500	-61.800	1996	06	2.00000	BNT	GRB
211.600	17.300	1996	06	2.12000	BNT	GRB
272.720	-35.190	1996	06	2.16647	BT	4B960602
74.580	-6.123	1996	06	2.49380	K/W	960602_T42664
67.100	-18.600	1996	06	2.50000	BNT	GRB
169.100	57.600	1996	06	3.28436	BNT	GRB
125.100	-34.700	1996	06	3.69000	BNT	GRB
170.800	33.700	1996	06	4.06000	BNT	GRB
317.600	-17.400	1996	06	4.69000	BNT	GRB
349.900	-28.000	1996	06	4.70902	BNT	GRB
313.900	-26.930	1996	06	4.85264	BT	4B960604
154.260	-1.980	1996	06	5.34019	BT	4B960605-
244.060	52.800	1996	06	5.54972	BT	4B960605-
299.290	-23.510	1996	06	7.25604	BT	4B960607-
282.700	-32.500	1996	06	7.68993	BNT	GRB
48.430	75.100	1996	06	7.90366	BT	4B960607-
255.950	-13.090	1996	06	8.64829	BT	4B960608-
311.650	56.360	1996	06	8.80674	BT	4B960608-
100.000	36.500	1996	06	9.75000	BNT	GRB

Continued on next column

Continued from previous column

RA deg	DEC deg	Year	Month	Day	Cat.	GRB Name
312.000	-45.900	1996	06	9.88000	BNT	GRB
328.240	-29.350	1996	06	10.89101	BT	4B960610
169.600	75.900	1996	06	11.12000	BNT	GRB
282.900	65.300	1996	06	11.62000	BNT	GRB
22.250	6.340	1996	06	12.23787	BT	4B960612
276.530	-66.460	1996	06	13.00260	BT	4B960613-
221.700	35.970	1996	06	13.57024	BT	4B960613-
212.410	43.970	1996	06	14.73821	BT	4B960614
107.700	-31.800	1996	06	14.94000	BNT	GRB
110.930	51.130	1996	06	15.08782	BT	4B960615-
237.370	64.820	1996	06	15.17155	BT	4B960615-
295.470	-65.970	1996	06	15.99903	BT	4B960615-
171.430	43.980	1996	06	16.29449	BT	4B960616-
168.440	-38.960	1996	06	16.55212	BT	4B960616-
109.130	62.700	1996	06	16.76963	BT	4B960616-
242.300	17.200	1996	06	16.80131	BNT	GRB
154.900	-32.200	1996	06	16.84021	BNT	GRB
310.110	-44.720	1996	06	17.15207	BT	4B960617-
161.140	-30.900	1996	06	17.88190	BT	4B960617-
199.380	53.050	1996	06	18.09259	BT	4B960618
125.800	52.700	1996	06	18.94000	BNT	GRB
152.000	76.100	1996	06	19.50000	BNT	GRB
206.880	27.780	1996	06	20.22611	BT	4B960620
21.100	-84.000	1996	06	20.86094	BNT	GRB
357.190	10.860	1996	06	21.09736	BT	4B960621-
90.710	31.760	1996	06	21.20030	BT	4B960621-
290.500	25.340	1996	06	21.27414	BT	4B960621-
280.500	-55.700	1996	06	21.87788	BNT	GRB
71.640	57.530	1996	06	21.93297	BT	4B960621-
218.200	-16.900	1996	06	22.69036	BNT	GRB
180.780	7.590	1996	06	23.05473	BT	4B960623-
287.040	-45.580	1996	06	23.13934	BT	4B960623-
201.300	4.500	1996	06	23.38000	BNT	GRB
163.700	-59.730	1996	06	23.38314	BT	4B960623-
359.000	0.050	1996	06	23.75745	BT	4B960623-
178.580	-10.460	1996	06	24.10924	BT	4B960624-
98.960	32.050	1996	06	24.14321	BT	4B960624-
149.400	-56.500	1996	06	25.19000	BNT	GRB
110.590	-8.210	1996	06	25.19615	BT	4B960625
350.000	1.500	1996	06	25.95204	BNT	GRB
324.060	34.660	1996	06	26.80156	BT	4B960626
326.980	48.280	1996	06	28.22249	BT	4B960628
40.700	-11.800	1996	06	28.86616	BNT	GRB
104.400	13.900	1996	06	29.47957	BNT	GRB
108.660	19.430	1996	07	2.04109	BT	4B960702-
36.780	-15.530	1996	07	2.63294	BT	4B960702-
108.000	-10.500	1996	07	3.02241	BNT	GRB
142.000	-9.000	1996	07	3.31931	BeS	960703A

Continued on next column

Continued from previous column

RA deg	DEC deg	Year	Month	Day	Cat.	GRB Name
4.620	-7.750	1996	07	3.57146	BeS	960703B
330.400	-54.790	1996	07	3.75742	BeS	960703C
358.290	-7.300	1996	07	4.67264	BT	4B960704
16.800	53.300	1996	07	4.70097	BNT	GRB
29.450	-0.290	1996	07	5.03453	BT	4B960705
348.000	-66.800	1996	07	6.25182	BNT	GRB
320.950	82.510	1996	07	7.42825	BeS	960707A
189.270	-1.780	1996	07	7.51728	BT	4B960707-
162.390	-14.340	1996	07	7.68502	BeS	960707B
71.200	-77.700	1996	07	7.86345	BNT	GRB
221.870	-7.970	1996	07	8.62854	BT	4B960708-
307.030	9.800	1996	07	8.83995	BT	4B960708-
346.480	-30.660	1996	07	10.44777	BT	4B960710
130.130	12.470	1996	07	13.71902	BT	4B960713-
169.290	85.450	1996	07	13.82330	BT	4B960713-
3.430	35.500	1996	07	15.03365	BT	4B960715-
81.760	48.840	1996	07	15.31473	BT	4B960715-
312.990	51.860	1996	07	15.47170	BT	4B960715-
17.500	-2.900	1996	07	15.69000	BNT	GRB
83.300	41.300	1996	07	15.75000	BNT	GRB
55.420	-10.530	1996	07	16.09316	BT	4B960716
7.020	16.960	1996	07	17.19168	BT	4B960717
72.500	3.400	1996	07	17.38000	BNT	GRB
29.800	52.200	1996	07	19.88000	BNT	GRB
262.650	49.080	1996	07	20.48395	BeS	960720
228.820	10.490	1996	07	22.01876	BT	4B960722-
52.040	-77.150	1996	07	22.17259	BT	4B960722-
29.640	31.670	1996	07	22.29522	BT	4B960722-
94.990	43.250	1996	07	23.19865	BeS	960723A
357.700	-64.700	1996	07	24.44000	BNT	GRB
275.760	37.050	1996	07	25.06269	BT	4B960725
90.300	45.100	1996	07	25.73550	BeS	960725
89.700	45.300	1996	07	25.75000	BNT	GRB
140.300	-31.000	1996	07	25.94398	BNT	GRB
94.800	69.100	1996	07	27.84255	BNT	GRB
265.900	-56.700	1996	07	27.96914	BNT	GRB
201.100	-18.900	1996	07	28.06000	BNT	GRB
253.620	-6.770	1996	07	29.07422	BT	4B960729
292.700	-53.500	1996	07	30.19000	BNT	GRB
277.940	-56.540	1996	07	30.81612	BeS	960730
150.010	25.410	1996	07	30.85646	BT	4B960730-
199.530	-18.290	1996	07	31.14089	BT	4B960731-
43.930	12.510	1996	07	31.24032	BeS	960731
125.540	37.370	1996	07	31.86446	BT	4B960731-
230.000	21.000	1996	08	1.65905	BeS	960801B
204.200	-13.400	1996	08	2.25000	BNT	GRB
249.520	30.530	1996	08	2.92155	BeS	960802
166.270	40.360	1996	08	3.36126	BT	4B960803-

Continued on next column

Continued from previous column

RA deg	DEC deg	Year	Month	Day	Cat.	GRB Name
1.900	8.600	1996	08	3.63880	BNT	GRB
338.020	-50.130	1996	08	3.78150	BT	4B960803-
120.400	-44.600	1996	08	4.31000	BNT	GRB
218.000	3.200	1996	08	4.48471	BNT	GRB
357.400	25.800	1996	08	4.75000	BNT	GRB
281.250	-52.120	1996	08	4.81436	BT	4B960804-
218.670	68.200	1996	08	4.97843	BT	4B960804-
186.030	76.360	1996	08	5.89522	BeS	960805A
175.800	-7.100	1996	08	5.93128	BNT	GRB
319.980	1.030	1996	08	6.67955	BT	4B960806-
182.930	-2.190	1996	08	6.93653	BeS	960806
46.700	-42.700	1996	08	7.62000	BNT	GRB
157.530	32.130	1996	08	7.82600	BT	4B960807
85.250	37.020	1996	08	8.69588	BT	4B960808
185.290	-34.600	1996	08	10.28440	BeS	960810A
102.000	-11.000	1996	08	10.28907	BeS	960810B
118.500	-15.900	1996	08	10.56000	BNT	GRB
5.150	8.280	1996	08	10.96596	BT	4B960810-
156.600	-42.000	1996	08	11.06000	BNT	GRB
250.900	-17.600	1996	08	11.94000	BNT	GRB
97.020	39.000	1996	08	12.58640	BT	4B960812
89.820	14.910	1996	08	13.24039	BT	4B960813-
172.000	27.100	1996	08	13.83450	BNT	GRB
186.970	41.960	1996	08	13.90785	BT	4B960813-
192.490	-48.550	1996	08	14.68111	BT	4B960814
265.330	-58.010	1996	08	15.41698	BT	4B960815
187.710	56.550	1996	08	16.09453	BT	4B960816
211.200	29.300	1996	08	17.31000	BNT	GRB
126.400	9.500	1996	08	17.40981	BNT	GRB
208.700	-13.600	1996	08	17.42022	BNT	GRB
76.400	-32.750	1996	08	18.66852	BT	4B960818
87.100	50.770	1996	08	19.85859	BT	4B960819
325.900	15.400	1996	08	22.25000	BNT	GRB
351.240	65.670	1996	08	24.07073	BT	4B960824
238.200	17.900	1996	08	24.46219	BNT	GRB
160.600	-27.600	1996	08	25.38000	BNT	GRB
63.920	-3.490	1996	08	25.72729	BT	4B960825
37.300	-48.100	1996	08	25.77866	BNT	GRB
69.700	-24.000	1996	08	26.22525	BNT	GRB
191.100	28.300	1996	08	26.69000	BNT	GRB
191.100	15.800	1996	08	26.69000	BNT	GRB
107.600	-33.300	1996	08	28.45509	BNT	GRB
58.800	65.200	1996	08	30.25435	BNT	GRB
130.010	-36.800	1996	08	30.27601	BT	GRB960830
159.000	24.100	1996	08	30.98896	BNT	GRB
327.820	40.180	1996	08	31.29004	BT	GRB960831-
242.760	22.930	1996	08	31.43647	BT	GRB960831-
14.100	18.400	1996	09	1.17598	BNT	GRB

Continued on next column

Continued from previous column

RA deg	DEC deg	Year	Month	Day	Cat.	GRB Name
40.200	19.200	1996	09	1.58000	BNT	GRB
348.300	66.100	1996	09	1.76469	BNT	GRB
194.700	-4.700	1996	09	2.44479	BNT	GRB
284.700	-6.100	1996	09	4.54895	BNT	GRB
272.900	63.700	1996	09	5.02972	BNT	GRB
327.800	17.000	1996	09	5.70861	BNT	GRB
329.550	30.290	1996	09	6.80250	BT	GRB960906-
65.100	-41.470	1996	09	6.94432	BT	GRB960906-
143.930	49.870	1996	09	7.28485	BT	GRB960907-
320.100	-5.060	1996	09	7.33235	BT	GRB960907-
68.500	66.400	1996	09	7.84450	BNT	GRB
166.100	-16.600	1996	09	8.12067	BNT	GRB
291.098	59.703	1996	09	8.28968	K/W	960908_T25028
187.190	-63.230	1996	09	8.58469	BT	GRB960908
25.880	-7.800	1996	09	9.86160	BeS	960909
311.800	30.600	1996	09	11.12000	BNT	GRB
251.500	-12.600	1996	09	12.24392	BNT	GRB
95.140	76.860	1996	09	12.58157	BeS	960912
197.610	-44.630	1996	09	12.99520	BT	GRB960912-
137.370	-39.860	1996	09	13.16914	BT	GRB960913-
88.200	-42.000	1996	09	13.25000	BNT	GRB
75.800	48.300	1996	09	13.25000	BNT	GRB
69.500	-9.000	1996	09	13.94787	BNT	GRB
182.580	-23.450	1996	09	13.96204	BeS	960913
114.100	-60.400	1996	09	14.01997	BNT	GRB
285.000	-67.000	1996	09	16.35499	BeS	960916C
206.000	32.000	1996	09	16.63557	BeS	960916D
153.960	57.550	1996	09	16.99189	BeS	960916E
206.800	53.100	1996	09	17.16679	BNT	GRB
313.870	-33.890	1996	09	17.93233	BeS	960917
233.340	21.570	1996	09	19.93611	BeS	960919
223.220	-25.350	1996	09	21.33670	BT	GRB960921-
345.270	-28.550	1996	09	21.62765	BeS	960921
223.900	-70.800	1996	09	21.88000	BNT	GRB
256.330	57.350	1996	09	23.02656	BeS	960923
178.800	-35.000	1996	09	23.38000	BNT	GRB
88.270	20.000	1996	09	23.82414	BT	GRB960923-
37.280	2.700	1996	09	24.48740	BT	GRB960924
29.260	-13.860	1996	09	25.14393	BT	GRB960925
199.560	74.130	1996	09	27.15791	BeS	960927
282.000	48.000	1996	09	27.49177	BNT	GRB
263.300	14.100	1996	09	27.56000	BNT	GRB
59.350	-2.490	1996	09	29.01200	BT	GRB960929-
110.000	-44.000	1996	09	29.27526	BeS	960929
23.700	42.400	1996	09	29.56000	BNT	GRB
54.470	45.320	1996	09	29.72928	BT	GRB960929-
30.900	29.000	1996	09	30.50000	BNT	GRB
63.090	38.220	1996	10	1.85432	BT	GRB961001-

Continued on next column

Continued from previous column

RA deg	DEC deg	Year	Month	Day	Cat.	GRB Name
42.790	59.030	1996	10	1.87020	BT	GRB961001-
129.890	29.990	1996	10	2.70757	BT	GRB961002
284.200	-15.600	1996	10	3.25000	BNT	GRB
237.000	27.300	1996	10	3.44000	BNT	GRB
80.600	-35.550	1996	10	4.79068	BeS	961004
274.650	-28.880	1996	10	6.37231	BeS	961006
244.300	23.800	1996	10	6.75000	BNT	GRB
104.320	-30.060	1996	10	6.79950	BT	GRB961006-
258.690	29.570	1996	10	8.22291	BeS	961008
218.330	-26.630	1996	10	9.08622	BT	GRB961009-
94.040	80.060	1996	10	9.38836	BT	GRB961009-
110.200	-79.000	1996	10	9.56000	BNT	GRB
130.200	-80.230	1996	10	9.56788	BT	GRB961009-
267.400	61.100	1996	10	9.75000	BNT	GRB
147.400	-70.700	1996	10	10.25000	BNT	GRB
105.900	-71.600	1996	10	10.75000	BNT	GRB
142.900	7.000	1996	10	11.33705	BNT	GRB
210.000	-21.000	1996	10	11.81406	BeS	961011
277.000	-13.400	1996	10	13.12000	BNT	GRB
192.900	53.700	1996	10	13.88000	BNT	GRB
332.730	-29.550	1996	10	14.00588	BT	GRB961014
305.000	45.000	1996	10	15.44219	BeS	961015A
29.000	21.000	1996	10	15.49514	BeS	961015B
220.030	30.100	1996	10	15.67273	BT	GRB961015
130.000	63.600	1996	10	16.77039	BNT	GRB
162.800	42.400	1996	10	17.25000	BNT	GRB
115.160	-4.680	1996	10	17.25581	BT	GRB961017-
37.160	-10.680	1996	10	17.46995	BT	GRB961017-
286.610	31.660	1996	10	17.62713	BT	GRB961017-
248.700	-55.200	1996	10	19.50000	BNT	GRB
321.870	-84.180	1996	10	19.88070	BT	GRB961019
73.740	8.430	1996	10	20.11921	BT	GRB961020
154.900	-4.500	1996	10	21.03573	BNT	GRB
267.640	-12.950	1996	10	22.28045	BT	GRB961022-
159.630	-38.760	1996	10	22.79242	BeS	961022
328.400	9.300	1996	10	23.08976	BeS	961023
33.900	23.900	1996	10	24.25000	BNT	GRB
331.200	-58.200	1996	10	24.30782	BNT	GRB
42.400	-18.900	1996	10	25.44000	BNT	GRB
281.420	21.990	1996	10	25.53123	BT	GRB961025
99.320	41.880	1996	10	26.25822	BeS	961026
202.890	26.010	1996	10	26.40544	BT	GRB961026-
40.600	59.700	1996	10	26.77294	BNT	GRB
67.380	-42.380	1996	10	27.48897	BT	GRB961027-
68.740	-54.290	1996	10	27.50142	BT	GRB961027-
59.360	-52.620	1996	10	29.27405	BT	GRB961029-
59.790	-48.890	1996	10	29.28184	BT	GRB961029-
276.740	67.130	1996	10	30.59085	BT	GRB961030

Continued on next column

Continued from previous column

RA deg	DEC deg	Year	Month	Day	Cat.	GRB Name
150.100	51.900	1996	10	30.94000	BNT	GRB
311.900	-25.000	1996	11	2.23773	BNT	GRB
271.440	28.130	1996	11	2.48500	BT	GRB961102
301.400	23.100	1996	11	2.88000	BNT	GRB
219.900	25.600	1996	11	4.19000	BNT	GRB
273.560	14.070	1996	11	5.53066	BT	GRB961105
296.900	68.700	1996	11	6.49803	BeS	961106
211.500	-41.000	1996	11	6.68045	BNT	GRB
43.800	41.500	1996	11	7.14689	BNT	GRB
86.900	-1.200	1996	11	7.86387	BNT	GRB
182.900	15.200	1996	11	7.96138	BNT	GRB
357.700	37.900	1996	11	8.94000	BNT	GRB
61.100	59.000	1996	11	10.31223	BeS	961110
311.470	28.510	1996	11	10.51432	BT	GRB961110
343.400	-11.600	1996	11	11.12000	BNT	GRB
175.690	-35.780	1996	11	11.56302	BT	GRB961111-
330.000	-0.600	1996	11	11.62000	BNT	GRB
86.340	34.390	1996	11	11.96535	BT	GRB961111-
300.400	28.400	1996	11	12.75000	BNT	GRB
226.000	-5.900	1996	11	13.93198	BNT	GRB
88.400	-22.200	1996	11	13.95066	BNT	GRB
58.630	-31.130	1996	11	15.03828	BT	GRB961115
115.500	61.100	1996	11	15.81324	BNT	GRB
61.270	60.660	1996	11	16.68335	BT	GRB961116
63.600	23.000	1996	11	19.44000	BNT	GRB
286.800	43.600	1996	11	20.35223	BeS	961120
286.800	43.600	1996	11	20.38000	BNT	GRB
67.600	60.600	1996	11	23.69000	BNT	GRB
278.000	10.000	1996	11	25.01722	BeS	961125A
304.690	-53.520	1996	11	25.31918	BT	GRB961125
326.000	-47.000	1996	11	25.32483	BeS	961125B
150.340	36.720	1996	11	26.28008	BeS	961126
16.900	65.400	1996	11	28.06000	BNT	GRB
247.230	24.400	1996	11	30.21796	BT	GRB961130
43.700	-29.100	1996	11	30.44000	BNT	GRB
202.200	-62.600	1996	12	2.43315	BNT	GRB
336.670	20.550	1996	12	2.77154	BT	GRB961202
28.100	-36.330	1996	12	6.19824	BT	GRB961206
7.900	-51.900	1996	12	6.38000	BNT	GRB
109.300	-52.300	1996	12	7.62000	BNT	GRB
327.800	-37.100	1996	12	8.19000	BNT	GRB
316.000	-33.000	1996	12	8.22520	BeS	961208A
138.200	-54.300	1996	12	8.56000	BNT	GRB
61.400	-44.900	1996	12	8.78973	BeS	961208B
57.500	-46.000	1996	12	8.81000	BNT	GRB
130.700	-24.900	1996	12	9.31000	BNT	GRB
188.600	33.400	1996	12	9.88000	BNT	GRB
248.300	-34.300	1996	12	10.12421	BNT	GRB

Continued on next column

Continued from previous column

RA deg	DEC deg	Year	Month	Day	Cat.	GRB Name
281.710	54.820	1996	12	11.08069	BeS	961211
296.110	41.260	1996	12	11.86204	BT	GRB961211-
182.860	34.480	1996	12	12.17212	BT	GRB961212
238.500	79.700	1996	12	12.31000	BNT	GRB
190.560	44.540	1996	12	13.52343	BT	GRB961213
186.300	57.300	1996	12	13.56000	BNT	GRB
207.440	-18.540	1996	12	14.39443	BT	GRB961214
69.710	-21.480	1996	12	16.68683	BT	GRB961216
251.300	50.600	1996	12	16.88000	BNT	GRB
347.200	26.100	1996	12	16.94000	BNT	GRB
19.900	-0.800	1996	12	17.81000	BNT	GRB
281.630	-28.550	1996	12	18.03502	BT	GRB961218-
97.750	-21.730	1996	12	18.81634	BT	GRB961218-
305.000	64.100	1996	12	19.56000	BNT	GRB
210.400	-34.000	1996	12	19.56000	BNT	GRB
2.600	-0.700	1996	12	20.00000	BNT	GRB
6.900	17.330	1996	12	20.22351	BeS	961220
302.900	-12.100	1996	12	22.50009	BeS	961222
86.320	36.600	1996	12	23.87229	BT	GRB961223
271.500	41.300	1996	12	24.12492	BNT	GRB
319.500	14.500	1996	12	24.42434	BeS	961224A
322.000	13.700	1996	12	24.44000	BNT	GRB
11.920	41.130	1996	12	24.45130	BT	GRB961224-
182.840	-64.640	1996	12	24.73736	BeS	961224B
171.310	-2.850	1996	12	25.42170	BT	GRB961225
21.040	78.250	1996	12	26.24365	BT	GRB961226
186.900	-15.300	1996	12	27.62000	BNT	GRB
160.280	-53.600	1996	12	28.02081	BeS	961228
268.030	27.170	1996	12	28.94716	BT	GRB961228-
4.150	-59.060	1996	12	28.99906	BT	GRB961228-
37.520	-80.620	1996	12	30.58940	BT	GRB961230
108.700	-11.700	1996	12	31.31000	BNT	GRB
329.960	-21.920	1997	01	1.26516	BeS	970101
179.080	-6.850	1997	01	3.21984	BT	GRB970103
107.000	-46.000	1997	01	4.14324	BeS	970104
315.660	57.520	1997	01	5.12356	BT	GRB970105
12.500	-61.100	1997	01	5.15631	BNT	GRB
36.000	-51.200	1997	01	8.62000	BNT	GRB
1.230	-53.610	1997	01	8.71807	BeS	970108
50.100	61.900	1997	01	10.44000	BNT	GRB
280.550	54.380	1997	01	10.96727	BT	GRB970110
232.060	19.600	1997	01	11.40556	BeS	970111
154.000	25.100	1997	01	11.69000	BNT	GRB
325.300	22.700	1997	01	11.94000	BNT	GRB
310.800	-23.900	1997	01	15.12000	BNT	GRB
47.200	46.300	1997	01	16.38000	BNT	GRB
123.450	-11.150	1997	01	16.48705	BeS	970116
280.300	4.900	1997	01	16.50348	BNT	GRB

Continued on next column

Continued from previous column

RA deg	DEC deg	Year	Month	Day	Cat.	GRB Name
181.300	-49.300	1997	01	16.69000	BNT	GRB
306.400	-60.200	1997	01	17.06000	BNT	GRB
106.500	-14.200	1997	01	17.24520	BNT	GRB
101.000	-74.000	1997	01	17.61587	BeS	970117B
322.740	32.170	1997	01	19.30938	BT	GRB970119
218.300	82.000	1997	01	19.50000	BNT	GRB
109.200	9.200	1997	01	20.62000	BNT	GRB
196.090	60.830	1997	01	20.96490	BT	GRB970120
139.900	-20.900	1997	01	21.31000	BNT	GRB
261.000	-45.000	1997	01	22.48709	BeS	970122
290.000	-53.300	1997	01	22.85954	BNT	GRB
96.000	51.000	1997	01	23.35876	BeS	970123
92.400	-32.100	1997	01	24.49599	BNT	GRB
127.100	-36.900	1997	01	24.81799	BNT	GRB
201.100	-33.400	1997	01	26.25000	BNT	GRB
40.500	68.000	1997	01	26.38000	BNT	GRB
281.800	23.900	1997	01	26.38000	BNT	GRB
265.700	-20.800	1997	01	27.63709	BNT	GRB
275.260	24.680	1997	01	28.34656	BT	GRB970128
59.000	-75.700	1997	01	28.44000	BNT	GRB
28.000	3.000	1997	01	28.98274	BeS	970128
98.100	47.700	1997	01	29.56000	BNT	GRB
287.700	34.400	1997	01	31.19000	BNT	GRB
289.000	-1.000	1997	01	31.90323	BeS	970131A
253.790	36.590	1997	01	31.90707	BeS	970131B
55.130	-19.440	1997	02	1.66263	BT	GRB970201-
178.140	-42.350	1997	02	1.93443	BT	GRB970201-
39.900	69.000	1997	02	2.09516	BNT	GRB
49.580	-28.790	1997	02	2.29912	BT	GRB970202
251.000	32.000	1997	02	3.06384	BeS	970203
44.800	31.300	1997	02	3.38000	BNT	GRB
8.630	-4.300	1997	02	3.77266	BT	GRB970203
136.600	-71.500	1997	02	5.06000	BNT	GRB
25.100	-62.700	1997	02	5.12000	BNT	GRB
170.010	16.570	1997	02	6.00924	BT	GRB970206
171.500	26.200	1997	02	6.06000	BNT	GRB
101.700	47.600	1997	02	6.30764	BNT	GRB
2.100	-19.300	1997	02	7.89189	BNT	GRB
242.930	38.540	1997	02	11.06105	BT	GRB970211-
95.610	-30.870	1997	02	11.15157	BT	GRB970211-
242.110	10.250	1997	02	11.62050	BT	GRB970211-
333.200	71.400	1997	02	14.00686	BNT	GRB
294.900	4.300	1997	02	14.31567	BNT	GRB
339.810	15.750	1997	02	14.44890	BT	GRB970214-
199.270	-12.780	1997	02	14.66771	BT	GRB970214-
158.400	-37.000	1997	02	15.81389	BNT	GRB
330.000	0.800	1997	02	18.10353	BNT	GRB
328.020	69.910	1997	02	19.27641	BT	GRB970219

Continued on next column

Continued from previous column

RA deg	DEC deg	Year	Month	Day	Cat.	GRB Name
33.600	68.800	1997	02	21.15925	BeS	970221A
16.800	66.500	1997	02	21.19000	BNT	GRB
297.100	44.900	1997	02	21.31000	BNT	GRB
342.800	-69.700	1997	02	21.42949	BeS	970221B
308.000	-10.000	1997	02	22.99546	BeS	970222
330.200	-26.100	1997	02	23.31000	BNT	GRB
142.440	35.460	1997	02	23.35160	BT	GRB970223
190.700	24.800	1997	02	23.61113	BNT	GRB
240.000	60.800	1997	02	23.75097	BeS	970223
65.270	-37.040	1997	02	24.20935	BT	GRB970224
233.900	57.600	1997	02	25.69730	BNT	GRB
278.800	-46.100	1997	02	25.88322	BNT	GRB
138.100	59.200	1997	02	26.12000	BNT	GRB
335.500	-36.660	1997	02	26.39249	BT	GRB970226-
45.440	-26.260	1997	02	26.42942	BT	GRB970226-
322.790	-30.660	1997	02	27.38031	BT	GRB970227-
93.690	49.880	1997	02	27.55876	BT	GRB970227-
75.490	11.770	1997	02	28.12362	BeS	970228
7.930	-54.540	1997	03	2.53904	BeS	970302A
275.920	21.020	1997	03	2.77947	BeS	970302B
130.000	-3.000	1997	03	3.02567	BeS	970303
345.800	59.400	1997	03	3.95215	BNT	GRB
343.200	-14.100	1997	03	4.28345	BNT	GRB
219.930	-9.330	1997	03	4.33618	BT	GRB970304
18.340	21.360	1997	03	6.11690	BeS	970306
245.700	58.000	1997	03	6.52531	BNT	GRB
204.400	-87.300	1997	03	6.88000	BNT	GRB
349.000	-42.000	1997	03	7.81187	BeS	970307
166.540	10.650	1997	03	8.19399	BT	GRB970308
241.500	-35.200	1997	03	9.92024	BNT	GRB
76.200	-34.900	1997	03	10.06000	BNT	GRB
84.300	59.400	1997	03	10.25000	BNT	GRB
224.570	-7.650	1997	03	11.07518	BT	GRB970311
20.700	-1.900	1997	03	11.35031	BeS	970311A
320.000	16.000	1997	03	11.36333	BeS	970311B
26.600	7.100	1997	03	11.38000	BNT	GRB
354.510	33.850	1997	03	12.48659	BT	GRB970312
118.100	-53.700	1997	03	13.21402	BNT	GRB
179.000	6.000	1997	03	13.40692	BeS	970313
133.030	68.600	1997	03	13.74955	BT	GRB970313
106.000	31.000	1997	03	14.16750	BeS	970314
352.630	-41.700	1997	03	15.34801	BT	GRB970315-
2.150	60.720	1997	03	15.65341	BeS	970315A
130.620	-52.400	1997	03	15.92618	BT	GRB970315-
339.710	-23.150	1997	03	17.02039	BeS	970317A
111.750	68.900	1997	03	17.97256	BeS	970317B
135.240	56.240	1997	03	18.35000	BT	GRB970318
94.990	51.390	1997	03	21.70109	BT	GRB970321

Continued on next column

Continued from previous column

RA deg	DEC deg	Year	Month	Day	Cat.	GRB Name
307.800	23.710	1997	03	23.31749	BT	GRB970323
290.300	51.800	1997	03	23.41509	BNT	GRB
129.900	24.500	1997	03	23.71210	BNT	GRB
206.600	-37.000	1997	03	23.81000	BNT	GRB
9.060	-22.840	1997	03	24.09888	BT	GRB970324
266.000	-26.000	1997	03	25.52693	BeS	970325
359.280	-67.630	1997	03	26.34459	BeS	970326A
133.980	-23.920	1997	03	26.58237	BT	GRB970326-
94.000	-40.000	1997	03	26.75228	BeS	970326B
348.880	15.400	1997	03	27.13884	BT	GRB970327-
27.900	39.970	1997	03	27.65932	BT	GRB970327-
2.020	19.590	1997	03	28.16455	BT	GRB970328-
116.790	41.790	1997	03	28.44724	BT	GRB970328-
173.550	31.040	1997	03	29.04211	BT	GRB970329-
169.740	8.800	1997	03	29.54563	BT	GRB970329-
352.500	0.000	1997	03	30.15689	BNT	GRB
347.740	-19.120	1997	03	30.37424	BeS	970330A
332.000	29.000	1997	03	30.50916	BeS	970330B
304.600	2.260	1997	03	30.59115	BT	GRB970330-
332.400	8.800	1997	03	31.88000	BNT	GRB
212.080	85.720	1997	03	31.89258	BT	GRB970331
310.110	34.300	1997	04	2.07378	BT	GRB970402-
9.170	42.090	1997	04	2.34713	BT	GRB970402-
222.570	-69.320	1997	04	2.92958	BeS	970402
73.170	-44.600	1997	04	3.00017	BT	GRB970403-
45.630	8.350	1997	04	3.66201	BT	GRB970403-
74.200	16.500	1997	04	4.31000	BNT	GRB
180.290	36.010	1997	04	4.71838	BT	GRB970404-
73.650	-53.280	1997	04	4.72929	BT	GRB970404-
216.280	-41.790	1997	04	4.83755	BT	GRB970404-
133.300	-12.900	1997	04	5.03027	BNT	GRB
98.840	22.840	1997	04	5.15418	BeS	970405A
201.000	38.000	1997	04	6.01225	BeS	970406A
341.030	-67.850	1997	04	6.17306	BT	GRB970406-
50.810	-24.640	1997	04	6.26358	BeS	970406B
287.600	-30.300	1997	04	6.29509	BeS	970406C
287.300	-28.200	1997	04	6.31000	BNT	GRB
174.280	2.660	1997	04	7.49715	BeS	970407
184.400	41.800	1997	04	7.81000	BNT	GRB
143.040	48.920	1997	04	7.82710	BT	GRB970407-
162.620	10.690	1997	04	8.08767	BT	GRB970408-
167.970	7.390	1997	04	8.24826	BT	GRB970408-
150.500	31.000	1997	04	9.31000	BNT	GRB
15.070	36.300	1997	04	9.78344	BT	GRB970409
333.200	-39.800	1997	04	10.51321	BNT	GRB
56.970	34.340	1997	04	11.41141	BT	GRB970411
111.500	1.840	1997	04	14.30177	BT	GRB970414-
99.600	0.200	1997	04	14.38000	BNT	GRB

Continued on next column

Continued from previous column

RA deg	DEC deg	Year	Month	Day	Cat.	GRB Name
352.110	37.500	1997	04	14.54229	BT	GRB970414-
21.350	-26.470	1997	04	14.67019	BT	GRB970414-
42.530	-11.760	1997	04	15.65765	BeS	970415
228.200	-1.400	1997	04	15.81000	BNT	GRB
309.250	-38.880	1997	04	16.92543	BT	GRB970416
332.000	10.000	1997	04	16.96803	BeS	970416
295.660	55.770	1997	04	17.57890	BT	GRB970417-
56.530	8.610	1997	04	17.59787	BeS	970417B
41.520	17.120	1997	04	17.65770	BT	GRB970417-
331.000	11.000	1997	04	17.75855	BeS	970417C
240.420	-63.040	1997	04	19.25853	BeS	970419
212.990	-15.910	1997	04	20.84309	BeS	970420
25.900	-36.800	1997	04	21.25000	BNT	GRB
290.910	6.410	1997	04	23.72099	BT	GRB970423
54.480	5.130	1997	04	24.18618	BT	GRB970424-
266.610	-44.340	1997	04	24.33809	BT	GRB970424-
18.000	64.000	1997	04	24.41417	BeS	970424A
198.040	-17.530	1997	04	24.42330	BeS	970424B
209.300	-45.500	1997	04	25.69000	BNT	GRB
66.000	-71.800	1997	04	26.12000	BNT	GRB
312.700	59.430	1997	04	26.49900	BT	GRB970426
299.400	-15.600	1997	04	27.31000	BNT	GRB
181.350	-8.370	1997	04	27.52914	BeS	970427
280.400	-9.500	1997	04	27.54993	BNT	GRB
289.640	41.980	1997	04	27.86843	BT	GRB970427-
179.400	36.200	1997	04	27.88000	BNT	GRB
229.400	1.700	1997	04	28.27061	BNT	GRB
225.390	11.040	1997	04	29.29987	BT	GRB970429-
34.720	26.980	1997	04	29.48361	BeS	970429
259.710	44.930	1997	04	30.80459	BeS	970430
176.700	64.300	1997	05	1.12000	BNT	GRB
148.820	-22.320	1997	05	1.36688	BT	GRB970501
304.000	42.000	1997	05	2.42369	BeS	970502
207.400	20.100	1997	05	2.75000	BNT	GRB
170.660	70.180	1997	05	3.24038	BT	GRB970503
95.000	-23.000	1997	05	4.34265	BeS	970504
164.640	-29.640	1997	05	4.53809	BT	GRB970504-
157.290	-9.970	1997	05	4.97968	BT	GRB970504-
264.860	18.420	1997	05	5.06201	BT	GRB970505
88.300	40.700	1997	05	6.06000	BNT	GRB
30.000	-10.000	1997	05	6.65402	BeS	970506
89.220	83.480	1997	05	7.70955	BT	GRB970507
189.200	-63.500	1997	05	7.91822	BNT	GRB
286.500	-4.800	1997	05	8.89692	BNT	GRB
103.370	79.280	1997	05	8.90402	BeS	970508
192.380	20.100	1997	05	9.55829	BeS	970509
284.880	68.660	1997	05	10.11955	BT	GRB970510-
12.840	-0.840	1997	05	10.76991	BT	GRB970510-

Continued on next column

Continued from previous column

RA deg	DEC deg	Year	Month	Day	Cat.	GRB Name
0.500	19.690	1997	05	11.62509	BT	GRB970511
333.300	33.300	1997	05	11.69000	BNT	GRB
194.400	36.300	1997	05	13.72257	BNT	GRB
67.610	-60.890	1997	05	14.09325	BT	GRB970514
199.500	-27.300	1997	05	14.23314	BNT	GRB
65.300	-17.660	1997	05	16.82868	BT	GRB970516
333.580	17.320	1997	05	17.01317	BeS	970517A
112.110	-15.410	1997	05	17.37827	BeS	970517B
119.000	-36.000	1997	05	17.53666	BeS	970517C
77.000	17.000	1997	05	18.30014	BeS	970518
85.300	48.700	1997	05	18.38000	BNT	GRB
213.460	-63.580	1997	05	19.54268	BT	GRB970519
33.730	51.040	1997	05	21.40125	BT	GRB970521
187.100	-23.000	1997	05	22.06000	BNT	GRB
235.720	-12.970	1997	05	22.85182	BT	GRB970522
39.440	-38.050	1997	05	23.52072	BT	GRB970523-
111.080	43.870	1997	05	23.95938	BT	GRB970523-
88.200	-29.900	1997	05	24.41736	BNT	GRB
261.730	33.380	1997	05	25.11115	BT	GRB970525
149.500	50.800	1997	05	25.36790	BeS	970525
142.600	57.400	1997	05	25.38000	BNT	GRB
287.100	-14.900	1997	05	26.00517	BNT	GRB
1.120	12.940	1997	05	26.07880	BeS	970526
149.700	-42.300	1997	05	26.56000	BNT	GRB
160.400	-64.300	1997	05	27.56000	BNT	GRB
234.400	-0.900	1997	05	29.59850	BNT	GRB
155.820	13.050	1997	05	29.62807	BT	GRB970529
323.330	-75.800	1997	05	30.19450	BT	GRB970530
263.300	-84.100	1997	05	31.62000	BNT	GRB
105.250	-13.850	1997	06	3.40912	BeS	970603A
177.050	62.310	1997	06	3.98265	BeS	970603B
301.900	41.800	1997	06	4.75000	BNT	GRB
89.984	-66.617	1997	06	4.82575	K/W	970604_T71345
148.680	60.790	1997	06	5.33918	BT	GRB970605
181.900	-72.500	1997	06	5.50000	BNT	GRB
35.000	23.100	1997	06	7.44000	BNT	GRB
354.200	-38.700	1997	06	7.50000	BNT	GRB
113.482	-19.680	1997	06	8.56751	K/W	970608_T49032
195.480	37.050	1997	06	9.08542	BeS	970609
61.780	-5.500	1997	06	9.34309	BT	GRB970609-
32.700	41.800	1997	06	10.41961	BeS	970610
16.000	22.400	1997	06	10.44000	BNT	GRB
36.100	4.400	1997	06	10.75000	BNT	GRB
193.800	-42.000	1997	06	11.06543	BNT	GRB
78.370	-3.310	1997	06	11.34826	BeS	970611
273.100	57.000	1997	06	11.81000	BNT	GRB
272.620	8.420	1997	06	12.30454	BeS	970612A
290.230	43.520	1997	06	12.60308	BeS	970612B

Continued on next column

Continued from previous column

RA deg	DEC deg	Year	Month	Day	Cat.	GRB Name
117.570	62.150	1997	06	12.85985	BT	GRB970612-
106.850	28.190	1997	06	13.22466	BeS	970613
199.810	-16.600	1997	06	13.41994	BT	GRB970613-
273.370	24.980	1997	06	13.63339	BT	GRB970613-
317.350	-46.180	1997	06	14.32487	BT	GRB970614-
234.690	62.200	1997	06	14.96367	BeS	970614
201.900	-30.600	1997	06	15.00000	BNT	GRB
32.330	33.030	1997	06	16.07723	BT	GRB970616-
20.440	-7.120	1997	06	16.75740	BeS	970616
346.300	-18.500	1997	06	16.94000	BNT	GRB
204.180	-73.270	1997	06	17.01040	BT	GRB970617
160.900	10.100	1997	06	17.69000	BNT	GRB
161.700	10.600	1997	06	17.71141	BeS	970617A
226.860	48.460	1997	06	18.50381	BT	GRB970618
333.200	67.700	1997	06	19.67412	BNT	GRB
279.500	-40.190	1997	06	23.22456	BeS	970623
154.680	-45.420	1997	06	24.43661	BT	GRB970624
77.170	-79.635	1997	06	25.27410	K/W	970625_T23681
102.253	5.135	1997	06	26.07221	K/W	970626_T06239
154.000	-9.400	1997	06	26.76753	BNT	GRB
190.800	-72.700	1997	06	26.94000	BNT	GRB
227.740	39.980	1997	06	27.04473	BT	GRB970627-
120.840	42.280	1997	06	27.30074	BeS	970627A
285.240	-18.360	1997	06	27.84262	BT	GRB970627-
10.000	-44.800	1997	06	28.23810	BNT	GRB
24.060	6.220	1997	06	28.30755	BT	GRB970628-
298.470	-38.250	1997	06	28.58700	BT	GRB970628-
45.920	-24.020	1997	06	28.86573	BeS	970628B
29.620	25.040	1997	06	29.59496	BeS	970629
326.700	-21.400	1997	06	29.88000	BNT	GRB
272.650	32.300	1997	07	1.46931	BeS	970701
74.820	-16.000	1997	07	4.04742	BeS	970704
210.700	-59.650	1997	07	4.53667	BT	GRB970704-
173.600	-3.400	1997	07	5.84454	BNT	GRB
191.970	7.380	1997	07	7.09093	BT	GRB970707-
344.780	-12.950	1997	07	7.79760	BT	GRB970707-
141.120	-21.160	1997	07	8.14720	BT	GRB970708-
153.610	-54.330	1997	07	8.57381	BT	GRB970708-
263.030	32.620	1997	07	9.28830	BT	GRB970709-
315.910	-31.300	1997	07	9.56331	BeS	970709
244.600	20.700	1997	07	9.62000	BNT	GRB
49.100	-2.400	1997	07	12.31000	BNT	GRB
19.780	-32.050	1997	07	12.53829	BT	GRB970712
161.550	-14.350	1997	07	13.26142	BT	GRB970713-
274.480	58.650	1997	07	13.63708	BeS	970713A
127.120	58.450	1997	07	13.87311	BeS	970713B
12.250	32.360	1997	07	14.12358	BT	GRB970714-
6.290	-29.340	1997	07	14.44928	BT	GRB970714-

Continued on next column

Continued from previous column

RA deg	DEC deg	Year	Month	Day	Cat.	GRB Name
4.400	-22.900	1997	07	14.56000	BNT	GRB
270.470	-64.560	1997	07	15.51601	BT	GRB970715
114.190	-58.520	1997	07	16.17607	BT	GRB970716
52.500	40.600	1997	07	19.39079	BNT	GRB
277.400	-7.400	1997	07	20.79300	BNT	GRB
229.690	-33.160	1997	07	20.93502	BT	GRB970720
292.200	26.200	1997	07	22.06109	BNT	GRB
114.460	-33.100	1997	07	23.21588	BT	GRB970723
199.500	46.700	1997	07	24.38000	BNT	GRB
286.420	48.970	1997	07	25.20221	BT	GRB970725-
12.950	36.210	1997	07	25.95183	BT	GRB970725-
64.100	-8.900	1997	07	26.94000	BNT	GRB
283.000	46.800	1997	07	28.44000	BNT	GRB
258.520	-57.460	1997	07	31.83895	BT	GRB970731
101.040	29.550	1997	08	1.26512	BT	GRB970801
308.000	-54.300	1997	08	1.31000	BNT	GRB
219.100	-13.600	1997	08	1.69000	BNT	GRB
215.070	3.320	1997	08	2.14269	BT	GRB970802-
101.970	-1.980	1997	08	2.70487	BT	GRB970802-
146.370	59.800	1997	08	3.77010	BT	GRB970803
68.000	81.600	1997	08	4.50000	BNT	GRB
227.900	-30.100	1997	08	6.86231	BNT	GRB
224.710	-40.720	1997	08	7.34597	BT	GRB970807-
289.440	-38.700	1997	08	7.76747	BT	GRB970807-
92.800	-19.900	1997	08	7.98279	BNT	GRB
9.100	34.000	1997	08	8.14619	BNT	GRB
183.930	66.830	1997	08	9.11520	BT	GRB970809-
159.300	-65.520	1997	08	9.65160	BT	GRB970809-
307.430	-29.170	1997	08	10.90693	BT	GRB970810
183.900	-13.400	1997	08	11.89339	BNT	GRB
305.900	-14.400	1997	08	12.06000	BNT	GRB
98.900	-33.500	1997	08	12.12154	BNT	GRB
111.000	13.000	1997	08	12.15233	BeS	970812
145.100	-28.500	1997	08	13.92887	BNT	GRB
306.790	38.220	1997	08	14.01225	BT	GRB970814
242.180	81.500	1997	08	15.50492	BeS	970815
91.570	44.970	1997	08	16.09566	BeS	970816
313.400	63.600	1997	08	16.56000	BNT	GRB
277.430	36.630	1997	08	17.35312	BT	GRB970817-
50.300	50.500	1997	08	17.80670	BeS	970817
246.110	50.500	1997	08	17.99871	BT	GRB970817-
319.720	18.980	1997	08	18.75496	BeS	970818
95.210	68.930	1997	08	20.23404	BeS	970820
117.000	15.000	1997	08	21.45790	BeS	970821
226.070	-76.990	1997	08	21.61808	BT	GRB970821
300.000	27.300	1997	08	23.38000	BNT	GRB
191.630	33.170	1997	08	24.24279	BT	GRB970824-
221.870	39.260	1997	08	24.72484	BeS	970824A

Continued on next column

Continued from previous column

RA deg	DEC deg	Year	Month	Day	Cat.	GRB Name
115.330	36.660	1997	08	24.88563	BT	GRB970824-
29.200	-47.800	1997	08	25.47030	BeS	970825A
43.600	-46.400	1997	08	25.50000	BNT	GRB
89.260	-10.180	1997	08	25.91867	BeS	970825B
168.440	-3.370	1997	08	26.40626	BT	GRB970826
287.600	-23.800	1997	08	27.29978	BeS	970827A
288.700	-22.600	1997	08	27.31000	BNT	GRB
134.650	-51.640	1997	08	27.41382	BeS	970827B
131.100	-8.000	1997	08	28.12197	BNT	GRB
269.220	59.420	1997	08	28.73932	BT	GRB970828
7.800	12.700	1997	08	29.33639	BNT	GRB
226.050	1.530	1997	08	29.39559	BT	GRB970829
340.200	-32.200	1997	08	30.11248	BNT	GRB
85.750	-47.330	1997	08	31.73589	BeS	970831
210.830	24.010	1997	09	2.19085	BT	GRB970902-
351.026	7.329	1997	09	2.31899	K/W	970902_T27561
74.740	-30.410	1997	09	2.42384	BT	GRB970902-
17.600	13.890	1997	09	3.48529	BT	GRB970903-
237.750	-58.440	1997	09	3.72579	BeS	970903
95.390	-55.360	1997	09	4.45632	BT	GRB970904
220.330	57.610	1997	09	6.11573	BT	GRB970906
168.300	19.800	1997	09	6.25000	BNT	GRB
228.900	45.600	1997	09	6.69000	BNT	GRB
346.900	11.260	1997	09	7.13587	BT	GRB970907-
175.470	-17.340	1997	09	7.27039	BeS	970907
273.470	38.690	1997	09	7.47201	BT	GRB970907-
111.740	24.450	1997	09	8.30059	BT	GRB970908-
342.370	-35.520	1997	09	8.51882	BT	GRB970908-
176.800	40.200	1997	09	9.81000	BNT	GRB
316.640	-45.440	1997	09	10.05109	BeS	970910
22.700	-26.100	1997	09	10.31000	BNT	GRB
100.510	32.140	1997	09	10.47649	BT	GRB970910-
350.700	-23.800	1997	09	11.94675	BNT	GRB
341.230	45.300	1997	09	12.62373	BT	GRB970912-
55.700	39.100	1997	09	12.69000	BNT	GRB
181.280	-23.460	1997	09	12.91139	BT	GRB970912-
144.800	7.400	1997	09	14.09995	BNT	GRB
297.300	43.700	1997	09	14.56000	BNT	GRB
17.200	73.300	1997	09	14.94000	BNT	GRB
238.970	61.760	1997	09	15.65227	BT	GRB970915
210.400	-15.700	1997	09	16.81000	BNT	GRB
302.000	29.000	1997	09	17.00000	BNT	GRB
233.800	-36.800	1997	09	17.83984	BNT	GRB
94.300	24.400	1997	09	17.88000	BNT	GRB
31.490	40.180	1997	09	18.40377	BT	GRB970918-
29.390	-67.580	1997	09	18.66971	BT	GRB970918-
194.980	45.460	1997	09	19.15626	BeS	970919A
140.390	-4.740	1997	09	19.76000	BeS	970919B

Continued on next column

Continued from previous column

RA deg	DEC deg	Year	Month	Day	Cat.	GRB Name
298.550	59.560	1997	09	19.92378	BeS	970919C
235.883	-24.831	1997	09	21.97023	K/W	970921-T83828
280.500	20.300	1997	09	21.99882	BNT	GRB
328.000	62.000	1997	09	22.10135	BeS	970922B
230.720	49.470	1997	09	23.38917	BT	GRB970923
29.000	-41.000	1997	09	23.48565	BeS	970923
289.600	70.800	1997	09	23.76799	BNT	GRB
95.000	-54.000	1997	09	24.11037	BeS	970924
287.850	0.520	1997	09	24.57665	BT	GRB970924
346.970	54.600	1997	09	25.29450	BT	GRB970925-
326.840	-8.420	1997	09	25.94671	BT	GRB970925-
60.300	60.200	1997	09	26.28947	BNT	GRB
345.130	-4.360	1997	09	26.43382	BT	GRB970926-
139.420	18.280	1997	09	26.84844	BT	GRB970926-
161.500	-39.100	1997	09	26.94000	BNT	GRB
313.700	40.400	1997	09	26.95578	BT	GRB970926-
311.100	-3.000	1997	09	27.00000	BNT	GRB
168.300	78.630	1997	09	28.09847	BeS	970928
281.450	-84.510	1997	09	30.00068	BT	GRB970930-
40.400	-19.900	1997	09	30.65459	BeS	970930
270.240	-88.000	1997	09	30.92986	BT	GRB970930-
182.300	-72.600	1997	10	1.96512	BNT	GRB
8.420	47.250	1997	10	2.73723	BeS	971002
193.370	-7.960	1997	10	2.90084	BT	GRB971002-
205.400	-33.300	1997	10	4.15547	BNT	GRB
354.550	-24.600	1997	10	4.57929	BT	GRB971004-
324.430	83.290	1997	10	4.82339	BT	GRB971004-
331.170	-56.250	1997	10	5.05273	BeS	971005
249.770	53.230	1997	10	6.22010	BT	GRB971006
221.720	-17.070	1997	10	7.66390	BeS	971007
38.090	-48.390	1997	10	8.15606	BT	GRB971008
255.960	-31.060	1997	10	9.34306	BeS	971009A
273.510	-66.240	1997	10	9.78953	BeS	971009B
206.080	-59.720	1997	10	11.49367	BeS	971011
329.720	40.980	1997	10	12.33403	BT	GRB971012
167.030	2.660	1997	10	13.36347	BT	GRB971013-
197.500	72.900	1997	10	13.63745	BNT	GRB
84.800	25.500	1997	10	13.88000	BNT	GRB
221.750	-63.870	1997	10	13.99802	BeS	971013
284.810	-52.840	1997	10	14.22532	BeS	971014
114.700	-69.000	1997	10	14.95118	BNT	GRB
265.710	12.910	1997	10	15.15964	BeS	971015
280.800	-79.200	1997	10	15.25000	BNT	GRB
279.990	18.620	1997	10	15.35253	BT	GRB971015-
192.630	28.430	1997	10	15.90551	BT	GRB971015-
51.780	49.320	1997	10	16.48260	BT	GRB971016
35.800	81.000	1997	10	17.00000	BNT	GRB
246.700	47.400	1997	10	18.50000	BNT	GRB

Continued on next column

Continued from previous column

RA deg	DEC deg	Year	Month	Day	Cat.	GRB Name
153.000	6.000	1997	10	19.62214	BeS	971019
212.000	63.200	1997	10	19.66467	BNT	GRB
149.000	-54.000	1997	10	20.16931	BeS	971020
28.790	-45.210	1997	10	20.23455	BT	GRB971020
3.600	-5.300	1997	10	21.16550	BNT	GRB
69.600	21.000	1997	10	21.30396	BNT	GRB
147.030	3.410	1997	10	21.71409	BT	GRB971021
11.000	-64.000	1997	10	22.49813	BeS	971022A
54.000	-65.000	1997	10	22.81971	BeS	971022B
246.320	29.260	1997	10	23.35847	BT	GRB971023-
288.080	51.520	1997	10	23.46683	BeS	971023B
191.440	-36.600	1997	10	23.49898	BT	GRB971023-
276.210	49.470	1997	10	24.48163	BeS	971024A
141.000	80.000	1997	10	24.56020	BeS	971024B
147.300	40.300	1997	10	24.78390	BNT	GRB
104.540	25.630	1997	10	24.93258	BT	GRB971024-
138.000	13.200	1997	10	26.19000	BNT	GRB
205.700	59.200	1997	10	27.11354	BeS	971027A
194.600	67.500	1997	10	27.12000	BNT	GRB
185.500	20.100	1997	10	27.29630	BNT	GRB
309.000	-51.000	1997	10	27.36973	BeS	971027B
275.900	29.200	1997	10	27.81000	BNT	GRB
199.250	-1.690	1997	10	28.27698	BT	GRB971028
213.900	-4.900	1997	10	28.86951	BeS	971028
101.120	24.670	1997	10	29.06164	BeS	971029
66.870	-44.970	1997	10	29.25959	BT	GRB971029-
243.030	70.630	1997	10	29.70005	BT	GRB971029-
281.300	-64.400	1997	10	30.21875	BNT	GRB
347.800	-6.300	1997	10	30.81000	BNT	GRB
359.000	13.100	1997	11	1.25000	BNT	GRB
205.500	-78.200	1997	11	1.81948	BNT	GRB
181.100	38.600	1997	11	2.06468	BeS	971102A
280.000	-37.000	1997	11	2.07623	BeS	971102B
287.700	-59.600	1997	11	2.25000	BNT	GRB
3.500	2.200	1997	11	3.31362	BeS	971103
32.000	-36.200	1997	11	3.81000	BNT	GRB
290.840	-38.510	1997	11	4.85324	BT	GRB971104
65.700	42.500	1997	11	5.16425	BNT	GRB
193.800	-23.100	1997	11	6.12000	BNT	GRB
253.100	-1.800	1997	11	6.65116	BNT	GRB
236.070	-70.440	1997	11	8.12008	BT	GRB971108
118.100	42.800	1997	11	8.38000	BNT	GRB
42.300	12.600	1997	11	9.00000	BNT	GRB
65.000	47.600	1997	11	10.19000	BNT	GRB
301.900	-34.100	1997	11	10.56000	BNT	GRB
241.670	50.370	1997	11	10.78692	BeS	971110
215.500	30.200	1997	11	10.81000	BNT	GRB
35.600	-30.500	1997	11	11.13337	BNT	GRB

Continued on next column

Continued from previous column

RA deg	DEC deg	Year	Month	Day	Cat.	GRB Name
168.500	71.500	1997	11	12.09807	BNT	GRB
216.570	-76.630	1997	11	13.67281	BT	GRB971113
342.900	49.800	1997	11	13.82995	BNT	GRB
57.000	-50.000	1997	11	14.51463	BeS	971114
84.630	41.690	1997	11	15.76573	BT	GRB971115-
60.890	-4.750	1997	11	15.80928	BT	GRB971115-
74.000	20.300	1997	11	17.31662	BNT	GRB
38.700	78.500	1997	11	17.69000	BNT	GRB
176.400	1.200	1997	11	18.14970	BNT	GRB
113.910	-73.700	1997	11	18.33574	BT	GRB971118-
36.000	3.000	1997	11	18.86332	BeS	971118
319.190	-57.650	1997	11	18.92234	BT	GRB971118-
38.500	56.600	1997	11	19.25000	BNT	GRB
155.760	76.410	1997	11	20.89926	BT	GRB971120
288.000	-71.000	1997	11	21.50000	BNT	GRB
187.630	-9.320	1997	11	21.50427	BT	GRB971121
72.580	-9.790	1997	11	22.03926	BT	GRB971122-
118.870	-30.720	1997	11	22.61161	BT	GRB971122-
232.900	6.300	1997	11	22.89007	BNT	GRB
300.490	78.470	1997	11	22.89561	BeS	971122
73.500	-9.200	1997	11	22.99780	BNT	GRB
1.700	18.700	1997	11	23.50000	BNT	GRB
9.700	6.000	1997	11	23.87654	BNT	GRB
255.200	-87.100	1997	11	24.01638	BT	GRB971124
140.800	15.600	1997	11	25.06000	BNT	GRB
223.340	-13.260	1997	11	25.30682	BT	GRB971125-
304.470	12.320	1997	11	25.78807	BT	GRB971125-
225.610	31.930	1997	11	27.00326	BeS	971127
29.300	53.600	1997	11	27.44000	BNT	GRB
140.500	82.700	1997	11	28.93315	BNT	GRB
223.820	-12.070	1997	11	30.12537	BT	GRB971130-
199.710	-28.710	1997	11	30.64586	BT	GRB971130-
111.000	21.000	1997	11	30.85395	BeS	971130
230.820	36.330	1997	12	1.23889	BT	GRB971201
42.900	15.400	1997	12	1.25000	BNT	GRB
338.400	59.900	1997	12	1.81729	BNT	GRB
36.150	-14.300	1997	12	2.56588	BT	GRB971202
322.300	-42.500	1997	12	3.25000	BNT	GRB
195.830	-34.510	1997	12	4.19022	BT	GRB971204
117.840	4.130	1997	12	6.53506	BeS	971206A
161.050	-5.780	1997	12	6.80611	BeS	971206B
56.000	1.000	1997	12	6.91509	BeS	971206C
264.950	-6.090	1997	12	7.26896	BT	GRB971207-
95.070	3.380	1997	12	7.43395	BT	GRB971207-
91.200	56.000	1997	12	7.81000	BNT	GRB
133.740	-4.590	1997	12	7.83613	BeS	971207A
138.200	71.000	1997	12	7.87375	BeS	971207B
131.400	71.100	1997	12	7.88000	BNT	GRB

Continued on next column

Continued from previous column

RA deg	DEC deg	Year	Month	Day	Cat.	GRB Name
50.000	-12.000	1997	12	8.19944	BeS	971208A
356.460	77.940	1997	12	8.32542	BeS	971208B
241.350	62.210	1997	12	9.96569	BT	GRB971209
176.910	-51.950	1997	12	10.32192	BeS	971210
7.700	15.300	1997	12	10.52737	BNT	GRB
253.480	32.710	1997	12	10.89127	BT	GRB971210-
223.000	10.200	1997	12	12.41875	BNT	GRB
306.690	-44.950	1997	12	12.92891	BeS	971212
345.350	-6.700	1997	12	13.72515	BT	GRB971213
209.300	58.500	1997	12	14.06000	BNT	GRB
179.120	65.200	1997	12	14.97271	BeS	971214B
214.900	-11.000	1997	12	16.08535	BNT	GRB
357.020	-23.420	1997	12	16.32294	BT	GRB971216
91.000	-29.200	1997	12	18.47696	BNT	GRB
248.000	31.000	1997	12	18.52968	BeS	971218
41.620	61.470	1997	12	18.60764	BT	GRB971218-
116.170	16.670	1997	12	18.69811	BT	GRB971218-
220.400	-9.400	1997	12	19.32359	BNT	GRB
240.000	-45.000	1997	12	19.44534	BeS	971219A
356.440	34.730	1997	12	19.81670	BT	GRB971219
33.230	-38.550	1997	12	20.17123	BeS	971220
205.440	58.840	1997	12	20.81367	BT	GRB971220-
73.740	4.690	1997	12	21.50945	BT	GRB971221
289.930	-17.810	1997	12	22.48396	BT	GRB971222
316.900	60.200	1997	12	22.73263	BNT	GRB
193.200	27.400	1997	12	22.83336	BNT	GRB
144.400	20.200	1997	12	22.93125	BNT	GRB
221.650	50.530	1997	12	23.02642	BeS	971223A
75.000	-26.000	1997	12	23.39931	BeS	971223B
312.000	-43.000	1997	12	23.44191	BeS	971223C
151.900	2.000	1997	12	25.73351	BNT	GRB
265.120	64.650	1997	12	25.75039	BT	GRB971225
194.400	59.250	1997	12	27.34939	BeS	971227
138.000	-29.000	1997	12	28.28866	BeS	971228A
155.180	62.230	1997	12	28.34125	BT	GRB971228
34.400	26.900	1997	12	28.62074	BeS	971228B
50.600	-58.100	1997	12	28.91449	BNT	GRB
340.290	-68.340	1997	12	29.42470	BeS	971229
305.150	-9.530	1997	12	30.37792	BT	GRB971230-
147.610	-19.150	1997	12	30.46394	BT	GRB971230-
148.549	-12.954	1997	12	30.96933	K/W	971230..T83750
205.070	35.050	1998	01	1.14403	BeS	980101
236.690	-75.040	1998	01	3.44355	BeS	980103A
133.850	1.480	1998	01	3.66751	BeS	980103B
74.800	-58.200	1998	01	3.90303	BNT	GRB
37.200	51.660	1998	01	5.03104	BeS	980105
210.000	61.000	1998	01	6.51193	BNT	GRB
106.990	12.790	1998	01	6.55292	BT	GRB980106

Continued on next column

Continued from previous column

RA deg	DEC deg	Year	Month	Day	Cat.	GRB Name
286.000	4.000	1998	01	6.60527	BeS	980106
75.600	14.400	1998	01	7.48086	BNT	GRB
190.240	-7.190	1998	01	7.57593	BT	GRB980107
311.000	-20.950	1998	01	8.77925	BT	GRB980108
6.480	-63.020	1998	01	9.05030	BeS	980109
168.490	-55.510	1998	01	9.32375	BT	GRB980109-
270.010	-40.310	1998	01	10.80869	BT	GRB980110
40.510	71.640	1998	01	12.32644	BeS	980112B
136.110	-24.790	1998	01	12.35388	BT	GRB980112-
266.970	10.710	1998	01	12.59427	BT	GRB980112-
261.030	-23.830	1998	01	13.17183	BT	GRB980113
193.900	19.900	1998	01	13.23861	BNT	GRB
251.000	25.310	1998	01	14.28997	BT	GRB980114
161.600	13.300	1998	01	14.35697	BNT	GRB
315.310	37.790	1998	01	16.61374	BT	GRB980116
296.000	40.000	1998	01	16.62611	BeS	980116
306.300	9.300	1998	01	18.04015	BNT	GRB
96.000	0.000	1998	01	18.49570	BeS	980118
109.100	-13.200	1998	01	19.39755	BNT	GRB
293.000	-21.000	1998	01	21.94633	BeS	980121
272.220	80.300	1998	01	24.27403	BeS	980124A
8.690	45.510	1998	01	24.81222	BT	GRB980124-
192.200	-62.700	1998	01	24.87337	BeS	980124B
345.580	-15.830	1998	01	24.94528	BT	GRB980124-
97.160	1.480	1998	01	25.43132	BT	GRB980125-
350.680	35.810	1998	01	25.86075	BT	GRB980125-
81.100	27.500	1998	01	26.16129	BNT	GRB
245.650	-62.320	1998	01	26.86185	BT	GRB980126
36.000	-29.000	1998	01	27.04088	BeS	980127
148.300	-66.700	1998	01	28.38431	BNT	GRB
287.430	-64.920	1998	01	29.63870	BeS	980129
278.700	6.500	1998	01	29.92919	BNT	GRB
357.700	-4.200	1998	01	30.57167	BNT	GRB
313.500	60.900	1998	01	30.63640	BNT	GRB
135.600	41.700	1998	01	30.77559	BNT	GRB
194.200	41.700	1998	01	31.22785	BNT	GRB
329.400	37.300	1998	01	31.77749	BNT	GRB
357.500	22.900	1998	02	1.91472	BNT	GRB
151.400	-44.500	1998	02	2.23102	BNT	GRB
46.240	-52.710	1998	02	2.58782	BT	GRB980202
333.340	49.590	1998	02	3.24262	BT	GRB980203-
3.460	-17.650	1998	02	3.94940	BeS	980203B
146.400	-37.400	1998	02	5.22898	BeS	980205
14.720	46.180	1998	02	6.39811	BT	GRB980206
82.200	-53.500	1998	02	6.67316	BNT	GRB
101.270	5.800	1998	02	7.19736	BT	GRB980207-
193.100	49.500	1998	02	7.67375	BNT	GRB
318.630	-11.750	1998	02	7.75815	BT	GRB980207-

Continued on next column

Continued from previous column

RA deg	DEC deg	Year	Month	Day	Cat.	GRB Name
75.990	-32.200	1998	02	8.52318	BeS	980208A
60.970	-75.490	1998	02	8.53542	BeS	980208B
249.400	-8.400	1998	02	9.91434	BNT	GRB
171.500	-46.000	1998	02	10.69576	BNT	GRB
112.600	-29.000	1998	02	11.55838	BNT	GRB
243.200	21.400	1998	02	12.53179	BNT	GRB
239.210	-38.360	1998	02	13.01231	BT	GRB980213-
251.840	68.090	1998	02	13.69865	BT	GRB980213-
11.100	-23.800	1998	02	13.73991	BNT	GRB
6.200	-10.600	1998	02	13.75057	BNT	GRB
354.790	-32.350	1998	02	14.26899	BT	GRB980214-
229.150	1.780	1998	02	14.51013	BT	GRB980214-
341.700	-52.570	1998	02	15.76711	BT	GRB980215
183.290	56.640	1998	02	18.15652	BT	GRB980218-
90.730	-10.110	1998	02	18.63387	BT	GRB980218-
217.330	-65.800	1998	02	18.99147	BT	GRB980218-
250.990	-54.720	1998	02	19.57828	BT	GRB980219
53.500	-27.800	1998	02	21.13383	BNT	GRB
114.600	-27.800	1998	02	21.72104	BNT	GRB
31.210	28.510	1998	02	22.10134	BeS	980222
219.500	7.600	1998	02	22.15552	BNT	GRB
189.770	-29.220	1998	02	22.39765	BT	GRB980222-
219.850	27.940	1998	02	23.53104	BT	GRB980223
305.300	-42.600	1998	02	23.88706	BeS	980223
138.700	53.200	1998	02	24.44325	BNT	GRB
56.600	8.700	1998	02	24.55559	BNT	GRB
186.000	18.000	1998	02	24.87099	BeS	980224
126.170	14.440	1998	02	25.35375	BT	GRB980225
243.000	-10.000	1998	02	26.47840	BeS	980226
95.810	-63.740	1998	02	26.68913	BT	GRB980226
54.900	22.800	1998	02	26.71946	BNT	GRB
24.510	13.430	1998	02	28.28064	BT	GRB980228-
293.100	-24.600	1998	02	28.60592	BNT	GRB
90.490	44.100	1998	02	28.70418	BT	GRB980228-
184.000	24.000	1998	02	28.96642	BeS	980228
204.400	32.200	1998	03	1.12944	BNT	GRB
148.360	34.880	1998	03	1.25485	BT	GRB980301-
348.500	16.450	1998	03	1.32340	BT	GRB980301-
98.550	-31.040	1998	03	1.37425	BT	GRB980301-
1.370	47.690	1998	03	1.52938	BT	GRB980301-
31.300	-7.290	1998	03	2.20802	BT	GRB980302
181.200	-6.900	1998	03	2.57646	BNT	GRB
193.600	18.600	1998	03	4.40376	BNT	GRB
18.400	44.800	1998	03	4.61185	BeS	980304
192.200	-40.000	1998	03	5.37685	BNT	GRB
239.900	-64.700	1998	03	6.16178	BNT	GRB
7.050	-45.510	1998	03	6.39794	BeS	980306B
341.630	-56.740	1998	03	6.73207	BeS	980306C

Continued on next column

Continued from previous column

RA deg	DEC deg	Year	Month	Day	Cat.	GRB Name
188.600	36.800	1998	03	6.97765	BNT	GRB
273.290	35.440	1998	03	8.22268	BT	GRB980308
310.230	-48.060	1998	03	9.00500	BT	GRB980309-
223.780	-14.290	1998	03	9.71459	BT	GRB980309-
75.190	-60.720	1998	03	10.02534	BT	GRB980310-
242.410	-60.470	1998	03	10.58172	BeS	980310A
142.760	-48.240	1998	03	12.95108	BT	GRB980312
285.990	-38.160	1998	03	13.04948	BT	GRB980313-
31.850	42.330	1998	03	13.37803	BeS	980313
75.840	20.360	1998	03	15.11802	BeS	980315A
74.650	31.570	1998	03	15.30895	BeS	980315B
180.090	74.620	1998	03	15.51683	BT	GRB980315-
0.470	-40.220	1998	03	15.85977	BT	GRB980315-
68.900	17.600	1998	03	17.98740	BNT	GRB
10.260	-26.970	1998	03	19.37361	BT	GRB980319
226.360	-38.790	1998	03	20.01286	BT	GRB980320
82.000	29.000	1998	03	20.68228	BeS	980320
42.250	7.590	1998	03	21.25434	BeS	980321
34.030	61.700	1998	03	22.10226	BT	GRB980322
66.000	29.000	1998	03	24.47552	BeS	980324A
208.790	-53.640	1998	03	25.14918	BT	GRB980325-
305.800	-0.300	1998	03	25.38440	BNT	GRB
61.360	53.240	1998	03	25.61546	BT	GRB980325-
266.290	-21.270	1998	03	26.18523	BT	GRB980326-
129.110	-18.880	1998	03	26.88811	BeS	980326
103.900	22.600	1998	03	27.93285	BT	GRB980327
105.670	38.830	1998	03	29.15586	BeS	980329A
273.690	59.150	1998	03	29.43819	BT	GRB980329-
260.100	12.800	1998	03	29.44091	BNT	GRB
172.300	-63.200	1998	03	29.64221	BeS	980329B
224.920	-24.010	1998	03	30.00106	BeS	980330
131.360	-24.670	1998	03	31.27924	BT	GRB980331-
191.360	-44.940	1998	03	31.70689	BT	GRB980331-
125.700	18.270	1998	04	1.18882	BeS	980401A
35.440	-3.510	1998	04	1.38266	BeS	980401B
198.550	-62.390	1998	04	1.53222	BeS	980401C
138.000	-35.900	1998	04	1.64662	BNT	GRB
198.120	62.140	1998	04	2.90912	BT	GRB980402
279.550	46.410	1998	04	3.96935	BeS	980403
69.240	-49.950	1998	04	4.70255	BT	GRB980404-
0.000	11.800	1998	04	4.78807	BeS	980404
339.340	20.060	1998	04	5.45737	BT	GRB980405
176.430	63.330	1998	04	6.45677	BT	GRB980406
31.000	-56.000	1998	04	6.71811	BeS	980406B
104.990	1.120	1998	04	7.76177	BT	GRB980407
64.000	27.000	1998	04	7.78588	BeS	980407
206.370	9.830	1998	04	9.08929	BeS	980409
327.300	17.100	1998	04	13.39847	BNT	GRB

Continued on next column

Continued from previous column

RA deg	DEC deg	Year	Month	Day	Cat.	GRB Name
93.590	8.520	1998	04	13.86988	BT	GRB980413
95.760	0.050	1998	04	16.25573	BT	GRB980416
182.000	2.000	1998	04	16.59209	BeS	980416
300.590	17.760	1998	04	17.27128	BT	GRB980417-
67.810	-8.440	1998	04	17.70829	BT	GRB980417-
134.250	9.240	1998	04	19.60152	BT	GRB980419
130.000	78.000	1998	04	19.88108	BeS	980419
292.810	26.560	1998	04	20.42143	BeS	980420
170.910	-30.410	1998	04	21.05561	BT	GRB980421-
355.070	-38.680	1998	04	21.81618	BT	GRB980421-
220.150	34.920	1998	04	21.94724	BeS	980421
265.690	0.140	1998	04	22.65293	BT	GRB980422
161.190	-58.040	1998	04	23.11506	BT	GRB980423
93.330	5.180	1998	04	24.06398	BeS	980424
174.000	23.000	1998	04	25.44576	BeS	980425A
293.730	-52.820	1998	04	25.90912	BeS	980425B
206.730	-29.700	1998	04	26.45090	BeS	980426
96.060	82.190	1998	04	26.72862	BT	GRB980426-
225.170	-21.890	1998	04	27.65313	BeS	980427
151.900	48.400	1998	04	29.20582	BNT	GRB
313.600	-8.100	1998	04	29.23719	BNT	GRB
130.170	22.810	1998	04	29.36523	BeS	980429
293.370	-66.890	1998	04	30.04500	BT	GRB980430-
91.900	14.200	1998	04	30.11898	BNT	GRB
241.230	28.930	1998	04	30.33461	BT	GRB980430-
307.600	-42.100	1998	04	30.67527	BNT	GRB
223.870	23.360	1998	05	1.92994	BT	GRB980501
115.960	15.110	1998	05	3.08784	BT	GRB980503
325.900	-52.300	1998	05	4.18547	BNT	GRB
323.600	50.700	1998	05	4.37835	BNT	GRB
195.500	-34.400	1998	05	6.29470	BNT	GRB
334.080	20.460	1998	05	8.17183	BeS	980508
271.350	-18.780	1998	05	8.50863	BT	GRB980508-
128.200	70.500	1998	05	8.74354	BNT	GRB
45.500	-18.200	1998	05	9.39144	BNT	GRB
66.990	1.940	1998	05	11.08016	BeS	980511
270.180	-27.560	1998	05	12.97883	BT	GRB980512
135.500	30.500	1998	05	13.53773	BNT	GRB
127.620	-54.840	1998	05	13.90375	BeS	980513
319.520	-67.230	1998	05	15.70856	BeS	980515
89.000	-4.000	1998	05	16.47473	BeS	980516
160.300	-44.500	1998	05	18.26214	BNT	GRB
162.060	-42.490	1998	05	18.28288	BT	GRB980518-
330.700	58.420	1998	05	18.40777	BT	GRB980518-
207.100	-43.900	1998	05	18.69346	BNT	GRB
306.100	-79.000	1998	05	18.78111	BeS	980518A
350.560	77.250	1998	05	19.51414	BeS	980519B
265.500	-59.000	1998	05	20.28891	BNT	GRB

Continued on next column

Continued from previous column

RA deg	DEC deg	Year	Month	Day	Cat.	GRB Name
349.800	-24.100	1998	05	20.60205	BeS	980520B
353.710	-11.320	1998	05	20.80021	BeS	980520C
304.100	-47.300	1998	05	22.82427	BNT	GRB
198.710	-42.400	1998	05	23.03266	BT	GRB980523
336.100	-50.600	1998	05	23.36120	BNT	GRB
48.700	-27.500	1998	05	24.24154	BNT	GRB
248.300	56.400	1998	05	24.37468	BNT	GRB
157.610	-17.860	1998	05	25.10789	BeS	980525
65.900	6.500	1998	05	25.15920	BNT	GRB
248.010	-52.300	1998	05	26.29823	BT	GRB980526
344.250	45.170	1998	05	27.25679	BT	GRB980527-
108.410	14.580	1998	05	27.28853	BT	GRB980527-
276.930	24.150	1998	05	27.34862	BeS	980527
197.390	5.050	1998	05	27.57029	BT	GRB980527-
148.310	-27.290	1998	05	30.04211	BT	GRB980530-
194.220	57.350	1998	05	30.95268	BT	GRB980530-
222.560	-52.100	1998	06	1.27755	BT	GRB980601
313.500	24.100	1998	06	2.53852	BNT	GRB
264.300	44.500	1998	06	5.59178	BeS	980605
71.000	-21.000	1998	06	6.37656	BeS	980606
16.100	-55.900	1998	06	6.71925	BNT	GRB
332.000	1.100	1998	06	7.35831	BNT	GRB
197.870	37.110	1998	06	9.29045	BT	GRB980609-
116.300	-12.300	1998	06	9.61678	BNT	GRB
320.520	-18.650	1998	06	9.85574	BT	GRB980609-
53.010	25.830	1998	06	10.47860	BT	GRB980610
96.262	-32.492	1998	06	10.82809	K/W	980610_T71546
275.270	55.020	1998	06	11.03403	BT	GRB980611-
278.620	76.050	1998	06	11.23703	BT	GRB980611-
308.000	5.100	1998	06	11.38225	BNT	GRB
294.600	-81.500	1998	06	12.70096	BNT	GRB
154.440	71.480	1998	06	13.20215	BeS	980613
58.000	65.000	1998	06	13.60867	BNT	GRB
116.400	-36.280	1998	06	14.36869	BT	GRB980614
352.800	-52.800	1998	06	14.59726	BNT	GRB
242.000	-32.000	1998	06	15.11610	BeS	980615A
43.000	19.000	1998	06	15.42519	BeS	980615B
17.000	4.500	1998	06	15.97752	BNT	GRB
213.320	36.370	1998	06	16.56174	BeS	980616
147.300	5.300	1998	06	16.91023	BNT	GRB
55.950	-3.820	1998	06	17.11935	BeS	980617
56.700	-23.210	1998	06	17.28666	BT	GRB980617-
222.490	48.900	1998	06	17.53031	BT	GRB980617-
269.200	6.400	1998	06	17.94524	BNT	GRB
295.700	-33.600	1998	06	18.21361	BNT	GRB
151.100	9.200	1998	06	18.38212	BNT	GRB
27.400	79.900	1998	06	19.25512	BNT	GRB
345.170	54.200	1998	06	19.50076	BT	GRB980619

Continued on next column

Continued from previous column

RA deg	DEC deg	Year	Month	Day	Cat.	GRB Name
105.521	-41.107	1998	06	19.55012	K/W	980619_T47530
247.000	-49.900	1998	06	22.59126	BNT	GRB
312.000	45.000	1998	06	22.84837	BeS	980622
184.900	-7.900	1998	06	22.85447	BNT	GRB
216.100	85.100	1998	06	23.13439	BNT	GRB
174.900	-38.510	1998	06	24.41859	BT	GRB980624-
185.370	10.070	1998	06	24.49889	BT	GRB980624-
69.500	-10.100	1998	06	24.93255	BNT	GRB
355.900	-18.900	1998	06	25.17558	BNT	GRB
58.870	-72.530	1998	06	26.05971	BT	GRB980626-
131.200	56.800	1998	06	26.81231	BNT	GRB
17.650	-72.980	1998	06	26.94429	BeS	980626B
159.710	-0.230	1998	06	27.18089	BeS	980627A
180.200	22.830	1998	06	27.52539	BeS	980627B
183.140	57.950	1998	06	28.62609	BT	GRB980628
252.100	-42.700	1998	06	29.03035	BNT	GRB
308.460	44.290	1998	06	29.06528	BeS	980629
271.700	53.600	1998	06	29.37473	BNT	GRB
281.000	45.500	1998	06	29.71036	BNT	GRB
158.300	-11.400	1998	07	1.76890	BNT	GRB
138.000	39.000	1998	07	1.77718	BeS	980701
230.100	25.300	1998	07	3.03418	BNT	GRB
359.780	8.580	1998	07	3.18249	BeS	980703
228.000	3.270	1998	07	3.57534	BT	GRB980703-
58.700	53.600	1998	07	3.61904	BNT	GRB
301.200	-7.800	1998	07	3.70975	BNT	GRB
157.100	34.900	1998	07	5.26811	BeS	980705
334.700	53.800	1998	07	5.27083	BNT	GRB
320.200	19.350	1998	07	5.77039	BT	GRB980705
298.280	33.560	1998	07	6.65138	BeS	980706A
162.000	57.330	1998	07	6.66652	BeS	980706B
198.000	49.700	1998	07	6.74059	BeS	980706C
308.000	-37.000	1998	07	6.90322	BeS	980706D
245.770	-45.120	1998	07	7.38207	BT	GRB980707-
72.370	24.650	1998	07	7.68378	BT	GRB980707-
174.800	58.400	1998	07	8.08580	BNT	GRB
151.600	-53.500	1998	07	8.23394	BNT	GRB
14.380	-19.580	1998	07	8.60978	BT	GRB980708
12.600	-31.900	1998	07	9.19643	BeS	980709A
332.400	-7.700	1998	07	9.83617	BNT	GRB
85.300	16.160	1998	07	10.18620	BT	GRB980710
140.500	-21.500	1998	07	10.86315	BNT	GRB
243.100	33.590	1998	07	11.12684	BT	GRB980711
331.900	8.300	1998	07	12.21508	BeS	980712A
292.600	-47.670	1998	07	12.25278	BeS	980712B
66.700	20.700	1998	07	12.39823	BNT	GRB
4.860	-30.740	1998	07	12.87925	BT	GRB980712-
119.700	-28.200	1998	07	13.15398	BeS	980713

Continued on next column

Continued from previous column

RA deg	DEC deg	Year	Month	Day	Cat.	GRB Name
282.810	58.910	1998	07	14.45234	BT	GRB980714
327.000	43.000	1998	07	14.82259	BeS	980714
313.700	-20.700	1998	07	15.40839	BeS	980715
99.210	3.280	1998	07	16.38145	BT	GRB980716
129.000	27.000	1998	07	18.04905	BeS	980718
318.960	-46.430	1998	07	18.12392	BT	GRB980718-
195.970	49.370	1998	07	18.55287	BT	GRB980718-
192.700	35.900	1998	07	20.47198	BNT	GRB
272.930	27.010	1998	07	20.71126	BT	GRB980720
36.000	-28.000	1998	07	20.92786	BeS	980720
43.050	35.250	1998	07	22.72045	BT	GRB980722
145.870	-16.430	1998	07	23.59370	BT	GRB980723
127.750	-31.320	1998	07	24.51965	BeS	980724
193.920	-0.770	1998	07	24.85742	BT	GRB980724-
138.000	5.400	1998	07	25.43456	BNT	GRB
109.010	32.810	1998	07	27.87880	BT	GRB980727-
294.390	-12.420	1998	07	27.97887	BT	GRB980727-
88.000	-56.000	1998	07	28.36707	BeS	980728
164.200	-42.400	1998	07	28.62360	BNT	GRB
343.900	-50.400	1998	07	28.64068	BNT	GRB
127.630	8.600	1998	07	28.70699	BT	GRB980728
237.400	-51.200	1998	07	28.75129	BNT	GRB
302.800	-42.100	1998	07	28.82545	BNT	GRB
205.600	0.500	1998	07	31.89067	BNT	GRB
240.400	-48.300	1998	08	1.14954	BNT	GRB
178.620	-45.540	1998	08	2.18812	BeS	980802A
252.640	-32.160	1998	08	2.33419	BeS	980802B
273.900	-64.500	1998	08	3.13590	BNT	GRB
141.190	57.980	1998	08	3.56691	BT	GRB980803
115.320	-23.930	1998	08	5.56733	BeS	980805
309.200	15.800	1998	08	5.97911	BNT	GRB
123.120	-4.110	1998	08	8.32686	BeS	980808A
138.200	30.000	1998	08	8.44738	BNT	GRB
196.210	45.020	1998	08	8.80578	BT	GRB980808-
155.800	-1.900	1998	08	8.91201	BeS	980808B
334.700	7.100	1998	08	10.18455	BeS	980810A
349.930	24.640	1998	08	10.77470	BeS	980810B
337.900	33.200	1998	08	11.19116	BNT	GRB
266.800	3.510	1998	08	11.28133	BeS	980811
103.600	21.600	1998	08	11.90328	BNT	GRB
145.100	15.700	1998	08	12.20424	BeS	980812A
337.300	33.900	1998	08	12.21954	BeS	980812B
128.690	25.690	1998	08	13.97003	BT	GRB980813
310.850	61.250	1998	08	14.56479	BT	GRB980814
153.300	6.800	1998	08	14.60878	BNT	GRB
210.940	-32.220	1998	08	15.89023	BeS	980815
133.300	-12.900	1998	08	19.13754	BNT	GRB
192.920	28.470	1998	08	19.36282	BeS	980819

Continued on next column

Continued from previous column

RA deg	DEC deg	Year	Month	Day	Cat.	GRB Name
7.100	45.100	1998	08	19.38013	BNT	GRB
311.320	5.200	1998	08	20.43388	BT	GRB980820
84.000	-19.000	1998	08	20.97589	BeS	980820
123.500	-12.000	1998	08	21.71951	BT	GRB980821
114.100	66.500	1998	08	26.78485	BNT	GRB
116.050	33.060	1998	08	27.56837	BT	GRB980827
146.410	20.730	1998	08	28.81812	BT	GRB980828
240.000	-54.200	1998	08	29.22280	BeS	980829A
92.000	-49.000	1998	08	30.61251	BeS	980830
315.400	-0.300	1998	08	30.83726	BNT	GRB
284.490	25.030	1998	09	2.69157	BT	GRB980902
139.910	-41.540	1998	09	3.14934	BeS	980903
58.000	-34.000	1998	09	4.27969	BeS	980904A
125.990	-53.710	1998	09	4.36285	BeS	980904B
84.180	-9.750	1998	09	4.56223	BT	GRB980904-
29.300	65.300	1998	09	5.18491	BNT	GRB
78.100	-10.000	1998	09	7.46744	BeS	980907
183.700	-54.300	1998	09	8.02884	BeS	980908
256.503	37.635	1998	09	8.95213	K/W	980908_T82263
195.070	-21.150	1998	09	10.70676	BeS	980910A
205.490	27.470	1998	09	10.83498	BeS	980910B
8.760	8.300	1998	09	13.23130	BT	GRB980913
10.800	6.500	1998	09	13.23129	BNT	GRB
115.300	-35.000	1998	09	13.41914	BNT	GRB
353.400	76.600	1998	09	16.26733	BNT	GRB
57.300	-10.400	1998	09	16.84866	BeS	980916
259.500	49.300	1998	09	17.23014	BNT	GRB
320.200	58.370	1998	09	17.25898	BT	GRB980917
162.500	-7.500	1998	09	17.40844	BeS	980917
134.700	26.880	1998	09	18.57635	BeS	980918
309.290	78.290	1998	09	19.81172	BeS	980919
344.000	42.000	1998	09	20.09904	BeS	980920A
199.180	-6.270	1998	09	20.55474	BeS	980920B
125.400	-11.800	1998	09	20.89866	BNT	GRB
202.470	21.530	1998	09	21.43988	BT	GRB980921
258.950	5.070	1998	09	22.23768	BeS	980922
58.140	41.690	1998	09	22.97741	BT	GRB980922-
336.700	26.900	1998	09	23.02970	BNT	GRB
235.300	-32.700	1998	09	23.34928	BeS	980923
210.600	-3.600	1998	09	23.71473	BNT	GRB
76.950	-80.600	1998	09	23.84083	BT	GRB980923
65.950	-26.050	1998	09	24.62803	BT	GRB980924
162.400	67.900	1998	09	25.09496	BNT	GRB
323.000	14.000	1998	09	25.83663	BeS	980925
339.300	-32.600	1998	09	26.21641	BNT	GRB
255.770	49.510	1998	09	28.46713	BT	GRB980928
166.250	-22.990	1998	09	29.91086	BeS	980929
199.500	-45.900	1998	10	2.06326	BeS	981002

Continued on next column

Continued from previous column

RA deg	DEC deg	Year	Month	Day	Cat.	GRB Name
203.200	36.400	1998	10	2.27084	BNT	GRB
156.700	-3.300	1998	10	4.87039	BNT	GRB
275.240	44.050	1998	10	5.75029	BeS	981005
56.700	-21.200	1998	10	7.54618	BNT	GRB
23.200	39.000	1998	10	7.62436	BNT	GRB
202.300	-15.300	1998	10	8.85469	BNT	GRB
188.420	36.620	1998	10	9.04757	BT	GRB981009-
300.000	-30.200	1998	10	9.10360	BNT	GRB
351.500	-36.700	1998	10	9.12184	BNT	GRB
135.000	53.000	1998	10	9.32358	BNT	GRB
264.000	-16.370	1998	10	9.89538	BT	GRB981009-
37.910	-60.070	1998	10	11.81662	BT	GRB981011
210.500	-9.900	1998	10	12.89672	BNT	GRB
212.500	27.900	1998	10	13.18668	BNT	GRB
22.500	23.200	1998	10	14.77454	BNT	GRB
287.820	-80.320	1998	10	15.20303	BT	GRB981015-
301.200	63.100	1998	10	15.28139	BNT	GRB
121.540	20.190	1998	10	15.54128	BT	GRB981015-
316.400	8.700	1998	10	16.20280	BNT	GRB
42.080	50.280	1998	10	16.70205	BT	GRB981016
211.000	52.000	1998	10	17.02647	BeS	981017
58.100	11.600	1998	10	17.81826	BNT	GRB
109.400	-11.500	1998	10	18.01899	BeS	981018
107.200	6.700	1998	10	19.06950	BNT	GRB
318.700	-36.700	1998	10	19.92135	BeS	981019
282.700	-17.200	1998	10	20.16634	BNT	GRB
243.920	-5.430	1998	10	20.61565	BT	GRB981020
133.700	57.740	1998	10	21.40034	BT	GRB981021-
357.160	1.670	1998	10	21.96403	BT	GRB981021-
146.800	38.800	1998	10	22.25096	BeS	981022A
287.900	8.000	1998	10	22.65332	BNT	GRB
14.890	48.920	1998	10	22.75140	BeS	981022B
111.900	-5.030	1998	10	22.96421	BeS	981022C
84.900	30.700	1998	10	24.02141	BNT	GRB
339.940	-63.580	1998	10	27.97532	BT	GRB981027
252.500	3.000	1998	10	28.56642	BNT	GRB
4.000	-6.000	1998	10	30.05558	BeS	981030
200.200	48.640	1998	10	30.13023	BT	GRB981030
358.400	-14.100	1998	10	31.06572	BNT	GRB
278.250	-24.570	1998	10	31.40399	BT	GRB981031
170.300	-6.600	1998	11	1.22191	BeS	981101
290.700	18.400	1998	11	1.31181	BNT	GRB
228.200	-48.400	1998	11	1.69501	BNT	GRB
159.800	27.900	1998	11	2.08580	BNT	GRB
277.051	-48.335	1998	11	2.33050	K/W	981102_T28554
26.600	-42.240	1998	11	3.56975	BT	GRB981103
104.340	12.410	1998	11	4.09444	BT	GRB981104
126.900	10.900	1998	11	4.38471	BNT	GRB

Continued on next column

Continued from previous column

RA deg	DEC deg	Year	Month	Day	Cat.	GRB Name
284.800	-5.700	1998	11	4.45958	BNT	GRB
351.000	41.000	1998	11	4.72035	BeS	981104
171.080	-52.440	1998	11	5.05984	BT	GRB981105
136.900	-25.100	1998	11	5.38306	BNT	GRB
323.800	58.400	1998	11	6.44536	BeS	981106
127.200	-5.900	1998	11	6.53763	BNT	GRB
317.000	20.000	1998	11	7.00902	BeS	981107
154.400	-24.600	1998	11	10.40633	BNT	GRB
168.940	-44.600	1998	11	10.95322	BeS	981110
110.880	65.590	1998	11	11.28034	BT	GRB981111-
173.000	-62.000	1998	11	11.47883	BeS	981111
248.130	48.060	1998	11	11.58404	BT	GRB981111-
203.000	7.000	1998	11	12.16372	BeS	981112
284.000	10.000	1998	11	15.24813	BNT	GRB
212.800	3.600	1998	11	16.43118	BNT	GRB
2.100	-62.700	1998	11	16.65133	BNT	GRB
217.600	-65.700	1998	11	17.13459	BNT	GRB
294.940	-1.300	1998	11	17.28383	BT	GRB981117
186.900	60.600	1998	11	18.02932	BNT	GRB
206.900	-34.300	1998	11	20.16154	BNT	GRB
15.510	42.330	1998	11	21.05989	BeS	981121
145.700	64.300	1998	11	21.65169	BNT	GRB
151.700	-36.300	1998	11	22.98302	BNT	GRB
342.830	-52.560	1998	11	24.83366	BT	GRB981124
134.200	22.100	1998	11	25.01133	BNT	GRB
254.630	29.870	1998	11	25.35166	BeS	981125A
202.310	61.860	1998	11	25.87941	BeS	981125B
83.830	-11.820	1998	11	26.37147	BT	GRB981126
65.000	55.000	1998	11	26.72314	BeS	981126A
57.000	1.000	1998	11	26.80093	BeS	981126B
33.600	-27.700	1998	11	27.13835	BNT	GRB
155.510	-41.420	1998	11	27.63243	BT	GRB981127
131.690	39.350	1998	11	28.80285	BT	GRB981128
60.300	38.400	1998	11	28.86065	BNT	GRB
100.930	-14.470	1998	11	29.65580	BT	GRB981129
311.900	38.000	1998	11	29.68159	BNT	GRB
348.930	-12.830	1998	11	30.03686	BT	GRB981130
10.800	-0.900	1998	12	1.43161	BNT	GRB
214.300	-40.100	1998	12	1.79498	BNT	GRB
324.240	-16.060	1998	12	1.87329	BT	GRB981201
161.460	32.910	1998	12	3.04119	BeS	981203A
293.340	-27.240	1998	12	3.30418	BeS	981203B
53.400	-55.900	1998	12	4.43808	BNT	GRB
90.990	43.730	1998	12	5.23708	BT	GRB981205
168.900	40.100	1998	12	7.54402	BNT	GRB
295.900	8.800	1998	12	8.30459	BNT	GRB
351.580	-18.770	1998	12	10.56655	BT	GRB981210
7.500	-9.800	1998	12	11.65075	BNT	GRB

Continued on next column

Continued from previous column

RA deg	DEC deg	Year	Month	Day	Cat.	GRB Name
332.520	-9.730	1998	12	11.85392	BT	GRB981211
129.400	45.600	1998	12	12.53904	BNT	GRB
194.730	23.240	1998	12	15.58986	BeS	981215B
298.000	-2.800	1998	12	15.93413	BNT	GRB
226.400	17.200	1998	12	16.22866	BeS	981216A
277.000	-15.000	1998	12	16.75038	BeS	981216B
293.500	74.000	1998	12	17.07995	BNT	GRB
65.000	51.000	1998	12	18.43774	BNT	GRB
218.900	-43.610	1998	12	19.39292	BT	GRB981219
233.000	-31.000	1998	12	19.80943	BeS	981219B
117.700	-43.300	1998	12	20.10066	BNT	GRB
55.640	17.150	1998	12	20.91141	BeS	981220
286.580	-9.870	1998	12	21.04140	BT	GRB981221-
283.680	3.610	1998	12	21.10483	BeS	981221A
150.380	24.530	1998	12	21.73442	BeS	981221B
145.900	67.100	1998	12	22.67338	BNT	GRB
322.100	-31.300	1998	12	23.07999	BNT	GRB
191.940	12.510	1998	12	23.50781	BT	GRB981223
106.400	-1.400	1998	12	23.83113	BNT	GRB
94.900	13.200	1998	12	25.02701	BNT	GRB
352.420	-23.920	1998	12	26.40801	BeS	981226A
267.150	-24.400	1998	12	26.44934	BeS	981226B
89.700	44.500	1998	12	27.37546	BNT	GRB
112.390	38.380	1998	12	27.78120	BT	GRB981227
321.600	-62.600	1998	12	28.42774	BNT	GRB
285.760	31.310	1998	12	28.51638	BeS	981228
73.600	-13.600	1998	12	28.75277	BNT	GRB
326.690	61.420	1998	12	29.39103	BeS	981229
76.100	-61.800	1998	12	30.20363	BNT	GRB
30.100	-1.700	1998	12	30.32148	BNT	GRB
43.700	9.310	1998	12	30.93745	BT	GRB981230
90.620	0.030	1998	12	31.04728	BT	GRB981231-
335.680	-51.750	1998	12	31.96412	BT	GRB981231-
20.600	19.700	1998	12	31.97648	BNT	GRB
54.300	-71.800	1999	01	1.21492	BNT	GRB
277.380	39.330	1999	01	2.21294	BeS	990102A
287.000	-10.500	1999	01	2.33933	BNT	GRB
218.350	-24.040	1999	01	2.39845	BT	GRB990102-
203.480	2.740	1999	01	2.57777	BeS	990102B
235.600	58.200	1999	01	2.88198	BNT	GRB
140.070	76.390	1999	01	3.40946	BT	GRB990103
141.800	-13.600	1999	01	3.83523	BNT	GRB
191.710	-33.400	1999	01	4.09294	BT	GRB990104-
268.100	74.500	1999	01	4.45836	BeS	990104A
129.960	1.190	1999	01	4.66829	BeS	990104B
131.700	3.500	1999	01	4.99019	BNT	GRB
306.610	4.330	1999	01	5.36793	BeS	990105
28.900	-21.600	1999	01	7.14105	BNT	GRB

Continued on next column

Continued from previous column

RA deg	DEC deg	Year	Month	Day	Cat.	GRB Name
358.000	-52.600	1999	01	8.13024	BNT	GRB
62.130	-12.110	1999	01	8.34799	BT	GRB990108
295.000	47.100	1999	01	8.59008	BNT	GRB
232.000	5.500	1999	01	8.73926	BNT	GRB
160.830	-72.400	1999	01	9.06694	BT	GRB990109
319.500	-49.200	1999	01	9.47516	BNT	GRB
287.100	9.700	1999	01	10.36043	BNT	GRB
272.000	-24.000	1999	01	11.38007	BeS	990111A
43.850	38.270	1999	01	11.49816	BT	GRB990111-
173.650	27.820	1999	01	11.74884	BeS	990111B
118.600	-45.600	1999	01	12.08178	BNT	GRB
277.240	-18.190	1999	01	12.59538	BT	GRB990112
66.910	31.730	1999	01	13.00119	BT	GRB990113
342.700	-61.800	1999	01	13.42796	BNT	GRB
78.700	49.300	1999	01	14.44441	BNT	GRB
264.300	32.300	1999	01	15.61431	BNT	GRB
19.660	-1.290	1999	01	17.31274	BT	GRB990117-
316.360	-22.020	1999	01	17.88351	BT	GRB990117-
188.000	41.000	1999	01	17.98352	BeS	990117B
67.800	68.100	1999	01	18.23317	BNT	GRB
299.000	19.000	1999	01	18.52542	BeS	990118B
20.000	69.300	1999	01	19.08219	BNT	GRB
228.400	-24.400	1999	01	19.54186	BNT	GRB
235.740	-1.410	1999	01	19.59745	BT	GRB990119
10.200	-7.580	1999	01	20.39838	BeS	990120
332.100	-6.500	1999	01	20.58300	BNT	GRB
292.800	-5.500	1999	01	21.51974	BNT	GRB
186.900	63.100	1999	01	21.52463	BNT	GRB
63.000	-49.000	1999	01	22.34505	BeS	990122
73.200	41.600	1999	01	22.71033	BNT	GRB
87.700	-4.400	1999	01	23.06757	BNT	GRB
231.370	44.750	1999	01	23.40775	BeS	990123A
320.610	-60.810	1999	01	23.55535	BeS	990123B
328.700	-65.300	1999	01	24.77072	BNT	GRB
97.200	11.000	1999	01	25.76116	BNT	GRB
62.720	-43.930	1999	01	26.28128	BT	GRB990126-
268.100	33.300	1999	01	26.44676	BNT	GRB
321.140	-24.300	1999	01	26.60003	BeS	990126
312.900	-65.800	1999	01	27.33091	BNT	GRB
269.660	-37.100	1999	01	28.39419	BT	GRB990128-
304.900	-41.900	1999	01	28.43116	BeS	990128
319.250	-43.180	1999	01	28.47069	BT	GRB990128-
100.980	-19.080	1999	01	29.15392	BT	GRB990129-
94.920	-12.280	1999	01	29.21934	BT	GRB990129-
204.170	-28.290	1999	01	29.72513	BT	GRB990129-
11.000	39.500	1999	01	30.32615	BNT	GRB
19.000	-71.000	1999	01	30.56044	BeS	990130
175.590	56.970	1999	01	30.69113	BT	GRB990130

Continued on next column

Continued from previous column

RA deg	DEC deg	Year	Month	Day	Cat.	GRB Name
243.900	30.600	1999	01	31.37215	BNT	GRB
339.500	5.600	1999	01	31.62505	BNT	GRB
303.000	-21.000	1999	01	31.81021	BeS	990131
315.850	-1.780	1999	02	2.14968	BeS	990202A
336.060	38.430	1999	02	2.65148	BeS	990202B
324.930	23.500	1999	02	3.65372	BT	GRB990203
31.560	1.420	1999	02	4.01701	BT	GRB990204
131.600	63.200	1999	02	4.34918	BNT	GRB
199.500	12.600	1999	02	4.96282	BNT	GRB
276.190	22.850	1999	02	5.01351	BT	GRB990205
247.410	8.750	1999	02	6.21559	BT	GRB990206-
75.000	-61.500	1999	02	6.25398	BNT	GRB
112.100	60.400	1999	02	6.66043	BeS	990206
215.930	5.130	1999	02	7.03991	BT	GRB990207
287.100	-35.600	1999	02	7.12671	BNT	GRB
152.900	-9.700	1999	02	7.64464	BNT	GRB
166.000	51.000	1999	02	7.80642	BeS	990207
303.080	16.130	1999	02	8.04456	BeS	990208A
296.100	-39.400	1999	02	8.17551	BeS	990208B
190.300	58.900	1999	02	8.30653	BNT	GRB
108.110	50.110	1999	02	10.18629	BeS	990210
36.870	-28.470	1999	02	10.44014	BT	GRB990210-
22.100	43.800	1999	02	10.58859	BNT	GRB
205.700	-25.600	1999	02	11.23787	BNT	GRB
230.860	-10.040	1999	02	12.32668	BT	GRB990212
334.800	65.200	1999	02	12.81781	BNT	GRB
203.020	-27.810	1999	02	13.01423	BT	GRB990213-
275.090	-49.060	1999	02	13.29176	BT	GRB990213-
145.890	51.720	1999	02	13.40698	BeS	990213
76.000	-0.400	1999	02	14.66044	BNT	GRB
237.700	-48.800	1999	02	14.86841	BNT	GRB
153.900	-34.200	1999	02	16.02423	BNT	GRB
316.000	4.000	1999	02	16.07785	BeS	990216A
274.940	-40.340	1999	02	16.27111	BeS	990216B
45.510	-53.100	1999	02	17.22461	BeS	990217
72.900	37.700	1999	02	18.85361	BNT	GRB
297.200	-24.900	1999	02	20.00237	BNT	GRB
163.050	55.600	1999	02	20.50229	BeS	990220
35.900	-66.110	1999	02	21.04051	BT	GRB990221-
297.800	-10.450	1999	02	21.32855	BT	GRB990221-
62.200	-2.600	1999	02	22.54031	BNT	GRB
40.300	-42.300	1999	02	23.25574	BNT	GRB
215.700	26.800	1999	02	23.39304	BNT	GRB
245.100	-13.600	1999	02	23.52772	BNT	GRB
170.600	49.800	1999	02	23.96676	BNT	GRB
205.660	-34.090	1999	02	25.62771	BT	GRB990225-
232.940	-18.730	1999	02	25.81861	BeS	990225
244.470	10.660	1999	02	26.35750	BeS	990226

Continued on next column

Continued from previous column

RA deg	DEC deg	Year	Month	Day	Cat.	GRB Name
146.480	-52.620	1999	02	26.69314	BT	GRB990226-
180.070	-29.950	1999	02	27.75418	BT	GRB990227
172.540	-40.730	1999	02	28.18110	BT	GRB990228-
25.200	-30.000	1999	02	28.43738	BNT	GRB
44.440	22.330	1999	02	28.61554	BT	GRB990228-
79.100	13.400	1999	02	28.97084	BNT	GRB
176.300	60.400	1999	03	1.94991	BNT	GRB
255.630	66.030	1999	03	2.31162	BT	GRB990302
188.700	-43.000	1999	03	2.34444	BNT	GRB
317.680	-16.590	1999	03	3.16598	BT	GRB990303-
330.920	-41.250	1999	03	3.37696	BT	GRB990303-
8.320	-58.250	1999	03	4.42750	BT	GRB990304-
220.190	-26.910	1999	03	4.93650	BT	GRB990304-
316.800	18.300	1999	03	5.39874	BNT	GRB
209.780	45.730	1999	03	5.58211	BT	GRB990305-
155.090	-49.480	1999	03	5.77097	BT	GRB990305-
283.130	16.850	1999	03	6.50914	BT	GRB990306-
315.010	13.450	1999	03	6.69895	BeS	990306
275.890	-1.250	1999	03	6.82939	BT	GRB990306-
19.200	14.590	1999	03	7.45119	BeS	990307
48.190	69.210	1999	03	8.12838	BeS	990308A
189.180	3.550	1999	03	8.21883	BT	GRB990308-
190.100	-61.400	1999	03	8.74122	BNT	GRB
64.720	70.100	1999	03	8.82470	BeS	990308B
27.300	-59.500	1999	03	8.90002	BNT	GRB
15.900	-45.500	1999	03	9.54382	BNT	GRB
232.000	66.000	1999	03	10.35750	BeS	990310
43.950	19.250	1999	03	11.92482	BeS	990311B
303.000	-31.000	1999	03	12.20300	BeS	990312A
107.350	-59.170	1999	03	12.37762	BT	GRB990312
189.000	9.000	1999	03	12.69146	BeS	990312B
338.000	52.000	1999	03	13.39019	BeS	990313
184.010	-12.860	1999	03	14.83696	BeS	990314
71.940	62.280	1999	03	15.00681	BT	GRB990315-
5.710	-63.000	1999	03	15.69132	BeS	990315
197.800	-24.700	1999	03	15.77097	BNT	GRB
46.300	28.400	1999	03	16.39946	BNT	GRB
152.080	-4.440	1999	03	16.40324	BT	GRB990316-
102.450	-6.200	1999	03	16.52014	BT	GRB990316-
180.200	8.400	1999	03	16.75015	BNT	GRB
244.900	1.650	1999	03	18.13530	BeS	990318A
348.500	-5.000	1999	03	18.41748	BNT	GRB
18.100	7.600	1999	03	18.92578	BNT	GRB
138.000	-49.000	1999	03	19.52958	BeS	990319
286.450	31.610	1999	03	19.90331	BT	GRB990319
65.840	38.310	1999	03	20.18966	BT	GRB990320-
5.700	6.700	1999	03	20.95970	BeS	990320
42.260	0.230	1999	03	21.82579	BT	GRB990321

Continued on next column

Continued from previous column

RA deg	DEC deg	Year	Month	Day	Cat.	GRB Name
12.490	-68.320	1999	03	22.16940	BeS	990322
152.400	-35.000	1999	03	22.25275	BNT	GRB
29.000	-36.800	1999	03	23.07086	BNT	GRB
208.070	24.660	1999	03	23.37352	BeS	990323
249.500	20.200	1999	03	23.46417	BNT	GRB
246.760	-25.630	1999	03	23.59958	BT	GRB990323-
332.580	-76.540	1999	03	23.72890	BT	GRB990323-
276.300	0.500	1999	03	24.88199	BNT	GRB
287.600	21.500	1999	03	25.24641	BNT	GRB
53.300	-7.500	1999	03	25.39706	BNT	GRB
143.014	-24.897	1999	03	27.26517	K/W	990327_T22911
150.080	-47.170	1999	03	28.14187	BeS	990328
28.400	-66.300	1999	03	28.70907	BNT	GRB
358.700	20.800	1999	03	29.04175	BNT	GRB
80.900	41.400	1999	03	29.46231	BNT	GRB
72.440	68.340	1999	03	29.95578	BT	GRB990329
61.410	0.690	1999	03	30.19435	BT	GRB990330-
35.610	-16.480	1999	03	30.75768	BeS	990330A
160.650	34.310	1999	03	30.81001	BeS	990330B
223.700	36.900	1999	03	31.00833	BNT	GRB
2.780	19.440	1999	03	31.21762	BT	GRB990331
33.270	-9.400	1999	04	1.26522	BT	GRB990401
202.400	-31.100	1999	04	1.98038	BNT	GRB
339.900	-32.700	1999	04	2.69513	BNT	GRB
301.410	-19.020	1999	04	3.09907	BeS	990403A
298.870	-5.050	1999	04	3.40837	BT	GRB990403-
355.300	-19.400	1999	04	3.69106	BeS	990403B
251.200	31.180	1999	04	3.86165	BT	GRB990403-
301.270	-47.160	1999	04	4.46343	BT	GRB990404-
112.600	-53.500	1999	04	4.70402	BNT	GRB
305.650	-72.190	1999	04	4.81637	BT	GRB990404-
166.000	-16.000	1999	04	5.13078	BeS	990405
288.006	21.880	1999	04	5.34792	K/W	990405_T30059
306.100	30.300	1999	04	6.85628	BeS	990406
346.000	-38.000	1999	04	7.58003	BeS	990407
266.690	49.080	1999	04	7.99931	BT	GRB990407
258.530	4.570	1999	04	8.39897	BT	GRB990408
6.300	53.300	1999	04	9.96824	BeS	990409
329.840	-83.440	1999	04	11.18440	BeS	990411
50.750	-67.610	1999	04	11.71725	BT	GRB990411-
264.000	2.800	1999	04	12.20348	BNT	GRB
135.820	-58.300	1999	04	12.46008	BT	GRB990412
323.300	-4.000	1999	04	12.67273	BNT	GRB
180.000	-18.440	1999	04	13.32926	BT	GRB990413
302.100	55.500	1999	04	13.37612	BNT	GRB
12.400	4.400	1999	04	14.54566	BNT	GRB
238.460	-45.810	1999	04	14.77223	BT	GRB990414
330.457	59.988	1999	04	15.02659	K/W	990415_T02297

Continued on next column

Continued from previous column

RA deg	DEC deg	Year	Month	Day	Cat.	GRB Name
71.830	-3.450	1999	04	15.12582	BT	GRB990415
130.300	36.600	1999	04	16.51022	BNT	GRB
111.310	-38.140	1999	04	16.71205	BT	GRB990416
135.300	-47.600	1999	04	16.78701	BNT	GRB
285.900	61.100	1999	04	18.00398	BNT	GRB
349.200	13.900	1999	04	18.41109	BNT	GRB
34.680	-12.830	1999	04	20.64152	BT	GRB990420-
305.070	26.240	1999	04	20.96601	BT	GRB990420-
47.700	-79.100	1999	04	21.12343	BNT	GRB
93.000	-44.400	1999	04	21.76128	BNT	GRB
111.110	-57.490	1999	04	23.09799	BT	GRB990423
88.870	-60.330	1999	04	24.13370	BT	GRB990424-
157.970	11.910	1999	04	24.34462	BT	GRB990424-
84.000	36.640	1999	04	24.92318	BT	GRB990424-
332.670	-7.410	1999	04	25.09684	BT	GRB990425-
58.810	-42.140	1999	04	25.45312	BT	GRB990425-
259.500	-10.000	1999	04	25.73920	BNT	GRB
263.040	-22.410	1999	04	26.39497	BT	GRB990426
354.140	-19.270	1999	04	27.65552	BT	GRB990427
132.860	-15.070	1999	04	28.39236	BT	GRB990428
286.100	6.000	1999	04	29.41152	BNT	GRB
299.150	69.540	1999	04	30.29995	BT	GRB990430
347.400	-7.700	1999	05	1.71436	BNT	GRB
19.300	-48.700	1999	05	2.34583	BNT	GRB
82.430	41.310	1999	05	2.92317	BT	GRB990502
130.300	58.400	1999	05	3.35457	BNT	GRB
248.900	-58.300	1999	05	4.47375	BeS	990504A
54.880	-19.340	1999	05	4.50819	BT	GRB990504
321.261	-9.495	1999	05	4.78225	K/W	990504_T67586
227.690	-47.680	1999	05	5.32718	BT	GRB990505
178.670	-26.750	1999	05	6.47466	BeS	990506A
186.900	9.600	1999	05	6.49382	BNT	GRB
196.000	-48.000	1999	05	6.81078	BeS	990506B
33.100	-49.200	1999	05	6.94295	BNT	GRB
140.250	2.780	1999	05	6.99579	BT	GRB990506-
13.780	-24.450	1999	05	7.10576	BT	GRB990507-
137.560	65.900	1999	05	7.82564	BeS	990507
227.210	75.980	1999	05	8.73143	BT	GRB990508
234.000	-25.300	1999	05	9.86047	BNT	GRB
10.970	-67.310	1999	05	10.26726	BT	GRB990510-
204.530	-80.500	1999	05	10.36747	BeS	990510
265.700	8.600	1999	05	10.77718	BNT	GRB
205.610	42.370	1999	05	11.61142	BT	GRB990511
262.700	7.300	1999	05	12.21684	BNT	GRB
326.720	-4.670	1999	05	13.67096	BT	GRB990513-
339.450	-75.010	1999	05	13.82517	BeS	990513B
43.560	-27.810	1999	05	15.05297	BT	GRB990515
354.500	25.600	1999	05	15.10662	BNT	GRB

Continued on next column

Continued from previous column

RA deg	DEC deg	Year	Month	Day	Cat.	GRB Name
85.620	56.090	1999	05	16.87170	BeS	990516A
266.000	-43.060	1999	05	16.97519	BeS	990516B
253.550	-3.640	1999	05	16.99610	BeS	990516C
235.250	19.200	1999	05	18.06047	BeS	990518A
343.330	-38.680	1999	05	18.72112	BeS	990518B
204.300	-73.400	1999	05	18.92839	BNT	GRB
317.780	-27.080	1999	05	19.64138	BT	GRB990519
175.300	-26.600	1999	05	20.00153	BNT	GRB
134.600	63.800	1999	05	20.08544	BNT	GRB
198.000	22.000	1999	05	20.51304	BeS	990520
40.100	21.500	1999	05	20.63554	BNT	GRB
206.000	25.000	1999	05	21.96725	BeS	990521
39.380	27.070	1999	05	22.17622	BT	GRB990522
130.950	-62.090	1999	05	23.23883	BT	GRB990523-
235.960	-60.410	1999	05	23.58248	BT	GRB990523-
51.840	52.980	1999	05	23.78249	BT	GRB990523-
268.640	5.900	1999	05	25.01613	BeS	990525
177.000	6.500	1999	05	25.21004	BNT	GRB
163.500	36.000	1999	05	25.51751	BNT	GRB
343.700	-71.800	1999	05	25.77973	BNT	GRB
163.100	-58.200	1999	05	26.51521	BNT	GRB
285.700	15.100	1999	05	26.54714	BeS	990526
294.940	-45.160	1999	05	27.14770	BT	GRB990527-
344.560	-20.000	1999	05	27.58120	BT	GRB990527-
199.930	49.350	1999	05	27.775917	BT	GRB990527-
65.860	-15.920	1999	05	28.40434	BT	GRB990528
15.750	-32.660	1999	05	30.66909	BT	GRB990530
52.350	36.540	1999	05	31.66417	BT	GRB990531
342.200	-81.900	1999	05	31.97709	BNT	GRB
105.000	-32.000	1999	06	1.62608	BeS	990601
220.000	-19.000	1999	06	3.55471	BeS	990603A
55.100	-36.300	1999	06	3.77183	BeS	990603B
48.000	-16.000	1999	06	3.78354	BeS	990603C
263.760	3.070	1999	06	3.80486	BeS	990603D
298.380	8.610	1999	06	3.96492	BT	GRB990603-
69.810	-63.610	1999	06	4.69554	BeS	990604A
91.090	38.050	1999	06	4.83311	BeS	990604B
86.390	34.740	1999	06	5.02118	BT	GRB990605
65.500	-16.900	1999	06	5.48799	BNT	GRB
93.700	-14.500	1999	06	5.61383	BNT	GRB
151.000	48.000	1999	06	6.05010	BeS	990606
271.600	59.800	1999	06	6.12875	BNT	GRB
62.350	-41.250	1999	06	10.51792	BT	GRB990610-
105.700	-16.600	1999	06	10.65631	BNT	GRB
306.620	20.870	1999	06	10.92278	BT	GRB990610-
282.120	-65.440	1999	06	11.21326	BT	GRB990611-
65.700	-5.700	1999	06	11.26520	BNT	GRB
228.120	48.010	1999	06	11.42165	BeS	990611A

Continued on next column

Continued from previous column

RA deg	DEC deg	Year	Month	Day	Cat.	GRB Name
343.200	-47.090	1999	06	11.49794	BeS	990611B
111.680	-38.910	1999	06	14.59775	BT	GRB990614
342.000	-1.000	1999	06	15.19905	BeS	990615
173.920	-56.080	1999	06	15.65826	BT	GRB990615
255.700	-12.500	1999	06	16.32440	BNT	GRB
137.600	-43.000	1999	06	16.38012	BNT	GRB
84.220	4.750	1999	06	16.44503	BT	GRB990616
214.660	-61.310	1999	06	18.16275	BeS	990618A
42.300	2.400	1999	06	18.20331	BNT	GRB
169.700	-65.500	1999	06	18.43579	BeS	990618B
118.100	-34.200	1999	06	18.47503	BNT	GRB
223.310	-42.030	1999	06	19.54308	BT	GRB990619
334.400	-21.300	1999	06	19.57929	BNT	GRB
84.200	3.700	1999	06	19.98304	BNT	GRB
17.400	-31.500	1999	06	20.37199	BNT	GRB
268.540	-18.140	1999	06	20.47457	BT	GRB990620-
6.090	14.350	1999	06	20.56745	BT	GRB990620-
133.000	-3.000	1999	06	20.94875	BeS	990620
132.900	58.100	1999	06	21.50859	BeS	990621
116.000	24.000	1999	06	22.43781	BeS	990622A
50.230	-42.220	1999	06	22.67024	BT	GRB990622-
79.430	-29.730	1999	06	22.86602	BeS	990622B
133.100	-48.300	1999	06	23.53042	BNT	GRB
82.000	-2.000	1999	06	24.88445	BeS	990624
6.640	-31.200	1999	06	25.01706	BeS	990625
359.000	-76.000	1999	06	27.16696	BeS	990627A
27.100	-77.080	1999	06	27.20895	BeS	990627B
115.000	-26.000	1999	06	30.65229	BeS	990630
34.530	21.690	1999	07	1.14980	BT	GRB990701-
171.000	39.000	1999	07	1.46119	BeS	990701
216.740	34.310	1999	07	1.89728	BT	GRB990701-
117.900	39.500	1999	07	3.11042	BNT	GRB
175.280	79.230	1999	07	3.45647	BT	GRB990703
184.790	-3.800	1999	07	4.72940	BeS	990704A
194.510	49.220	1999	07	5.15456	BT	GRB990705-
8.700	13.400	1999	07	5.19590	BNT	GRB
81.360	6.170	1999	07	5.55970	BT	GRB990705-
77.380	-72.150	1999	07	5.66765	BeS	990705
289.900	-4.900	1999	07	6.48282	BNT	GRB
314.790	-15.040	1999	07	6.60235	BeS	990706
278.630	-53.570	1999	07	6.85525	BT	GRB990706-
128.100	36.400	1999	07	7.39389	BNT	GRB
328.250	24.990	1999	07	7.60392	BT	GRB990707-
102.700	-53.000	1999	07	7.63427	BeS	990707A
72.410	21.840	1999	07	7.81895	BeS	990707B
269.860	-42.130	1999	07	8.85684	BT	GRB990708-
178.130	57.510	1999	07	8.96653	BeS	990708
116.510	6.430	1999	07	9.49208	BT	GRB990709-

Continued on next column

Continued from previous column

RA deg	DEC deg	Year	Month	Day	Cat.	GRB Name
299.030	44.600	1999	07	9.66420	BeS	990709
313.000	-21.000	1999	07	11.30627	BeS	990711A
288.700	-3.500	1999	07	11.56841	BeS	990711B
66.070	29.220	1999	07	11.90963	BeS	990711C
126.520	8.650	1999	07	12.32314	BeS	990712A
337.960	-73.400	1999	07	12.69655	BeS	990712B
281.340	11.790	1999	07	12.78839	BT	GRB990712-
45.500	3.500	1999	07	13.01611	BNT	GRB
319.310	-53.290	1999	07	13.15066	BT	GRB990713-
186.000	-60.000	1999	07	13.40835	BeS	990713A
310.460	-27.280	1999	07	13.90163	BeS	990713B
231.190	19.660	1999	07	14.75959	BeS	990714
296.520	-13.530	1999	07	15.11652	BT	GRB990715-
229.040	19.560	1999	07	15.52994	BT	GRB990715-
117.900	53.700	1999	07	15.59088	BNT	GRB
154.420	44.510	1999	07	15.99972	BeS	990715
282.780	-53.470	1999	07	16.16668	BT	GRB990716-
337.260	-44.610	1999	07	16.26984	BT	GRB990716-
104.000	-13.000	1999	07	17.71684	BeS	990717
52.100	-27.400	1999	07	18.46947	BNT	GRB
286.920	1.330	1999	07	18.50478	BeS	990718
342.600	-2.300	1999	07	18.78081	BNT	GRB
224.510	10.860	1999	07	19.59170	BT	GRB990719
270.764	9.158	1999	07	19.70758	K/W	990719_T61135
32.900	2.100	1999	07	19.91917	BeS	990719
160.800	-38.900	1999	07	20.00031	BeS	990720A
189.000	-41.000	1999	07	20.35406	BeS	990720B
11.800	-33.360	1999	07	20.87893	BT	GRB990720
82.000	2.200	1999	07	20.89733	BNT	GRB
199.000	-55.200	1999	07	21.59731	BNT	GRB
213.380	35.530	1999	07	22.30785	BT	GRB990722-
149.690	-54.440	1999	07	22.88941	BT	GRB990722-
217.570	22.400	1999	07	24.13580	BT	GRB990724
299.700	-29.400	1999	07	24.68139	BNT	GRB
12.560	32.740	1999	07	25.15812	BT	GRB990725
15.500	-9.900	1999	07	25.47472	BeS	990725
25.200	76.100	1999	07	25.58990	BNT	GRB
289.000	77.000	1999	07	26.12469	BeS	990726
3.910	-14.940	1999	07	26.38796	BT	GRB990726
343.400	43.000	1999	07	26.40263	BNT	GRB
271.700	-6.000	1999	07	27.55890	BeS	990727
225.800	41.700	1999	07	28.06671	BNT	GRB
320.200	61.800	1999	07	28.32547	BNT	GRB
209.620	-56.840	1999	07	28.46094	BT	GRB990728
290.500	79.100	1999	07	28.65708	BNT	GRB
141.360	74.800	1999	07	30.79110	BeS	990730A
53.030	-10.290	1999	07	30.86346	BeS	990730B
34.750	40.500	1999	08	2.04495	BT	GRB990802-

Continued on next column

Continued from previous column

RA deg	DEC deg	Year	Month	Day	Cat.	GRB Name
279.190	4.950	1999	08	2.79741	BT	GRB990802-
53.100	24.000	1999	08	2.95079	BNT	GRB
258.630	-2.030	1999	08	3.27056	BT	GRB990803
80.600	31.700	1999	08	3.66626	BeS	990803
294.100	-11.200	1999	08	3.79936	BNT	GRB
241.200	5.000	1999	08	5.22157	BNT	GRB
47.650	-68.120	1999	08	6.60286	BeS	990806B
31.100	68.900	1999	08	6.69639	BNT	GRB
260.824	68.516	1999	08	6.69640	K/W	990806_T60168
338.610	20.520	1999	08	7.91373	BT	GRB990807
301.760	-12.990	1999	08	8.30226	BT	GRB990808
355.200	48.700	1999	08	9.43595	BNT	GRB
88.870	43.400	1999	08	9.52159	BT	GRB990809
29.400	-10.400	1999	08	10.18016	BNT	GRB
358.070	1.730	1999	08	10.30895	BT	GRB990810-
325.580	2.060	1999	08	10.74293	BT	GRB990810-
124.100	7.400	1999	08	10.77030	BNT	GRB
154.780	-66.080	1999	08	14.38690	BeS	990814A
164.320	6.620	1999	08	14.90306	BeS	990814B
187.970	6.700	1999	08	16.11439	BeS	990816
31.200	15.400	1999	08	17.37501	BNT	GRB
196.680	39.370	1999	08	17.55225	BT	GRB990817
225.000	50.000	1999	08	19.76951	BeS	990819
245.700	-45.100	1999	08	19.86182	BNT	GRB
262.600	34.100	1999	08	20.50959	BNT	GRB
120.000	58.000	1999	08	20.96400	BeS	990820
70.000	34.000	1999	08	21.46023	BeS	990821B
111.570	-38.070	1999	08	22.50249	BeS	990822
23.300	68.770	1999	08	22.79672	BT	GRB990822-
264.370	-28.670	1999	08	23.54220	BT	GRB990823
136.930	-31.500	1999	08	24.16470	BT	GRB990824-
325.970	35.840	1999	08	24.45177	BT	GRB990824-
71.080	58.560	1999	08	25.65512	BT	GRB990825
253.500	21.600	1999	08	26.94927	BNT	GRB
264.000	52.000	1999	08	27.83513	BeS	990827
249.410	-13.010	1999	08	28.56972	BT	GRB990828
221.000	-66.600	1999	08	28.81041	BNT	GRB
261.000	27.000	1999	08	29.13883	BeS	990829A
338.600	-2.180	1999	08	29.23866	BT	GRB990829-
250.600	-66.800	1999	08	29.54821	BeS	990829B
2.000	-73.100	1999	08	29.66471	BNT	GRB
259.180	-57.220	1999	08	29.90044	BT	GRB990829-
269.600	72.900	1999	08	30.66598	BNT	GRB
66.380	-38.800	1999	09	1.16147	BT	GRB990901
58.230	62.490	1999	09	2.15416	BT	GRB990902
133.300	-66.900	1999	09	2.24723	BNT	GRB
207.300	-47.000	1999	09	2.52934	BNT	GRB
237.000	52.000	1999	09	3.23762	BeS	990903

Continued on next column

Continued from previous column

RA deg	DEC deg	Year	Month	Day	Cat.	GRB Name
337.020	71.730	1999	09	3.80204	BT	GRB990903
226.370	-59.340	1999	09	4.61139	BT	GRB990904-
301.750	-27.750	1999	09	4.66503	BT	GRB990904-
55.200	-7.200	1999	09	5.69138	BNT	GRB
95.400	46.130	1999	09	5.94370	BeS	990905
197.900	19.400	1999	09	6.43725	BNT	GRB
58.320	1.390	1999	09	6.74284	BT	GRB990906
112.700	-69.400	1999	09	7.73277	BeS	990907
103.230	-74.980	1999	09	8.01292	BeS	990908
28.530	-29.460	1999	09	9.32725	BT	GRB990909
14.600	-64.200	1999	09	10.07219	BNT	GRB
85.060	-18.270	1999	09	12.97737	BT	GRB990912
153.000	46.000	1999	09	13.28607	BeS	990913A
43.510	37.690	1999	09	14.61961	BT	GRB990914
273.200	-21.900	1999	09	15.68003	BNT	GRB
97.100	71.870	1999	09	15.96900	BeS	990915B
42.000	61.000	1999	09	17.59594	BeS	990917A
85.900	-14.900	1999	09	17.60764	BeS	990917B
155.300	25.800	1999	09	17.82290	BeS	990917C
320.290	19.090	1999	09	17.84199	BT	GRB990917
262.080	1.970	1999	09	18.23142	BeS	990918
69.400	74.000	1999	09	19.57104	BeS	990919
135.900	-26.200	1999	09	19.99581	BNT	GRB
195.100	42.900	1999	09	22.68882	BNT	GRB
83.900	7.300	1999	09	23.24444	BNT	GRB
334.000	-1.000	1999	09	23.67767	BeS	990923
15.500	45.500	1999	09	24.41463	BNT	GRB
228.610	4.110	1999	09	25.23719	BT	GRB990925-
50.070	46.070	1999	09	25.37365	BT	GRB990925-
317.000	56.000	1999	09	25.95179	BeS	990925
350.600	-6.100	1999	09	26.37793	BNT	GRB
67.000	-33.000	1999	09	26.58593	BNT	GRB
65.300	18.000	1999	09	28.24580	BNT	GRB
11.630	-63.250	1999	09	30.95875	BT	GRB990930
6.160	36.760	1999	10	1.05729	BT	GRB991001
62.000	-24.700	1999	10	1.44983	BNT	GRB
153.000	-26.900	1999	10	1.59469	BNT	GRB
292.800	-41.700	1999	10	2.17405	BeS	991002A
202.300	73.200	1999	10	2.78560	BNT	GRB
25.160	3.750	1999	10	2.95073	BeS	991002B
306.300	-55.000	1999	10	3.64027	BNT	GRB
329.940	-15.620	1999	10	4.07854	BT	GRB991004-
229.780	-20.910	1999	10	4.18034	BT	GRB991004-
251.900	-6.400	1999	10	4.26494	BeS	991004A
40.580	-24.330	1999	10	4.28122	BT	GRB991004-
210.750	-19.040	1999	10	4.55163	BT	GRB991004-
146.000	18.000	1999	10	4.63376	BeS	991004B
48.380	-72.600	1999	10	5.14574	BeS	991005

Continued on next column

Continued from previous column

RA deg	DEC deg	Year	Month	Day	Cat.	GRB Name
329.000	37.900	1999	10	5.17668	BNT	GRB
309.600	-53.300	1999	10	5.43903	BNT	GRB
342.330	6.200	1999	10	5.45100	BT	GRB991005-
97.730	45.800	1999	10	6.42661	BT	GRB991006-
102.380	10.210	1999	10	6.78936	BT	GRB991006-
213.100	7.200	1999	10	6.85925	BNT	GRB
234.180	-3.390	1999	10	7.07602	BT	GRB991007
95.000	-73.500	1999	10	7.43292	BNT	GRB
171.100	-15.000	1999	10	9.20422	BNT	GRB
257.270	-46.920	1999	10	9.70134	BT	GRB991009
159.810	-22.280	1999	10	11.06303	BeS	991011A
334.770	-15.910	1999	10	11.35859	BT	GRB991011-
287.100	6.100	1999	10	11.41632	BeS	991011B
203.420	-17.870	1999	10	11.57137	BeS	991011C
320.700	-20.200	1999	10	12.01439	BNT	GRB
218.430	46.300	1999	10	12.19094	BT	GRB991012
123.940	8.560	1999	10	13.85987	BeS	991013B
193.100	-43.800	1999	10	14.67473	BNT	GRB
102.780	11.600	1999	10	14.91149	BeS	991014
11.640	8.940	1999	10	15.27705	BT	GRB991015
35.300	41.500	1999	10	15.94777	BNT	GRB
10.700	-57.100	1999	10	16.46594	BNT	GRB
232.000	27.200	1999	10	17.70492	BNT	GRB
224.030	-3.680	1999	10	18.79354	BeS	991018
257.930	39.640	1999	10	19.00538	BT	GRB991019-
113.200	47.300	1999	10	19.63213	BNT	GRB
8.480	-1.320	1999	10	19.82412	BT	GRB991019-
104.100	86.700	1999	10	20.19228	BNT	GRB
261.520	-62.800	1999	10	20.56970	BT	GRB991020
346.280	-30.920	1999	10	21.08242	BT	GRB991021
1.000	-24.660	1999	10	22.77262	BeS	991022
227.000	41.300	1999	10	23.51999	BNT	GRB
233.950	-26.520	1999	10	23.59392	BT	GRB991023
86.300	-46.800	1999	10	24.20810	BNT	GRB
257.250	44.020	1999	10	25.70590	BT	GRB991025
51.000	-69.000	1999	10	26.54325	BeS	991026B
343.600	-16.000	1999	10	27.41438	BNT	GRB
325.970	-5.650	1999	10	27.53446	BT	GRB991027
80.940	-23.770	1999	10	28.36874	BT	GRB991028
342.960	-72.350	1999	10	29.26146	BT	GRB991029
358.100	38.600	1999	10	29.50590	BNT	GRB
123.000	-47.520	1999	10	30.07364	BeS	991030
46.800	47.300	1999	10	30.08224	BNT	GRB
25.000	5.000	1999	11	1.15720	BeS	991101
203.490	-61.330	1999	11	1.18030	BT	GRB991101-
259.370	78.120	1999	11	1.63058	BT	GRB991101-
276.700	80.500	1999	11	1.63056	BNT	GRB
320.950	15.140	1999	11	3.77964	BeS	991103

Continued on next column

Continued from previous column

RA deg	DEC deg	Year	Month	Day	Cat.	GRB Name
53.130	55.080	1999	11	4.71329	BeS	991104
214.500	40.000	1999	11	5.24287	BNT	GRB
259.000	-8.000	1999	11	5.34186	BeS	991105A
16.000	48.000	1999	11	5.44412	BeS	991105B
180.750	-66.800	1999	11	5.69498	BeS	991105C
39.240	60.630	1999	11	6.79412	BeS	991106
155.800	-54.410	1999	11	7.33578	BT	GRB991107
260.200	23.800	1999	11	7.34524	BNT	GRB
166.300	-11.900	1999	11	7.67362	BNT	GRB
314.400	75.400	1999	11	7.85854	BNT	GRB
3.640	-54.890	1999	11	8.28200	BeS	991108
164.400	-52.800	1999	11	8.41696	BNT	GRB
65.700	-18.300	1999	11	9.24200	BNT	GRB
107.000	35.300	1999	11	9.63553	BNT	GRB
276.860	75.570	1999	11	9.76023	BT	GRB991109
227.000	24.000	1999	11	9.87617	BeS	991109
39.700	-25.900	1999	11	10.11620	BNT	GRB
121.100	25.800	1999	11	11.38819	BNT	GRB
241.460	25.320	1999	11	12.92250	BT	GRB991112
116.200	-0.800	1999	11	13.67729	BNT	GRB
3.420	32.850	1999	11	13.94514	BT	GRB991113
297.100	21.600	1999	11	14.27016	BNT	GRB
37.000	-2.700	1999	11	14.52936	BNT	GRB
274.330	36.700	1999	11	14.55234	BT	GRB991114
142.200	-64.100	1999	11	15.35704	BNT	GRB
294.220	40.440	1999	11	15.78344	BeS	991115
267.000	-71.000	1999	11	16.60492	BeS	991116
207.060	-42.490	1999	11	17.90709	BT	GRB991117
311.000	-65.000	1999	11	19.60689	BeS	991119
105.500	-7.700	1999	11	19.83361	BNT	GRB
151.200	-37.700	1999	11	19.86400	BNT	GRB
51.190	-56.610	1999	11	20.24086	BeS	991120
153.400	-28.700	1999	11	20.31330	BNT	GRB
301.590	-61.570	1999	11	21.47343	BT	GRB991121
176.200	-48.300	1999	11	22.17571	BNT	GRB
214.840	-59.790	1999	11	22.30661	BT	GRB991122
266.000	21.000	1999	11	22.37814	BeS	991122B
157.180	26.940	1999	11	23.21442	BT	GRB991123-
182.960	-26.950	1999	11	23.92741	BT	GRB991123-
142.000	84.000	1999	11	24.27919	BeS	991124A
174.200	8.000	1999	11	25.82345	BNT	GRB
205.100	-1.700	1999	11	27.06566	BNT	GRB
164.900	-39.100	1999	11	27.45323	BNT	GRB
16.480	-10.440	1999	11	27.62153	BT	GRB991127
121.000	78.000	1999	11	28.25278	BeS	991128
38.520	-33.700	1999	11	29.33809	BT	GRB991129-
229.900	-36.200	1999	11	29.39926	BNT	GRB
313.730	57.530	1999	11	29.52648	BeS	991129

Continued on next column

Continued from previous column

RA deg	DEC deg	Year	Month	Day	Cat.	GRB Name
114.800	40.610	1999	11	30.54652	BeS	991130
167.900	-10.900	1999	12	1.02086	BNT	GRB
327.610	27.200	1999	12	1.48602	BT	GRB991201
245.000	35.000	1999	12	1.95225	BeS	991201
314.200	-59.500	1999	12	2.60362	BNT	GRB
248.000	-11.000	1999	12	5.71083	BeS	991205A
21.000	-35.000	1999	12	5.93391	BeS	991205B
337.600	-43.700	1999	12	5.95672	BeS	991205C
359.000	4.000	1999	12	9.79969	BeS	991209B
297.160	-45.450	1999	12	10.00984	BT	GRB991210-
302.630	-45.580	1999	12	10.43616	BT	GRB991210-
293.010	-75.690	1999	12	10.62510	BT	GRB991210-
215.260	11.720	1999	12	11.19076	BT	GRB991211-
17.350	15.450	1999	12	11.59314	BT	GRB991211-
317.000	22.000	1999	12	12.28708	BeS	991212
107.610	42.590	1999	12	13.54064	BT	GRB991213
189.080	59.770	1999	12	14.99517	BT	GRB991214
79.880	11.180	1999	12	16.67172	BeS	991216B
115.300	48.500	1999	12	17.25253	BeS	991217
64.800	-12.700	1999	12	17.43876	BNT	GRB
124.500	22.700	1999	12	18.11465	BNT	GRB
61.600	-58.700	1999	12	18.96919	BNT	GRB
302.640	8.780	1999	12	19.77108	BT	GRB991219
50.400	51.900	1999	12	20.42631	BNT	GRB
221.000	-5.600	1999	12	20.66715	BNT	GRB
274.300	40.200	1999	12	21.19972	BNT	GRB
180.500	-62.300	1999	12	21.86786	BNT	GRB
307.000	-18.200	1999	12	22.27940	BNT	GRB
129.000	60.400	1999	12	22.39699	BNT	GRB
283.100	9.900	1999	12	24.05316	BNT	GRB
56.600	-8.200	1999	12	24.31235	BNT	GRB
144.200	-23.700	1999	12	25.50309	BNT	GRB
276.040	-12.710	1999	12	26.32206	BT	GRB991226
269.000	11.000	1999	12	26.96457	BeS	991226B
71.100	44.300	1999	12	27.09953	BNT	GRB
21.670	-13.130	1999	12	28.18615	BT	GRB991228-
167.460	34.440	1999	12	28.48600	BT	GRB991228-
277.000	-37.500	1999	12	28.68906	BNT	GRB
317.870	8.140	1999	12	29.50603	BT	GRB991229-
332.870	33.590	1999	12	29.63291	BT	GRB991229-
39.300	32.300	1999	12	31.32977	BNT	GRB
300.770	28.490	2000	01	1.05554	BT	GRB000101
213.200	-13.900	2000	01	2.32071	BNT	GRB
184.800	-12.200	2000	01	3.43910	BNT	GRB
167.900	-57.990	2000	01	3.98274	BT	GRB000103
145.170	-66.120	2000	01	4.06162	BeS	000104A
169.300	22.000	2000	01	4.35103	BNT	GRB
223.240	70.390	2000	01	4.60152	BeS	000104B

Continued on next column

Continued from previous column

RA deg	DEC deg	Year	Month	Day	Cat.	GRB Name
199.300	8.300	2000	01	6.25002	BNT	GRB
187.680	34.570	2000	01	7.03066	BT	GRB000107-
119.000	-20.000	2000	01	7.85832	BeS	000107B
285.760	-29.150	2000	01	7.90594	BeS	000107C
236.350	-78.820	2000	01	8.70008	BeS	000108
120.410	43.720	2000	01	8.85649	BT	GRB000108-
248.880	-28.530	2000	01	9.43569	BeS	000109
312.000	70.000	2000	01	10.19358	BeS	000110
148.900	44.500	2000	01	10.65025	BT	GRB000110
134.730	-16.560	2000	01	11.11248	BT	GRB000111
95.900	-34.500	2000	01	11.16653	BNT	GRB
28.700	77.600	2000	01	11.49478	BNT	GRB
312.100	-3.800	2000	01	12.63248	BNT	GRB
163.270	19.890	2000	01	13.39586	BT	GRB000113
214.000	-65.000	2000	01	14.37259	BeS	000114
152.500	-41.040	2000	01	14.51789	BT	GRB000114-
107.400	-25.300	2000	01	14.59538	BNT	GRB
121.640	39.560	2000	01	14.84551	BT	GRB000114-
283.600	9.300	2000	01	14.94580	BNT	GRB
116.550	-15.790	2000	01	15.61773	BeS	000115
245.000	45.000	2000	01	16.57221	BeS	000116
236.600	16.500	2000	01	17.16327	BNT	GRB
206.000	-27.100	2000	01	19.52245	BNT	GRB
203.000	-12.000	2000	01	19.54830	BeS	000119B
205.200	-77.700	2000	01	21.91557	BNT	GRB
254.510	58.590	2000	01	22.86177	BT	GRB000122
318.070	14.100	2000	01	23.57618	BeS	000123
355.710	-32.310	2000	01	23.72946	BT	GRB000123-
6.300	25.900	2000	01	25.04248	BNT	GRB
0.560	35.520	2000	01	26.29028	BeS	000126
327.610	-42.670	2000	01	26.34434	BT	GRB000126-
357.800	-7.400	2000	01	26.47146	BNT	GRB
136.870	64.490	2000	01	26.55684	BT	GRB000126-
118.000	5.040	2000	01	26.97674	BT	GRB000126-
273.000	-41.000	2000	01	27.14746	BeS	000127
64.700	2.100	2000	01	29.03106	BNT	GRB
18.300	5.000	2000	01	29.09221	BNT	GRB
228.050	21.960	2000	01	30.05391	BT	GRB000130
68.300	-34.500	2000	01	30.61103	BNT	GRB
261.800	-58.400	2000	01	31.19677	BNT	GRB
93.960	-52.030	2000	01	31.62358	BT	GRB000131
140.070	15.910	2000	02	1.12650	BT	GRB000201-
31.410	56.890	2000	02	1.77052	BT	GRB000201-
5.240	-17.890	2000	02	2.37782	BT	GRB000202
329.060	-88.400	2000	02	3.43600	BT	GRB000203
345.960	68.230	2000	02	4.26580	BT	GRB000204
8.410	30.180	2000	02	5.36102	BeS	000205A
203.000	14.600	2000	02	5.52718	BeS	000205B

Continued on next column

Continued from previous column

RA deg	DEC deg	Year	Month	Day	Cat.	GRB Name
28.100	18.200	2000	02	6.10628	BeS	000206
210.000	63.000	2000	02	6.45683	BNT	GRB
255.700	78.500	2000	02	6.86659	BNT	GRB
236.200	-39.600	2000	02	7.23861	BNT	GRB
150.200	-11.000	2000	02	7.55251	BNT	GRB
330.000	-7.300	2000	02	7.85514	BNT	GRB
289.700	59.250	2000	02	7.99747	BeS	000207
28.900	-22.840	2000	02	8.18138	BeS	000208A
82.000	-16.000	2000	02	8.38343	BeS	000208B
221.000	-36.300	2000	02	9.08826	BNT	GRB
74.200	50.500	2000	02	10.16238	BNT	GRB
29.810	-40.670	2000	02	10.36395	BeS	000210
334.900	58.600	2000	02	11.19961	BNT	GRB
3.200	24.000	2000	02	11.52343	BeS	000211
329.000	72.000	2000	02	12.71287	BeS	000212
16.090	35.620	2000	02	12.93825	BT	GRB000212
176.000	-29.100	2000	02	13.59644	BNT	GRB
136.770	4.800	2000	02	13.91156	BT	GRB000213
283.570	-66.450	2000	02	14.04236	BeS	000214A
319.000	-49.000	2000	02	14.23910	BeS	000214B
255.300	-28.600	2000	02	15.64135	BNT	GRB
296.800	-10.900	2000	02	16.05697	BNT	GRB
344.300	-29.300	2000	02	17.28774	BNT	GRB
247.100	-0.900	2000	02	17.33850	BNT	GRB
91.700	3.400	2000	02	17.37844	BNT	GRB
16.560	36.510	2000	02	17.44938	BeS	000217
272.720	-56.970	2000	02	17.87506	BT	GRB000217-
2.435	-79.530	2000	02	18.67992	K/W	000218.T58744
162.000	-40.700	2000	02	18.92684	BNT	GRB
274.160	84.140	2000	02	19.68045	BT	GRB000219
182.040	65.950	2000	02	20.19774	BT	GRB000220
217.500	-41.500	2000	02	20.22642	BNT	GRB
299.400	-67.200	2000	02	21.87965	BNT	GRB
125.760	77.700	2000	02	21.98553	BT	GRB000221
53.990	60.600	2000	02	22.57252	BeS	000222
0.900	-77.400	2000	02	23.14492	BNT	GRB
317.300	55.400	2000	02	23.22824	BNT	GRB
298.800	-27.400	2000	02	24.95149	BeS	000224
110.560	0.530	2000	02	25.06632	BeS	000225
113.300	17.300	2000	02	25.16750	BNT	GRB
143.680	29.820	2000	02	26.16098	BT	GRB000226-
330.030	16.890	2000	02	26.42561	BT	GRB000226-
327.000	-10.000	2000	02	26.53551	BeS	000226
245.600	50.700	2000	02	26.79844	BNT	GRB
43.330	-7.490	2000	02	27.90002	BeS	000227
236.520	65.160	2000	02	28.14242	BT	GRB000228
206.400	20.600	2000	02	28.26811	BNT	GRB
296.730	47.870	2000	02	29.11461	BT	GRB000229

Continued on next column

Continued from previous column

RA deg	DEC deg	Year	Month	Day	Cat.	GRB Name
168.200	-56.500	2000	02	29.34889	BNT	GRB
354.860	75.780	2000	03	1.10687	BeS	000301A
239.000	0.000	2000	03	1.51926	BeS	000301B
215.000	-6.000	2000	03	1.52853	BeS	000301C
58.200	54.280	2000	03	2.11834	BT	GRB000302-
174.460	30.660	2000	03	2.59892	BeS	000302
73.100	-0.600	2000	03	3.11558	BNT	GRB
275.830	62.050	2000	03	3.19897	BT	GRB000303
159.900	48.000	2000	03	5.41406	BNT	GRB
322.800	15.400	2000	03	6.06875	BNT	GRB
349.500	-56.700	2000	03	6.19711	BNT	GRB
69.730	-10.170	2000	03	6.51015	BT	GRB000306-
226.070	40.920	2000	03	6.75037	BeS	000306
88.490	6.800	2000	03	7.91027	BT	GRB000307
224.900	-41.100	2000	03	9.29594	BNT	GRB
127.510	-10.860	2000	03	10.34492	BT	GRB000310-
5.400	-1.460	2000	03	10.63003	BeS	000310
320.290	37.920	2000	03	12.22494	BeS	000312
96.210	11.040	2000	03	12.86865	BT	GRB000312-
29.800	-62.100	2000	03	13.12547	BNT	GRB
229.100	-19.370	2000	03	13.18728	BT	GRB000313-
197.890	10.250	2000	03	13.88407	BT	GRB000313-
137.710	50.660	2000	03	14.36925	BeS	000314
27.220	32.660	2000	03	17.90224	BT	GRB000317
3.700	-36.500	2000	03	18.09068	BNT	GRB
164.700	-33.600	2000	03	18.14966	BNT	GRB
172.770	-13.860	2000	03	19.18265	BT	GRB000319
82.480	4.440	2000	03	20.34406	BT	GRB000320
310.600	-50.000	2000	03	20.58575	BNT	GRB
49.240	36.390	2000	03	21.91189	BT	GRB000321
170.300	59.000	2000	03	22.25514	BNT	GRB
193.000	48.820	2000	03	23.37646	BeS	000323
207.020	-24.040	2000	03	24.21544	BT	GRB000324
267.600	-13.500	2000	03	24.90849	BNT	GRB
333.360	-26.360	2000	03	26.22148	BT	GRB000326-
270.840	-63.470	2000	03	26.64266	BT	GRB000326-
316.000	55.000	2000	03	27.94302	BeS	000327
246.800	-40.500	2000	03	28.37377	BNT	GRB
155.500	50.600	2000	03	30.32487	BNT	GRB
312.400	32.000	2000	03	30.35916	BT	GRB000330-
308.000	3.100	2000	03	30.79940	BNT	GRB
358.310	39.260	2000	03	30.87325	BeS	000330
169.400	-15.020	2000	03	31.15831	BT	GRB000331-
19.110	-46.290	2000	03	31.29178	BT	GRB000331-
135.200	47.700	2000	03	31.44586	BNT	GRB
32.000	59.770	2000	03	31.98868	BT	GRB000331-
185.300	-33.600	2000	04	1.75411	BNT	GRB
296.290	80.600	2000	04	1.89579	BT	GRB000401

Continued on next column

Continued from previous column

RA deg	DEC deg	Year	Month	Day	Cat.	GRB Name
318.000	25.000	2000	04	2.12212	BeS	000402A
343.530	6.650	2000	04	2.60484	BeS	000402B
275.100	-10.700	2000	04	3.15277	BNT	GRB
228.400	-26.300	2000	04	3.17572	BNT	GRB
146.800	28.100	2000	04	3.52001	BNT	GRB
57.200	24.690	2000	04	3.56461	BT	GRB000403
322.900	9.700	2000	04	3.86274	BNT	GRB
129.100	27.400	2000	04	4.02462	BNT	GRB
189.400	-52.600	2000	04	4.44170	BNT	GRB
174.300	-29.900	2000	04	5.46096	BNT	GRB
226.900	-52.500	2000	04	5.89567	BNT	GRB
75.800	-34.500	2000	04	7.03265	BNT	GRB
157.980	-70.060	2000	04	7.12961	BeS	000407
132.900	-43.800	2000	04	7.25053	BNT	GRB
254.350	-71.850	2000	04	8.00484	BT	GRB000408-
138.510	67.220	2000	04	8.10819	BT	GRB000408-
257.600	-24.000	2000	04	8.55825	BNT	GRB
180.000	50.700	2000	04	8.83249	BNT	GRB
264.370	80.820	2000	04	9.62535	BeS	000409
101.300	15.000	2000	04	10.50297	BNT	GRB
197.200	-57.000	2000	04	10.58874	BNT	GRB
209.940	-12.480	2000	04	10.72052	BT	GRB000410
212.900	16.600	2000	04	10.97983	BNT	GRB
53.100	4.900	2000	04	12.34172	BNT	GRB
201.370	-59.780	2000	04	12.48811	BeS	000412
119.400	-8.100	2000	04	13.20545	BNT	GRB
175.470	68.270	2000	04	15.01122	BeS	000415
134.850	69.420	2000	04	15.36157	BT	GRB000415-
199.390	-29.980	2000	04	15.69330	BT	GRB000415-
277.300	26.200	2000	04	16.34961	BNT	GRB
258.500	-65.700	2000	04	16.60625	BNT	GRB
222.390	2.930	2000	04	17.98273	BT	GRB000417
69.800	76.150	2000	04	18.89604	BeS	000418
64.500	33.700	2000	04	18.99929	BNT	GRB
330.070	48.280	2000	04	19.09223	BeS	000419
139.060	-44.660	2000	04	20.05759	BT	GRB000420-
16.450	27.180	2000	04	20.48926	BeS	000420A
129.260	-14.590	2000	04	20.59874	BeS	000420B
104.100	54.200	2000	04	20.71035	BNT	GRB
313.810	-63.010	2000	04	20.75046	BeS	000420C
94.600	-28.900	2000	04	21.05317	BNT	GRB
174.910	16.980	2000	04	21.51637	BeS	000421
233.060	71.800	2000	04	24.37808	BT	GRB000424-
105.030	53.980	2000	04	24.76259	BT	GRB000424-
315.000	-47.000	2000	04	25.22605	BeS	000425
358.600	19.400	2000	04	29.34946	BNT	GRB
98.340	-4.420	2000	04	29.42178	BeS	000429
27.400	-56.000	2000	04	29.65376	BNT	GRB

Continued on next column

Continued from previous column

RA deg	DEC deg	Year	Month	Day	Cat.	GRB Name
8.200	4.700	2000	04	29.85675	BNT	GRB
65.700	-65.000	2000	04	30.54846	BNT	GRB
266.600	-80.000	2000	04	30.61630	BNT	GRB
346.300	-6.000	2000	05	1.35650	BNT	GRB
68.000	9.000	2000	05	2.14125	BeS	000502A
253.940	-46.680	2000	05	2.14804	BT	GRB000502
252.000	-41.000	2000	05	2.55457	BeS	000502B
171.800	-63.500	2000	05	2.62568	BeS	000502C
23.400	-31.300	2000	05	3.72020	BNT	GRB
1.000	-34.800	2000	05	4.11244	BNT	GRB
38.100	18.100	2000	05	4.44509	BNT	GRB
37.800	-77.700	2000	05	4.71573	BNT	GRB
85.200	-6.900	2000	05	4.71962	BNT	GRB
87.500	-32.200	2000	05	6.01515	BNT	GRB
258.000	-9.000	2000	05	6.42826	BeS	000506
20.700	-4.100	2000	05	6.86216	BNT	GRB
232.000	-32.000	2000	05	7.54780	BeS	000507
272.900	-50.400	2000	05	7.70478	BNT	GRB
202.720	3.780	2000	05	8.01977	BT	GRB000508-
253.540	-20.380	2000	05	8.79920	BT	GRB000508-
89.890	2.390	2000	05	8.89605	BT	GRB000508-
83.300	25.300	2000	05	8.95361	BNT	GRB
344.190	-39.270	2000	05	9.94226	BT	GRB000509
331.240	-36.110	2000	05	11.05010	BeS	000511A
265.400	-14.200	2000	05	11.16273	BNT	GRB
295.580	-8.700	2000	05	11.75206	BeS	000511B
48.700	38.000	2000	05	11.76734	BNT	GRB
125.200	-19.100	2000	05	12.25228	BNT	GRB
338.910	-45.110	2000	05	13.47332	BT	GRB000513-
160.730	-12.010	2000	05	13.74367	BT	GRB000513-
259.000	-25.300	2000	05	14.76625	BNT	GRB
34.900	-11.900	2000	05	14.83892	BNT	GRB
35.070	-14.830	2000	05	16.39311	BeS	000516
107.980	76.740	2000	05	17.23368	BeS	000517A
71.330	53.910	2000	05	18.23740	BeS	000518
346.160	1.170	2000	05	19.34597	BeS	000519
266.900	-16.200	2000	05	19.98375	BNT	GRB
234.740	-0.310	2000	05	20.46917	BT	GRB000520
5.960	-6.250	2000	05	21.40817	BT	GRB000521
109.190	-41.360	2000	05	24.00632	BT	GRB000524
270.500	-25.800	2000	05	24.83129	BNT	GRB
169.000	10.000	2000	05	25.25594	BeS	000525
280.220	-39.440	2000	05	25.43349	BT	GRB000525
261.100	-43.800	2000	05	25.82740	BNT	GRB
231.290	-10.320	2000	05	26.41776	BT	GRB000526
0.000	0.000	2000	05	26.97795	K/W	000526_T84494
161.350	-34.000	2000	05	28.36555	BeS	000528
218.000	39.000	2000	05	29.00267	BeS	000529A

Continued on next column

Continued from previous column

RA deg	DEC deg	Year	Month	Day	Cat.	GRB Name
2.280	-61.530	2000	05	29.36333	BeS	000529B
91.000	24.000	2000	06	4.35488	BeS	000604
247.000	52.000	2000	06	6.07950	BeS	000606
38.497	17.142	2000	06	7.10057	K/W	000607_T08689
229.037	-7.973	2000	06	8.81594	K/W	000608_T70497
133.000	52.000	2000	06	13.02204	BeS	000613
233.140	73.800	2000	06	15.26236	BeS	000615A
35.610	-17.870	2000	06	15.68929	BeS	000615B
89.000	21.000	2000	06	18.37199	BeS	000618
276.000	-59.000	2000	06	20.03795	BeS	000620A
113.820	69.200	2000	06	20.23163	BeS	000620B
247.000	-3.000	2000	06	21.08392	BeS	000621
296.000	6.000	2000	06	23.04498	BeS	000623
90.000	-26.000	2000	06	26.86631	BeS	000626
51.000	22.000	2000	06	27.19593	BeS	000627
104.000	53.000	2000	06	29.01965	BeS	000629
221.810	41.220	2000	06	30.02152	BeS	000630
150.283	-52.117	2000	07	1.30047	K/W	000701_T25961
115.000	-31.000	2000	07	4.12469	BeS	000704
314.695	-53.653	2000	07	7.20107	K/W	000707_T17372
111.000	-3.000	2000	07	18.86608	BeS	000718B
20.000	-51.000	2000	07	23.44451	BeS	000723
176.300	17.400	2000	07	27.82131	BeS	000727
53.000	-44.000	2000	08	1.04940	BeS	000801
299.580	23.530	2000	08	11.64584	BeS	000811
177.000	-14.000	2000	08	19.34415	BeS	000819
196.000	-21.000	2000	08	20.69844	BeS	000820
359.000	22.000	2000	08	21.09505	BeS	000821
69.226	-67.193	2000	08	21.38877	K/W	000821_T33589
19.000	61.000	2000	08	28.74697	BeS	000828A
155.000	-24.000	2000	08	28.95988	BeS	000828B
141.000	-49.000	2000	08	30.48551	BeS	000830B
353.550	6.350	2000	08	30.99296	BeS	000830C
327.000	59.000	2000	09	3.54294	BeS	000903A
134.000	-6.000	2000	09	3.64748	BeS	000903C
11.000	-23.000	2000	09	3.98280	BeS	000903D
12.000	5.000	2000	09	4.55465	BeS	000904
272.000	47.000	2000	09	6.87557	BeS	000906
244.000	-81.000	2000	09	15.16549	BeS	000915
85.000	29.000	2000	09	16.59377	BeS	000916
94.000	34.000	2000	09	22.88994	BeS	000922
48.000	-39.000	2000	09	24.69487	BeS	000924
146.000	12.000	2000	09	26.87715	BeS	000926
106.061	-4.477	2000	09	28.07274	K/W	000928_T06285
240.090	-56.810	2000	10	4.61905	BeS	001004
67.000	53.000	2000	10	11.42140	BeS	001011A
275.770	-50.900	2000	10	11.66306	BeS	001011C
203.000	-44.000	2000	10	13.75947	BeS	001013

Continued on next column

Continued from previous column

RA deg	DEC deg	Year	Month	Day	Cat.	GRB Name
257.930	35.340	2000	10	19.99950	BeS	001019
196.000	15.000	2000	10	22.01271	BeS	001022A
275.000	-79.000	2000	10	22.21867	BeS	001022B
68.257	-76.184	2000	10	22.24197	K/W	001022_T20905
275.349	-5.107	2000	10	25.82604	K/W	001025_T71369
119.000	42.000	2000	11	1.91147	BeS	001101
190.000	-15.000	2000	11	6.72069	BeS	001106
233.000	48.000	2000	11	8.88819	BeS	001108
277.530	55.300	2000	11	9.39112	BeS	001109
196.000	-6.000	2000	11	10.51214	BeS	001110
34.000	-7.000	2000	11	15.58797	BeS	001115
42.000	-2.000	2000	11	18.34704	BeS	001118A
171.000	-76.000	2000	11	18.86361	BeS	001118B
101.000	-65.000	2000	12	1.54787	BeS	001201A
77.000	-4.000	2000	12	4.09973	BeS	001204A
40.290	12.900	2000	12	4.33413	BeS	001204B
260.000	41.000	2000	12	5.62465	BeS	001205
49.000	-36.000	2000	12	6.40071	BeS	001206A
209.000	-49.000	2000	12	6.89560	BeS	001206C
98.163	-62.886	2000	12	7.10204	K/W	001207_T08815
7.000	-74.000	2000	12	12.39840	BeS	001212A
102.400	36.440	2000	12	12.62318	BeS	001212B
192.000	-42.000	2000	12	14.24939	BeS	001214A
40.000	2.000	2000	12	15.20596	BeS	001215A
298.000	-17.000	2000	12	15.60734	BeS	001215B
71.000	-54.000	2000	12	16.59262	BeS	001216
195.000	44.000	2000	12	17.68089	BeS	001217
102.000	18.000	2000	12	18.08759	BeS	001218
50.000	56.000	2000	12	19.31631	BeS	001219A
269.000	-33.000	2000	12	26.39218	BeS	001226A
350.000	-39.000	2000	12	26.84356	BeS	001226B
317.370	63.510	2001	01	4.72326	BeS	010104B
323.260	-49.520	2001	01	9.10979	BeS	010109
141.000	55.000	2001	01	11.78019	BeS	010111
325.000	39.000	2001	01	13.20483	BeS	010113
158.000	-64.000	2001	01	14.15546	BeS	010114
150.000	12.000	2001	01	19.01383	BeS	010119A
283.460	12.020	2001	01	19.43029	BeS	010119B
141.000	-45.000	2001	01	21.72820	BeS	010121
99.000	24.000	2001	01	23.09631	BeS	010123
179.290	49.750	2001	01	26.38248	BeS	010126B
349.000	-27.000	2001	01	26.85196	BeS	010126C
118.000	-59.000	2001	02	3.19266	BeS	010203
33.000	48.000	2001	02	8.17248	BeS	010208B
131.000	39.000	2001	02	8.60159	BeS	010208C
8.000	28.000	2001	02	9.21596	BeS	010209A
335.000	-17.000	2001	02	11.94000	BeS	010211
219.000	47.000	2001	02	12.72670	BeS	010212B

Continued on next column

Continued from previous column

RA deg	DEC deg	Year	Month	Day	Cat.	GRB Name
77.000	-43.000	2001	02	12.99807	BeS	010212C
257.340	39.260	2001	02	13.12318	BeS	010213
157.900	5.511	2001	02	13.52471	HET	GRB010213
265.240	48.580	2001	02	14.36675	BeS	010214
315.000	2.000	2001	02	20.80618	BeS	010220A
293.000	10.000	2001	02	20.85510	BeS	010220B
39.250	61.770	2001	02	20.95213	BeS	010220C
223.050	43.020	2001	02	22.30767	BeS	010222A
106.000	26.000	2001	02	22.87064	BeS	010222B
242.000	-64.000	2001	02	26.80223	BeS	010226A
181.000	31.000	2001	02	26.89390	BeS	010226B
173.000	3.000	2001	03	1.24221	BeS	010301
294.000	55.000	2001	03	3.63574	BeS	010303
316.590	53.210	2001	03	4.22142	BeS	010304
159.000	-29.000	2001	03	7.68589	BeS	010307
37.000	-60.000	2001	03	8.65205	BeS	010308
19.000	-2.000	2001	03	9.52351	BeS	010309
33.000	-5.000	2001	03	17.26953	BeS	010317
204.000	-14.000	2001	03	21.50575	BeS	010321
107.780	20.080	2001	03	24.48088	BeS	010324
19.000	25.000	2001	03	25.27646	BeS	010325
132.960	-38.300	2001	03	26.13537	BeS	010326
35.000	-67.000	2001	03	30.60304	BeS	010330
301.000	36.000	2001	04	2.56676	BeS	010402
15.000	10.000	2001	04	4.35265	BeS	010404
158.000	46.000	2001	04	6.03907	BeS	010406
84.000	37.000	2001	04	7.30343	BeS	010407A
68.000	40.000	2001	04	7.94175	BeS	010407C
13.000	-2.000	2001	04	11.54862	BeS	010411A
218.000	-11.000	2001	04	11.67091	BeS	010411B
290.910	13.620	2001	04	12.90728	BeS	010412
218.000	-88.000	2001	04	14.99132	BeS	010414
200.000	-30.000	2001	04	15.79980	BeS	010415B
342.000	-1.000	2001	04	18.34170	BeS	010418
159.000	-3.000	2001	04	20.94301	BeS	010420
13.000	28.000	2001	04	27.06830	BeS	010427A
319.000	24.000	2001	04	27.38894	BeS	010427B
98.000	-36.000	2001	04	27.55145	BeS	010427C
342.112	-65.623	2001	04	27.78071	K/W	010427_T67452
8.000	-4.000	2001	04	30.96076	BeS	010430
286.710	-70.180	2001	05	1.27601	BeS	010501
16.000	-33.000	2001	05	4.11373	BeS	010504
41.000	10.000	2001	05	5.26838	BeS	010505A
192.000	0.000	2001	05	5.49016	BeS	010505B
347.000	81.000	2001	05	7.38346	BeS	010507B
47.000	-1.000	2001	05	10.02970	BeS	010510
307.000	54.000	2001	05	11.69058	BeS	010511
55.000	-69.000	2001	05	14.69605	BeS	010514

Continued on next column

Continued from previous column

RA deg	DEC deg	Year	Month	Day	Cat.	GRB Name
22.000	-7.000	2001	05	15.09759	BeS	010515A
161.680	-57.780	2001	05	18.27996	BeS	010518A
138.000	-51.000	2001	05	18.35038	BeS	010518B
257.000	-39.000	2001	05	22.86930	BeS	010522
56.000	8.000	2001	05	28.13918	BeS	010528
84.000	3.000	2001	06	2.49801	BeS	010602
84.000	33.000	2001	06	5.61148	BeS	010605
349.000	-31.000	2001	06	11.31829	BeS	010611A
270.820	-32.130	2001	06	12.10640	BeS	010612A
328.000	-30.000	2001	06	12.40973	BeS	010612B
63.000	28.000	2001	06	16.06811	BeS	010616
3.907	44.111	2001	06	16.23292	K/W	010616_T20124
259.000	27.000	2001	06	17.12005	BeS	010617
95.000	22.000	2001	06	18.67126	BeS	010618B
123.000	-64.000	2001	06	19.12391	BeS	010619A
321.000	28.000	2001	06	23.14670	BeS	010623
38.000	-83.000	2001	06	24.56632	BeS	010624
160.452	-55.825	2001	06	24.56631	K/W	010624_T48929
303.000	39.000	2001	06	26.10132	BeS	010626
18.016	13.030	2001	06	28.04869	K/W	010628_T04206
248.160	-18.720	2001	06	29.51465	BeS	010629A
94.000	11.000	2001	06	29.79927	BeS	010629B
67.000	12.000	2001	07	5.17653	BeS	010705
149.000	27.000	2001	07	10.98209	BeS	010710B
118.000	17.000	2001	07	21.16448	BeS	010721
266.000	-4.000	2001	07	23.70133	BeS	010723
279.000	55.000	2001	07	27.04611	BeS	010727A
276.000	-26.000	2001	07	27.52074	BeS	010727C
175.030	-7.950	2001	07	28.80882	BeS	010728
244.000	42.000	2001	07	30.49906	BeS	010730
177.000	12.000	2001	08	2.35787	BeS	010802
328.000	-2.000	2001	08	18.57859	BeS	010818A
167.000	-2.000	2001	08	18.87338	BeS	010818B
180.000	-12.000	2001	08	20.85848	BeS	010820
267.000	-75.000	2001	08	25.75205	BeS	010825
299.000	41.000	2001	08	26.75418	BeS	010826
251.000	31.000	2001	09	8.75006	BeS	010908
274.000	26.000	2001	09	10.10476	BeS	010910
127.000	23.000	2001	09	13.86712	BeS	010913
140.000	52.000	2001	09	17.29483	BeS	010917
343.900	40.930	2001	09	21.21933	BeS	010921
302.070	18.030	2001	09	23.39200	BeS	010923
272.000	-29.000	2001	09	30.56947	BeS	010930
187.000	-64.000	2001	10	1.93861	BeS	011001
190.000	-5.000	2001	11	4.41809	BeS	011104
294.000	28.000	2001	11	16.14936	BeS	011116
173.630	-76.030	2001	11	21.78273	BeS	011121
45.000	-9.000	2001	11	26.41947	BeS	011126

Continued on next column

Continued from previous column

RA deg	DEC deg	Year	Month	Day	Cat.	GRB Name
46.362	3.825	2001	11	30.26361	HET	GRB011130
168.810	-21.940	2001	12	11.79816	BeS	011211
170.000	-31.000	2001	12	12.06661	BeS	011212
75.019	32.127	2001	12	12.16947	HET	GRB011212
43.000	54.000	2001	12	16.12179	BeS	011216
220.000	-16.000	2001	12	17.48828	BeS	011217
129.000	-8.000	2001	12	22.44101	BeS	011222
16.000	33.000	2001	12	30.32382	BeS	011230A
82.000	67.000	2001	12	30.36692	BeS	011230B
178.000	-34.000	2001	12	31.14915	BeS	011231
11.000	-40.000	2002	01	2.87348	BeS	020102A
84.000	-19.000	2002	01	2.88058	BeS	020102B
84.000	52.000	2002	01	13.08624	BeS	020113A
283.691	68.930	2002	01	13.08626	K/W	020113_T07452
0.000	0.000	2002	01	16.91166	K/W	020116_T78766
326.917	69.564	2002	01	17.53135	K/W	020117_T45909
125.000	4.000	2002	01	19.18553	BeS	020119B
58.000	69.000	2002	01	19.67418	BeS	020119C
143.206	-11.460	2002	01	24.44531	HET	GRB020124
123.774	36.742	2002	01	27.87321	HET	GRB020127
205.000	-51.000	2002	02	9.32635	BeS	020209
154.000	27.000	2002	02	12.98057	BeS	020212B
48.700	36.300	2002	02	21.33869	BeS	020221
190.762	-14.552	2002	03	5.49682	HET	GRB020305
62.000	27.000	2002	03	5.62943	BeS	020305
262.187	38.706	2002	03	6.79029	K/W	020306_T68280
6.000	-9.000	2002	03	8.25485	BeS	020308
351.000	-56.000	2002	03	9.29034	BeS	020309
57.000	54.000	2002	03	11.05660	BeS	020311
155.837	12.744	2002	03	17.76077	HET	GRB020317
43.000	-7.000	2002	03	20.24641	BeS	020320
242.760	-83.700	2002	03	21.18105	BeS	020321
270.210	81.100	2002	03	22.16084	BeS	020322
98.633	-37.423	2002	03	26.45351	K/W	020326_T39182
152.000	-39.000	2002	03	27.06890	BeS	020327A
337.000	60.000	2002	03	27.10148	BeS	020327B
199.142	-17.875	2002	03	31.68922	HET	GRB020331
339.000	-80.000	2002	04	1.70524	BeS	020401
209.540	-31.390	2002	04	5.02887	BeS	020405
151.000	53.000	2002	04	9.39396	BeS	020409A
131.310	66.690	2002	04	9.88302	BeS	020409B
14.910	-7.110	2002	04	13.68072	BeS	020413
240.000	-81.000	2002	04	14.07458	BeS	020414
4.000	68.000	2002	04	16.32863	BeS	020416
349.000	-44.000	2002	04	17.23353	BeS	020417
120.080	-48.650	2002	04	18.36010	BeS	020418
143.000	76.000	2002	04	26.99739	BeS	020426
26.557	47.412	2002	05	25.18536	K/W	020525_T16014

Continued on next column

Continued from previous column

RA deg	DEC deg	Year	Month	Day	Cat.	GRB Name
228.688	-19.360	2002	05	31.01828	HET	GRB020531
306.271	49.820	2002	06	2.72951	K/W	020602_T63030
311.060	7.170	2002	06	25.47626	HET	GRB020625
152.217	54.873	2002	07	15.63502	K/W	020715_T54866
47.522	-74.688	2002	07	31.01893	K/W	020731_T01635
315.560	-53.770	2002	08	1.54076	HET	GRB020801
309.699	-5.393	2002	08	12.44565	HET	GRB020812
296.658	-19.588	2002	08	13.11411	HET	GRB020813
351.849	6.269	2002	08	19.62333	HET	GRB020819
144.152	46.095	2002	08	28.24002	K/W	020828_T20737
342.252	-20.930	2002	09	3.42058	HET	GRB020903
6.737	18.929	2002	10	4.50433	HET	GRB021004
359.805	50.642	2002	10	16.43682	HET	GRB021016
4.347	-1.617	2002	10	21.77986	HET	GRB021021
58.452	37.953	2002	11	4.29240	HET	GRB021104
39.217	48.849	2002	11	12.14463	HET	GRB021112
23.485	40.453	2002	11	13.27705	HET	GRB021113
296.983	28.391	2002	11	25.74890	INT	021125
121.932	21.244	2002	12	1.22921	K/W	021201_T19803
122.250	6.739	2002	12	11.47123	HET	GRB021211
282.625	31.900	2002	12	19.31521	INT	021219
250.493	74.039	2002	12	26.62060	K/W	021226_T53620
47.320	2.738	2003	01	1.86367	K/W	030101_T74621
88.757	-27.201	2003	01	5.60711	K/W	030105_T52454
287.307	84.230	2003	01	10.40245	K/W	030110_T34772
169.626	15.038	2003	01	15.14067	HET	GRB030115
102.170	66.676	2003	01	17.73354	K/W	030117_T63378
202.093	30.673	2003	01	31.31862	INT	030131
116.269	-34.926	2003	02	6.45873	K/W	030206_T39634
93.308	-65.316	2003	02	10.59094	K/W	030210_T51057
173.255	25.899	2003	02	26.15731	HET	GRB030226
74.388	20.485	2003	02	27.36257	INT	030227A
267.925	-25.312	2003	03	20.42487	INT	030320
166.527	-21.906	2003	03	23.91456	HET	GRB030323
204.295	-0.323	2003	03	24.13383	HET	GRB030324
182.711	-9.352	2003	03	28.47289	HET	GRB030328
161.203	21.479	2003	03	29.48420	HET	GRB030329
166.711	-2.883	2003	04	16.46110	HET	GRB030416
163.721	-6.990	2003	04	18.41619	HET	GRB030418
183.276	-20.933	2003	04	29.44610	HET	GRB030429
286.375	6.307	2003	05	1.13197	INT	030501
148.436	11.723	2003	05	1.86447	K/W	030501_T74690
239.758	-33.488	2003	05	19.58674	HET	GRB030519
30.185	59.014	2003	05	23.59085	K/W	030523_T51049
256.009	-22.650	2003	05	28.54379	HET	GRB030528
145.125	-56.342	2003	05	29.82868	INT	030529
64.930	-14.036	2003	06	7.09672	K/W	030607_T08357
258.914	19.037	2003	06	29.14356	K/W	030629_T12404

Continued on next column

Continued from previous column

RA deg	DEC deg	Year	Month	Day	Cat.	GRB Name
327.374	-27.702	2003	07	23.26964	HET	GRB030723
308.444	-50.764	2003	07	25.49057	HET	GRB030725
272.044	-20.656	2003	08	13.41115	HET	GRB030813
326.946	-48.180	2003	08	21.23028	HET	GRB030821
322.695	21.996	2003	08	23.36992	HET	GRB030823
1.260	19.927	2003	08	24.69971	HET	GRB030824
89.655	-66.189	2003	09	16.91618	K/W	030916_T79158
84.265	82.452	2003	09	26.70309	K/W	030926_T60747
269.703	67.615	2003	09	29.60226	K/W	030929_T52035
339.192	0.096	2003	10	26.06003	K/W	031026_T05187
49.677	28.366	2003	10	26.23314	HET	GRB031026
72.434	17.474	2003	11	11.69807	HET	GRB031111A
59.770	34.605	2003	11	11.82741	HET	GRB031111B
104.237	-74.513	2003	11	18.26825	K/W	031118_T23176
120.626	-39.851	2003	12	3.91770	INT	031203B
84.770	-41.872	2003	12	8.89905	K/W	031208_T77678
245.344	-12.641	2003	12	14.42425	K/W	031214_T36655
84.232	62.089	2003	12	18.26951	K/W	031218_T23285
69.893	7.373	2003	12	20.14580	HET	GRB031220
178.051	-46.788	2004	01	6.74664	INT	040106
281.156	52.390	2004	01	29.37382	K/W	040129_T32297
102.640	25.540	2004	02	10.46611	K/W	040210_T40272
249.876	-41.933	2004	02	23.56127	INT	040223A
153.051	-7.326	2004	02	28.00884	HET	GRB040228B
102.854	-65.894	2004	03	12.00181	K/W	040312_T00156
234.492	-21.244	2004	03	22.31187	K/W	040322_T26945
208.469	-52.354	2004	03	23.54382	INT	040323A
329.877	-2.659	2004	03	24.43142	K/W	040324_T37274
115.225	68.215	2004	04	3.21392	INT	040403
130.338	32.320	2004	04	13.54854	K/W	040413_T47394
280.505	1.981	2004	04	22.29033	INT	040422A
226.684	-24.794	2004	04	23.41292	HET	GRB040423
232.899	-39.721	2004	04	25.68414	HET	GRB040425
221.958	-44.252	2004	05	11.54289	HET	GRB040511
195.050	-3.580	2004	06	24.34832	INT	040624
311.943	-40.237	2004	07	1.54230	HET	GRB040701
313.471	-28.225	2004	07	9.04037	HET	GRB040709
279.608	57.691	2004	07	19.05315	K/W	040719_T04591
238.302	-56.470	2004	07	30.09191	INT	040730A
358.532	-35.074	2004	08	10.59417	HET	GRB040810
246.535	-44.684	2004	08	12.25130	INT	040812
348.462	-36.901	2004	08	16.34721	K/W	040816_T29998
344.744	-10.934	2004	08	25.14618	HET	GRB040825A
341.640	-2.408	2004	08	25.68169	HET	GRB040825B
229.256	-16.141	2004	08	27.49382	INT	040827A
60.822	-72.495	2004	08	31.68781	K/W	040831_T59426
270.850	-25.250	2004	09	3.76248	INT	040903
359.223	-1.001	2004	09	12.59186	HET	GRB040912

Continued on next column

Continued from previous column

RA deg	DEC deg	Year	Month	Day	Cat.	GRB Name
345.376	-5.583	2004	09	16.00243	HET	GRB040916
148.046	-17.016	2004	09	21.67102	K/W	040921_T57975
31.581	16.024	2004	09	24.49457	HET	GRB040924
13.603	-33.866	2004	10	4.09517	HET	GRB041004
13.719	1.201	2004	10	6.51260	HET	GRB041006
81.039	-41.897	2004	10	7.08482	K/W	041007_T07328
335.921	47.558	2004	10	10.01043	K/W	041010_T00900
225.801	-11.545	2004	10	13.95583	K/W	041013_T82584
4.692	66.853	2004	10	15.46635	INT	041015
26.182	-4.402	2004	10	16.19420	HET	GRB041016
100.798	20.395	2004	12	11.48040	HET	GRB041211
353.900	23.000	2004	12	11.99841	INT	041211D
58.171	-52.271	2004	12	13.29140	K/W	041213_T25176
164.793	-17.942	2004	12	17.31140	Swi	041217
24.782	71.342	2004	12	18.65693	INT	041218A
6.154	62.847	2004	12	19.07104	Swi	041219A
167.674	-33.458	2004	12	19.65195	Swi	041219B
343.926	-76.744	2004	12	19.85456	Swi	041219C
291.288	60.598	2004	12	20.95726	Swi	041220
100.204	-37.068	2004	12	23.58771	Swi	041223
56.192	-6.663	2004	12	24.84789	Swi	041224
79.689	73.329	2004	12	26.85716	Swi	041226
336.642	5.032	2004	12	28.45086	Swi	041228
216.254	80.770	2004	12	31.91030	K/W	041231_T78649
112.626	-17.902	2005	01	11.28648	K/W	050111_T24751
222.048	-41.307	2005	01	12.46553	K/W	050112_T40222
358.479	65.939	2005	01	17.53653	Swi	050117
157.901	-11.475	2005	01	23.43257	HET	GRB050123
192.877	13.039	2005	01	24.47920	Swi	050124
278.115	42.384	2005	01	26.50063	Swi	050126
219.587	-34.765	2005	01	28.18050	Swi	050128
252.800	-3.080	2005	01	29.83547	INT	050129
290.584	-38.730	2005	02	2.14948	Swi	050202
291.386	42.478	2005	02	8.48641	K/W	050208_T42025
126.537	19.684	2005	02	9.06367	HET	GRB050209
290.005	46.006	2005	02	12.89181	K/W	050212_T77051
348.403	49.328	2005	02	15.09409	Swi	050215A
174.463	40.797	2005	02	15.10675	Swi	050215B
234.312	-13.838	2005	02	16.31010	K/W	050216_T26792
166.416	-40.681	2005	02	19.52779	Swi	050219A
81.306	-57.758	2005	02	19.87906	Swi	050219B
271.394	-62.465	2005	02	23.13132	Swi	050223
282.309	-9.152	2005	03	6.14806	Swi	050306
190.899	6.302	2005	03	12.23631	K/W	050312_T20417
306.476	-42.591	2005	03	15.87480	Swi	050315
49.695	-46.386	2005	03	18.65598	Swi	050318
154.172	43.581	2005	03	19.39674	Swi	050319
6.871	-71.377	2005	03	26.41245	Swi	050326

Continued on next column

Continued from previous column

RA deg	DEC deg	Year	Month	Day	Cat.	GRB Name
112.487	-28.828	2005	03	28.14255	K/W	050328_T12316
247.873	2.185	2005	04	1.59740	Swi	050401
34.410	-50.180	2005	04	6.66583	Swi	050406
180.563	10.867	2005	04	8.68254	HET	GRB050408
41.070	-50.379	2005	04	9.05455	K/W	050409_T04712
89.757	79.605	2005	04	10.51012	Swi	050410
181.099	-1.193	2005	04	12.23892	Swi	050412
188.485	21.058	2005	04	16.46162	Swi	050416A
133.848	11.186	2005	04	16.94160	Swi	050416B
44.334	-18.541	2005	04	18.45874	Swi	050418
307.341	73.678	2005	04	21.17491	Swi	050421
324.507	55.788	2005	04	22.32824	Swi	050422
202.443	42.674	2005	05	2.09321	INT	050502A
142.535	16.987	2005	05	2.39282	Swi	050502B
201.005	40.703	2005	05	4.33400	INT	050504A
141.760	30.266	2005	05	5.97385	Swi	050505
48.063	-11.064	2005	05	7.94674	Swi	050507
310.573	54.076	2005	05	9.07395	Swi	050509A
189.046	28.974	2005	05	9.16689	Swi	050509B
193.283	-44.843	2005	05	9.94854	HET	GRB050509C
290.025	-6.771	2005	05	13.19449	K/W	050513_T16804
192.526	30.451	2005	05	20.00462	INT	050520A
200.147	24.792	2005	05	22.25024	INT	050522
278.142	26.335	2005	05	25.00200	Swi	050525A
90.254	-15.800	2005	05	27.27265	K/W	050527_T23557
353.524	45.957	2005	05	28.17135	Swi	050528
39.982	-25.175	2005	06	3.27020	Swi	050603
300.180	9.139	2005	06	7.38291	Swi	050607
186.742	-63.137	2005	06	26.15703	INT	050626
227.241	-59.399	2005	07	1.48818	Swi	050701
345.375	-38.976	2005	07	9.94209	HET	GRB050709
77.722	64.924	2005	07	12.58366	Swi	050712
320.585	77.072	2005	07	13.18683	Swi	050713A
307.821	60.936	2005	07	13.50507	Swi	050713B
43.586	69.126	2005	07	14.00412	INT	050714A
169.691	-15.547	2005	07	14.94481	Swi	050714B
155.641	-0.029	2005	07	15.93780	Swi	050715
338.593	38.683	2005	07	16.52505	Swi	050716
214.348	-50.541	2005	07	17.43810	Swi	050717
253.453	-28.386	2005	07	21.18697	Swi	050721
246.175	-27.526	2005	07	24.52372	Swi	050724
200.024	-32.064	2005	07	26.20854	Swi	050726
286.920	36.756	2005	07	30.46577	K/W	050730_T40242
212.069	-3.754	2005	07	30.83221	Swi	050730
204.144	-21.930	2005	08	1.76947	Swi	050801
219.283	27.799	2005	08	2.42225	Swi	050802
350.650	5.788	2005	08	3.80139	Swi	050803
340.010	-36.061	2005	08	5.56241	K/W	050805_T48592

Continued on next column

Continued from previous column

RA deg	DEC deg	Year	Month	Day	Cat.	GRB Name
303.361	-36.937	2005	08	7.45747	HET	GRB050807
35.333	11.069	2005	08	9.84405	K/W	050809_T72926
242.001	11.244	2005	08	13.28137	Swi	050813
264.196	46.324	2005	08	14.48538	Swi	050814
293.584	9.139	2005	08	15.72591	Swi	050815
358.751	24.871	2005	08	19.68328	Swi	050819
337.416	19.560	2005	08	20.27423	Swi	050820A
135.607	-72.640	2005	08	20.99337	Swi	050820B
14.835	-76.738	2005	08	21.45536	K/W	050821_T39343
51.106	-46.030	2005	08	22.15936	Swi	050822
84.067	-69.164	2005	08	24.49841	K/W	050824_T43062
12.264	22.602	2005	08	24.96685	Swi	050824
21.265	-75.222	2005	08	25.14896	K/W	050825_T12869
87.761	-2.658	2005	08	26.26262	Swi	050826
64.294	18.219	2005	08	27.78976	Swi	050827
277.273	62.611	2005	08	29.28624	K/W	050829_T24731
13.770	14.189	2005	09	4.07759	Swi	050904
52.802	-14.621	2005	09	6.43895	Swi	050906
20.457	-12.950	2005	09	8.23786	Swi	050908
13.710	-38.856	2005	09	11.66637	Swi	050911
81.688	-28.014	2005	09	15.47410	Swi	050915A
219.109	-67.411	2005	09	15.89102	Swi	050915B
135.979	-51.406	2005	09	16.69157	Swi	050916
267.620	-25.411	2005	09	18.65044	INT	050918
271.096	-32.042	2005	09	22.57176	INT	050922
5.790	-5.607	2005	09	22.62639	Swi	050922B
317.383	-8.764	2005	09	22.83044	Swi	050922C
303.490	34.329	2005	09	25.37817	Swi	050925
350.984	-31.515	2005	10	1.46639	Swi	051001
110.807	9.510	2005	10	6.85455	Swi	051006
202.865	42.103	2005	10	8.68983	Swi	051008
270.513	-52.799	2005	10	12.71243	Swi	051012
122.814	-18.299	2005	10	16.22466	Swi	051016A
132.123	13.629	2005	10	16.76955	Swi	051016B
29.112	9.077	2005	10	21.55691	HET	GRB051021
126.059	-45.534	2005	10	21.98049	Swi	051021B
359.000	19.597	2005	10	22.54720	HET	GRB051022
27.163	47.808	2005	10	28.56668	HET	GRB051028
148.814	69.512	2005	11	3.39287	K/W	051103_T33943
265.279	34.916	2005	11	5.26853	Swi	051105A
9.468	-40.479	2005	11	5.46230	INT	051105A
9.474	-40.488	2005	11	5.46228	INT	051105B
330.316	40.850	2005	11	9.05024	Swi	051109A
345.469	38.663	2005	11	9.36087	Swi	051109B
348.136	18.367	2005	11	11.24978	Swi	051111
311.353	-19.730	2005	11	11.32487	K/W	051111_T28068
187.242	-26.395	2005	11	13.64068	Swi	051113
226.290	60.154	2005	11	14.17463	Swi	051114

Continued on next column

Continued from previous column

RA deg	DEC deg	Year	Month	Day	Cat.	GRB Name
228.398	30.868	2005	11	17.45231	Swi	051117A
85.205	-19.286	2005	11	17.55757	Swi	051117B
301.677	-37.147	2005	11	27.95505	K/W	051127_T82515
330.192	-57.622	2005	12	10.24052	Swi	051210
104.054	32.679	2005	12	11.11811	HET	GRB051211
345.673	55.081	2005	12	11.92091	INT	051211B
252.084	-59.233	2005	12	13.30074	Swi	051213
350.622	70.116	2005	12	20.54462	INT	051220A
328.715	16.888	2005	12	21.07727	Swi	051221A
312.378	53.041	2005	12	21.83565	Swi	051221B
125.231	31.949	2005	12	27.75505	Swi	051227
328.839	-1.837	2006	01	2.88713	Swi	060102
297.485	46.356	2006	01	5.28434	Swi	060105
147.013	31.935	2006	01	8.61056	Swi	060108
282.735	32.011	2006	01	9.70464	Swi	060109
72.737	28.428	2006	01	10.33424	Swi	060110
276.193	37.600	2006	01	11.18271	Swi	060111A
286.456	70.380	2006	01	11.84425	Swi	060111B
195.275	-4.735	2006	01	14.52744	INT	060114
54.007	17.339	2006	01	15.54723	Swi	060115
84.698	-5.438	2006	01	16.35934	Swi	060116
327.912	-59.982	2006	01	17.28475	Swi	060117
137.489	45.675	2006	01	21.93396	HET	GRB060121
179.750	45.513	2006	01	23.93241	Swi	060123
77.097	69.727	2006	01	24.66310	Swi	060124
229.250	-36.922	2006	01	30.20589	INT	060130
35.809	38.377	2006	02	2.36175	Swi	060202
226.916	-14.041	2006	02	3.31176	K/W	060203_T26936
103.463	71.841	2006	02	3.99693	Swi	060203
232.243	-39.458	2006	02	4.55531	INT	060204A
211.805	27.675	2006	02	4.60722	Swi	060204B
202.933	35.046	2006	02	6.19922	Swi	060206
57.727	27.015	2006	02	10.20752	Swi	060210
58.381	21.489	2006	02	11.40221	Swi	060211A
75.085	14.959	2006	02	11.66337	Swi	060211B
50.380	16.910	2006	02	18.14897	Swi	060218
241.851	32.309	2006	02	19.95006	Swi	060219
255.053	-24.214	2006	02	21.65316	INT	060221C
55.186	-17.134	2006	02	23.25306	Swi	060223A
254.238	-30.812	2006	02	23.82020	Swi	060223B
39.126	-46.739	2006	02	23.97416	K/W	060223_T84166
180.107	-27.548	2006	02	28.51883	K/W	060228_T44827
226.108	47.637	2006	03	3.94640	K/W	060303_T81768
41.097	-2.163	2006	03	6.03415	Swi	060306
199.967	-63.713	2006	03	6.64072	K/W	060306_T55358
45.780	12.827	2006	03	12.06682	Swi	060312
66.625	-10.858	2006	03	13.00840	Swi	060313
176.379	60.038	2006	03	19.03869	Swi	060319

Continued on next column

Continued from previous column

RA deg	DEC deg	Year	Month	Day	Cat.	GRB Name
274.230	-36.710	2006	03	22.95858	Swi	060322
174.421	50.000	2006	03	23.60597	Swi	060323
233.444	-15.235	2006	03	31.27897	HET	GRB060331
282.338	8.327	2006	04	3.55020	Swi	060403
291.287	13.746	2006	04	13.77804	Swi	060413
51.021	-10.514	2006	04	15.76020	K/W	060415_T65681
236.431	-3.640	2006	04	18.12926	Swi	060418
343.629	62.730	2006	04	21.02735	Swi	060421
7.359	36.787	2006	04	24.17801	Swi	060424
211.925	-5.710	2006	04	25.70675	K/W	060425_T61063
124.177	62.657	2006	04	27.48832	Swi	060427
98.385	22.855	2006	04	27.99435	K/W	060427_T85912
285.217	-9.550	2006	04	28.10457	INT	060428C
123.540	-37.167	2006	04	28.14083	Swi	060428A
235.369	62.016	2006	04	28.37128	Swi	060428B
115.569	-24.850	2006	04	29.51377	K/W	060429_T44389
328.374	44.002	2006	05	1.34374	Swi	060501
240.937	66.604	2006	05	2.12745	Swi	060502A
278.927	52.618	2006	05	2.72547	Swi	060502B
331.772	-27.815	2006	05	5.27501	Swi	060505
89.911	75.250	2006	05	7.07861	Swi	060507
95.860	-1.163	2006	05	10.32185	Swi	060510A
239.259	78.591	2006	05	10.34878	Swi	060510B
195.748	41.209	2006	05	12.96760	Swi	060512
127.277	73.561	2006	05	15.10270	Swi	060515
71.170	-18.126	2006	05	16.28027	Swi	060516
322.954	2.895	2006	05	22.09119	Swi	060522
232.834	0.288	2006	05	26.68646	Swi	060526
149.579	0.314	2006	06	2.89736	Swi	060602A
337.224	-10.945	2006	06	4.76319	Swi	060604
322.128	-6.071	2006	06	5.76094	Swi	060605
329.705	-22.496	2006	06	7.21682	Swi	060607A
42.043	14.755	2006	06	7.98106	Swi	060607B
320.877	-53.027	2006	06	14.53043	Swi	060614
107.381	73.360	2006	06	14.79422	K/W	060614_T68621
357.069	-17.904	2006	07	7.89605	Swi	060707
292.352	-49.796	2006	07	8.18801	K/W	060708_T16243
7.831	-33.751	2006	07	8.51110	Swi	060708
184.067	35.540	2006	07	12.88037	Swi	060712
227.855	-6.544	2006	07	14.63333	Swi	060714
170.857	28.982	2006	07	17.38031	Swi	060717
18.420	-48.381	2006	07	19.28515	Swi	060719
112.137	48.193	2006	07	25.66840	K/W	060725_T57750
16.644	-41.390	2006	07	28.93369	Swi	060728
95.287	-62.221	2006	07	29.80033	Swi	060729
212.989	16.988	2006	08	1.51128	Swi	060801
112.219	-27.225	2006	08	4.31134	Swi	060804
220.928	12.580	2006	08	5.19987	Swi	060805A

Continued on next column

Continued from previous column

RA deg	DEC deg	Year	Month	Day	Cat.	GRB Name
252.520	31.591	2006	08	7.61221	Swi	060807
111.890	-29.844	2006	08	13.95166	Swi	060813
221.338	20.591	2006	08	14.95994	Swi	060814
18.132	55.796	2006	08	25.12498	Swi	060825
287.158	-6.639	2006	09	1.78053	INT	060901A
237.731	44.984	2006	09	4.04399	Swi	060904A
58.218	-0.729	2006	09	4.10491	Swi	060904B
40.709	30.362	2006	09	6.35610	Swi	060906
31.828	0.335	2006	09	8.37317	Swi	060908
5.285	20.971	2006	09	12.58049	Swi	060912A
271.204	-19.872	2006	09	12.73068	INT	060912B
276.900	-50.994	2006	09	19.32545	Swi	060919
254.623	12.341	2006	09	23.21684	Swi	060923A
238.193	-30.907	2006	09	23.48479	Swi	060923B
346.122	3.943	2006	09	23.56462	Swi	060923C
263.926	13.039	2006	09	26.70049	Swi	060926
329.547	5.370	2006	09	27.58860	Swi	060927
263.148	29.825	2006	09	29.82987	Swi	060929
304.512	-23.635	2006	09	30.37792	INT	060930
220.356	48.726	2006	10	2.04410	Swi	061002
293.820	-4.404	2006	10	3.50998	K/W	061003_T44061
97.795	-45.903	2006	10	4.82675	Swi	061004
110.998	-79.195	2006	10	6.69851	Swi	061006
46.299	-50.496	2006	10	7.42233	Swi	061007
91.675	29.527	2006	10	19.17994	Swi	061019
145.146	-21.953	2006	10	21.65218	Swi	061021
300.912	-48.243	2006	10	25.77504	INT	061025A
270.992	-82.239	2006	10	27.42711	Swi	061027
97.193	46.290	2006	10	28.05998	Swi	061028
148.394	-17.022	2006	11	2.04203	Swi	061102
70.062	8.074	2006	11	8.23198	K/W	061108_T20042
336.284	-2.252	2006	11	10.49122	Swi	061110A
323.912	6.872	2006	11	10.91581	Swi	061110B
77.944	-27.845	2006	11	11.45452	K/W	061111_T39270
147.228	-13.188	2006	11	21.64061	Swi	061121
303.833	15.517	2006	11	22.33118	INT	061122A
86.615	64.204	2006	11	26.36662	Swi	061126
266.939	-65.514	2006	12	1.34127	K/W	061201_T29486
332.079	-74.568	2006	12	1.66571	Swi	061201
105.255	-74.602	2006	12	2.34149	Swi	061202
144.521	15.613	2006	12	10.51434	Swi	061210
160.403	-21.152	2006	12	17.15287	Swi	061217
149.260	-35.217	2006	12	18.17021	Swi	061218
358.254	46.524	2006	12	22.14505	Swi	061222A
105.353	-25.866	2006	12	22.17433	Swi	061222B
352.581	26.823	2007	01	3.86573	Swi	070103
159.422	-53.202	2007	01	7.50368	Swi	070107
0.934	-52.978	2007	01	10.30743	Swi	070110

Continued on next column

Continued from previous column

RA deg	DEC deg	Year	Month	Day	Cat.	GRB Name
74.961	7.806	2007	01	13.49756	K/W	070113_T42988
221.303	54.529	2007	01	24.36241	K/W	070124_T31311
33.503	-73.553	2007	01	26.10655	Swi	070126
104.526	-48.349	2007	01	29.92324	K/W	070129_T79768
36.995	11.728	2007	01	29.98275	Swi	070129
10.877	42.454	2007	02	1.64110	K/W	070201_T55390
18.895	-44.245	2007	02	7.87551	K/W	070207_T75644
197.891	61.942	2007	02	8.38234	Swi	070208
46.213	-47.376	2007	02	9.14840	Swi	070209
260.220	69.345	2007	02	19.04880	Swi	070219
34.800	68.800	2007	02	20.19760	Swi	070220
205.526	-26.897	2007	02	22.31384	K/W	070222_T27115
153.453	43.132	2007	02	23.05210	Swi	070223
178.988	-13.355	2007	02	24.85275	Swi	070224
120.578	-46.302	2007	02	27.93193	Swi	070227
148.154	10.440	2007	03	6.69546	Swi	070306
263.685	-37.945	2007	03	9.41740	INT	070309
87.534	3.375	2007	03	11.07829	INT	070311A
48.486	-42.950	2007	03	18.31176	Swi	070318
227.634	-17.157	2007	03	21.78632	K/W	070321_T67937
40.337	-66.989	2007	03	26.68694	Swi	070326
65.113	-34.079	2007	03	28.16242	Swi	070328
269.533	-63.799	2007	03	30.95244	Swi	070330
198.956	16.530	2007	04	6.03517	Swi	070406
107.342	1.061	2007	04	11.84205	Swi	070411
181.525	40.133	2007	04	12.06045	Swi	070412
302.130	7.370	2007	04	18.71972	INT	070418B
182.755	39.903	2007	04	19.41627	Swi	070419A
315.709	-31.266	2007	04	19.44729	Swi	070419B
121.245	-45.564	2007	04	20.26266	Swi	070420
28.871	-27.603	2007	04	27.35497	Swi	070427
297.695	-32.420	2007	04	29.06609	Swi	070429A
328.006	-38.857	2007	04	29.13130	Swi	070429B
347.203	10.711	2007	05	6.23331	Swi	070506
312.832	-78.382	2007	05	8.17937	Swi	070508
237.874	-78.657	2007	05	9.11698	Swi	070509
268.720	-31.697	2007	05	12.25432	K/W	070512_T21972
195.487	28.622	2007	05	16.86211	K/W	070516_T74485
277.556	-62.305	2007	05	17.47289	Swi	070517
254.219	55.289	2007	05	18.60163	Swi	070518
193.255	75.005	2007	05	20.54525	Swi	070520A
121.886	57.588	2007	05	20.73950	Swi	070520B
242.659	30.260	2007	05	21.28554	Swi	070521
283.717	20.648	2007	05	29.53366	Swi	070529
6.714	74.315	2007	05	31.09049	Swi	070531
2.004	-29.756	2007	06	11.08141	Swi	070611
121.355	37.258	2007	06	12.11025	Swi	070612A
261.716	-8.747	2007	06	12.26479	Swi	070612B

Continued on next column

Continued from previous column

RA deg	DEC deg	Year	Month	Day	Cat.	GRB Name
270.625	-63.043	2007	06	14.21197	K/W	070614_T18314
44.295	-4.397	2007	06	15.09765	INT	070615
32.096	56.946	2007	06	16.68720	Swi	070616
323.806	-24.809	2007	06	21.97059	Swi	070621
115.271	-20.281	2007	06	28.61183	Swi	070628
354.707	66.257	2007	07	4.83747	Swi	070704
267.744	-68.924	2007	07	7.67267	INT	070707B
42.933	30.241	2007	07	14.13925	Swi	070714A
57.853	28.294	2007	07	14.20797	Swi	070714B
3.144	-28.530	2007	07	21.41745	Swi	070721A
33.128	-2.198	2007	07	21.44014	Swi	070721B
27.824	-18.610	2007	07	24.45405	Swi	070724A
17.629	57.673	2007	07	24.97580	Agi	070724B
56.296	-39.330	2007	07	29.01797	Swi	070729
328.581	-15.740	2007	07	31.39817	Swi	070731
36.903	-55.517	2007	08	2.29682	Swi	070802
245.057	-59.957	2007	08	5.83038	Swi	070805
6.761	1.180	2007	08	8.76944	Swi	070808
203.767	-22.119	2007	08	9.80714	Swi	070809
189.947	10.747	2007	08	10.09157	Swi	070810A
8.952	8.822	2007	08	10.63839	Swi	070810B
233.781	68.617	2007	09	10.73159	K/W	070910_T63208
25.819	-33.484	2007	09	11.24843	Swi	070911
264.608	-28.706	2007	09	12.31416	INT	070912A
228.737	-24.278	2007	09	13.02550	Swi	070913
0.765	-60.264	2007	09	15.35753	K/W	070915_T30890
293.923	2.420	2007	09	17.31523	Swi	070917
100.968	72.250	2007	09	20.16682	Swi	070920A
0.127	-34.844	2007	09	20.87815	Swi	070920B
184.623	-38.294	2007	09	23.80235	Swi	070923
253.217	-22.029	2007	09	25.66166	INT	070925C
149.707	-59.763	2007	10	1.68875	Swi	071001
301.857	10.954	2007	10	3.32008	Swi	071003
335.294	-23.147	2007	10	6.27894	Swi	071006
151.571	44.303	2007	10	8.91384	Swi	071008
288.040	-32.385	2007	10	10.15361	Swi	071010A
150.531	45.733	2007	10	10.86513	Swi	071010B
338.054	66.159	2007	10	10.93081	Swi	071010C
8.395	61.132	2007	10	11.52793	Swi	071011
279.501	33.846	2007	10	13.50647	Swi	071013
164.685	53.822	2007	10	18.35950	Swi	071018
119.666	32.857	2007	10	20.29336	Swi	071020
340.573	23.764	2007	10	21.40385	Swi	071021
355.065	31.784	2007	10	25.17285	Swi	071025
354.163	-31.630	2007	10	28.11373	Swi	071028B
119.828	21.473	2007	10	28.73682	Swi	071028A
121.930	11.090	2007	10	30.36995	K/W	071030_T31964
6.399	-58.048	2007	10	31.04625	Swi	071031

Continued on next column

Continued from previous column

RA deg	DEC deg	Year	Month	Day	Cat.	GRB Name
48.179	62.524	2007	11	1.74567	Swi	071101
295.600	14.645	2007	11	4.48707	Agi	071104
289.913	2.048	2007	11	9.85839	INT	071109
260.213	-80.884	2007	11	12.76633	Swi	071112B
39.218	28.368	2007	11	12.77288	Swi	071112C
335.026	-63.442	2007	11	17.61813	Swi	071117
299.839	70.130	2007	11	18.37311	Swi	071118
276.576	47.102	2007	11	22.05793	Swi	071122
160.285	11.223	2007	11	26.08733	K/W	071126_T07545
220.039	-26.667	2007	11	29.00272	Swi	071129
149.585	8.972	2007	12	4.24898	K/W	071204_T21511
58.132	-55.959	2007	12	27.84291	Swi	071227
97.871	70.621	2008	01	9.56888	K/W	080109_T49151
225.264	-10.875	2008	01	20.72810	INT	080120
137.235	41.841	2008	01	21.89577	Swi	080121
338.974	-64.930	2008	01	23.18191	Swi	080123
105.297	-7.840	2008	01	29.25469	Swi	080129
261.632	-53.190	2008	01	30.46804	Swi	080130
48.209	24.329	2008	02	3.09788	K/W	080203_T08456
98.261	62.782	2008	02	5.33045	Swi	080205
207.514	7.492	2008	02	7.89608	Swi	080207
251.259	13.826	2008	02	10.32645	Swi	080210
231.145	-22.739	2008	02	12.73233	Swi	080212
123.000	22.000	2008	02	12.96168	Agi	080212B
355.941	12.159	2008	02	18.83937	Swi	080218A
177.927	-53.086	2008	02	18.99846	Swi	080218B
168.805	38.396	2008	02	22.25760	K/W	080222_T22257
68.719	56.939	2008	02	22.43128	K/W	080222_T37262
265.137	-12.827	2008	02	23.81909	INT	080223A
228.220	-14.697	2008	02	29.71179	Swi	080229A
199.221	-64.878	2008	02	29.98126	Agi	080229B
112.019	-70.231	2008	03	3.38235	Swi	080303
270.000	-24.000	2008	03	3.89905	Agi	080303B
136.629	35.151	2008	03	7.47465	Swi	080307
220.040	-0.164	2008	03	10.35970	Swi	080310
155.124	41.701	2008	03	15.10071	Swi	080315
2.270	-28.268	2008	03	17.46646	K/W	080317_T40302
256.204	65.934	2008	03	18.02212	K/W	080318_T01910
206.352	44.080	2008	03	19.24007	Swi	080319A
217.919	36.300	2008	03	19.25890	Swi	080319B
259.006	55.393	2008	03	19.51801	Swi	080319C
99.479	23.982	2008	03	19.71191	Swi	080319D
177.763	57.162	2008	03	20.19280	Swi	080320
277.906	36.516	2008	03	25.17311	Swi	080325
80.490	47.523	2008	03	28.33546	Swi	080328
169.278	30.607	2008	03	30.15366	Swi	080330
183.000	20.000	2008	04	7.86256	Agi	080407
114.678	33.305	2008	04	8.75889	Agi	080408

Continued on next column

Continued from previous column

RA deg	DEC deg	Year	Month	Day	Cat.	GRB Name
84.304	5.078	2008	04	9.05760	Swi	080409
131.723	-73.170	2008	04	11.81110	K/W	080411_T70079
37.961	-71.297	2008	04	11.88579	Swi	080411
287.301	-27.677	2008	04	13.12105	Swi	080413A
326.138	-19.981	2008	04	13.36889	Swi	080413B
287.300	-27.700	2008	04	13.80991	Agi	080413
272.133	-18.829	2008	04	14.93989	INT	080414B
26.510	69.469	2008	04	26.55789	Swi	080426
165.331	51.682	2008	04	30.82850	Swi	080430
286.686	68.803	2008	05	3.51821	Swi	080503
329.467	38.961	2008	05	6.74052	Swi	080506
233.721	56.424	2008	05	7.32292	Agi	080507
322.820	0.710	2008	05	14.41385	Agi	080514B
3.166	32.564	2008	05	15.25084	Swi	080515
120.661	-26.146	2008	05	16.01189	Swi	080516
102.274	50.741	2008	05	17.89087	Swi	080517
280.179	-54.964	2008	05	20.93083	Swi	080520
20.769	-64.060	2008	05	23.89017	Swi	080523
268.449	80.143	2008	05	24.17569	Swi	080524
186.000	0.000	2008	05	30.67473	Agi	080530
19.177	-9.239	2008	06	2.06282	Swi	080602
279.409	62.735	2008	06	3.47096	INT	080603A
176.554	68.061	2008	06	3.81821	Swi	080603B
236.960	20.557	2008	06	4.31043	Swi	080604
262.130	4.010	2008	06	5.99163	Swi	080605
194.964	15.910	2008	06	7.25517	Swi	080607
262.000	-24.000	2008	06	9.95115	Agi	080609
213.274	5.169	2008	06	13.39955	INT	080613A
173.806	-7.102	2008	06	13.46709	Swi	080613B
237.667	-62.044	2008	06	23.43435	Swi	080623
298.442	56.265	2008	06	25.51980	Agi	080625
45.944	75.481	2008	07	1.42612	Swi	080701
355.616	-5.424	2008	07	2.04909	Swi	080702B
313.049	72.278	2008	07	2.49355	Swi	080702A
101.822	-63.211	2008	07	3.79182	Swi	080703
32.627	33.100	2008	07	7.35270	Swi	080707
245.000	-20.000	2008	07	9.76103	Agi	080709
8.259	19.484	2008	07	10.30081	Swi	080710
41.900	8.500	2008	07	14.08625	Fer	080714B
187.500	-74.000	2008	07	14.42502	Fer	080714C
188.104	-60.274	2008	07	14.74509	Swi	080714
214.700	9.900	2008	07	15.95047	Fer	080715A
147.300	-70.000	2008	07	17.54346	Fer	080717A
153.200	-61.300	2008	07	19.52895	Fer	080719A
98.500	-43.900	2008	07	20.31600	Fer	080720A
224.481	-11.709	2008	07	21.43421	Swi	080721
274.461	-6.910	2008	07	23.18014	Swi	080723A
176.800	-60.200	2008	07	23.55719	Fer	080723B

Continued on next column

Continued from previous column

RA deg	DEC deg	Year	Month	Day	Cat.	GRB Name
113.300	-19.700	2008	07	23.91346	Fer	080723C
105.300	71.100	2008	07	23.98452	Fer	080723D
358.300	32.900	2008	07	24.40117	Fer	080724A
121.699	-13.984	2008	07	25.43489	Swi	080725
354.800	8.900	2008	07	25.54125	Fer	080725B
20.398	13.913	2008	07	26.00000	Agi	080726
208.416	-18.572	2008	07	27.24837	Swi	080727A
276.871	1.173	2008	07	27.34264	Swi	080727B
32.638	64.130	2008	07	27.96360	Swi	080727C
245.400	4.600	2008	07	30.52032	Fer	080730A
246.600	28.700	2008	07	30.78586	Fer	080730B
154.300	40.700	2008	08	2.38554	Fer	080802A
270.729	-32.329	2008	08	2.63358	Swi	080802
108.000	22.000	2008	08	3.01563	Agi	080803B
300.100	82.800	2008	08	3.77178	Fer	080803A
107.500	20.300	2008	08	4.45564	Fer	080804B
328.675	-53.189	2008	08	4.97238	Swi	080804
314.231	-62.433	2008	08	5.32053	Swi	080805
322.700	47.900	2008	08	5.49572	Fer	080805B
174.500	-23.100	2008	08	5.58410	Fer	080805C
94.600	57.800	2008	08	6.58416	Fer	080806A
241.800	46.700	2008	08	6.89561	Fer	080806B
101.700	-16.000	2008	08	7.99343	Fer	080807A
107.400	-33.800	2008	08	8.45143	Fer	080808A
33.600	5.400	2008	08	8.56514	Fer	080808B
96.700	-14.400	2008	08	8.77199	Fer	080808C
91.700	61.400	2008	08	9.80802	Fer	080809A
356.783	0.310	2008	08	10.54875	Swi	080810
176.700	-33.200	2008	08	12.88859	Fer	080812A
240.900	-47.800	2008	08	15.91673	Fer	080815A
156.200	42.600	2008	08	16.50299	Fer	080816A
289.500	-6.800	2008	08	16.98883	Fer	080816B
148.900	-16.300	2008	08	17.16123	Fer	080817A
80.200	-17.100	2008	08	17.72023	Fer	080817B
60.400	-6.900	2008	08	18.57945	Fer	080818A
98.100	7.400	2008	08	18.94501	Fer	080818B
238.600	32.600	2008	08	21.33156	Fer	080821A
63.560	25.760	2008	08	22.87699	Swi	080822B
89.800	-42.400	2008	08	23.36265	Fer	080823A
122.400	-2.800	2008	08	24.90897	Fer	080824A
234.000	-4.700	2008	08	25.59292	Fer	080825C
209.281	-68.943	2008	08	25.74074	Agi	080825B
221.300	-12.300	2008	08	28.18902	Fer	080828B
221.900	3.200	2008	08	29.79000	Fer	080829A
160.100	30.800	2008	08	30.36824	Fer	080830A
211.200	-51.700	2008	08	31.05295	Fer	080831A
259.100	-23.200	2008	08	31.92110	Fer	080831B
86.790	51.256	2008	09	3.05027	Swi	080903

Continued on next column

Continued from previous column

RA deg	DEC deg	Year	Month	Day	Cat.	GRB Name
214.200	-30.300	2008	09	4.88617	Fer	080904A
287.663	-18.865	2008	09	5.49924	Swi	080905A
96.900	-69.800	2008	09	5.57048	Fer	080905C
301.746	-62.568	2008	09	5.70538	Swi	080905B
182.800	-6.400	2008	09	6.21194	Fer	080906B
228.055	-80.540	2008	09	6.56477	Swi	080906
25.800	-7.200	2008	09	12.36037	Fer	080912A
65.741	-25.127	2008	09	13.28257	Swi	080913
45.100	-3.000	2008	09	13.73509	Fer	080913B
17.911	-76.042	2008	09	15.00196	Swi	080915A
213.088	-11.491	2008	09	15.66221	Swi	080915B
119.800	-56.600	2008	09	16.00886	Fer	080916C
336.289	-57.026	2008	09	16.40648	Swi	080916A
163.632	69.061	2008	09	16.61443	Swi	080916B
22.000	14.000	2008	09	18.40598	Agi	080918
265.221	-42.375	2008	09	19.00362	Swi	080919
219.500	44.400	2008	09	19.78999	Fer	080919B
121.600	8.900	2008	09	20.26793	Fer	080920A
270.837	-22.508	2008	09	22.46083	INT	080922
72.800	32.500	2008	09	24.76571	Fer	080924A
96.100	18.200	2008	09	25.77495	Fer	080925A
61.300	27.400	2008	09	27.47954	Fer	080927A
95.061	-55.176	2008	09	28.62606	Swi	080928
276.576	-8.754	2008	10	1.88729	Agi	081001
262.376	16.566	2008	10	3.57375	INT	081003A
259.100	35.400	2008	10	3.64396	Fer	081003C
285.025	16.691	2008	10	3.86676	INT	081003B
295.284	8.323	2008	10	4.55992	K/W	081004_T48376
142.000	-67.400	2008	10	6.60387	Fer	081006A
172.200	-61.000	2008	10	6.87194	Fer	081006B
339.963	-40.146	2008	10	7.22491	Swi	081007
279.968	-57.433	2008	10	8.83205	Swi	081008
250.500	18.400	2008	10	9.13956	Fer	081009A
64.600	14.200	2008	10	9.69002	Fer	081009B
220.363	33.548	2008	10	11.02002	Swi	081011
69.700	4.500	2008	10	12.04540	Fer	081012B
30.184	-17.627	2008	10	12.54888	Swi	081012
255.572	-23.330	2008	10	16.28606	INT	081016A
14.582	-43.536	2008	10	16.82447	Swi	081016B
109.000	-15.200	2008	10	17.47404	Fer	081017B
230.209	-32.790	2008	10	17.98486	Swi	081017
190.300	-25.600	2008	10	21.39824	Fer	081021A
205.400	16.600	2008	10	22.36441	Fer	081022A
226.584	12.409	2008	10	22.59986	Swi	081022
27.891	61.352	2008	10	24.24514	Swi	081024A
145.800	-10.800	2008	10	24.85109	Fer	081024C
322.900	21.200	2008	10	24.89075	Fer	081024B
245.298	60.466	2008	10	25.34863	Swi	081025

Continued on next column

Continued from previous column

RA deg	DEC deg	Year	Month	Day	Cat.	GRB Name
121.893	2.305	2008	10	28.01736	Swi	081028A
16.000	-27.200	2008	10	28.53829	Fer	081028B
346.776	-68.179	2008	10	29.07218	Swi	081029
213.300	-18.500	2008	11	1.16713	Fer	081101C
95.836	-0.112	2008	11	1.49064	Swi	081101
207.500	-28.000	2008	11	1.53153	Fer	081101B
225.300	22.000	2008	11	2.36459	Fer	081102B
331.178	52.991	2008	11	2.73934	Swi	081102
100.500	-54.722	2008	11	4.39910	Swi	081104
3.950	3.470	2008	11	5.56374	Agi	081105
215.800	38.700	2008	11	5.61379	Fer	081105B
51.000	17.100	2008	11	7.32085	Fer	081107A
330.798	-54.711	2008	11	9.29313	Swi	081109A
111.700	21.400	2008	11	10.60119	Fer	081110A
289.100	35.000	2008	11	10.67975	INT	081110C
170.300	56.300	2008	11	13.23024	Fer	081113A
190.600	63.300	2008	11	15.89060	Fer	081115A
82.572	-43.305	2008	11	18.62264	Swi	081118
54.600	-43.300	2008	11	18.87562	Fer	081118B
346.500	30.000	2008	11	19.18434	Fer	081119A
205.400	-9.100	2008	11	20.61776	Fer	081120A
89.282	-60.612	2008	11	21.85801	Swi	081121
339.100	40.000	2008	11	22.51959	Fer	081122A
151.400	-2.100	2008	11	22.61350	Fer	081122B
340.100	-14.600	2008	11	24.05985	Fer	081124A
42.700	-18.900	2008	11	25.49559	Fer	081125A
323.526	48.714	2008	11	26.89873	Swi	081126
332.075	6.858	2008	11	27.29523	Swi	081127
20.800	38.123	2008	11	28.72134	Swi	081128
63.200	-54.900	2008	11	29.16116	Fer	081129A
34.200	45.400	2008	11	30.21158	Fer	081130A
13.200	-5.500	2008	11	30.62865	Fer	081130B
228.789	44.427	2008	12	3.58138	Swi	081203B
233.071	63.514	2008	12	3.58138	Swi	081203A
63.300	-62.600	2008	12	4.00375	Fer	081204C
150.800	30.500	2008	12	4.51697	Fer	081204B
349.773	-60.221	2008	12	4.69786	INT	081204
120.100	32.800	2008	12	6.27492	Fer	081206A
353.300	-31.900	2008	12	6.60383	Fer	081206B
54.300	-8.600	2008	12	6.98739	Fer	081206C
112.400	70.500	2008	12	7.67971	Fer	081207A
45.300	63.500	2008	12	9.98051	Fer	081209A
70.485	-11.263	2008	12	10.84692	Swi	081210
168.231	53.845	2008	12	11.26044	Swi	081211B
328.082	-33.818	2008	12	11.49178	Swi	081211A
12.900	-33.900	2008	12	13.17340	Fer	081213A
125.600	54.000	2008	12	15.78376	Fer	081215A
228.600	-50.700	2008	12	15.87978	Fer	081215B

Continued on next column

Continued from previous column

RA deg	DEC deg	Year	Month	Day	Cat.	GRB Name
129.200	7.600	2008	12	16.53056	Fer	081216A
116.800	26.800	2008	12	17.98251	Fer	081217A
15.801	-24.542	2008	12	21.68138	Swi	081221
22.748	-34.095	2008	12	22.20415	Swi	081222
112.500	33.200	2008	12	23.41941	Fer	081223A
201.700	75.100	2008	12	24.88745	Fer	081224A
234.100	-64.600	2008	12	25.25650	Fer	081225A
120.478	-69.014	2008	12	26.04418	Swi	081226A
193.000	26.800	2008	12	26.15616	Fer	081226C
25.500	-47.400	2008	12	26.50915	Fer	081226B
39.477	30.833	2008	12	28.05394	Swi	081228
172.600	56.900	2008	12	29.18683	Fer	081229A
310.000	22.800	2008	12	29.67500	Fer	081229B
37.330	-25.145	2008	12	30.85847	Swi	081230
207.600	-17.300	2008	12	30.87061	Fer	081230B
208.600	-35.800	2008	12	31.13960	Fer	081231A
77.800	-31.600	2009	01	1.75812	Fer	090101A
128.248	33.107	2009	01	2.12205	Swi	090102
302.409	4.744	2009	01	7.20005	Swi	090107A
284.800	59.600	2009	01	7.68105	Fer	090107B
260.800	46.000	2009	01	8.02017	Fer	090108A
0.400	-32.900	2009	01	8.32180	Fer	090108B
129.600	51.800	2009	01	9.33229	Fer	090109A
251.656	0.067	2009	01	11.99885	Swi	090111
110.900	-30.400	2009	01	12.33152	Fer	090112A
192.300	25.400	2009	01	12.72935	Fer	090112B
32.067	33.436	2009	01	13.77823	Swi	090113
227.300	-41.500	2009	01	17.33475	Fer	090117B
121.600	-38.800	2009	01	17.63241	Fer	090117C
164.000	-58.200	2009	01	17.64029	Fer	090117A
49.865	18.478	2009	01	18.57919	Swi	090118
38.100	-72.200	2009	01	20.62665	Fer	090120A
6.794	-23.503	2009	01	23.32773	Swi	090123
3.848	81.365	2009	01	26.08420	Agi	090126A
189.200	34.100	2009	01	26.22665	Fer	090126B
224.900	41.200	2009	01	26.24483	Fer	090126C
269.105	-32.793	2009	01	29.88004	Swi	090129
352.300	21.200	2009	01	31.08983	Fer	090131A
92.051	-46.604	2009	02	1.74100	Swi	090201
274.300	-2.000	2009	02	2.34688	Fer	090202A
220.917	-27.848	2009	02	5.96058	Swi	090205
156.200	8.800	2009	02	6.61993	Fer	090206A
101.776	-51.180	2009	02	7.44965	K/W	090207_T38849
252.700	34.900	2009	02	7.77721	Fer	090207A
137.663	63.492	2009	02	9.01748	K/W	090209_T01509
330.600	-55.000	2009	02	13.23571	Fer	090213A
204.900	-8.400	2009	02	17.20605	Fer	090217A
26.500	59.200	2009	02	19.07382	Fer	090219A

Continued on next column

Continued from previous column

RA deg	DEC deg	Year	Month	Day	Cat.	GRB Name
118.600	45.000	2009	02	22.17858	Fer	090222A
358.200	61.000	2009	02	25.00861	Fer	090225A
3.300	-43.000	2009	02	27.30969	Fer	090227A
11.800	32.200	2009	02	27.77154	Fer	090227B
106.800	-24.300	2009	02	28.20371	Fer	090228A
357.600	36.700	2009	02	28.97571	Fer	090228B
338.142	26.639	2009	03	1.28883	Swi	090301A
352.800	9.500	2009	03	1.31502	Fer	090301B
195.900	-73.400	2009	03	4.21584	Fer	090304A
135.000	74.300	2009	03	5.05180	Fer	090305B
241.764	-31.572	2009	03	5.22212	Swi	090305A
137.000	57.000	2009	03	6.24451	Fer	090306C
231.204	-6.958	2009	03	6.96322	Swi	090306B
245.007	-28.647	2009	03	7.15737	Swi	090307A
172.700	-23.900	2009	03	7.16664	Fer	090307B
21.900	-54.300	2009	03	8.73362	Fer	090308B
183.545	-48.754	2009	03	8.75096	Swi	090308A
174.300	-49.500	2009	03	9.76744	Fer	090309B
284.978	-25.274	2009	03	9.97862	Swi	090309A
184.900	-34.200	2009	03	10.18947	Fer	090310A
198.400	8.086	2009	03	13.37948	Swi	090313
256.100	-38.900	2009	03	16.31091	Fer	090316A
283.300	-8.900	2009	03	19.62193	Fer	090319A
108.300	-43.300	2009	03	20.04526	Fer	090320C
238.000	-46.500	2009	03	20.41789	Fer	090320A
183.400	49.800	2009	03	20.80123	Fer	090320B
190.700	17.100	2009	03	23.00188	Fer	090323A
259.700	-7.400	2009	03	26.63252	Fer	090326A
33.100	-41.500	2009	03	27.40395	Fer	090327A
90.900	-42.000	2009	03	28.40054	Fer	090328A
155.700	33.400	2009	03	28.71325	Fer	090328B
160.200	-8.200	2009	03	30.27942	Fer	090330A
210.500	3.100	2009	03	31.68079	Fer	090331A
350.920	29.762	2009	04	1.00068	Swi	090401A
95.095	-8.963	2009	04	1.35793	Swi	090401B
67.100	47.200	2009	04	3.31438	Fer	090403A
239.233	35.518	2009	04	4.66424	Swi	090404
221.900	-9.200	2009	04	5.66298	Fer	090405A
68.979	-12.684	2009	04	7.43640	Swi	090407
302.100	1.100	2009	04	9.28752	Fer	090409A
334.956	15.419	2009	04	10.70685	Swi	090410
156.000	-68.900	2009	04	11.83793	Fer	090411A
38.500	5.100	2009	04	11.99149	Fer	090411B
1.300	-51.900	2009	04	12.06117	Fer	090412A
266.500	-9.200	2009	04	13.12219	Fer	090413A
34.993	-7.141	2009	04	17.55374	Swi	090417A
209.687	47.015	2009	04	17.63892	Swi	090417B
225.910	17.224	2009	04	18.37433	Swi	090418B

Continued on next column

Continued from previous column

RA deg	DEC deg	Year	Month	Day	Cat.	GRB Name
269.320	33.407	2009	04	18.46366	Swi	090418A
262.800	-28.200	2009	04	18.81626	Fer	090418C
197.006	-75.615	2009	04	19.57189	Swi	090419
88.600	31.300	2009	04	19.99659	Fer	090419B
294.746	40.398	2009	04	22.14949	Swi	090422
148.891	18.165	2009	04	23.33008	Swi	090423
189.531	16.829	2009	04	24.59177	Swi	090424
118.600	68.100	2009	04	25.37744	Fer	090425A
17.600	-19.200	2009	04	26.06638	Fer	090426B
189.082	32.978	2009	04	26.53388	Swi	090426
82.700	-9.700	2009	04	26.68997	Fer	090426C
210.000	-45.700	2009	04	27.64376	Fer	090427B
356.200	-34.600	2009	04	27.68777	Fer	090427C
235.900	13.500	2009	04	27.97670	Agi	090427
210.100	39.500	2009	04	28.44072	Fer	090428A
0.800	11.500	2009	04	28.55221	Fer	090428B
90.573	-52.389	2009	04	29.20392	Swi	090429A
210.672	32.167	2009	04	29.22920	Swi	090429B
260.000	54.300	2009	04	29.53016	Fer	090429C
125.210	6.200	2009	04	29.75275	Fer	090429D
267.800	-20.300	2009	05	2.77748	Fer	090502A
241.422	-28.385	2009	05	9.21531	Swi	090509
333.552	-26.598	2009	05	10.01597	Swi	090510
269.400	-57.900	2009	05	10.32476	Fer	090510B
161.900	51.300	2009	05	11.68422	Fer	090511A
269.800	-31.600	2009	05	13.91583	Fer	090513A
99.100	-72.900	2009	05	13.94138	Fer	090513B
12.300	-10.900	2009	05	14.00601	Fer	090514A
304.317	-24.400	2009	05	14.72647	Fer	090514B
316.033	-43.967	2009	05	14.73397	Fer	090514C
164.166	14.469	2009	05	15.19802	Swi	090515
122.200	-71.620	2009	05	16.13704	Fer	090516B
138.246	-11.848	2009	05	16.35266	Swi	090516A
15.700	-13.700	2009	05	16.85324	Fer	090516C
119.957	0.778	2009	05	18.07968	Swi	090518
211.200	-16.700	2009	05	18.24380	Fer	090518B
105.900	-56.700	2009	05	19.46212	Fer	090519B
142.317	0.190	2009	05	19.88120	Swi	090519
11.613	-8.000	2009	05	20.06755	Swi	090520
332.000	43.200	2009	05	20.83187	Fer	090520B
111.200	-19.700	2009	05	20.84953	Fer	090520C
131.300	-18.000	2009	05	20.87613	Fer	090520D
277.700	19.600	2009	05	22.34432	Fer	090522A
329.500	-67.400	2009	05	24.34579	Fer	090524A
108.601	-71.659	2009	05	25.21150	K/W	090525_T18274
134.900	-35.800	2009	05	28.17293	Fer	090528A
312.200	32.700	2009	05	28.51564	Fer	090528B
231.200	32.200	2009	05	29.30998	Fer	090529B

Continued on next column

Continued from previous column

RA deg	DEC deg	Year	Month	Day	Cat.	GRB Name
162.700	47.300	2009	05	29.56389	Fer	090529C
212.446	24.450	2009	05	29.59207	Swi	090529
179.400	26.590	2009	05	30.13771	Swi	090530
73.200	13.800	2009	05	30.76001	Fer	090530B
178.672	7.824	2009	05	31.07311	Swi	090531A
252.070	-36.015	2009	05	31.77495	Swi	090531B
248.940	-65.020	2009	06	2.56415	Fer	090602A
146.940	-70.490	2009	06	6.47093	Fer	090606A
191.194	44.108	2009	06	7.22936	Swi	090607
100.190	-37.410	2009	06	8.05239	Fer	090608A
84.200	35.420	2009	06	10.64822	Fer	090610A
275.990	-42.090	2009	06	10.72329	Fer	090610B
70.370	30.300	2009	06	10.88342	Fer	090610C
81.030	17.710	2009	06	12.61864	Fer	090612A
103.070	-3.710	2009	06	16.15674	Fer	090616A
78.890	15.650	2009	06	17.20832	Fer	090617A
294.008	78.352	2009	06	18.35311	Swi	090618
237.350	61.150	2009	06	20.40027	Fer	090620A
241.380	-43.020	2009	06	20.90111	Fer	090620B
10.987	61.938	2009	06	21.18244	Swi	090621A
257.490	-28.460	2009	06	21.41727	Fer	090621C
12.270	-22.580	2009	06	21.44705	Fer	090621D
313.455	69.034	2009	06	21.92182	Swi	090621B
309.000	-43.240	2009	06	23.10715	Fer	090623A
41.700	1.800	2009	06	23.91279	Fer	090623B
20.290	-6.430	2009	06	25.23403	Fer	090625A
2.262	-65.780	2009	06	25.55998	Fer	090625B
170.010	-33.500	2009	06	26.18899	Fer	090626A
136.440	14.440	2009	06	26.70747	Fer	090626B
237.038	-15.969	2009	06	28.88903	Swi	090628
8.480	17.670	2009	06	29.54261	Fer	090629A
146.550	-46.580	2009	06	30.31066	Fer	090630A
114.690	-42.070	2009	07	1.22495	Fer	090701A
175.888	11.501	2009	07	2.44487	INT	090702
0.770	9.680	2009	07	3.32920	Fer	090703A
208.205	22.790	2009	07	4.24153	Fer	090704A
296.350	25.880	2009	07	4.78265	Fer	090704B
205.070	-47.070	2009	07	6.28311	Fer	090706A
154.632	26.616	2009	07	8.15156	Swi	090708
289.944	60.728	2009	07	9.31845	Swi	090709A
93.522	64.081	2009	07	9.63035	Swi	090709B
139.610	-64.740	2009	07	11.84957	Fer	090711A
70.097	22.525	2009	07	12.16047	Swi	090712
284.800	-3.330	2009	07	13.02046	Fer	090713A
152.102	10.006	2009	07	15.72615	Swi	090715A
251.337	44.837	2009	07	15.87724	Swi	090715B
92.410	-62.480	2009	07	17.03440	Fer	090717A
246.950	22.970	2009	07	17.11148	Fer	090717B

Continued on next column

Continued from previous column

RA deg	DEC deg	Year	Month	Day	Cat.	GRB Name
243.760	-6.680	2009	07	18.71994	Fer	090718A
274.120	-36.390	2009	07	18.76230	Fer	090718B
341.270	-67.860	2009	07	19.06350	Fer	090719A
203.694	-10.335	2009	07	20.27648	Swi	090720
203.000	-54.800	2009	07	20.71038	Fer	090720B
67.400	-50.916	2009	07	21.24954	K/W	090721_T21560
281.880	-69.490	2009	07	25.83774	Fer	090725A
240.450	36.750	2009	07	26.21814	Fer	090726B
248.681	72.866	2009	07	26.94615	Swi	090726
315.917	64.937	2009	07	27.94604	Swi	090727
29.644	41.632	2009	07	28.61510	Swi	090728
252.580	30.460	2009	07	30.60773	Fer	090730A
84.330	34.090	2009	08	2.23545	Fer	090802A
267.020	-71.770	2009	08	2.66555	Fer	090802B
130.400	-11.300	2009	08	4.93982	Fer	090804A
300.027	-50.845	2009	08	5.62174	Fer	090805A
273.741	10.279	2009	08	7.62531	Swi	090807
326.900	7.230	2009	08	7.83193	Fer	090807B
328.665	-0.083	2009	08	9.73002	Swi	090809
95.250	0.160	2009	08	9.97795	Fer	090809B
168.930	-76.400	2009	08	10.65912	Fer	090810A
116.430	-17.480	2009	08	10.78107	Fer	090810B
277.050	22.220	2009	08	11.69572	Fer	090811A
353.200	-10.609	2009	08	12.25148	Swi	090812
225.065	88.571	2009	08	13.17411	Swi	090813
239.613	25.586	2009	08	14.03633	Swi	090814A
64.775	60.583	2009	08	14.05641	INT	090814B
332.480	58.920	2009	08	14.36784	Fer	090814C
307.650	45.720	2009	08	14.94964	Fer	090814D
41.030	-2.730	2009	08	15.30014	Fer	090815A
21.420	53.440	2009	08	15.43798	Fer	090815B
251.260	52.930	2009	08	15.94568	Fer	090815D
64.490	-65.943	2009	08	15.97337	Swi	090815C
63.966	44.123	2009	08	17.03572	Fer	090817A
49.080	-67.120	2009	08	19.60726	Fer	090819A
87.700	27.060	2009	08	20.02658	Fer	090820A
318.260	-18.580	2009	08	20.50922	Fer	090820B
49.530	-17.580	2009	08	23.13257	Fer	090823B
128.700	60.600	2009	08	23.67446	Agi	090823
46.650	59.810	2009	08	24.91828	Fer	090824A
140.620	-0.110	2009	08	26.06773	Fer	090826A
18.435	-50.899	2009	08	27.79613	Swi	090827
124.380	-26.140	2009	08	28.09917	Fer	090828A
329.230	-34.190	2009	08	29.67198	Fer	090829A
354.990	-9.360	2009	08	29.70185	Fer	090829B
145.100	50.970	2009	08	31.31709	Fer	090831A
108.294	-25.112	2009	08	31.89612	Swi	090831C
183.199	47.389	2009	09	1.56696	K/W	090901_T48984

Continued on next column

Continued from previous column

RA deg	DEC deg	Year	Month	Day	Cat.	GRB Name
290.980	53.110	2009	09	2.40145	Fer	090902A
264.939	27.324	2009	09	2.46190	Fer	090902B
100.855	50.235	2009	09	4.04243	Swi	090904A
264.194	-25.219	2009	09	4.05854	Swi	090904B
261.650	4.560	2009	09	4.58145	Fer	090904C
86.330	-38.850	2009	09	7.01678	Fer	090907A
81.060	20.500	2009	09	7.80819	Fer	090907B
282.250	3.540	2009	09	8.31380	Fer	090908A
174.140	-25.130	2009	09	8.34074	Fer	090908B
32.300	53.920	2009	09	9.48700	Fer	090909A
54.180	-25.030	2009	09	9.85408	Fer	090909B
296.230	72.280	2009	09	10.81237	Fer	090910A
188.046	61.475	2009	09	12.66006	Swi	090912
237.990	15.480	2009	09	15.64972	Swi	090915
126.582	25.941	2009	09	16.29218	Swi	090916
230.340	-11.690	2009	09	17.66087	Fer	090917A
299.730	-52.190	2009	09	20.03471	Fer	090920A
17.160	74.300	2009	09	22.53938	Fer	090922A
38.360	-73.080	2009	09	22.60465	Fer	090922B
69.730	-65.020	2009	09	24.62493	Fer	090924A
333.210	14.270	2009	09	25.38928	Fer	090925A
353.401	-66.324	2009	09	26.18087	Fer	090926A
46.310	-38.997	2009	09	26.91375	Swi	090926B
343.929	-70.973	2009	09	27.42171	Swi	090927
103.910	-43.530	2009	09	28.64566	Fer	090928A
51.700	-7.340	2009	09	29.18963	Fer	090929A
117.712	-0.645	2009	09	29.42300	Swi	090929B
41.920	-14.010	2009	10	2.68485	Fer	091002A
251.520	36.625	2009	10	3.19150	Fer	091003A
43.140	12.120	2009	10	5.67883	Fer	091005A
243.110	-31.040	2009	10	6.36027	Fer	091006A
298.669	-22.538	2009	10	10.11330	Fer	091010A
109.400	87.270	2009	10	12.78267	Fer	091012A
316.090	-49.500	2009	10	15.12897	Fer	091015B
210.800	25.490	2009	10	17.86139	Fer	091017A
214.400	-64.740	2009	10	17.98539	Fer	091017B
32.191	-57.546	2009	10	18.86689	Swi	091018
321.830	-23.080	2009	10	18.95718	Fer	091018B
226.030	80.330	2009	10	19.75047	Fer	091019A
175.727	50.977	2009	10	20.90051	Swi	091020
187.800	-13.400	2009	10	20.97679	Fer	091020B
215.420	25.950	2009	10	23.02065	Fer	091023A
339.240	56.885	2009	10	24.37223	Swi	091024
137.080	-23.650	2009	10	26.48528	Fer	091026B
276.657	-86.113	2009	10	26.54965	Swi	091026
60.166	-55.954	2009	10	29.16206	Swi	091029
249.000	23.540	2009	10	30.61338	Fer	091030B
41.670	21.540	2009	10	30.82809	Fer	091030A

Continued on next column

Continued from previous column

RA deg	DEC deg	Year	Month	Day	Cat.	GRB Name
70.580	-59.080	2009	10	31.50033	Fer	091031A
29.800	-33.680	2009	11	1.14343	Fer	091101A
72.622	-72.527	2009	11	2.60738	Swi	091102
170.600	11.300	2009	11	3.91240	Fer	091103A
208.723	47.391	2009	11	4.36762	Swi	091104
49.130	60.320	2009	11	6.76195	Fer	091106A
182.350	38.940	2009	11	7.63472	Fer	091107A
309.252	-44.177	2009	11	9.20675	Swi	091109A
247.720	42.310	2009	11	9.89491	Fer	091109C
112.750	-54.092	2009	11	9.90906	Swi	091109B
137.813	-45.909	2009	11	11.64027	INT	091111
257.751	-36.729	2009	11	12.73705	Swi	091112
208.410	37.170	2009	11	12.92768	Fer	091112B
219.227	-78.548	2009	11	14.13041	K/W	091114_T11266
307.760	71.460	2009	11	15.17697	Fer	091115A
246.540	-73.940	2009	11	17.08015	Fer	091117B
148.142	-79.954	2009	11	17.92738	K/W	091117_T80126
226.810	-21.790	2009	11	20.19074	Fer	091120A
110.860	0.570	2009	11	22.16273	Fer	091122A
337.820	13.350	2009	11	23.08055	Fer	091123B
297.110	-29.180	2009	11	23.29765	Fer	091123A
83.250	-19.270	2009	11	26.33293	Fer	091126A
47.400	31.500	2009	11	26.38900	Fer	091126B
36.581	-18.948	2009	11	27.97622	Swi	091127
127.690	1.730	2009	11	28.28512	Fer	091128A
203.149	34.086	2009	11	30.74935	Swi	091130B
27.840	11.940	2009	12	1.08858	Fer	091201A
257.500	-1.900	2009	12	2.07230	Fer	091202B
13.860	9.080	2009	12	2.21924	Fer	091202C
138.831	62.544	2009	12	2.96542	INT	091202
12.670	-50.190	2009	12	7.33345	Fer	091207A
0.295	65.680	2009	12	8.36528	Swi	091208A
29.411	16.881	2009	12	8.40969	Swi	091208B
260.960	38.290	2009	12	9.00052	Fer	091209A
283.250	17.550	2009	12	15.23434	Fer	091215A
294.490	71.910	2009	12	19.46164	Fer	091219A
166.770	4.810	2009	12	20.44225	Fer	091220A
55.798	23.243	2009	12	21.87005	Swi	091221
203.230	76.350	2009	12	23.19109	Fer	091223A
231.270	54.730	2009	12	23.51104	Fer	091223B
331.170	18.260	2009	12	24.37334	Fer	091224A
296.940	2.600	2009	12	27.29391	Fer	091227A
101.530	0.680	2009	12	30.25983	Fer	091230B
132.915	-53.882	2009	12	30.26910	INT	091230
51.650	77.170	2009	12	30.71197	Fer	091230C
199.360	-60.700	2009	12	31.20594	Fer	091231A
241.260	3.290	2009	12	31.54015	Fer	091231B
307.320	-27.000	2010	01	1.02765	Fer	100101A

Continued on next column

Continued from previous column

RA deg	DEC deg	Year	Month	Day	Cat.	GRB Name
23.327	84.980	2010	01	1.30133	K/W	100101_T26034
70.660	18.690	2010	01	1.98768	Fer	100101B
112.366	-34.482	2010	01	3.73787	INT	100103A
6.310	-21.240	2010	01	7.07398	Fer	100107A
247.029	15.539	2010	01	11.17557	Swi	100111A
240.140	-75.100	2010	01	12.41756	Fer	100112A
3.333	-0.817	2010	01	15.46897	Swi	100115A
305.020	14.450	2010	01	16.89653	Fer	100116A
11.280	-1.586	2010	01	17.87939	Swi	100117A
9.260	-37.370	2010	01	18.09970	Fer	100118A
299.308	-53.149	2010	01	19.76765	Swi	100119A
79.200	-2.710	2010	01	22.61640	Fer	100122A
338.370	-18.740	2010	01	26.46048	Fer	100126A
21.190	-24.750	2010	01	30.72875	Fer	100130A
78.570	20.830	2010	01	30.77680	Fer	100130B
120.400	16.450	2010	01	31.72983	Fer	100131A
115.670	-54.350	2010	02	1.58770	Fer	100201A
96.225	4.793	2010	02	3.77161	Swi	100203A
50.780	-47.890	2010	02	4.02354	Fer	100204A
273.070	-52.780	2010	02	4.56578	Fer	100204B
91.290	-20.940	2010	02	4.85838	Fer	100204C
141.385	31.740	2010	02	5.17966	Swi	100205A
133.920	-23.020	2010	02	5.49003	Fer	100205B
47.168	13.175	2010	02	6.56256	Swi	100206A
307.860	-27.730	2010	02	7.66522	Fer	100207A
321.780	-15.780	2010	02	7.72118	Fer	100207B
260.250	27.530	2010	02	8.38581	Fer	100208A
244.380	16.080	2010	02	10.10057	Fer	100210A
132.250	29.490	2010	02	11.43999	Fer	100211A
134.270	32.220	2010	02	12.54983	Fer	100212B
356.445	49.492	2010	02	12.58845	Swi	100212A
349.379	43.370	2010	02	13.93597	Swi	100213A
124.320	43.464	2010	02	13.95734	Swi	100213B
154.263	35.524	2010	02	16.42153	Swi	100216A
206.640	-11.940	2010	02	18.19359	Fer	100218A
330.930	37.790	2010	02	19.02587	Fer	100219B
154.202	-12.555	2010	02	19.63595	Swi	100219A
27.120	-17.410	2010	02	21.36836	Fer	100221A
104.500	3.700	2010	02	23.10983	Fer	100223A
269.560	-17.080	2010	02	24.11175	Fer	100224B
83.467	-7.994	2010	02	24.63900	Swi	100224A
310.300	-59.400	2010	02	25.11494	Fer	100225A
352.850	15.030	2010	02	25.24937	Fer	100225B
314.270	0.210	2010	02	25.58022	Fer	100225C
147.910	34.010	2010	02	25.70299	Fer	100225D
199.830	15.620	2010	02	28.54353	Fer	100228A
117.990	18.630	2010	02	28.87347	Fer	100228B
110.140	-15.680	2010	03	1.06758	Fer	100301A

Continued on next column

Continued from previous column

RA deg	DEC deg	Year	Month	Day	Cat.	GRB Name
201.850	19.830	2010	03	1.22345	Fer	100301B
195.504	74.568	2010	03	2.82854	Swi	100302A
76.200	60.460	2010	03	4.00371	Fer	100304A
260.140	-21.920	2010	03	4.53355	Fer	100304B
168.373	42.381	2010	03	5.37891	Swi	100305A
216.040	-29.370	2010	03	6.19891	Fer	100306A
129.420	32.970	2010	03	7.92813	Fer	100307A
303.410	-27.770	2010	03	11.51799	Fer	100311A
172.710	-52.580	2010	03	13.28777	Fer	100313A
186.370	11.720	2010	03	13.50853	Fer	100313B
208.900	30.140	2010	03	15.36056	Fer	100315A
251.953	71.819	2010	03	16.09931	Swi	100316A
163.499	-45.464	2010	03	16.33444	Swi	100316B
32.309	-67.992	2010	03	16.37360	Swi	100316C
107.599	-56.275	2010	03	16.53113	Swi	100316D
210.960	21.190	2010	03	18.61070	Fer	100318A
21.320	-12.440	2010	03	22.04525	Fer	100322A
188.870	-18.660	2010	03	23.54218	Fer	100323A
98.612	-9.735	2010	03	24.01490	Swi	100324A
39.672	-19.287	2010	03	24.17195	Fer	100324B
209.140	-79.100	2010	03	25.24634	Fer	100325B
330.240	-26.470	2010	03	25.27509	Fer	100325A
131.240	-28.180	2010	03	26.29381	Fer	100326A
314.700	0.450	2010	03	26.40162	Fer	100326B
155.940	47.030	2010	03	28.14079	Fer	100328A
202.080	-0.900	2010	03	30.30893	Fer	100330A
326.380	-6.970	2010	03	30.85611	Fer	100330B
302.987	-11.067	2010	03	31.88099	Agi	100331B
290.813	-8.257	2010	04	1.29690	Swi	100401A
77.790	26.860	2010	04	6.75794	Fer	100406A
130.020	21.480	2010	04	10.35553	Fer	100410A
78.130	61.330	2010	04	10.74012	Fer	100410B
210.610	47.910	2010	04	11.51594	Fer	100411A
356.826	51.270	2010	04	13.36297	Swi	100413B
266.223	15.835	2010	04	13.73157	Swi	100413A
192.112	8.692	2010	04	14.09748	Fer	100414A
261.310	50.380	2010	04	17.16648	Fer	100417A
295.810	9.840	2010	04	17.78866	Fer	100417B
256.358	11.457	2010	04	18.88204	Swi	100418A
123.460	-4.390	2010	04	20.00841	Fer	100420B
296.090	55.755	2010	04	20.22410	Swi	100420A
350.680	-25.660	2010	04	21.91653	Fer	100421A
136.471	21.487	2010	04	23.02429	Swi	100423A
119.670	5.780	2010	04	23.24405	Fer	100423B
209.453	1.512	2010	04	24.68937	Swi	100424A
246.720	-48.850	2010	04	24.72928	Fer	100424B
7.790	43.350	2010	04	24.87630	Fer	100424C
299.161	-26.463	2010	04	25.11858	Swi	100425A

Continued on next column

Continued from previous column

RA deg	DEC deg	Year	Month	Day	Cat.	GRB Name
312.895	49.602	2010	04	25.41570	K/W	100425_T35916
89.171	-3.461	2010	04	27.35550	Swi	100427A
89.090	-69.960	2010	04	29.99990	Fer	100429A
131.010	18.380	2010	05	2.35628	Fer	100502A
147.480	3.960	2010	05	3.55421	Fer	100503A
255.575	-35.590	2010	05	4.80624	Swi	100504A
102.140	58.590	2010	05	6.65265	Fer	100506A
2.900	-79.010	2010	05	7.57727	Fer	100507A
76.263	-20.744	2010	05	8.38937	Swi	100508A
355.800	-35.600	2010	05	10.81050	Fer	100510A
109.290	-4.650	2010	05	11.03468	Fer	100511A
169.606	3.617	2010	05	13.08829	Swi	100513A
321.040	22.250	2010	05	13.87914	Fer	100513B
328.821	29.170	2010	05	14.78748	Swi	100514A
275.470	27.010	2010	05	15.46747	Fer	100515A
274.410	-8.200	2010	05	16.36853	Fer	100516A
297.680	18.660	2010	05	16.39628	Fer	100516B
100.930	-28.990	2010	05	17.07162	Fer	100517B
40.630	-44.320	2010	05	17.13183	Fer	100517C
243.590	-10.370	2010	05	17.15426	Fer	100517D
10.440	4.430	2010	05	17.24296	Fer	100517E
52.730	-71.870	2010	05	17.63887	Fer	100517F
304.789	-24.555	2010	05	18.48168	INT	100518A
191.490	57.410	2010	05	19.20374	Fer	100519A
6.990	9.397	2010	05	22.15685	Swi	100522A
251.820	41.040	2010	05	25.74404	Fer	100525A
230.792	25.623	2010	05	26.68484	Swi	100526A
0.777	-37.913	2010	05	26.79211	Swi	100526B
226.830	19.780	2010	05	27.79488	Fer	100527A
311.119	27.810	2010	05	28.07501	Fer	100528A
289.730	31.040	2010	05	30.73740	Fer	100530A
248.300	-73.190	2010	06	4.28721	Fer	100604A
273.430	-67.600	2010	06	5.77443	Fer	100605A
350.617	-66.234	2010	06	6.80047	Swi	100606A
30.540	20.450	2010	06	8.38202	Fer	100608A
90.480	42.780	2010	06	9.78346	Fer	100609A
63.530	13.740	2010	06	12.54469	Fer	100612A
352.000	-1.830	2010	06	12.72646	Fer	100612B
224.760	40.870	2010	06	14.49819	Fer	100614B
263.534	49.232	2010	06	14.90169	Swi	100614A
177.208	-19.483	2010	06	15.08267	Swi	100615A
342.910	3.090	2010	06	16.77260	Fer	100616A
84.618	-27.012	2010	06	19.01466	Swi	100619A
80.100	-51.680	2010	06	20.11909	Fer	100620A
315.309	-51.102	2010	06	21.12745	Swi	100621A
103.830	37.350	2010	06	21.45230	Fer	100621B
160.860	14.720	2010	06	21.52936	Fer	100621C
15.796	-39.091	2010	06	25.77255	Swi	100625A

Continued on next column

Continued from previous column

RA deg	DEC deg	Year	Month	Day	Cat.	GRB Name
338.260	20.290	2010	06	25.89080	Fer	100625B
225.943	-31.653	2010	06	28.34491	Swi	100628A
231.210	27.810	2010	06	29.80143	Fer	100629A
43.109	-2.224	2010	07	1.48985	Fer	100701B
245.693	-56.549	2010	07	2.04429	Swi	100702A
133.639	-24.202	2010	07	4.14940	Swi	100704A
263.972	30.178	2010	07	4.95779	K/W	100704_T82753
255.160	46.890	2010	07	6.69327	Fer	100706A
351.070	-6.570	2010	07	7.03240	Fer	100707A
142.530	17.380	2010	07	9.60246	Fer	100709A
255.209	28.390	2010	07	13.60840	INT	100713A
82.060	13.000	2010	07	13.98026	Fer	100713B
106.370	51.140	2010	07	14.67180	Fer	100714A
307.940	61.300	2010	07	14.68565	Fer	100714B
299.270	-54.710	2010	07	15.47729	Fer	100715A
287.060	-0.660	2010	07	17.37160	Fer	100717A
304.310	19.530	2010	07	17.44568	Fer	100717B
121.830	-46.180	2010	07	18.15983	Fer	100718B
298.470	41.430	2010	07	18.79609	Fer	100718A
112.319	-5.857	2010	07	19.14649	Swi	100719A
304.870	-67.140	2010	07	19.31132	Fer	100719B
231.410	18.560	2010	07	19.82509	Fer	100719C
113.300	5.400	2010	07	19.98894	Fer	100719D
238.770	-15.610	2010	07	22.09626	Fer	100722A
31.810	56.230	2010	07	22.29056	Fer	100722B
119.599	75.856	2010	07	24.02924	Fer	100724A
194.569	-11.095	2010	07	24.02939	Swi	100724A
166.468	-26.667	2010	07	25.30060	Swi	100725A
290.029	76.955	2010	07	25.47539	Swi	100725B
154.187	-21.417	2010	07	27.23770	Swi	100727A
88.753	-15.259	2010	07	28.09611	Swi	100728A
44.051	0.296	2010	07	28.43883	Swi	100728B
339.790	-22.230	2010	07	30.46267	Fer	100730A
2.482	47.752	2010	08	2.24000	Swi	100802A
248.970	27.450	2010	08	4.10378	Fer	100804A
299.846	52.618	2010	08	5.17549	Swi	100805A
22.800	34.190	2010	08	5.30014	Fer	100805B
112.720	-35.930	2010	08	5.84479	Fer	100805C
55.283	67.665	2010	08	7.38418	Swi	100807A
124.770	-1.610	2010	08	10.04901	Fer	100810A
345.870	15.860	2010	08	11.10821	Fer	100811A
108.140	62.190	2010	08	11.78066	Fer	100811B
22.479	-17.990	2010	08	14.15985	Swi	100814A
122.820	18.490	2010	08	14.35099	Fer	100814B
102.120	-26.660	2010	08	16.00881	Fer	100816B
351.738	26.568	2010	08	16.02629	Swi	100816A
279.600	-50.040	2010	08	19.49763	Fer	100819A
258.790	-18.510	2010	08	20.37290	Fer	100820A

Continued on next column

Continued from previous column

RA deg	DEC deg	Year	Month	Day	Cat.	GRB Name
20.706	5.848	2010	08	23.72610	Swi	100823A
253.440	-56.570	2010	08	25.28737	Fer	100825A
33.657	-65.051	2010	08	26.79627	K/W	100826_T68797
284.000	-23.190	2010	08	26.95721	Fer	100826A
193.900	71.890	2010	08	27.45543	Fer	100827A
115.450	-3.990	2010	08	29.37439	Fer	100829B
90.409	30.314	2010	08	29.87649	Fer	100829A
161.260	33.650	2010	08	31.65100	Fer	100831A
27.252	22.751	2010	09	1.56539	Swi	100901A
48.626	30.970	2010	09	2.81382	Swi	100902A
306.040	42.310	2010	09	2.98981	Fer	100902B
172.907	-16.185	2010	09	4.06508	Swi	100904A
31.542	14.919	2010	09	5.63072	Swi	100905A
262.650	13.080	2010	09	5.90721	Fer	100905B
28.697	55.634	2010	09	6.57601	Swi	100906A
177.290	-40.630	2010	09	7.75083	Fer	100907A
73.951	54.654	2010	09	9.37778	INT	100909A
238.100	-34.620	2010	09	10.81787	Fer	100910A
151.320	58.990	2010	09	11.81643	Fer	100911A
315.664	65.676	2010	09	15.06325	Swi	100915A
85.394	25.095	2010	09	15.24282	Fer	100915B
151.960	-59.380	2010	09	16.77862	Fer	100916A
289.250	-17.120	2010	09	17.21071	Swi	100917A
308.410	-45.960	2010	09	18.86271	Fer	100918A
163.240	6.020	2010	09	19.88352	Fer	100919A
356.980	-25.190	2010	09	22.62480	Fer	100922A
106.120	39.600	2010	09	23.84387	Fer	100923A
0.672	7.004	2010	09	24.16537	Swi	100924A
222.750	-72.350	2010	09	26.59518	Fer	100926A
43.580	-11.100	2010	09	26.69438	Fer	100926B
223.037	-28.542	2010	09	28.09713	Swi	100928A
166.330	62.290	2010	09	29.23533	Fer	100929A
243.620	33.330	2010	09	29.31463	Fer	100929B
183.030	-24.940	2010	09	29.91650	Fer	100929C
323.350	-27.470	2010	10	2.27878	Fer	101002A
175.850	2.490	2010	10	3.24384	Fer	101003A
232.220	-43.990	2010	10	4.42627	Fer	101004A
328.882	37.060	2010	10	8.69670	Swi	101008A
75.932	-33.853	2010	10	9.28774	K/W	101009_T24860
47.190	43.560	2010	10	10.19013	Fer	101010A
48.274	-65.990	2010	10	11.70735	Swi	101011A
292.080	-49.640	2010	10	13.41161	Fer	101013A
26.940	-51.070	2010	10	14.17491	Fer	101014A
73.160	15.460	2010	10	15.55836	Fer	101015A
133.040	-4.620	2010	10	16.24324	Fer	101016A
291.377	-35.141	2010	10	17.43943	Swi	101017A
27.470	-26.550	2010	10	17.61909	Fer	101017B
189.607	23.129	2010	10	20.98659	Swi	101020A

Continued on next column

Continued from previous column

RA deg	DEC deg	Year	Month	Day	Cat.	GRB Name
0.870	-23.710	2010	10	21.00932	Fer	101021A
0.460	47.340	2010	10	21.06287	Fer	101021B
317.949	-65.389	2010	10	23.95153	Swi	101023A
37.395	62.275	2010	10	24.14336	K/W	101024_T12386
66.465	-77.261	2010	10	24.48576	Swi	101024A
240.190	-8.490	2010	10	25.14605	Fer	101025A
263.700	-0.370	2010	10	26.03421	Fer	101026A
79.020	43.970	2010	10	27.22952	Fer	101027A
166.390	-16.389	2010	10	30.66422	Swi	101030A
184.120	-7.470	2010	10	31.62468	Fer	101031A
13.550	45.750	2010	11	1.74414	Fer	101101A
266.040	-29.000	2010	11	1.89871	Fer	101101B
284.680	-37.030	2010	11	2.84036	Fer	101102A
265.758	23.631	2010	11	4.74856	K/W	101104_T64676
161.020	-7.080	2010	11	4.80989	Fer	101104A
168.330	22.430	2010	11	7.01140	Fer	101107A
292.218	39.359	2010	11	12.92399	Fer	101112A
100.100	9.620	2010	11	12.98398	Fer	101112B
29.080	0.210	2010	11	13.48306	Fer	101113A
303.193	14.029	2010	11	14.02280	Swi	101114A
32.000	-81.200	2010	11	16.48087	Fer	101116A
57.190	-26.870	2010	11	17.49636	Fer	101117C
172.991	-72.651	2010	11	17.80096	Swi	101117B
226.490	59.610	2010	11	19.68545	Fer	101119A
135.160	1.910	2010	11	23.95249	Fer	101123A
84.770	-22.550	2010	11	26.19754	Fer	101126A
290.310	7.890	2010	11	27.09304	Fer	101127A
70.950	-11.320	2010	11	27.10244	Fer	101127B
145.470	-35.200	2010	11	28.32227	Fer	101128A
155.921	-17.645	2010	11	29.65244	Swi	101129A
271.540	1.010	2010	11	29.72599	Fer	101129B
274.610	26.620	2010	11	30.07355	Fer	101130B
1.955	-16.196	2010	12	1.41792	Swi	101201A
254.020	58.480	2010	12	2.15410	Fer	101202A
191.910	55.670	2010	12	4.34327	Fer	101204B
167.548	-20.434	2010	12	4.99547	Swi	101204A
322.100	-39.100	2010	12	5.30862	Fer	101205A
164.080	-38.110	2010	12	6.03631	Fer	101206A
175.750	8.720	2010	12	7.53589	Fer	101207A
212.400	4.040	2010	12	8.20344	Fer	101208A
280.940	-59.020	2010	12	8.49793	Fer	101208B
31.840	10.060	2010	12	11.48466	Fer	101211A
241.297	21.905	2010	12	13.45096	Swi	101213A
260.990	-64.510	2010	12	13.84892	Fer	101213B
0.690	-28.270	2010	12	14.74796	Fer	101214A
181.130	-31.060	2010	12	14.99307	Fer	101214A
284.270	-20.970	2010	12	16.72075	Fer	101216A
74.586	-2.527	2010	12	19.10520	Swi	101219A

Continued on next column

Continued from previous column

RA deg	DEC deg	Year	Month	Day	Cat.	GRB Name
12.259	-34.556	2010	12	19.68603	Swi	101219B
241.570	46.140	2010	12	20.57637	Fer	101220A
2.700	27.200	2010	12	20.86382	Fer	101220B
250.550	48.220	2010	12	23.83354	Fer	101223A
285.939	45.706	2010	12	24.22723	Swi	101224A
289.140	-55.250	2010	12	24.57845	Fer	101224B
290.160	34.460	2010	12	24.61357	Fer	101224C
325.170	-38.660	2010	12	24.99832	Fer	101224D
60.680	32.770	2010	12	25.37701	Fer	101225B
0.204	44.574	2010	12	25.77621	Swi	101225A
186.790	-83.550	2010	12	27.19478	Fer	101227A
240.500	-24.500	2010	12	27.40633	Fer	101227B
150.870	-49.440	2010	12	27.53595	Fer	101227C
191.710	17.640	2010	12	31.06725	Fer	101231A
264.260	36.540	2011	01	1.20163	Fer	110101A
105.500	34.580	2011	01	1.50581	Fer	110101B
245.877	7.617	2011	01	2.78640	Swi	110102A
85.110	-17.120	2011	01	5.87685	Fer	110105A
79.295	64.199	2011	01	6.64255	Swi	110106A
134.155	47.005	2011	01	6.89325	Swi	110106B
299.130	42.040	2011	01	7.88602	Fer	110107A
11.620	-9.640	2011	01	8.97660	Fer	110108A
329.936	26.470	2011	01	12.17521	Swi	110112A
10.600	64.410	2011	01	12.93397	Fer	110112B
130.870	47.590	2011	01	17.36448	Fer	110117A
129.510	-12.880	2011	01	17.62601	Fer	110117B
226.570	-39.550	2011	01	18.85716	Fer	110118A
348.589	5.982	2011	01	19.93123	Swi	110119A
61.600	-12.000	2011	01	20.66643	Fer	110120A
246.970	28.030	2011	01	23.80399	Fer	110123A
53.830	36.350	2011	01	24.78413	Fer	110124A
331.350	-46.210	2011	01	25.89408	Fer	110125A
193.871	28.108	2011	01	28.07260	Swi	110128A
111.510	38.250	2011	01	30.23047	Fer	110130A
183.790	72.910	2011	01	31.77961	Fer	110131A
137.489	88.610	2011	02	1.39940	Swi	110201A
1.820	-17.400	2011	02	4.17860	Fer	110204A
359.730	-80.440	2011	02	5.02714	Fer	110205B
164.603	67.533	2011	02	5.08520	Swi	110205A
312.690	-55.850	2011	02	5.58843	Fer	110205C
333.700	1.610	2011	02	6.20181	Fer	110206B
92.355	-58.807	2011	02	6.75561	INT	110206A
12.540	-10.790	2011	02	7.47037	Swi	110207A
179.000	-58.430	2011	02	7.95864	Fer	110207B
22.487	-20.561	2011	02	8.88248	Swi	110208A
329.700	-21.930	2011	02	9.16537	Fer	110209A
13.108	7.778	2011	02	10.41159	Swi	110210A
69.025	43.716	2011	02	12.04801	Swi	110212A

Continued on next column

Continued from previous column

RA deg	DEC deg	Year	Month	Day	Cat.	GRB Name
311.330	-74.500	2011	02	12.55039	Fer	110212B
42.978	49.278	2011	02	13.22047	Swi	110213A
41.768	0.952	2011	02	13.60542	Swi	110213B
6.280	27.540	2011	02	13.87559	Fer	110213C
274.740	32.350	2011	02	17.59082	Fer	110217A
185.490	16.580	2011	02	20.76136	Fer	110220A
15.180	66.050	2011	02	21.24397	Fer	110221A
345.386	87.586	2011	02	23.87291	Swi	110223A
150.340	-68.329	2011	02	23.89292	Swi	110223B
199.290	35.770	2011	02	26.98925	Fer	110226A
148.720	-54.040	2011	02	27.00866	Fer	110227A
25.240	15.890	2011	02	27.22929	Fer	110227B
232.730	-9.940	2011	02	27.41959	Fer	110227C
10.270	-45.670	2011	02	28.01110	Fer	110228A
245.090	16.410	2011	02	28.79156	Fer	110228B
229.350	29.400	2011	03	1.21439	Fer	110301A
122.350	2.910	2011	03	2.04296	Fer	110302A
322.930	33.270	2011	03	4.07122	Fer	110304A
260.877	-15.810	2011	03	5.27640	Swi	110305A
193.120	15.640	2011	03	7.97162	Fer	110307A
117.590	34.290	2011	03	11.81205	Fer	110311A
157.500	-5.259	2011	03	12.74696	Swi	110312A
279.205	17.537	2011	03	15.99796	Swi	110315A
46.700	-67.580	2011	03	16.13868	Fer	110316A
338.292	-15.278	2011	03	18.55161	Swi	110318A
211.691	-51.577	2011	03	18.64385	Swi	110318B
356.510	-66.008	2011	03	19.09492	Swi	110319A
207.960	-51.580	2011	03	19.62830	Fer	110319C
326.088	-56.774	2011	03	19.81530	Swi	110319B
13.310	-21.810	2011	03	21.34563	Fer	110321A
99.040	-48.900	2011	03	22.55813	Fer	110322A
117.650	43.100	2011	03	28.52036	Fer	110328B
251.233	57.590	2011	03	28.54010	Swi	110328A
6.660	25.990	2011	03	31.60355	Fer	110331A
268.560	26.870	2011	04	1.91967	Fer	110401A
197.432	61.247	2011	04	2.00899	Swi	110402A
186.022	15.726	2011	04	7.58797	Swi	110407A
97.410	-11.950	2011	04	7.99788	Fer	110407B
238.700	-34.320	2011	04	9.17871	Fer	110409A
30.940	-15.950	2011	04	10.13255	Fer	110410A
337.170	-21.960	2011	04	10.77176	Fer	110410B
210.300	-64.990	2011	04	11.62865	Fer	110411B
291.427	67.706	2011	04	11.81540	Swi	110411A
133.491	13.488	2011	04	12.31483	Swi	110412A
352.670	32.330	2011	04	13.93830	Fer	110413A
97.876	24.349	2011	04	14.32100	Swi	110414A
213.820	9.050	2011	04	15.54124	Fer	110415A
2.164	-37.877	2011	04	20.46000	Swi	110420A

Continued on next column

Continued from previous column

RA deg	DEC deg	Year	Month	Day	Cat.	GRB Name
320.045	-41.277	2011	04	20.94596	Swi	110420B
277.230	50.800	2011	04	21.75741	Fer	110421A
226.690	43.020	2011	04	22.02903	Fer	110422B
112.057	75.100	2011	04	22.65411	Swi	110422A
293.310	-11.120	2011	04	24.75806	Fer	110424A
219.930	-8.720	2011	04	26.62947	Fer	110426A
128.440	19.940	2011	04	28.33825	Fer	110428B
5.300	64.800	2011	04	28.38785	Fer	110428A
147.060	67.950	2011	04	30.37515	Fer	110430A
70.510	-10.900	2011	05	3.14475	Fer	110503B
132.799	52.211	2011	05	3.73316	Swi	110503A
16.810	-32.300	2011	05	5.20343	Fer	110505A
180.810	-34.000	2011	05	9.14212	Fer	110509A
74.650	-26.980	2011	05	9.47518	Fer	110509B
214.100	-45.420	2011	05	11.61612	Fer	110511A
296.090	-73.760	2011	05	17.45319	Fer	110517A
190.150	6.290	2011	05	17.57277	Fer	110517A
85.600	47.300	2011	05	17.90195	Fer	110517B
261.638	-23.426	2011	05	19.09185	Swi	110519A
71.010	-85.930	2011	05	20.30169	Fer	110520B
134.363	56.418	2011	05	20.85333	Swi	110520A
57.540	-62.340	2011	05	21.47846	Fer	110521B
120.132	45.818	2011	05	21.66078	Swi	110521A
228.910	55.530	2011	05	22.25576	Fer	110522A
184.460	49.330	2011	05	22.29586	Fer	110522B
180.570	-26.810	2011	05	22.63329	Fer	110522C
219.030	-15.420	2011	05	23.34438	Fer	110523A
102.480	-16.420	2011	05	26.71460	Fer	110526A
44.790	-6.870	2011	05	28.62412	Fer	110528A
118.330	67.910	2011	05	29.03383	Fer	110529A
172.600	8.790	2011	05	29.26228	Fer	110529B
340.620	1.860	2011	05	29.81056	Fer	110529C
282.045	61.953	2011	05	30.64655	Swi	110530A
190.510	11.850	2011	05	31.44804	Fer	110531A
310.710	11.480	2011	06	1.68074	Fer	110601A
14.950	52.460	2011	06	5.18301	Fer	110605A
242.090	-3.140	2011	06	5.77973	Fer	110605B
327.830	44.590	2011	06	9.18485	Fer	110609A
317.630	-38.160	2011	06	9.42507	Fer	110609B
308.205	74.827	2011	06	10.63995	Swi	110610A
336.860	-3.470	2011	06	13.63109	Fer	110613A
274.450	-34.020	2011	06	16.64821	Fer	110616A
176.808	-71.688	2011	06	18.36639	Fer	110618A
147.050	-7.480	2011	06	18.75991	Fer	110618B
133.960	19.460	2011	06	22.15786	Fer	110622A
65.020	-15.950	2011	06	24.90585	Fer	110624A
315.330	-39.440	2011	06	25.57876	Fer	110625B
286.751	6.755	2011	06	25.88088	Swi	110625A

Continued on next column

Continued from previous column

RA deg	DEC deg	Year	Month	Day	Cat.	GRB Name
131.910	5.560	2011	06	26.44785	Fer	110626A
69.370	25.010	2011	06	29.17359	Fer	110629A
5.620	-37.660	2011	07	2.18714	Fer	110702A
155.390	-29.300	2011	07	3.55712	Fer	110703A
156.024	40.099	2011	07	5.15083	Fer	110705A
122.960	28.800	2011	07	5.36370	Fer	110705B
100.080	6.140	2011	07	6.20213	Fer	110706A
94.150	-50.770	2011	07	6.47657	Fer	110706B
9.060	31.730	2011	07	6.72774	Fer	110706C
347.470	7.110	2011	07	6.97698	Fer	110706D
340.121	53.960	2011	07	8.19683	INT	110708A
155.380	23.120	2011	07	9.46312	Fer	110709C
238.895	40.918	2011	07	9.64200	Swi	110709A
156.210	-41.790	2011	07	9.86169	Fer	110709D
164.668	-23.470	2011	07	9.89767	Swi	110709B
229.090	48.400	2011	07	10.95406	Fer	110710A
237.665	-46.237	2011	07	15.55127	Swi	110715A
329.680	-76.980	2011	07	16.01759	Fer	110716A
308.470	-7.850	2011	07	17.18045	Fer	110717A
312.840	-14.840	2011	07	17.31940	Fer	110717B
24.570	34.578	2011	07	19.25638	Swi	110719A
198.650	-44.290	2011	07	20.17676	Fer	110720A
332.456	-38.628	2011	07	21.19981	Fer	110721A
215.060	5.000	2011	07	22.69394	Fer	110722A
8.280	62.740	2011	07	22.70956	Fer	110722B
270.140	-25.200	2011	07	25.23590	Fer	110725A
286.713	56.070	2011	07	26.06296	Swi	110726A
317.710	2.470	2011	07	26.21111	Fer	110726B
166.600	20.110	2011	07	28.05582	Fer	110728A
353.390	4.970	2011	07	29.14243	Fer	110729A
263.080	-22.780	2011	07	30.00827	Fer	110730A
335.100	-2.890	2011	07	30.66023	Fer	110730B
280.513	-28.536	2011	07	31.46493	Swi	110731A
248.270	-57.060	2011	08	1.33453	Fer	110801B
89.415	80.958	2011	08	1.82618	Swi	110801A
300.420	-11.440	2011	08	3.78293	Fer	110803A
112.040	2.380	2011	08	6.93439	Fer	110806A
57.322	-44.177	2011	08	8.26313	Swi	110808A
172.170	-13.930	2011	08	9.46081	Fer	110809A
77.760	1.710	2011	08	12.89941	Fer	110812B
61.240	34.560	2011	08	13.23670	Fer	110813A
336.040	-45.840	2011	08	17.19111	Fer	110817A
317.373	-63.981	2011	08	18.85959	Swi	110818A
139.490	-76.640	2011	08	19.66522	Fer	110819A
90.510	21.630	2011	08	20.47621	Fer	110820C
343.203	70.298	2011	08	20.73503	Swi	110820A
152.050	1.320	2011	08	24.00914	Fer	110824A
44.896	15.407	2011	08	25.10198	Fer	110825A

Continued on next column

Continued from previous column

RA deg	DEC deg	Year	Month	Day	Cat.	GRB Name
251.310	-80.280	2011	08	25.26541	Fer	110825B
164.059	53.817	2011	08	27.00130	Swi	110827A
110.580	-23.810	2011	08	28.57517	Fer	110828A
352.350	33.660	2011	08	31.28156	Fer	110831A
141.280	-15.790	2011	09	1.23037	Fer	110901A
164.210	42.080	2011	09	3.00910	Fer	110903B
197.061	58.985	2011	09	3.11082	Fer	110903A
359.690	35.900	2011	09	4.12380	Fer	110904A
190.400	-28.850	2011	09	4.16292	Fer	110904B
323.740	23.940	2011	09	4.53078	Fer	110904C
26.320	17.650	2011	09	6.30224	Fer	110906B
347.340	-24.220	2011	09	9.11595	Fer	110909A
258.580	-66.980	2011	09	11.07062	Fer	110911A
310.830	-0.713	2011	09	15.55606	Swi	110915A
77.548	1.925	2011	09	15.76689	Agi	110915B
4.110	40.360	2011	09	16.01599	Fer	110916A
279.970	66.430	2011	09	19.63352	Fer	110919A
87.570	38.760	2011	09	20.33838	Fer	110920A
209.820	-27.560	2011	09	20.54565	Fer	110920A
6.090	-5.830	2011	09	21.44361	Fer	110921C
294.094	36.355	2011	09	21.57731	Swi	110921A
17.970	-27.750	2011	09	21.91163	Fer	110921B
323.400	-10.890	2011	09	23.83470	Fer	110923A
69.440	10.430	2011	09	26.10667	Fer	110926A
257.745	36.547	2011	09	28.07744	Swi	110928A
153.400	34.290	2011	09	28.18046	Fer	110928B
288.190	-62.210	2011	09	29.18673	Fer	110929A
187.310	-53.660	2011	09	30.56425	Fer	110930A
340.010	-15.330	2011	10	1.80415	Fer	111001A
276.760	-62.320	2011	10	3.46528	Fer	111003A
223.315	-19.722	2011	10	5.33697	Swi	111005A
340.300	75.800	2011	10	5.39796	Fer	111005B
60.439	-32.708	2011	10	8.92567	Swi	111008A
220.750	-5.670	2011	10	8.99238	Fer	111008B
183.040	-56.820	2011	10	9.28172	Fer	111009A
87.090	43.980	2011	10	10.23651	Fer	111010A
183.540	-31.700	2011	10	10.65997	Fer	111010B
69.800	41.880	2011	10	10.70874	Fer	111010C
77.020	-14.960	2011	10	10.89877	Fer	111010D
37.960	-12.530	2011	10	11.09386	Fer	111011A
154.010	68.090	2011	10	12.45599	Fer	111012A
97.220	67.050	2011	10	12.81087	Fer	111012B
220.650	-58.410	2011	10	15.42723	Fer	111015A
153.826	27.474	2011	10	16.77574	Swi	111016A
8.100	-7.010	2011	10	17.65652	Fer	111017A
106.080	66.140	2011	10	18.59501	Fer	111018B
271.482	-3.880	2011	10	18.72667	Swi	111018A
124.180	81.290	2011	10	18.78489	Fer	111018C

Continued on next column

Continued from previous column

RA deg	DEC deg	Year	Month	Day	Cat.	GRB Name
287.029	-38.031	2011	10	20.27348	Swi	111020A
275.871	-23.666	2011	10	22.67157	Swi	111022A
108.927	49.663	2011	10	22.71741	Swi	111022B
104.500	-33.110	2011	10	22.85375	Fer	111022C
162.740	-44.940	2011	10	24.72156	Fer	111024B
91.230	-1.750	2011	10	24.89586	Fer	111024C
325.620	-35.520	2011	10	25.07831	Fer	111025A
244.256	-47.435	2011	10	26.28297	Swi	111026A
44.785	57.101	2011	10	29.40602	Swi	111029A
327.111	-10.532	2011	11	3.44112	Swi	111103A
265.691	1.605	2011	11	3.45767	Swi	111103B
201.580	-43.160	2011	11	3.94798	Fer	111103C
153.480	7.280	2011	11	5.45667	Fer	111105A
129.487	-66.520	2011	11	7.03500	Swi	111107A
315.460	-38.530	2011	11	7.07623	Fer	111107B
118.248	-41.588	2011	11	9.12345	Swi	111109A
133.730	-33.350	2011	11	9.45315	Fer	111109B
129.980	44.650	2011	11	9.87311	Fer	111109C
223.720	28.810	2011	11	12.90820	Fer	111112A
4.320	-7.520	2011	11	13.40986	Fer	111113B
268.080	-20.010	2011	11	14.23316	Fer	111114A
12.702	23.021	2011	11	17.50950	Swi	111117A
27.160	-16.110	2011	11	17.52640	Fer	111117B
344.600	-37.340	2011	11	20.55583	Fer	111120A
154.746	-46.670	2011	11	21.68500	Swi	111121A
154.845	-20.639	2011	11	23.75927	Swi	111123A
94.060	4.630	2011	11	24.30845	Fer	111124A
276.057	51.461	2011	11	26.79007	Swi	111126A
103.700	3.500	2011	11	27.81044	Fer	111127A
307.415	-52.722	2011	11	29.67933	Swi	111129A
190.485	32.993	2011	12	1.59913	Swi	111201A
53.220	33.470	2011	12	3.05352	Fer	111203A
242.830	-22.150	2011	12	3.60886	Fer	111203B
336.651	-31.414	2011	12	4.56769	Swi	111204A
164.880	-17.940	2011	12	7.51199	Fer	111207B
92.924	-39.504	2011	12	7.59513	Swi	111207A
290.215	40.669	2011	12	8.35291	Swi	111208A
14.350	-46.799	2011	12	9.30009	Swi	111209A
191.493	-7.173	2011	12	10.60906	Swi	111210A
153.091	11.182	2011	12	11.92885	Agi	111211A
310.442	-68.585	2011	12	12.39105	Swi	111212A
349.582	32.440	2011	12	15.58620	Swi	111215A
185.990	5.830	2011	12	16.38925	Fer	111216A
267.600	-56.050	2011	12	20.48641	Fer	111220A
10.160	-29.770	2011	12	21.73855	Fer	111221A
179.193	69.036	2011	12	22.61939	Fer	111222A
13.158	51.573	2011	12	25.16015	Swi	111225A
21.500	3.870	2011	12	26.79512	Fer	111226A

Continued on next column

Continued from previous column

RA deg	DEC deg	Year	Month	Day	Cat.	GRB Name
330.650	14.470	2011	12	28.45336	Fer	111228B
150.063	18.284	2011	12	28.65605	Swi	111228A
76.561	-84.687	2011	12	29.94296	Swi	111229A
150.190	33.430	2011	12	30.68274	Fer	111230A
242.610	-22.120	2011	12	30.81912	Fer	111230B
185.870	52.910	2012	01	1.35425	Fer	120101A
276.224	24.713	2012	01	2.09439	Swi	120102A
341.150	-23.160	2012	01	2.41599	Fer	120102B
203.690	40.070	2012	01	5.58375	Fer	120105A
66.129	64.050	2012	01	6.59472	Swi	120106A
246.400	-69.930	2012	01	7.38351	Fer	120107A
251.330	30.800	2012	01	9.82363	Fer	120109A
95.340	5.000	2012	01	11.05101	Fer	120111A
263.230	-75.640	2012	01	14.43309	Fer	120114B
317.904	57.036	2012	01	14.68066	Swi	120114A
16.240	33.927	2012	01	16.75449	Swi	120116A
124.862	-7.178	2012	01	18.70858	Swi	120118B
166.570	47.870	2012	01	18.89775	Fer	120118C
120.029	-9.076	2012	01	19.16979	Swi	120119A
139.650	-61.330	2012	01	19.22904	Fer	120119B
65.960	-33.920	2012	01	19.35382	Fer	120119C
134.720	35.470	2012	01	20.43154	Fer	120120A
235.670	-39.340	2012	01	21.10132	Fer	120121B
208.900	-1.340	2012	01	21.25052	Fer	120121C
249.363	-23.963	2012	01	21.40439	Swi	120121A
96.580	16.530	2012	01	22.30007	Fer	120122A
26.520	-8.510	2012	01	29.31197	Fer	120129B
30.440	59.282	2012	01	29.58040	Fer	120129A
150.040	-17.450	2012	01	30.69943	Fer	120130A
64.960	9.480	2012	01	30.90619	Fer	120130B
323.300	58.560	2012	01	30.93790	Fer	120130C
203.508	22.774	2012	02	2.90277	INT	120202A
339.300	-46.590	2012	02	3.81208	Fer	120203A
292.580	-3.570	2012	02	4.05356	Fer	120204A
243.417	25.900	2012	02	5.28548	Fer	120205A
73.450	58.410	2012	02	6.94880	Fer	120206A
54.650	-58.520	2012	02	10.64981	Fer	120210A
87.781	-24.795	2012	02	11.49893	Swi	120211A
303.400	-48.100	2012	02	12.35263	Fer	120212B
43.086	-18.043	2012	02	12.38289	Swi	120212A
300.987	65.413	2012	02	13.01897	Swi	120213A
183.490	5.760	2012	02	13.60607	Fer	120213B
30.057	8.790	2012	02	15.02865	Swi	120215A
122.440	36.770	2012	02	17.80822	Fer	120217A
298.730	32.700	2012	02	17.90414	Fer	120217B
319.764	-25.463	2012	02	18.03428	Swi	120218A
101.850	-1.370	2012	02	18.27572	Fer	120218B
274.850	-31.110	2012	02	19.56346	Fer	120219B

Continued on next column

Continued from previous column

RA deg	DEC deg	Year	Month	Day	Cat.	GRB Name
129.862	51.006	2012	02	19.60426	Swi	120219A
206.130	-57.360	2012	02	20.20997	Fer	120220A
299.550	26.490	2012	02	22.02056	Fer	120222A
340.000	-36.410	2012	02	22.11938	Fer	120222A
219.610	-7.460	2012	02	23.93320	Fer	120223A
40.937	-17.779	2012	02	24.19440	Swi	120224A
118.420	41.340	2012	02	24.28227	Fer	120224B
331.060	10.180	2012	02	24.89800	Fer	120224C
87.590	52.350	2012	02	26.44741	Fer	120226B
302.930	48.665	2012	02	26.87103	Fer	120226A
84.760	8.500	2012	02	27.39081	Fer	120227A
256.730	-88.860	2012	02	27.72548	Fer	120227B
20.033	-35.796	2012	02	29.60777	Swi	120229A
122.426	29.642	2012	03	2.08031	Swi	120302A
24.090	9.710	2012	03	2.72221	Fer	120302B
127.150	-61.120	2012	03	4.06098	Fer	120304A
277.280	-46.220	2012	03	4.24847	Fer	120304B
47.549	28.495	2012	03	5.81771	Swi	120305A
219.123	79.674	2012	03	8.25947	Swi	120308A
30.750	55.220	2012	03	8.58757	Fer	120308B
273.075	14.297	2012	03	11.23169	Swi	120311A
258.551	-13.068	2012	03	11.63067	Swi	120311B
251.812	23.881	2012	03	12.67116	Swi	120312A
17.890	-48.730	2012	03	14.41151	Fer	120314A
57.016	-56.288	2012	03	16.00767	Fer	120316A
69.850	-45.440	2012	03	19.98269	Fer	120319A
212.517	8.682	2012	03	20.49740	Swi	120320A
211.100	-45.230	2012	03	23.16168	Fer	120323B
340.407	29.717	2012	03	23.50717	Fer	120323A
291.081	24.140	2012	03	24.24943	Swi	120324A
273.906	69.248	2012	03	26.05589	Swi	120326A
246.854	-29.415	2012	03	27.12171	Swi	120327A
170.410	23.760	2012	03	27.41793	Fer	120327B
241.607	-39.322	2012	03	28.12939	Swi	120328A
228.140	22.800	2012	03	28.26830	Fer	120328B
26.370	-54.840	2012	03	31.05494	Fer	120331A
58.057	-17.658	2012	04	1.22517	Swi	120401A
223.730	-10.400	2012	04	2.66945	Fer	120402B
42.458	40.489	2012	04	3.04541	Swi	120403A
54.302	-89.029	2012	04	3.85690	Swi	120403B
235.002	12.883	2012	04	4.53544	Swi	120404A
159.630	-17.000	2012	04	10.58472	Fer	120410A
38.070	-7.240	2012	04	11.92530	Fer	120411A
29.440	-24.670	2012	04	12.05465	Fer	120412A
38.910	7.060	2012	04	12.91991	Fer	120412B
213.540	16.730	2012	04	15.07636	Fer	120415A
190.690	4.910	2012	04	15.89145	Fer	120415B
150.460	61.270	2012	04	15.95786	Fer	120415C

Continued on next column

Continued from previous column

RA deg	DEC deg	Year	Month	Day	Cat.	GRB Name
187.402	-63.017	2012	04	19.53918	INT	120419A
47.890	-52.190	2012	04	20.24870	Fer	120420A
109.260	10.760	2012	04	20.85779	Fer	120420B
136.915	13.974	2012	04	22.30004	Swi	120422A
111.537	-65.631	2012	04	26.08975	Fer	120426A
285.490	-13.680	2012	04	26.58498	Fer	120426B
224.935	29.311	2012	04	27.05379	Fer	120427A
114.700	50.210	2012	04	27.15322	Fer	120427B
165.980	-8.760	2012	04	29.00286	Fer	120429A
133.040	-32.230	2012	04	29.48407	Fer	120429B
47.250	18.520	2012	04	30.97967	Fer	120430A
329.940	46.830	2012	05	4.46782	Fer	120504A
200.280	-24.200	2012	05	4.94454	Fer	120504B
172.220	-33.720	2012	05	6.12850	Fer	120506A
195.390	38.310	2012	05	9.61948	Fer	120509A
186.930	-55.240	2012	05	10.90030	Fer	120510B
226.930	-60.490	2012	05	11.63805	Fer	120511A
325.558	13.636	2012	05	12.11232	Fer	120512A
140.790	74.990	2012	05	13.53056	Fer	120513A
283.002	-4.258	2012	05	14.05057	Swi	120514A
180.250	20.550	2012	05	19.72101	Fer	120519A
45.860	35.280	2012	05	20.94890	Fer	120520A
148.692	-49.422	2012	05	21.24979	Swi	120521A
197.016	-52.742	2012	05	21.38042	Swi	120521B
214.288	42.144	2012	05	21.97369	Swi	120521C
56.070	54.850	2012	05	22.36061	Fer	120522B
358.150	-15.610	2012	05	24.13397	Fer	120524A
66.280	-32.230	2012	05	26.30325	Fer	120526A
295.130	6.500	2012	05	28.44167	Fer	120528A
175.960	78.830	2012	05	30.12062	Fer	120530A
290.400	1.220	2012	05	31.39350	Fer	120531A
198.794	4.326	2012	06	3.43900	Fer	120603A
163.870	-7.400	2012	06	4.21981	Fer	120604A
113.580	-2.790	2012	06	4.34283	Fer	120604B
243.610	41.510	2012	06	5.45296	Fer	120605A
229.980	-26.120	2012	06	8.48879	Fer	120608A
313.260	12.640	2012	06	8.77677	Fer	120608B
67.320	13.000	2012	06	9.57958	Fer	120609A
324.680	-44.790	2012	06	11.10834	Fer	120611A
126.723	-17.598	2012	06	12.08703	Swi	120612A
211.880	34.560	2012	06	12.68039	Fer	120612B
39.670	-37.910	2012	06	12.68732	Fer	120612C
79.690	56.440	2012	06	16.62975	Fer	120616A
77.310	75.850	2012	06	18.12766	Fer	120618A
213.570	-2.110	2012	06	18.91915	Fer	120618B
190.740	-25.020	2012	06	19.88422	Fer	120619A
4.773	7.167	2012	06	24.30863	Fer	120624A
170.886	8.933	2012	06	24.93045	Swi	120624B

Continued on next column

Continued from previous column

RA deg	DEC deg	Year	Month	Day	Cat.	GRB Name
51.260	51.070	2012	06	25.11859	Fer	120625A
176.160	-0.600	2012	06	29.56541	Fer	120629A
352.300	42.495	2012	06	30.00000	Swi	120630A
80.338	-58.531	2012	07	1.00000	Swi	120701A
182.730	-45.700	2012	07	1.65403	Fer	120701B
227.800	36.760	2012	07	2.89119	Fer	120702A
69.490	34.740	2012	07	3.41750	Fer	120703B
210.510	46.260	2012	07	3.49788	Fer	120703C
339.353	-29.726	2012	07	3.72595	Swi	120703A
291.060	-34.440	2012	07	7.80020	Fer	120707A
318.400	-50.100	2012	07	9.88311	Fer	120709A
120.390	-31.140	2012	07	10.09950	Fer	120710A
94.690	-71.000	2012	07	11.11451	Fer	120711A
331.710	59.996	2012	07	11.13267	Swi	120711B
127.880	-31.830	2012	07	11.44646	Fer	120711C
169.598	-20.051	2012	07	12.57115	Swi	120712A
161.680	40.660	2012	07	13.22603	Fer	GRB120713226
167.975	-30.625	2012	07	14.32414	Swi	120714A
355.412	-46.196	2012	07	14.88804	Swi	120714B
272.150	58.790	2012	07	15.06615	Fer	GRB120715066
304.530	59.410	2012	07	16.57711	Fer	GRB120716577
308.230	12.310	2012	07	16.71185	Fer	GRB120716712
204.290	-43.450	2012	07	19.14584	Fer	GRB120719146
230.489	13.249	2012	07	22.53711	Swi	120722A
245.193	3.535	2012	07	24.27711	Swi	120724A
163.260	25.090	2012	07	27.35392	Fer	GRB120727354
37.760	16.360	2012	07	27.68078	Fer	GRB120727681
101.790	-42.470	2012	07	28.43431	Fer	GRB120728434
137.085	-54.437	2012	07	28.93415	Swi	120728A
13.078	49.936	2012	07	29.45572	Swi	120729A
245.730	-47.370	2012	08	1.92038	Fer	GRB120801920
44.833	13.762	2012	08	2.33392	Swi	120802A
269.531	-6.733	2012	08	3.30713	Swi	120803A
314.223	53.298	2012	08	3.46257	Swi	120803B
233.951	-28.768	2012	08	4.03766	Swi	120804A
30.130	-21.510	2012	08	5.70581	Fer	GRB120805706
216.536	5.853	2012	08	5.89455	Swi	120805A
308.990	6.330	2012	08	6.00705	Fer	GRB120806007
241.273	-47.455	2012	08	7.29835	Swi	120807A
43.658	-31.675	2012	08	11.01424	Fer	GRB120811014
257.184	-22.735	2012	08	11.10785	Swi	120811A
199.690	62.297	2012	08	11.64921	Swi	120811C
26.190	22.450	2012	08	14.20084	Fer	GRB120814201
90.570	33.130	2012	08	14.80286	Fer	GRB120814803
273.976	-52.125	2012	08	15.09303	Swi	120815A
282.133	-6.981	2012	08	16.80456	Swi	120816A
259.970	-9.070	2012	08	17.05706	Fer	GRB120817057
8.310	-26.428	2012	08	17.16839	Swi	120817B

Continued on next column

Continued from previous column

RA deg	DEC deg	Year	Month	Day	Cat.	GRB Name
250.692	-38.377	2012	08	17.28451	Swi	120817A
171.540	49.420	2012	08	19.04753	Fer	GRB120819048
235.887	-7.304	2012	08	19.54877	Swi	120819A
186.640	-12.310	2012	08	20.58498	Fer	GRB120820585
181.720	80.560	2012	08	22.62774	Fer	GRB120822628
70.920	17.630	2012	08	24.59445	Fer	GRB120824594
222.740	-71.890	2012	08	27.21557	Fer	GRB120827216
337.870	-80.040	2012	08	30.21172	Fer	GRB120830212
76.710	-27.840	2012	08	30.29657	Fer	GRB120830297
110.030	17.530	2012	08	30.70251	Fer	GRB120830702
144.020	-16.210	2012	08	31.90106	Fer	GRB120831901
355.960	16.990	2012	09	5.65719	Fer	GRB120905657
74.736	-9.323	2012	09	7.01693	Swi	120907A
268.670	-35.790	2012	09	8.87327	Fer	GRB120908873
230.640	-25.790	2012	09	8.93819	Fer	GRB120908938
275.735	-59.432	2012	09	9.07087	Swi	120909A
357.966	63.090	2012	09	11.29760	Swi	120911A
146.400	26.959	2012	09	13.84608	Swi	120913A
213.660	-14.508	2012	09	13.99720	Swi	120913B
267.940	1.820	2012	09	14.14354	Fer	GRB120914144
209.350	67.320	2012	09	15.00048	Fer	GRB120915000
283.560	-1.110	2012	09	15.47366	Fer	GRB120915474
82.040	-19.220	2012	09	16.08491	Fer	GRB120916085
205.810	36.660	2012	09	16.17269	Fer	GRB120916173
181.042	-32.762	2012	09	18.46956	Swi	120918A
298.000	-38.070	2012	09	19.05166	Fer	GRB120919052
213.420	-46.310	2012	09	19.30882	Fer	GRB120919309
303.530	-66.160	2012	09	19.81646	Fer	GRB120919816
27.120	-26.120	2012	09	20.00316	Fer	GRB120920003
96.420	-64.770	2012	09	21.87713	Fer	GRB120921877
234.758	-20.181	2012	09	22.93782	Swi	120922A
303.781	6.255	2012	09	23.21951	Swi	120923A
318.390	58.380	2012	09	26.33538	Fer	GRB120926335
59.720	-37.200	2012	09	26.42588	Fer	GRB120926426
24.610	-45.580	2012	09	26.75318	Fer	GRB120926753
136.606	0.420	2012	09	27.94498	Swi	120927A
276.029	-5.667	2012	10	1.76600	Swi	121001A
137.460	-11.020	2012	10	4.21063	Fer	GRB121004211
195.170	-2.090	2012	10	5.02977	Fer	GRB121005030
149.730	25.400	2012	10	5.33973	Fer	GRB121005340
340.970	-3.100	2012	10	8.42420	Fer	GRB121008424
260.204	41.123	2012	10	11.46910	Swi	121011A
33.420	14.580	2012	10	12.72380	Fer	GRB121012724
320.010	-53.430	2012	10	14.63820	Fer	GRB121014638
166.645	-29.105	2012	10	14.84162	Swi	121014A
288.820	-1.602	2012	10	17.80796	Swi	121017A
43.470	62.140	2012	10	19.23275	Fer	GRB121019233
313.860	-4.380	2012	10	23.32242	Fer	GRB121023322

Continued on next column

Continued from previous column

RA deg	DEC deg	Year	Month	Day	Cat.	GRB Name
70.481	-12.255	2012	10	24.12236	Swi	121024A
248.750	27.730	2012	10	25.32396	Swi	121025A
4.310	-47.540	2012	10	27.03772	Fer	GRB121027038
63.598	-58.839	2012	10	27.31422	Swi	121027A
271.903	-2.298	2012	10	28.21147	Swi	121028A
52.560	-25.070	2012	10	28.28001	Fer	GRB121028280
226.770	-28.200	2012	10	29.35023	Fer	GRB121029350
170.772	-3.513	2012	10	31.95174	Swi	121031A
258.470	14.090	2012	11	2.06444	Fer	GRB121102064
270.896	-16.951	2012	11	2.10211	Swi	121102A
72.140	14.080	2012	11	4.62657	Fer	GRB121104627
83.216	54.520	2012	11	8.74142	Swi	121108A
6.840	-42.570	2012	11	9.33816	Fer	GRB121109338
78.980	-55.440	2012	11	12.80607	Fer	GRB121112806
313.170	59.820	2012	11	13.54356	Fer	GRB121113544
180.880	-74.790	2012	11	16.45862	Fer	GRB121116459
279.140	44.930	2012	11	17.01780	Fer	GRB121117018
31.617	7.432	2012	11	17.36870	Swi	121117A
299.379	65.654	2012	11	18.57563	Fer	GRB121118576
311.650	-16.920	2012	11	19.57864	Fer	GRB121119579
52.670	46.470	2012	11	22.56351	Fer	GRB121122564
355.450	6.340	2012	11	22.87001	Fer	GRB121122870
35.262	45.139	2012	11	22.88533	Fer	GRB121122885
307.334	-11.873	2012	11	23.41853	Swi	121123A
30.520	-18.790	2012	11	23.44162	Fer	GRB121123442
87.930	49.550	2012	11	24.60564	Fer	GRB121124606
228.519	55.318	2012	11	25.35587	Swi	121125A
177.530	38.540	2012	11	25.46861	Fer	GRB121125469
164.410	-64.480	2012	11	27.91389	Fer	GRB121127914
300.589	54.301	2012	11	28.21223	Swi	121128A
13.473	-42.929	2012	12	1.51785	Swi	121201A
256.790	23.942	2012	12	2.18061	Swi	121202A
238.590	-49.710	2012	12	5.50700	Fer	GRB121205507
326.800	-8.232	2012	12	9.91610	Swi	121209A
202.540	17.770	2012	12	10.08057	Fer	GRB121210081
195.575	30.173	2012	12	11.57433	Swi	121211A
72.370	8.630	2012	12	11.69517	Fer	GRB121211695
177.787	78.052	2012	12	12.28904	Swi	121212A
13.880	-85.440	2012	12	16.41894	Fer	GRB121216419
153.708	-62.354	2012	12	17.30402	Swi	121217A
153.710	-62.350	2012	12	17.31252	Fer	GRB121217313
31.070	48.280	2012	12	20.31126	Fer	GRB121220311
214.260	33.550	2012	12	21.91632	Fer	GRB121221916
50.110	21.370	2012	12	23.29954	Fer	GRB121223300
310.450	-34.830	2012	12	25.41729	Fer	GRB121225417
168.620	-30.413	2012	12	26.79841	Swi	121226A
190.095	-50.588	2012	12	29.20858	Swi	121229A
315.590	-11.940	2012	12	29.53303	Fer	GRB121229533

Continued on next column

Continued from previous column

RA deg	DEC deg	Year	Month	Day	Cat.	GRB Name
335.470	-17.780	2012	12	31.44541	Fer	GRB121231445
311.435	49.838	2013	01	2.75756	Swi	130102A
174.090	25.920	2013	01	4.72091	Fer	GRB130104721
66.670	29.740	2013	01	6.82873	Fer	GRB130106829
28.760	63.380	2013	01	6.99474	Fer	GRB130106995
17.450	19.240	2013	01	9.20586	Fer	GRB130109206
236.030	52.190	2013	01	12.28620	Fer	GRB130112286
196.290	-31.940	2013	01	12.35264	Fer	GRB130112353
310.190	-15.320	2013	01	14.01880	Fer	GRB130114019
171.090	22.620	2013	01	15.71573	Fer	GRB130115716
38.240	15.750	2013	01	16.41544	Fer	GRB130116415
341.240	2.810	2013	01	17.08694	Fer	GRB130117087
278.300	40.980	2013	01	18.48159	Fer	GRB130118482
211.310	-49.490	2013	01	21.83472	Fer	GRB130121835
194.307	59.003	2013	01	22.98899	Swi	130122A
301.210	-57.210	2013	01	27.29853	Fer	GRB130127299
251.050	-17.070	2013	01	27.74333	Fer	GRB130127743
189.630	-14.480	2013	01	31.51057	Fer	GRB130131511
171.091	48.064	2013	01	31.58081	Swi	130131A
173.957	15.033	2013	01	31.79870	Swi	130131B
105.640	41.920	2013	02	4.48393	Fer	GRB130204484
269.100	49.430	2013	02	6.48165	Fer	GRB130206482
140.387	-58.193	2013	02	6.81699	Swi	130206A
181.600	50.930	2013	02	8.68361	Fer	GRB130208684
33.590	-27.580	2013	02	9.96090	Fer	GRB130209961
147.524	-42.330	2013	02	11.15037	Swi	130211A
99.090	-8.100	2013	02	13.90551	Fer	GRB130213905
325.020	-1.830	2013	02	14.13687	Fer	GRB130214137
56.930	-0.290	2013	02	14.80025	Fer	GRB130214800
43.486	13.387	2013	02	15.06354	Swi	130215A
3.110	59.380	2013	02	15.64880	Fer	GRB130215649
58.866	2.036	2013	02	16.79042	Swi	130216B
67.901	14.670	2013	02	16.92736	Swi	130216A
96.720	6.800	2013	02	17.68842	Fer	GRB130217688
69.310	-69.130	2013	02	18.26141	Fer	GRB130218261
169.290	-22.250	2013	02	19.19731	Fer	GRB130219197
211.600	12.220	2013	02	19.62586	Fer	GRB130219626
303.730	40.830	2013	02	19.77490	Fer	GRB130219775
306.200	31.740	2013	02	20.96445	Fer	GRB130220964
205.900	59.720	2013	02	24.37017	Fer	GRB130224370
257.280	53.940	2013	02	28.11114	Fer	GRB130228111
240.750	-55.210	2013	02	28.21247	Fer	GRB130228212
98.930	53.570	2013	03	4.40964	Fer	GRB130304410
178.870	-60.290	2013	03	4.65752	Fer	GRB130304658
116.774	52.037	2013	03	5.48560	Swi	130305A
73.320	-1.560	2013	03	5.52625	Fer	GRB130305526
279.475	-11.682	2013	03	6.99376	Swi	130306A
155.996	22.998	2013	03	7.12621	Fer	GRB130307126

Continued on next column

Continued from previous column

RA deg	DEC deg	Year	Month	Day	Cat.	GRB Name
319.520	10.770	2013	03	7.23772	Fer	GRB130307238
142.340	-17.230	2013	03	10.84006	Fer	GRB130310840
236.438	-0.355	2013	03	13.67235	Swi	130313A
206.210	46.770	2013	03	14.14672	Fer	GRB130314147
157.541	-51.794	2013	03	15.53162	Swi	130315A
200.740	8.120	2013	03	18.45592	Fer	GRB130318456
195.539	-71.259	2013	03	20.56012	Fer	GRB130320560
255.430	0.050	2013	03	24.04195	Fer	GRB130324042
30.440	62.060	2013	03	25.00540	Fer	GRB130325005
122.780	-18.900	2013	03	25.20271	Fer	GRB130325203
91.984	55.732	2013	03	27.07470	Swi	130327A
215.300	-74.480	2013	03	27.35005	Fer	GRB130327350
164.470	29.640	2013	03	31.56649	Fer	GRB130331566
199.900	-46.680	2013	04	3.86583	Fer	GRB130403866
30.750	1.540	2013	04	4.42755	Fer	GRB130404428
146.580	-42.160	2013	04	4.84032	Fer	GRB130404840
28.290	56.490	2013	04	4.87652	Fer	GRB130404877
157.780	-62.050	2013	04	6.28823	Fer	GRB130406288
109.660	-27.860	2013	04	6.33376	Fer	GRB130406334
138.210	42.830	2013	04	6.35390	Fer	GRB130406354
53.530	44.170	2013	04	7.80050	Fer	GRB130407800
118.770	66.340	2013	04	8.65304	Fer	GRB130408653
134.398	-32.363	2013	04	8.91086	Swi	130408A
30.520	44.100	2013	04	9.95972	Fer	GRB130409960
99.280	24.700	2013	04	16.69036	Fer	GRB130416690
51.210	-18.250	2013	04	16.77006	Fer	GRB130416770
149.045	13.674	2013	04	18.79228	Swi	130418A
216.530	-17.540	2013	04	18.84358	Fer	GRB130418844
355.278	9.900	2013	04	19.56284	Swi	130419A
196.118	59.421	2013	04	20.31145	Swi	130420A
122.680	-11.430	2013	04	20.34308	Fer	GRB130420343
117.060	-69.030	2013	04	20.42233	Fer	GRB130420422
183.095	54.376	2013	04	20.53925	Swi	130420B
18.990	-72.220	2013	04	25.32727	Fer	GRB130425327
173.150	27.706	2013	04	27.32496	Swi	130427A
314.900	-22.548	2013	04	27.55603	Swi	130427B
66.762	71.061	2013	05	2.32722	Fer	GRB130502327
138.579	-0.134	2013	05	2.74340	Swi	130502A
214.720	-11.550	2013	05	3.21422	Fer	GRB130503214
272.459	-16.320	2013	05	4.08720	Swi	130504A
347.952	-5.739	2013	05	4.31393	Fer	GRB130504314
91.631	3.834	2013	05	4.97844	Fer	GRB130504978
137.060	17.485	2013	05	5.34894	Swi	130505A
344.470	-70.470	2013	05	5.95505	Fer	GRB130505955
319.740	-20.530	2013	05	7.54488	Fer	GRB130507545
305.351	34.966	2013	05	8.71450	Swi	130508A
240.850	-40.220	2013	05	9.07795	Fer	GRB130509078
133.860	-11.510	2013	05	9.83939	Fer	GRB130509839

Continued on next column

Continued from previous column

RA deg	DEC deg	Year	Month	Day	Cat.	GRB Name
105.710	-9.870	2013	05	10.87734	Fer	GRB130510877
196.654	18.709	2013	05	11.47971	Swi	130511A
144.775	-5.244	2013	05	13.31806	INT	130513A
296.278	-7.974	2013	05	14.30117	Swi	130514A
147.600	-18.970	2013	05	14.56010	Fer	GRB130514560
283.436	-54.283	2013	05	15.05645	Swi	130515A
312.840	-14.950	2013	05	15.42952	Fer	GRB130515430
146.770	11.260	2013	05	15.75476	Fer	GRB130515755
41.860	42.660	2013	05	17.78071	Fer	GRB130517781
321.555	-20.148	2013	05	18.45183	Swi	130518B
289.720	-4.150	2013	05	18.55079	Fer	GRB130518551
355.671	47.478	2013	05	18.57995	Swi	130518A
87.568	14.470	2013	05	21.95088	Swi	130521A
134.150	17.620	2013	05	22.51008	Fer	GRB130522510
22.290	29.730	2013	05	23.09455	Fer	GRB130523095
39.490	-63.070	2013	05	23.19841	Fer	GRB130523198
309.282	-24.726	2013	05	27.59826	Swi	130527A
175.790	-2.520	2013	05	27.62656	Fer	GRB130527627
352.700	27.810	2013	05	28.50314	Fer	GRB130528503
139.405	87.300	2013	05	28.69541	Swi	130528A
24.274	-64.143	2013	05	29.46904	Swi	130529A
160.950	25.230	2013	05	30.71902	Fer	GRB130530719
86.859	82.910	2013	06	3.24968	Swi	130603A
172.222	17.063	2013	06	3.65919	Swi	130603B
292.180	-24.860	2013	06	4.03346	Fer	GRB130604033
250.166	68.225	2013	06	4.28780	Swi	130604A
134.536	-33.477	2013	06	5.98729	Swi	130605A
339.370	12.490	2013	06	6.31632	Fer	GRB130606316
218.574	-22.131	2013	06	6.49692	Fer	GRB130606497
249.390	29.796	2013	06	6.87823	Swi	130606A
24.597	41.492	2013	06	8.96830	Swi	130608A
152.680	24.124	2013	06	9.12856	Swi	130609A
53.776	-40.168	2013	06	9.90185	Swi	130609B
224.414	28.187	2013	06	10.13348	Swi	130610A
238.840	-25.230	2013	06	11.53774	Fer	GRB130611538
259.771	16.729	2013	06	12.14053	Swi	130612A
247.940	31.020	2013	06	12.45642	Fer	GRB130612456
324.180	-33.890	2013	06	14.99734	Fer	GRB130614997
184.860	69.620	2013	06	15.39800	Fer	GRB130615398
274.963	-68.161	2013	06	15.40608	Swi	130615A
74.730	-60.060	2013	06	17.56447	Fer	GRB130617564
74.420	61.190	2013	06	20.49800	Fer	GRB130620498
312.740	24.460	2013	06	22.61520	Fer	GRB130622615
194.610	35.510	2013	06	23.12960	Fer	GRB130623130
203.590	49.030	2013	06	23.39611	Fer	GRB130623396
20.723	-77.784	2013	06	23.48802	Swi	130623A
284.680	10.670	2013	06	23.69889	Fer	GRB130623699
107.430	36.040	2013	06	23.79017	Fer	GRB130623790

Continued on next column

Continued from previous column

RA deg	DEC deg	Year	Month	Day	Cat.	GRB Name
337.320	11.450	2013	06	24.09301	Fer	GRB130624093
343.336	82.171	2013	06	25.29212	Swi	130625A
273.128	-9.525	2013	06	26.45212	Swi	130626A
24.890	4.930	2013	06	26.59551	Fer	GRB130626596
184.415	-37.114	2013	06	27.37156	Swi	130627A
181.914	-55.706	2013	06	27.50058	Swi	130627B
6.290	-5.070	2013	06	28.53058	Fer	GRB130628531
312.830	6.100	2013	06	28.85974	Fer	GRB130628860
170.010	60.060	2013	06	30.27176	Fer	GRB130630272
97.790	-60.130	2013	07	1.06049	Fer	GRB130701060
357.224	36.100	2013	07	1.17897	Swi	130701A
325.940	-30.890	2013	07	1.76077	Fer	GRB130701761
218.810	12.250	2013	07	2.00374	Fer	GRB130702004
292.160	10.390	2013	07	2.95069	Fer	GRB130702951
65.560	-14.460	2013	07	4.55981	Fer	GRB130704560
156.300	47.410	2013	07	5.39796	Fer	GRB130705398
299.360	56.480	2013	07	6.90009	Fer	GRB130706900
54.450	-21.040	2013	07	7.50543	Fer	GRB130707505
17.474	0.003	2013	07	8.48824	Swi	130708A
287.370	-31.050	2013	07	15.90567	Fer	GRB130715906
348.870	45.340	2013	07	16.35161	Fer	GRB130716352
179.581	63.057	2013	07	16.44228	Swi	130716A
256.590	-13.570	2013	07	17.73357	Fer	GRB130717734
89.038	-11.591	2013	07	19.24154	Swi	130719A
243.500	14.970	2013	07	20.11575	Fer	GRB130720116
338.030	-9.400	2013	07	20.58172	Fer	GRB130720582
119.860	-47.450	2013	07	22.02073	Fer	GRB130722021
260.670	-2.979	2013	07	22.34675	Swi	130722A
352.410	-22.310	2013	07	22.99041	Fer	GRB130722990
217.770	-16.860	2013	07	23.09206	Fer	GRB130723092
230.060	0.624	2013	07	25.48416	Swi	130725A
42.450	64.820	2013	07	25.52686	Fer	GRB130725527
214.233	-11.124	2013	07	25.73574	Swi	130725B
330.790	-65.540	2013	07	27.69814	Swi	130727A
133.750	-60.360	2013	07	30.24328	Fer	GRB130730243
80.280	-7.620	2013	08	2.73047	Fer	GRB130802730
220.256	-2.499	2013	08	3.41866	Swi	130803A
280.030	-76.150	2013	08	4.02310	Fer	GRB130804023
35.907	67.525	2013	08	6.11913	Swi	130806A
269.801	-27.616	2013	08	7.43453	Swi	130807A
162.720	33.380	2013	08	8.25317	Fer	GRB130808253
192.890	-17.040	2013	08	11.18613	Fer	GRB130811186
92.387	-13.285	2013	08	12.93255	Swi	130812A
204.030	56.340	2013	08	13.79124	Fer	GRB130813791
164.710	49.570	2013	08	15.42023	Fer	GRB130815420
112.370	-2.150	2013	08	15.66033	Fer	GRB130815660
197.093	-58.996	2013	08	16.07425	Swi	130816A
170.049	-57.527	2013	08	16.20391	Swi	130816B

Continued on next column

Continued from previous column

RA deg	DEC deg	Year	Month	Day	Cat.	GRB Name
192.290	57.580	2013	08	18.94067	Fer	GRB130818941
124.720	-33.760	2013	08	19.39414	Fer	GRB130819394
314.100	-12.000	2013	08	21.67393	Fer	GRB130821674
27.940	-3.219	2013	08	22.66270	Swi	130822A
259.797	28.215	2013	08	28.30556	Fer	GRB130828306
188.250	27.890	2013	08	28.80826	Fer	GRB130828808
182.426	46.520	2013	08	29.23858	Swi	130829A
258.510	6.000	2013	08	29.67224	Fer	GRB130829672
142.970	-0.550	2013	08	30.86446	Fer	GRB130830864
350.970	-51.570	2013	08	30.92122	Fer	GRB130830921
267.450	61.030	2013	08	31.05849	Fer	GRB130831058
358.635	29.431	2013	08	31.54463	Swi	130831A
192.454	-29.187	2013	08	31.57522	Swi	130831B
82.130	-0.127	2013	09	3.03301	Fer	GRB130903033
275.890	-2.310	2013	09	5.37652	Fer	GRB130905377
194.110	4.200	2013	09	6.22188	Fer	GRB130906222
279.390	-53.380	2013	09	6.43502	Fer	GRB130906435
236.630	-25.100	2013	09	7.76026	Fer	GRB130907760
215.898	45.602	2013	09	7.90362	Swi	130907A
219.160	-7.200	2013	09	8.67666	Fer	GRB130908677
198.180	-20.790	2013	09	9.81677	Fer	GRB130909817
47.606	13.999	2013	09	12.35760	Swi	130912A
341.960	1.294	2013	09	13.01969	Swi	130913A
297.350	-11.730	2013	09	19.17338	Fer	GRB130919173
59.800	48.520	2013	09	19.35214	Fer	GRB130919352
207.281	-10.353	2013	09	19.46347	Swi	130919A
242.220	-48.290	2013	09	19.98488	Fer	GRB130919985
28.770	-7.140	2013	09	24.25473	Fer	GRB130924255
78.590	39.260	2013	09	24.91043	Fer	GRB130924910
41.183	-26.134	2013	09	25.16416	Fer	GRB130925164
41.186	-26.146	2013	09	25.17458	Swi	130925A
83.430	55.300	2013	09	25.54564	Fer	GRB130925546
306.910	-44.190	2013	09	28.53652	Fer	GRB130928537
200.930	2.800	2013	09	29.37515	Fer	GRB130929375
135.028	-47.554	2013	09	29.40038	Swi	130929A
190.725	-35.511	2013	09	30.79829	Swi	130930A
8.304	25.557	2013	10	1.23431	Swi	131001A
253.103	82.036	2013	10	2.28774	Swi	131002A
75.135	-75.701	2013	10	2.45449	Swi	131002B
296.108	-2.952	2013	10	4.90351	Swi	131004A
325.380	-26.630	2013	10	6.36691	Fer	GRB131006367
139.360	-0.870	2013	10	6.84019	Fer	GRB131006840
328.000	-25.980	2013	10	8.85837	Fer	GRB131008858
32.526	-4.412	2013	10	11.74138	Fer	GRB131011741
100.500	-19.100	2013	10	14.21459	Fer	GRB131014215
15.050	21.430	2013	10	14.51292	Fer	GRB131014513
98.473	-19.897	2013	10	18.53319	Swi	131018A
304.410	23.110	2013	10	18.67268	Fer	GRB131018673

Continued on next column

Continued from previous column

RA deg	DEC deg	Year	Month	Day	Cat.	GRB Name
209.000	51.100	2013	10	20.11280	Fer	GRB131020113
329.120	-25.350	2013	10	21.35192	Fer	GRB131021352
290.544	-64.599	2013	10	24.51829	Swi	131024A
144.464	44.284	2013	10	24.89966	Swi	131024B
56.950	72.190	2013	10	28.07572	Fer	GRB131028076
333.400	-56.940	2013	10	28.09573	Fer	GRB131028096
200.785	48.298	2013	10	29.97278	Fer	GRB131029973
110.280	-1.370	2013	10	29.99021	Fer	GRB131029990
61.450	-62.800	2013	10	30.65308	Fer	GRB131030653
186.290	-5.340	2013	10	30.79150	Fer	GRB131030791
345.074	-5.380	2013	10	30.87243	Swi	131030A
29.618	-1.603	2013	10	31.48161	Swi	131031A
74.100	-28.010	2013	11	2.62204	Fer	GRB131102622
348.948	-44.645	2013	11	3.92182	Swi	131103A
70.973	-63.005	2013	11	5.08662	Swi	131105A
353.600	33.880	2013	11	8.02411	Fer	GRB131108024
156.501	9.662	2013	11	8.86245	Fer	GRB131108862
9.810	8.160	2013	11	10.37293	Fer	GRB131110373
69.268	-17.259	2013	11	10.49527	Swi	131110A
157.990	-41.520	2013	11	13.48307	Fer	GRB131113483
332.354	-31.761	2013	11	17.02366	Swi	131117A
213.270	-2.470	2013	11	17.76632	Fer	GRB131117766
349.863	-66.833	2013	11	18.95761	Fer	GRB131118958
47.960	-24.010	2013	11	19.78111	Fer	GRB131119781
278.937	-12.026	2013	11	20.60968	Swi	131120A
261.670	33.380	2013	11	22.48965	Fer	GRB131122490
152.555	57.740	2013	11	22.89237	INT	131122A
53.240	-20.880	2013	11	23.54303	Fer	GRB131123543
109.260	49.970	2013	11	25.68948	Fer	GRB131125689
215.430	53.530	2013	11	26.16262	Fer	GRB131126163
332.714	36.596	2013	11	27.42471	Swi	131127A
49.400	-5.670	2013	11	27.47987	Fer	GRB131127480
306.090	-0.810	2013	11	27.59188	Fer	GRB131127592
246.300	33.920	2013	11	27.69567	Fer	GRB131127696
355.305	31.293	2013	11	28.62944	Swi	131128A
344.005	-21.650	2013	12	2.63344	Swi	131202A
169.660	21.250	2013	12	2.90649	Fer	GRB131202906
309.670	-69.670	2013	12	4.93678	Fer	GRB131204937
131.573	-60.181	2013	12	5.38794	Swi	131205A
136.500	-33.200	2013	12	9.54719	Fer	GRB131209547
253.880	72.600	2013	12	9.96269	Fer	GRB131209963
271.340	-40.610	2013	12	11.51030	Fer	GRB131211510
273.630	18.110	2013	12	12.81423	Fer	GRB131212814
183.940	-6.340	2013	12	14.70550	Fer	GRB131214705
104.070	68.260	2013	12	15.29775	Fer	GRB131215298
94.674	-41.627	2013	12	16.08093	Fer	GRB131216081
86.590	30.600	2013	12	17.10847	Fer	GRB131217108
227.730	25.160	2013	12	17.18296	Fer	GRB131217183

Continued on next column

Continued from previous column

RA deg	DEC deg	Year	Month	Day	Cat.	GRB Name
163.722	-14.177	2013	12	24.14245	Swi	131224B
301.309	-64.943	2013	12	26.24142	Swi	131226A
67.369	28.879	2013	12	27.19781	Swi	131227A
85.236	-4.401	2013	12	29.27736	Swi	131229A
91.110	64.290	2013	12	30.52879	Fer	GRB131230529
73.050	4.840	2013	12	30.80845	Fer	GRB131230808
10.110	-2.420	2013	12	31.19810	Fer	GRB131231198
211.915	1.332	2014	01	2.88723	Swi	140102A
232.114	37.752	2014	01	3.02133	Swi	140103A
218.810	-8.900	2014	01	4.73059	Fer	GRB140104731
208.220	50.170	2014	01	5.06460	Fer	GRB140105065
252.880	19.030	2014	01	5.74760	Fer	GRB140105748
2.340	-8.750	2014	01	6.34495	Fer	GRB140106345
325.129	58.749	2014	01	8.72132	Swi	140108A
102.740	29.760	2014	01	9.77090	Fer	GRB140109771
24.090	-25.050	2014	01	9.87739	Fer	GRB140109877
28.900	-36.260	2014	01	10.26294	Fer	GRB140110263
50.640	-69.290	2014	01	10.41116	Fer	GRB140110411
31.860	65.160	2014	01	10.81359	Fer	GRB140110814
8.440	11.990	2014	01	12.06026	Fer	GRB140112060
75.630	3.180	2014	01	13.18328	Fer	GRB140113183
329.370	18.130	2014	01	13.62391	Fer	GRB140113624
188.498	27.942	2014	01	14.49838	Swi	140114A
210.030	-61.410	2014	01	15.86341	Fer	GRB140115863
94.860	-48.860	2014	01	15.89944	Fer	GRB140115899
330.999	-17.937	2014	01	18.06391	Swi	140118A
56.080	15.090	2014	01	22.59708	Fer	GRB140122597
64.180	38.480	2014	01	24.52675	Fer	GRB140124527
208.700	31.280	2014	01	26.81507	Fer	GRB140126815
37.851	-1.594	2014	01	29.14165	Swi	140129A
183.400	-10.320	2014	01	29.49932	Fer	GRB140129499
326.764	26.215	2014	01	29.53552	Swi	140129B
166.110	62.530	2014	02	4.54656	Fer	GRB140204547
315.260	-8.520	2014	02	6.27515	Fer	GRB140206275
145.321	66.762	2014	02	6.30370	Swi	140206A
81.328	32.488	2014	02	9.31316	Swi	140209A
115.840	-13.590	2014	02	11.09075	Fer	GRB140211091
124.233	20.237	2014	02	11.51601	Swi	140211A
105.166	-73.136	2014	02	13.80668	Swi	140213A
104.129	41.787	2014	02	15.17164	Swi	140215A
194.040	31.460	2014	02	16.33061	Fer	GRB140216331
359.390	76.750	2014	02	17.04285	Fer	GRB140217043
347.480	44.540	2014	02	18.42673	Fer	GRB140218427
221.930	50.000	2014	02	19.31869	Fer	GRB140219319
156.440	7.460	2014	02	19.82398	Fer	GRB140219824
141.120	-30.400	2014	02	23.49521	Fer	GRB140223495
2.780	20.370	2014	02	24.38214	Fer	GRB140224382
23.740	39.480	2014	02	24.78842	Fer	GRB140224788

Continued on next column

Continued from previous column

RA deg	DEC deg	Year	Month	Day	Cat.	GRB Name
221.492	14.993	2014	02	26.42917	Swi	140226A
235.310	31.550	2014	02	27.73827	Fer	GRB140227738
69.521	-34.249	2014	03	1.64223	Swi	140301A
253.862	-12.875	2014	03	2.34234	Swi	140302A
30.653	33.480	2014	03	4.55730	Swi	140304A
354.180	-27.030	2014	03	4.84896	Fer	GRB140304849
344.497	15.448	2014	03	5.62523	Swi	140305A
38.367	60.100	2014	03	6.14566	Fer	GRB140306146
350.160	73.030	2014	03	8.71017	Fer	GRB140308710
39.040	-25.230	2014	03	11.45283	Fer	GRB140311453
183.650	62.810	2014	03	11.61751	Fer	GRB140311618
209.293	0.607	2014	03	11.87866	Swi	140311A
252.333	52.733	2014	03	11.88506	Swi	140311B
184.049	20.225	2014	03	18.00633	Swi	140318A
136.010	81.530	2014	03	19.96424	Fer	GRB140319964
281.843	-11.188	2014	03	20.09219	Swi	140320A
145.541	60.279	2014	03	20.39305	INT	140320B
134.417	71.200	2014	03	20.55370	INT	140320C
250.300	-69.450	2014	03	22.42435	Fer	GRB140322424
356.975	-79.916	2014	03	23.43277	Swi	140323A
283.120	-6.150	2014	03	27.06465	Fer	GRB140327065
320.040	17.970	2014	03	28.56002	Fer	GRB140328560
92.350	-41.080	2014	03	29.27178	Fer	GRB140329272
145.698	-32.229	2014	03	29.29489	Fer	GRB140329295
328.068	-57.745	2014	03	30.18049	Fer	GRB140330180
134.860	2.755	2014	03	31.24292	Swi	140331A
207.592	5.971	2014	04	2.00701	Swi	140402A
14.890	78.890	2014	04	4.03016	Fer	GRB140404030
172.730	33.180	2014	04	4.17138	Fer	GRB140404171
101.810	-6.950	2014	04	4.90020	Fer	GRB140404900
119.100	-26.890	2014	04	5.03267	Fer	GRB140405033
357.550	5.630	2014	04	6.11960	Fer	GRB140406120
70.100	13.540	2014	04	6.14361	Fer	GRB140406144
290.723	-12.585	2014	04	8.55271	Swi	140408A
145.032	-65.826	2014	04	12.93112	Swi	140412A
65.439	-51.188	2014	04	13.00671	Swi	140413A
195.310	56.902	2014	04	14.25450	Swi	140414A
45.680	13.820	2014	04	14.69349	Fer	GRB140414693
35.410	43.910	2014	04	16.06020	Fer	GRB140416060
127.001	46.234	2014	04	19.17142	Swi	140419A
164.540	-62.620	2014	04	22.19358	Fer	GRB140422194
197.276	49.838	2014	04	23.35547	Swi	140423A
174.490	-13.950	2014	04	26.51496	Fer	GRB140426515
131.910	27.490	2014	04	27.70163	Fer	GRB140427702
2.006	68.172	2014	04	28.90600	Fer	GRB140428906
194.365	28.331	2014	04	28.94502	Swi	140428A
338.600	34.850	2014	04	29.97548	Fer	GRB140429975
146.380	-36.880	2014	04	30.71625	Fer	GRB140430716

Continued on next column

Continued from previous column

RA deg	DEC deg	Year	Month	Day	Cat.	GRB Name
102.942	23.033	2014	04	30.85667	Swi	140430A
171.880	24.640	2014	05	1.13867	Fer	GRB140501139
62.780	43.250	2014	05	1.49665	Fer	GRB140501497
319.172	48.975	2014	05	2.35440	Swi	140502A
276.806	-55.556	2014	05	6.88028	Swi	140506A
255.467	46.780	2014	05	8.12772	Fer	GRB140508128
350.530	-63.780	2014	05	8.17895	Fer	GRB140508179
272.100	72.530	2014	05	8.62877	Fer	GRB140508629
46.564	-62.662	2014	05	9.09876	Swi	140509A
329.760	-30.060	2014	05	11.09527	Fer	GRB140511095
26.250	-24.910	2014	05	11.99525	Fer	GRB140511995
289.366	-15.087	2014	05	12.81376	Swi	140512A

Concluded

# Bibliography

- [1] Paciesas W. S. et al. The fourth batse gamma-ray burst catalog (revised). *ApJS*, 122(2):465, 1999. URL <http://stacks.iop.org/0067-0049/122/i=2/a=465>.
- [2] Qin Y.-P., Xie G.-Z., Xue S.-J., Liang E.-W., Zheng X.-T., Mei D.-C. The Hardness-Duration Correlation in the Two Classes of Gamma-Ray Bursts. *Public. Astron. Soc. of Jap.*, 52:759, October 2000. doi: 10.1093/pasj/52.5.759.
- [3] Burrows D. N. et al. X-ray flares in early GRB afterglows. *Royal Society of London Philosophical Transactions Series A*, 365:1213–1226, May 2007. doi: 10.1098/rsta.2006.1970.
- [4] Mészáros P. Gamma-Ray Bursts. *Rept. Prog. Phys.*, 69:2259–2322, 2006. URL <http://arxiv.org/abs/astro-ph/0605208>.
- [5] Band D. et al. BATSE observations of gamma-ray burst spectra. I - Spectral diversity. *ApJ*, 413:281–292, August 1993. doi: 10.1086/172995.
- [6] Sari R., Piran T., Narayan R. Spectra and Light Curves of Gamma-Ray Burst Afterglows. *Astroph. Journal Lett.*, 497:L17–L20, April 1998. doi: 10.1086/311269.
- [7] Hurley K. et al. The solar X-ray/cosmic gamma-ray burst experiment aboard ULYSSES. *Astrop. Jour. Suppl. Ser.*, 92:401–410, January 1992.
- [8] Imager IBIS. URL [http://integral.esac.esa.int/integ\\_payload\\_imager.html](http://integral.esac.esa.int/integ_payload_imager.html).
- [9] Schoemer J., Leitner S., Chi T. THE "EYES" OF THE COMPTON GAMMA RAY OBSERVATORY. URL <http://heasarc.gsfc.nasa.gov/docs/cgro/epo/vu/overview/gro/gro.html>.
- [10] Boella G., Butler R. C., Perola G. C., Piro L., Scarsi L., Bleeker J. A. M. BeppoSAX, the wide band mission for X-ray astronomy. *Astron. Astrophys. Suppl. Ser.*, 122:299–307, April 1997. doi: 10.1051/aas:1997136.

- [11] Frontera F. et al. The Gamma-Ray Burst Catalog Obtained with the Gamma-Ray Burst Monitor Aboard BeppoSAX. *Astroph. Jour. Suppl. Ser.*, 180(1):192, 2009. URL <http://stacks.iop.org/0067-0049/180/i=1/a=192>.
- [12] Shirasaki Y. et al. Design and Performance of the Wide-Field X-Ray Monitor on Board the High-Energy Transient Explorer 2. *Publ. Astron. Soc. Japan*, 55: 1033–1049, October 2003.
- [13] Swift’s Burst Alert Telescope (BAT), . URL [http://swift.gsfc.nasa.gov/about\\_swift/bat\\_desc.html](http://swift.gsfc.nasa.gov/about_swift/bat_desc.html).
- [14] Dewdney P. E., Turner W., Millenaar R., McCool R., Lazio J., Cornwel T. J. Ska1 system baseline design. *SKA - RfP documentation*, (SKA-TEL-SKO-DD-001):1–98, March 2013. URL [www.skatelescope.org](http://www.skatelescope.org).
- [15] Clark B. G. Coherence in Radio Astronomy. In Taylor G. B., Carilli C. L., Perley R. A., editors, *Synthesis Imaging in Radio Astronomy II*, volume 180 of *Astronomical Society of the Pacific Conference Series*, page 1, 1999.
- [16] Thompson A. R. Fundamentals of Radio Interferometry. In Taylor G. B., Carilli C. L., Perley R. A., editors, *Synthesis Imaging in Radio Astronomy II*, volume 180 of *Astronomical Society of the Pacific Conference Series*, page 11, 1999.
- [17] Taylor G. B., Carilli C. L., Perley R. A., editors. *Synthesis Imaging in Radio Astronomy II*, volume 180 of *Astronomical Society of the Pacific Conference Series*, 1999.
- [18] Chandra P., Frail D. A. A Radio-selected Sample of Gamma-Ray Burst Afterglows. *ApJ*, 746(2):156, 2012. URL <http://stacks.iop.org/0004-637X/746/i=2/a=156>.
- [19] Panaitescu A., Kumar P. Fundamental Physical Parameters of Collimated Gamma-Ray Burst Afterglows. *Astroph. Journal Lett.*, 560:L49–L53, October 2001. doi: 10.1086/324061.
- [20] Yost S. A., Harrison F. A., Sari R., Frail D. A. A Study of the Afterglows of Four Gamma-Ray Bursts: Constraining the Explosion and Fireball Model. *Astroph. Journal*, 597:459–473, November 2003. doi: 10.1086/378288.
- [21] Hancock P. J., Gaensler B. M., Murphy T. Two populations of gamma-ray burst radio afterglows. *Astroph. Journal*, 776(2):106, 2013. URL <http://stacks.iop.org/0004-637X/776/i=2/a=106>.

- [22] Mészáros P., Rees M. J., Wijers R. A. M. J. Viewing Angle and Environment Effects in Gamma-Ray Bursts: Sources of Afterglow Diversity. *Astroph. Journal*, 499:301–308, May 1998. doi: 10.1086/305635.
- [23] Sari R., Piran T., Halpern J. P. Jets in Gamma-Ray Bursts. *Astroph. Journal lett.*, 519:L17–L20, July 1999. doi: 10.1086/312109.
- [24] Chevalier R. A., Li Z.-Y. Wind Interaction Models for Gamma-Ray Burst Afterglows: The Case for Two Types of Progenitors. *Astroph. Journal*, 536:195–212, June 2000. doi: 10.1086/308914.
- [25] Dai Z. G., Cheng K. S. Afterglow Emission from Highly Collimated Jets with Flat Electron Spectra: Application to the GRB 010222 Case? *Astroph. Journal lett.*, 558:L109–L112, September 2001. doi: 10.1086/323566.
- [26] Zhang B., Mészáros P. Gamma-Ray Bursts: progress, problems & prospects. *International Journal of Modern Physics A*, 19:2385–2472, 2004. doi: 10.1142/S0217751X0401746X.
- [27] Sari R., Mészáros P. Impulsive and Varying Injection in Gamma-Ray Burst Afterglows. *Astroph. Journal Lett.*, 535:L33–L37, May 2000. doi: 10.1086/312689.
- [28] Rees M. J., Mészáros P. Refreshed Shocks and Afterglow Longevity in Gamma-Ray Bursts. *Astroph. Journal Lett.*, 496:L1–L4, March 1998. doi: 10.1086/311244.
- [29] Bélanger G. IBIS Observer’s Manual, March 2011. URL [http://integral.esac.esa.int/A09/A09\\_IBIS\\_om.pdf](http://integral.esac.esa.int/A09/A09_IBIS_om.pdf).
- [30] Instruments: JEM-X, . URL <http://sci.esa.int/integral/31175-instruments/?fobjectid=31175&fbodylongid=721>.
- [31] Instruments: OMC, . URL <http://sci.esa.int/integral/31175-instruments/?fobjectid=31175&fbodylongid=722>.
- [32] NASA’s HEASARC. About the Compton Gamma Ray Observatory.
- [33] Parmar A. N. et al. The low-energy concentrator spectrometer on-board the BeppoSAX X-ray astronomy satellite. *Astron. Astrophys. Suppl. Ser.*, 122:309–326, April 1997. doi: 10.1051/aas:1997137.
- [34] Boella G. et al. The medium-energy concentrator spectrometer on board the BeppoSAX X-ray astronomy satellite. *Astron. Astrophys. Suppl. Ser.*, 122:327–340, April 1997. doi: 10.1051/aas:1997138.

- [35] Frontera F. et al. The high energy instrument PDS on-board the BeppoSAX X-ray astronomy satellite. *Astron. Astrophys. Suppl. Ser.*, 122:357–369, April 1997. doi: 10.1051/aas:1997140.
- [36] Jager R. et al. The Wide Field Cameras onboard the BeppoSAX X-ray Astronomy Satellite. *Astron. Astrophys. Suppl. Ser.*, 125:557–572, November 1997. doi: 10.1051/aas:1997243.
- [37] Soft X-ray Camera and Boresight Camera, . URL <http://space.mit.edu/HETE/sxc.html>.
- [38] Wide Field X-ray Monitor , . URL <http://space.mit.edu/HETE/wxm.html>.
- [39] Swift’s X-Ray Telescope (XRT) , . URL [http://swift.gsfc.nasa.gov/about\\_swift/xrt\\_desc.html](http://swift.gsfc.nasa.gov/about_swift/xrt_desc.html).
- [40] Swift’s Ultraviolet/Optical Telescope (UVOT), . URL [http://swift.gsfc.nasa.gov/about\\_swift/uvot\\_desc.html](http://swift.gsfc.nasa.gov/about_swift/uvot_desc.html).
- [41] Tavani M. et al. Science with AGILE, November, 30 2004. URL <http://agile.asdc.asi.it/a-science-27.pdf>.
- [42] GBM Requirements and Capabilities. URL <http://f64.nsstc.nasa.gov/gbm/instrument/description/character.html>.
- [43] Strong I. B., Klebesadel R. W., Olson R. A. A Preliminary Catalog of Transient Cosmic Gamma-Ray Sources Observed by the VELA Satellites. *Astroph. Journal Lett.*, 188:L1, February 1974. doi: 10.1086/181415.
- [44] Norris J. P., Marani G. F., Bonnell J. T. Connection between Energy-dependent Lags and Peak Luminosity in Gamma-Ray Bursts. *Astophysical Journal*, 534:248–257, May 2000. doi: 10.1086/308725.
- [45] Koshut T. M., Paciesas W. S., Kouveliotou C., van Paradijs J., Pendleton G. N., Fishman G. J., Meegan C. A. T<sub>90</sub> as a Measurement of the Duration of GRBs. In *American Astronomical Society Meeting Abstracts #186*, volume 27 of *Bulletin of the American Astronomical Society*, page 886, May 1995.
- [46] Dezalay J.-P., Barat C., Talon R., Syunyaev R., Terekhov O., Kuznetsov A. Short cosmic events - A subset of classical GRBs? In Paciesas W. S., Fishman G. J., editors, *American Institute of Physics Conference Series*, volume 265 of *American Institute of Physics Conference Series*, pages 304–309, 1992.
- [47] Kouveliotou C. et al. Identification of two classes of gamma-ray bursts. *Astroph. Journal Lett.*, 413:L101–L104, August 1993. doi: 10.1086/186969.

- [48] Eichler D., Livio M., Piran T., Schramm D. N. Nucleosynthesis, neutrino bursts and gamma-rays from coalescing neutron stars. *Nature*, 340:126–128, July 1989. doi: 10.1038/340126a0.
- [49] Fryer C. L., Mészáros P. Neutrino-driven Explosions in Gamma-Ray Bursts and Hypernovae. *Astroph. Journal*, 588:L25–L28, May 2003. doi: 10.1086/375412.
- [50] MacFadyen A. I., Woosley S. E. Collapsars: Gamma-Ray Bursts and Explosions in “Failed Supernovae”. *Astroph. Journal*, 524:262–289, October 1999. doi: 10.1086/307790.
- [51] Ruffert M., Janka H.-T., Takahashi K., Schaefer G. Coalescing neutron stars - a step towards physical models. II. Neutrino emission, neutron tori, and gamma-ray bursts. *A&A*, 319:122–153, March 1997.
- [52] Ruffert M., Janka H.-T. Colliding neutron stars. Gravitational waves, neutrino emission, and gamma-ray bursts. *A&A*, 338:535–555, October 1998.
- [53] Blandford R. D., Znajek R. L. Electromagnetic extraction of energy from Kerr black holes. *MNRAS*, 179:433–456, May 1977.
- [54] Li L.-X. Making Clean Energy with a Kerr Black Hole: A Tokamak Model for Gamma-Ray Bursts. *Astroph. Journal*, 544:375–380, November 2000. doi: 10.1086/317215.
- [55] Lee H. K., Wijers R. A. M. J., Brown G. E. The Blandford-Znajek process as a central engine for a gamma-ray burst. *Phys. Rep.*, 325:83–114, 2000. doi: 10.1016/S0370-1573(99)00084-8.
- [56] Mészáros P., Rees M. J. Poynting Jets from Black Holes and Cosmological Gamma-Ray Bursts. *Astroph. Journal Lett.*, 482:L29–L32, June 1997. doi: 10.1086/310692.
- [57] van Putten M. H. P. M. Gamma-ray bursts: LIGO//VIRGO sources of gravitational radiation. *Phys. Rep.*, 345:1–59, April 2001. doi: 10.1016/S0370-1573(01)00014-X.
- [58] Thompson C. A Model of Gamma-Ray Bursts. *MNRAS*, 270:480, October 1994.
- [59] Zhang B. et al. Physical Processes Shaping Gamma-Ray Burst X-Ray Afterglow Light Curves: Theoretical Implications from the Swift X-Ray Telescope Observations. *Astroph. Journal*, 642:354–370, May 2006. doi: 10.1086/500723.
- [60] Nousek J. A. et al. Evidence for a Canonical Gamma-Ray Burst Afterglow Light Curve in the Swift XRT Data. *Astroph. Journal*, 642:389–400, May 2006. doi: 10.1086/500724.

- [61] Fong W. et al. Demographics of the Galaxies Hosting Short-duration Gamma-Ray Bursts. *Astroph. Journal*, 769:56, May 2013. doi: 10.1088/0004-637X/769/1/56.
- [62] Leibler C. N., Berger E. The Stellar Ages and Masses of Short Gamma-ray Burst Host Galaxies: Investigating the Progenitor Delay Time Distribution and the Role of Mass and Star Formation in the Short Gamma-ray Burst Rate. *Astroph. Journal*, 725:1202–1214, December 2010. doi: 10.1088/0004-637X/725/1/1202.
- [63] Nakar E. Short-hard gamma-ray bursts. *Phys. Rep.*, 442:166–236, April 2007. doi: 10.1016/j.physrep.2007.02.005.
- [64] Burrows D. N. et al. Jet Breaks in Short Gamma-Ray Bursts. II. The Collimated Afterglow of GRB 051221A. *Astroph. Journal*, 653:468–473, December 2006. doi: 10.1086/508740.
- [65] Norris J. P., Bonnell J. T. Short Gamma-Ray Bursts with Extended Emission. *ApJ*, 643(1):266, 2006. URL <http://stacks.iop.org/0004-637X/643/i=1/a=266>.
- [66] Proga D., Zhang B. The late time evolution of gamma-ray bursts: ending hyperaccretion and producing flares. *Mon. Not. R. Astron. Soc.*, 370:L61–L65, July 2006. doi: 10.1111/j.1745-3933.2006.00189.x.
- [67] Mészáros P., Rees M. J. Gamma-Ray Bursts. *ArXiv e-prints*, January 2014.
- [68] Rezzolla L., Giacomazzo B., Baiotti L., Granot J., Kouveliotou C., Aloy M. A. The Missing Link: Merging Neutron Stars Naturally Produce Jet-like Structures and Can Power Short Gamma-ray Bursts. *Astrops. Journal Lett.*, 732:L6, May 2011. doi: 10.1088/2041-8205/732/1/L6.
- [69] Bloom J. S., Prochaska J. X. Constraints on the diverse progenitors of grbs from the largescale environments. *AIP Conference Proceedings*, 836(1), 2006.
- [70] Savaglio S., Glazebrook K., Le Borgne D. Grb host studies (ghosts). *AIP Conference Proceedings*, 836(1), 2006.
- [71] Stanek K. Z. et al. Protecting Life in the Milky Way: Metals Keep the GRBs Away. *Acta Astron.*, 56:333–345, December 2006.
- [72] Le Floc'h E. et al. Are the hosts of gamma-ray bursts sub-luminous and blue galaxies? *A&A*, 400:499–510, March 2003. doi: 10.1051/0004-6361:20030001.
- [73] Le Floch E., Charmandaris V., Forrest B., Mirabel F., Armus L., Devost D. Missing grb host galaxies in deep midinfrared observations: implications on the use of grbs as star formation tracers. *AIP Conference Proceedings*, 836(1), 2006.

- [74] Natarajan P., Albanna B., Hjorth J., Ramirez-Ruiz E., Tanvir N., Wijers R. The redshift distribution of gamma-ray bursts revisited. *MNRAS*, 364:L8–L12, November 2005. doi: 10.1111/j.1745-3933.2005.00094.x.
- [75] Ciardi B., Loeb A. Expected Number and Flux Distribution of Gamma-Ray Burst Afterglows with High Redshifts. *Astroph. Journal*, 540:687–696, September 2000. doi: 10.1086/309384.
- [76] Lamb D. Q., Reichart D. E. Gamma-Ray Bursts as a Probe of the Very High Redshift Universe. *Astroph. Journal*, 536:1–18, June 2000. doi: 10.1086/308918.
- [77] Gou L. J., Mészáros P.
- [78] Galama T. J. et al. An unusual supernova in the error box of the  $\gamma$ -ray burst of 25 April 1998. *Nat.*, 395:670–672, October 1998. doi: 10.1038/27150.
- [79] Hjorth J. et al. A very energetic supernova associated with the  $\gamma$ -ray burst of 29 March 2003. *Nat.*, 423:847–850, June 2003. doi: 10.1038/nature01750.
- [80] Malesani D. et al. SN 2003lw and GRB 031203: A Bright Supernova for a Faint Gamma-Ray Burst. *Astroph. Journal Lett.*, 609:L5–L8, July 2004. doi: 10.1086/422684.
- [81] Della Valle M. Supernova and GRB connection: Observations and Questions. In Holt S. S., Gehrels N., Nousek J. A., editors, *Gamma-Ray Bursts in the Swift Era*, volume 836 of *American Institute of Physics Conference Series*, pages 367–379, May 2006. doi: 10.1063/1.2207923.
- [82] Sollerman J. et al. Supernova 2006aj and the associated X-Ray Flash 060218. *Astronom. Astroph.*, 454:503–509, August 2006. doi: 10.1051/0004-6361:20065226.
- [83] Della Valle M. et al. Evidence for supernova signatures in the spectrum of the late-time bump of the optical afterglow of GRB 021211. *Astronom. Astroph.*, 406: L33–L37, July 2003. doi: 10.1051/0004-6361:20030855.
- [84] Soderberg A. M. et al. An HST Search for Supernovae Accompanying X-Ray Flashes. *Astroph. Journal*, 627:877–887, July 2005. doi: 10.1086/430405.
- [85] Della Valle M., Malesani D., Benetti S., Chincarini G., Stella L., Tagliaferri G. Supernova 2005nc and GRB 050525A. *IAU Circ.*, 8696:1, March 2006.
- [86] van Putten M. H. P. M. LIGO/VIRGO Searches for Gravitational Radiation in Hypernovae. *Astroph. Journal Lett.*, 575:L71–L74, August 2002. doi: 10.1086/342781.

- [87] Villasenor J. S. et al. Discovery of the short  $\gamma$ -ray burst GRB 050709. *Nature*, 437:855–858, October 2005. doi: 10.1038/nature04213.
- [88] Ruffini R., Bianco C. L., Fraschetti F., Xue S.-S., Chardonnet P. Relative Space-time Transformations in Gamma-Ray Bursts. *Astroph. Journal Lett.*, 555:L107–L111, July 2001. doi: 10.1086/323175.
- [89] Ruffini R., Bianco C. L., Chardonnet P., Fraschetti F., Vitagliano L., Xue S.-S. New perspectives in physics and astrophysics from the theoretical understanding of Gamma-Ray Bursts. In Novello M., Perez Bergliaffa S. E., editors, *Cosmology and Gravitation*, volume 668 of *American Institute of Physics Conference Series*, pages 16–107, June 2003. doi: 10.1063/1.1587092.
- [90] Berezhiani Z., Bombaci I., Drago A., Frontera F., Lavagno A. Gamma-Ray Bursts from Delayed Collapse of Neutron Stars to Quark Matter Stars. *Astroph. Journal*, 586:1250–1253, April 2003. doi: 10.1086/367756.
- [91] Cheng K. S., Dai Z. G. Conversion of neutron stars to strange stars as a possible origin of  $\gamma$ -ray bursts. *Phys. Rev. Lett.*, 77:1210–1213, Aug 1996. doi: 10.1103/PhysRevLett.77.1210. URL <http://link.aps.org/doi/10.1103/PhysRevLett.77.1210>.
- [92] Drago A., Lavagno A., Parenti I. Burning of a hadronic star into a quark or a hybrid star. *Astroph. Journal*, 659(2):1519, 2007. URL <http://stacks.iop.org/0004-637X/659/i=2/a=1519>.
- [93] Tanvir N. R. et al. A  $\gamma$ -ray burst at a redshift of  $z \sim 8.2$ . *Nature*, 461:1254–1257, October 2009. doi: 10.1038/nature08459.
- [94] Cucchiara A. et al. A Photometric Redshift of  $z \sim 9.4$  for GRB 090429B. *ApJ*, 736:7, July 2011. doi: 10.1088/0004-637X.
- [95] Robertson B. E., Ellis R. S. Connecting the Gamma Ray Burst Rate and the Cosmic Star Formation History: Implications for Reionization and Galaxy Evolution. *Astroph. Journal*, 744:95, January 2012. doi: 10.1088/0004-637X/744/2/95.
- [96] Kistler M. D., Yüksel H., Beacom J. F., Hopkins A. M., Wyithe J. S. B. The Star Formation Rate in the Reionization Era as Indicated by Gamma-Ray Bursts. *Astroph. Journal Lett.*, 705:L104–L108, November 2009. doi: 10.1088/0004-637X/705/2/L104.
- [97] Donaghy T. Q. et al. HETE-2 Localizations and Observations of Four Short Gamma-Ray Bursts: GRBs 010326B, 040802, 051211 and 060121. *ArXiv Astrophysics e-prints*, May 2006.

- [98] Norris J. P., Bonnell J. T. Short Gamma-Ray Bursts with Extended Emission. *Astroph. Journal*, 643:266–275, May 2006. doi: 10.1086/502796.
- [99] Bernardini M. G., Bianco C. L., Caio L., Dainotti M. G., Guida R., Ruffini R. GRB 970228 and a class of GRBs with an initial spikelike emission. *Astron. Astroph.*, 474:L13–L16, October 2007. doi: 10.1051/0004-6361:20078300.
- [100] Dainotti M. G. *The Long Gamma-Ray Bursts and their Connection with Supernovae within the "fireshell model"*. PhD thesis, Università degli studi di Roma "La Sapienza", 2008.
- [101] Barthelmy S. D. et al. An origin for short  $\gamma$ -ray bursts unassociated with current star formation. *Nat.*, 438:994–996, December 2005. doi: 10.1038/nature04392.
- [102] Amati L. The  $E_{p,i}$ - $E_{iso}$  correlation in gamma-ray bursts: updated observational status, re-analysis and main implications. *Mon. Not. R. Astron. Soc.*, 372:233–245, October 2006. doi: 10.1111/j.1365-2966.2006.10840.x.
- [103] Burrows D. N. et al. Relativistic jet activity from the tidal disruption of a star by a massive black hole. *Nature*, 476:421–424, August 2011. doi: 10.1038/nature10374.
- [104] Cavallo G., Rees M. J. A qualitative study of cosmic fireballs and gamma-ray bursts. *Mon. Not. R. Astron. Soc.*, 183:359–365, May 1978.
- [105] Shemi A., Piran T. The appearance of cosmic fireballs. *Astrophys. J. Lett.*, 365: L55–L58, December 1990. doi: 10.1086/185887.
- [106] Paczynski B. Gamma-ray bursters at cosmological distances. *Astrophys. J. Lett.*, 308:L43–L46, September 1986. doi: 10.1086/184740.
- [107] Goodman J. Are gamma-ray bursts optically thick? *Astrophys. J. Lett.*, 308:L47–L50, September 1986. doi: 10.1086/184741.
- [108] Paczynski B. Super-Eddington winds from neutron stars. *Astrophys. J.*, 363: 218–226, November 1990. doi: 10.1086/169332.
- [109] Harding A. K., Baring M. G. Escape of High-Energy Photons from Relativistically Expanding Gamma-Ray Burst Sources. In Fishman G. J., editor, *Gamma-Ray Bursts*, volume 307 of *American Institute of Physics Conference Series*, page 520, 1994.
- [110] Mészáros P. Gamma-Ray Burst Models: General Requirements and Predictions. In Böhringer H., Morfill G. E., Trümper J. E., editors, *Seventeenth Texas Symposium on Relativistic Astrophysics and Cosmology*, volume 759 of *Annals of the New York Academy of Sciences*, page 440, 1995. doi: 10.1111/j.1749-6632.1995.tb17581.x.

- [111] Lyutikov M. The electromagnetic model of gamma-ray bursts. *New Journal of Physics*, 8:119, July 2006. doi: 10.1088/1367-2630/8/7/119.
- [112] Rybicki G. B., Lightman A. P. *Radiative processes in astrophysics*. 1979.
- [113] Paczynski B. Cosmological gamma-ray bursts. *Acta Astron.*, 41:257–267, 1991.
- [114] Mészáros P., Laguna P., Rees M. J. Gasdynamics of relativistically expanding gamma-ray burst sources - Kinematics, energetics, magnetic fields, and efficiency. *Astroph. Journal*, 415:181–190, September 1993. doi: 10.1086/173154.
- [115] Rees M. J., Meszaros P. Relativistic fireballs - Energy conversion and time-scales. *MNRAS*, 258:41P–43P, September 1992.
- [116] Rees M. J., Meszaros P. Unsteady outflow models for cosmological gamma-ray bursts. *Astroph. Journal Lett.*, 430:L93–L96, August 1994. doi: 10.1086/187446.
- [117] Meszaros P., Rees M. J. Relativistic fireballs and their impact on external matter - Models for cosmological gamma-ray bursts. *Astroph. Journal*, 405:278–284, March 1993. doi: 10.1086/172360.
- [118] Meszaros P., Rees M. J. Gamma-Ray Bursts: Multiwaveband Spectral Predictions for Blast Wave Models. *Astroph. Journal Lett.*, 418:L59, December 1993. doi: 10.1086/187116.
- [119] Achterberg A., Gallant Y. A., Kirk J. G., Guthmann A. W. Particle acceleration by ultrarelativistic shocks: theory and simulations. *Mon. Not. R. Astron. Soc.*, 328:393–408, December 2001. doi: 10.1046/j.1365-8711.2001.04851.x.
- [120] Blandford R., Eichler D. Particle acceleration at astrophysical shocks: A theory of cosmic ray origin. *Phys. Rep.*, 154:1–75, October 1987. doi: 10.1016/0370-1573(87)90134-7.
- [121] Ellison D. C., Double G. P. Nonlinear particle acceleration in relativistic shocks. *Astroparticle Physics*, 18:213–228, December 2002. doi: 10.1016/S0927-6505(02)00142-1.
- [122] Keshet U., Waxman E. Energy Spectrum of Particles Accelerated in Relativistic Collisionless Shocks. *Physical Review Letters*, 94(11):111102, March 2005. doi: 10.1103/PhysRevLett.94.111102.
- [123] Lemoine M., Pelletier G. Particle Transport in Tangled Magnetic Fields and Fermi Acceleration at Relativistic Shocks. *Astroph. Journal Lett.*, 589:L73–L76, June 2003. doi: 10.1086/376353.

- [124] Sokolov I. V., Roussev I. I., Fisk L. A., Lee M. A., Gombosi T. I., Sakai J. I. Diffusive Shock Acceleration Theory Revisited. *Astroph. Journal Lett.*, 642:L81–L84, May 2006. doi: 10.1086/504406.
- [125] Baring M. G., Braby M. L. A Study of Prompt Emission Mechanisms in Gamma-Ray Bursts. *Astroph. Journal*, 613:460–476, September 2004. doi: 10.1086/422867.
- [126] Hededal C. B., Haugbølle T., Frederiksen J. T., Nordlund Å. Non-Fermi Power-Law Acceleration in Astrophysical Plasma Shocks. *Astroph. Journal Lett.*, 617:L107–L110, December 2004. doi: 10.1086/427387.
- [127] Rieger F. M., Duffy P. Particle Acceleration in Gamma-Ray Burst Jets. *Astroph. Journal Lett.*, 632:L21–L24, October 2005. doi: 10.1086/497634.
- [128] Meszaros P., Rees M. J., Papathanassiou H. Spectral properties of blast-wave models of gamma-ray burst sources. *Astroph. Journal*, 432:181–193, September 1994. doi: 10.1086/174559.
- [129] Bykov A. M., Meszaros P. Electron Acceleration and Efficiency in Nonthermal Gamma-Ray Sources. *Astroph. Journal Lett.*, 461:L37, April 1996. doi: 10.1086/309999.
- [130] Rybicki G. B., Lightman A. P. *Radiative processes in astrophysics*. 1979.
- [131] Dermer C. D., Chiang J., Mitman K. E. Beaming, Baryon Loading, and the Synchrotron Self-Compton Component in Gamma-Ray Bursts. *Astroph. Journal*, 537:785–795, July 2000. doi: 10.1086/309061.
- [132] Sari R., Esin A. A. On the Synchrotron Self-Compton Emission from Relativistic Shocks and Its Implications for Gamma-Ray Burst Afterglows. *Astroph. Journal*, 548:787–799, February 2001. doi: 10.1086/319003.
- [133] Palmer D. M. et al. A giant  $\gamma$ -ray flare from the magnetar SGR 1806 - 20. *Nature*, 434:1107–1109, April 2005. doi: 10.1038/nature03525.
- [134] Ghisellini G., Celotti A. Quasi-thermal Comptonization and Gamma-Ray Bursts. *Astroph. Journal Lett.*, 511:L93–L96, February 1999. doi: 10.1086/311845.
- [135] Sari R., Piran T., Narayan R. Spectra and Light Curves of Gamma-Ray Burst Afterglows. *Astroph. Journal Lett.*, 497:L17–L20, April 1998. doi: 10.1086/311269.
- [136] Mannheim K., Protheroe R. J., Rachen J. P. Cosmic ray bound for models of extragalactic neutrino production. *Phys. Rev. D*, 63(2):023003, January 2001. doi: 10.1103/PhysRevD.63.023003.

- [137] Li Z.-Y., Chevalier R. A. Wind Interaction Models for the Afterglows of GRB 991208 and GRB 000301C. *Astroph. Journal*, 551:940–945, April 2001. doi: 10.1086/320239.
- [138] Eichler D., Levinson A. A Compact Fireball Model of Gamma-Ray Bursts. *Astroph. Journal*, 529:146–150, January 2000. doi: 10.1086/308245.
- [139] Preece R. D., Briggs M. S., Mallozzi R. S., Pendleton G. N., Paciesas W. S., Band D. L. The BATSE Gamma-Ray Burst Spectral Catalog. I. High Time Resolution Spectroscopy of Bright Bursts Using High Energy Resolution Data. *Astroph. Journal, Suppl.*, 126:19–36, January 2000. doi: 10.1086/313289.
- [140] Rossi E. M., Beloborodov A. M., Rees M. J. Neutron-loaded outflows in gamma-ray bursts. *Monthly Notices of the Royal Astronomical Society*, 369(4): 1797–1807, 2006. doi: 10.1111/j.1365-2966.2006.10417.x. URL <http://mnras.oxfordjournals.org/content/369/4/1797.abstract>.
- [141] Rosswog S., Ramirez-Ruiz E., Davies M. B. High-resolution calculations of merging neutron stars - III. Gamma-ray bursts. *Mon. Not. R. Astron. Soc.*, 345:1077–1090, November 2003. doi: 10.1046/j.1365-2966.2003.07032.x.
- [142] Proga D. On Magnetohydrodynamic Jet Production in the Collapsing and Rotating Envelope. *Astroph. Journal*, 629:397–402, August 2005. doi: 10.1086/431276.
- [143] Panaiteescu A., Mészáros P. Gamma-Ray Bursts from Upscattered Self-absorbed Synchrotron Emission. *Astroph. Journal Lett.*, 544:L17–L21, November 2000. doi: 10.1086/317301.
- [144] Panaiteescu A., Mészáros P. Simulations of Gamma-Ray Bursts from External Shocks: Time Variability and Spectral Correlations. *Astroph. Journal*, 492:683–695, January 1998. doi: 10.1086/305056.
- [145] Rau A., Greiner J., Schwarz R. Constraining the GRB collimation with a survey for orphan afterglows. *Astron. and Astroph.*, 449:79–88, April 2006. doi: 10.1051/0004-6361:20054317.
- [146] Panaiteescu A., Mészáros P. Radiative Regimes in Gamma-Ray Bursts and Afterglows. *Astroph. Journal*, 501:772–779, July 1998. doi: 10.1086/305856.
- [147] Panaiteescu A., Mészáros P. Rings in Fireball Afterglows. *Astroph. Journal Lett.*, 493:L31–L34, January 1998. doi: 10.1086/311127.
- [148] Amati L. et al. Intrinsic spectra and energetics of BeppoSAX Gamma-Ray Bursts with known redshifts. *A&A*, 390:81–89, July 2002. doi: 10.1051/0004-6361:20020722.

- [149] Ghirlanda G., Magliocchetti M., Ghisellini G., Guzzo L. On the correlation of short gamma-ray bursts and clusters of galaxies. *Mon. Not. R. Astron. Soc.*, 368: L20–L24, May 2006. doi: 10.1111/j.1745-3933.2006.00147.x.
- [150] Spruit H. C. Gamma-ray bursts from X-ray binaries. *A&A*, 341:L1–L4, January 1999.
- [151] Metzger M. R. et al. Spectral constraints on the redshift of the optical counterpart to the  $\gamma$ -ray burst of 8 May 1997. *Nature*, 387:878–880, June 1997. doi: 10.1038/43132.
- [152] Mészáros P. Gamma-Ray Burst Models: General Requirements and Predictions. In Böhringer H., Morfill G. E., Trümper J. E., editors, *Seventeenth Texas Symposium on Relativistic Astrophysics and Cosmology*, volume 759 of *Annals of the New York Academy of Sciences*, page 440, 1995. doi: 10.1111/j.1749-6632.1995.tb17581.x.
- [153] Dermer C. D. External Shock Interactions of GRB Blast Waves and the Swift Observations. In Holt S. S., Gehrels N., Nousek J. A., editors, *Gamma-Ray Bursts in the Swift Era*, volume 836 of *American Institute of Physics Conference Series*, pages 97–102, May 2006. doi: 10.1063/1.2207865.
- [154] Spitkovsky A. Simulations of relativistic collisionless shocks: shock structure and particle acceleration. *AIP Conference Proceedings*, 801(1), 2005.
- [155] Wheeler J. C., Yi I., Höflich P., Wang L. Asymmetric Supernovae, Pulsars, Magnetars, and Gamma-Ray Bursts. *Astroph. Journal*, 537:810–823, July 2000. doi: 10.1086/309055.
- [156] Castro-Tirado A. J. et al. Decay of the GRB 990123 Optical Afterglow: Implications for the Fireball Model. *Science*, 283:2069, March 1999. doi: 10.1126/science.283.5410.2069.
- [157] Derishev E. V., Kocharovsky V. V., Kocharovsky V. V. The Neutron Component in Fireballs of Gamma-Ray Bursts: Dynamics and Observable Imprints. *Astroph. Journal*, 521:640–649, August 1999. doi: 10.1086/307574.
- [158] Nousek J. A. et al. Evidence for a canonical gamma-ray burst afterglow light curve in the swift xrt data. *Astrophysical Journal*, 642(1):389, 2006. URL <http://stacks.iop.org/0004-637X/642/i=1/a=389>.
- [159] Retter A. et al. GRB 050813: possible short Swift-BAT GRB. *GRB Coordinates Network*, 3788:1, 2005.
- [160] Dado S., Dar A., De Rújula A. On the optical and X-ray afterglows of gamma ray bursts. *A&A*, 388:1079–1105, June 2002. doi: 10.1051/0004-6361:20020537.

- [161] Dar A., de Rújula A. Towards a complete theory of gamma-ray bursts. *Phys. Rep.*, 405:203–278, December 2004. doi: 10.1016/j.physrep.2004.09.008.
- [162] Sari R. Hydrodynamics of Gamma-Ray Burst Afterglow. *Astroph. Journal Lett.*, 489:L37–L40, November 1997. doi: 10.1086/310957.
- [163] Waxman E. Angular Size and Emission Timescales of Relativistic Fireballs. *Astroph. Journal Lett.*, 491:L19–L22, December 1997. doi: 10.1086/311057.
- [164] Mészáros P., Rees M. J. Optical and Long-Wavelength Afterglow from Gamma-Ray Bursts. *Astroph. Journal*, 476:232–237, February 1997.
- [165] Paczyński B., Rhoads J. E. Radio Transients from Gamma-Ray Bursters. *Astroph. Journal Lett.*, 418:L5, November 1993. doi: 10.1086/187102.
- [166] Katz J. I. Radio and optical emission: Spectral shapes and breaks in GRB. In Fishman G. J., editor, *Gamma-Ray Bursts*, volume 307 of *American Institute of Physics Conference Series*, page 529, January 1994.
- [167] Katz J. I., Piran T. Persistent Counterparts to Gamma-Ray Bursts. *Astroph. Journal*, 490:772–778, December 1997.
- [168] Waxman E. Gamma-Ray-Burst Afterglow: Supporting the Cosmological Fireball Model, Constraining Parameters, and Making Predictions. *Astroph. Journal Lett.*, 485:L5–L8, August 1997. doi: 10.1086/310809.
- [169] Waxman E.  $\gamma$ -Ray Burst Afterglow: Confirming the Cosmological Fireball Model. *Astroph. Journal Lett.*, 489:L33–L36, November 1997. doi: 10.1086/310960.
- [170] van Paradijs J., Kouveliotou C., Wijers R. A. M. J. Gamma-Ray Burst Afterglows. *Annu. Rev. Astron. Astroph.*, 38:379–425, 2000. doi: 10.1146/annurev.astro.38.1.379.
- [171] Dai Z. G., Lu T. The Afterglow of GRB 990123 and a Dense Medium. *Astroph. Journal Lett.*, 519:L155–L158, July 1999. doi: 10.1086/312127.
- [172] Livio M., Waxman E. Toward a Model for the Progenitors of Gamma-Ray Bursts. *Astroph. Journal*, 538:187–191, July 2000. doi: 10.1086/309120.
- [173] Wijers R. A. M. J., Rees M. J., Meszaros P. Shocked by GRB 970228: the afterglow of a cosmological fireball. *Mon. Not. R. Astron. Soc.*, 288:L51–L56, July 1997.
- [174] Wijers R. A. M. J., Galama T. J. Physical Parameters of GRB 970508 and GRB 971214 from Their Afterglow Synchrotron Emission. *Astroph. Journal*, 523:177–186, September 1999. doi: 10.1086/307705.

- [175] Lazzati D., Begelman M. C. Universal GRB Jets from Jet-Cocoon Interaction in Massive Stars. *Astroph. Journal*, 629:903–907, August 2005. doi: 10.1086/430877.
- [176] Matzner C. D. Supernova hosts for gamma-ray burst jets: dynamical constraints. *MNRAS*, 345:575–589, October 2003. doi: 10.1046/j.1365-8711.2003.06969.x.
- [177] Mészáros P., Rees M. J. Collapsar Jets, Bubbles, and Fe Lines. *Astroph. Journal Lett.*, 556:L37–L40, July 2001. doi: 10.1086/322934.
- [178] Waxman E., Mészáros P. Collapsar Uncorking and Jet Eruption in Gamma-Ray Bursts. *Astroph. Journal*, 584:390–398, February 2003. doi: 10.1086/345536.
- [179] Peer A., Mészáros P.
- [180] Aloy M. A., Müller E., Ibáñez J. M., Martí J. M., MacFadyen A. Relativistic Jets from Collapsars. *Astroph. Journal Lett.*, 531:L119–L122, March 2000. doi: 10.1086/312537.
- [181] Scully S., Stecker F. On the spectrum of ultrahigh energy cosmic rays and the -ray burst origin hypothesis. *Astroparticle Physics*, 16(3):271 – 276, 2002. ISSN 0927-6505. doi: [http://dx.doi.org/10.1016/S0927-6505\(01\)00133-5](http://dx.doi.org/10.1016/S0927-6505(01)00133-5). URL <http://www.sciencedirect.com/science/article/pii/S0927650501001335>.
- [182] INTEGRAL: The INTERNational Gamma-Ray Astrophysics Laboratory. A project of the European Space Agency , .
- [183] INTEGRAL Scientific Payload. URL [http://integral.esac.esa.int/integ\\_payload.html](http://integral.esac.esa.int/integ_payload.html).
- [184] Roques J.-P., Diehl R. Spectrometer SPI. URL [http://integral.esac.esa.int/integ\\_payload\\_spectro.html](http://integral.esac.esa.int/integ_payload_spectro.html).
- [185] NASA. Appendix G to the NASA RESEARCH ANNOUNCEMENT for the COMPTON GAMMA RAY OBSERVATORY GUEST INVESTIGATOR PROGRAM. URL [http://heasarc.nasa.gov/docs/cgro/nra/appendix\\_g.html](http://heasarc.nasa.gov/docs/cgro/nra/appendix_g.html).
- [186] HEASARC. The burst and transient source experiment (batse), . URL <http://heasarc.gsfc.nasa.gov/docs/cgro/cgro/batse.html>.
- [187] The Imaging Compton Telescope (COMPTEL). URL <http://heasarc.gsfc.nasa.gov/docs/cgro/cgro/comptel.html>.
- [188] Schoenfelder V. et al. Instrument description and performance of the Imaging Gamma-Ray Telescope COMPTEL aboard the Compton Gamma-Ray Observatory. *"Astroph. Jour. Supp. Ser."*, 86:657–692, June 1993. doi: 10.1086/191794.

- [189] HEASARC. The energetic gamma ray experiment telescope (egret), . URL <http://heasarc.gsfc.nasa.gov/docs/cgro/cgro/egret.html>.
- [190] HEASARC. The oriented scintillation spectrometer experiment (osse), . URL <http://heasarc.gsfc.nasa.gov/docs/cgro/cgro/osse.html>.
- [191] Manzo G., Giarrusso S., Santangelo A., Ciralli F., Fazio G., Piraino S., Segreto A. The high pressure gas scintillation proportional counter on-board the BeppoSAX X-ray astronomy satellite. *Astron. Astrophys. Suppl. Ser.*, 122:341–356, April 1997. doi: 10.1051/aas:1997139.
- [192] Citterio O., Conti G., Mattaini E., Sacco B., Santambrogio E. Optics for X-ray concentrators on board of the Astronomy Satellite SAX, 1986. URL <http://dx.doi.org/10.1117/12.966567>.
- [193] Conti G. et al. X-ray characteristics of the Italian X-Ray Astronomy Satellite (SAX) flight mirror units, 1994. URL <http://dx.doi.org/10.1117/12.193179>.
- [194] Boella G., Butler R. C., Perola G. C., Piro L., Scarsi L., Bleeker J. A. M. BeppoSAX, the wide band mission for X-ray astronomy. *A&AS*, 122:299–307, April 1997. doi: 10.1051/aas:1997136.
- [195] Manzo G., Davelaar J., Peacock A., Andresen R., Taylor B. A fluorescent gated gas scintillation proportional counter for high energy X-ray spectroscopy. *Nuclear Instruments and Methods*, 177(2–3):595–603, 1980. ISSN 0029-554X. doi: 10.1016/0029-554X(80)90078-6. URL <http://www.sciencedirect.com/science/article/pii/0029554X80900786>.
- [196] Gedanken A., Jortner J., Raz B., Szöke A. Electronic Energy Transfer Phenomena in Rare Gases. *The Journal of Chemical Physics*, 57(8):3456–3469, 1972. doi: 10.1063/1.1678779. URL <http://scitation.aip.org/content/aip/journal/jcp/57/8/1.1063/1.1678779>.
- [197] About the Swift Gamma-Ray Burst Mission. URL [http://swift.gsfc.nasa.gov/about\\_swift/#science](http://swift.gsfc.nasa.gov/about_swift/#science).
- [198] Barthelmy S. D. et al. The Burst Alert Telescope (BAT) on the SWIFT Midex Mission. *Space Science Rev.*, 120:143–164, October 2005. doi: 10.1007/s11214-005-5096-3.
- [199] Barthelmy S. D. Burst Alert Telescope (BAT) on the Swift MIDEX mission. In Flanagan K. A., Siegmund O. H., editors, *X-Ray and Gamma-Ray Instrumentation for Astronomy XI*, volume 4140 of *Society of Photo-Optical Instrumentation Engineers (SPIE) Conference Series*, pages 50–63, December 2000.

- [200] Burrows D. N. et al. Swift X-Ray Telescope. In Flanagan K. A., Siegmund O. H., editors, *X-Ray and Gamma-Ray Instrumentation for Astronomy XI*, volume 4140 of *Society of Photo-Optical Instrumentation Engineers (SPIE) Conference Series*, pages 64–75, December 2000.
- [201] Hill J. E. et al. Laboratory x-ray CCD camera electronics: a test bed for the Swift X-Ray Telescope. In Flanagan K. A., Siegmund O. H., editors, *X-Ray and Gamma-Ray Instrumentation for Astronomy XI*, volume 4140 of *Society of Photo-Optical Instrumentation Engineers (SPIE) Conference Series*, pages 87–98, December 2000.
- [202] AGILE Mission Overview. URL <http://agile.asdc.asi.it/overview.html>.
- [203] Tavani M. et al. The AGILE mission and its scientific instrument. In *Society of Photo-Optical Instrumentation Engineers (SPIE) Conference Series*, volume 6266 of *Society of Photo-Optical Instrumentation Engineers (SPIE) Conference Series*, July 2006. doi: 10.1117/12.673207.
- [204] Barbiellini G. et al. The AGILE scientific instrument. In Ritz S., Gehrels N., Shrader C. R., editors, *Gamma 2001: Gamma-Ray Astrophysics*, volume 587 of *American Institute of Physics Conference Series*, pages 774–778, October 2001. doi: 10.1063/1.1419498.
- [205] Fermi Spacecraft and Instruments - Fermi Instruments , . URL [http://www.nasa.gov/mission\\_pages/GLAST/spacecraft/index.html](http://www.nasa.gov/mission_pages/GLAST/spacecraft/index.html).
- [206] The Fermi LAT instrument. URL <http://www-glast.stanford.edu/instrument.html>.
- [207] The SKA Organization. The History of the SKA Project. [www.skatelescope.org](http://www.skatelescope.org/), ”The History of the SKA Project”, 2013. URL <http://www.skatelescope.org/project/history-of-the-skaproject>.
- [208] Carilli C. L., Rawlings S. Motivation, key science projects, standards and assumptions. *New Astronomy Reviews*, 48:979–984, December 2004. doi: 10.1016/j.newar.2004.09.001.
- [209] Staley T. D. et al. Automated rapid follow-up of Swift gamma-ray burst alerts at 15 GHz with the AMI Large Array. *MNRAS*, 428:3114–3120, February 2013. doi: 10.1093/mnras/sts259.
- [210] Anderson G. E. et al. Probing the bright radio flare and afterglow of GRB 130427A with the Arcminute Microkelvin Imager. *MNRAS*, 440:2059–2065, May 2014. doi: 10.1093/mnras/stu478.

- [211] Ghirlanda G., Burlon D., Ghisellini G., Salvaterra R., Bernardini M., et al. GRB orphan afterglows in present and future radio transient surveys. 2014.
- [212] Feretti L., Prandoni I., Brunetti G., Burigana C., Capetti A., Della Valle M., Ferrara A., Ghirlanda G., Govoni F., Molinari S., A. P., Scaramella R., Testi L., Tozzi P., Umana G., Wolter A., editors. *Italian SKA White Book*. INAF Press, Rome, 2014. ISBN ISBN 978-88-98985-00-5.
- [213] Capozziello S., De Laurentis M., Ruggeri A. C. Dark energy observational tests and the SKA perspective. In Feretti L., Prandoni I., Brunetti G., Burigana C., Capetti A., Della Valle M., Ferrara A., Ghirlanda G., Govoni F., Molinari S., A. P., Scaramella R., Testi L., Tozzi P., Umana G., Wolter A., editors, *Italian SKA White Book*. INAF Press, 2014. ISBN ISBN 978-88-98985-00-5.
- [214] Amati L., Ruggeri A., Stratta G., Capozziello S., De Laurentis M., Della Valle M., Luongo O. The SKA contribution to GRB cosmology. *Science with the Square Kilometre Array*, Accepted.
- [215] Cornwell T., Braun R., Briggs D. S. Deconvolution. In Taylor G. B., Carilli C. L., Perley R. A., editors, *Synthesis Imaging in Radio Astronomy II*, volume 180 of *Astronomical Society of the Pacific Conference Series*, page 151, 1999.
- [216] Frail D. A. et al. An Energetic Afterglow from a Distant Stellar Explosion. *Astroph. Journal Lett.*, 646:L99–L102, August 2006. doi: 10.1086/506934.
- [217] Frail D. A. The Radio Afterglows of Gamma-Ray Bursts. In Marcaide J.-M., Weiler K. W., editors, *IAU Colloq. 192: Cosmic Explosions, On the 10th Anniversary of SN1993J*, page 451, 2005. doi: 10.1007/3-540-26633-X\_61.
- [218] Racusin J. L. et al. Jet Breaks and Energetics of Swift Gamma-Ray Burst X-Ray Afterglows. *Astroph. Journal*, 698:43–74, June 2009. doi: 10.1088/0004-637X/698/1/43.
- [219] Bloom J. S., Frail D. A., Sari R. The Prompt Energy Release of Gamma-Ray Bursts using a Cosmological k-Correction. *Astron. Journal*, 121:2879–2888, June 2001. doi: 10.1086/321093.
- [220] Frail D. A. et al. Beaming in Gamma-Ray Bursts: Evidence for a Standard Energy Reservoir. *Astroph. Journal Lett.*, 562:L55–L58, November 2001. doi: 10.1086/338119.
- [221] Nysewander M., Fruchter A. S., Pe'er A. A Comparison of the Afterglows of Short- and Long-duration Gamma-ray Bursts. *Astroph. Journal*, 701:824–836, August 2009. doi: 10.1088/0004-637X/701/1/824.

- [222] Gehrels N. et al. Correlations of Prompt and Afterglow Emission in Swift Long and Short Gamma-Ray Bursts. *Astroph. Journal*, 689:1161–1172, December 2008. doi: 10.1086/592766.
- [223] de Pasquale M. et al. The BeppoSAX catalog of GRB X-ray afterglow observations. *A&A*, 455:813–824, September 2006. doi: 10.1051/0004-6361:20053950.
- [224] Sakamoto T. et al. The First Swift BAT Gamma-Ray Burst Catalog. *Astrop. Journal Suppl. Series*, 175:179–190, March 2008. doi: 10.1086/523646.
- [225] Sakamoto T. et al. The Second Swift Burst Alert Telescope Gamma-Ray Burst Catalog. *Astrop. Journal Suppl. Series*, 195:2, July 2011. doi: 10.1088/0067-0049/195/1/2.
- [226] Evans P. A. et al. An online repository of Swift/XRT light curves of  $\gamma$ -ray bursts. *A&A*, 469:379–385, July 2007. doi: 10.1051/0004-6361:20077530.
- [227] Schlegel D. J., Finkbeiner D. P., Davis M. Maps of Dust Infrared Emission for Use in Estimation of Reddening and Cosmic Microwave Background Radiation Foregrounds. *Astrop. Journal*, 500:525–553, June 1998. doi: 10.1086/305772.
- [228] Berger E., Kulkarni S. R., Frail D. A. The Nonrelativistic Evolution of GRBs 980703 and 970508: Beaming-independent Calorimetry. *Astroph. Journal*, 612: 966–973, September 2004. doi: 10.1086/422809.
- [229] van der Horst A. J. et al. Detailed study of the GRB 030329 radio afterglow deep into the non-relativistic phase. *A&A*, 480:35–43, March 2008. doi: 10.1051/0004-6361:20078051.
- [230] Hancock P. J., Gaensler B. M., Murphy T. Visibility Stacking in the Quest for Type Ia Supernova Radio Emission. *Astroph. Journal Lett.*, 735:L35, July 2011. doi: 10.1088/2041-8205/735/2/L35.
- [231] White R. L., Helfand D. J., Becker R. H., Glikman E., de Vries W. Signals from the Noise: Image Stacking for Quasars in the FIRST Survey. *Astrop. Journal*, 654:99–114, January 2007. doi: 10.1086/507700.
- [232] Piran T. Gamma-ray bursts and the fireball model. *Phys. Rep.*, 314:575–667, June 1999. doi: 10.1016/S0370-1573(98)00127-6.
- [233] Komissarov S. S. Shock dissipation in magnetically dominated impulsive flows. *Mon. Not. R. Astron. Soc.*, 422:326–346, May 2012. doi: 10.1111/j.1365-2966.2012.20609.x.

- [234] Zhang B. Open questions in GRB physics. *Comptes Rendus Physique*, 12:206–225, April 2011. doi: 10.1016/j.crhy.2011.03.004.
- [235] Ruggeri A. C., Dainotti M. G., Capozziello S. Possible detection of Gamma Ray Bursts in the radio band by the Square Kilometre Array. *Mon. Not. R. Astron. Soc.*, Submitted, 2015.
- [236] Galli, M. et al. Agile mini-calorimeter gamma-ray burst catalog. *A&A*, 553:A33, 2013. doi: 10.1051/0004-6361/201220833. URL <http://dx.doi.org/10.1051/0004-6361/201220833>.
- [237] Pal’shin V. D. et al. Interplanetary network localizations of konus short gamma-ray bursts. *ApJS*, 207(2):38, 2013. URL <http://stacks.iop.org/0067-0049/207/i=2/a=38>.
- [238] Longo, F. et al. Upper limits on the high-energy emission from gamma-ray bursts observed by agile-grid. *A&A*, 547:A95, 2012. doi: 10.1051/0004-6361/201016238. URL <http://dx.doi.org/10.1051/0004-6361/201016238>.
- [239] Hurley K. et al. The interplanetary network supplement to the fermi gbm catalog of cosmic gamma-ray bursts. *ApJS*, 207(2):39, 2013. doi: 10.1088/0067-0049/207/2/39. URL <http://stacks.iop.org/0067-0049/207/i=2/a=39>.
- [240] Frontera F. et al. The Gamma-Ray Burst Catalog Obtained with the Gamma-Ray Burst Monitor Aboard BeppoSAX. *ApJS*, 180:192–223, January 2009. doi: 10.1088/0067-0049.
- [241] Stern B. E., Tikhomirova Y., Kompaneets D., Svensson R., Poutanen J. An Off-Line Scan of the BATSE Daily Records and a Large Uniform Sample of Gamma-Ray Bursts. *ApJ*, 563(1):80, 2001. URL <http://stacks.iop.org/0004-637X/563/i=1/a=80>.
- [242] Kommers J. M., Lewin W. H. G., Kouveliotou C., van Paradijs J., Pendleton G. N., Meegan C. A., Fishman G. J. A Nontriggered Burst Supplement to the BATSE Gamma-Ray Burst Catalogs. *ApJS*, 134:385–454, June 2001. doi: 10.1086/320856.
- [243] Schönfelder V. et al. The first COMPTEL source catalogue. *Astron. Astrophys. Suppl. Ser.*, 143(2):145–179, 2000. doi: 10.1051/aas:2000101. URL <http://dx.doi.org/10.1051/aas:2000101>.
- [244] Meegan C. A. et al. The 4b batse gamma-ray burst catalog. *AIP Conference Proc.*, 428(1), 1998.
- [245] Meegan C. A. et al. The Third BATSE Gamma-Ray Burst Catalog. *ApJS*, 106:65, September 1996. doi: 10.1086/192329.

- [246] Paciesas W. S. et al. The Fermi GBM Gamma-Ray Burst Catalog: The First Two Years. *ApJS*, 199(1):18, 2012. URL <http://stacks.iop.org/0067-0049/199/i=1/a=18>.
- [247] von Kienlin A. et al. The Second Fermi GBM Gamma-Ray Burst Catalog: The First Four Years. *ApJS*, 211(1):13, 2014. URL <http://stacks.iop.org/0067-0049/211/i=1/a=13>.
- [248] Gruber D. et al. The fermi gbm gamma-ray burst spectral catalog: Four years of data. *ApJS*, 211(1):12, 2014. URL <http://stacks.iop.org/0067-0049/211/i=1/a=12>.
- [249] Goldstein A. et al. The fermi gbm gamma-ray burst spectral catalog: The first two years. *ApJS*, 199(1):19, 2012. URL <http://stacks.iop.org/0067-0049/199/i=1/a=19>.
- [250] Minaev P. Y., Pozanenko A. S., Molkov S. V., Grebenev S. A. Catalog of Short Gamma-Ray Transients Detected in the SPI/INTEGRAL Experiment. *ArXiv e-prints*, 1405.3784, May 2014.
- [251] Bošnjak, Ž., Götz, D., Bouchet, L., Schanne, S., Cordier, B. The spectral catalogue of integral gamma-ray bursts. *A&A*, 561:A25, 2014. doi: 10.1051/0004-6361/201322256. URL <http://dx.doi.org/10.1051/0004-6361/201322256>.
- [252] Mereghetti S. Ten years of the INTEGRAL Burst Alert System (IBAS). *ArXiv e-prints*, 1302.5347, February 2013.
- [253] Sakamoto T. et al. The Second Swift Burst Alert Telescope Gamma-Ray Burst Catalog. *ApJS*, 195(1):2, 2011. URL <http://stacks.iop.org/0067-0049/195/i=1/a=2>.
- [254] Hurley K. et al. The ULYSSES Supplement to the BATSE 3B Catalog of Cosmic Gamma-Ray Bursts. *ApJS*, 120(2):399, 1999. URL <http://stacks.iop.org/0067-0049/120/i=2/a=399>.
- [255] Terekhov O. V. et al. A catalog of cosmic gamma-ray bursts registered by the PHEBUS instrument of the GRANAT Observatory, December 1989-May 1991. *Astronomy Letters*, 20:265–299, May 1994.
- [256] Terekhov O. V. et al. Catalog of cosmic gamma-ray bursts detected with the PHOEBUS instrument aboard the GRANAT observatory between June 1991 and December 1992. *Astronomy Letters*, 21:73–98, January 1995.

- [257] Tkachenko A. Y. et al. A catalog of cosmic gamma-ray bursts recorded by PHEBUS/Granat: January 1993-September 1994. *Astronomy Letters*, 24:722–741, November 1998.
- [258] Tkachenko A. Y., Terekhov O. V., Sunyaev R. A., Kuznetsov A. V., Barat C., Dezelay J.-P., Vedrenne G. A Catalog of Cosmic Gamma-Ray Bursts Detected by the PHEBUS Instrument on the Granat Observatory: October 1994-December 1996. *Astronomy Letters*, 28:353–365, June 2002. doi: 10.1134/1.1484135.
- [259] Millenaar R. P., Bolton R. C. Figures of merit for ska configuration analysis. *SKA - RfP documentation*, (WP3050.020.000TR001 rev. C):1–10, December 2010. URL [http://www.skatelescope.org/wp-content/uploads/2012/06/91\\_Figures-of-Merit-for-SKA-configuration-analysis-RevC.pdf](http://www.skatelescope.org/wp-content/uploads/2012/06/91_Figures-of-Merit-for-SKA-configuration-analysis-RevC.pdf).
- [260] Binney J., Merrifield M. *Galactic Astronomy*. 1998.
- [261] Preece R. D. et al. BATSE Observations of Gamma-Ray Burst Spectra. IV. Time-resolved High-Energy Spectroscopy. *Astroph. Journal*, 496:849–862, March 1998. doi: 10.1086/305402.
- [262] Tavani M. A Shock Emission Model for Gamma-Ray Bursts. II. Spectral Properties. *Astroph. Journal*, 466:768, August 1996. doi: 10.1086/177551.
- [263] Phillips M. M. The absolute magnitudes of Type IA supernovae. *APJ*, 413:L105–L108, August 1993. doi: 10.1086/186970.
- [264] Greiner J. <http://www.mpe.mpg.de/~jcg/grbgen.html>.
- [265] Capozziello S., De Laurentis M., Luongo O., Ruggeri A. Cosmographic Constraints and Cosmic Fluids. *Galaxies*, 1:216–260, December 2013. doi: 10.3390/galaxies1030216.
- [266] Chevallier M., Polarski D. Accelerating Universes with Scaling Dark Matter. *International Journal of Modern Physics D*, 10:213–223, 2001. doi: 10.1142/S0218271801000822.
- [267] Linder E. V. Exploring the Expansion History of the Universe. *Physical Review Letters*, 90(9):091301, March 2003. doi: 10.1103/PhysRevLett.90.091301.
- [268] Hořava P. Quantum gravity at a Lifshitz point. *Phys. Rev. D*, 79(8):084008, April 2009. doi: 10.1103/PhysRevD.79.084008.
- [269] Hořava P. Spectral Dimension of the Universe in Quantum Gravity at a Lifshitz Point. *Physical Review Letters*, 102(16):161301, April 2009. doi: 10.1103/PhysRevLett.102.161301.

- [270] Weinberg S. *Gravitation and Cosmology: Principles and Applications of the General Theory of Relativity*. July 1972.
- [271] Stephani H., Kramer D., MacCallum M., Hoenselaers C., Herlt E. *Exact solutions of Einstein's field equations*. 2003.
- [272] Leavitt H. S. 1777 variables in the Magellanic Clouds. *Annals of Harvard College Observatory*, 60:87–108, 1908.
- [273] Inserra C., Smartt S. J. Superluminous Supernovae as Standardizable Candles and High-redshift Distance Probes. *Astroph. Journal*, 796:87, December 2014. doi: 10.1088/0004-637X/796/2/87.
- [274] Hubble E. A Relation between Distance and Radial Velocity among Extra-Galactic Nebulae. *Proc. of the National Academy of Science*, 15:168–173, March 1929. doi: 10.1073/pnas.15.3.168.
- [275] Liang E., Zhang B. Model-independent Multivariable Gamma-Ray Burst Luminosity Indicator and Its Possible Cosmological Implications. *Astrop. Journal*, 633: 611–623, November 2005. doi: 10.1086/491594.
- [276] Ghirlanda G., Ghisellini G., Lazzati D. The Collimation-corrected Gamma-Ray Burst Energies Correlate with the Peak Energy of Their  $\nu F_{\nu}$  Spectrum. *Astrop. Journal*, 616:331–338, November 2004. doi: 10.1086/424913.
- [277] Dainotti M. G., Cardone V. F., Capozziello S. A time-luminosity correlation for -ray bursts in the X-rays. *MNRAS*, 391(1):L79–L83, 2008. doi: 10.1111/j.1745-3933.2008.00560.x. URL <http://mnras.oxfordjournals.org/content/391/1/L79.abstract>.



## *Acknowledgements II*

Poco prima dell'una di notte, entrati nell'ultimo giorno per la sottomissione di questa tesi di dottorato, mi sembra più che giusto rilassarmi un po' scrivendo una sacrosanta sfilza di ringraziamenti ed ovviamente questa parte non sarà soggetta a correzioni.

Tirando le somme, l'esperienza del dottorato è stata certamente positiva e descriverla nella sua interezza non è possibile in poche righe. Tuttavia, posso dire che sicuramente mi ha fatto maturare ulteriormente, mettendomi davanti a difficoltà, imprevisti e sorprese che non avrei mai potuto vedere percorrendo un'altra strada. Alla fine dei tre anni, effettivamente ci si sente diversi, più arricchiti (ovviamente non nel senso monetario del termine). Quasi inconsapevolmente, si acquista la qualità di saper valutare meglio le persone, comprendendo sempre più che nella vita contano i fatti e non le parole. Alla fine della fiera, si sa sempre chi vale e chi no.

Senza annoiare più del dovuto, passiamo a quella lista che, a giudicare dall'ora, mancherà di qualche nome. Invocando il valore dell'amicizia, confido che gli assenti non mi insulteranno.

Senza dubbio alcuno, il primo della lista è il Prof. Paolo Strolin che, 5 anni orsono, incoraggiò a seguire il percorso della ricerca scientifica un giovane(?) e acerbo(??) laureato che bussò alla sua porta. Ricordo come ieri la sua prima frase: "Dottorato di ricerca??! Lasci perdere!!". Ovviamente il discorso si concluse diversamente e, per questo, un grazie da parte mia nei suoi riguardi è il minimo.

Passiamo ora a uno dei pilastri del dottorato in *Fisica Fondamentale ed Applicata*. Nonostante mi definisca un pilone di prima linea, la colonna a cui tutti i dottorandi fanno riferimento è il nostro ottimo segretario, Guido Celentano. Seppur molti di voi sanno quanto io possa essere molesto, lui ancora risponde alle mie pignolerie con una cortesia notevole e, oltre a rispondere, a volte e lui stesso a iniziare i discorsi con me. Guido, grazie per aver semplificato e reso leggero questi 3 anni di dottorato.

Allo studio accanto, il buon (padre) Nicola, a cui un saluto non si può rifiutare.

Grazie anche alle guardie del servizio di sicurezza del Dipartimento di Fisica che hanno sempre evitato di spararmi durante gli orari notturni. Sono sempre stati tolleranti e di una cortesia unica; se ho concluso in tempo è stato anche per loro concessione.

Passiamo ora ai compagni di avventura. Fortuna ha voluto che anche in questa parentesi di vita sono stato circondato da splendide persone e nominare tutti i colleghi mischiati tra 7 cicli di dottorato sarebbero troppi. Prima che il sonno obnubili del tutto la mia mente, ringrazio intanto Susan ed Atanu che ho stressato fino alla fine con domande sugli usi e modi di dire inglesi, per evitare di scrivere in *Italish*. Sono anche riuscito a importunare Deborah che spontaneamente mi chiese se mi serviva una mano. Come poter rifiutare?

In ordine sparso potrei nominare Mariano, Lorenzo (paziente alfa della sindrome - ancora solo teorizzata - sul progressivo decadimento mentale dei dottorandi), Behzad, Hassan, Fatema, Andrea, Akif, Filippo, Paolino, Fabio e Serena (che in realtà non è una dottoranda, ma mi deve un pacco di Mikado), ma potrei continuare a snocciolarne altri. Ragazzi, a tutti voi, sinceramente, grazie!!

Nominando Filippo, mi sono ricordato i compagni di basket (preziosissimi) con cui ho passato ore divertentissime, che dissipavano lo stress di una giornata di lavoro. Gerardo, Gegè, Luigi, Alessandro, Stefano, Lucio, ecc ecc ecc.

Agli amici di sempre, Clizia e Pietro, che per una cosa e l'altra mi hanno accompagnato durante questi tre anni. Vorrei sottolineare che, seppur leggermente sfasati e dislocati in posti diversissimi, tutti e tre abbiamo spesso avuto idee molto simili sul dottorato ricerca. Pur essendo in fascia non protetta, stendiamo un velo di silenzio...

Anche voi, grazie!

Siccome non sarebbe corretto rompere le scatole ai soli amici, come potevo non coinvolgere anche mio fratello? Christian, grazie mille per l'ausilio che mi ha fatto guadagnare parecchio tempo che altrimenti avrei tolto alla scrittura della tesi. Grazie per essere stato presente quando ho chiesto il tuo aiuto!

Ovviamente non posso non ringraziare Gianfranca e Tristano, con cui mi sono consultato per motivo di studio, consigli vari e partite di calcetto. Ma lo stesso vale per Peppe Longo a cui ogni tanto ho chiesto dei pareri, nonché a Mariafelicia, Orlando e Maria Giovanna.

Pensavate che stessi finendo e... vi sbagliavate!

Dottorandi in azienda? Presenti!! Riccardo, come potersi dimenticare del mio collega dottorando aziendale, come pure della prossima neo mamma, Mena. È stato un piacere dividere con voi opinioni e consigli sul da farsi.

Un buon dottorando in azienda non è all'altezza del suo dottorato se non saluta i colleghi SAM. Cominciando con Elena e Renato, Alessandro, Tommaso e Luca, che ringrazio per avermi seguito dall'inizio alla fine (senza comunque scordare R. C., che non so se se può essere nominato) una riga a parte va a Salvatore, con cui ho interagito molto nell'arco di questi anni ed è stato un punto di riferimento e un amico in SAM e con cui ho lavorato nel progetto dello SKA. Salvo, se la plafoniera è attaccata al soffitto, siamo d'accordo che occorre un 40% in più per svitare la lampadina??

Un grazie anche a Jean e Louwrens che mi hanno praticamente permesso di arrampicarmi sulla prima antenna di MeerKAT in mezzo al deserto del Karoo. Esperienza incredibile, come per il ritorno: in volo charter e al posto di copilota, accanto a Jerard.

Infine, ricordiamoci tutti che "se da un testo prendi le cose utili e togli quelle che non ti servono, hai finito!".

**Fratello, amici e colleghi, a tutti voi, di tutto cuore, grazie!!!**